MECHANISM AND ROLE OF CALCIUM IN EXCITATION-MUCUS SECRETION COUPLING IN HUMAN COLONIC EPITHELIUM

By

SIU KEI CHRISTY KAM

A thesis submitted for the degree of Doctor of Philosophy

School of Biological Sciences
University of East Anglia

September 2015

Abstract

Defective mucus barrier function is one of the contributing factors for inflammatory bowel disease (IBD) pathogenesis. Understanding the regulation of mucus secretion is essential for developing new therapies. Cholinergic signals have been shown to stimulate mucus secretion, but the mechanism is not fully understood. The aim of this study was to investigate the molecular mechanism of calcium (Ca^{2+}) coupling mucus (MUC2) secretion in colonic goblet cells in situ, using an ex-vivo 3D model native human colonic crypt model system.

Immunohistochemistry revealed the presence of cholinergic neurons in close proximity to the basal membrane of the crypts, where the muscarinic receptor (M3AchR) was expressed. Fura-2 Ca^{2+} imaging demonstrated that Carbachol (Cch) evoked Ca^{2+} signals at the human colonic crypt base via M3AchR activation, which then spread to all cell types along the crypt-axis. Surprisingly, pharmacological inhibition of the canonical 2nd messenger IP3 pathway had no major effect on Ca^{2+} signal generation, and depleting the ER Ca^{2+} store demonstrated Cch-induced Ca^{2+} mobilisation from other intracellular organelles, including lysosomes. Inhibition of pathways and 2nd messengers which mobilise Ca^{2+} from lysosomal stores – including chemicals targeting CD38, NOX1, NAADP and TPC – profoundly suppressed Cch-induced Ca^{2+} signals. Furthermore, inhibition of this cholinergic coupled calcium signalling pathway prevented MUC2 mucus secretion from colonic crypt goblet cells in situ.

This is the first study to demonstrate that M3AchR activation mobilises Ca^{2+} from acidic lysosomes in the human colonic epithelium. These findings also implicate NAADP as the key 2nd messenger which mediates this pathway via activation of two pore channels. Modulation of Ca^{2+} release from acidic stores may serve as a potential target for treating IBD and other gastrointestinal pathologies.

Declaration

I declare that this thesis represents my own work, except where due acknowledgement is made, and that it has not been previously included in a thesis, dissertation or report submitted to this University or to any other institution for a degree, diploma or other qualifications.

Christy Kam

PhD candidate

Acknowledgements

This project would not have been possible without the support of many people.

First of all, I would like to thank the Norwich Research Park (NRP) for awarding me the postgraduate studentship which supported me financially throughout my studies.

I would like to thank my primary supervisor Dr. Mark Williams for his amiable and beneficial guidance throughout the whole project. Thank you for sharing your excitement about colonic crypts with me.

I am extremely appreciative to Dr. Alyson Parris for her help and suggestions for the experiments, both of which were invaluable to me. It was an absolute pleasure to work with you for the past 4 years. Every time when I was unclear on something, you always talked me through it. I really appreciate it.

Special thanks to Dr. Paul Thomas for his expert help with the confocal imaging and analysis. You repeatedly saved my life over the past four years by fixing the confocal microscope for me, so that I could manage to keep imaging long into the night.

I am grateful for the collaboration and contributions to the current work from past master students including Martin, Hakeemah and George.

Thanks also go to the past and present members of Dr. Ian Clark's and Dr. Andrea Munsterberg's lab for their help. I am especially thankful to Ian for allowing me to do some PCR work in his lab.

I would like to take this opportunity to thank my partner Jamie. Thank you for all your unconditional support for the past four years. I would like to thank my family, especially my aunt Joyce and my cousin Fiona for their support. Last, to all my friends, especially Linh and Hinnah. Thanks to all of you for listening to me and for keeping me going.

Glossary

Ach	Acetylcholine
ACTB	Beta actin
2APB	2-Aminoethoxydiphenyl borate
ASC	Active stem cell
ATP	Adenosine triphosphate
B2M	Beta-2 microglobulin
Baf	Bafilomycin
BMP	Bone morphogenetic protein
BSA	Bovine Serum Albumin
Ca^{2+}	Calcium
cADPR	Cyclic ADP-ribose
CaM	Calmodulin
CBCC	Crypt base columnar cell
Cch	Cabachol
CCK	Cholecystokinin
CD	Crohn's disease
CDC	Centre for Disease Control and Prevention
CD38	ADP ribosyl cyclase
CGA	Chromogranin A
CHAT	Choline acetyltransferase
CHQ	Chloroquine
CHRM	Cholinergic receptor, muscarinic (Gene)
CICR	Calcium induced calcium release
Cl^-	Chloride ion
CNS	Central nervous system
COX	Cyclooxygenase
CPZ	Chlorpromazine hydrochloride
CRAC	Calcium Release-Activated Channels
Ct	Threshold cycle
Cys	Cysteine
DAG	Diacylglycerol
DAMP	Danger-associated molecular patterns

DHPR	Di-hydropyridine receptor
DMSO	Dimethyl sulfoxide
DPI	Diphenyleneiodonium
DTT	Dithiothreitol
DZM	Diltiazem
Ecad	E-cadherin
E-C coupling	Excitation contraction coupling
EDTA	Ethylenediaminetetraacetic acid
EGF	Epidermal growth factor
ENS	Enteric nervous system
EP-R	Prostaglandin E receptors
ER	Endoplasmic reticulum
ERAD	Endoplasmic reticulum associated degradation
Fcgbp	Fc gamma binding protein
GALT	Gut associated lymphoid tissue
$GdCl^3$	Gadolinium III Chloride
GDP	Guanosine diphosphate
GEFs	Guanine nucleotide exchange factors
GI	Gastrointestinal
GISTs	Gastrointestinal stromal tumors
GPCR	G-protein coupled receptor
GPN	Glycyl-L-phenylalanine-beta-naphthylamide
GTP	Guanosine triphosphate
GWAS	Genome-wide association study
H_2O_2	Hydrogen peroxide
HCO_3^-	Bicarbonate
HCX	Hydrogen/calcium exchanger
HEK293 cell	Human embryonic kidney 293 cell
IBD	Inflammatory bowel diseases
IL-10	Interleukin-10
IMM	Inner mitochondrial membrane
IP3/ ITP	Inositol triphosphate

IP3R/ ITPR	Inositol triphosphate receptor
ISC	Intestinal stem cell
KDEL	Lysine, Aspartic acid, Glutamic acid, Leucine (ER retention protein sequence)
KO	Knockout
La^{3+}	Lanthanum ions
LAMP-1	Lysosomal-associated membrane protein 1
LC3	Microtubule-associated protein 1A/1B-light chain 3
LGR5	Leucine-rich repeat-containing G-protein coupled receptor 5
LPS	Lipopolysaccharide
M cells	Microfold cells
M1AchR	Muscarinic acetylcholine receptor 1
M3AchR	Muscarinic acetylcholine receptor 3
M5AchR	Muscarinic acetylcholine receptor 5
MβC	Methyl-beta-cyclodextrin
MCU	Mitochondrial uniporter
Mg^{2+}	Magnesium
MUC2	Mucin 2
NAADP	Nicotinic acid adenine dinucleotide phosphate
NAD	Nicotinamide adenine dinucleotide
NADP	Nicotinamide adenine dinucleotide phosphate
NAchR	Nicotinic acetylcholine receptor
NADPH oxidase	Nicotinamide adenine dinucleotide phosphate-oxidase
NCX	Sodium calcium exchanger
NKCC1	Na-K-Cl cotransporter
NLR	NOD-like receptor
NOD2	Nucleotide-binding oligomerisation domain-containing protein 2
NOX1	NADPH oxidase 1
OCT	Organic cation transporter
OLFM4	Olfactomedin 4
OMM	Outer mitochondrial membrane
P2RX4	P2X purinoceptor 4
PA	Phosphatidic acid

PAMP	Pathogen-associated molecular patterns
PBS	Phosphate buffer saline
PC	Phosphatidylcholine
PFA	Paraformaldehyde
PGE2	Prostaglandin E2
PIP2	Phosphatidylinositol 4,5-bisphosphate
PKC	Protein Kinase C
PLA	Phospholipase A
PLC	Phospholipase C
PLD	Phospholipase D
PMCA	Plasma membrane calcium ATPase
PNS	Peripheral nervous system
PTP	Permeability transition pore
PTS	Proline, Threonine, Serine
QSC	Quiescent stem cell
RELMβ	Resistin-like molecule beta
ROS	Reactive oxygen species
RT-qPCR	Reverse transcription-quantitative polymerase chain reaction
RYR	Ryanodine receptor
SERCA / ATP2A	Smooth ER calcium ATPase/ gene
SOCE	Store-operated calcium entry
SPDEF	SAM pointed domain ETS factor
SR	Sarcoplasmic reticulum
STIM-1	Stromal interaction molecule-1
TM	Transmembrane
T-tubule	Transverse-tubule
TFF	Trefoil factor
Tg	Thapsigargin
TGF-β	Transforming growth factor-beta
TNF-α	Tumour necrosis factor-alpha
TPCs	Two pore channels
TPCN	Two pore channels (Gene)

TRP	Transient receptor potential
TUJ-1 / TU-20	anti- neuronal class III beta-tubulin
UC	Ulcerative colitis
UPR	Unfolded protein response
VAChT	Vesicular acetylcholine transferase
VDAC	Voltage dependent anion channel
V-type	Vacuolar type
XBP-1	X-box binding protein-1
XesC	Xestospongin C

Table of Contents

Table of Figures

Chapter 1: General Introduction

Mucosal barrier in health and diseases

The gastrointestinal (GI) tracts of vertebrate species are incredibly interesting biological systems, which must fulfil a number of contrasting functions. They must be able to digest food, without digesting themselves. They also contain billions of bacteria – some commensal, some pathogenic, some somewhere in between – and thus must allow the concomitant survival and existence of both parties. The intestinal mucosal barrier provides the first line of defence against these bacteria and toxins, as well as host-derived digestive enzymes (Johansson, et al., 2013). It consists of three protective components: cell junctions, mucus layers and anti-microbial peptides (Groschwitz, 2009). The innermost layer of the mucosa is composed of a single layer of epithelial cells inwardly facing the lumen of the GI tract. This intact epithelial cell layer is sealed by apical junctional complexes including the tight and adherens junctions (Figure 1.1 left). Tight junctions form a physical barrier which control the paracellular transport across the epithelium; whereas the adherens junctions maintain the integrity and polarity of the epithelium (Giepmans, et al., 2009). Coating the epithelial layer is the key defence mechanism: the mucus barrier. The colon is protected by two mucus layers: the outer layer harbours the commensals, while the inner layer is usually impenetrable to bacteria (Figure 1.1 right) (Hansson, et al., 2010). In healthy colonic epithelium, interaction with microbes is minimised by the secretion of anti-microbial peptides, primarily defensins, and by the functional mucus barrier (Antoni, et al., 2014).

Intestinal barrier dysfunction – where the physical barrier between luminal bacteria and the intestinal mucosa is defective – is emerging as a risk factor for some subsets of inflammatory bowel diseases (IBDs) (Antoni, et al., 2014). Defective mucus production has been reported in various immune mediated diseases. Insufficient or absent mucus layers allows bacteria to come into direct contact with epithelial cells. Mouse models devoid of such layers have been shown to develop severe colitis and eventually colon cancer (Velcich, et al., 2002; Van der Sluis, et al., 2006; Heazlewood, et al., 2008; Hansson, et al., 2010; Balzola, et al., 2013), which resembles the phenotype of human disease. Changes in mucus composition have also been shown to affect the makeup of microbial populations (Fritz, et al., 2011). In addition, tight junction barrier dysfunction has also been shown to contribute to the development of IBD (Hollander, 1988; Groschwitz, et al., 2009; Salim, et al., 2011; Hering, et al., 2012). Thus, the mucosal and mucus barriers play an important role in GI defence, with intestinal permeability potentially being one of the key factors contributing to colonic diseases such as IBD.

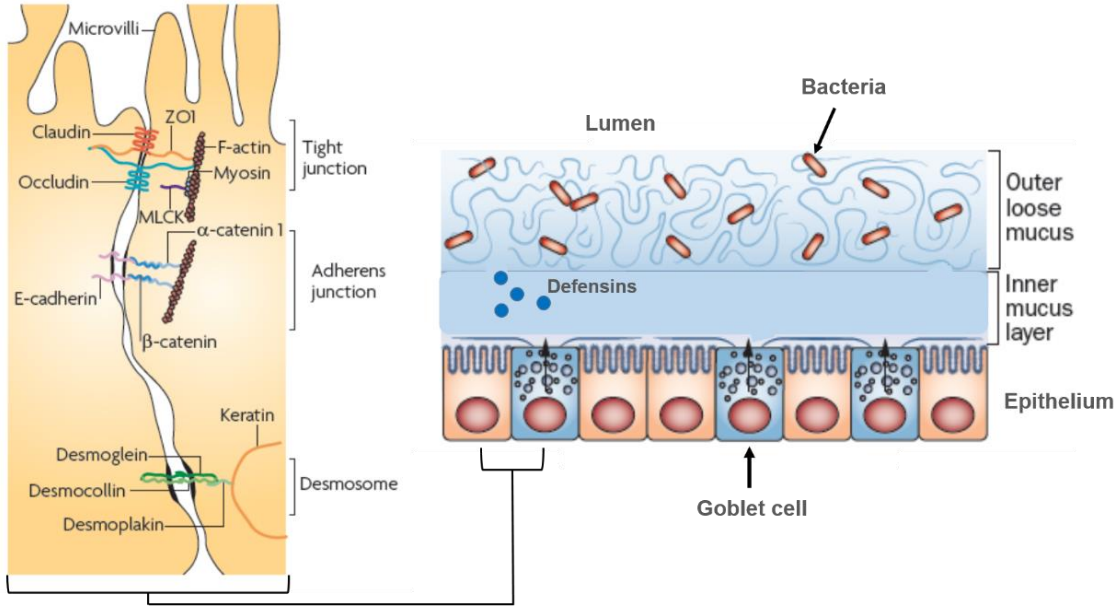

Figure 1.1 Colonic defence barrier

The colonic mucosa is composed of a single layer of epithelial cells (right). Each cell is connected by junctional complexes including tight and adherens junctions that control paracellular transport and maintain the integrity & polarity of the epithelium respectively (left). The key defence mechanism of the colonic epithelium is the surface mucus coatings that are produced by colonic goblet cells. The outer mucus layer harbours the commensals, while the inner mucus layer is normally sterile. Microbial-epithelial interactions are further minimised by the secretion of anti-microbial peptides such as defensins by Paneth-like cells (goblet cells) at the colonic crypt base.

(Figures from Turner, 2009 (Left) and partially adapted from Johansson, et al., 2013 (Right))

IBDs are major health problems in developed countries which can greatly impair the quality of life of the patients. IBDs are characterised by chronic or relapsing gastrointestinal inflammation (Jawad, et al., 2011; CDC, 2015). Based on their clinical and histopathological features, IBDs can be categorised into ulcerative colitis (UC) and Crohn's disease (CD). CD can affect all of the digestive systems (from mouth to anus), whereas the inflammation observed in UC is restricted to the colon (Gersemann, et al., 2011). 30-40% of genetic risk loci are shared between the diseases despite their phenotypic differences (Zhernakova, et al., 2009; Budarf, et al., 2009; Fritz, et al., 2011), and patients with chronic uncontrolled colitis (CD or UC) have a significantly higher risk of developing colorectal cancer (Coussens, et al., 2002; Sheng, et al., 2011; Jawad, et al., 2011). The risk of UC-associated colorectal cancer elevates after seven years of extensive colonic disease (Guagnozzi, et al., 2012). Based on a meta-analysis of 41 cumulative studies, IBD-associated colorectal cancer in UC patients was 2% at 10 years, 8% at 20 years, and 18% after 30 years of disease (Eaden, et al., 2001). Although colorectal cancer occurs in a minority of IBD patients (1%), it accounts for approximately 20% of IBD-related deaths (Basseri, et al., 2011). The worldwide incidence rate of UC varies between 2.2-14.3/ 100,000 persons, whereas CD varies between 3.1-14.6/100,000 persons (CDC, 2014). While the precise aetiology of the diseases remains unclear, it is believed that they are caused by complex interactions between genetic, environmental and immune-regulatory factors. This would involve: (1) the luminal bacteria and dietary factors; (2) the intestinal epithelial barrier; and (3) the innate and adaptive immune systems.

The vast majority of research into the pathophysiology of UC has mainly concentrated on immunological aspects (Cader, et al., 2013; Geremia, et al., 2014). However, the role of defects in the production and maintenance of the mucus layer have not been extensively addressed. Increased intestinal permeability was reported as early as the 1980s in children with active small-bowel CD (Pearson, et al., 1982), a phenomenon that has been suggested as a predictor of relapse in CD patients (Wyatt, et al., 1993). More recently, barrier dysfunction was also described in UC patients (Arslan, et al., 2001; Welcker, et al., 2004). These findings, alongside MUC2 knockout (KO) mouse phenotypes, inform a hypothesis that defective mucus layers and tight junction abnormalities might contribute to disease progression. However, it remains to be shown whether permeability changes are primary events in disease development or secondary effects triggered by inflammation.

By highlighting disease-associated genetic polymorphisms, genome-wide associated studies (GWAS) have implicated a number of genes as potential contributors to IBD susceptibility, particularly nucleotide-binding oligomerisation domain-containing protein 2 (NOD2), a

regulator of autophagy (Hugot, et al., 2001; Ogura, et al., 2001; Van Limbergen, et al., 2009; Fritz, et al., 2011). These genomic data have brought NOD2, autophagy and endoplasmic reticulum (ER) stress responses to light as a focus of IBD research for the past few years. For example, ER stress and the unfolded protein response (UPR) have recently been shown to be involved in the regulation of mucus secretion (Walter et al, 2011).

The current gold standard treatment for moderate to severe IBD patients consists of anti-inflammatory therapy (such as anti-tumour necrosis factor, or TNF). However these treatments can be considered to be targeting the symptoms rather than the underlying cause of the disease, which is typically unknown. Recent studies have implicated the cholinergic nervous system in mediating gut immune responses (Pavlov, et al., 2003; Pavlov, et al., 2008). Cholinergic signalling has additionally been shown to play a role in cell proliferation (Wessler, et al., 2008; Takahashi, et al., 2014), axon guidance (Xu, et al., 2011), muscle contraction (Parkman, et al., 1999; Gosens, et al., 2006), fluid secretion (Javed, at al., 1992; O'Malley, et al., 1995; Reynolds, et al., 2007) and mucus secretion (Halm and Halm, 2000), and cholinergic-mediated MAchR activation has been shown to mobilise intracellular Ca^{2+} (Lindqvist, et al., 1998; Lindqvist, 2000). These findings imply that there are connections between cholinergic signals, intracellular Ca^{2+} mobilisation and mucus secretion; however there is no specific evidence thus far regarding the underlying mechanisms of how cholinergic signals could mediate Ca^{2+} signal generation and how this relates to the regulation of mucus barrier function. Therefore the research question of this thesis asks what are these mechanisms, and how do they function, with the contention that it could potentially form the basis of a therapy for treating IBD.

1.1 Neuronal-epithelial cells interaction

1.1.1 Structure and function of the human colon

The human large intestine consists of the cecum, colon, rectum and anus, in order, totalling around one and a half meters in length. The colon is separated into four regions (Figure 1.2): the ascending colon (which passes upwards from the cecum on the right), transverse colon (the longest section which arches across), descending colon (passing downwards on the left) and sigmoid colon (the 'S' shaped region connecting to the rectum and anus). The primary function of the large intestine is to absorb water from the remaining indigestible food matter (stool) (Grays, 1918; NIH National Cancer Institute). Mucus is secreted by colonic goblet cells into the gut lumen where in addition to its protective barrier functions it serves as a lubricant for the stool passing through the colon due to peristalsis. The stool is stored in the sigmoid colon and it normally takes about 36 hours for the content to be emptied into the rectum and passed out the body from the anus.

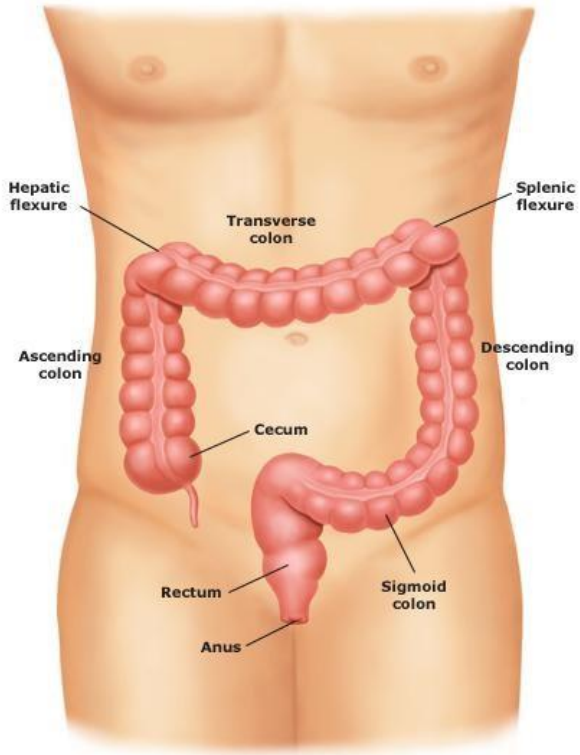

(Figure from Colorectal Cancer Association of Canada)

Figure 1.2 Anatomy of the human Colon

The large intestine consists of the cecum, colon, rectum and anus. The colon is further separated into four regions: ascending, transverse, descending and the sigmoid colon. The hepatic flexure (adjacent to liver) is a sharp bend between ascending and transverse colon. The splenic flexure (near spleen) is a sharp bend between transverse and descending colon. The primary function of the colon is to absorb water from the remaining indigestible food matter.

1.1.2 Mucin distribution along the GI tract

The major functional components of the colonic barrier are mucin glycoproteins, the organisation of which varies along the GI tract (Atuma, et al., 2001). Similar to the large intestine, the stomach is protected by a relatively thick sterile firm inner mucus layer, where the loose outer layer contains low numbers of bacteria compared to the colon (Figure 1.3). This thick inner layer is believed to protect the lining from the acidic digestive enzymes. The mucins 5AC (MUC5AC) and MUC6 are the major mucin subtypes produced by stomach goblet cells. The MUC2 glycoprotein is the major type of gel-forming mucin found in the small and large intestines (Matsuo et al., 1997). In the small intestine, both the inner and outer mucus layers are very thin, and the mucins are produced by goblet cells and Paneth cells (Stappenbeck, 2009). Both thin mucus layers seem to facilitate the absorption of nutrients and minerals from the digested food (Ermund, et al., 2013B). Mucin production in the colon comes predominately from goblet cells (McGuckin et al., 2011). The large intestine is also protected by two layers of mucus, with the loose outer mucus layer (being the habitat of millions of commensals) being the thickest among the entire GI tract (Hansson, et al., 2010) (Figure 1.3). These bacteria have several useful functions such as synthesising vitamins (K and H), processing food waste (fermenting indigestible dietary fibre for the generation of short chain fatty acids) and protecting us from the actions of harmful bacteria. Thus, the thickness of the mucus layer correlates with the specific function of the different regions of the GI tract. However, the regulation of mucus secretion remains poorly understood.

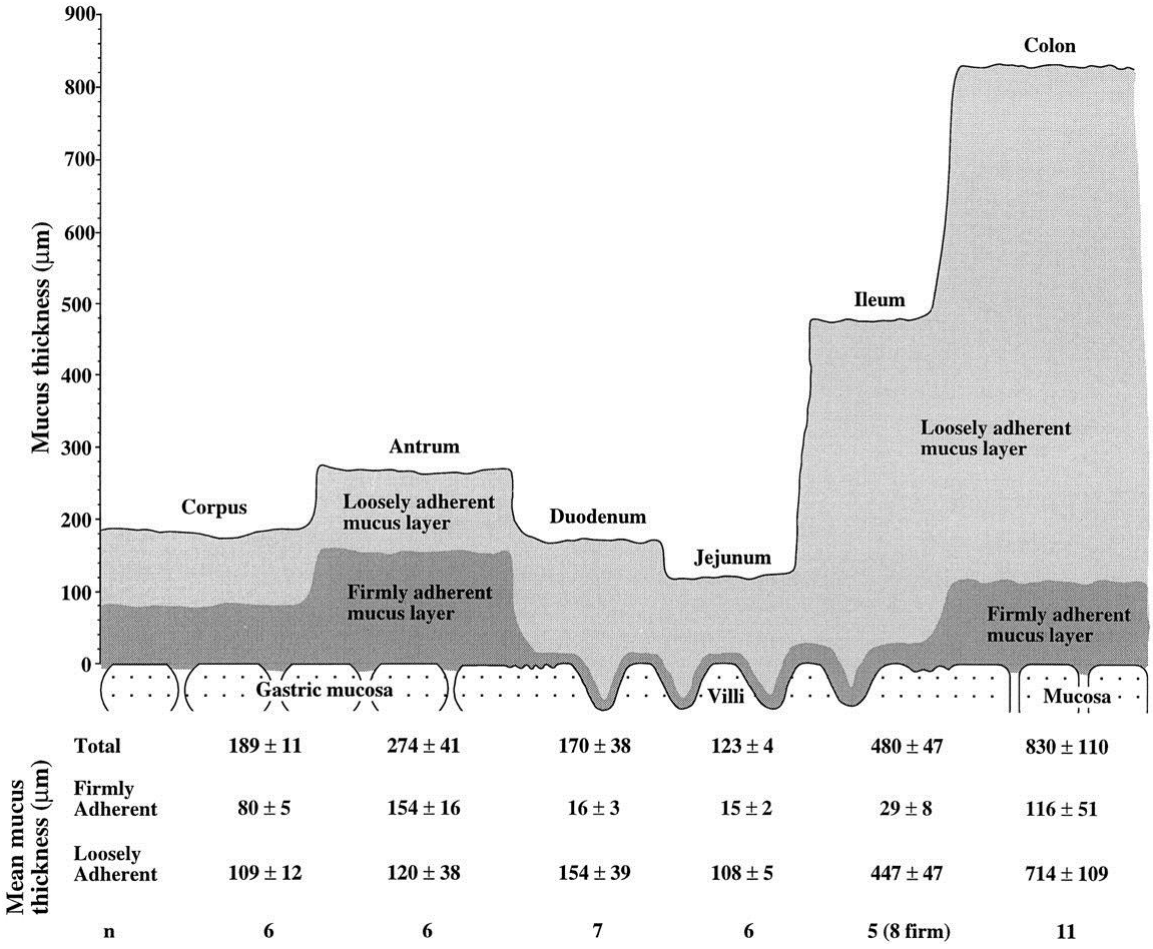

Mean mucus thickness (μm)

Total	189 ± 11	274 ± 41	170 ± 38	123 ± 4	480 ± 47	830 ± 110
Firmly Adherent	80 ± 5	154 ± 16	16 ± 3	15 ± 2	29 ± 8	116 ± 51
Loosely Adherent	109 ± 12	120 ± 38	154 ± 39	108 ± 5	447 ± 47	714 ± 109
n	6	6	7	6	5 (8 firm)	11

Figure 1.3 Schematic diagram of the gastrointestinal mucosal barrier.

The diagram shows the thickness of the two translucent mucus layers of the rat GI tract. The loose outer mucus layer (light grey) is continuous along the GI tract and can be easily removed by careful suction, while the firm inner mucus layer (dark grey) is relatively thicker and continuous only in the stomach (antrum) and colon. In the small intestine (duodenum, jejunum and ileum), the inner mucus layer (dark grey) is relatively thin, and exhibits a patchy distribution (non-continuous) and is absent from some individual villi according to some studies.

(Figure from Atuma, et al., 2001)

1.1.3 Anatomy of the intestinal mucosa

The mucosa is the innermost layer surrounding the lumen of the GI tract. Both the small and large gut wall are composed of the following four layers (outer to inner): serosa or adventitia (connective tissue), muscularis externa (two layers of smooth muscle, longitudinal and circular), submucosa (dense and irregular connective tissue) and mucosa (Figures 1.4 and 1.6). The mucosa itself is further divided into three layers (inner to outer): epithelium, lamina propria (connective tissue), and muscularis mucosae (thin layer of smooth muscle) (Jaladanki, et al., 2011). The surface of the small intestinal epithelium has numerous finger-like protrusions called villi projecting into the lumen, which increases the surface area for absorption. These villi are closely associated with the pocket-like invaginations called Crypts of Lieberkühn (Figures 1.4 and 1.5). By contrast, villi are absent in the colon and the surface lining of the colonic epithelium is flat, pocked with numerous crypts (composed of a single layer of epithelial cells) that penetrate into the underlying submucosa (Figures 1.4 and 1.6) (Jaladanki, et al., 2011; Simons, et al., 2011a). These epithelial cells are under constant self-renewal, being replaced every 4-5 days, with the stem cells located at the base of the crypts providing the proliferative activity of the crypt (Van der Flier, et al., 2009; Clevers, 2013a and b). The study of crypt biology is therefore faced with a number of relative technical difficulties, being complex physiological units composed of a heterogeneous mix of rapidly dividing cells. Furthermore, despite being highly prevalent – it has been estimated that there are about 20 million crypts in the human colon (Potten, et al., 2003) – given their location they are relatively inaccessible, which can make data or sample acquisition more difficult.

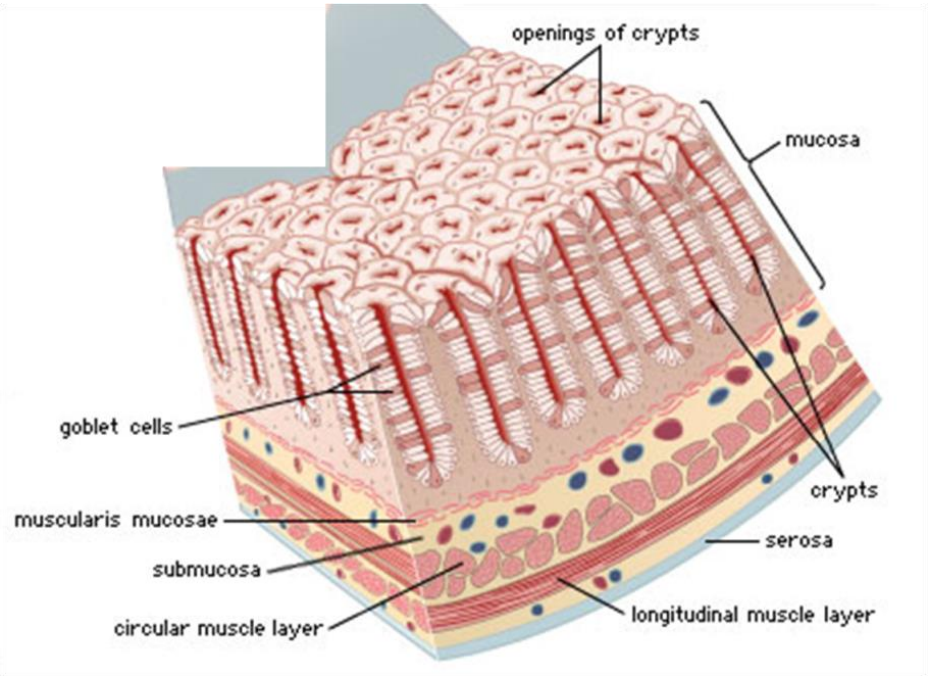

Figure 1.4 Structures of the colonic mucosa.

The large intestinal wall is composed of four layers (from bottom to top): serosa, muscularis externa (longitudinal and circular smooth muscle layers), submucosa and the mucosa. The mucosa is further divided into three layers: muscularis mucosae (thin layer of smooth muscle), lamina propria (connective tissues) and the single epithelial cell layer folded into structures called Crypts of Lieberkühn. Openings of crypts face towards the gut lumen that are the passageways for fluid and mucus secretion. Goblet cells are one of the epithelial cell types embedded in crypts and are responsible for synthesis and secretion of mucus.

(Figure from Encyclopaedia Britannica)

1.1.4 The organisation of human colonic crypt and the importance of stem cell niche

The four major epithelial cell lineages present in the colonic crypt are: (1) the enterocytes or columnar cells, (2) the mucus-secreting goblet cells, (3) peptide hormone-secreting enteroendocrine cells and (4) tuft cells (Figure 1.5). Paneth cells and microfold (M) cells (other epithelial cell lineages found in the small intestine) are not detected in the colon (Cheng, et al., 1974b; Van der Flier, et al., 2009; Gerbe, et al., 2011; Simons, et al., 2011a). However, Paneth-like cells (goblet cells expressing the Paneth cell marker cKit) have been demonstrated to be present at the mouse colonic crypt base (Rothenberg, et al., 2012). These crypt base goblet cells have an intermediate gene signature between goblet and Paneth cells, but their functional significance remains uncertain (Date and Sato, 2015). All these cell types are terminally differentiated and are derived from the multipotent intestinal stem cells (ISCs) located at the bottom of the crypt (Figure 1.5) (Bjerknes, et al., 1981a and b; Simons, et al., 2011a and b; Gerbe, et al., 2012).

The most abundant cell type in the colon are columnar cells, which make up more than 80% of intestinal epithelia. These cells are highly polarised and have a basal nucleus and an apical brush border, which plays a dual role in absorption and secretion (Cheng, et al., 1974b; Van der Flier, et al., 2009). Goblet cells play a major role in mucosal defence by secreting mucins. They also secrete other bioactive molecules believed to help protect and repair the epithelium and maintain mucosal barrier integrity, such as trefoil factors (TFF), resistin-like molecule beta (RELMβ) and Fc-gamma binding proteins (Fcgbp) (Kim, et al., 2010). In addition, the proportion of goblet cells increases from the duodenum (~4%) to the descending colon (~16%) (Karam, 1999). Enteroendocrine cells are present throughout the intestinal epithelium, which represents approximately 1% of all intestinal lineage. They produce peptide hormones which are secreted basally in an endocrine or paracrine manner (Tsubouchi, et al., 1979). Based on their morphology and specific hormone expression, 15 different enteroendocrine cell subtypes have been identified (Schonhoff, et al., 2004). Tuft cells are very rare cell types identified which constitute roughly 0.4% of total epithelia (Bjerknes, et al., 2012; Gerbe, et al., 2012). Their precise function is unknown but is probably related to sensing the chemical content of the lumen (Hofer, et al., 1996; Clevers, 2013a and b). All four lineages move up the crypt axis and are shed into the lumen after a few days while undergoing apoptosis. In addition, relatively long lived Paneth cells (2-3 months) at the base of small intestinal crypts produce lysozymes, antimicrobials, and defensins, which are stored in apical granules awaiting secretion, allowing them to play a major role in innate immunity in the small intestine (Bjerknes, et al., 1981b; Date and Sato, 2015). During

differentiation, Paneth cells move downward to the base of crypt and are suggested to regulate the stem cell niche by providing Wnt, Notch and EGF signalling to the stem cells (Bjerknes and Cheng, 1981a and b; Abdul khalek, et al., 2010; Sato, et al., 2011; Simons and Clevers, 2011a; Date and Sato, 2015). M cells are expressed at the surface of the gut associated lymphoid tissue (GALT) in the small intestine, where they transport luminal antigens to immune cells such as dendritic cells and macrophages (Neutra, 1998).

Due to the high turnover of cells there is a strong pressure to maintain homeostasis of the intestinal epithelium. The ISCs are $Lgr5^{+}$ (Barker, et al., 2007) and were first identified as crypt base columnar cells (CBCC) undergoing continuous cell cycling by Cheng and Leblond in 1974. These ISCs are crucial for the renewal of the differentiated progeny within the intestinal epithelial layer (Leblond and Stevens, 1947; Medema, et al., 2011; Clevers, 2013a) and play a major role in maintaining the cellular organisation of the mucosa. Briefly, the stem cells proliferate and exit the stem cell zone at the base of crypt and start to differentiate into one epithelial cell lineage; once committed the lineage will further mature upon migration up along the crypt axis (Bjerknes and Cheng, 1981a and b). Moreover, extensive evidence demonstrates the importance of Wnt and Notch signalling pathways in maintaining the ISC niche and regulating normal crypt dynamics (Pinto, et al., 2003; van Leeuwen, et al., 2009; Ogaki, et al., 2013). Furthermore, reactive oxygen species (ROS) has recently emerged as an important mediator of stem cell homeostasis in various systems, in particular, Rac1-dependent ROS has also been shown to drive stem cell proliferation and regeneration in mouse model of colorectal cancer (Myant, et al., 2013).

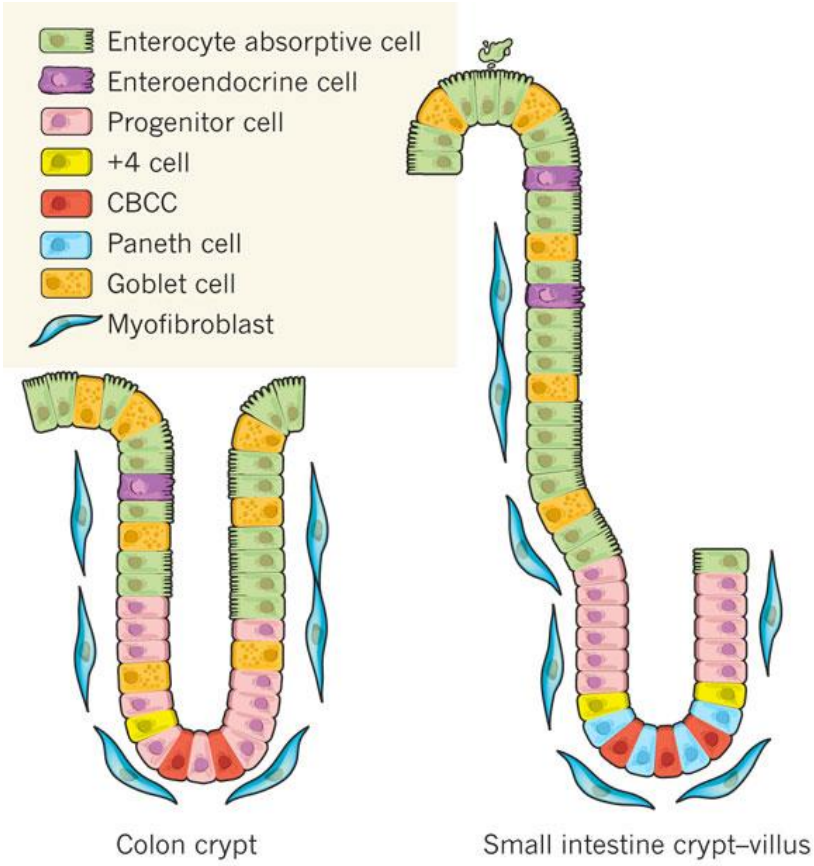

Figure 1.5 Characterisation of intestinal epithelial cell lineages in crypt and villus

The epithelium is composed of a variety of cell types. Intestinal stem cells (ISCs) are $Lgr5^{+}$ and were first identified as crypt base columnar cells (CBCC, red) located at the base of the crypt. These stem cells are involved in the generation of progenitor cells (pink) that subsequently differentiate into other epithelial cell lineages including enterocytes (green), goblet cells (orange), enteroendocrine cells (purple), and Paneth cells (small intestinal crypt only, light blue); and they play an important role in the renewal and repair of the epithelium. Some studies have suggested the presence of +4 cells (quiescent stem cell population, yellow) that function to replenish the active stem cell population after crypt injury. Other newly identified epithelial cell lineages including tuft cells and M cells (small intestine only) are not shown in this figure. The subepithelial myofibroblast (dark blue, alpha-smooth muscle actin-positive (α-SMA^{+}) mesenchymal cells in the lamina propria) has also been shown to be involved in growth and repair, tumorigenesis and fibrosis of the intestine.

(Figure from Medema, et al., 2011)

1.1.5 Enteric nervous system

The enteric nervous system (ENS), called the second brain by some, is embedded in the wall of the GI tract. It contains 200-600 million neurons which are distributed in many thousands of small ganglia. The majority of these ganglia can be found in the myenteric (Auerbach's) plexuses located between the inner and outer layer of the muscularis externa; and in the submucosal (Meissner's) plexuses located in the submucosa (Figure 1.6) (Bowen, R. 2006; Furness, J. 2008). Both plexuses receive central nervous system (CNS) signals via the parasympathetic and sympathetic systems, which can control the activation and inhibition of the gastrointestinal functions respectively. The ENS is also an autonomous system, which includes a number of efferent-, afferent- and interneurons (the neural circuits) which make the system capable of reflex actions and signal transduction in the absence of the CNS input (Furness, et al., 2014).

The function of the ENS is to control blood flow, motor functions, mucosal transport and secretions, and also to modulate immune and endocrine functions. All these events are interlinked and are operated in concert by independent enteric neural networks, including the muscle motor neurons, secreto-motor neurons, and vasodilator neurons (Costa, et al., 2000). To perform their functions, the primary afferent (sensory) neurons sense thermal, chemical and mechanical stimuli; the signals are then conveyed by interneurons which act directly on different effector cells including the smooth muscle, mucosal glands, blood vessels and epithelial cells (Costa, et al., 2000).

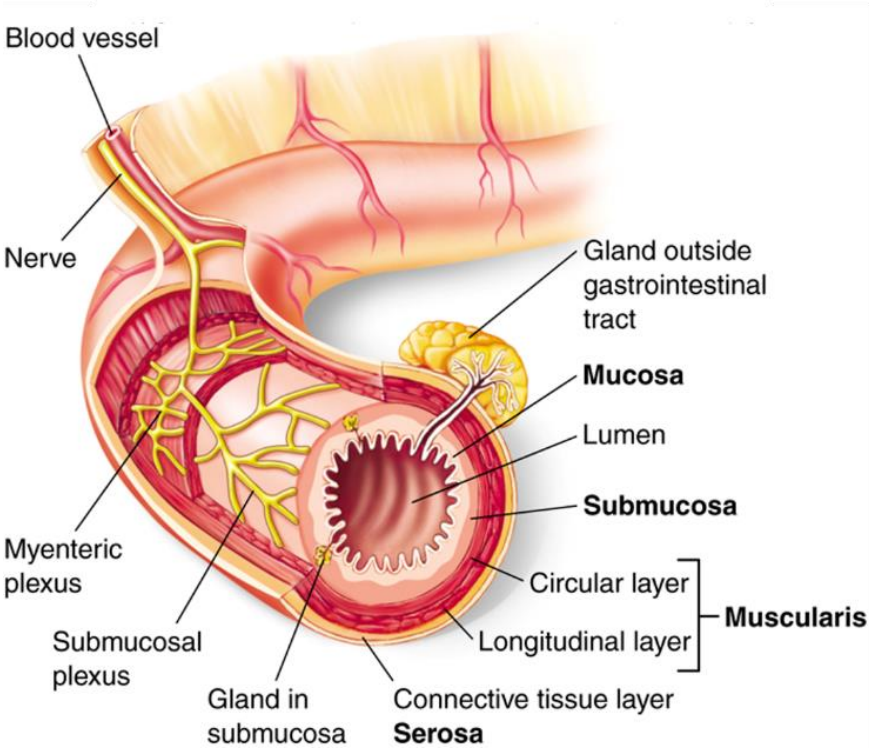

Figure 1.6 Enteric nervous systems.

The wall of the GI tract is innervated with a few hundred millions of neurons (enteric nervous systems) and these neurons are distributed in many thousands of small ganglia. The majority of these ganglia are found in the myenteric (Auerbach's) plexuses located between the two layers of the muscularis externa; and in the submucosal (Meissner's) plexuses located in the submucosa. Some nerve (axon) terminals are further extended from the submucosa into the mucosa (crypts) (Figures 3.1, 3.2 and 3.4). The functions of the ENS are to control blood flow, motility, transport of fluid, secretion of mucus, and also to modulate immune and endocrine functions.

(Figure from McGraw Hill text book Human physiology)

1.1.5.1 Cholinergic innervation of the colonic epithelium

The colonic epithelium is under the neuronal control of the ENS. The neurons that extend from the submucosal plexus into the mucosa can be cholinergic and non-cholinergic. These cholinergic neuronal networks are the major source of the neurotransmitter Ach in the intestine. Other classical neurotransmitters such as dopamine, serotonin and histamine are also well known regulators of gut physiology. Cholinergic innervation has been detected by vesicular acetylcholine transporter (VAChT) labelling (Schafer, et al., 1998). In particular, the release of Ach into the neuro-epithelial junction stimulating ion secretion from intestinal mucosa is a well-known phenomenon (Brown, et al., 1997). Chloride (Cl^-) secretion in the colonic mucosa mediated by cholinergic stimulus has been mostly studied in animal models (McCulloch, et al., 1987; Diener, et al., 1989; Javed, et al., 1992; O'Malley, et al., 1995) and more recently in humans (Cliff, et al., 1998; Reynolds, et al., 2007; Toumi, et al., 2011). In addition, cholinergic agents via the muscarinic receptor signal transduction have also been shown to accelerate mucus exocytosis from goblet cells throughout the intestines of rats (Neutra, et al., 1982). All these studies strengthen the role of neurotransmitters in regulating gastrointestinal functions.

Ach functions as a neuromodulator in both the CNS and peripheral nervous systems (PNS). It is also a major neurotransmitter in the autonomic nervous system. Ach was first identified by Henry Hallett Dale in 1915 when he demonstrated its role on heart tissue. It was later identified as the first neurotransmitter when Otto Loewi described the function of the chemical when it was released from the vagus nerve. Ach is a fast-acting neurotransmitter, synthesised by the enzyme choline acetyl transferase (ChAT) from its two immediate precursors – choline and acetyl coenzyme A (Figure 1.7) (Tucek, 1983; Wurtman, et al., 2008). This event is dependent on the Na^+ dependent CHT1 transporter (high-affinity choline transporter/SLC5A7 (solute carrier family 5 member 7)) for transferring the Ach precursor choline into the cytosol of the cholinergic nerve endings (Ribeiro, et al., 2006). The source of this choline is thought to be either hydrolysis by cholinesterase from the released Ach or from the breakdown of phosphatidylcholine (Wurtman, et al., 2008). Following synthesis by ChAT, Ach is then loaded into synaptic vesicles by vesicular Ach transporter (VAChT / SLC18A3) prior to being released by exocytosis (Parsons, et al., 1987; Parsons, 2000). These synaptic vesicles accumulate thousands of Ach molecules to form a quantum, in which this process is driven by an electrochemical gradient generated by a proton ATPase (Parsons, 2000) (Figure 1.7). However, VAChT acts very slowly, thus serving as a limiting factor for maintaining Ach release (Varoqui and Erickson 1996). Moreover, ChAT and VAChT have been

suggested to be co-regulated, as the gene encoding VAChT was discovered to be located within an intron of the ChAT gene (Erickson, et al., 1996). Both ChAT and VAChT are required for cholinergic neurotransmission. Since ChAT protein expression is concentrated at the nerve endings of cholinergic neurons, and VAChT is predominantly expressed in synaptic vesicles in the same location (Gilmor, et al., 1996), both ChAT and VAChT proteins have been used as markers for cholinergic neurons in immunohistochemical studies (Ichigawa, et al., 1997).

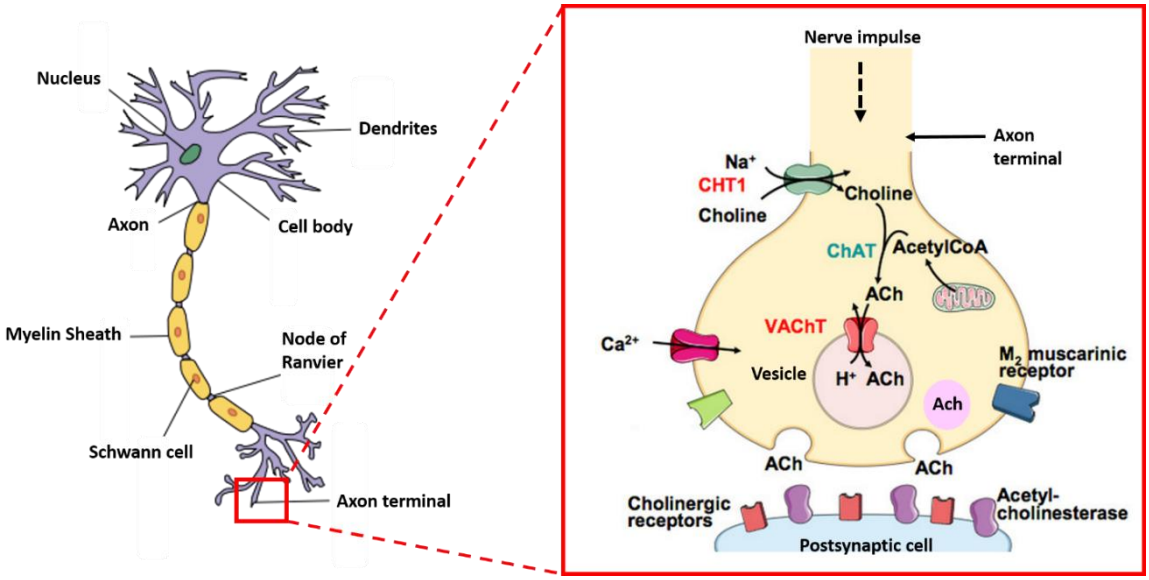

Figure 1.7 Acetylcholine synthesis and secretion at the cholinergic synapse

A typical neuron consists of complex dendritic arbors that receive electrochemical (synaptic) inputs from other neurons, a cell body (containing the nucleus) and an axon that transfers signals to postsynaptic cells (neurons or other effector cells) (left). Ca^{2+} serves multiple complex and integrated functions, including the control of dendritic responses to neurotransmitters; and the initiation of neurotransmitter Ach release from presynaptic cholinergic axon terminals (red box) upon a nerve impulse (right). At nerve endings, ChAT is the enzyme responsible for Ach synthesis in the presence of the substrate choline, while VAChT is responsible for transferring Ach into secretory vesicles. Upon release, Ach binds to cholinergic receptors on the membrane of the postsynaptic cell.

(Figure from New World Encyclopaedia-Nervous system (Left); figure partially adapted from quizlet.com images- cholinergic synapse (Right))

1.1.5.2 Non-neuronal Ach in the regulation of intestinal physiology

The traditional view of Ach acting solely as a neurotransmitter has been revised after significant amount of studies demonstrated the production of Ach in non-neuronal cholinergic systems (Keely, 2011; Grando, et al., 2012). It was first observed by Sastry and Sadavongvivad in 1979, and subsequently Ach synthesis has been identified in a range of non-neuronal cells including lymphocytes (Kawashima, et al., 2000), epithelial cells (Wessler, et al., 2003), vascular endothelial cells (Kirkpatrick, et al., 2001), and keratinocytes (Grando, et al., 1993). Evidence is mainly provided by ChAT labelling, Ach content (measured by HPLC or microdialysis) and muscarinic receptor expression (Wessler, et al., 2008). However, our knowledge about the mechanism of the non-neuronal Ach release is still very limited. In the airway epithelium, organic cation transporters (OCT) subtypes 1 and 2 have been shown to mediate non-neuronal Ach release (Lips, et al., 2005; Kummer, et al., 2006). Since OCTs are widely expressed in most cells, they can be considered appropriate candidates for non-neuronal Ach transport.

In the intestine, non-neuronal Ach release was first identified by Klapproth et al in 1997 in rats and humans, and again in humans by Jönsson et al in 2007. However, the physiological relevance of this regulation is still poorly understood. Recent findings by Yajima et al (2011) and Bader et al (2014) provide valuable insights into the non-neuronal Ach regulation of gut physiology. They demonstrated that the fatty acid propionate stimulates non-neuronal Ach release which coupled to chloride secretion in the rat colon. In addition, they also showed the expression of ChAT and OCT transporters in the colonic epithelial cells. These observations fully support a model in which synthesis and release of Ach occurs in the colon without cholinergic innervation, and that the release of endogenous epithelial Ach in response to short chain fatty acids (the contribution of microbiota) could play an important role in regulating goblet cell mucus exocytosis and maintaining the barrier function.

Moreover, by using mouse crypt-villus organoids that lack nerves and immune cells, Takahashi and colleagues (2014) demonstrated that endogenously synthesised Ach regulates growth and differentiation via muscarinic receptor activation. Thus, Ach is not only a neurotransmitter, but can also function as an intercellular messenger that integrates different aspects of intestinal physiology. Taken together, these studies open up new insights about the non-neuronal regulation of gut physiology and a potential target for developing new therapies for colonic diseases.

1.1.6 Muscarinic Acetylcholine Receptor signalling

The two main classes of Ach receptors are the nicotinic (NAchR) and muscarinic receptors (MAchR) (Wess, 2003). The concept of these receptors was first described by Dale in 1914, and confirmed by Loewi, Dale and others between 1921 and 1934. MAchRs were named because they are selectively activated by muscarine, a natural product of the mushroom *Amanita muscaria* which can mimic the actions of parasympathetic neurons. Its action can be blocked by atropine, a derivative from the plant *Atropa bella-donna* (Hulme, et al., 1990). MAchRs are expressed in both the CNS and PNS, in particular in the target organs of parasympathetic neurons (van koppen, et al., 2003). It has been shown that they modulate a variety of physiological functions such as smooth muscle contraction and secretions from glands (Caulfield, 1993).

1.1.6.1 G-protein coupled receptor

MAchR belongs to the seven-transmembrane receptor superfamily, which interact with heterotrimeric guanine nucleotide binding regulatory proteins (G proteins) to activate signal transduction. G proteins are composed of alpha (α), beta (β) and gamma (γ) subunits. These proteins are categorised by their α-subunits into four broad types: $G\alpha_s$, $G\alpha_i$, $G\alpha_q$ and $G\alpha_{12/13}$ (Sanders, 1998). In addition, five isotypes of β and at least 12 γ subunits have been identified (Sanders, 1998). The α-subunit is critical for normal functioning of the G protein. In its inactive state it binds GDP: upon G protein activation, the exchange of bound GDP with GTP leads to dissociation of the βγ subunit (figure 1.8). The α-subunit then in turn interacts with the effector protein to stimulate or inhibit the release of intracellular second messengers (Weiss, et al., 1988). The βγ subunit was originally shown to be required for the GDP-GTP exchange at the α subunit of the G protein (Florio, et al., 1989), but more recent studies have revealed their role in regulating signal transduction (Katz, et al., 1992). Significant amount of studies have shown the existence of G-protein coupled receptor (GPCR) as dimers/ oligomers, that appears to be assembled either in the ER or at the cell surface (Devi, 2001). Heteromerisation of GPCR has emerged as an important process in recent years for receptor function specification that mediate distinct biological responses (Milligan, et al., 2009; Ferre, et al., 2014).

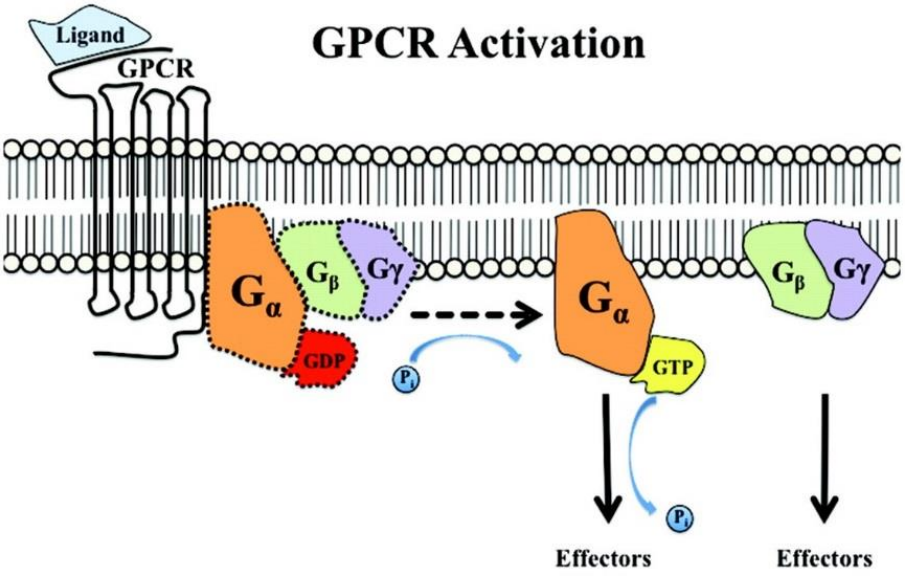

Figure 1.8 G-protein coupled receptor signal transduction

GPCR are seven transmembrane receptors that activate intracellular signal transduction. Ligand binding causes a conformation change of the receptor, exchanging of GDP to GTP of the α-subunit dissociates the βγ subunits. The GTP bound α-subunit then activates downstream signal transduction, whereas the βγ subunit has also been shown to activate further effector functions.

(Figure from Belmonte, et al., 2011)

In mammals, five subtypes of MAchR have been identified, termed M1 to M5 (or M1AchR to M5AchR) (Bonner, et al., 1987). Each receptor subtype is encoded by a different gene (*CHRM1-5*) (Bonner, et al., 1987; Nathanson, 2000). The odd-numbered receptors (M1, M3 and M5) are coupled to the pertussis toxin-insensitive $G\alpha_{q/11}$ and $G\alpha_{13}$ proteins, which activate phospholipase A2 (PLA2), phospholipase C (PLC) and phospholipase D (PLD) (Fukada, et al., 1987; Wess, et al., 1989); whereas the even numbers (M2 and M4) are coupled to pertussis toxin-sensitive $G\alpha_i$ and $G\alpha_o$ proteins, which inhibit adenylyl cyclase (Peralta, et al., 1988; Caulfield, 1993; Felder,1995; Caulfield and Birdsall, 1998; Rümenapp, et al., 2001). These different receptor subtypes can couple to a diverse array of signalling pathways via these G proteins (Ashkenazi, et al., 1989). With regards to the gut, signalling through M1, M2 and M3 receptors has been shown to influence intestinal activity such as motility and secretion (Cooke, 2000; Harrington, et al., 2010).

In most model systems, MAchR activation increases intracellular Ca^{2+} concentration $[Ca^{2+}]$ up to 20-fold (Budd, et al., 1999). Activation of different MAchR subtypes can mediate different signal transduction pathways. Activation signals via PLA2 catalyses the hydrolysis of

membrane phospholipids to form arachidonic acid and lysophospholipids. Arachidonic acid is then converted to a variety of eicosanoids (bioactive fatty acid derivatives) such as prostaglandins, thromboxanes and leukotrienes, whereas lysophospholipids are recycled within the membrane (Felder, 1995). The release of arachidonic acid and eicosanoids upon MAchR activation has been shown in a variety of tissues including the heart, muscle and brain (Abdel-Latif, 1986). Moreover, activation signals via PLD promotes the hydrolysis of phosphatidylcholine (PC) into choline and phosphatidic acid (PA) (Figure 1.9) (Felder, 1995; Liscovitch, et al., 2000). In most cells studied, PLC and PLD are stimulated simultaneously after agonist induced receptor activation, but through independent processes (Liscovitch, 1991).

1.1.6.2 Muscarinic receptor mediated intracellular calcium signalling in the ER

ER is a highly dynamic organelle. In addition to its role in protein synthesis and packaging, it is also the major intracellular Ca^{2+} store within the cell that mediates many signalling processes (Berridge, 2002). The ER intraluminal [Ca^{2+}] is about 0.5 mM (Alvarez, et al., 2002). Ca^{2+} homeostasis in the ER is predominantly controlled by three mechanisms: refilling of the store is maintained by the continuous activity of the sarco/endoplasmic reticulum Ca^{2+} ATPase (SERCA) pump and capacitive Ca^{2+} entry (or store-operated Ca^{2+} entry (SOCE)) (Takemura, et al., 1989; Putney, 2001; Putney, 2008), while efflux is mediated through the Ca^{2+}-induced Ca^{2+} release (CICR) response (Berridge, 2002). Inositol 1,4,5 triphosphate receptors (IP3Rs) and Ryanodine receptors (RYRs) are the two main Ca^{2+} channels on the ER membrane.

The most common MAchR signal transduction is via the activation of PLC (Budd, et al., 1999). Upon Ach binding, M3AchR activation initiates conformational change of the receptor, promoting its association with the heterotrimeric G protein ($G\alpha_q\beta\gamma$). The activation of the G protein causes the dissociation of βγ subunits from the α-subunit, freeing the α-subunit to travel along the cell membrane and activate additional PLC molecules. PLC in turn initiates phosphatidyl-inositol 4, 5 bisphosphate (PIP2) hydrolysis (a drastic decrease of membrane PIP2 levels by 75% within seconds of agonist stimulation) to generate diacylglycerol (DAG) and inositol 1,4,5 triphosphate (InsP3 or IP3) (Felder, 1995; Budd, et al., 1999). IP3 then translocate to the ER where it binds to the IP3R and promotes Ca^{2+} release from the ER Ca^{2+} store into the cytosol (Felder, 1995; Nahorski, et al., 1997). Increase in cytosolic [Ca^{2+}] in turn activates the IP3R and RYR and induce the CICR response (Ca^{2+} waves) in the entire cell

(Figure 1.9) (Taylor and Dale, 2012). This mobilisation of intracellular Ca^{2+} then initiates a variety of physiological responses such as transcription of genes, muscle contraction and fluid secretion (Caulfield, 1993; Billington, et al., 2002; Gerthoffer, 2005; Kong and Tobin, 2011). The ER store depletion mediated by IP3 is then refilled by the SOCE mechanism. The magnitude and kinetics of the CICR and SOCE responses in a cell are dependent on the precise intracellular channel isoforms and their subcellular localisation in the ER. Meanwhile, DAG binds to and activates PKC (Felder, 1995). While the molecular mechanisms of DAG and PKC signalling are not fully understood, and the immediate downstream effects of PKC are unclear, PKC has been shown to activate downstream effectors in regulating proliferation, differentiation, cell migration, cell death and secretion (Nishizuka, 1989; Kai, et al., 1994). In addition, DAG can also be converted to PA by DAG kinase (Kanoh, et al., 2002), which might terminate signalling downstream of DAG. MAchR activation has been shown to activate the ectoenzyme CD38 (ADP-ribosyl cyclase), causing it to synthesise Cyclic ADP Ribose (cADPR) and nicotinic acid adenine dinucleotide phosphate (NAADP) (Higashida, et al., 2001a and b). However, it is unclear whether CD38 signalling is downstream of PKC.

To sum up, Ca^{2+} release from the ER amplifies cytosolic Ca^{2+} signals, but there are also multiple feedback mechanisms that prevent Ca^{2+} overload such as mitochondrial Ca^{2+} uptake and extrusion from cell via Na^{+}/Ca^{2+} exchanger (NCX) on the plasma membrane. The uptake of Ca^{2+} by the mitochondria accelerates the decline in cytosolic [Ca^{2+}], which can influence the Ca^{2+} signal transduction cascade. Because all intracellular Ca^{2+} channels on the ER membrane are governed by different regulatory mechanisms, the control of Ca^{2+} homeostasis in the ER remains relatively complex.

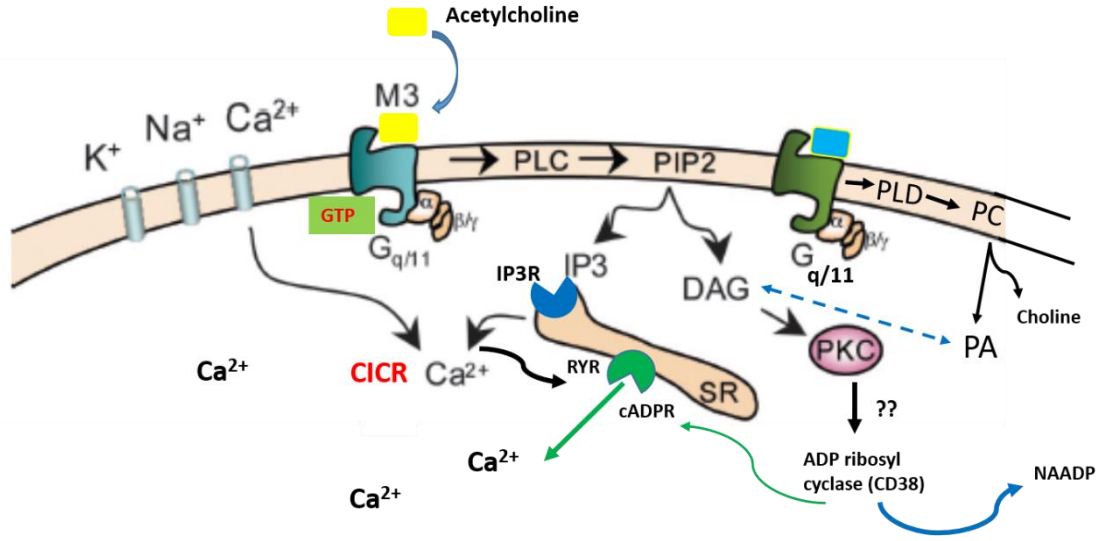

Figure 1.9 Schematic diagram of the M3AchR signal transduction pathways upon Ach stimulation.

The binding of Ach to M3AchR triggers the dissociation of βγ subunits from α subunit of the G protein. The alpha (α) subunit travels along the plasma membrane and activates phospholipase C (PLC). PLC then initiates the hydrolysis of phosphatidyl-inositol 4, 5 bisphosphate (PIP2) into inositol 1,4,5 triphosphate (IP3) and diacylglycerol (DAG). Subsequent translocation of the 2nd messenger IP3 to the ER membrane allows its binding to the IP3R and triggers intracellular Ca^{2+} mobilisation from the ER store. Localised increase in cytosolic [Ca^{2+}] further activates IP3 receptor (IP3R) and ryanodine receptor (RYR) on the ER membrane and induces Ca^{2+}-induced Ca^{2+} release (CICR) response. Meanwhile, DAG activates the downstream signalling molecule protein kinase C (PKC). It is currently unclear whether PKC directly activates CD38 upon M3AchR activation or via some upstream signalling molecules potentially phosphatidic acid (PA, converted from DAG) and/ or NADPH oxidases (not shown). CD38 is an enzyme synthesising both 2nd messenger Cyclic ADP Ribose (cADPR) and nicotinic acid adenine dinucleotide phosphate (NAADP) that could also trigger cytosolic [Ca^{2+}] increase upon binding to RYR and Two pore channel (TPC) respectively. Through independent processes, phospholipase D (PLD) can also be activated upon PLC activation. PLD then promotes the hydrolysis of phosphatidylcholine (PC) into choline and PA, suggesting PA might be an important effector for M3AchR signal transduction pathway.

(Partially adapted from Gerthoffer 2005)

1.2 Intracellular calcium signalling

Ca^{2+} is an important 2nd messenger, which helps control almost every cellular activity. Our modern understanding of the role of Ca^{2+} began with the studies by Sydney Ringer in early 1880s when he first demonstrated that Ca^{2+} ions were indispensable for certain physiological functions, such as muscle contraction, cell adhesion and the development of fertilized eggs (Ringer, 1883- 1894, reviewed by Miller, 2004). In particular, his observation that extracellular Ca^{2+} removal abolishes contraction of the frog heart suggested that the influx of Ca^{2+} ion across the cell membrane might regulate intracellular activity (reviewed by Miller, 2004). In 2002, Bers suggested that Ringer's observation was due to depolarisation-triggered Ca^{2+} entry through the plasma membrane, triggering CICR via the RYR in the ER membrane (Bers, 2002). Thus, while the extracellular Ca^{2+} signal was not directly responsible for heart contraction, it triggers a huge intracellular release of Ca^{2+} from the ER store. These studies provided the first lines of evidence that regulation of Ca^{2+} entry is important for physiological functions, building on the concept of Ca^{2+} ion storage within intracellular organelles that was established in 1965. Sandow demonstrated that the major source of Ca^{2+} triggering striated muscle contraction was indeed also coming from the sarcoplasmic reticulum (SR) (Sandow, 1965). Subsequently in 1984, Streb discovered that IP3 stimulates Ca^{2+} release from non-mitochondrial Ca^{2+} store in pancreatic acinar cells (Streb, 1984). Later studies confirmed that the ER is the major intracellular source of Ca^{2+} in most cells (Berridge & Irvine, 1984; Berridge & Irvine, 1989). Previous studies had also suggested the possible role for IP3 in releasing Ca^{2+} from other intracellular organelles into the cytosol including the Golgi apparatus (Pinton, et al., 1998), nucleus (Gerasimenko, et al., 1995; Marchenko, et al., 2005) and secretory vesicles (Gerasimenko, et al., 1996). Our current understanding of the spatiotemporal complexity in the regulation of cytosolic [Ca^{2+}] relies mainly on the extracellular Ca^{2+} (~ 1.2mM) and the intracellular Ca^{2+} stores (>100μM), while the resting cytosolic [Ca^{2+}] is approximately 50-100nM, which generates a concentration gradient across the plasma and organelles membranes (Streb, et al., 1984; Pozzan, et al., 1994). Recent studies have identified several other intracellular Ca^{2+} channels that are unrelated to IP3R and RYR, in mediating Ca^{2+} signal transduction. In particular, Two pore channels (TPCs) have been shown to regulate Ca^{2+} release from intracellular acidic organelles (Brailoiu, et al., 2009; Calcraft, et al., 2009; Zong, et al., 2009; Patel, et al., 2010; Zhu, et al., 2010). Finally, the transient receptor potential cation (TRPC) channels not only mediate Ca^{2+} influx through the plasma membrane, but several receptor subtypes such as TRPV (vanilloid) and TRPML (mucolipin) may also mediate Ca^{2+} release from intracellular stores (Puertollano, et al., 2009; Gees, et al., 2010). At present,

it is widely appreciated that Ca^{2+} signals generated through different mechanisms act via different channels and through different pathways. All such channels do not function alone, instead working in concert to maintain intracellular Ca^{2+} homeostasis.

1.2.1 Intracellular calcium homeostasis and physiological responses

Intracellular Ca^{2+} homeostasis involves dynamic processes which dictate the balance between (1) Ca^{2+} entry into and extrusion from cells; and (2) Ca^{2+} uptake into and release from organelles (Sneyd, et al., 1995; Brini and Carafoli, 2009). Eukaryotic cells contain various Ca^{2+} transport systems (channels), belonging to a number of different subtypes and subcellular locations, which make the transport process relatively complex. These channels are mainly localised on the plasma membrane, and the membranes of the intracellular organelles including the ER, Golgi, mitochondria and endo-lysosomes. The plasma membrane typically contains three Ca^{2+} transport systems: the plasma membrane Ca^{2+} ATPases (PMCA), Na^{+}/ Ca^{2+} exchanger (NCX), and the Ca^{2+} channels (CRAC, TRPC). The first two systems are involved in the removal of cytosolic Ca^{2+} into the extracellular space, while the latter one is involved in extracellular Ca^{2+} entry into cell (Brini and Carafoli, 2009). The ER and mitochondria have long been known to be key players in regulating cytosolic [Ca^{2+}], whereas the role of the endo-lysosomes has come to our attention more recently, in the late 2000s. The major intracellular Ca^{2+} channels (IP3R, RYR), ATPase pump (SERCA) in the ER, and endo-lysosomal stores (TPC) will be discussed in the following sections.

As discussed previously, elevation of cytosolic [Ca^{2+}] mediates certain cellular responses. The physiological outcomes are very diverse, ranging from extremely rapid events such as muscle contraction and neuro-secretion, to more orchestrated responses such as cell division, differentiation and apoptosis (Dupont, et al., 2011). In the human colon, Ca^{2+} signalling has been shown to be important for fluid secretion and tissue renewal of the colonic epithelium (Lindqvist, 2000; Reynolds, 2007). Chronic disruptions of Ca^{2+} homeostasis have also been shown to be causative in the development of certain diseases such as neurodegeneration (Mattson, et al., 2003), heart failure (Scoote, et al., 2004) and cognitive deficits in senescence (Toescu, et al., 2004). Therefore, the balance between the supply and removal of cytosolic Ca^{2+} is key to maintain homeostasis.

1.2.1.1 Spatial and temporal aspects of calcium oscillations

MAchR induced Ca^{2+} signals (oscillations or waves) in a cell can vary with respect to time and space (Lechleiter, et al., 1991b; Berridge, 1993). The two general properties of Ca^{2+} oscillations are: (1) each Ca^{2+} spike or oscillation is primarily due to intracellular release-transient phase. (2) The oscillations rapidly run down in the absence of extracellular Ca^{2+}, indicating the requirement of Ca^{2+} influx to maintain the system-plateau phase (Thomas, et al., 1996; Bird, et al., 2005; Dupont, 2011). Oscillations and waves of cytosolic Ca^{2+} were first described by Prince and Berridge in 1973 and Woods et al in 1987, respectively (Prince and Berridge, 1973; Woods, et al., 1987). It is now known to be a common phenomenon in a wide range of cell types upon agonist stimulation of second messengers, revealed through a number of experimental devices. IP3-dependent release of Ca^{2+} from ER stores via IP3R is considered to be one of the hallmark models of Ca^{2+} oscillation. By using Ca^{2+} specific fluorescent dye such as Fura-2 AM and Fluo-4 AM, the spatial and temporal dynamics of these Ca^{2+} oscillations in cells can be visualised. Temporal events of Ca^{2+} oscillations have been measured experimentally with photomultipliers as average recordings from whole cells or as regions of interest within a cell or structure (Sneyd, et al., 1995). Ca^{2+} waves are transient and repetitive (Berridge, 1990a and b), yet imaging techniques have clearly indicated that Ca^{2+} oscillations are not uniformly distributed, but rather initiated in a specific site of the cell and then propagated to other regions of the cell (Sneyd, et al., 1995). Upon PLC activation in a restricted region of the cell, newly-generated IP3 is then free to diffuse outwards, stimulating Ca^{2+} release by binding to IP3R on the ER membrane (Rooney, et al., 1993). The size of the cell can also influence the appearance of such Ca^{2+} waves. In very large cells, such as Xenopus oocytes, the Ca^{2+} wave can be organised into complex spatiotemporal patterns such as rotating spirals or multiple concentric circles (Lechleiter, et al., 1991a).

Intercellular communication is required for transmitting regulatory signals in multicellular organisms (Figure 1.12). Intercellular Ca^{2+} waves are one form of communication that allows a single cell to interact with multiple adjacent cells (Sneyd, et al., 1995). These waves were first observed in epithelial and glial cell cultures in response to neurotransmitters, and are now commonly observed in many other cell types (Sanderson, et al., 1994). However, these spatiotemporal patterns of $[Ca^{2+}]$ are not fully understood. One popular proposed model is that IP3 generated by mechanical stimulation in the stimulated/ initiator cell diffuses from cell to cell through gap junctions to spread the Ca^{2+} signals (Sneyd, et al., 1995).

It has become increasingly clear that periodic discharges and/or entry of Ca^{2+} is the common signalling pattern in both excitable and non-excitable cells. In excitable cells such as

myocardium, Ca^{2+} signals are initiated by the Ca^{2+} action potential (electrical or nerve impulse) on the plasma membrane (Hess, et al., 1986) and then amplified by the release of intracellular Ca^{2+} (Fabiato, 1983). In non-excitable cells such as epithelial cells, Ca^{2+} signals initiate from the discharge of ER stored Ca^{2+} into the cytosol. However, a study by Bird and Putney demonstrated that some non-excitable cells do not require Ca^{2+} influx to drive oscillations, which seems at odds with the original two proposed general properties of Ca^{2+} oscillations (Bird and Putney, 2005). In the human epithelial kidney (HEK293) cell line, methacholine (a MAchR agonist) induced Ca^{2+} oscillation is sustained by SOCE. Bird and Putney demonstrated that this Ca^{2+} oscillation can also be sustained when the cells are treated with high concentrations of Gadolinium (III) Chloride ($GdCl^3$, 1mM) that blocks the transcellular Ca^{2+} fluxes across the plasma membrane via the PMCA. These findings suggest that the mechanisms underlying Ca^{2+} oscillations can be intrinsic to the intracellular milieu and that Ca^{2+} entry is not a requirement if Ca^{2+} ions were prevented from being pumped out of the cell (Bird and Putney, 2005). Presently, controversy remains about the precise mode of Ca^{2+} entry associated with Ca^{2+} oscillations.

1.2.2 Intracellular calcium channels

1.2.2.1 Inositol 1,4,5 triphosphate receptors

In addition to being one of the major Ca^{2+} release channels expressed in the ER membranes of most cell types, IP3Rs are also expressed in the Golgi apparatus, secretory vesicles and in plasma membrane of some specialised cells (Dellis, et al., 2006; Taylor, et al., 2010; Yoo, et al., 2010). In mammals, three IP3R isoforms (IP3R1, 2 and 3) have been identified. All these IP3Rs are regulated by both IP3 and Ca^{2+} (Finch, et al., 1991; Marchant and Taylor, 1997; Foskett, et al., 2007), albeit with different affinities of IP3 binding. The general consensus of the receptor sensitivity hierarchy is that IP3R2 > IP3R1 > IP3R3 (Tu, et al., 2005a; Tu, et al., 2005b; Iwai, et al., 2007). In addition, expression levels of the receptor (Dellis, 2006), subcellular distribution of the receptor (Petersen, et al., 1999), and the presence of accessory proteins (Patterson, 2004), can also influence IP3R sensitivity. Opening of IP3Rs upon IP3 stimulation allows Ca^{2+} movement across the ER membrane into the cytosol (Foskett, et al., 2007). Each ten millisecond (10 ms) opening of the IP3R can mediate a large Ca^{2+} flux (approximately 10^4 Ca^{2+} ions) into the cytosol (Vais, et al., 2010). Moreover, a single IP3R opening may be sufficient to evoke a cellular response (Ca^{2+} blips). The presence of IP3 causes IP3R clustering, and the coordinated opening of several IP3Rs culminates in Ca^{2+} puffs. With sufficient IP3, these individual Ca^{2+} puffs culminate to form a regenerative Ca^{2+} wave which spreads across the entire cell (Figure 1.10) (Bootman, et al., 1997; Demuro and Parker, 2008).

Ca^{2+} regulation of IP3Rs is biphasic. A moderate increase of cytosolic [Ca^{2+}] augments the receptor response to IP3, whereas high cytosolic [Ca^{2+}] inhibits the IP3R (Iino, 1987; Finch, 1991; Marshall and Taylor 1993). This Ca^{2+} mediated inhibition of IP3R is probably due to direct Ca^{2+} binding to the IP3R or the formation of Ca^{2+}complexes with accessory proteins such as calmodulin (CaM) (Hirota, et al, 1999; Nadif, et al., 2002; Taylor and Laude, 2002). Previous studies have suggested the presence of essential Ca^{2+} binding sites on the IP3R. Marshall and Taylor (1994) suggested that there are distinct stimulatory and inhibitory Ca^{2+} binding sites on the IP3R, and that the essential role of IP3 is to promote the binding of Ca^{2+} to the stimulatory binding site to mediate opening of the channel (Marshall and Taylor, 1994). However, a study by Mak and colleagues revised the initial model of inhibition, by suggesting that the absence or presence of IP3 controls the switching of a single Ca^{2+} binding site from being inhibitory to stimulatory respectively (Mak, et al., 2003). This model suggests that IP3 not only alleviates Ca^{2+} inhibition but also promotes Ca^{2+} binding to the IP3R (Marchant and Taylor, 1997; Adkins and Taylor, 1999). However, the molecular mechanism of inhibition remains unclear. In experimental condition, IP3Rs can be blocked by the non-specific

inhibitor 2-amino-ethyl diphenylboronate (2-APB, Bootman, et al., 2002) or the specific inhibitor Xestospongin C (Xes C, Gafni, et al., 1997), in which 2-APB has been shown to block IP3 mediated Ca^{2+} release without affecting IP3 binding (Maruyama, et al., 1997). Moreover, high concentrations of caffeine have also been shown to inhibit IP3-mediated Ca^{2+} release (Parker and Ivorra, 1991) without affecting IP3 binding (Worley, et al., 1987). Since caffeine can also stimulate the RYR (Endo, 1977), it becomes difficult to differentiate Ca^{2+}signals released from these two receptors upon activation.

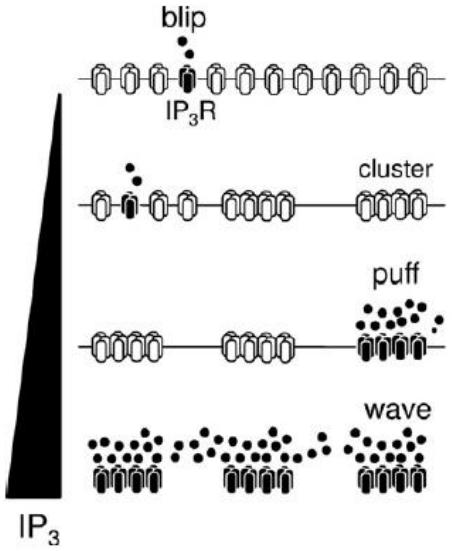

Figure 1.10 Calcium oscillation event evoked by IP3.

(Top) Single IP3R opening mediated by low [IP3] evokes Ca^{2+} blips. The presence of IP3 causes IP3R clustering which facilitates Ca^{2+} interaction with IP3-bound IP3Rs. Several IP3-bound neighbouring receptors in a cluster open simultaneously and generate the Ca^{2+} puff. The diffusion of Ca^{2+} from one puff site to another ignites a regenerative Ca^{2+} wave at neighbouring sites.

(Figure from Taylor and Dale 2012)

1.2.2.2 Ryanodine receptors

RYR are the largest known ion channels (>2MDa) (Takeshima, et al., 1989; Otsu, et al., 1990) which are expressed primarily on the sarcoplasmic reticulum (SR) of muscle cells and endoplasmic reticulum (ER) of other cell types. In mammals, there are three RYR isoforms (RYR1, 2 and 3) which share 66% sequence identity. All three isoforms were first identified as expressed in excitable muscle cells (Lanner, et al., 2010), in which RYR1 and RYR2 are crucial for excitation contraction (E-C) coupling in skeletal and cardiac muscle respectively (Takeshima, et al., 1989; Lai, et al., 1989a; Otsu, et al., 1990; Lewartowski, 2000; Lamb, 2000). However, the activation mechanism of RYR in E-C coupling is different between skeletal and cardiac muscles. In both scenarios, activation of RYR mediates SR Ca^{2+} release. In skeletal muscle, the depolarisation of transverse tubules (t-tubules) activates RYR via the voltage sensor dihydropyridine receptor (DHPR, also known as L-type Ca^{2+} channels) (Tanabe, et al., 1990; Nakai, et al., 1998); whereas in cardiac muscle, E-C coupling depends primarily on Ca^{2+} influx through DHPR. (Endo, 1977; Sham, et al., 1995).

RYRs are homotetramers and their activation can be regulated by caffeine (Endo, 1977) and cyclic ADP-Ribose (cADPR, Takasawa, et al., 1993; Ozawa, et al., 1999; Ogunbayo, et al., 2011) or by direct interaction with Ca^{2+} ions (Lanner, et al., 2010). In addition, ryanodine (a plant alkaloid), can also regulate RYR function by binding to it with high affinity and specificity, hence the receptors' name. Low, nanomolar concentrations of ryanodine lock the channels in an open state (allowing Ca^{2+} release), whereas high concentrations (> 100 μM) inhibit receptor opening (Meissner, et al., 1986; Lai, et al., 1989b; McGrew, et al., 1989). In addition, millimolar magnesium (Mg^{2+}) (Meissner, et al., 1997; Laver, et al., 1997) or micromolar ruthenium red concentrations (Miyamoto, et al., 1982) have also been shown to inhibit RYR activity.

RYRs are considered to be one of the key players in regulating intracellular Ca^{2+} release in many cell types. In particular, they have been found to regulate anion secretion in non-excitable rat colonic epithelial cells (Kocks, et al., 2002). However, the activation mechanism of RYR has not been clearly elucidated. Similar to IP3R (with which they share an overall 17% sequence identity) (Mignery, et al., 1989), RYR mediates Ca^{2+} release from the ER store. Depleted or emptied SR/ER stores are then refilled with Ca^{2+} via their membranous SERCA.

1.2.2.3 Calcium pumps

SERCA, a P-type II ATPase, is another key player of Ca^{2+} signalling in the ER. The SERCA pump, first discovered in 1961 in a cell fraction derived from skeletal muscle tissue, is involved in many aspects of signal transduction and cellular function (Clapham, 2007). This fraction was later shown to contain the vesicles of the SR which accumulate Ca^{2+} at the expense of hydrolysing ATP (Ebashi, et al., 1962). Further studies extended the analysis to the ER of all cells, revealing SERCA as one of the main control systems of cytoplasmic Ca^{2+} in all cells.

In mammals, three SERCA isoforms (SERCA1-3) have been identified which are encoded by three highly homologous genes (*ATP2A1-3*) (Arai, et al., 1994). Diversity within these genes is generated by alternative splicing; at least 11 SERCA splice variants have been observed (Periasamy, et al., 2007). The main function of the SERCA pump is to transfer cytosolic Ca^{2+} into the ER for storage by utilising ATP, maintaining Ca^{2+} homeostasis within a cell (Wuytack, et al., 2002; Berridge, et al., 2003). Under experimental conditions, these pumps can be inhibited with lanthanum ions (La^{3+}) and orthovanadate (Szász, et al., 1978), or more latterly with specific small molecule inhibitors such as thapsigargin (Tg) (Thastrup, et al., 1990), now the most commonly used pharmacological tool for store-operated pathway. SERCA has been shown to play a role in certain human diseases: the loss of SERCA3 expression has been linked to the progression of colon carcinogenesis (Brouland, et al., 2005), underlining the importance of ER Ca^{2+} homeostasis in health.

In response to agonist induced ER store depletion, there is a functional coupling between the SERCA pump and SOCE mechanism, in which extensive Ca^{2+} influx into the cytosol via the SOCE mediated Ca^{2+} release-activated Ca^{2+} channel (CRAC) is rapidly taken up by SERCA into the ER (Takemura, et al., 1989; Thastrup, et.al., 1990). This highly regulated mechanism not only avoids Ca^{2+} overload in the cytoplasm, but also maintains the [Ca^{2+}] gradient for proper physiological functions.

1.2.2.4 ER Calcium store homeostasis - Store-operated calcium entry

Ca^{2+} signalling events are highly coordinated and linked, and it is widely accepted that (1) the increase in cytosolic [Ca^{2+}] is mediated by Ca^{2+} release from intracellular stores and also (2) the increase of Ca^{2+} flux across the plasma membrane (Putney, et al., 2008). As discussed previously, intracellular Ca^{2+} release is mediated by IP3 derived from PLC activation at the plasma membrane, whereas Ca^{2+} entry to the cytosol results from the activation of SOCE (capacitive Ca^{2+} entry) (Putney, 1986; Putney, 2014). Between 1986 and 2005 there were several important findings regarding SOCE. By using the fluorescent Ca^{2+} indicator Fura-2, Takemura and colleagues demonstrated for the first time that Ca^{2+} entry to the cytosol is independent of agonist-induced receptor activation of PLC on the plasma membrane (Takemura, et al., 1989). The use of Tg provided solid evidence that Ca^{2+} influx refilling the intracellular ER store is not a consequence of receptor activation (Jackson, et al., 1988; Takemura, et al., 1989). Tg was subsequently shown to deplete Ca^{2+} stores by blocking the SERCA pump (Thastrup, et al., 1990). Since Tg has no effect on ER permeability, store-operated Ca^{2+} influx must occur across the plasma membrane directly into the cytoplasm. If this is the case, then there should be an electrical current associated with this process. In 1992, Marcus Hoth and Reinhold Penner identified the store-operated current I_{crac} as the Ca^{2+} release-activated Ca^{2+} channel (CRAC) current (Hoth and Penner, 1992).

A number of studies have aimed to characterise the store-operated Ca^{2+} influx channels – now commonly known as the CRAC channels – in the plasma membrane. In 1993, Hardie and Minke put forth the idea that transient receptor potential cation (TRPC) channels might be the store-operated Ca^{2+} influx channels (Hardie and Minke, 1993). TRPCs were first described in Drosophila as light-activated Ca^{2+} permeable cation channels (Montell, et al., 1989; Hardie and Minke, 1992). Seven mammalian genes, designated *TRPC1-7*, were eventually found to encode the canonical TRPC channels (Montell, et al., 2002). Subsequent electrophysiological studies of these TRPC channels suggested that they did not likely form the basis of I_{crac} (Hurst, et al., 1998). However, discrepancies in the findings between different laboratories means that the question remains unresolved (Cahalan, 2009; Yuan, et al., 2009). TRPC1 protein overexpression is however capable of increasing Ca^{2+} influx following store depletion (Rao, et al., 2006), and this effect was demonstrated to be dependent on the CRAC channel subunit Orai1 (Kwong, et al., 2008). Therefore, it remains possible that TRPC1 protein may interact with or couple to the store-operated CRAC channels for Ca^{2+} entry.

The discovery of the ER Ca^{2+} sensors-STIM1 (stromal interaction molecule 1) and 2 by Zhang and colleagues in 2005 further expanded our current understanding of SOCE (Zhang, et al., 2005). Both STIM1 and 2 proteins contain a Ca^{2+} binding EF-hand motif facing the ER lumen, which is a key component of STIM for sensing Ca^{2+} levels. STIM1 is a single transmembrane protein residing in both the ER and plasma membranes (Dziadek, et al., 2007). When the ER store is full, STIM1 is distributed uniformly on the ER membranes, with the EF-hand motif of STIM1 bound to Ca^{2+} (Zhang, et al., 2005; Liou, et al., 2005). In response to IP3 mediated ER store depletion, Ca^{2+} ions dissociate from the EF-hand motif and trigger oligomerisation of STIM1 and migration towards the ER-plasma membrane junction. The concomitant relocation of Orai1 within the plasma membrane allows the two proteins to interact and induces SOCE (Prakriya, et al., 2006; Navarro-Borelly, et al., 2008; Luik, et al., 2008). Orai has been shown to function as pore forming subunits of the CRAC channels (Putney, 2011). Opening of the CRAC channels allows rapid Ca^{2+} influx into the cytosol. Since overexpressing Orai1 and STIM1 augments the I_{crac} current by 50-100 fold, these two proteins fully reconstitute the function of the I_{crac} (Peinelt, et al., 2006; Soboloff, et al., 2006). In addition, STIM2 has been shown to be a more sensitive Ca^{2+} sensor than STIM1, but the efficacy of STIM2 activation is lower and its function is less clear (Shim, et al., 2015). A recent study has demonstrated the role of STIM2 in promoting the recruitment of STIM1 to the ER-plasma membrane junction (Ong, et al., 2015). In summary, STIM is a true ER [Ca^{2+}] sensor, in that it triggers SOCE only in response to a decrease in ER [Ca^{2+}] rather than an increase in cytosolic [Ca^{2+}] (Putney, 2011). Therefore, SOCE is identified as a mechanism for refilling the intracellular ER Ca^{2+} store following agonist-receptor dependent or independent depletion.

1.2.3 Role of mitochondria in Calcium homeostasis

Mitochondria were the first intracellular organelles associated with Ca^{2+} handling (Slater, et al., 1953), when the electrochemical gradient (or membrane potential) was found to be the driving force for Ca^{2+} influx into the mitochondria (Scarpa, et al., 1970; Selwyn et al., 1970; Rottenberg, et al., 1974). Accumulation of Ca^{2+} in the mitochondrial matrix requires it to cross two membranes: the outer mitochondrial membrane (OMM, permeable to solutes such as Ca^{2+}) and the inner mitochondrial membrane (IMM, which is ion-impermeable) (Rizzuto, et al., 2012). OMM permeability is dependent on the expression level of the voltage dependent anion channels (VDACs), whereas the mitochondrial Ca^{2+} uniporter (MCU) is involved in transporting Ca^{2+} across the ion impermeable IMM (Rizzuto, et al., 2012). VDACs, also known as the mitochondrial porins, are the key players in crosstalk between the mitochondria and the rest of the cell (Rizzuto, et al., 2012). Mitochondrial Ca^{2+} efflux, on the other hand, is dependent on the Na^{+}/Ca^{2+} (NCX) or H^{+}/Ca^{2+} (HCX) exchangers, or "antiporters" (Crompton, et al., 1978; Carafoli, et al., 2012). 2APB, a non-specific IP3R inhibitor, has also been shown to block Ca^{2+} efflux from mitochondria possibly inhibiting the NCX (Prakriya, et al., 2001). Moreover, in response to mitochondrial Ca^{2+} overload and oxidative stress, Ca^{2+} and other small molecules (<1.5kDA) may also escape the mitochondrial matrix through the opening of the mitochondrial permeability transition pore (PTP) (Elrod, et al., 2010; Barsukova, et al., 2011). PTP is a voltage and Ca^{2+} dependent channel which is also sensitive to cyclosporine A (CsA). Their properties have been well defined through extensive research, but uncertainty remains about the exact molecular identity of PTP (Halestrap, 2009). Thus, both Ca^{2+} uptake and extrusion mechanisms allow mitochondria to operate as a reversible Ca^{2+} storage compartment in the cytoplasm.

Mitochondria can move through the cytosol in a Ca^{2+} dependent manner, which makes the relationships between mitochondria and Ca^{2+} signalling even more dynamic (Yi, et al., 2004; Brough, et al., 2005). This strategic trafficking of mitochondria can keep cytosolic Ca^{2+} signalling to a specific subcellular region. Mitochondria are capable of forming close contacts with the ER (Rizzuto, et al.,1998), the Golgi (Dolman, et al., 2005) and also the plasma membrane (Frieden, et al., 2005), allowing them to affect their Ca^{2+} modulatory roles at each of these sites. The transfer of Ca^{2+} from the ER via IP3R to the mitochondrial matrix is also crucial for mitochondrial-specific functions, including the regulation of cell survival/death (Giorgi, et al., 2008; Harr, et al., 2010). A substantial number of studies were performed in different cell models, and a "two pool" system of Ca^{2+} in ER-mitochondrial interplay was observed: (1) The rapid Ca^{2+} uptake into mitochondria suppresses local Ca^{2+} signals and

prevents the formation of Ca^{2+} waves via IP3R and RYR on the ER membrane; (2) ATP and reactive oxygen species (ROS) production as a result of Ca^{2+} uptake induce local Ca^{2+} responses and further sustain CICR in the cytosol (Deluca, et al., 1961; Vasington, et al., 1962). Rather than just causing cell damage, ROS have been implicated in physiological cell signalling (Goldhaber, et al., 2000; Hidalgo, et al., 2008). However, our understanding of the role of ROS in regulating Ca^{2+} homeostasis in physiological conditions is still unclear. Furthermore, ATP depletion has been shown to block Ca^{2+} release from internal stores and also inhibit SOCE (Gamberucci, et al., 1994). Hence, mitochondria seem to be capable of regulating numerous components of the Ca^{2+} signalling cascade, at various levels including Ca^{2+} uptake and extrusion by the mitochondria, Ca^{2+} release via IP3R and RYR on the ER membrane, and Ca^{2+} influx via store operated channels (Rizzuto, et al., 2012). The mitochondrial Ca^{2+} handling remains complex and unresolved. Our current understanding is that mitochondrial Ca^{2+} uptake not only happens during pathological conditions but also during physiological Ca^{2+} responses.

1.2.4 Calcium signalling in the acidic organelles – Lysosomes

Mobilisation of Ca^{2+} from intracellular stores is a common signal transduction mechanism in both plants and animals. The temporal and spatial aspects of cytoplasmic [Ca^{2+}] can be controlled through the interplay between different intracellular organelles through a range of Ca^{2+} channels. The ER, as the major intracellular Ca^{2+} store, has been the key focus of research for decades. Recently, the acidic organelles have also emerged as important Ca^{2+} stores for regulating cellular and physiological functions. These acidic Ca^{2+} stores are organelles with acidic lumens such as the endosomes, lysosomes, secretory vesicles and lysosome-related organelles (Morgan, et al., 2011). These acidic organelles not only store Ca^{2+}, but also release Ca^{2+} and evoke downstream responses such as cell differentiation (Brailoiu, et al., 2006; Aley, et al., 2010; Zhang, et al., 2013), vesicle trafficking (Ruas, et al., 2010; Ruas, et al., 2014) and exocytosis (Davis, et al., 2012). Lysosomal exocytosis plays an important role in secretion and plasma membrane repair. These findings suggested that the cell can mobilise additional intracellular source of Ca^{2+} to drive different cellular processes.

Ca^{2+} storage in the lysosomes requires active ion transport across the lysosomal membrane. This process is dependent on the transmembrane vacuolar-type proton ATPase (V-type H^+ ATPase) (Lemons and Thoene, 1991). The H^+ ATPase not only promotes the acidification of the intracellular compartment via the neighbouring chloride channel, it also mediates the uptake of Ca^{2+} via H^+-driven antiporter (Beyenbach, et al., 2006). Loss of protons from a lysosome is likely to diminish Ca^{2+} release due to the incapability to refill the acidic stores. The uptake of Ca^{2+} into the acidic stores can be blocked by vacuolar proton pump inhibitors such as bafilomycin (Baf) and also by protonophores such as nigericin which dissipates the proton gradient across lysosome membranes (Galione, 2006).

1.2.4.1 NAADP: A new intracellular messenger

The discovery of NAADP as the 2^{nd} messenger for mobilising acidic Ca^{2+} stores was based on a landmark study in 1987 by Clapper and colleagues, in which they showed that both NAD and NADP release sequestered Ca^{2+} from IP3-desensitised sea urchin egg homogenates (i.e. Percoll-purified intracellular vesicles). This finding was remarkable because two 2^{nd} messengers, cADPR and NAADP, were later discovered, and these two molecules were suggested to target distinct Ca^{2+} channels (Clapper, et al., 1987). cADPR is a product of the enzymatic conversion from NAD (Lee, et al., 1999), whereas NAADP was initially thought to be a contaminant in the commercial sources of NADP: the two structures are closely related,

with NAADP only different from NADP due to the substitution of a nicotinamide moiety with nicotinic acid (Galione, 2006).

NAADP was later confirmed as a potent Ca^{2+} mobilising molecule (Lee, et al., 1995), and the nature of the NAADP-sensitive Ca^{2+} store was further investigated by Genazzani and Galione in 1996. By using high concentrations of the SERCA inhibitor Tg (which depleted the ER Ca^{2+} store), NAADP was revealed to still be capable of releasing Ca^{2+} in egg homogenate and in intact eggs. CD38 was later identified as the enzyme responsible for synthesising both NAADP and cADPR, the latter of which was later shown to be an agonist of RYR (Lee, 1997; Ogunbayo, et al., 2011).

The intracellular actions of NAADP were further explored. In 2002, Churchill and colleagues demonstrated that reserve granules (the functional equivalent of a lysosome in the sea urchin egg) and lysosome-related organelles are targets of NAADP in sea urchin eggs. Disruption of these acidic organelles (by osmotic permeabilisation) using GPN (glycyl-phenylalanyl-napthylamide) selectively abolished the effects of NAADP. In addition, application of Baf prevented organelle acidification and blocked Ca^{2+} uptake into these stores, which also eliminate NAADP mediated Ca^{2+} mobilisation. Thus, this study identified a novel acidic Ca^{2+} store regulated by NAADP, which was distinguishable from the ER Ca^{2+} release mediated by IP3R and RYR (Churchill, et al., 2002).

The action of NAADP was further investigated in mammalian cells, starting with mouse pancreatic acinar cells being shown to be responsive to NAADP (Galione, 2005). NAADP has also been shown to be very potent in these cells, with < 50nM concentrations capable of producing a robust Ca^{2+} current independent of extracellular Ca^{2+} (Cancela, et al., 1999). Moreover, by using both GPN and Baf , the role of NAADP was further confirmed in a variety of mammalian cells including pancreatic beta cells (Yamasaki, et al., 2004), smooth muscle (Kinnear, et al., 2004), neurons (Brailoiu, et al., 2005), endothelial cells (Brailoiu, G.C. et al., 2010b) and breast cancer cells (Schrlau, et al., 2008), efforts that were aided through use of the antagonist “trans-Ned 19”, which has also been shown to block NAADP signalling (Naylor, et al., 2009). These findings further reinforce the concept of NAADP as a mediator of acidic store Ca^{2+} release in both mammalian and non-mammalian species. Subsequent studies have revealed the physiological role of NAADP such as in angiogenesis, cardiac function, fertilisation, immunology and autophagy (Galione, 2015). Activation of NAADP has been shown to be agonist specific. The brain/gut peptide cholecystokinin (CCK but not acetylcholine) has been shown to recruit NAADP in pancreatic acinar cells (Yamasaki, et al.,

2005), which raises the possibility that NAADP might be recruited by other neurotransmitters such as Ach in other cell types and systems.

1.2.4.2 NAADP sensitive calcium channels

The identity of the NAADP receptor (endo-lysosomal ion channel) has been the subject of debate. The TRPC family member mucolipins (TRPMLs), of which three mammalian isoforms have been identified (TRPML1-3), are one of the best characterised endo-lysosomal ion channels (Puertollano, et al., 2009). These TRPML channels have been linked to Ca^{2+} dependent membrane trafficking of the endo-lysosomal system, in which Ca^{2+} is required for the fusion of lysosomes with other acidic organelles (Luzio, et al., 2007) and the plasma membrane (Luzio, et al., 2010). Depletion of TRPML1 from the lysosomes of myocytes using siRNA has been shown to reduce NAADP mediated Ca^{2+} release. This suggests that TRPML1 is an NAADP receptor (Zhang, et al., 2009). Defects in lysosomal Ca^{2+} handling due to TRPML1 mutations have been shown to disrupt membrane trafficking and contribute to the lysosomal storage disease mucolipidosis IV (Bargal, et al., 2000). Thus, NAADP extends the role of lysosomal Ca^{2+} signalling as well as membrane trafficking. Several other ion channels such as TRPC subfamily members (TRPM2, TRPV2) and P2X purinergic receptor 4 (P2RX4), all located within the endo-lysosomal system, have also been touted as potential candidate NAADP receptors, but the definitive evidence for their involvement in NAADP mediated signalling are lacking (Patel, et al., 2010).

TPCs are a family of proteins that have gained recognition in recent years as major regulators of endosomal-lysosomal Ca^{2+} release (Figure 1.11) (Morgan, et al., 2015). TPCs were first cloned in 2000 by Ishibashi and colleagues (Ishibashi, et al., 2000). The function of TPCs had remained mysterious for some time until 2005, when a TPC in the model plant species *Arabidopsis thaliana* was revealed by overexpression and knockdown studies to be a slow vacuolar Ca^{2+} release channel (Peiter, et al., 2005), which mediates long-range Ca^{2+} waves (Choi, et al., 2014).

In sea urchin egg cell lysate model, NAADP receptors were initially found to be insensitive to Ca^{2+} feedback (Morgan, et al., 2011). However, similar to TRPML channels, growing evidence suggests that TPCs are also mediated by Ca^{2+} to regulate membrane traffic. An initial investigation in 2010 confirmed that TPC2 present in lipid bilayers or discrete lysosomes functions as a Ca^{2+} permeable channel (Pitt, et al., 2010, Schieder, et al., 2010). By using Ca^{2+} imaging and electrophysiological techniques, different laboratories have subsequently

revealed that TPC1 (Rybalchenko, et al., 2012; Pitt, et al., 2014) and TPC2 (Brailoiu, et al., 2010a; Schieder, et al., 2010; Pitt, et al., 2010) are Ca^{2} permeable NAADP target channels (Ogunbayo, et al., 2011). In addition, TPCs not only signal in response to Ca^{2+} flux, but also to changes in pH and membrane potential, which might be important for the regulation of autophagy (Morgan, et al., 2015). In humans, two TPCs (TPC1 and TPC2) were identified. TPC2 is primarily expressed in late-endosomes/lysosomes, while TPC1 appeared to be express in endosomes (Brailoiu, et al., 2009; Calcraft, et al., 2009; Ruas, et al., 2010).

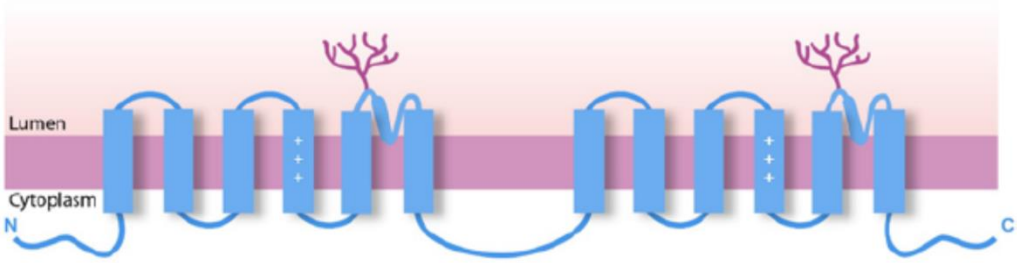

Figure 1.11 Predicted transmembrane domain structure of animal TPCs.

All TPCs share the same membrane topology, which is the two well-defined 6-TM (transmembrane) homologous domains. The pore loop is present on the luminal side of the receptor between the 5th and 6th TM domains of the 6-TM segment. Positively charged residues are present on the 4th TM domain and the tree-like symbol represent the glycosylation site of the receptor.

(Figure from Morgan, et al., 2015)

The hypothesis that TPCs are NAADP sensitive channels is supported by a substantial number of studies (Calcraft, et al., 2009; Brailoiu, et al., 2009; Zong, et al., 2009). However, these findings were recently challenged by two high profile papers in late 2012 which described TPCs as lipid-regulated Na^+ channels. Both studies concluded that TPCs were NAADP insensitive in both wild type mouse cells or in cell lines overexpressing TPCs (Wang, et al., 2012; Cang, et al., 2013). However, these studies used 2mM of Mg^{2+} in their assays, while cytosolic Mg^{2+} has recently been shown to potently inhibit TPCs function with an affinity of 60-130µM (Jha, et al., 2014; Morgan, et al., 2015); which suggests the TPCs in their systems were inactive.

Overexpression of TPCs enhances NAADP dependent responses (Calcraft, et al., 2009; Ruas, et al., 2010; Churamani, et al., 2013; Jha, et al., 2014; Lin-Moshier, et al., 2014). Similarly, TPC down-regulation by RNA interference attenuates responses to NAADP (Brailoiu, et al., 2009; Calcraft, et al., 2009; Zhang, et al., 2013), and similar results have been observed in TPC knockout mouse models (Arndt, et al., 2014; Ruas, et al., 2015). NAADP sensitivity was restored upon re-expression of wild type TPCs, but not with mutant TPCs that have impairment in Ca^{2+} permeability nor with TRPML1 (mucolipins, Ruas, et al., 2015). Taken together, these findings suggest that TPCs are NAADP targets expressed on the membrane of acidic organelles. However, it is still unclear whether NAADP binds directly to TPC or via an accessory protein (Patel, et al., 2011). For instance, by using [^{32}P] NAADP molecules, several studies have suggested the possible indirect interaction of TPC with an unknown low molecular weight NAADP binding protein that mediates channel activation (Ruas, et al., 2010; Lin-Moshier, et al., 2012; Walseth, et al., 2012). It is now widely appreciated that TPCs contribute to both the control of endo-lysosomal trafficking and the regulation of diverse cellular activities via Ca^{2+} release from acidic stores. Upon ER Ca^{2+} store depletion, TPC2 has been shown to modulate SOCE by its association with STIM1 and Orai 1 in human megakaryoblastic leukaemia (MEG01) cells (Lopez, et al., 2012).

1.2.4.3 Lysosomal-ER interaction via NAADP

Pancreatic acinar cells were the first whole mammalian cell type used for testing NAADP function. In this model, Cancela and colleagues (1999) demonstrated that the NAADP mediated Ca^{2+} response was attenuated in the presence of ER Ca^{2+} channel inhibition. This observation was in contrast to findings in a sea urchin egg homogenate model, which suggested that NAADP initiates a small local release of Ca^{2+} by TPCs that is subsequently amplified by the ER through the process of CICR via IP3R and or RYR (Berridge, 1999).

Lysosomes and the ER are often closely associated (Kinnear, et al., 2008). In HEK293 cells overexpressing TPC2, there was a biphasic effect of the Ca^{2+} transient waves. Pre-treatment of cells with Tg and heparin selectively blocked the 2^{nd} large Ca^{2+} waves, whereas pre-treatment with Baf eliminated the entire NAADP-stimulated Ca^{2+} response. Thus, the 2^{nd} large Ca^{2+} waves should be a result of the ER Ca^{2+} release. These findings suggest that the initial phase of Ca^{2+} release is dependent on the acidic stores, while the 2^{nd} transient was triggered by Ca^{2+} release from the acidic stores (Calcraft, et al., 2009). In order to raise local $[Ca^{2+}]$, it is likely that multiple endo-lysosomes act in concert to release Ca^{2+} at a specific site in close proximity to IP3R and RYR (Zhu, et al., 2010). Substantial evidence also suggests that TPCs could preferentially interact with IP3R or RYR in different cell types. Hence in HEK cells, TPC2 effectively triggers IP3R activation (Brailoiu, et al., 2010a); while in vascular smooth muscle cells, TPCs couple selectively to RYR even in the presence of IP3R (Kinnear, et al., 2004). Furthermore, not all NAADP evoked Ca^{2+} signals will be converted to a global CICR, as the signal could be removed by mitochondrial uptake. However once IP3R or RYR get activated by previous Ca^{2+} release from acidic stores, it is likely that a regenerative Ca^{2+} wave will be produced throughout the entire cell (Boittin, et al., 2002; Zhu, et al., 2010). Thus, the Ca^{2+} signals were generated by the interplay of multiple Ca^{2+} stores in which the acidic stores provide the initial key signals for subsequent Ca^{2+} waves.

However, very little is known about the interactions between these Ca^{2+} signalling organelles and the role of NAADP in the colon, and what its functional significance might be.

1.2.5 Cholinergic stimulated calcium signalling in human colonic epithelium

1.2.5.1 Intercellular communication in polarized epithelium

As described previously, the epithelial cell surface is linked by cell-cell adhesion junctions. The three major connections are the tight junctions, gap junctions and the adherens junctions (Figure 1.12).

Tight junctions are intercellular adhesions which form physical barriers between the extracellular space and epithelium. They are normally found at the apical membrane of a cell, where they play an important role in maintaining the apical-basal polarity of the epithelium. The major function of the tight junction is to restrict paracellular transport (transport of substances through the intercellular space between cells) across epithelial cell sheets, and to serve as a barrier between the apical and basolateral membrane for intramembrane diffusion (Giepmans, et al., 2009). Depletion of extracellular Ca^{2+} ions has been shown to impair the formation of tight junctions (Cereijido, et al., 1993), which suggests an important role of Ca^{2+} in maintaining epithelial cell integrity and polarity.

Gap (or 'nexus') junctions are clusters of channels on the lateral plasma membrane which provide direct intercellular communication between epithelial cells through the transmission of 2^{nd} messengers such as molecules, ions and electrical impulses (Rose, 1971). In particular, both Ca^{2+} ions and IP3 molecules have been shown to move passively through gap junctions (Sanderson, et al., 1990). Gap junction channels are formed by hexameric assemblies of the integral membrane proteins 'connexins' (Goodenough, et al., 1996). Since multiple connexin isoforms are expressed in most cell types, the formation of homomeric or heteromeric connexons can be observed (Falk, et al., 1997). The diversity of these channels has been shown to correspond to a range of physiological properties including single- or multiple-channel conductance states (Takens-Kwak and Jongsma, 1992), and selectivity and permeability to certain molecules and ions (Veenstra, et al., 1995; Bevans, et al., 1998; Harris, 2007).

Adherens junctions are cell-cell microdomains that physically connect neighbouring epithelial cells and provide the adherent strength (Fristrom, 1988). In mammals, these adherens junctions are located at the basal side of the tight junctions, which help to define each cell's apical-basal axis. They are composed of proteins including cadherins and catenins, while E-cadherin is the most abundant integral membrane protein expressed in the epithelia. Interaction of E-cadherin with extracellular Ca^{2+} has been shown to strengthen the cell-cell interaction and integrity of the epithelium (Perez-Moreno, et al., 2003).

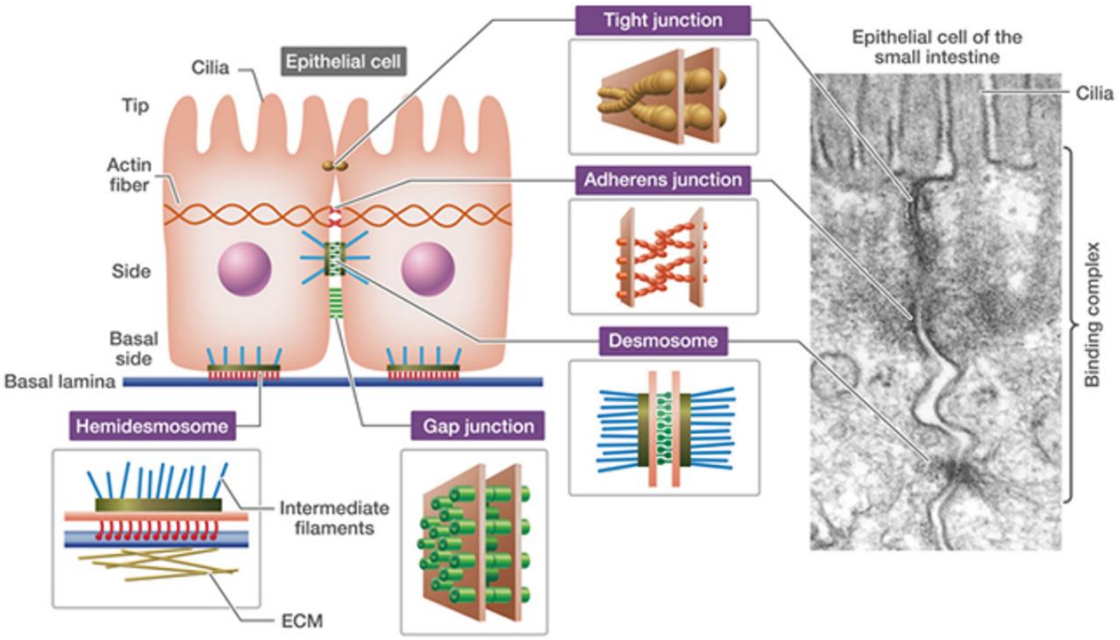

Figure 1.12 Multiple levels of cell-cell junctions that connect epithelial cells.

Epithelial cells are connected to each other via junctional complexes. These junctions are present on the plasma membrane of the epithelial cells and play various roles. Tight junctions form the first line of defence between the epithelia and the extracellular space. Gap junctions allow intercellular communication between cells, whereas cell-cell connections (integrity) are maintained by adherens junctions and desmosome. The epithelial cell sheet is attached to the basal lamina via hemidesmosome.

(Figure from Life Science web textbook by University of Tokyo)

1.2.5.2 Cholinergic signalling mediated secretion in the colonic epithelium

Over the past 30 years there have been a considerable number of studies investigating the role of cholinergic signalling in mediating secretion in the colonic epithelium. However, most of these studies were based on animal models such as guinea pig, rat, mouse and rabbit (Bradbury, et al., 1980; Zimmerman, et al., 1982; Camilleri, et al., 1982; Phillips, et al., 1984; Kuwahara, et al., 1987; Diener, et al., 1989; Javed, et al., 1992; O'Malley, et al., 1995; Haberberger, et al., 2006), which do not necessarily accurately reflect human biology. Since the early 1990s, some studies began to be performed using human colon cancer cell lines such as HT-29 (Phillips, et al., 1993; Bou- Hanna, et al., 1994; Bertrand, et al., 1999; Stanley, et al., 1999; Oprins, et al., 2000; Himmerkus, et al., 2010) and T-84 (Tabcharani, et al., 1994; Cliff, et al., 1998; Banks, et al., 2004; Hassan, et al., 2012), which provided evidence of cholinergic signalling in a human tissue model. However, the polarity and topology of the colonic epithelium is lost in these cell lines, which might affect Ca^{2+} signal generation properties relative to the tissues from which these lines derive. Cholinergic stimulation has been shown to mobilise intracellular Ca^{2+} in all cells, however, the underlying mechanism of the Ca^{2+} signal generation in coupling the physiological function of the human colonic crypts has never been shown.

1.2.5.3 Association of intracellular calcium signals and colonic crypt physiology

A 3-D human colonic crypt culture model has been developed in our lab, which made it possible to perform functional studies on the native human colonic epithelium. Using this model, cholinergic stimulated Ca^{2+} mobilisation in the native human colonic epithelium was first shown by Susanne Lindqvist. By using Ca^{2+} sensitive fluorescence imaging, she demonstrated that Ach initiated a Ca^{2+} signal in the base of the crypt (via M3AchR activation), which then propagated along the crypt-axis towards the surface epithelium. In conjunction with experiments on the HT-29 colon cell line, Lindqvist concluded that there is a fundamental role for Ach-induced Ca^{2+} signals in regulating cellular homeostasis of the colonic epithelium (Lindqvist, et al., 1998; Lindqvist, et al., 2002). Subsequent work by Amy Reynolds in our lab investigated the cholinergic regulation of fluid secretion and tissue renewal in the human colonic epithelium. She demonstrated for the first time that internalisation of the Na-K-2Cl co-transporter (NKCC1) attenuates the cholinergic secretory response in a Ca^{2+} dependent manner, identifying NKCC1 as a major modulator of colonic crypt fluid secretion. She further observed that cholinergic stimulation of colonic epithelium regulates fluid secretion in the short term (minutes to hours), and tissue renewal in the long

term (days) (unpublished data). Both of these studies provided important information informing this thesis, regarding Ca^{2+} signalling in the regulation of physiological function in human colonic crypt.

Our lab has repeatedly demonstrated that cholinergic stimulation of MAchR mobilises intracellular Ca^{2+} in the native human colonic epithelium (Lindqvist, 2000; Reynolds, 2007). This Ca^{2+} signal is observed within 30 seconds of cholinergic stimulation. This Ca^{2+} wave appears to initiate at the apical pole of cells at the base of crypt, near the stem cell niche; the signal then diffuses to the basal pole of the initiator cell, before it propagates further up the entire crypt axis (Figure 1.13). The intercellular communication that permits signal transduction is believed to be mediated via gap junctions in the lateral membrane of the epithelial cells. However, the mechanism of the regulation remains unclear. Based on immunohistochemistry findings, we speculate that $Lgr5^{+}$ stem cells are the Ca^{2+} initiator cells at the colonic crypt base (Figure 4.2B, unpublished data). This could be due to their close proximity with the cholinergic neurons which provide the activation signals. Further study is required to confirm this finding, and to discover why specifically stem cells are the initiator cells when all epithelial cells express MAchR.

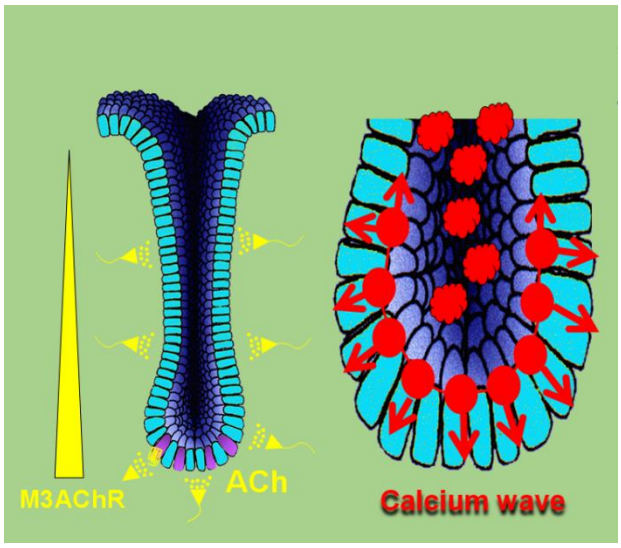

Figure 1.13 Schematic diagram of Ca^{2+} wave propagation along the colonic crypt-axis upon a cholinergic stimulation.

Binding of Ach to M3AchR on the basal pole of the crypt triggers Ca^{2+} mobilisation at the crypt base. The Ca^{2+} signal initiates at the apical pole of initiator cells and exhibits both intracellular propagation to basal pole, and intercellular propagation along the entire crypt axis via gap junctions.

(Figure is courtesy of Mark Williams)

1.3 Mucin secreting goblet cells

1.3.1 Goblet Cell biology and function

One of the major known physiological roles of colonic crypts is to produce the mucus which forms the protective and lubricative barrier that lines the gut, a feat which is made possible by the actions of mucin-secreting goblet cells. Goblet cells were first described in the GI tract by Bizzozero in 1892 (reviewed by Cheng, et al., 1974a). They were so-named due to the cup-like appearance of the cytoplasm that holds mucus granules below the apical membrane (Figure 1.15). They are one of the several secretory cell types found in the intestines, scattered among the columnar cells in the epithelium (Figure 1.5). Their main function is to secrete mucins, trefoil peptides, Fc gamma binding protein (Fcgbp) and RELM-β, which are the major components of the mucus barrier layer formed between the gut lumen and the epithelial surface (Kim, et al., 2010). Goblet cells are morphologically indistinguishable from other epithelial cells in the absence of mucin. Based on studies of rabbit colon, goblet cells have been shown to undergo several morphological changes during their life. Once propagated from the stem cell niche, immature goblet cells rapidly begin to synthesise and secrete mucin granules (Radwan, et al., 1990). These immature cells are large and pyramidal in shape due to the shedding of cytoplasm, organelles and mucin granules; this causes their cell volume to diminish throughout migration upwards to the colonic surface (Radwan, et al., 1990). In addition, based on the level of maturation along the crypt axis and the location along the GI tract, intestinal goblet cell subpopulations produce and secrete different mucin species (Kim, et al., 2010). In the colon, goblet cells synthesise and secrete the mucin MUC2. The mucus, with MUC2 being the major component, also contains several abundant proteins such as CLCA1, ZG16, FCGBP and AGR2, although their functions remain largely unknown (Johansson, et al., 2008; Birchenough, et al., 2015). However, AGR2, an ER protein that is secreted into mucus, has been suggested to promote MUC2 folding in the ER by building intramolecular disulphide bonds (McGuckin, et al., 2011a). In addition, $AGR2^{-/-}$ mice have less filled goblet cells and a poorly developed inner colon mucus layer. These mice are more susceptible to colon inflammation. The high concentration of AGR2 in secreted mucus throughout the GI tract suggests they may also play some extracellular role (Bergström, et al., 2014). While our current knowledge of goblet cell biology is still very limited, studies from the past 10 years suggest that there are several types of goblet cells in the GI tract, which function in different ways.

MUC2 polymers are densely packed into secretory granules due to the low pH and high Ca^{2+} in this compartment. Once secretion takes place, the densely packed MUC2 polymers expand

over 1000-fold into large net-like structures (Johansson, et al., 2013). This process is dependent on increasing pH and the removal of a single Ca^{2+} ion (Ridley, et al., 2014). Experimentally, bicarbonate has been shown to be an ideal solution for raising pH and precipitating Ca^{2+} (Gustafsson, et al., 2012b). In the small intestine, the enterocytes adjacent to goblet cells provide the required bicarbonate for mucin unfolding (Gustafsson, et al., 2012b), whereas in the large intestine, goblet cells supply their own bicarbonate via the bestrophin-2 bicarbonate transporter (Yu, et al., 2010). Regulated granule secretion and compound exocytosis are the two major methods of mucus secretion. Regulated mucus secretion has been extensively studied in airway goblet cells. In this model, exocytosis of vesicles (granules) through fusion with the plasma membrane was shown to be mediated by typical exocytosis components such as the SNARE proteins: Syntaxin, VAMP8 and SNAP23 and the scaffolding protein Munc18 in both basal and stimulated secretion (Adler, et al., 2013). Although not yet closely studied, mucus secretion in the small and large intestines probably follow similar mechanisms. Moreover, compound exocytosis in goblet cells is more dramatic in that most mucus theca fused together in the cytoplasm and emptied their mucin content all at once that causes a 100-1000 fold expansion in mucin volume. To date, molecular studies of goblet cells compound exocytosis are not available, but morphological studies demonstrate the explosion of goblet cells during the secretion process (Specian & Neutra et al. 1980). Based on mucus turnover and renewal studies (by detecting mucin biosynthesis with azide-modified N-acetylgalactosamine, GalNAz), rapid mucin synthesis and secretion were observed in goblet cells on colon surface epithelium. In contrast, goblet cells at the colonic crypt base accumulate mucus granules over time, and secretion is much slower (Johansson, 2012). In addition, mucin biosynthesis and secretion was shown to be faster in small intestinal villi goblet cells than crypt goblet cells (Johansson, 2012). Thus, goblet cells play a pivotal role in maintaining the homeostasis of the gut microenvironment through the production of mucins.

1.3.1.1 Other potential goblet cell functions

The assumed primary function of intestinal goblet cells is to synthesise and secrete mucus. Recent studies have demonstrated that a sub-population of goblet cells exists in the small intestine which are capable of acquiring and presenting luminal antigens to $CD103^{+}$ dendritic cells in the lamina propria (McDole, et al., 2012; Howe, et al., 2014), implying a role in gut immunity. This antigen uptake was shown to be augmented by cholinergic agonists via muscarinic receptor 4 stimulation (Knoop, et al., 2015). This finding further supports the

existence of different goblet cell subsets along the GI tract that is mediated by cholinergic signalling.

1.3.2 Intestinal goblet cell development

Goblet cells are one of the principal cell types in the human colon which appear early in development, at around 9 to 10 weeks gestation in human foetal small intestines (Kim, et al., 2010). Previous studies in mouse small intestinal epithelium (Cheng, et al., 1974a and b) suggested that goblet cells were derived from some "poorly differentiated" cells called oligomucous cells at the crypt base, which contained very few of the mucus granules that identify goblet cells. Both oligomucous and mature goblet cells were shown to be present in the intestinal epithelium, but they are indistinguishable in the adult tissues. A later study by Gordon and colleagues demonstrated that goblet cells arise from multipotent stem cells residing at the mouse intestinal crypt base (Gordon, et al., 1992). It is now widely appreciated that goblet cells are sequentially derived from the long-lived $Lgr5^{+}$ ISC and shorter-lived secretory progenitor cells (Figure 1.5) (Barker, et al., 2007). Some studies have suggested the presence of two stem cell populations in the mouse small intestinal crypt: an active stem cell (ASC) population, responsible for proliferation and crypt maintenance, and a quiescent stem cell (QSC) population (typified by Bmi1 expression, which is a +4 cell marker) which replenishes the ASC population after crypt injury (Potten, et al., 2009; Yan, et al., 2012). This theory was later challenged by more recent studies, in which transcriptomic and proteomic approaches as well as lineage tracing knock-in mouse models suggested that the proposed quiescent stem cell marker Bmi1 is robustly expressed in $Lgr5^{+}$ stem cells (Muñoz, et al., 2012; Itzkovitz, et al., 2012). In addition, the Notch ligand DII1 has been recently used as a marker for the early secretory progenitors (van Es, et al., 2012). Thus identifying the definitive ISC population remains an active area of investigation (Carulli, et al., 2014).

Goblet cells form a constantly renewing population of very short lived cells. In mice, it has been shown that they migrate from the base to the top of crypt and are sloughed into the intestinal lumen within 2-3 days (Merzel and Leblond, 1969). However, the mechanism driving intestinal cell death (goblet cells included) during normal homeostasis is not clear. One recent study by Eisenhoffer and colleagues suggested that the overcrowding due to constant epithelial renewal forces extrusion of live cells, which is important for controlling the numbers of epithelial cell and maintaining the cellular organisation of the colonic mucosa (Eisenhoffer, et al., 2012).

ISCs are subject to the control of different molecular pathways and transcription factors to maintain intestinal homeostasis. Wnt signalling is important for stem cell establishment and crypt development in the intestine. It is required for the proliferation of stem and progenitor cells, and has been implicated in regulating epithelial cell differentiation, possibly via a Wnt-

Notch cross talk mechanism (Crosnier, et al., 2006). In addition, aberrant Wnt signalling has been observed in most cases of colorectal and intestinal cancers (White, et al., 2012). Notch signalling is involved in determining the cell fate decisions, and thus lineage specification, of intestinal cells. However, it is unclear when exactly such signalling occurs, and whether it targets progenitor cells or some intermediate (van der Flier and Clevers, 2009). Notch signalling has been shown to favour the development of absorptive cell lineages (enterocytes) relative to secretory cell lineages including Paneth, goblet and enteroendocrine cells (van Es, et al., 2005; Gerbe, et al., 2011). Based on mouse models, colonic goblet cell differentiation has been shown to be regulated by the transcription factors Math1 (the mouse homologue of human Hath1) and Krüppel-like factor 4 (KLF4), as well as the Notch and Wnt signalling pathways (Gregorieff, et al., 2005; Gregorieff, et al., 2009). Other signalling pathways including Bone Morphogenetic Proteins (BMP), Hedgehog, Hippo, Eph/ Ephrin and EGF/ Erb B have also been shown to play important roles in stem cell function (Crosnier, et al., 2006; Vanuytsel, et al., 2013). However, relevant data from humans is very limited due to the difficulties in culturing human stem cells.

Activation of Notch and its downstream target Hes1 blocks the basic Helix Loop Helix transcription factor Math1/ATOH1, in which Math1 is an essential determinant of secretory lineage commitment (Fre, et al., 2005; Stanger, et al., 2005). In contrast, inhibition of Notch pathway (by γ-secretase blockage) causes a rapid differentiation into the secretory cell lineages (Yang, et al., 2001; van Es, et al., 2005; Zecchini, et al., 2005; van Es, et al., 2010; Reynolds, 2014). Thus Notch signalling regulates epithelial cell fate in a Math1 dependent manner. The transcription factor SPDEF (SAM pointed domain ETS factor), which acts downstream of Math1, has also been shown to be important for goblet cell differentiation and maturation in the intestinal epithelium (Gregorieff, et al., 2009; Noah, et al., 2010). Apart from controlling cell fate, Notch signalling is also required for stem cell proliferation and survival in a Math1 independent manner (Crosnier, et al., 2005; Fre, et al., 2005; Stanger, et al., 2005; VanDussen, et al., 2012). Therefore Notch is capable of regulating distinct aspects of epithelial cell homeostasis. Moreover, the activation of KLF4, a zinc-finger transcription factor expressed in crypt intestinal goblet cells (Ghaleb, et al., 2011) is also involved in the terminal differentiation of goblet cells in mice (Katz, et al., 2002; Yu, et al., 2012). KLF4 has been identified as a tumour suppressor gene in colorectal cancer (Zhao, et al., 2004; Zhang, et al., 2006), and studies have shown inhibition of KLF4 expression as a result of Notch signalling (Ghaleb, et al., 2008; Zheng, et al., 2009). Furthermore, several studies have also suggested the involvement of E74-like factor 3 (Elf3) (Ng, et al., 2002; Kwon, et al., 2009) and

OASIS (ER stress transducer) (Asada, et al., 2012) in the terminal differentiation of goblet cells in mice.

1.3.3 Mucin structure, function and biosynthesis

Mucin is the major component of the mucus layer. A total of 20 different mucins have been described in humans, 15 of which being expressed in some region of the GI tract. Depending on their structure and location, mucins are subdivided into membrane-bound and secretory forms (Johansson, et al., 2011; MuGuckin et al., 2011b). Membrane-bound mucins are so-called due to the presence of a transmembrane domain which allows them to anchor to the cell membrane. These proteins consist of a large N-terminal extracellular, and a short cytoplasmic C-terminal domain (Hattrup, et al., 2008), and are primarily expressed at the apical side of epithelial cells. While the function of transmembrane mucins is only partially understood, they number a large proportion of known mucins, including: MUC1, MUC3A, MUC3B, MUC4, MUC11, MUC12, MUC13, MUC15, MUC16, MUC17, MUC20 and MUC21 (Imai, et al., 2013). The glycocalyx, a fuzz-like coating covering the surface of the microvilli of enterocytes, is composed of these cell surface mucins (Williams, et al., 2001; McGuckin, et al., 2011b). This glycocalyx is believed to function as a protective barrier, and is probably involved in apical cell surface sensing and signalling (Singh, et al., 2006; Hattrup, et al., 2008).

Secretory mucins, which can be gel-forming or non-gel-forming, include: MUC2, MUC5AC, MUC5B, MUC6, MUC7, MUC8, MUC9 and MUC19. MUC5AC is mainly expressed in tracheal-bronchial and gastric mucosa. Although lesser amounts of MUC5AC and MUC6 were detected in the colon, MUC2 is the major secretory mucin that is constitutively synthesised by colonic goblet cells (McGuckin, et al., 2011b). MUC2 molecules are large glycoproteins, whose protein core is characterised by multiple tandem repeat sequences with a high proportion of proline, theronine and serine residues (forming “PTS domains”) (Figure 1.14 B). The protein core is resistant to host proteolytic enzymes due to the high number of intra-molecular disulphide bonds and the glycan coating that shields the potential cleavage site (Johansson, et al., 2011; MuGuckin et al., 2011b). The hydroxyl residues of MUC2 get heavily O-glycosylated (Figure 1.14A); these post-translational modifications make up approximately 80% of the mature MUC2 mass. These O-linked oligosaccharides are densely packed, which functions to maintain the integrity of the mucin polymer. They also possess significant water holding capacity that provides the gel-like properties of mucins. The N- and C-terminal regions of MUC2 are poorly glycosylated, and mostly consist of cysteine residues (Figure 1.14

B). Secretory mucins (including MUC2) often contain three N-terminal von Willebrand factor-like domains (termed D1, D2 and D3), while the C-terminal region contains only one D4 domain (Figure 1.14 B). Some evidence suggests that glycosylation can be altered in response to mucosal infection and inflammation (Johansson, et al., 2011; MuGuckin et al., 2011b).

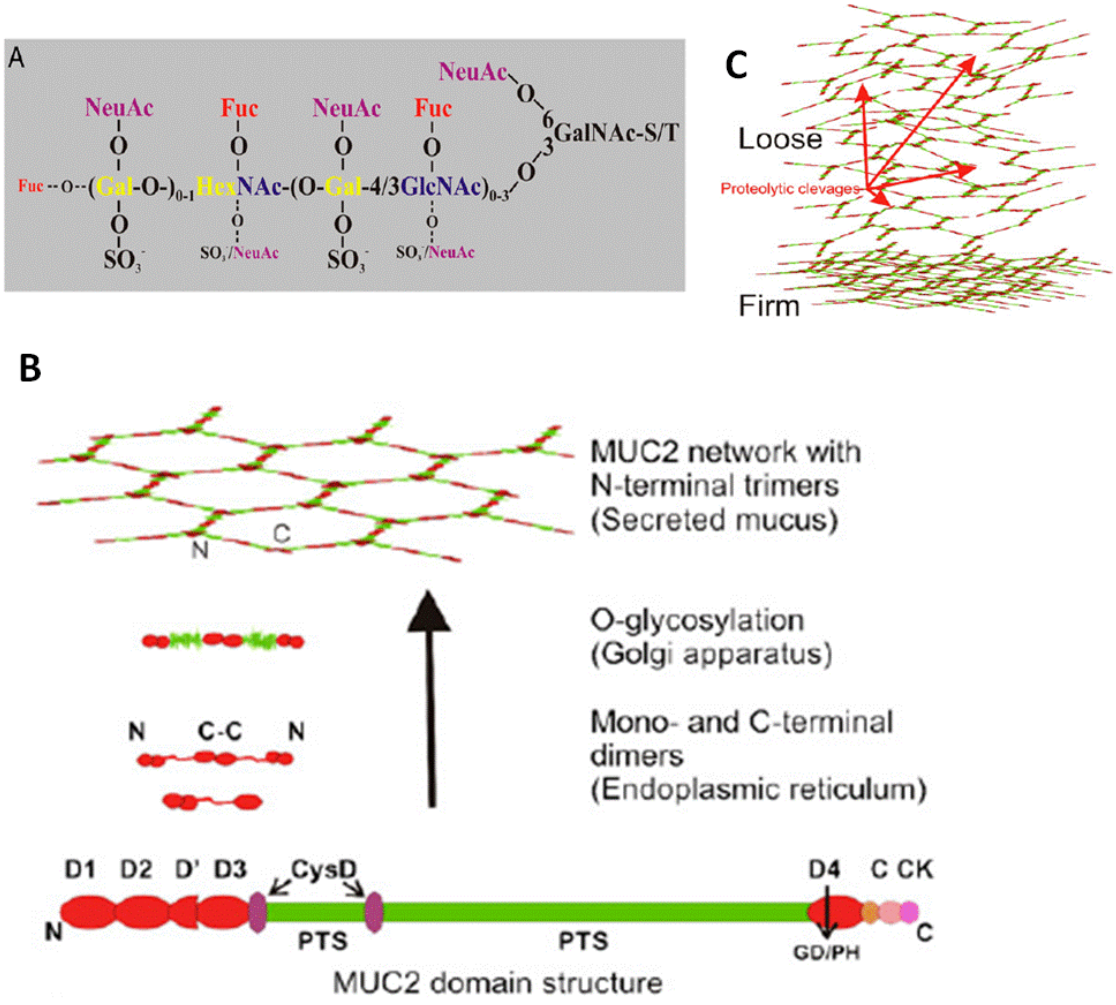

Figure 1.14 The MUC2 mucin network in mucus.

(A) MUC2 glycosylation sites. MUC2 mucin from human sigmoid colon has a relatively uniform O-glycan composition. (B) From bottom to top: MUC2 domain organisation (bottom). MUC2 has a central PTS domains that are rich in serine, threonine and proline residues, and these domains will subsequently become heavily glycosylated upon post-translational modification. The N- and C-terminal regions of MUC2 mostly consist of cysteine residues. Three von Willebrand factor-like domains (termed D1, D2 and D3) at the N-terminal, and only one D4 domain at the C-terminal region. MUC2 is synthesised in the ER, processed in the Golgi (middle), and released into the lumen from goblet cells (top). (C) The firm adherent mucus layer is converted to the loose outer layer by proteolytic cleavage of the cysteine residues of MUC2, expanded and dispersed to form a net-like structure.

(Figures from Johansson et al., 2011)

1.3.4 MUC2 packaging and secretion in goblet cell

Newly synthesized MUC2 proteins form homodimers in the ER via their C-termini concurrent with N-glycosylation, before subsequent O-glycosylation in the Golgi (Johansson, et al., 2011; Johansson, et al., 2013a). These heavily O-glycosylated MUC2 dimers are then densely packed into numerous apically-stored secretory vesicles (Figure 1.15). At this stage, the N-terminal ends of the dimers are coupled together by disulphide bonds into trimeric structures which give the native fresh mucus its viscous, sticky and hydrophobic properties (Caldara, et al., 2012). Due to the multimerisation, once released from the cell, MUC2 molecules expand to form large net-like structures (Figures 1.14B top and 1.15) (Johansson, et al., 2011; McGuckin et al., 2011b).

By using sprinkled charcoal, Lena Holm and others demonstrated the two layers of mucus in the rat colon (Holm, et al., 2012); the loose outer layer can be readily removed by suction, whereas the firm adherent inner layer required scraping to be removed (Atuma, et al., 2001; Brownlee, et al., 2003; Hansson, et al., 2010; Johansson, et al., 2011; MuGuckin et al., 2011b). The continuous release of MUC2 means that newly released mucins will interact with the already present inner mucus layer (Johansson, et al., 2012). This inner layer is about 50µm thick in mice and is renewed every 1-2 hours in the distal colon of live animals. In humans, the inner layer is around 200µm thick (Johansson, et al., 2012, Johansson, et al., 2013). The conversion of inner to outer mucus layers is mediated by proteolytic cleavage of cysteine residues of the mucus film (Figure 1.14C), that allow mucin to expand further, up to 3-4 times in volume. Because the outer layer pore size is larger, it allows freer movement of bacteria (Hansson, et al., 2010).

Due to the large size of the MUC2 protein, the high number of disulphide bonds and the oligomerisation into multimers, there is a relatively increased chance of misfolding during their biosynthesis (McGuckin, et al., 2011b). Correct protein folding is mediated by ER resident chaperones and enzymes. In normal conditions, the ER chaperone GRP78 (BiP) is bound by the transmembrane proteins IRE1, ATF6, and PERK, and thus rendered inactive. The accumulation of misfolded or unfolded proteins initiates the ER unfolded protein response (UPR) via the association with GRP78 (McGuckin, et al., 2010), which will lead to their removal by a process called ER associated degradation (ERAD) (Vembar, et al., 2008). Liberation of IRE1 and PERK facilitates the translation of the transcription factor X-box binding protein-1 (XBP-1). XBP-1 in turn induces a range of ER UPR-related genes such as chaperones and proteins involved in ERAD (Vembar, et al., 2008; Kaser, et al., 2008). Lack of XBP1 has been shown to cause accumulation of misfolded mucins, develop ER stress in

Paneth and goblet cells and subsequently lead to inflammation (Kaser, et al., 2008). In addition, activation of PERK inhibits global protein synthesis; the generation of active ATF6 also enhances the transcription of XBP-1 and other ER UPR genes. Thus, ER homeostasis is maintained by (1) elevating the degradation of misfolded proteins, (2) attenuating protein translation, (3) and increasing the protein folding capacity by upregulating the expression of ER chaperones (McGuckin, et al., 2011a).

Mucin granule exocytosis occurs in one of two modes: constitutively (unregulated baseline low-level secretion) and in response to extracellular stimuli (accelerated) (McGuckin et al., 2011a and b). Under normal physiological conditions, goblet cells continuously replenish the mucus layer. In the presence of potent secretagogues including hormones (neuropeptides) and inflammatory mediators (cytokines and lipids), there is a rapid increase in mucus exocytosis, with a maximum rate at 1-3 minutes after stimulation, followed by a much slower rate of release (Specian and Neutra, 1980; Phillips, et al., 1984; McGuckin, et al., 2011b; Johansson, 2012). However, the mechanisms underlying the formation of these layers are still under investigation. Mucus secretion was suggested to be mediated by various 2nd messengers that include intracellular Ca^{2+} (Seidler, et al., 1989; Davis, et al. 2008), cAMP and DAG. Current techniques available for detection of mucins included ELISA, dot/ slot blotting, Western blotting, use of lectins and antibodies on membranes, additionally immunohistochemistry and immunofluorescence on both tissues and cells (Harrop, et al., 2012).

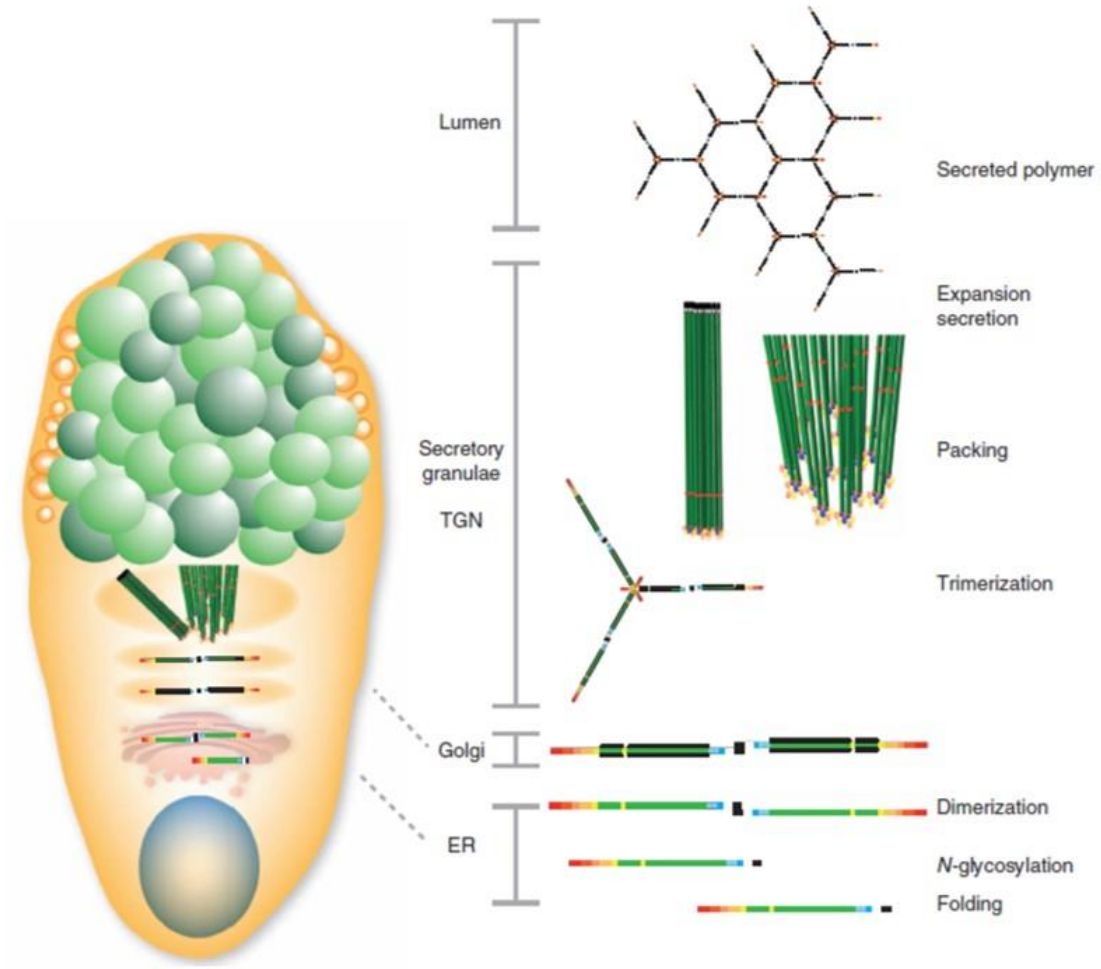

Figure 1.15 MUC2 mucin assembly in goblet cell.

MUC2 monomers are synthesised in the ER and dimerised via the C-terminals with concurrent N-glycosylation. These dimers then translocate to the Golgi where O-glycosylation occurs. The heavily O-glycosylated MUC2 then densely packed into the apically stored secretory granules. At this stage, the N-terminal ends of the dimers are coupled together by disulphide bonds into trimeric structures. Once released from cell, MUC2 multimers expand to form large net-like structures.

(Figure from Birchenough, et al., 2015)

1.3.5 Known mediators of goblet cell mucin secretion

Mucin secretion in goblet cells can be regulated by various mechanisms. Ach is the most studied Ca^{2+} mobilising agent that has been shown to induce mucus secretion in both the small and large intestines of mouse, rat, rabbit and the human colon (Specian & Neutra, 1980; Neutra, et al, 1982; Halm & Halm, 2000; Gustafsson, et al., 2012c; Ermund, et al., 2013b). Administration of Ach or Carbachol (Cch, non-degradable by cholinesterases) stimulates a rapid but transient increase in mucus secretion. Some previous studies have suggested that the small intestinal crypt goblet cells are more sensitive to cholinergic stimulation, while the villus goblet cells and colonic surface goblet cells are nonresponsive to the stimulus for mucus exocytosis (Gustafsson, et al., 2012a; Ermund, et al., 2013a and b). Histamine is another inducer that is mainly produced by immune cells such as basophils and mast cells. It is involved in local immune responses and can also act as a neurotransmitter. It has been shown to mediate mucus secretion in the airways of guinea pigs (Tamaoki, et al., 1997) and in the human colon, but not in the small intestine (Neutra, et al., 1982; Halm & Halm, 2000). Moreover, the prostaglandin E2 (PGE2) family is composed of lipid compounds that have been shown to induce mucus secretion in the rat colon and mouse small intestine, both via cAMP and Ca^{2+} dependent pathways. However, in the human colon PGE2 only appears to stimulate fluid secretion (Halm & Halm, 2000).

Colonic ischemia can be caused by disease or surgery. A recent study by Grootjans and colleagues demonstrated that the release of mucus by compound exocytosis prevented ischemia-induced tissue damage. Ischemia has been shown to cause the detachment of the inner mucus layer, allowing bacteria to penetrate the sterile crypts. Goblet cells seem tolerant to ischemia reperfusion injury, and they release mucus when circulation is restored. The growth of the newly formed mucus layer then washes off the bacteria from the epithelium (Grootjans, et al., 2013). Although the mechanisms for colonic crypt mucus compound exocytosis have not yet been identified, this mass release has been shown to be triggered by Ach (Neutra, et al., 1982; Plaisancié, et al., 1998).

1.3.6 Immunomodulation of goblet cell function

Interleukin-10 (IL-10) is an anti-inflammatory cytokine that has been shown to be critical for intestinal homeostasis. Bacterial-dependent colitis has been observed in mice deficient for IL-10 or its receptor (Kühn, et al., 1993; Sellon, et al., 1998). In addition, GWAS have

highlighted single nucleotide polymorphisms in the IL-10 loci, as well as IL-10 receptor mutations, as associated with IBD (Franke, et al., 2008; Begue, et al., 2011). ER stress is emerging as an important contributor to IBD pathogenesis (McGuckin, et al., 2010; Hasnain, et al., 2013). Mice lacking IL-10 develop colitis accompanied by ER stress (Shkoda, et al., 2007). TUDCA (a tertiary bile acid) has been suggested to play a role in resolving ER stress response in the small intestinal epithelial cell line Mode-K, that could be a potential drug to target IBD pathology (Berger and Haller, 2011). In addition, a study by Hasnain and colleagues recently demonstrated the role of IL-10 in modulating the ability of goblet cells to manage mucin biosynthesis and misfolding (Hasnain, et al., 2013). In another study, MUC2 production was shown to be decreased in IL-10 deficient mice (van der Sluis, et al., 2008). Thus, these studies demonstrate the role of anti-inflammatory cytokines in mediating goblet cell mucin secretion.

1.3.7 Other potential mediators of mucus secretion in goblet cells

Current studies have suggested that cellular processes including endocytosis, autophagy, ROS generation, and inflammasome activity appear to modulate mucin granules accumulation and secretion. For example, a study by Patel, et al demonstrated that the accumulation of goblet cell mucin granule in differentiated mouse intestinal cells was a result of the inhibition of clathrin-mediated endocytosis (Patel, et al., 2013). Electron microscopy revealed the expression of LC3β (an autophagosomal marker) and EEA1 (an endosomal marker) double positive vacuole, and this association was abrogated in endocytosis-inhibited cells. This finding potentially linked the autophagy and endocytosis pathways to mucus secretion. Autophagy is a process that links to immunity and inflammation (Levine, et al., 2011). Cells lacking autophagy proteins including Atg5, Atg14 and FIP200 also caused mucin granule accumulation in goblet cells. Fusion of autophagosomes and endosomes forms an intermediate structure called an amphisome (Sanchez-Wandelmer, et al., 2013) which closely resembles the LC3β and EEA1 double positive vacuoles (Figure 1.16). These amphisomes are the source of ROS (Patel, et al., 2013). Inhibition of endocytosis or knockout of autophagy genes have been shown to block NADPH oxidase (NOX) activity in these amphisome-like structures and result in a decrease of cellular ROS (Patel, et al., 2013). Administration of exogenous ROS mediates mucin secretion, which suggested a role of ROS in mucus regulation (Figure 1.16) (Brownlee, et al., 2007; Patel, et al., 2013).

Inflammasomes are another potential regulator of goblet cell mucus secretion. They are multiprotein complexes which comprise of a subset of NOD-like receptor (NLR) family members, and are linked to caspase 1 via the adaptor protein ASC (apoptosis-associated speck-like protein containing a CARD). NLRPs function as sensors for various pathogen-associated molecular patterns (PAMPs) and danger-associated molecular patterns (DAMPs). Activation of inflammasomes trigger pyroptosis, a proinflammatory and lytic mode of cell death (Lamkanfi, et al., 2014). Some NLRP subtypes have been shown to be expressed in mucosal epithelial cells which suggests their possible role in intestinal homeostasis (Chen, G. et al., 2011; Elinav, et al., 2011; Chen, G.Y. et al., 2014; Wlodarska, et al., 2014). NLRP6 inflammasomes are highly expressed by colonic goblet cells. Mice lacking NLRP6 displayed mucin granule accumulation, and thinner inner mucus layers compared to wild-type mice. This phenotype is similar to heterozygous Atg5 knockout mice (Patel, et al., 2013; Wlodarska, et al., 2014; Chen, G.Y. et al., 2014). In addition, NLRP6 knockout mice also possess elevated numbers of damaged mitochondria, which is a symptom of defective autophagy (Wlodarska, et al., 2014). Thus, these findings suggested the functional role of NLRP in intestinal mucin exocytosis through activation of autophagy in mice.

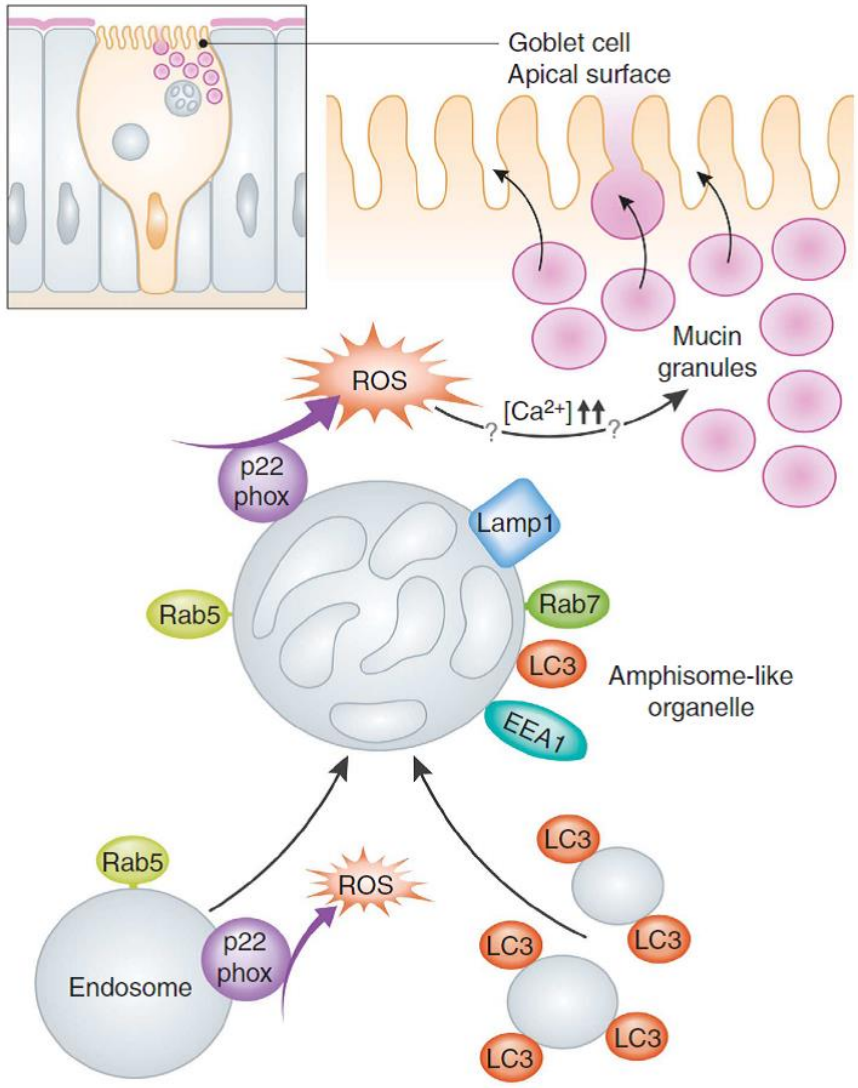

Figure 1.16 Proposed model of goblet cell mucus secretion mediated by ROS.

NADPH oxidase 1 (NOX1) is an endosomal enzyme in the colon that mediates the formation of ROS outside of the mitochondria. ROS is generated via the activation of NOX1 by forming a complex with RAC1 and p22 phox. These ROS were suggested to promote the fusion of $LC3^{+}$ vesicles with endosomes to form amphisome-like organelles. This compartment probably enhances the ROS production and in turn increase cytosolic [Ca^{2+}] through an unknown mechanism and lead to mucus secretion in goblet cells.

(Figure from Sanchez-Wandelmer, et al., 2013)

1.4 Hypothesis

Cholinergic stimulation of muscarinic acetylcholine receptor 3 (M3AchR) in native human colonic epithelium mobilises intracellular Ca^{2+} and regulates mucus secretion in colonic goblet cells.

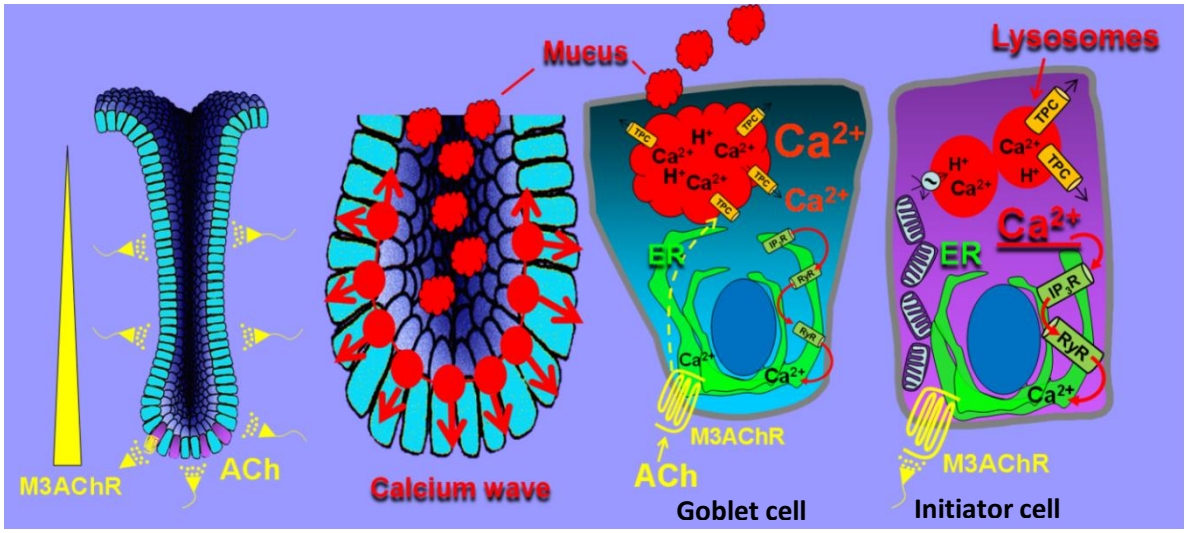

Figure 1.17 Illustration of the hypothesis to be tested.

(From left to right) Depictions of the neuronal-epithelial cell interactions in the human colonic epithelium via M3AchR. It has been well established in the Williams lab that the application of the neurotransmitter Ach or Cch stimulates a Ca^{2+} signal within seconds at the base of crypt near the stem cell niche. This Ca^{2+} signal (wave) appears to initiate at the apical pole of initiator cells at the base of crypt, before spreading to the basal pole of the cell and propagating further along the entire colonic crypt-axis via intercellular gap junctions. It is proposed that the cholinergic stimulated Ca^{2+} mobilisation from intracellular stores (ER, lysosomes) along the crypt-axis coordinates excitation secretion coupling of mucus in the human colonic goblet cells.

1.4.1 Aims of this study

Previous studies have demonstrated a close correlation between Ca^{2+} signalling and mucus secretion in several models, including: animal GI tracts (Neutra, et al., 1982; Seidler, et al., 1989; Hamada, et al., 1997; Yang, et al., 2013); human colon cancer cell lines (Mitrovic, et al., 2013); animal airways (Davis, et al. 2008); human airways (Sebille, et al., 1998; Denning, et al., 1998), and animal eyes (Dartt, et al., 2000). Cholinergic stimulated Ca^{2+} signals have been shown to regulate fluid secretion in the native human colonic epithelium (Reynolds, 2007). In addition, cholinergic stimulated mucus secretion was first demonstrated by Halm and Halm in the isolated human colonic crypt (Halm and Halm, 2000). However, the molecular mechanism of the cholinergic mediated Ca^{2+} signal generation in coupling mucus secretion is unclear. Recent advances in the field suggest that the acidic endo-lysosomal Ca^{2+} stores are the initiator of Ca^{2+} signal generation via the TPC. The intracellular organelles including the endosome ($EEA1^{+}$), lysosomes ($LAMP1^{+}$) and autophagosomes ($LC3^{+}$) are closely associated with each other. This arrangement suggests a possible cross-talk mechanism between Ca^{2+} and ROS in regulating mucus secretion.

The aim of the current study is to investigate the role that cholinergic stimulation of the muscarinic acetylcholine receptor 3 (M3AchR) and mobilisation of intracellular Ca^{2+} plays in the coordination of excitation-mucus secretion coupling in human colonic crypts. The hypothesis will be tested by addressing the following objectives:

(1) Characterisation of the cellular and molecular machinery of excitation-mucus secretion coupling in human colonic crypts

(2) Investigation of cholinergic regulated Ca^{2+} signal generation

(3) Investigation of Ca^{2+} excitation-mucus secretion coupling in the human colonic crypts

(4) Exploration of the interplay between Ca^{2+} and ROS in mucus secretion

Chapter 2: Materials and Methods

2.1 Materials

2.1.1 Chemicals and reagents

Chemicals, reagents, buffers and medium	Supplier
Agarose	Sigma- Aldrich
Bovine serum albumin (BSA)	Sigma- Aldrich
Calcium chloride (CaCl)	BDH Prolabo (VWR International)
D-Glucose	Fisher Scientific
Dimethyl sulfoxide (DMSO)	Sigma- Aldrich
Disodium hydrogen phosphate (Na_2HPO_4)	Fisons Scientific Apparatus
DMEM	Invitrogen
Donkey serum	Sigma
Ethanol	Sigma
Fluo-4 AM	Invitrogen (Molecular Probe)
Fura-2 AM	Invitrogen (Molecular Probe)
HEPES	Fisher Scientific
Hoechst 33342 solution	Life Technologies
Magnesium chloride (MgCl)	Fluka (Sigma-Aldrich)
Matrigel	BD Biosciences
Paraformaldehyde (PFA)	Sigma- Aldrich
Phosphate buffered saline (Dulbecco A) Tablets	OXOID
Potassium chloride (KCl)	Fisher Scientific
ROSstar^{TM} 550	LI-COR
Sodium bicarbonate ($NaHCO_3$)	Fisher Scientific
Sodium chloride (NaCl)	Fisher Scientific
Triton-X 100	Roche
VECTASHIELD	Vector laboratories
Xylene	Sigma

2.1.2 Buffers

Buffer	Formula
HEPES Buffered Saline (HBS), pH 7.4	KCl (5mM), NaCl (140mM), HEPES (10mM), D-glucose (5.5mM), Na2HPO4 (1mM), NaHCO3 (10mM), MgCl (0.5mM), CaCl (1mM) for 1 litre
Citrate Buffer, pH 6	Tri-sodium citrate 2.94 g in 1litre of H_2O (10mM)

2.1.3 RNA isolation, RT-PCR and PCR reagents

Name	Supplier
RNA later® Solution	Ambion life technologies
E.Z.N.A total RNA kit 1	OMEGA bio-tek
SuperScript® II Reverse Transcriptase	Invitrogen life technologies
RNasin® ribonuclease inhibitor	Promega
Oligo(dT) primer	Promega
PCR nucleotide mix	Promega
GoTaq® G2 polymerase	Promega
Low Molecular Weight DNA Ladder	New England Biolabs

2.1.4 Requirement of Bicarbonate in HBS buffer

Bicarbonate (HCO_3^-) is a crucial biochemical component of many physiological pH buffering systems. HCO_3^- is secreted into the gut lumen by diffusing into the mucus layers to aid in the neutralisation of acid generated by microbial fermentation (Allen, et al., 2005). A previous study has demonstrated the increase in diffusivity and hydration of mucus with the presence of extracellular (exogenous) HCO_3^- in airway cells (Chen, et al., 2010), suggesting HCO_3^- is required for decreasing the viscosity and increasing transportability of mucus. In cultured ex-vivo segments of mouse small intestine the presence or absence of HCO_3^- had no effect on the rate of basal mucus secretion. While HCO_3^- was shown to enhance mucus secretion when stimulated by secretagogues such as PGE2 or 5-hydroxytryptamine (5-HT), and the secretagogue-induced mucus secretion was reduced by half in the absence of HCO_3^- (Garcia, et al., 2009). These findings suggest the concurrent HCO_3^- secretion is a requirement for normal mucus secretion. In addition, inhibition or in the absence of HCO_3^- did not affect fluid secretion rates, suggesting the role of HCO_3^- in mucus secretion was independent of fluid secretion (Garcia, et al., 2009). In order to investigate the secretagogue (Cch)-induced mucus

secretion in the human colonic epithelium, HCO_3^- was included in the HBS buffer for all the experiments conducted in the current study.

2.2 Methods

2.2.1 Human colorectal tissue samples

This study is performed in accordance with the Norfolk and Norwich University Hospital UK and approval by the East of England National Research Ethics Committee (LREC 97/124). Human colorectal tissue biopsies were obtained with informed consent from patients undergoing recto-sigmoid endoscopy and from cancer patients undergoing colectomy (right hemi-colon or left hemi-colon or anterior resection). The histologically-normal mucosa samples were obtained at least 10cm away from tumour sites, and only used if there was no apparent intestinal pathology.

2.2.2 Micro-dissected native human colonic crypts

Biopsies and surgical tissue samples were fixed with 4% PFA for one hour and then washed with PBS. After micro-dissection, single micro-dissected crypts were embedded in Matrigel and post-fixed with 4% PFA before further immuno-staining procedures.

2.2.3 Vibratome sectioning of human colonic biopsies

Human colon biopsies or surgical samples were fixed immediately with 4% PFA for one hour. The samples were then washed with PBS 2-3 times. Fixed samples were cut into smaller pieces and embedded in 4% low melting temperature agarose gel, in a suitable orientation for sectioning. Tissues were sectioned with a Vibratome (Leica VT1000) to produce 70-100 µm thick sections, and were stored in PBS at 4˚C before further immuno-staining procedures.

2.2.4 Human colonic crypt isolation and culture

Human colonic crypts were isolated (as described in Reynolds et al., 2007 and Reynolds et al., 2014 supplementary methods), and provided by Dr. Alyson Parris in the Williams Laboratory. Briefly, tissues were washed with HBS and then transferred into Ca^{2+} and Mg^{2+} free HBS containing 1mM Dithiothreitol (DTT) and 1mM Diaminoethane-tetraacetic acid (EDTA) for one hour at room temperature. Crypts were then liberated through vigorous shaking; sedimented crypts were collected and mixed with Matrigel. A 20µl Matrigel suspension containing 50-100 crypts was seeded onto glass coverslips nested inside the wells

of a 12-well plate. After polymerisation of Matrigel at 37˚C for 15 min, isolated crypts were then flooded and cultured with 0.5ml of human colonic crypt culture medium (hCCCM, advanced F12/DMEM culture medium containing penicillin/streptomycin [100U/ml], L-glutamine [2mM], B27, N2, N-acetylcysteine [1mM], Hepes [10mM], A83-01 [0.5µM], human recombinant R-spondin-1 [500ng/ml], human recombinant Wnt 3A [100ng/ml], human recombinant Noggin [100ng/ml] or Gremlin-1 [200ng/ml], and human recombinant IGF-1 [50ng/ml]) at 37˚C with 5% CO_2 overnight prior to experimentation (Parris and Williams, 2015).

2.2.5 Single colonic epithelial cell isolation and culture

The isolated crypts were collected by centrifugation for 800rpm at 5 mins at 4˚C; and dissociated with TrypLE express in the presence of Y-27632 [10µM] and N-acetylcysteine [0.5mM] for 8 min at 37˚C with pipetting. After removal of cell clumps with a 20µm cell strainer, the dissociated colonic epithelial cells (including goblet cells) were then washed with culture medium and collected by centrifugation. 5000 epithelial cells were then re-suspended in 100µl of Matrigel, and a 20µl of Matrigel droplet was seeded onto glass coverslips contained within a 12-well plate. After polymerisation of Matrigel at 37˚C for 15 min, isolated single cells were then cultured with hCCCM as described above at 37˚C with 5% CO_2 overnight prior to experimentation.

2.2.6 Immunohistochemistry

Isolated human colonic crypts (Day1 - Day3 cultures) were used for live experiments. Crypts were washed once with PBS before fixation with 4% PFA for one hour on ice. The Vibratome sections, micro-dissected crypts or cultured crypts were then ready for immuno-staining procedures.

The samples were incubated with 1% SDS for 5 mins and then permeabilised with 0.5% Triton-X 100 for 30-35 minutes followed by a PBS wash. Non-specific binding was blocked with 10% donkey serum with 1% bovine serum albumin (BSA) for two hours. Depending on the protein of interest, the biopsy samples or cultured colonic crypts were incubated overnight with a combination of two to three primary antibodies (1:100 dilution) from different origin species at room temperature or 4˚C respectively (full list of antibodies as shown below in table 2.2.1). Samples were washed three times with PBS. Alexa fluor

conjugated donkey secondary antibodies (as listed in table 2.2.1) at half the concentration of the primary antibodies were used to detect the signals. Secondary antibodies were incubated for 2 to 5 hours at room temperature or 4˚C respectively. Non-specific labelling was determined by using primary antibody-negative controls. Samples were washed with PBS and mounted in VECTASHIELD containing Hoechst stain for labelling the cell nuclei. In conjunction with confocal microscopy (Zeiss LSM510-meta), the labelling can be visualised in thin optical sections (~ 1µm).

For live cell imaging of organelles, cultured colonic crypts were loaded at 37˚C for 2 hours with ER Tracker (5µM), Lyso Tracker (1µM) or Mito Tracker (0.5µM) diluted with serum-free DMEM. Samples were then washed twice with HBS and analysed by confocal microscopy.

2.2.6.1 Image analysis of immunohistochemistry

Fluorescent images were analysed by image analysis software including ImageJ (National Institutes of Health) and Volocity (Perkin Elmer). Fluorescence intensities of proteins of interest were measured by drawing regions of interest (ROI) on fluorescent images of colonic crypts. Values were background corrected. Mean readings were calculated for each treatment group and normalised to the mean intensity level of the control group as described in the equation below. Semi-quantitative analysis was presented using normalised mean ± standard error mean (SEM). For example, the MUC2 mucin content (as inferred from anti-MUC2 immunofluorescent intensities) in goblet cells was quantified by drawing a region of interest around the secretory vacuole of each goblet cell located at the base of colonic crypts using ImageJ. Mean MUC2 immunofluorescent intensities in goblet cells in each treatment group were calculated and normalised to the control group, as described above and presented as mean ± SEM.

$$\text{Normalized fluorescence intensity} = \frac{\text{Mean intensity value (treatment group)}}{\text{Mean intensity value (control group)}}$$

Table 2.2.1 Antibodies and Organelle Stains

Primary Antibody name	Species origin	Clonality	Working concentration	Supplier
anti-MUC2	Rabbit	Polyclonal	1:100	Santa Cruz
anti-MUC2	Mouse	Monoclonal	1:100	Abcam
anti-KDEL	Mouse	Monoclonal	1:100	Santa Cruz
anti-LAMP-1	Rabbit	Polyclonal	1:100	Abcam
anti-TPC1	Rabbit	Polyclonal	1:100	Abcam
anti-TPC2	Rabbit	Polyclonal	1:100	Abcam
anti-LC3	Mouse	Monoclonal	1:100	MBL
anti-LAMP-1 ascities/ concentrate	Mouse	Monoclonal	1:100	DSHB
anti-E-Cadherin	Goat	Polyclonal	1:100	R&D systems
anti-E-Cadherin	Mouse		1:100	BD Bioscience
anti-M1 muscarinic receptor (M1AchR)	Rabbit	Polyclonal	1:100	Research & Diagnostic Abs
anti-M3 muscarinic receptor (M3AchR)	Rabbit	Polyclonal	1:100	Research & Diagnostic Abs
anti-M5 muscarinic receptor (M5AchR)	Rabbit	Polyclonal	1:100	Research & Diagnostic Abs
anti-Choline acetyltransferase (CHAT)	Goat	Polyclonal	1:100	Millipore
anti-Ki67	Mouse	Monoclonal	1:100	DAKO
anti-beta tubulin III (Tuj-1)	Mouse	Monoclonal	1:100	Neuromics
anti-Tubulin, beta III isoform (TU-20)	Mouse	Monoclonal	1:100	Millipore
anti-Neurofilament	Mouse	Monoclonal	1:100	Abcam
anti-200kD Neurofilament Heavy	Mouse	Monoclonal	1:100	Abcam
anti-Neurofilament Light (NF-L)	Rabbit	Polyclonal	1:100	Millipore
anti-VesicularAcetylcholine Transporter (VAChT)	Rabbit	Polyclonal	1:100	Abcam
anti-CD38	Rabbit	Monoclonal	1:100	Abcam
anti-CD38	Mouse	Monoclonal	1:100	Abcam
anti-IP3R1	Rabbit	Polyclonal	1:100	Novus Biologicals
anti-IP3R2	Goat	Polyclonal	1:100	Santa Cruz

anti-IP3R3	Rabbit	Polyclonal	1:100	Novus Biologicals
anti-Ryanodine receptor (RYR)	Rabbit	Polyclonal	1:100	Abcam
anti-SERCA 1/2/3	Rabbit	Polyclonal	1:100	Santa Cruz
anti-DCAMKL-1	Rabbit	Polyclonal	1:100	Abcam
anti-OLFM4	Rabbit	Polyclonal	1:100	Abcam
anti-OLFM4	Rabbit	Polyclonal	1:100	LifeSpan BioSciences
anti-Lgr5	Mouse	Monoclonal	1:100	Origene
anti-Chromogranin A (CGA)	Rabbit	Polyclonal	1:100	Abcam
anti-Chromogranin A (CGA)	Mouse	Monoclonal	1:100	Abcam
anti-C-kit	Rabbit	Polyclonal	1:100	Abcam
anti-COX-1	Goat	Polyclonal	1:100	Santa Cruz
Secondary Antibody name	**Species origin**		**Working concentration**	**Supplier**
anti-goat Alexa Fluor 488	Donkey		1:200	Invitrogen
anti-goat Alexa Fluor 568	Donkey		1:200	Invitrogen
anti-rabbit Alexa Fluor 488	Donkey		1:200	Invitrogen
anti-rabbit Alexa Fluor 647	Donkey		1:200	Invitrogen
anti-mouse Alexa Fluor 488	Donkey		1:200	Invitrogen
anti-mouse Alexa Fluor 647	Donkey		1:200	Invitrogen
Other stains			**Working concentration**	**Supplier**
Rhodamine red- Wheat germ agglutinin (WGA)	Lectin		1:200	Vector Laboratories
Mito Tracker® (Organelle Stain)			0.5µM	Invitrogen
ER-Tracker™ (Organelle Stain)			5µM	Invitrogen
Lyso Tracker® (Organelle Stain)			1µM	Invitrogen

2.2.7 Gene expression analysis of muscarinic receptors and intracellular calcium channels in the human colonic mucosa

2.2.7.1 Isolation of total RNA and generation of cDNA

Human colon biopsies or freshly isolated colonic crypts were pelleted and placed in RNAlater®. Total RNA was isolated using the Omega Bio-tek Easy nucleic acid isolation kit according to the manufacturer's instructions. The concentration and purity of the total RNA was then measured by the NanoDrop Spectrophotometer. Purity of RNA samples with A260/A280 ratio between 2-2.2 was deemed acceptable for further experiments. RNA was then stored at minus 80˚C prior to use. First strand cDNA was prepared from 1 µg of total RNA using oligo-dT primers and Superscript II RT according to the manufacturer's instructions.

2.2.7.2 Conventional PCR

The presence of expression of the cholinergic neuronal markers (CHAT and VAChT), muscarinic acetylcholine receptor subtypes (M1-M5AchRs), intracellular Ca^{2+} channels (IP3Rs, RYRs and TPCs) and Ca^{2+} ATPase pump (SERCA) were assessed using reverse transcription PCR (RT- PCR). Gene-specific primers were designed to span intron-exon boundaries to avoid amplification from potential contaminating genomic DNA; primer sequences are listed below in table 2.2.2. Two µl of cDNA from RT reactions (as described above) was amplified using a G-Storm thermocycler. The conditions for amplification were as follows: initial denaturation for 5 mins at 95˚C followed by 40 cycles of; denaturation for 1 min at 95˚C; annealing for 50 sec using a touchdown PCR protocol (normally ranged from 55˚C to 65˚C, depending on the specific primer pairs), and extension for 1 min at 72˚C, followed by a final extension for 10 min at 72˚C. The PCR products were electrophoresed in 2.5% agarose gel and post stained with ethidium bromide, and then reviewed under UV-light with gel documentation system (UVP).

Table 2.2.2 Conventional PCR primers

Gene name	NCBI Reference	Primer L sequence	Primer R sequence	Product size (bp)
CHAT	NM_020985.3	GGACAACATCAGATCGGCCAC	GAACATCTCCGTGGTTGTGGG	300
Nested CHAT	NM_020985.3	TTTGTGAGAGCCGTGACTGA	ATCCATGAACATCTCGGGCA	195
SLC18A3 (VAChT)	NM_003055.2	CTGTAACATTCCCCTCGCCTTC	GCTGTGTCGACTAGGGCTATGC	299
Nested VAChT	NM_003055.2	TGGATGAAGCATACGATGGC	GAGGCCGCATAGTGAGACC	228
CHRM1	NM_000738.2	CAAGTGGCCTTCATTGGGATCAC	GCATTGCTGGCCACATAGTCC	260
CHRM2	NM_000739.2	GAGCTCCAATGACTCCACCTCAG	GGGAAGGAGGAGGCTTCTTTTTTG	298
CHRM3	NM_000740.2	CAACCTCGCCTTTGTTTCCAAAC	CCAGGATGTTGCCGATGATGG	242
CHRM4	NM_000741.3	GGCAGTTTGTGGTGGGTAAG	CGCTCTGCTTCATTAGTGGGC	248
CHRM5	NM_012125.3	GTCTGGCTTGTGACCTTTGGC	GGTGGGCTCAGAGAGAAACTG	278
ITPR1 (IP3R1)	NM_001099952.2	TGTCGGAATTAAAGGATCAGATGAC	CTGGTTGTTGTGGGTTGACATTC	102
ITPR2 (IP3R2)	NM_002223.3	GGAGCTCAAGGAGCAGATGAC	CAGGCAGGACACTGATGAAAG	150
ITPR3 (IP3R3)	NM_002224.3	AGCTCAAGGAGCAGATGACG	AGTGATGAGCATCCCCTGTTG	123
RYR1	NM_000540.2	AGAACACACGGGTCAGGAGTC	AGGGGCTTGCTGTGAGAATAAG	172
RYR2	NM_001035.2	CAGAACACACAGGACAGGAATC	GGGTTTTGGTTTTTAGAGGTGA	147
RYR3	NM_001036.4	CTGGCCATCATTCAAGGTCT	ACCCGTGTGCTCTGTTTCAT	231
ATP2A1 (SERCA1)	NM_004320.4	GGACAACACCCACTTTGAGG	GAGGATGAGGAAGTGCAGGG	211
ATP2A2 (SERCA2)	NM_001681.3	GACAATGGCGCTCTCTGTTC	CATGAGAATCACGGGCAAGG	250
ATP2A3 (SERCA3)	NM_005173.3	GAAATGTGCAATGCCCTCAACAG	GCAGGATGACAGGCAGAGATATC	214
TPCN1	NM_001143819.2	GCATCACCCTTGAGAAGGAAATC	GGCATGCTCCTCATACCACTC	233
TPCN2	NM_139075.3	GGCCAACAACTTCGATGACTTTG	TTGACCCAGATGACAGACGAC	165
GAPDH	NM_002046.5	GTCAGTGGTGGACCTGACCTG	TGCTGTAGCCAAATTCGTTG	245

2.2.8 Intracellular calcium imaging in human colonic crypt

Isolated human colonic crypts (Day 1 to Day 3 cultures) were loaded with Fura-2/AM (5 µM) for 2 hours at room temperature in the dark to monitor cytoplasmic Ca^{2+} levels. Crypts were washed twice with HBS and incubated with HBS for at least a further 30 minutes to allow de-esterification of the dye. The loaded samples were then transferred into a chamber located on the stage of an inverted fluorescent microscope (with X40 or X20 objectives) while maintained in HBS (200µl). Experimental agonists and antagonists (full list in Table 2.2.3 below) were diluted with HBS. The experimental solutions (agonist and/or antagonist) were administered by replacing the HBS buffer solution. Fura-2 in the loaded crypt was excited alternatively at 340 nm and 380 nm and the fluorescence at 510 nm was detected by a cooled CCD camera (Quantum, Roper Scientific, UK). The background-corrected F340/F380 ratios were calculated and monitored in real time. Fluorescent data were presented as pseudo-colour images (Figure 2.1) or traces (Figure 2.2). At the beginning of each experiment, regions of interest (ROI) were drawn along the crypt axis and the average ratio values (F340nm/ F380nm) of those regions were plotted with respect to time (Figure 2.1).

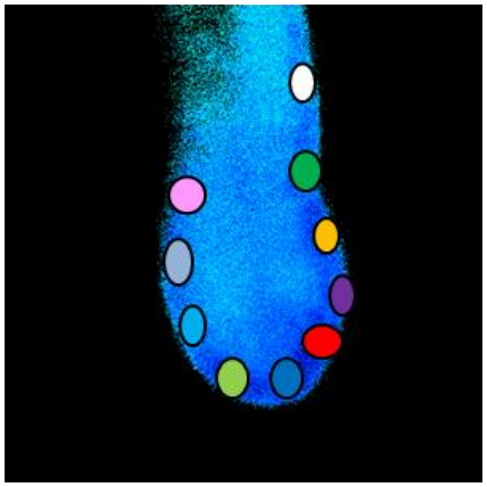

Figure 2.1 Fluorescence image of a Fura-2 loaded crypt.

Regions of interest (ROI) represented by circles as shown were drawn along the axis of the crypt. Each region is represented by a different colour in order to distinguish the signals from different regions.

2.2.8.1 Calcium imaging analysis

Since Ca^{2+} signals were reproducible in response to repeated applications of 10 µM Cch, a control Cch response was included in each antagonist experiment to which the experimental conditions can be compared. Measurement of the amplitude of the Ca^{2+} response is described in figure 2.2 below.

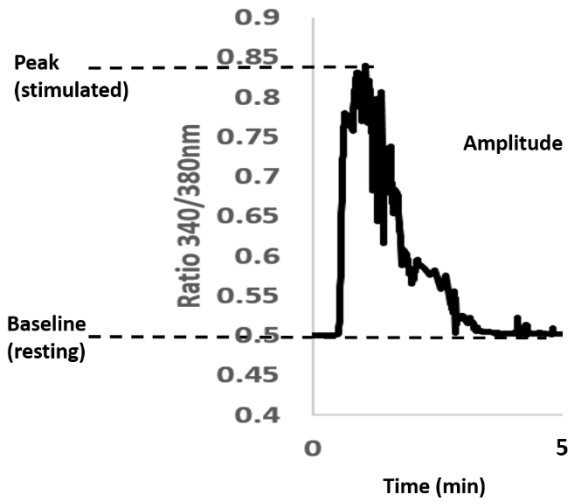

Figure 2.2 Changes of Fura-2 ratio with respect to time in response to Cch stimulation in ROI 1.

Human colonic crypts were loaded with Fura-2 AM to monitor intracellular Ca^{2+}. An increase in Fura-2 ratio represents an increase in cytosolic Ca^{2+} levels upon Cch stimulation. After background subtraction, the amplitude of the response was calculated by subtracting the baseline ratio from the peak ratio.

Table 2.2.3 Chemicals (agonist and antagonist) for live intracellular calcium experiments

Name	Function	Working concentration	Incubation time	Supplier
Carbachol (Cch)	Agonist	10 μM, 100 μM	1-2 min	Sigma
Methacholine	Agonist	10 μM	1-2 min	Sigma
U73122	Antagonist	10 μM	1 hr	Sigma
R59-022 (DAG kinase inhibitor)	Antagonist	10 μM	1 hr	TOCRIS
Sotrastaurin (PKC inhibitor)	Antagonist	20 μM	1 hr	AdooQ Bioscience
2AP-B	Antagonist	50 μM	1 hr	Sigma
Xestospongin C (XesC)	Antagonist	2 μM	1 hr	Calbiochem /TOCRIS
Ryanodine	Antagonist	50 μM	1 hr	TOCRIS
8 Bromo cADP ribose	Antagonist	30 μM	1 hr	Sigma
Thapsigargin (Tg)	Antagonist	1 μM	50 min	TOCRIS
Nicotinamide	Antagonist	20 mM	1-2 hrs	Sigma
Trans-Ned19	Antagonist	200 μM	1 hr	TOCRIS
Glycyl-L-phenylalanine-beta-naphthylamide (GPN)	Antagonist	200 μM	45 min	Sigma
Diltiazem (DZM)	Antagonist	300 μM	1 hr	TOCRIS
Bafilomycin (Baf)	Antagonist	2.5 μM	1 hr	TOCRIS
Chloroquine (CHQ)	Antagonist	100 μM	1 hr	Sigma
Methyl-beta-cyclodextrin (MβC)	Antagonist	10 mM	1 hr	Sigma
Hydroxy Dynasore	Antagonist	100 μM	1 hr	Sigma
BAPTA-AM	Antagonist	66 μM	1 hr	Sigma
Diphenyleneiodonium (DPI)	Antagonist	1 μM, 2.5 μM, 5 μM	1 hr	Sigma
VAS2870	Antagonist	56 μM	1 hr	Sigma
NSC 23766 (RAC inhibitor)	Antagonist	250 μM	1 hr	TOCRIS
Apocynin	Antagonist	100 μM	1 hr	TOCRIS

2.2.9 Intracellular ROS and calcium imaging in human colonic crypts

Similar to Fura-2 experiments, isolated human colonic crypts (Day 1 to Day 3 cultures) were loaded with both ROSstar 550 (100 µM, Invitrogen) and Fluo-4/AM (5 µM, Invitrogen) in HBS for 1.5-2 hours at room temperature in the dark to monitor cytoplasmic reactive oxygen species (ROS) and Ca^{2+} respectively. The crypts were then washed twice with HBS. Agonist (10 µM Cch or 10 µM methacholine) was administered by replacing the HBS buffer solution, and then changes in intracellular levels of ROS and calcium were monitored in real time by confocal microscopy.

2.2.10 Statistical analysis

Data were expressed as mean ± SEM. N = total number of subjects (i.e. patients), n = number of crypts derived from those 'N' subjects, and ng = number of goblet cells in each treatment group (that were analysed in 'n' crypts via analysis of the microscopy data). Differences between two groups were determined by paired or unpaired t-tests, while comparisons between more than two groups were determined by one-way ANOVA, followed by Bonferroni procedures and Tukey's post hoc analysis. For each test a P value of less than 0.05 was considered to be statistically significant.

Chapter 3 Results: Characterisation of the cellular and molecular machinery of excitation-mucus secretion coupling in human colonic crypts

3.1 Introduction

Activation of MAchRs by the neurotransmitter Ach has been shown previously to mobilise intracellular Ca^{2+} in the intestinal epithelium (Satoh, et al., 1995; Lindqvist, et al., 1998; Klaren, et al., 2001; Lindqvist, et al., 2002; Hirota & McKay, 2006; Reynolds, et al., 2007). Ach is thought to be primarily secreted by the cholinergic neurons of the enteric nervous system. However, evidence for cholinergic innervation in the human colonic epithelium remains limited. In recent years, some groups have initiated studies into the presence of the non-neuronal Ach system of the colonic epithelium. Findings by Yajima et al (2011) and Bader et al (2014) demonstrated that the fatty acid propionate stimulates non-neuronal Ach release which promoted chloride secretion in the rat colon. These observations fully support a model in which synthesis and release of Ach occurs in the colon without cholinergic innervation, and provides valuable insights into the regulation of gut physiology by neuronal and non-neuronal Ach.

A major function of the colon is to absorb water and to secrete fluid and mucus. Cholinergic signalling has been shown extensively to regulate electrolyte secretion in the colon (Zimmerman, et al., 1982; Javed, et al., 1992; O'Malley, et al., 1995; Cliff, et al., 1998; Banks, et al., 2004; Hassan, et al., 2012). Most of these studies were performed in animal models or on human colon cancer cell lines such as HT-29 and T-84. However, the polarity and topology of the intact colonic epithelium is compromised in these human cell lines, which may affect cellular signals generation with respect to the tissues from which these lines derive. A 3-D human colonic crypt culture model has therefore been developed in our lab where many features of colonic crypt morphology and function are maintained. These cultured crypts are proliferative, polarised, intact, and exhibit agonist-stimulated secretion coupling in culture.

Our lab has repeatedly demonstrated that cholinergic stimulation of M3AchR mobilises intracellular Ca^{2+} in this native human colonic crypt culture model (Lindqvist, et al., 2002; Reynolds, et al., 2007). However, the underlying mechanism of Ca^{2+} signal generation and role in coupling mucus secretion in the human colonic epithelium is unknown. Limited information is currently available regarding the cellular localisation of functional intracellular Ca^{2+} stores and the respective expression of the Ca^{2+} release channels in the human colonic

epithelium, and specifically in mucus secreting goblet cells. The present study investigated the expression patterns and localisation of cholinergic enteric neurons, and the potential for a non-neuronal Ach system in the human colonic epithelium. In addition, the colonic MAchR subtype expression and localisation has been confirmed. This initial series of experiments also aimed to characterise the Ca^{2+} signalling toolkit in our model, with a focus on goblet cells, in order to form the basis for further investigation of the cholinergic regulation of Ca^{2+} coupling mucus secretion.

Results

3.1.1 Neuronal-epithelial cell interactions

The colonic epithelium is under the control of the ENS. The neurons that extend from the submucosal plexus into the mucosa can be both cholinergic and non-cholinergic. In order to describe the spatial relationship of the enteric neurons and the colonic epithelium, human colon biopsies were fixed and sectioned with a vibratome. Mucosal sections were then stained with various neuronal markers including β-III Tubulin (TU-20 or TUJ 1), neurofilament light and heavy chain antibodies to visualise the localisation of enteric neurons. 10X magnification of the colonic mucosa revealed the presence of neurons surrounding the colonic crypts from the base to the surface epithelium (lumen-facing). The neurons were also detected in the muscularis mucosae and the submucosa (Figures 3.1). The neuronal network (branches) seem relatively dense in the sub-epithelial domain. Higher magnification, at 40X, not only revealed the close proximity of the enteric neurons with the crypts, it also demonstrated that nerve endings (axonal projections) touch and clasp the membrane of the crypt colonocytes (Figure 3.2A). Some of these interactions look invasive, in that they penetrate into the crypt. Images of the crypt equatorial layer further revealed and confirmed the penetration of some nerve endings into the single epithelial cell layer (Figure 3.2B). These nerve endings extended towards the apical membrane of the crypt cells which suggests that there is some site of interaction on the apical pole of colonic epithelial cells.

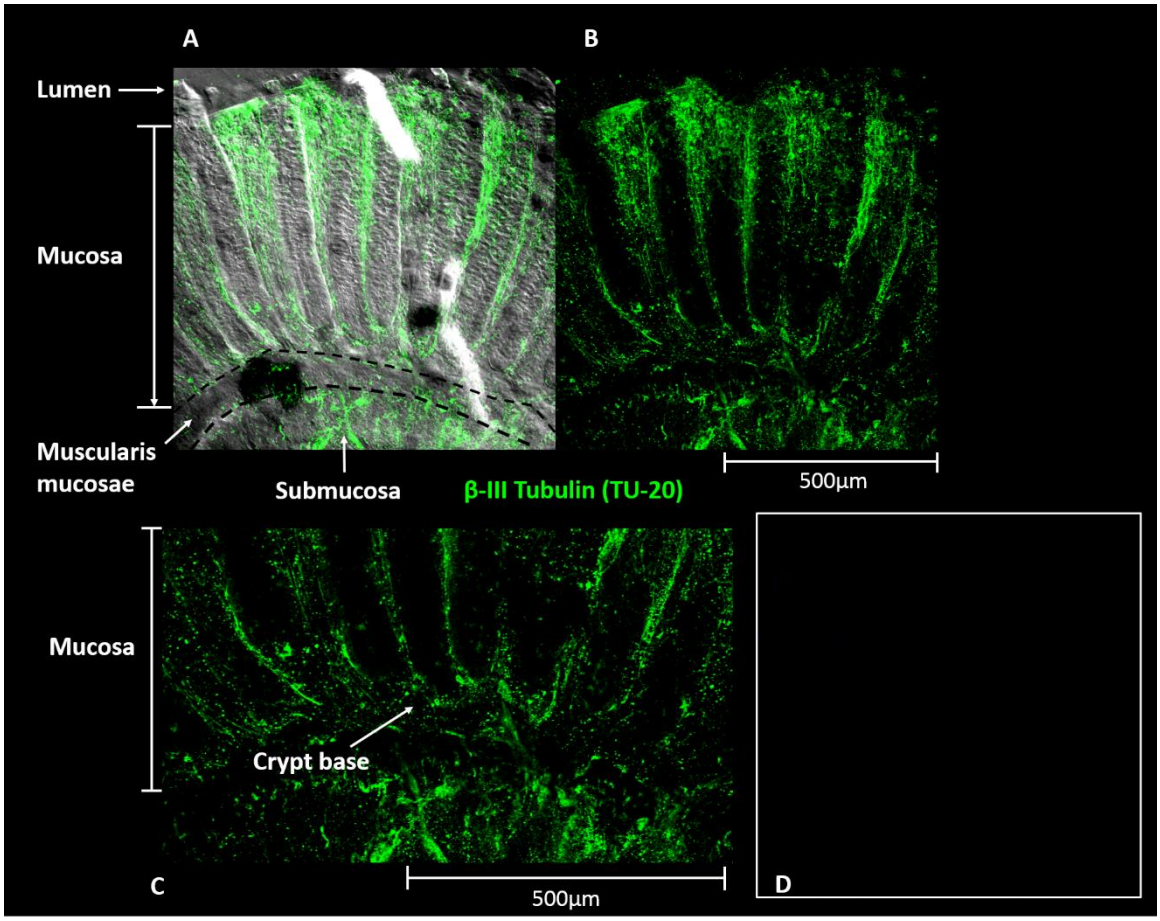

Figure 3.1 Enteric neuronal network in the colonic epithelium

Vibratome sections of human colon tissue biopsies were fixed and stained with anti-β-III tubulin (TU-20) antibody, and visualised with Alexa 488 conjugated secondary antibody. Images were taken with a Zeiss LSM 510 Meta confocal microscope using a x10 objective. (A) Overlay DIC image of the colonic mucosa and the supporting layers (muscularis mucosae and submucosa) and β-III tubulin (green); (B) β-III tubulin only (green) labelled colonic mucosa; (C) Enlarged image of (B); (D) No primary antibody (negative) control. Images are representative of N=2 subjects, n=4 sections derived from 2 subjects.

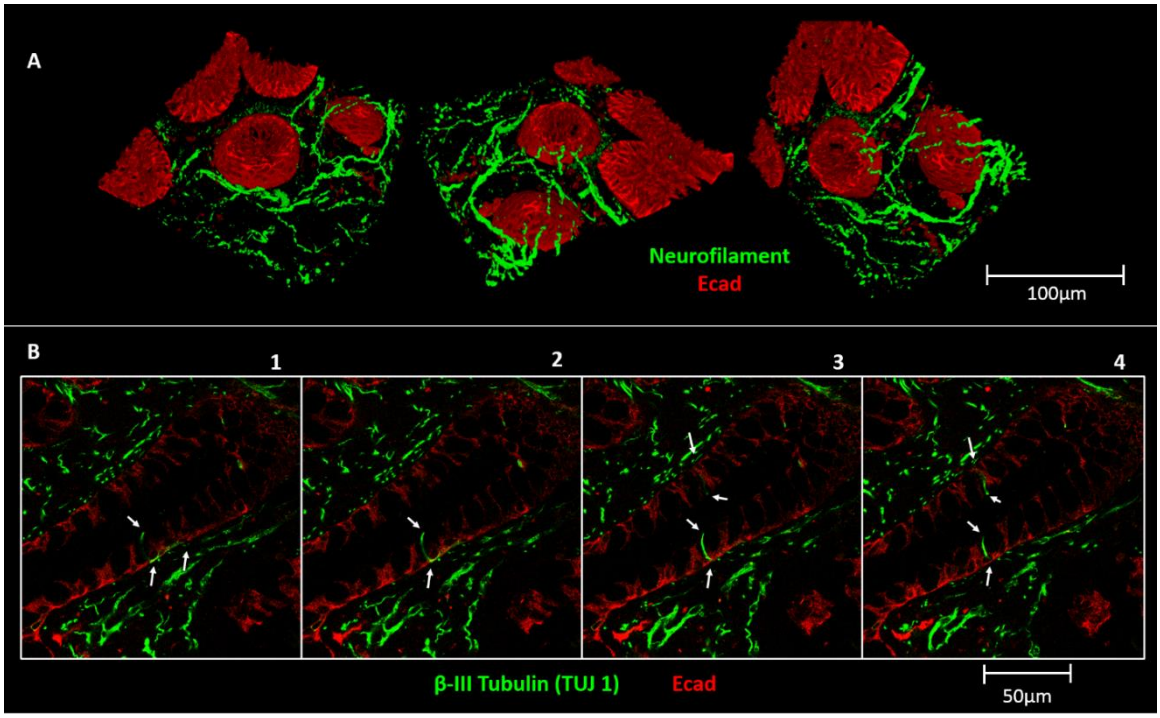

Figure 3.2 Interaction of enteric neurons with the colonic epithelium

Sections of human colonic mucosa fixed and stained with anti-neurofilament (green) and anti-Ecad (red) antibodies; or with anti-β-III tubulin (green) and anti-Ecad (red) antibodies. Optical sections (1µm thick) of the colonic mucosa were taken with a Zeiss LSM 510 Meta confocal microscope for 20-30µm with a x40 objective to generate the 3D z-stack images. (A) 3D reconstruction of the z-stack confocal images using the Volocity software (Perkin Elmer). Reconstructed image can be rotated through any axis to give a spatial appreciation of the neuronal-crypt morphology and interactions. (B) Consecutive z-stack images of the colonic mucosa to give an appreciation of the sequence of events from left to right. The nerve endings of the enteric neurons not only touch and clasp the surface of the crypt (A middle and right), but also penetrate into the epithelial cells (B white arrows). Images are representative of N=8 subjects, n≥40 sections derived from 8 subjects.

3.1.1.1 Cholinergic innervation of the human colonic epithelium

A substantial amount of work has demonstrated that the activation of MAchR by Ach – primarily secreted by the cholinergic enteric neurons – mobilises intracellular Ca^{2+} waves in the intestinal epithelium (Lindqvist, et al., 1998; Klaren, et al., 2001; Lindqvist, et al., 2002; Hirota & McKay, 2006; Reynolds, et al., 2007). Cholinergic neurons, a potential source of Ach, were specifically identified by the expression of CHAT and VAChT (see section 1.1.5.1). By using reverse transcription-PCR (RT-PCR), CHAT mRNA expression was demonstrated in both human colon biopsies and isolated colonic crypts (Figure 3.3), however, the expression level was relatively low (i.e. faint bands) with variations between individuals in both samples tested. By contrast, VAChT mRNA expression was undetectable during the initial RT-PCR reaction. By using nested PCR, a successive round of PCR amplification using another set of primers, the expression of both CHAT and VAChT mRNA was detectable in both set of samples. The expression and localisation of the cholinergic neurons were confirmed by labelling the mucosal sections with CHAT or VAChT antibodies in conjunction with other neuronal markers. CHAT positive or VAChT positive neurons are mainly located at the base of crypts, in the muscularis mucosae and submucosa (Figure 3.4 and Figure 3.11). X40 magnification reveals the close proximity of these cholinergic neurons with the colonic crypts, which provides a very short distance for Ach diffusion after release from nerve endings.

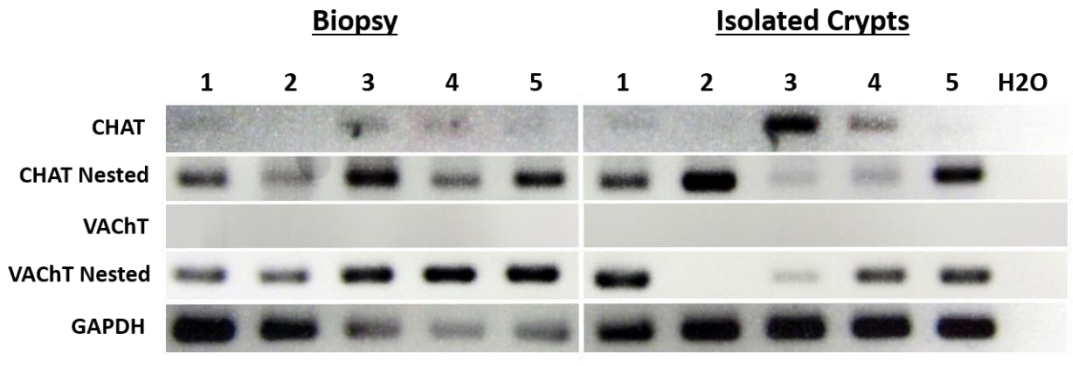

Figure 3.3 Cholinergic neuronal marker mRNA expression in human colon biopsies and isolated crypts.

Agarose gel electrophoresis showing RT-PCR products for CHAT and VAChT genes from human colon biopsies and isolated crypts, using specific primers designed to anneal across exon-exon boundaries to avoid amplification from potentially contaminating genomic DNA. Minimal or no expression was observed during first round PCR amplification of CHAT and VAChT respectively. PCR products from first round were further amplified for 40 cycles with the second set of primers for both genes (Nested). GAPDH is used as a positive control. No PCR product was detected in the no template (H_2O) control lanes. The above gels display mRNA expression of CHAT and VAChT from five random intact human colon biopsies and their corresponding isolated crypt samples.

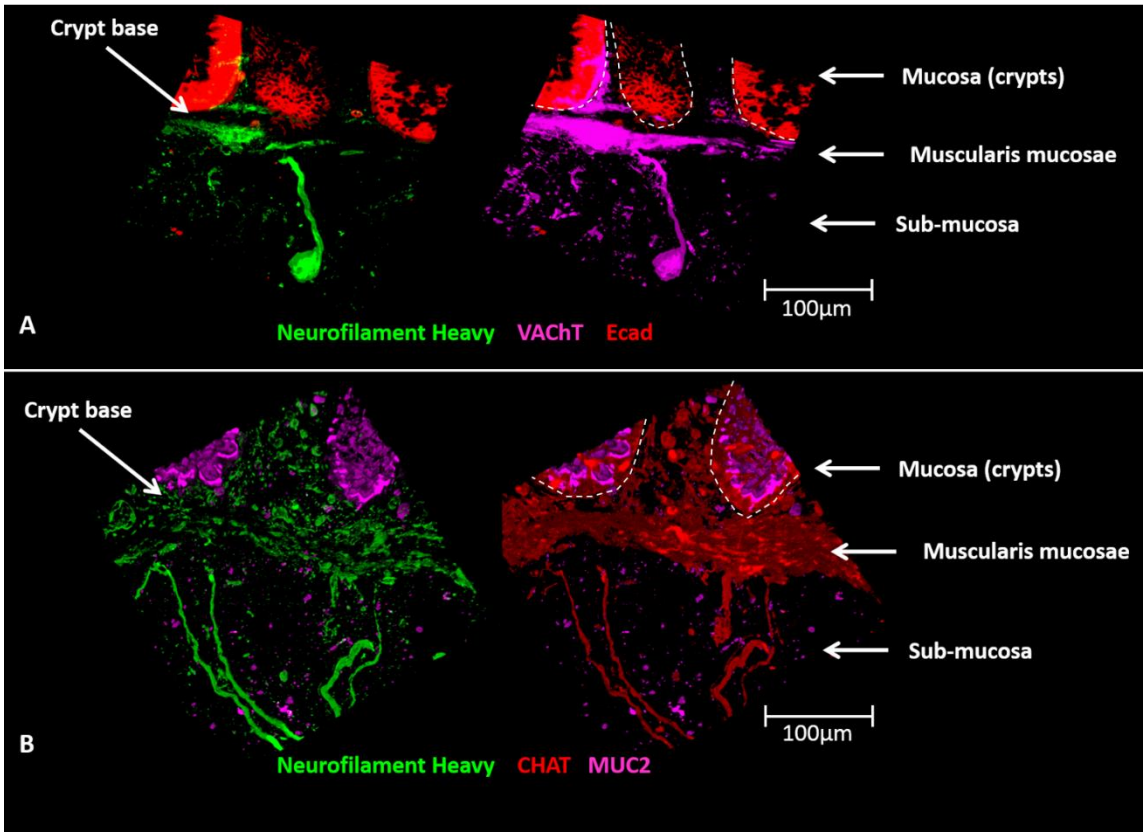

Figure 3.4 Immunolocalisation of neurofilament heavy, VAChT and CHAT in the human colonic epithelium.

Vibratome sections of human colon biopsy samples were fixed and stained with anti-200kD neurofilament heavy (green), anti-VAChT (pink) and anti-Ecad (red) antibodies (top panel); or with anti-200kD neurofilament heavy (green), anti-CHAT (red) and anti-MUC2 (pink) antibodies (bottom panel). Both Ecad and MUC2 were used to identify the location of the crypts. Images were taken simultaneously using the 488nm laser (green), the 568nm laser (red) and the 647nm laser designated pink that revealed overlapping signals of the cholinergic neuronal markers CHAT or VAChT with the general neuronal marker neurofilament heavy in the human colon. Both top and bottom panels show the inner layers of the gut wall including the bottom of the crypt (mucosa), the muscularis mucosae and the submucosa. White dotted lines mark the boundary of the crypts embedded in the lamina propria. Images were taken with a confocal microscope with a x40 objective. Images are representative of N=8 subjects, n≥40 sections derived from 8 subjects.

3.1.2 Potential non-neuronal Ach system in the human colon

The paradigm of Ach acting solely as a neurotransmitter has been revised after a substantial number of studies demonstrated the production of Ach in non-neuronal cholinergic systems, including the intestinal epithelium (Keely, 2011). CHAT is the enzyme responsible for Ach synthesis. As mentioned in the previous section, CHAT mRNA expression was detectable in isolated human colonic crypts that were absent of any neurons (Figure 3.3 right panel). The most striking observation was the presence of CHAT positive cells in both human colon biopsies and micro-dissected crypts (Figure 3.5). Immunohistochemical labelling also revealed that expression of CHAT protein on the basal membrane of the crypt, which co-localised with M3AchR under resting conditions (Figure 3.5B (iii). A previous study by Jönsson et al demonstrated the positive labelling of CHAT proteins in the human colonic epithelium: however they did not show the existence of these CHAT positive cells along the crypt-axis (Jönsson, et al., 2007). In the current study, these cells expressing CHAT were predominantly found among those between the base and the mid region of the crypt, where the proliferative immature cells reside. CHAT positive cells were also detectable between the mid to top region of the crypt but they were less numerous (Figure 3.5A).

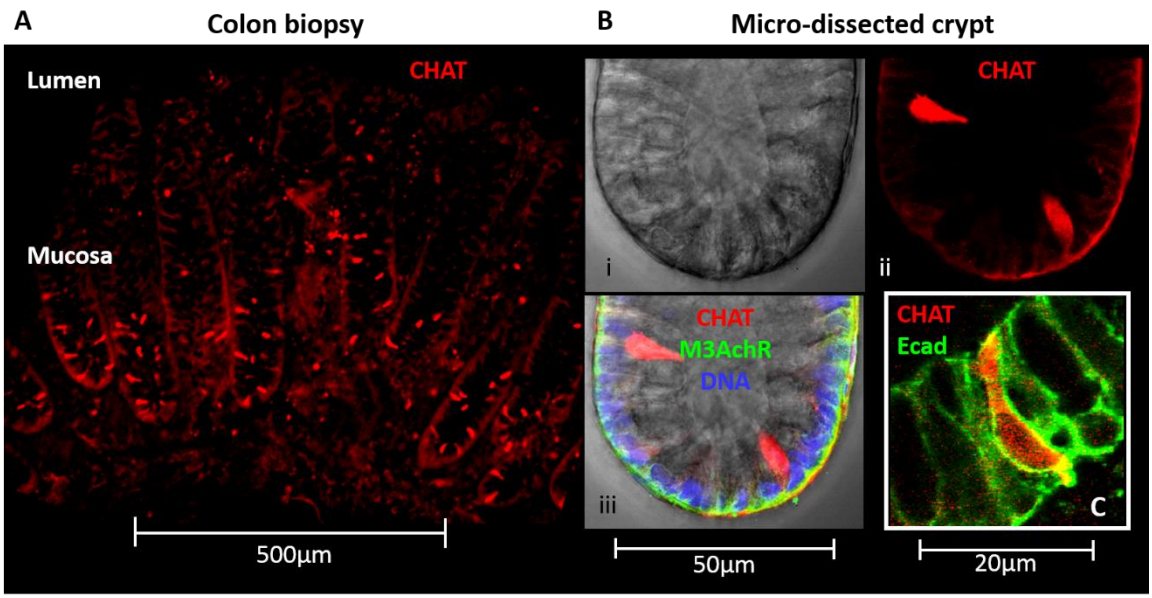

Figure 3.5 A non-neuronal Ach system in the human colonic epithelium

Sections of human colon biopsy were stained with anti-CHAT (red) antibody (A). Image was taken with a confocal microscope with a x10 objective. Microdissected crypts were labelled with anti-CHAT (red) and anti-M3AchR (green) antibodies, cell nuclei were stained with Hoechst (blue) B (iii). DIC image of a microdissected crypt base (B (i)); CHAT labelling (red) (B (ii)); A merged image of CHAT (red), M3AchR (green) and Hoechst (blue) (B (iii)). Images were taken with a x63 objective and were representative of N≥5 subjects, n≥25 crypts. Microdissected crypts were also labelled with anti-CHAT (red) and anti-Ecad (green) antibodies (C). The 2X zoom-in image was taken with a x63 objective (white box).

These CHAT positive cells represent a currently unknown cell type of epithelial origin expressed in the intact colonic epithelium, as confirmed by the Ecad labelling (Figure 3.5C). VAChT is a neurotransmitter transporter that is responsible for loading Ach into secretory vesicles for secretion. VAChT is predominantly expressed at the cholinergic nerve endings (Gilmor, et al., 1996; Parsons, 2000). VAChT positive labelling in the human colonic epithelium and in lamina propria cells was first demonstrated by Jönsson and colleagues, albeit only at the very top region of the crypt (Jönsson, et al., 2007). In addition to the previous observation that VAChT positive neurons were found near the base of the crypts in the muscularis mucosae and the submucosa (Figure 3.4A), they were also detected in the nerve fibers embedded in the lamina propria between the crypts (Figure 3.6A white arrows). Most importantly, VAChT positive signals were also detected in the human colonic epithelium (Figure 3.6A). In summary, CHAT, VAChT and M3AchR proteins are expressed in human colonic crypts, which suggests the existence of epithelial self-regulation by Ach in the absence of neuronal innervation.

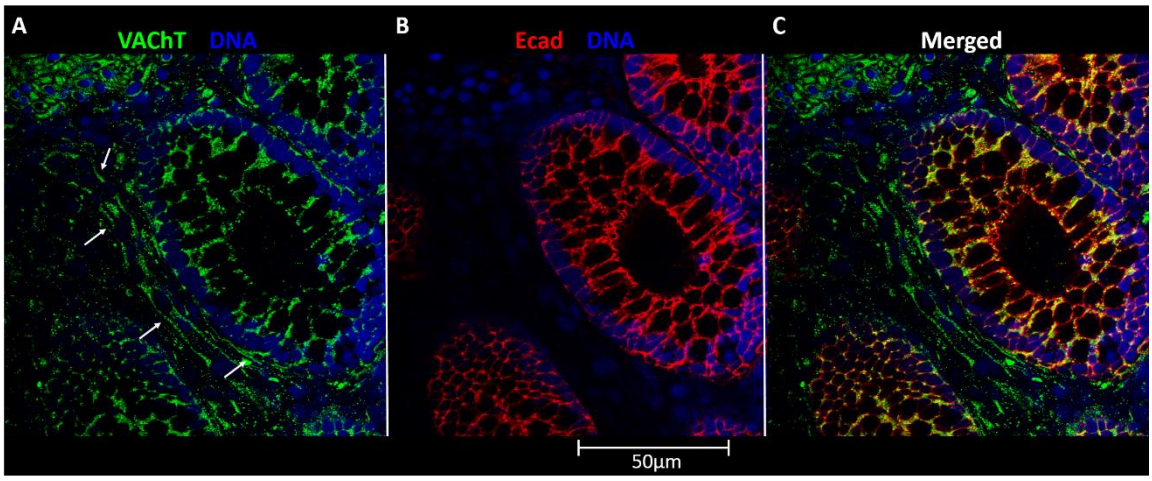

Figure 3.6 VAChT expression in the human colonic mucosa

Vibratome sections of the human colonic epithelium stained with anti-VAChT and anti-Ecad antibodies; cell nuclei were labelled with Hoechst. Images were taken with a confocal microscope with a x40 objective. (A) VAChT (green), cell nuclei (blue); (B) Ecad (red), cell nuclei (blue); and (C) a composite image of all three channels. Images are representative of N≥5 subjects, n≥25 sections derived from 5 subjects.

Attempts were made to identify the CHAT positive colonic epithelial cell type. Others have shown CHAT labelling in enteroendocrine cells (Jönsson, et al., 2007), however these images were in black and white and the data did not show double labelling with CHAT and the enteroendocrine cell marker, which generates equivocal conclusion. In this study, human colonic crypts were co-labelled with chromogranin A, an enteroendocrine cell marker, as well as CHAT. Immuno-reactivity of CHAT was observed in chromogranin A positive enteroendorcine cells, however there are also some cells that only exhibited CHAT labelling (Figure 3.7). In addition, the morphology of these CHAT single positive cells was different from the enteroendocrine cells expressing CHAT in that these cells are relatively long in shape, with the cytoplasm extended to the apical membrane of the crypt (Figure 3.7A and C). Conversely, the enteroendocrine cells exhibit a dense triangular basal domain and a very thin tail towards the apical pole of crypt (Figure 3.7B and D). Tuft cells are a newly identified epithelial cell type with unknown function (Gerbe, et al., 2012). Since tuft cells have a longer cell morphology, the CHAT positive cells were further investigated by staining with the tuft cell marker DCAMKL-1 which labels microtubules (Figure 3.8A). Positive labelling of DCAMKL-1 was detected in some CHAT positive cells (Figure 3.8B), but the staining pattern was different from that previously reported (Gerbe, et al., 2012; Westphalen, et al., 2014). There were also some CHAT positive cells that lacked DCAMKL-1 expression (Figure 3.8C). Thus, these results are inconclusive and further experiments are required to confirm the nature of these CHAT positive cells.

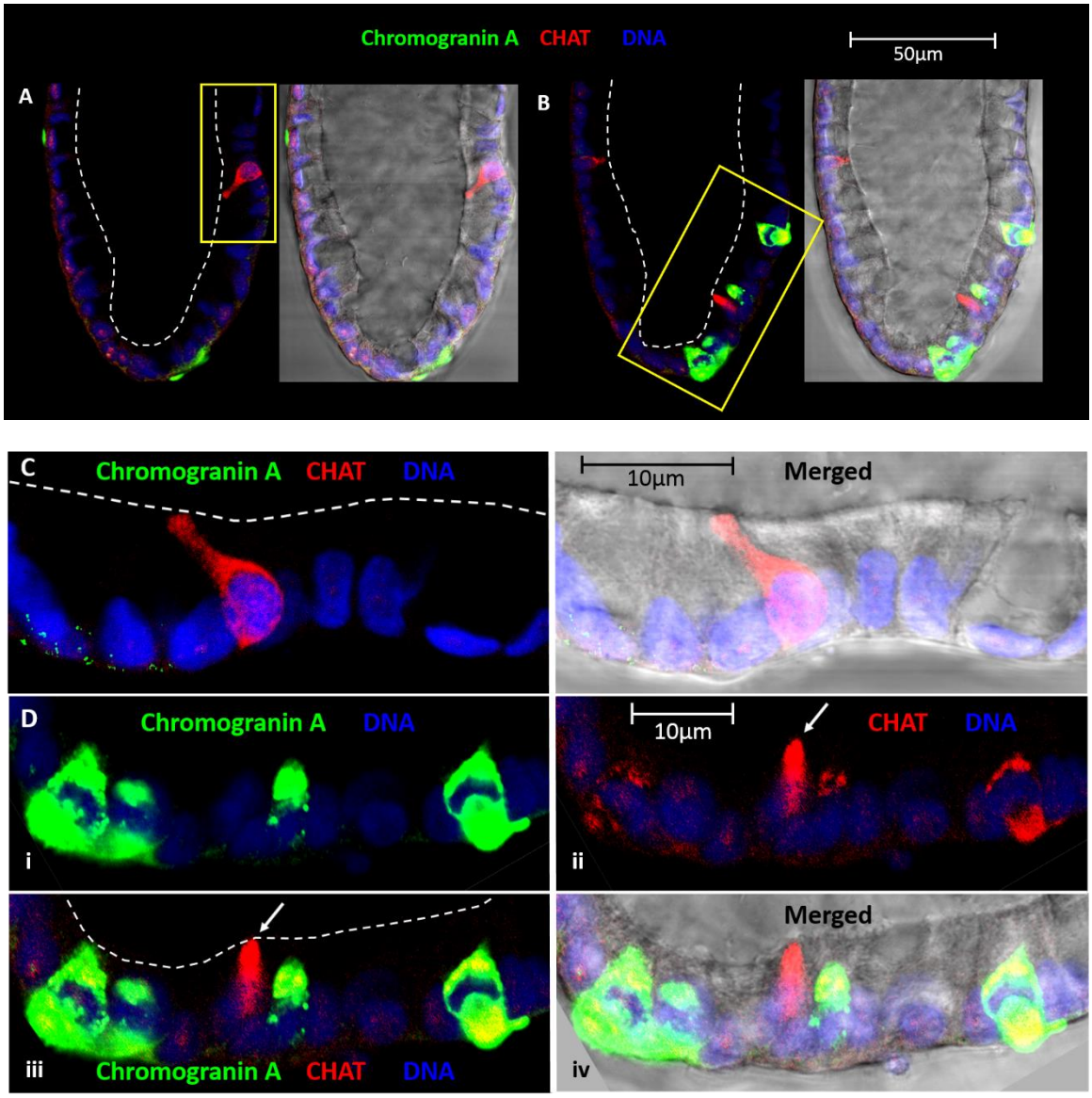

Figure 3.7 Characterisation of CHAT positive cells in the human colonic crypt

Human colonic crypts were labelled with anti-chromogranin A (green) and anti-CHAT (red) antibodies, cell nuclei were stained with Hoechst (blue). (A) and (B) are z-stack confocal images that show the presence of CHAT positive cells and enteroendocrine cells at different planes of focus in the same crypt. Images were taken with a x63 objective. (C) Enlarged zoom-in images of the yellow box in (A); composite image of the 3 channels (left); and a DIC image plus the 3 channels (right) clearly showing the basal and apical membrane of the epithelium. (D) Enlarged zoomed-in images of the yellow box in (B); (i) chromogranin A (green) and nuclei (blue); (ii) CHAT (red) and nuclei (blue); (iii) composite image of the 3 channels; (iv) DIC image overlaid with all three fluorescence channels. Dashed line shows the boundary of the apical membrane to the crypt lumen.

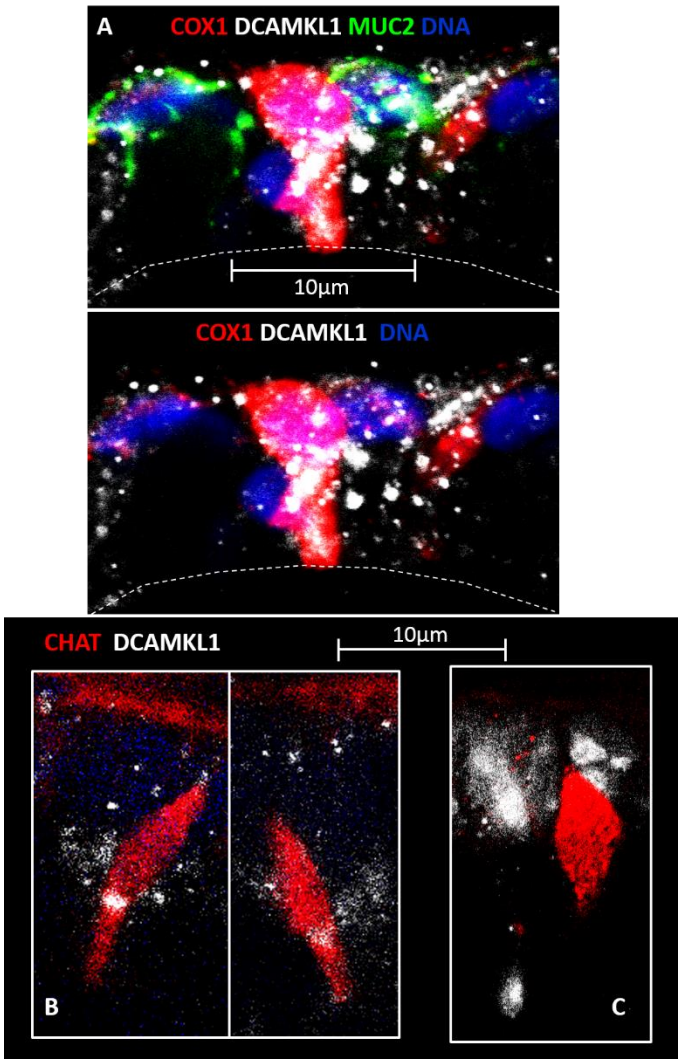

Figure 3.8 Immunolocalisation of tuft cell marker in CHAT positive cells

Enlarged epithelial layer was stained with anti-COX-1 (red), anti-DCAMKL-1 (white) and anti-MUC2 (green) antibodies; cell nuclei were stained with Hoechst (blue) (A). A composite image of all four channels: COX-1 (red), DCAMKL1 (white), MUC2 (green) and DNA (blue) (top). A merged image of COX1 (red), DCAMKL1 (white) and DNA (blue) (bottom). White dashed line shows the boundary of the crypt lumen. Enlarged epithelial layer was stained with anti-CHAT (red) and anti-DCAMKL-1 (white) antibodies, cell nuclei were stained with Hoechst (blue) (B). A composite image of CHAT (red) and DCAMKL1 (white) (C). All enlarged images were taken with a confocal microscope with a x63 objective.

3.1.3 MAchR subtype expression and localisation in human colonic crypts

MAchR expression in tissues of the GI tract or colon cancer cell lines was identified previously by RT-PCR and Western blot analysis that lacks information regarding its subcellular location; data for MAchR localisation in the human colon is very limited. Jönsson et al demonstrated the expression of M2AchR in the human colonic epithelium and in the smooth muscle layers (Jönsson, et al., 2007). Our lab demonstrated expression of the M3AchR protein on the basal membrane of human colonic crypts (Reynolds, et al., 2007). Furthermore, a recent study by Harrington and colleagues demonstrated the localisation of M1AchR, M2AchR and M3AchR expression in the human colon. They detected M3AchR but not M1AchR expression on the surface of colonic epithelial cells. M3AchR was also detected in myenteric nerve cell bodies. Both M2AchR and M3AchR were abundantly expressed in the circular and longitudinal muscles, while M1AchR expression was most abundant in myenteric and submucosal nerve cells (Harrington, et al., 2010). In this study, RT-PCR and immunohistochemistry were used to further characterise and confirm the expression and localisation of the MAchR subtypes in the human colonic epithelium.

M1AchR mRNA expression was detected in most four of the five human colon biopsy samples and its corresponding isolated crypt samples (Figure 3.9). The expression level of M1AchR was relatively low and varied between individuals. The highest M1AchR mRNA level was detected in subject 3 of the isolated crypt samples. M2AchR mRNA expression was only detected in two of the colon biopsy samples (subjects 2 and 3), and no expression was observed in the isolated crypt samples. Moreover, M3AchR mRNA was detected in all five colon biopsy and corresponding isolated crypt samples, with variation of the expression observed between individuals. M4AchR mRNA was however undetectable in all five colon biopsy samples, yet detected in three of the isolated crypt samples (subjects 3, 4 and 5). Finally, M5AchR mRNA was detected in most of the five colon biopsy samples and its corresponding isolated crypt samples. The expression level was relatively low in the biopsy samples, while three of the isolated crypt samples (subjects 3, 4 and 5) showed a higher level of expression. In summary, mRNA for M1AchR, M3AchR and M5AchR was detectable in most individuals, with subject 3 expressing the most MAchR subtypes in the colon.

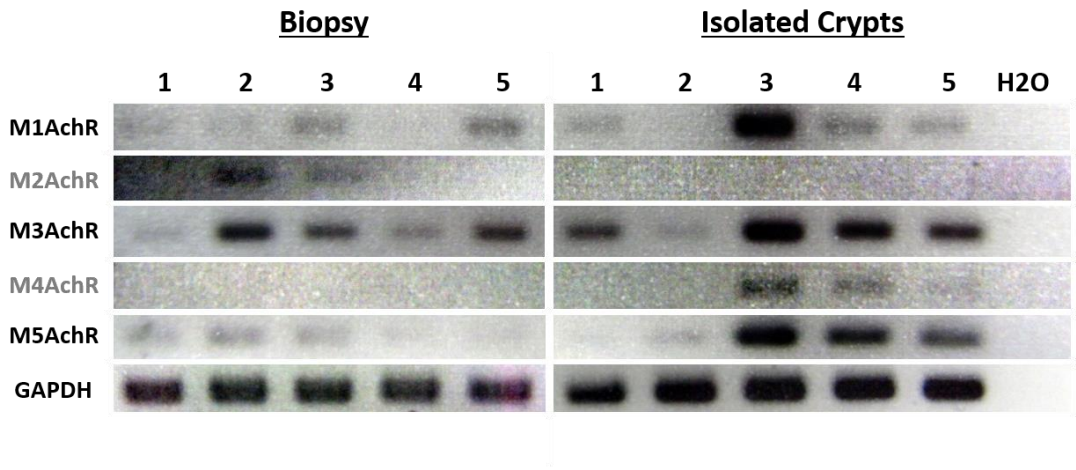

Figure 3.9 MAchR subtypes mRNA expression in the human colon biopsy and isolated colonic crypts

Agarose gel electrophoresis showing RT-PCR products from human colon biopsy and isolated crypts using specific primers for M1AchR to M5AchR genes designed to anneal across exon-exon boundaries to avoid amplification from potentially contaminating genomic DNA. GAPDH was used as a positive control. No bands were detected in the no template negative (H_2O) control. N=5 subjects.

Previously studies in our lab reported the M3AchR expression gradient along the crypt-axis, in which M3AchR protein was predominantly expressed at the crypt base (Lindqvist, et al., 2002; Reynolds, et al., 2007). Immunohistochemistry and confocal microscopy were used to further reveal the localisation of MAchR subtype expression in the colonic epithelium. Since M3AchR mRNA was expressed in most individuals, colon biopsies were fixed and stained with the primary antibody against M3AchR. Positive labelling was observed on both the basal membrane of the crypt and the nerve cell bodies in the lamina propria (Figure 3.10A). Given the mRNA data, M1AchR, M3AchR and M5AchR protein expression were targeted for immuno-labelling with primary antibodies, in both microdissected crypts from colon biopsy and isolated culture crypts. Positive immunofluorescence staining was observed for all three receptor subtypes, all of which was localised to the basal membrane at the crypt base (Figure 3.10B and C). In microdissected crypts, the expression intensity of M1AchR and M5AchR was relatively lower than M3AchR. While in isolated culture crypts, similar levels of expression were observed for all three receptor subtypes.

It is important to note that the cholinergic neurons are in close proximity with MAchRs expressed on the basal membrane of the crypt cells, which make the receptors accessible to Ach (Figure 3.10A and Figure 3.11). Thus, the conventional neuronal-epithelial cell interaction has been confirmed in the human colonic mucosa.

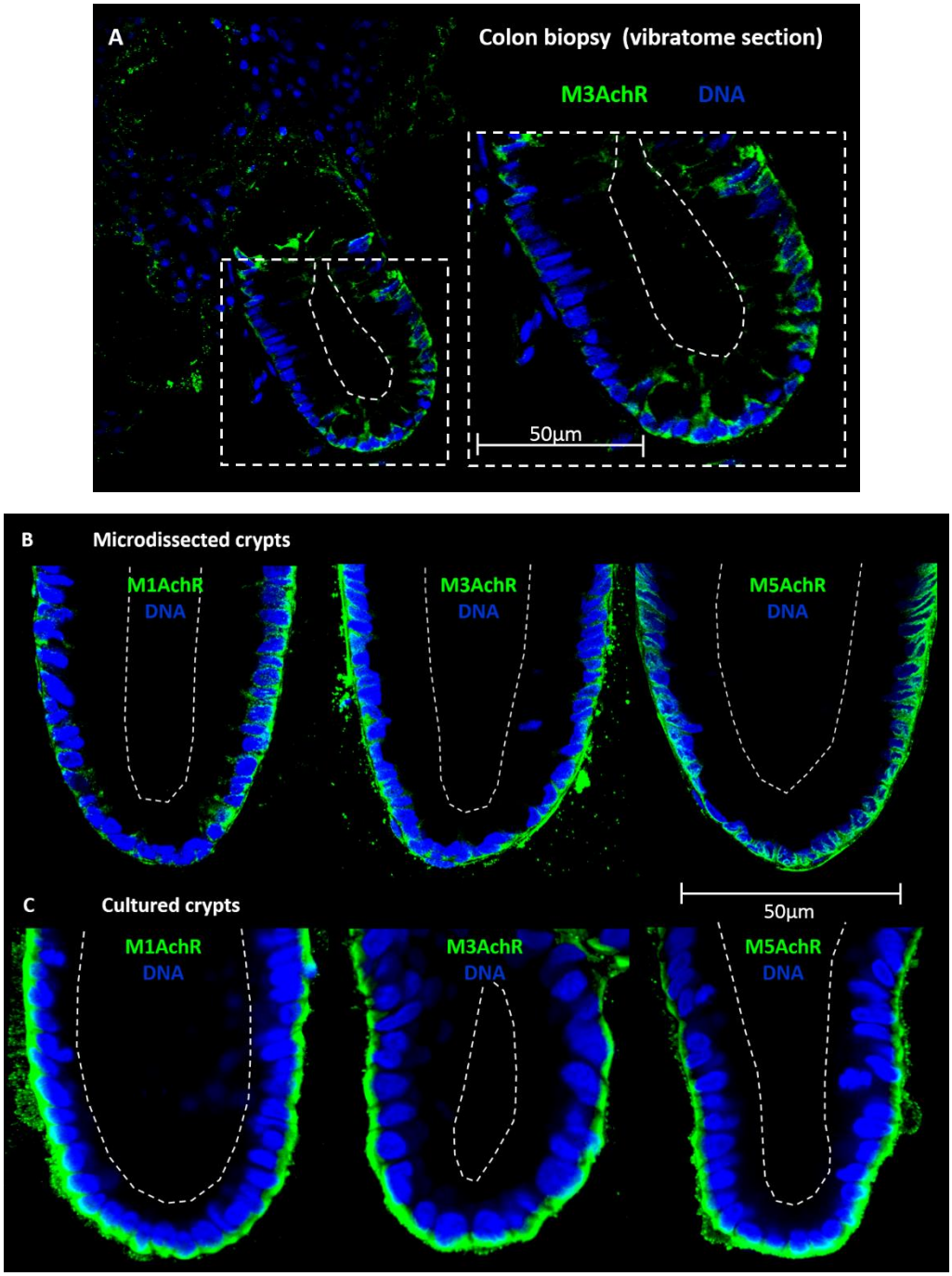

Figure 3.10 MAchR subtypes protein expression in human colonic epithelium.

(A) Sections of human colon biopsy were fixed and labelled with anti-M3AchR antibody (green) and cell nuclei were stained with Hoechst (blue). Image was taken with a x40 objective. Image was representative of N=2 subjects. (B) Microdissected crypts were labelled separately with anti-M1AchR, anti-M3AchR or anti-M5AchR antibodies (green), cell nuclei were labelled with Hoechst (blue). Images were representative of N=2 subjects, n=8 crypts. (C) Isolated culture crypts were stained as in (B). Images were representative of N=3 subjects, n=10 crypts. Dashed lines show the lumen of colonic crypt. Images of (B) and (C) were taken with a x63 objective.

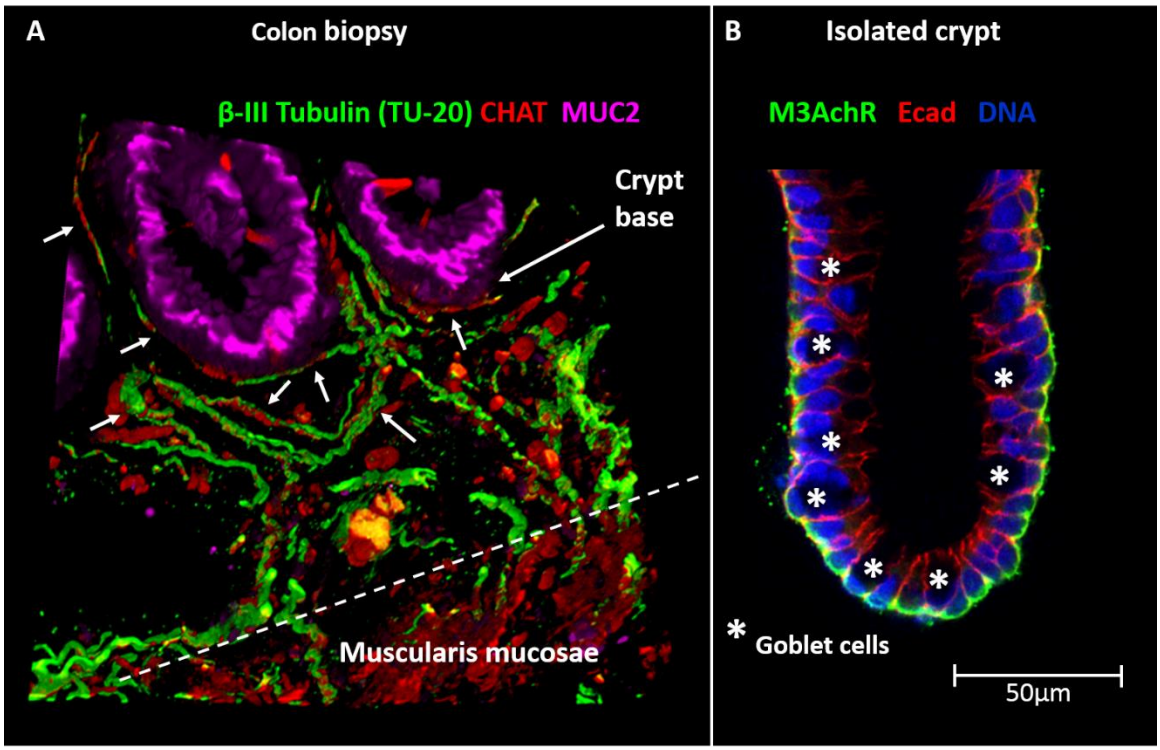

Figure 3.11 Cholinergic-epithelial cell interaction in the human colonic epithelium

Sections of human colon biopsy were stained with anti-β-III tubulin (green), anti-CHAT (red) and anti-MUC2 (pink) antibodies. MUC2 labelling was used to identify the location of the crypt. Composite image of the 3 channels was shown (A). Images were taken with a confocal microscope with a x40 objective. Cholinergic neurons were indicated by white arrows. These cholinergic neurons are expressed in the surroundings of the crypt base and in close proximity with the crypt. Dashed line shows the boundary between the mucosa and the underlying muscularis mucosae. Isolated culture crypts were labelled with anti-M3AchR (green) and anti-Ecad (red) antibodies, cell nuclei were stained with Hoechst (blue). A merged image of all three channels was shown (B). Goblet cells expressing M3AchR on their basal membrane were highlighted with an asterisk (*). Cholinergic-epithelial cell interaction was established with the presence of M3AchR on the basal membrane of the crypt which is in close proximity with the cholinergic neurons.

3.1.4 Isolated human colonic crypt culture model

Human colonic crypts were isolated from colorectal tissue biopsies obtained from patients undergoing recto-sigmoid endoscopy and from cancer patients undergoing colectomy. Samples were only used if there was no apparent intestinal pathology. Isolated crypts were embedded in Matrigel, affixed to glass coverslips, and placed in culture overnight prior to experimentation (Reynolds, et al., 2007; Reynolds et al., 2014 supplementary methods). This native crypt culture model allows us to study the cell biology and physiology of live human colonic epithelium. These isolated colonic crypts have similar dimensions to the microdissected crypts and the crypts from colon biopsies, and they resemble the intact colonic mucosa in many ways. The epithelial cells at the base of the cultured crypt are proliferative, which were identified by the immuno-labelling of the proliferation marker Ki67 (Figure 3.12A middle). Similar staining patterns were also observed in both microdissected crypts and vibratome sections of colon biopsies (Figure 3.12 B and C). Thus the hierarchy of proliferation at the crypt base is maintained in the culture system.

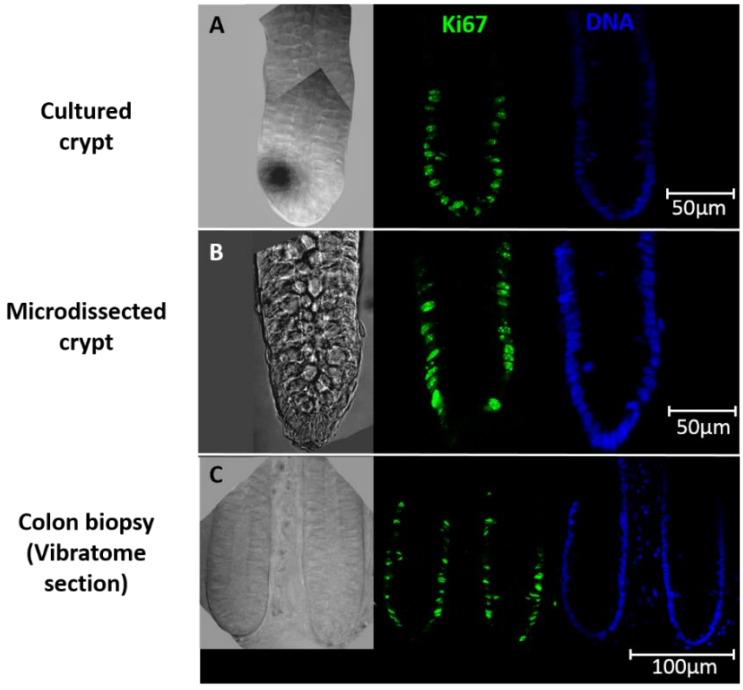

Figure 3.12 Proliferative potential of the isolated culture human colonic crypts

The isolated culture crypt (A), the microdissected crypt (B) and the vibratome section of the colon biopsy (C) were fixed and stained with anti-Ki67 antibody. Crypts or tissue sections were imaged with a Zeiss LSM 510 Meta confocal microscope using a x63 or x40 objective respectively. From left to right, DIC images of the respective crypt sample, the proliferative nuclei were labelled with anti-Ki67 (green), the cell nuclei were labelled with Hoechst stain (blue).

In addition, the single cell epithelial layer remained intact and polarised as shown by the Ecad labelling and the basal nuclei along the crypt-axis, respectively (Figure 3.13A and B). Cell division events were also observed at the lower region of the crypt as shown by Hoechst staining of the nuclei (Figure 3.13C white box). The colonic epithelium not only absorbs water, but also secretes fluid and mucus. Time-lapse microscopy of cultured human colonic crypts revealed particle flow through the crypt lumen in response to the secretagogue Ach (10µM) (Figure 3.14), suggesting that the cultured crypt model maintains the ability to secrete substances in response to stimuli.

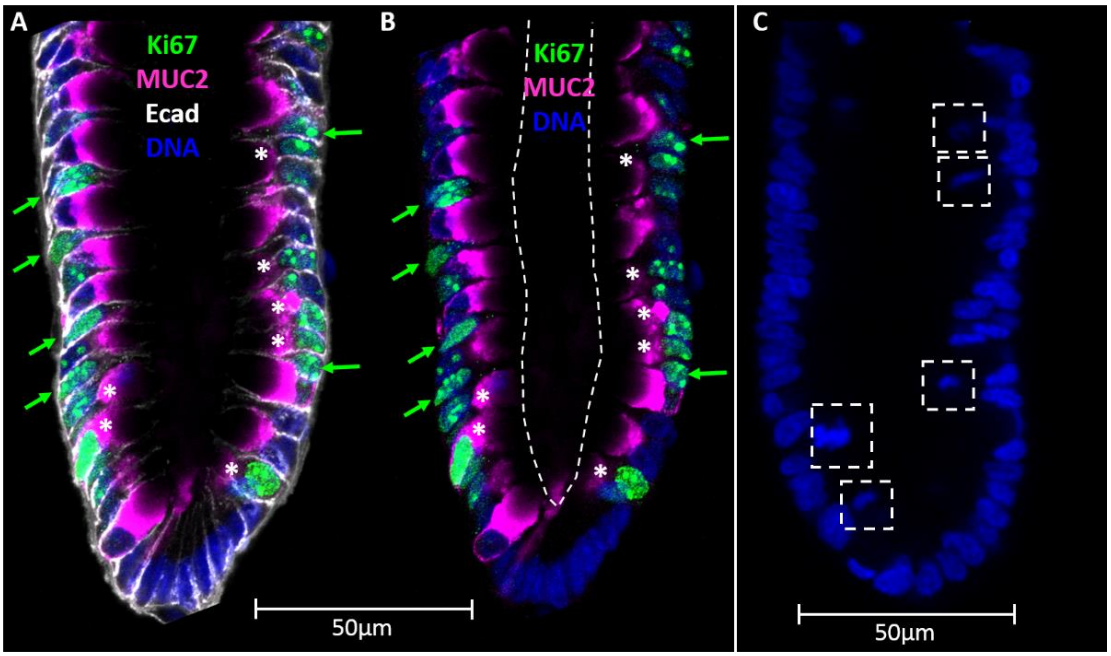

Figure 3.13 Proliferation and cell division in the intact human colonic crypt culture model

An isolated cultured crypt was fixed and labelled with anti-Ki67 (green), anti-MUC2 (pink), anti-Ecad (white) antibodies, and cell nuclei were stained with Hoechst (blue). Images were taken with a Zeiss LSM 510 Meta confocal microscope with a x63 objective. (A and B) Proliferative epithelial cells at the base of crypt were detected by anti-Ki67 staining and can be divided into goblet cells (Ki67 and MUC2 labelled, white asterisks), and non-goblet cell populations (green arrows). A composite image of all four channels: Ki67 (green), MUC2 (pink), Ecad (white) and DNA (blue) (A); a merged image of three channels: Ki67 (green), MUC2 (pink) and DNA (blue) (B). Colonocytes undergoing mitosis in culture as labelled by Hoechst stain (C, white box). White dotted line marks the boundary of the apical membrane to the crypt lumen.

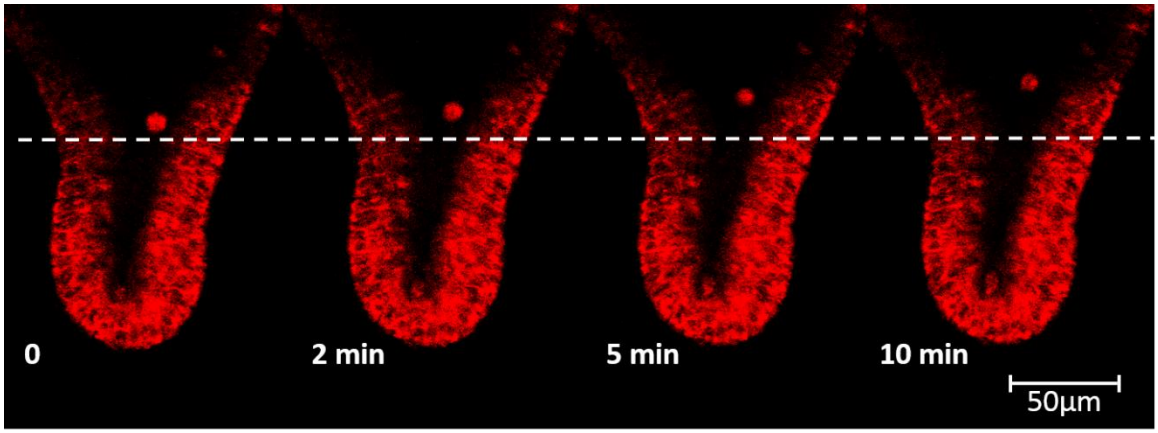

Figure 3.14 Secretagogue induced particle flow through the cultured crypt lumen.

Cultured crypts were loaded with ROSstar550 (red) and stimulated with Ach (10µM). Images were taken every 10s for 10 mins. Representative images were taken at the indicated time point. The dashed line marks the starting point of the particle moving up the crypt lumen.

3.1.5 Calcium signalling organelles in the cultured human colonic crypt

ER is the major intracellular Ca^{2+} store within a cell that has been the focus of Ca^{2+} signaling research for decades. The acidic lysosomes have recently emerged as other important Ca^{2+} stores for regulating cellular and physiological functions (Morgan, et al., 2011). Mitochondria are dynamic intracellular organelles that can operate as a reversible Ca^{2+} storage compartment in the cytoplasm (Rizzuto, et al., 2012). Mitochondrial Ca^{2+} uptake is capable to influence the generation of Ca^{2+} waves and the subsequent signal transduction (Rizzuto, et al., 1998; Brough, et al., 2005). In order to study intracellular Ca^{2+} signalling in the human colonic epithelium, immunofluorescence labelling and confocal microscopy were used to reveal the cellular location of these Ca^{2+} signalling organelles in polarised colonic epithelial cells (Figure 3.15).

As discussed previously, M3AchR is the predominant receptor subtype expressed at the basal pole of human colonic crypt cells (Figure 3.15A). The ER, stained against the retention peptide sequence KDEL, was localised at the basal pole of crypt cells, surrounding the nuclei (Figure 3.15B). Goblet cells are the key epithelial cell type studied in the current project, and were identified by the MUC2 mucin antibody labelling (Figure 3.15C). Mucus was detected in the ER, as specified by the prominent KDEL staining (Figures 3.15B and C), and in the cytoplasmic space of the goblet cells. The mitochondria were labelled with MitoTracker red, and the signals were found to be higher at the basal pole of crypt cells surrounding the nuclei (Figure 3.15G). This staining pattern strongly resembled the ER labelling, suggesting a close association between the two organelles. Moreover, the expression and localisation of the lysosomes were revealed by lysosome-associated membrane protein 1 (LAMP-1) antibody labelling in fixed tissues and by LysoTracker in live tissues (Figures 3.15E and F). Fluorescent signals were detected at the apical pole (towards crypt lumen) of crypt cells in both live and fixed tissues. However, low intensity signals were also observed at the basal pole of the crypt in the fixed tissue samples. In summary, M3AchRs are expressed at the basal pole of crypt cells including goblet cells, and were in close proximity with the ER. The ER major Ca^{2+} store and the acidic lysosomal Ca^{2+} stores were conversely located at the opposite pole of the colonic crypt cells. There was a strong association between the mitochondria and the ER at the basal pole of the crypt, however, the diffuse expression of the mitochondria suggested that they also interact with other intracellular organelles.

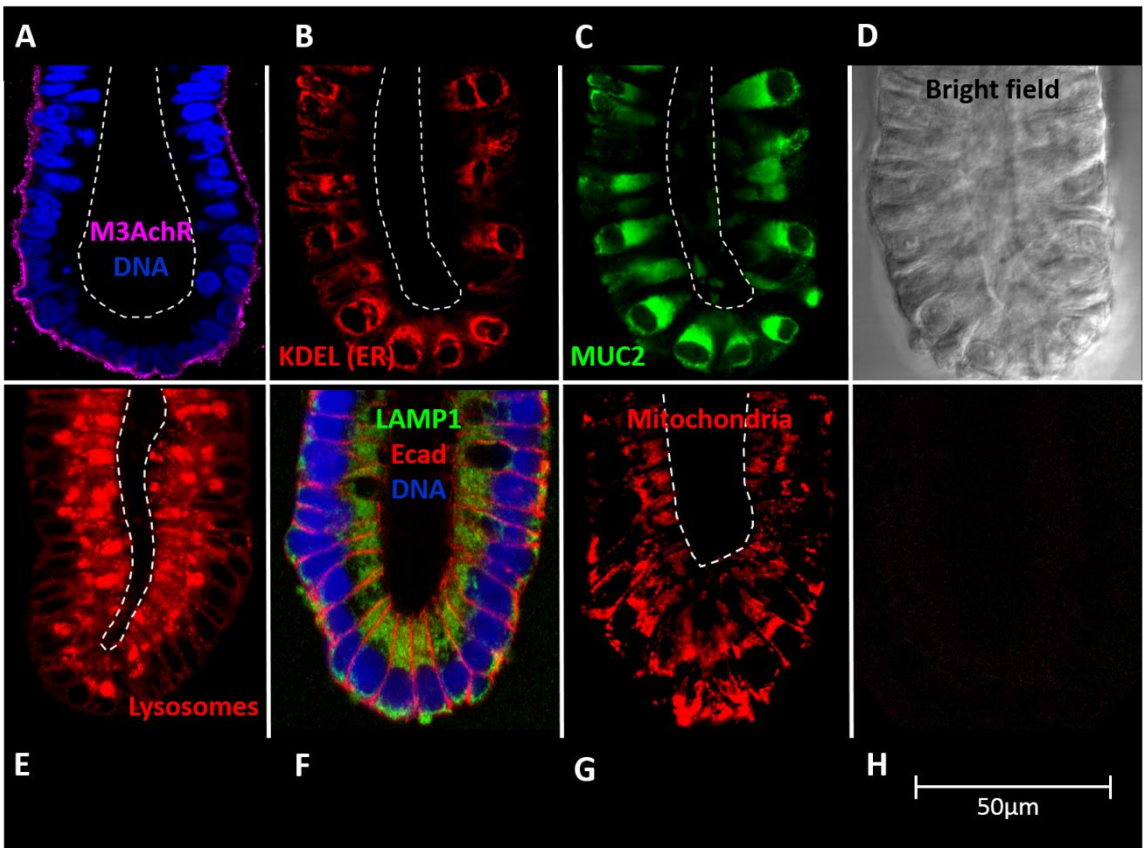

Figure 3.15 Localisation of the intracellular Ca^{2+} signalling organelles in human colonic crypts

Isolated culture crypts were fixed and labelled with the respective antibodies. (A) M3AchR immunolabelled (pink) and Hoechst stained cell nuclei (blue); (B) KDEL labelled ER (red); (C) MUC2 labelled goblet cells (green); (D) DIC image of a cultured crypt. (E) LysoTracker labelling of lysosomes in live crypts (red); (F) LAMP-1 labelled lysosomes in fixed crypt (green), Ecad (red) and Hoechst stained nuclei (blue); (G) MitoTracker labelling of the mitochondria (red); (H) no primary antibody (negative) control. Images were taken with a confocal microscope with a x63 objective. Dashed lines indicate the boundary of the apical membrane and the location of the crypt lumen. Images were representative of N≥5 subjects.

3.1.6 Intracellular calcium channel expression in the cultured human colonic crypt

Activation of M3AchR has been shown to mobilise intracellular Ca^{2+} from the ER store via the 2nd messenger IP3 (Berridge, 1993; Caulfield, 1993; Felder, 1995). Active IP3 translocates to the ER where it binds to IP3R (one of the major intracellular Ca^{2+} channels) on the ER membrane, causing the IP3R to open allowing Ca^{2+} mobilisation into the cytosol (Foskett, et al., 2007). The increase in cytosolic [Ca^{2+}] in turn activates IP3R and RYR on the ER membrane and induces the CICR response (Taylor and Dale, 2012). These regenerative Ca^{2+} waves have been shown to mediate certain physiological functions including intestinal motility and secretion, apoptosis and proliferation (Ehlert, et al., 2011). The depleted ER Ca^{2+} store is then refilled via the SERCA pump to maintain the ER Ca^{2+} homeostasis (Berridge, et al., 2003). In addition, mobilisation of the acidic lysosomal Ca^{2+} stores by NAADP via TPC have recently been appreciated to drive different cellular processes such as vesicle trafficking and exocytosis (Ruas, et al., 2010; Davis, et al., 2012). The expression of different intracellular Ca^{2+} channel subtypes and the subcellular location of these channels could influence the Ca^{2+} responses. It is thus important to identify the expression and cellular localisation of these intracellular Ca^{2+} channels in the colonic epithelial cells which control Ca^{2+} mobilisation. The expression of the IP3R and RYR subtypes have been previously characterised in the rat colonic epithelium (Siefjediers, et al., 2007; Prinz, et al., 2008), and little colocalisation of the two Ca^{2+} channels were observed. Information regarding the expression of these intracellular Ca^{2+} channels in the human colon is very limited. A recent study by Shibao and colleagues evaluated the expression of the IP3R subtypes in human colorectal carcinomas surgically resected from 116 patients (Shibao, et al., 2010). By using Western blots and immunohistochemistry, they found the expression of IP3R1 and IP3R2 in the normal colorectal mucosa and in colorectal cancer tissues, while IP3R3 expression was only observed in colorectal cancer. They concluded that the expression level of IP3R3 is directly associated with the aggressiveness of the tumour. RYR transcripts have previously been identified in the T84 human colon cancer cell line (Verma, et al., 1996). No information is currently available for TPC expression in the human colon.

In the current study, RT-PCR and immunohistochemistry were used to identify the expression and localisation of these intracellular Ca^{2+} channels in the human colonic epithelium. Transcripts of all three IP3R subtypes was detected in five isolated human colonic crypt samples (Figure 3.16). RYR1 mRNA was detected in four of the five isolated human crypt samples (all except subject 3), while RYR2 mRNA was only found in three human crypt samples (all donors except subjects 3 and 4). RYR3 transcripts were not investigated in the

current study. SERCA1 mRNA was detected in four of the five human crypt samples (once again all donors except subject 3), whereas SERCA2 and SERCA3 transcripts were detected in all five human crypt samples. In addition, both TPCN1 and TPCN2 mRNA were found to be expressed in all five of the isolated human crypt samples. Thus, most human subjects have message for at least one subtype of each intracellular Ca^{2+} channel gene detectable in their colon samples.

Localisation of the intracellular Ca^{2+} channel proteins in colonic epithelial cells was then investigated through immunofluorescence labelling and confocal microscopy (Figure 3.17). While strong yet diffuse IP3R1 protein labelling was observed in the human colonic epithelium, positive immunostaining was detected on the basal pole of the crypt, in the cell nuclei and in the cytoplasm of epithelial cells (Figure 3.17A). A similar staining pattern was observed for IP3R2 protein, but at much lower intensity (Figure 3.17B). In non-goblet epithelial cells, IP3R2 expression was diffuse; immunofluorescence signals were present near the basal and apical membranes of the crypt, in the cell nuclei and in the cytoplasm. In goblet cells, a distinctive IP3R2 staining pattern was observed in the cell nuclei. Positive IP3R2 labelling was also detected at the basal and apical membranes of the goblet cells and in the areas associated with the ER, while IP3R3 was mainly localised at the basal membrane of the colonic crypt (Figure 3.17C). RYR1 and/or RYR2 protein was also detected at the basal membrane of the crypt (Figure 3.17D). Furthermore, a diffuse expression of SERCA1, 2 and 3 proteins was detected in non-goblet epithelial cells (Figure 3.17F). Positive signals were found at the basal membrane, in the cell nuclei and in the cytoplasm. In goblet cells, labelling was detected at the basal membrane, in the cell nuclei and also in the area associated with the ER as defined by the KDEL labelling (Figure 3.17E).

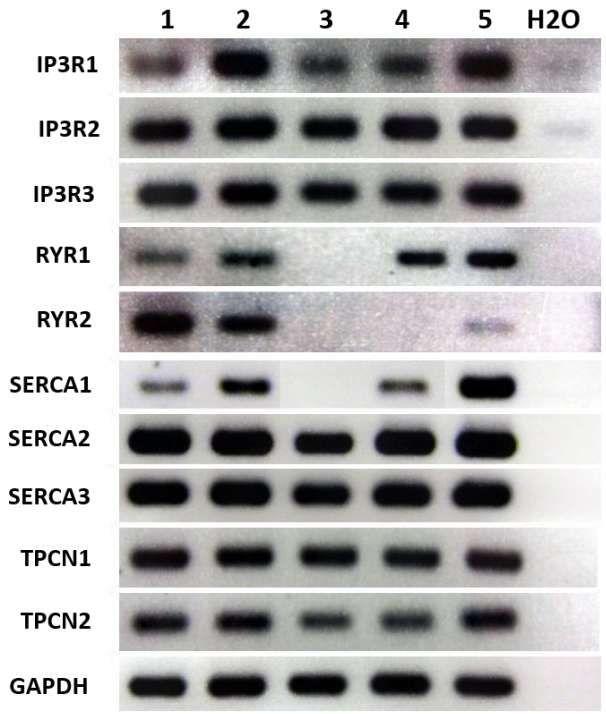

Figure 3.16 Intracellular Ca^{2+} channels mRNA expression in isolated human colonic crypts

Agarose gel electrophoresis showing RT-PCR products of the isolated human colonic crypt samples. Specific PCR primers for IP3R, RYR, SERCA and TPC transcripts were used that were designed to anneal across exon-exon boundaries to avoid amplification from potentially contaminating genomic DNA. GAPDH was used as the positive internal control. No bands were observed in most of the negative no template control (H_2O lane), except for a faint band observed in the IP3R1 and IP3R2 negative control lanes. However, the expression of both genes in the five samples is assumed to be real based on the strong intensity PCR products in the presence of template. N=5 subjects. Note that samples in lanes 3 and 4 in the SERCA1 gel were mistakenly run in the wrong order, and have therefore had the appropriate positions switched here for presentation purposes.

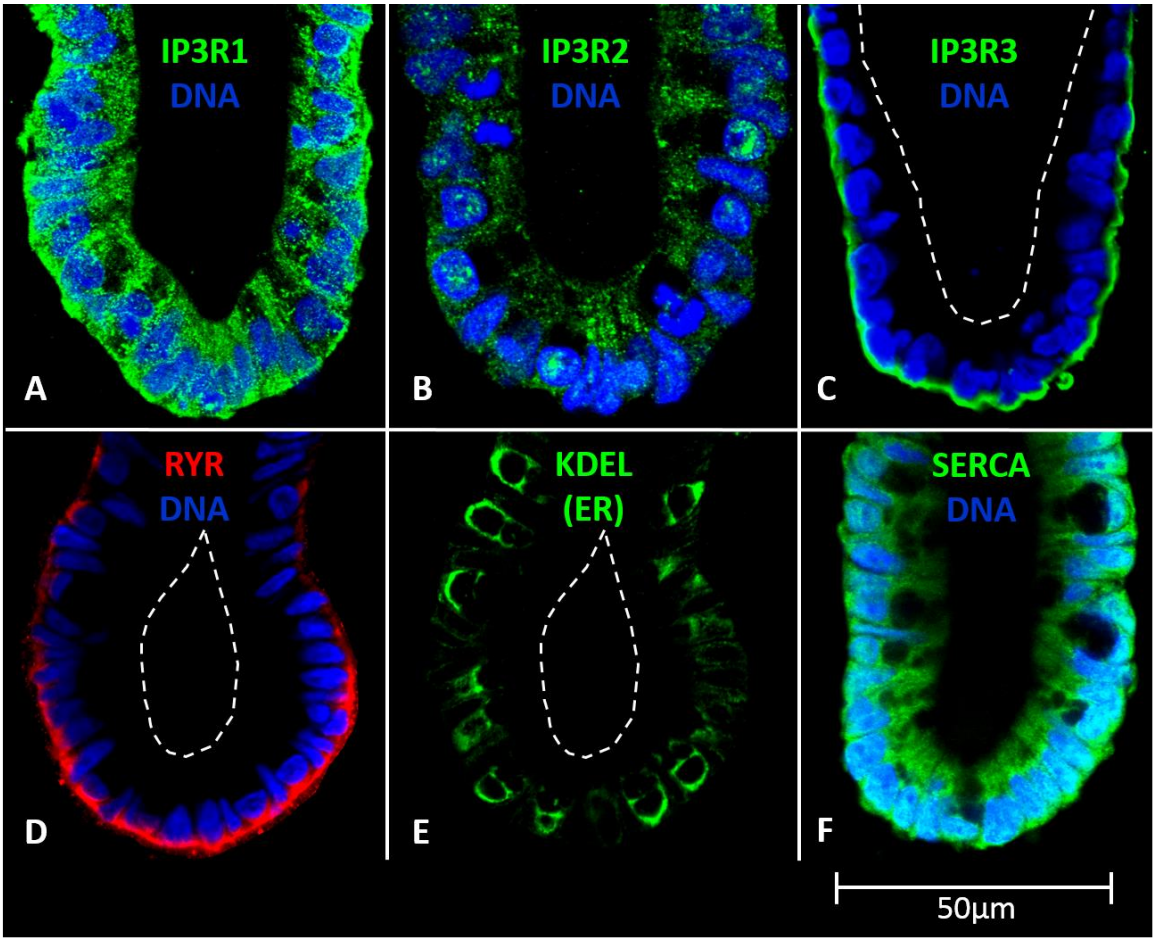

Figure 3.17 Immunolocalisation of the intracellular Ca^{2+} channels in the ER of colonic epithelial cells.

Isolated culture crypts were fixed and labelled with antibodies against different intracellular Ca^{2+} channels known to be expressed on the ER. Top row: (A) colonic crypts labelled with anti-IP3R1 antibody (green); (B) crypts stained with anti-IP3R2 antibody (green); (C) crypts labelled with anti-IP3R3 antibody (green). All cell nuclei were stained with Hoechst (blue). Bottom row: (D) crypts labelled with anti-RYR-1/2 antibody (red); (E) ER were stained with anti-KDEL antibody (green); and (F) crypts were stained with anti-SERCA antibody (green). Cell nuclei were stained with Hoechst (blue). Images were taken with a confocal microscope with a x63 objective. Dashed line indicated the location of the crypt lumen. Images were representative of N=3 subjects, n≥10 crypts for each antibody labelling.

Both TPC1 and TPC2 proteins were detected at the apical pole (towards crypt lumen) of colonic crypt cells (Figure 3.18A). TPC1 was previously found to be expressed in endosomes and lysosomes, whereas TPC2 was found on late endosomes and lysosomes (Ruas, et al., 2014). Similar to LAMP-1 labelling, the majority of the TPC2 signals resided at the apical pole of crypt cells, while minimal signals were also detected at the basal pole of the crypt (Figure 3.18B i and ii). Clusters of LAMP-1 and TPC2 labelled acidic organelles were observed between the mid-cell regions and the apical membrane of epithelial cells (Figure 3.18B iii). The human colonic epithelium is also equipped with the ectoenzyme CD38 which is responsible for the production of cADPR and NAADP, which act on RYR and TPC respectively. CD38 was found to be localised to both the apical and basal poles of crypts (Figure 3.18C ii), and was strongly associated with TPC2 (Figure 3.18C iii).

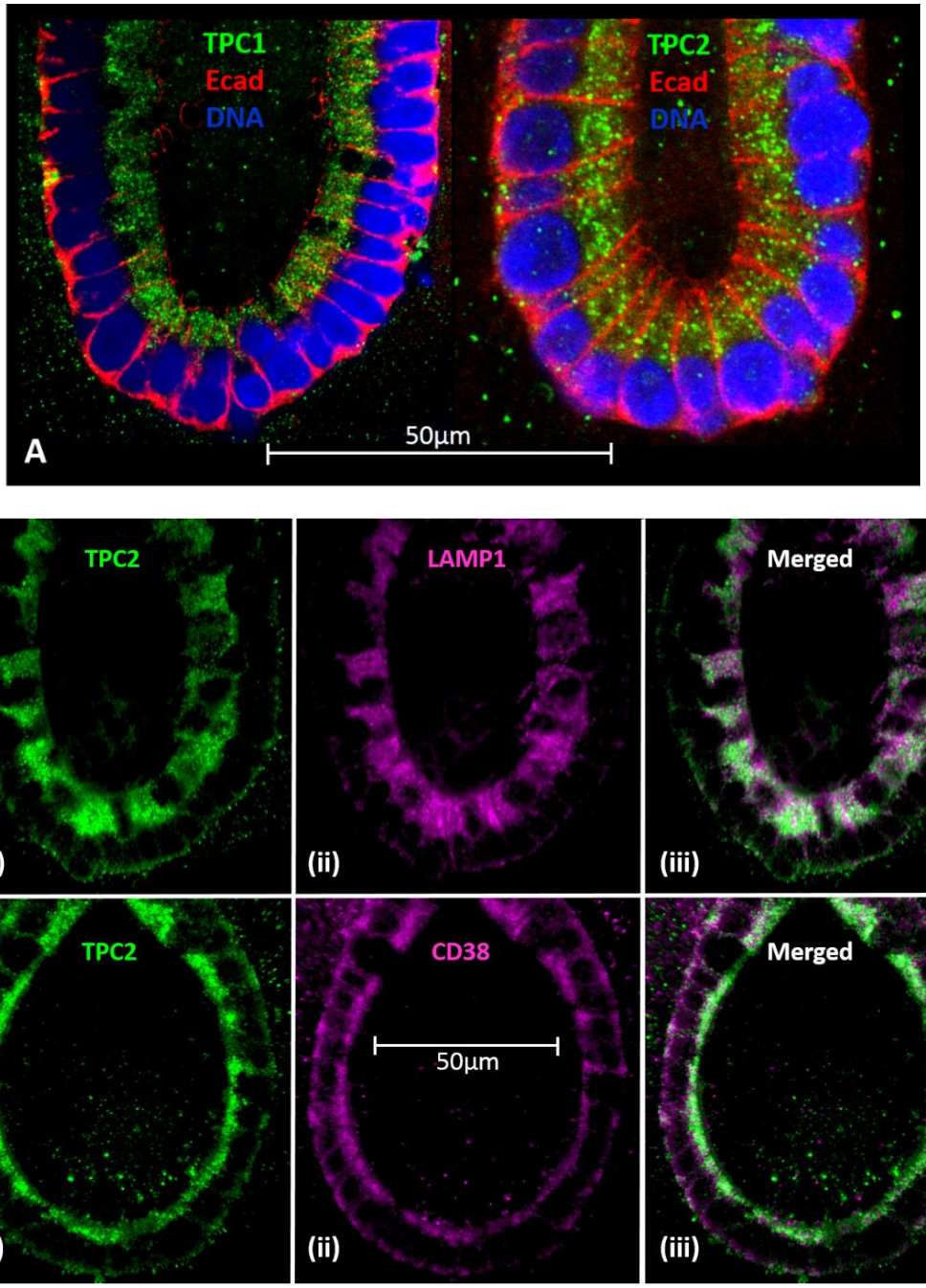

Figure 3.18 Immunolocalisation of TPCs, lysosomes and CD38 in the human colonic epithelial cells.

Top panel: (A) Isolated crypts were stained separately with anti-TPC1 (green) and anti-Ecad (red) antibodies (left), or anti-TPC2 (green) and anti-Ecad (red) antibodies (right), all cell nuclei were stained with Hoechst (blue). Bottom panel top row: (B) Crypts were labelled with anti-TPC2 (green) (i); anti-LAMP-1 (pink) (ii); a composite image of TPC2 (green) and LAMP1 (pink) (iii). Bottom row: (C) Crypts were stained with anti-TPC2 (green) (i); anti-CD38 (pink) (ii); and a composite image of TPC2 (green) and CD38 (pink) (iii). Images were taken with a confocal microscope with a x63 objective. Images were representative of N≥5 subjects, n≥10 crypts.

3.1.7 Calcium signalling organelles in human colonic goblet cells

The following section specifically focused on the expression of the Ca^{2+} signaling organelles in human colonic goblet cells *in situ*. The major function of the colonic goblet cells is to secrete mucus, which is primarily composed of the MUC2 mucin. Mature MUC2 proteins are densely packed into the acidic secretory granules (vesicles) before secretion. These mucus granules are mainly located at the apical pole of the goblet cells where the acidic lysosomes reside. Thus, there is a strong association between the acidic lysosomes and the mucus granules in goblet cells. MUC2 labelling not only identifies goblet cells within the colonic epithelium, it also demonstrates the quantity of mucus content within each goblet cells.

Under unstimulated basal conditions, different stages of mucus secretion were observed in goblet cells within the same crypt (Figure 3.19A middle), and can be separated into three stages: low, medium and high levels of secretion based on the mucus content within goblet cells. The amount of LAMP-1 labelled acidic lysosomes within a goblet cell was strongly associated with the MUC2 content. Higher LAMP-1 signals were detected in goblet cells with low levels of secretion, in which positive signals were detected in the centre of the cell near or underneath the ER in 2D view (Figure 3.19A white asterisks). Decreased LAMP-1 signals were observed in goblet cells with medium level of mucus secretion (Figure 3.19A pink asterisks), with labelling found near the ER and also beneath the lateral membrane, towards the apical poles of cells. Only weak LAMP-1 signals were detected in goblet cells with high level of secretion (Figure 3.19A green asterisks). The enlarged images demonstrate the expression of LAMP-1 in and around the nucleus, near the ER and in the cytosol of goblet cells. The highest intensity of LAMP-1 was detected beneath the lateral membrane towards the apical pole of cells (Figure 3.19 B and C). In addition, similar LAMP-1 expression patterns were observed in single goblet cells isolated from human colonic epithelium (Figure 3.19 D and E).

A functional crypt is composed of many different epithelial cell types connected to each other via cell junctions, including the tight and gap junctions. These cell-cell junctions are believed to mediate signal transduction and communication between cells. Development of the single cell epithelial model from native colonic tissue provided the opportunity to study the response of epithelial cells (including goblet cells) to a stimulus in the absence of neighbouring cells.

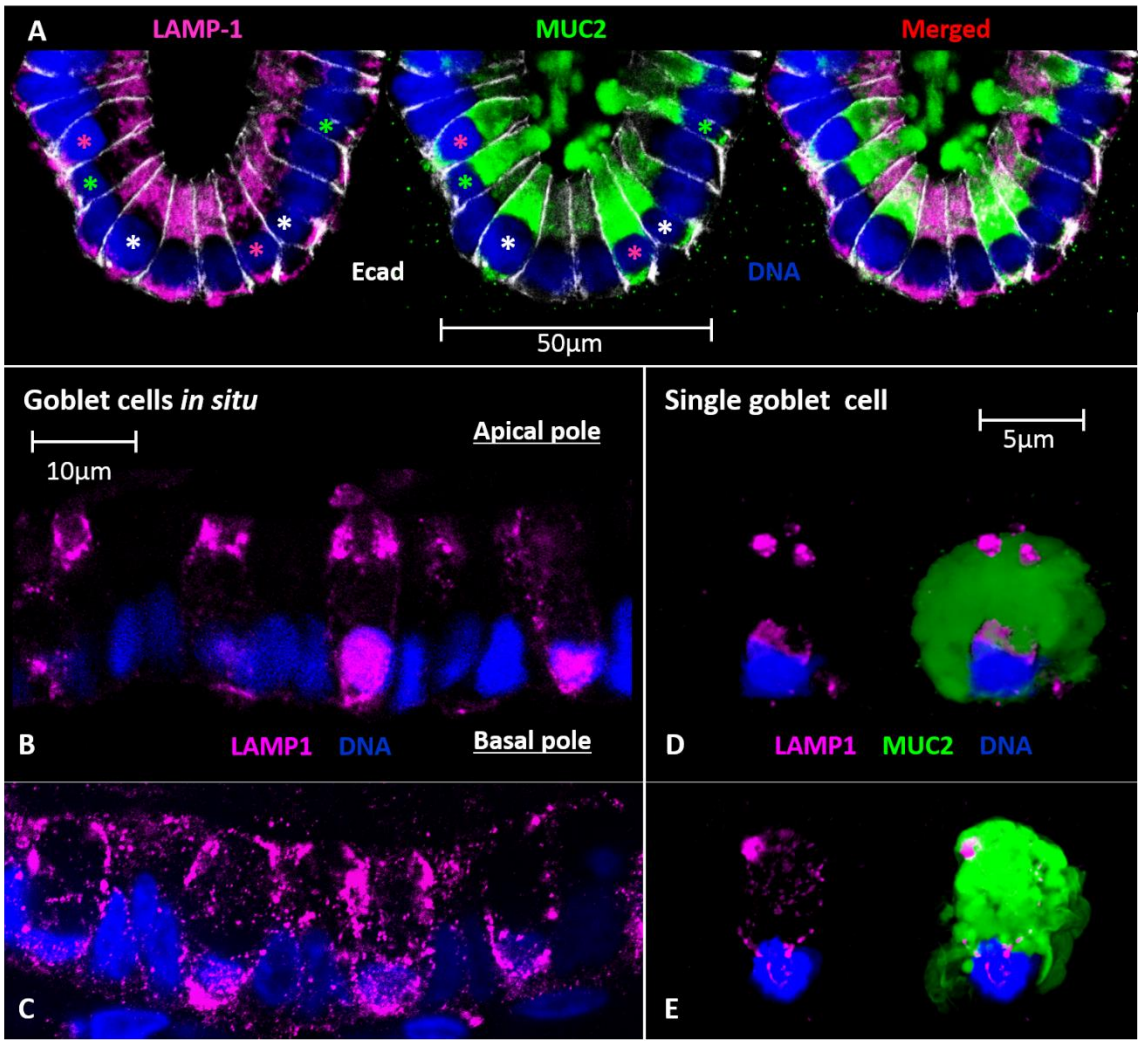

Figure 3.19 Localisation of acidic lysosomes in human colonic goblet cells

Cultured human colonic crypts were labelled with anti-LAMP-1, anti-MUC2 and anti-Ecad antibodies, and cell nuclei were stained with Hoechst (A). Images from left to right show representative crypts with the following combinations of stains: LAMP-1 (pink), Ecad (white) and Hoechst (blue); MUC2 (green), Ecad (white) and Hoechst (blue); a merged image of all 4 channels. MUC2 labelling shows the mucus status of goblet cells, characterised as having low levels of mucus secretion (white asterisks), medium levels of secretion (pink asterisks) or high levels of secretion (green asterisks). Enlarged images of goblet cells in situ (B and C); crypts were labelled with LAMP-1 (pink) and cell nuclei (blue). Single goblet cells (D and E) were stained with LAMP-1 (pink), MUC2 (green) and cell nuclei (blue). All images were taken with a x63 objective.

It is now widely accepted that TPCs are the lysosomal Ca^{2+} release channels. TPC1 was found to be expressed on endosomes and lysosomes (Ruas, et al., 2014): the detection of TPC1 proteins in the cytoplasm of goblet cells (Figure 3.20) therefore allowed the inference the location of the endo-lysosomes. These goblet cells were identified by another MUC2 antibody labelling predominantly the immature MUC2 protein which resides within the ER (Figure 3.20B). A 2D view reveals that clustering of the TPC1 and MUC2 signals occur within the region of the ER (Figure 3.20B cells highlighted with white asterisks). Similar to LAMP-1 labelling, TPC1 was localised in the region where the ER resides and beneath the lateral membrane towards the apical pole of cells. Moreover, prominent KDEL labelling was observed in the ER of goblet cells (Figure 3.21B), resembling the labelling of immature MUC2 (Figure 3.20B). TPC2 was found to be expressed mainly on late endosomes and lysosomes. Similar to TPC1 and LAMP-1 labelling, TPC2 signals were also detected in the cytoplasm of the goblet cells (Figure 3.21A white asterisks). Overlapping signals of TPC2 and the ER were observed in these mucus secreting goblet cells (Figure 3.21C), suggesting an association between the ER Ca^{2+} store and the TPC2 expressing lysosomal Ca^{2+} stores, which could possibly play a role in Ca^{2+} mediated mucus granule exocytosis.

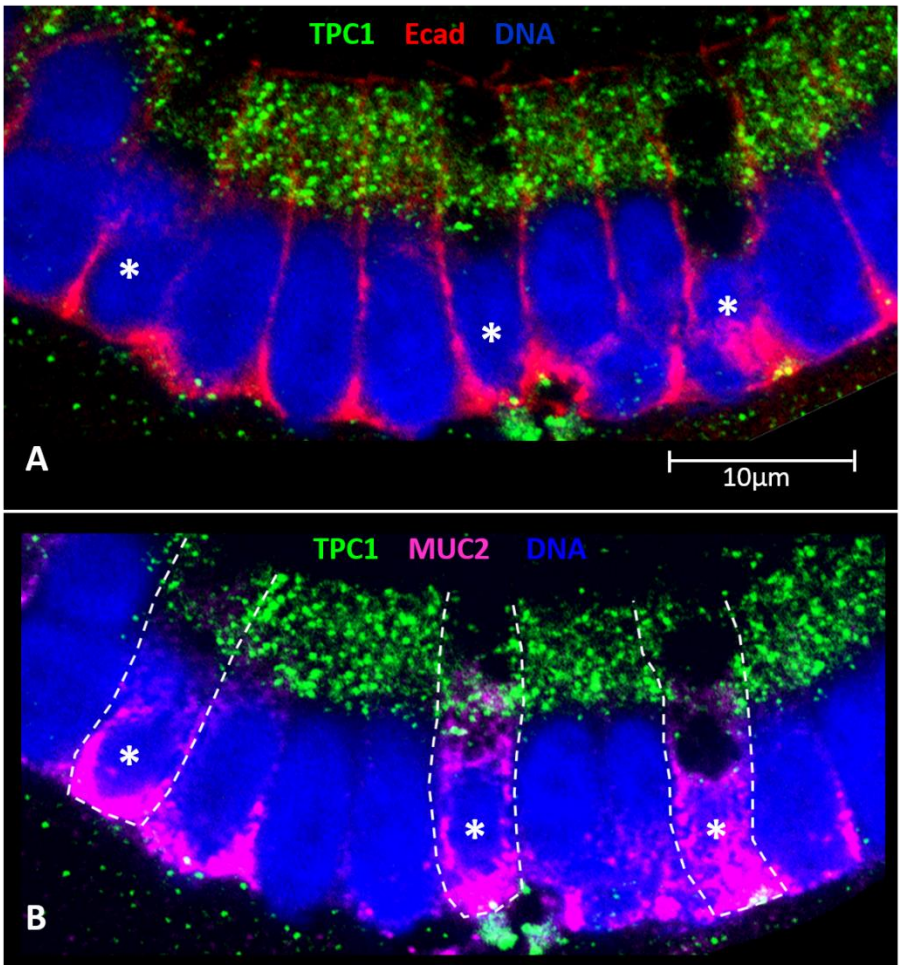

Figure 3.20 Immunolocalisation of TPC1 in human colonic goblet cells

Enlarged images of epithelial cell layer stained with anti-TPC1 (green), anti-Ecad (red) and anti-MUC2 (pink) antibodies, cell nuclei were stained with Hoechst (blue). A composite image of TPC1 (green), Ecad (red) and nuclei (blue) (A). A composite image of TPC1 (green), MUC2 (pink) and nuclei (blue) (B). White dashed lines mark the cell boundary of goblet cells. Asterisks highlight the goblet cells in the epithelial cell layer. All images were taken with a x63 objective.

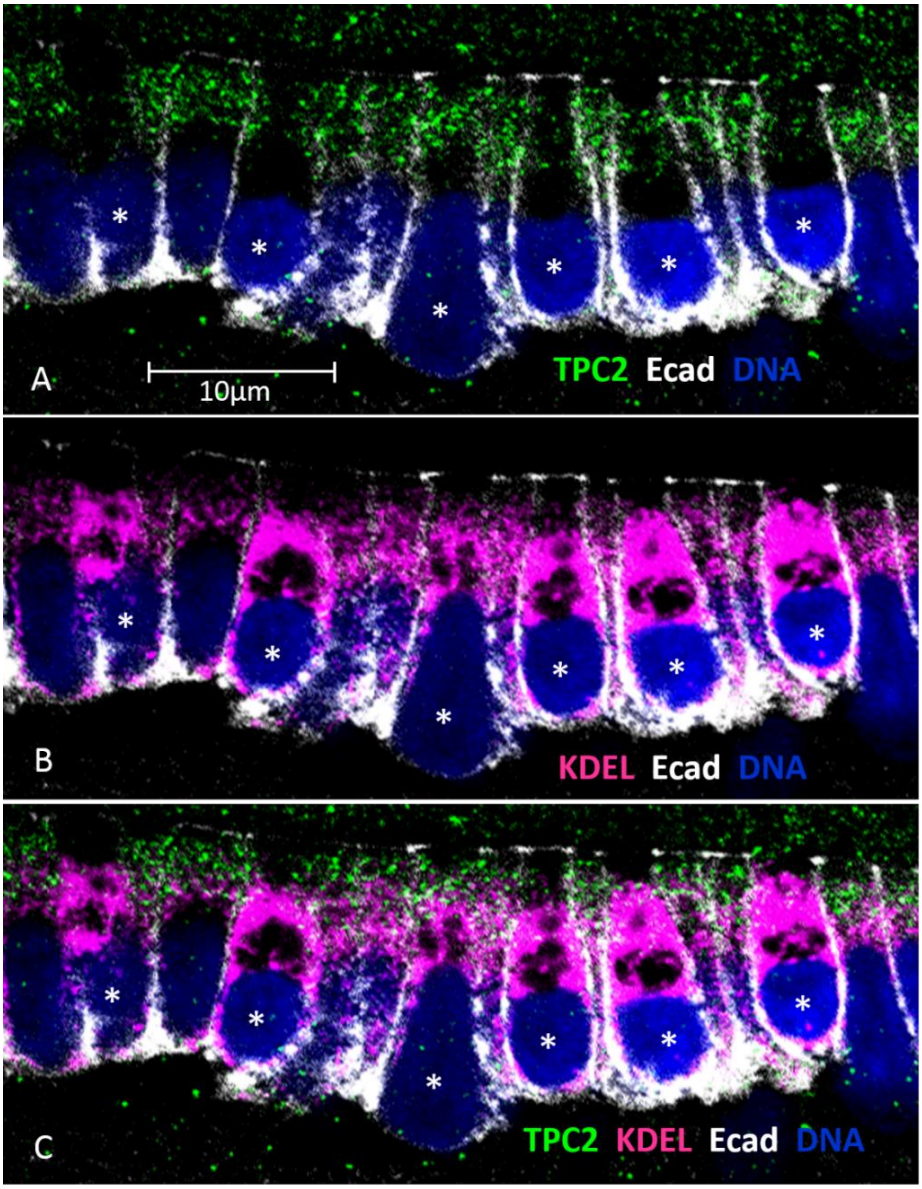

Figure 3.21 Immunolocalisation of TPC2 in human colonic goblet cells

Enlarged images of epithelial cell layer stained with anti-TPC2 (green), anti-Ecad (white) and anti-KDEL (pink) antibodies, cell nuclei were stained with Hoechst (blue). A composite image of TPC2 (green), Ecad (white), and nuclei (blue) (A); a merged image of KDEL (pink), Ecad (white) and nuclei (blue) (B); an overlaid image of all four channels: TPC2 (green), KDEL (pink), Ecad (white) and nuclei (blue) (C). Asterisks highlight the goblet cells in the epithelial cell layer. All images were taken with a x63 objective.

NAADP is the 2nd messenger responsible for mobilisation from lysosomal Ca^{2+} stores via the TPC (Calcraft, et al., 2009). CD38 is responsible for synthesising both NAADP and cADPR, it is therefore important to identify expression of the CD38 in goblet cells. CD38 expression was detected at the basal-lateral and apical membranes, and in the cytoplasm of the goblet cells in 2D view (Figure 3.22). CD38 immunoreactivity was occasionally observed in the nucleus of the goblet cells (Figure 3.22A).The basal expression pattern is consistent with the functional role of CD38 in synthesising cADPR, which acts on the RYR, which can be detected on the basal membrane of the colonic epithelial cells including goblet cells (Figure 3.17D). CD38 expression on the lateral and apical membranes was in close proximity to the LAMP-1 positive lysosomes (Figure 3.22A right), which may provide the major source of NAADP to act on the TPC. MUC2 labelling confirmed that goblet cells were indeed expressing CD38 (Figure 3.22B white asterisks). Thus, colonic goblet cells are equipped with all the necessary Ca^{2+} signalling organelles and Ca^{2+} channels to be capable of responding to cholinergic stimulation, even in the absence of neighbouring cells.

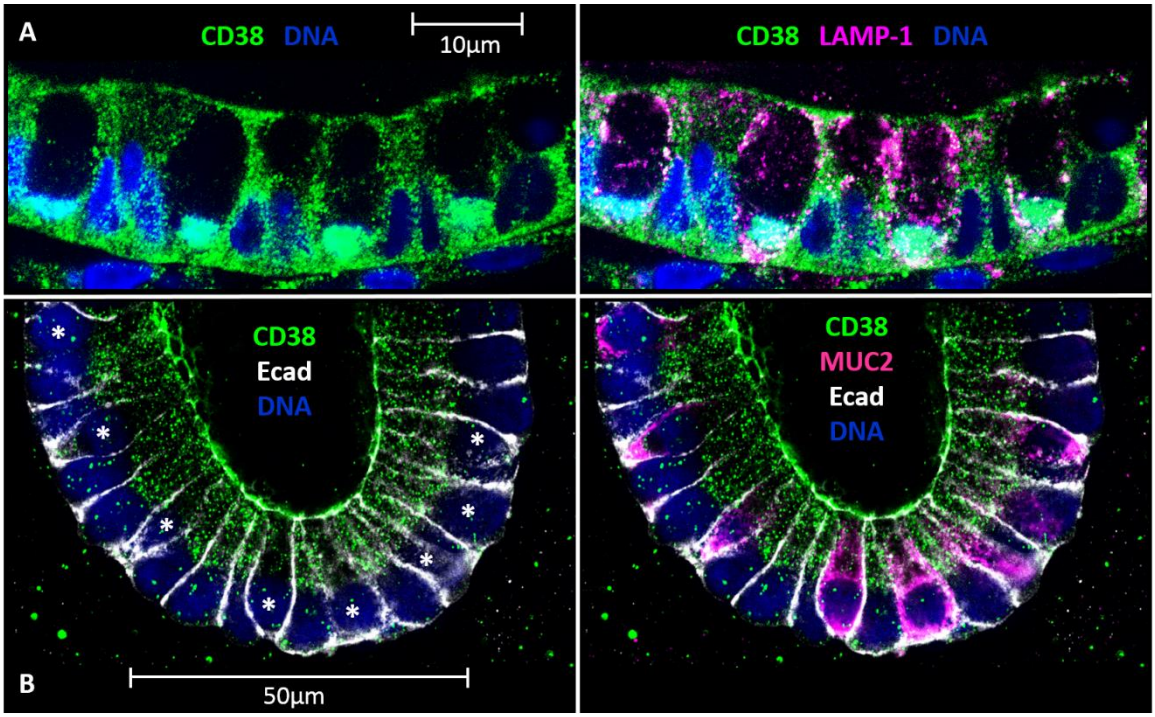

Figure 3.22 Expression of CD38 in human colonic goblet cells

Enlarged image of the epithelial layer. Sections were stained with anti-CD38 (green), anti-LAMP1 (pink) and cell nuclei were labelled with Hoechst (blue) (A). A composite image of CD38 (green) and cell nuclei (blue, left). An overlaid image of CD38 (green), LAMP1 (pink) and cell nuclei (blue, right). The seemingly hollow cytoplasmic domain is a common morphological feature of goblet cells. The base of a cultured crypt stained with anti-CD38 (green), anti-Ecad (white) and anti-MUC2 (pink) antibodies, with cell nuclei labelled with Hoechst (blue) (B). The image on the left is a composite image of 3 channels: CD38 (green), Ecad (white) and DNA (blue). The image on the right is a composite image of 4 channels: CD38 (green), MUC2 (pink), Ecad (white) and DNA (blue). White asterisks highlight goblet cells in the absence of MUC2 labelling. All images were taken with a x63 objective.

3.1.8 Discussion

3.1.8.1 Cholinergic-epithelial cell interactions

The enteric neurons innervating the colonic mucosa can be either cholinergic or non-cholinergic. In this study the spatial relationship of the neurons and colonic crypts were visualised by immunohistochemical labelling of fixed human colon biopsies. These enteric neurons were found to be present at the sub-epithelial layers including the muscularis mucosae and the submucosa, and also in the lamina propria surrounding the crypts, from the base to the surface epithelium. Nerve fibers were in close proximity with crypt cells (Figure 3.1). This observation is consistent with published findings regarding the location of enteric neurons in mouse intestinal crypts (Bjerknes & Cheng, 2001) as well as in the human colonic epithelium (Reynolds, et al., 2007). However, both of these studies only demonstrated the presence of the enteric neurons in the colonic mucosa with lower magnification 2D images, which therefore lack detailed information regarding the enteric neurons' interactions with the colonic epithelial cells. 3D reconstruction of a z-stack of images produced via confocal microscopy allows a much greater depth of investigation; reconstructed images can be rotated through different axes and angles, providing a better spatial appreciation of the neuronal-crypt morphology and sites of interaction (Figure 3.2A). The general view is that the enteric neurons lie in close proximity to – but do not penetrate – the colonic epithelium (Furness, 2006). Some nerve fibers, which are believed to be sensory, have been shown to penetrate the inner layers of stratified epithelium which line the oesophagus (Furness, 2006). Higher magnification of the colonic mucosal sections presented here not only reveals that some of axonal projections touch the surface of the crypt cells, but some were even found to penetrate through the single epithelial cell layer towards crypt lumen (Figure 3.2B). These nerve fibers could potentially be mucosal colonic sensory neurons responsible for sensing the luminal contents. However, the actual function of these penetrable nerve fibers is as yet unknown.

It has been long appreciated that cholinergic neurons are the major source of Ach in the colonic mucosa. CHAT is the enzyme responsible for synthesising Ach, while VAChT is responsible for Ach loading into vesicles prior to secretion. Since CHAT and VAChT are abundantly expressed in cholinergic nerve endings, both proteins have been used as cholinergic neuronal markers in immunohistochemical studies (Ichikawa, et al., 1997). In the human colonic mucosa, cholinergic innervation was primarily found at the base of the crypt, as well as in the muscularis mucosae and submucosa (Figure 3.4 and Figure 3.11). This observation further supports the previous finding that double immune-labelling of both

CHAT and neuronal markers was lacking (Reynolds, 2007). Similar to CHAT, VAChT positive neurons were found near the base of the crypts in the muscularis mucosae and the submucosa, and in the nerve fibers embedded in the lamina propria between the crypts (Figure 3.6A white arrows). The close proximity of the cholinergic neurons with the colonic epithelium may provide the shortest distance for Ach diffusion.

CHAT was also detected on the basal membrane of the colonic crypts, colocalised with M3AchR (Figure 3.5B iii). The presence of CHAT positive cells in the human colonic epithelium suggests the possible existence of a non-neuronal Ach system in the human colon. Jönsson and colleagues were the first group to demonstrate the positive immune-labelling of CHAT protein within the human colonic epithelium, yet they did not show the expression pattern of these cells along the crypt axis (Jönsson, et al., 2007). CHAT-positive cells are here found to be intact epithelial cells (Figure 3.5C), mainly present at the base to the mid region of the crypt, where the proliferative epithelial cells reside (Figure 3.5A). Most importantly, VAChT positive signals were also detected in the human colonic crypts (Figure 3.6A), consistent with the previous finding of VAChT expression in the human colon (Jönsson, et al., 2007). Thus, the human colonic epithelium is equipped with the machinery for a non-neuronal Ach system which strongly suggests the epithelial self-regulation in the absence of neuronal innervation. Moreover, recent studies have suggested the involvement of the organic cation transporters (OCT) in regulating non-neuronal Ach release in the rat colonic epithelium, in response to short chain fatty acids (Yajima, et al., 2011; Bader, et al., 2014). Yajima and colleagues demonstrated the role of OCT in Ach release in the absence of VAChT expression; in contrast Bader et al demonstrated the expression of VAChT in the rat colonic epithelium, yet VAChT blockade was ineffective in blocking the propionate induced short-circuit current and the release of Ach into the basolateral compartment. Thus, further experiments are required to investigate the functional role of VAChT within the human colonic epithelium; measurement of Ach level before and after the treatment with OCT or VAChT inhibitors is underway in our laboratory.

The identity and functions of the CHAT positive cells described here are currently unclear. Jönsson and colleagues have demonstrated CHAT labelling in enteroendocrine cells (Jönsson, et al., 2007). As enteroendocrine cells are known to be able to secrete hormones into the basolateral compartment, it is a reasonable supposition that these CHAT positive cells might fulfill a similar function with Ach, basal secretion of which could then bind to MAchR expressed on the basal membrane.

To confirm their findings, CHAT-positive cells were assessed for expression of the enteroendocrine cell marker chromogranin A (Figure 3.7). CHAT was indeed detected in enteroendocrine cells (Figure 3.7D), however some cells only exhibited CHAT labelling (Figure 3.7D iii white arrow), suggesting that these cells might represent previously undescribed epithelial cell types. Tuft cells are a newly identified epithelial cell type with unknown functions. Based on the cell morphology of the CHAT positive cells in the current study, they were further characterised by the tuft cell marker DCAMKL-1 (Figure 3.8). However, the results were inconclusive and further experiments are necessary to confirm the identity of these CHAT positive cells in the human colonic epithelium.

Previous studies have demonstrated the expression of M2AchR (Jönsson, et al., 2007) and M3AchR (Lindqvist, et al., 2002; Reynolds, et al., 2007; Harrington, et al., 2010) in the human colonic epithelium. However, no study so far has characterised all five MAchR subtypes in the human colon. In the current study, expression of all five MAchR mRNA were investigated. M3AchR was found to be the predominant subtype expressed in both colon biopsies and isolated crypt samples. M1AchR and M5AchR transcripts were also detected in both samples albeit at a lower level than M3AchR (Figure 3.9). These results suggest that M1AchR, M3AchR and M5AchR are the three major MAchR subtypes expressed in the human colon, which was confirmed by detection of all three receptors in microdissected and isolated cultured crypts (Figure 3.10). M2AchR mRNA was only detected in two of the five colon biopsy samples, but no expression was observed in isolated crypt samples. The explanation for this could be either that M2AchR is not expressed in the colonic mucosa, or the expression level was too low to be detected by conventional PCR. While M4AchR mRNA was undetectable in the colon biopsies, relatively higher expression was observed in three of the five isolated crypt samples suggesting that M4AchR transcription might be induced during the isolation processes. In addition, the overall mRNA expression level of each subtype was relatively higher in isolated crypt samples than in colon biopsy samples. This observation suggests that the receptor mRNA was either predominantly expressed in the colonic mucosa, or the isolated crypt samples provided a more concentrated mRNA sample for the PCR reaction. One other explanation would be the receptor transcripts were induced during the isolation processes. Moreover, not every individual showed concomitant expression of M1AchR, M3AchR and M5AchR in the colon. Since all three receptors couple to the G_q protein signal transduction pathway, it is possible that there is a functional compensation between these three receptor subtypes.

MAchR subtypes 1, 3 and 5 are expressed on the basal membrane of the cultured crypt model, which resembles the expression pattern on the microdissected crypts (Figure 3.10B and C). M3AchR expression at the base of the crypt was also consistent with the previous findings in our lab (Lindqvist, et al., 2002; Reynolds, et al., 2007). This native human colonic crypt culture model maintained many features of the intact colonic mucosa in both morphology and function; they are proliferative, polarised and intact, and also exhibit secretion coupling in culture in response to agonist stimulation (Figures 3.12, 3.13 and 3.14). This model allows us to study the cell biology and physiology of live colonic epithelium that is otherwise not possible to achieve in fixed colon biopsy tissues. Our lab has repeatedly demonstrated that cholinergic stimulation of M3AchR mobilises intracellular Ca^{2+} in this model (Lindqvist, et al., 2002; Reynolds, et al., 2007), and that these Ca^{2+} signals were shown to mediate fluid secretion via the Na-K-Cl cotransporter NKCC1 (Reynolds, et al., 2007). However, the intracellular Ca^{2+} stores responsible for this signal transduction is not known. In order to study the intracellular Ca^{2+} signalling in the live human colonic epithelium, the expression and localisation of the intracellular Ca^{2+} stores and the respective Ca^{2+} releasing channels were investigated in the cultured crypt.

3.1.8.2 Calcium signalling machineries in the human colonic epithelium

The ER – the major intracellular Ca^{2+} store within a cell – was found at the basal pole of the crypt epithelial cells surrounding the nucleus (Figure 3.15B). The ER is relatively large in size within the goblet cells as defined by the prominent KDEL labelling (Figures 3.15B and 3.21B). In a 2D equatorial view, the ER is located below the basal membrane and extends towards the middle of the cell. This large intracellular compartment is believed to be responsible for the continuous synthesis of mucus, protein chaperones and anti-microbial peptides to replenish the mucus barrier. In addition, the close proximity between the ER and M3AchR on the basal membrane of the crypt provides a short distance for IP3 diffusion and subsequent signal transduction. The acidic organelles such as the lysosomes and the secretory vesicles have recently emerged as other important cellular Ca^{2+} stores (Morgan, et al., 2011). Lysosomes were mainly located in the cytoplasm towards the apical pole of the cell (Figures 3.15E and 3.15F). Thus, the two intracellular Ca^{2+} pools were located at distinct opposite poles within the colonic epithelial cells in a 2D view. Low levels of lysosomes were also detected at the basal pole of the crypt in 2D view (Figure 3.15F and Figure 3.18B), which suggests that the lysosomes are localised in the cytoplasmic space surrounding the nucleus and the ER in a 3D view. These results further suggest that there is a close association

between the ER and lysosomal Ca^{2+} stores near the basal membrane and in the mid-region of the cell. Mitochondria are another important Ca^{2+} storage organelle. Ca^{2+} uptake into the mitochondria can influence the initial Ca^{2+} signal and subsequent transduction (Rizzuto, et al., 1998; Brough, et al., 2005; Ruzzuto, et al., 2012). Mitochondria are mainly localised at the basal pole of crypt in close association with the ER and the nucleus (Figure 3.15G). The transfer of Ca^{2+} from the ER via IP3R to the mitochondrial matrix has been shown to be crucial for mitochondrial-specific functions, including the regulation of cell survival/death (Giorgi, et al., 2008; Harr, et al., 2010; Giorgi, et al., 2012). Mitochondria were also found in the cytoplasm in close proximity to the region where the lysosomes reside (Figure 3.15G). The diffuse pattern of mitochondrial localisation suggests they are interacting with different intracellular organelles to monitor Ca^{2+} mobilisation within a cell.

Information regarding the expression patterns of the intracellular Ca^{2+} channels in human colonic epithelial cells are limited. In the current study, transcripts for all three IP3R isoforms were expressed in the colonic epithelium of all human subjects tested (Figure 3.16). RYR1 and RYR2 mRNA was also detected in most of the human samples. Lack of expression of both RYR isoforms in subject 3 could be a result of an extremely low transcript level of both RYR isoforms in this particular individual that could not be detected by conventional PCR, or this individual might express the RYR3 isoform which was not measured in the current study. Moreover, SERCA1 mRNA was detected in most subjects, while SERCA2 and SERCA3 mRNA were detected in all human subjects. The lack of the SERCA1 isoform would not be expected to cause a problem to that particular individual, as the function of the channel can be compensated by the two other SERCA isoforms. Furthermore, both TPC1 and TPC2 mRNA was also detected in all human subjects.

The expression and localisation of the intracellular Ca^{2+} channel proteins in the cultured crypt model was further confirmed by immunostaining. All IP3R subtypes were expressed in the colonic epithelium. Both IP3R1 and IP3R2 have similar patterns of localisation throughout the cell (Figure 3.17A and B), while IP3R3 expression was restricted to the basal membrane of the crypt (Figure 3.17C). One interesting observation is that the IP3R2 was expressed on the apical membranes of the crypt that are disparate from the ER. It is currently unknown whether this expression pattern is related to the acidic lysosomes and the secretory vesicles. The presence of IP3R3 in the normal colonic mucosa was in contrast with the findings from a recent cohort study that only found IP3R3 expression in colorectal cancer tissues (Shibao, et al., 2010). This discrepancy could be a result of induced receptor expression in the culture system or elevation of IP3R3 expression in the normal mucosa near the tumour tissues of

these five random patients. Moreover, both RYR and SERCA proteins were also expressed in the colonic epithelium in close proximity to the ER (Figure 3.17D and F). Furthermore, both TPC1 and TPC2 proteins were detected in the cytoplasm towards the apical pole of the cell, expression patterns which fully resemble the location of the lysosomes (Figure 3.18A). TPC2 has been found to be expressed primarily on late endosomes and lysosomes (Brailoiu, et al., 2009; Calcraft, et al., 2009; Ruas, et al., 2010). Double labelling of TPC2 and the lysosomal marker LAMP-1 in the same tissue revealed overlapping regions and clustering of the two markers, however co-localisation of these two markers was not observed (Figure 3.18B). In addition, the colonic epithelium also expressed the ectoenzyme CD38 that is responsible for the generation of both 2nd messenger cADPR and NAADP that act on RYR and TPCs respectively. CD38 expression was strongly associated with lysosomes and TPC2 labelling (Figure 3.18C), that is believed to provide the shortest distance for the diffusion of 2nd messengers. Hence, the human colonic crypt culture model is fully equipped with all relevant intracellular Ca^{2+} signalling organelles and channels, which form the basis for the investigation of Ca^{2+} coupling to mucus secretion.

Goblet cells are the mucus secreting cells embedded in the colonic epithelium. These cells normally possess a large round cytoplasmic space, that can be even sometimes be distinguished by the naked eye in a bright field image. MUC2 mucin labelling is commonly used to identify goblet cell populations in the epithelium, as well as providing information about the mucus content of the cell. Double immunostaining of the lysosomes and mucus granules revealed a strong association between these two organelles. Under unstimulated basal conditions, three levels (low, medium and high) of mucus secretion can be discerned in goblet cells. Higher numbers of LAMP-1 positive lysosomes in the cytoplasm of goblet cells during low levels of mucus secretion and vice versa (Figure 3.19A), suggests endocytosis and exocytosis of these acidic organelles might be important for the secretion of mucus granules. In general, almost all the cytoplasmic space of these goblet cells contains mucus granules. In comparison with other epithelial cell types, the lysosomal content is relatively low in goblet cells (Figure 3.19A left). These lysosomes are mainly located beneath the basolateral membranes and in the mid-cell region associated with the ER in 2D view. The strongest lysosomal labelling was found in the lateral membrane towards the apical membrane of the cell (Figure 3.19B and C), suggesting the mucus granules are flanked by the acidic lysosomes in a 2D view. If one were to transform these 2D data into the third dimension, it should produce an arrangement in which mucus granules are surrounded closely on all sides by acidic lysosomes, which are then poised to provide the Ca^{2+} signals for mucus exocytosis.

In addition, the expression patterns of both TPC1 and TPC2 in goblet cells resemble the lysosomal labelling (Figure 3.20 and Figure 3.21). Double immunolabelling of the ER and TPC2 revealed a close association in the region of the mature mucus granules (Figure 3.21C). In addition, goblet cells also express the ectoenzyme CD38 in close proximity to the ER, acidic lysosomes and the mucus granules (Figure 3.22), and are believed to be the source of 2^{nd} messengers for mobilising Ca^{2+} from both of the intracellular Ca^{2+} stores. These goblet cells should be capable of responding to agonist stimulation in the absence of neighbouring epithelial cells.

This first results chapter has confirmed the cholinergic-epithelial cell interactions in the human colonic epithelium. The spatio-temporal characteristics of the Cch-induced Ca^{2+} waves in this intact and polarised human colonic crypt culture model was firmly established. The machinery for non-neuronal Ach systems in the human colonic epithelium were also described, although the mechanism of regulation is currently unclear. Most importantly, the expression and localisation of the Ca^{2+} signalling toolkit in human colonic crypt epithelial cells (including goblet cells) was identified. This signalling toolkit includes the major intracellular Ca^{2+} stores, 2^{nd} messengers and Ca^{2+} release channels. The subcellular localisation and the complex interactions between these signalling elements generate Ca^{2+} signals with broad spatial and temporal properties. The basal location of the ER, IP3R and RYR, and the apical location of lysosomes, TPCs and CD38 in colonic epithelial cells provide a rationale for an investigation of the cellular consequences of cholinergic stimulation and the subsequent regulation of Ca^{2+} coupling mucus secretion in the human colonic epithelium.

Chapter 4 Results: The underlying mechanisms of the cholinergic stimulated calcium signal generation in human colonic crypts

4.1 Introduction

Ca^{2+} is an important 2nd messenger that is primarily stored inside the intracellular organelles including the ER, mitochondria and lysosomes within a cell (Berridge, 2002; Morgan, et al., 2011; Rizzuto, et al., 2012). An increase in intracellular [Ca^{2+}] derived from either the influx of extracellular Ca^{2+} or release from intracellular stores triggers a variety of cellular and physiological functions (Dupont, et al., 2011). Accordingly, movement of Ca^{2+} needs to be tightly regulated via the specific channels expressed on the plasma and organellar membranes. The intracellular Ca^{2+} channels expressed on the ER membrane include IP3R and RYR have been well studied for decades, whereas TPCs that mediate Ca^{2+} release from the acidic lysosomes have been gaining attention in recent years (Taylor and Dale, 2012). Cholinergic activated MAchR signalling has an established role in generating the 2nd messenger IP3, which binds to its receptor causing the mobilisation of Ca^{2+} from the ER store and the subsequent CICR response (Felder, 1995; Nahorski, et al., 1997). In addition, GPCR signalling, including MAchR activation, has also been suggested to upregulate CD38 activity (Higashida, et al., 1997a and b; Higashida, et al., 2001a and b); CD38 is an ectoenzyme that is responsible for the generation of two Ca^{2+} mobilising 2nd messengers: cADPR (an agonist for RYR) and NAADP (an activator of TPC) (Ogunbayo, et al., 2011). Thus, interactions between multiple Ca^{2+} releasing 2nd messengers and Ca^{2+} stores generate complexities and specificity of the Ca^{2+} signals (Galione, et al., 2002). Given the cellular and molecular characterisation of the colonic crypt Ca^{2+} signalling toolkit in the previous chapter, it is conceivable that in polarised epithelial cells MAchR activation stimulates multiple Ca^{2+} releasing messengers that mobilise Ca^{2+} from multiple organelles to generate a cholinergic-specific Ca^{2+} signature.

A close correlation between Ca^{2+} signalling and mucus secretion has been established in several model systems including animal GI tracts (Neutra, et al., 1982; Seidler, et al., 1989; Hamada, et al., 1997; Yang, et al., 2013) and human colon cancer cell lines (Mitrovic, et al., 2013). However, the underlying molecular mechanism of the cholinergic-mediated Ca^{2+} signal generation in the human colonic epithelium is yet to be described. This current work investigated three levels of interactions, from the intact tissue (i.e. colonic crypt), to single polarised epithelial cells, to the intracellular organelle that serve as Ca^{2+} stores (Figure 4.1). In the previous chapter, the cellular and molecular Ca^{2+} signalling machineries in the human

colonic crypt culture model were characterised. In this chapter, the cultured crypt model was further utilised to study the underlying mechanism of intracellular Ca^{2+} signal generation upon M3AchR activation in the human colonic crypt. This was achieved by combining fluorescence Ca^{2+} imaging, immunohistochemistry and confocal microscopy. Since isolated, single crypts are no longer embedded in the lamina propria, cholinergic signals were mimicked by the addition of Ach or Cch to the in vitro system.

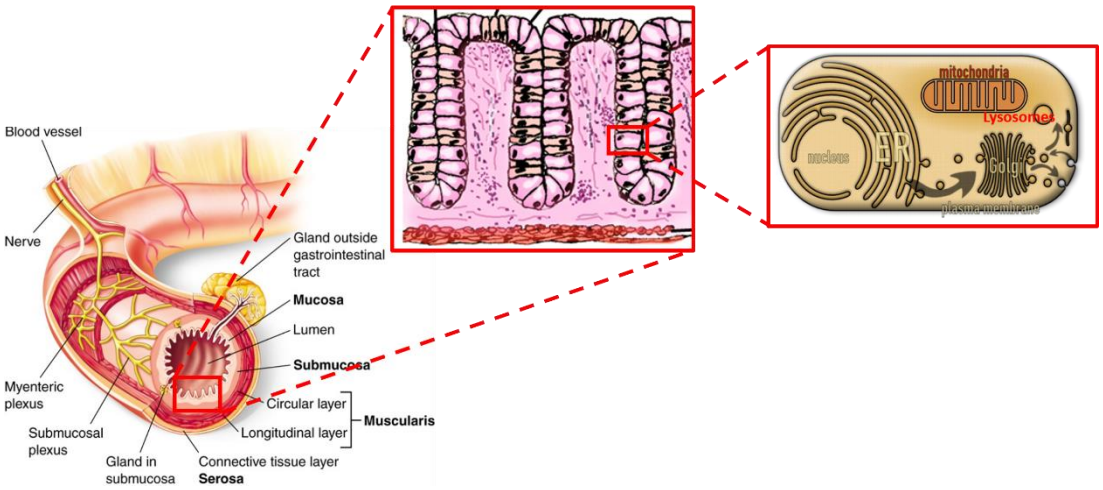

Figure 4.1 Cholinergic mediated signal transduction from the organ colon to individual epithelial cells.

Enteric cholinergic neurons are the major source of the neurotransmitter Ach in the colon (left). Ach is secreted at the enteric axon terminals in close proximity with the colonic epithelium (crypts, middle). The binding of Ach to the MAchR on the epithelial cell surface triggers intracellular Ca^{2+} signalling in the epithelial cells (right) that subsequently spread along the crypt-axis via gap junctional proteins.

(Figures from McGraw Hill text book Human physiology (left); cram Mm histology 1 epithelia flashcards (middle); ETH Zurich, Institute of Biochemistry, Kornmann group research page (right))

4.1.1 Cholinergic mediated calcium signalling in the human colonic epithelium

Application of Ach to both rat and human colonic crypts has previously been shown to mobilise Ca^{2+} in a wave-like manner, via the activation of M3AchR. These Ca^{2+} signals initiated at the base of the crypt and then propagated along the entire crypt-axis (Lindqvist, et al., 1998; Lindqvist, et al., 2002; Reynolds, et al., 2007). In order to investigate the underlying molecular mechanism of Ca^{2+} signal generation upon M3AchR activation, cholinergic mediated Ca^{2+} signals in cultured human colonic crypts were reproduced and the spatiotemporal characteristics were confirmed in the current study. Isolated human colonic crypts that had been cultured for 16 to 40 hours were loaded with the intracellular Ca^{2+}-sensitive dye Fura-2/AM (5µM) for 2 hours. In order to avoid the hydrolysis of Ach by endogenous cholinesterases, Cch (a cholinesterase-resistant Ach analogue) was used for all experiments in the current study. 10µM of Cch has been shown to be sufficient to evoke a biphasic Ca^{2+} response in human colonic crypts (Lindqvist, et al., 2002). Addition of Cch (10µM) elicited a significant increase of intracellular Ca^{2+} at the crypt base, as demonstrated in the pseudocolour images in Figure 4.2A (top panel) and the corresponding traces (Figure 4.2A bottom panel).

Specifically, the Ca^{2+} waves begin at the apical pole of the 'initiator' cells at the crypt base, then spread to the basal pole of cells before further propagating along the entire crypt-axis (Figure 4.2Ba). Region of interests (ROIs) drawn along the crypt demonstrate the progressive propagation of the Ca^{2+} signal along the crypt-axis following initiation at the crypt base (Figure 4.2A bottom left panel). Intracellular Ca^{2+} levels at the crypt-base increased to a peak level between 30-100 seconds after Cch administration and then plateaued, presumably due to ER store-operated or mitochondrial Ca^{2+} reuptake, and extrusion by plasma membrane Ca^{2+} ATPase. With the continuous presence of Cch, the intracellular [Ca^{2+}] does not return to resting levels (Figure 4.4 top Ca^{2+} trace). However, upon removal of the agonist, the cytosolic [Ca^{2+}] returned to baseline within 3-10 mins (Figures 4.3A and 4.4), which indicates some variability of the plateau phase persistence after agonist removal between different crypts/individuals. Thus sustained M3AchR activation elicits an intracellular [Ca^{2+}] above resting levels, and this behavior is maintained over a culture period of at least 3 days (data not shown). Also, these Cch-induced Ca^{2+} waves have previously been shown to exhibit similar spatial characteristics regardless of the age and gender of the patients (Lindqvist, 2000).

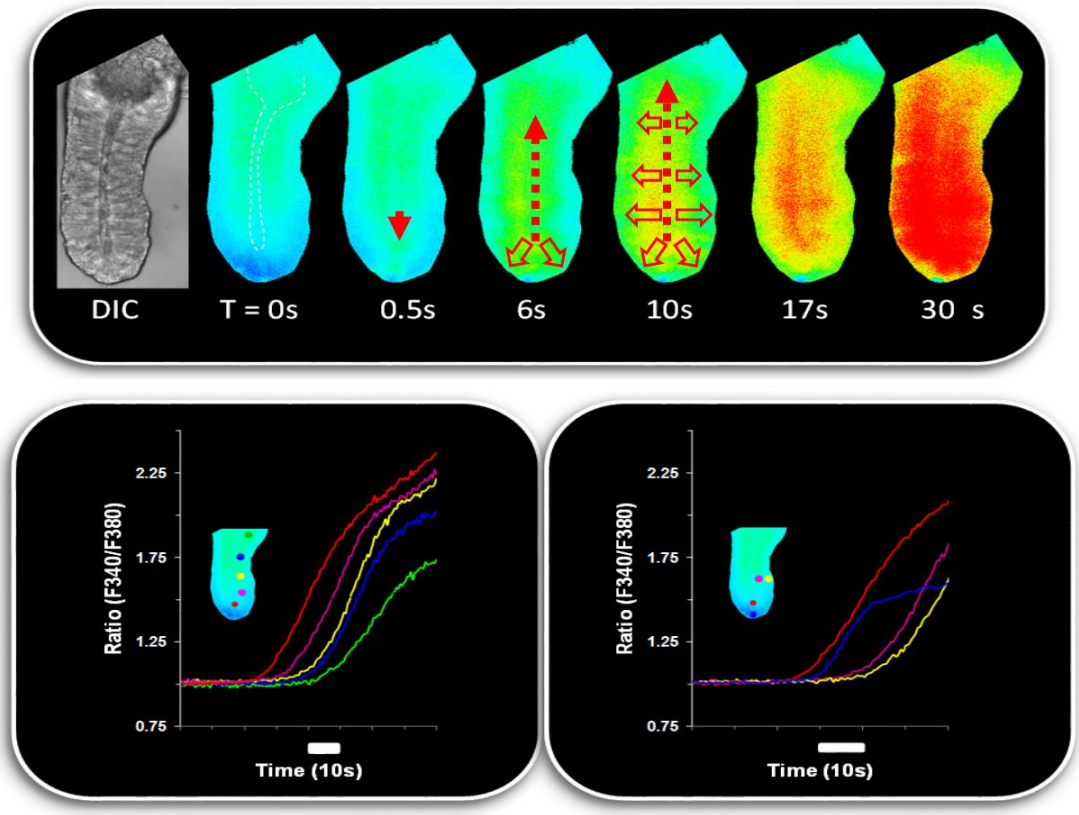

Figure 4.2A Spatio-temporal characteristics of Cch-induced human colonic crypt Ca^{2+} waves.

Application of Cch (10µM) to a day-1 cultured human colonic crypt loaded with Fura-2/AM (5µM). Upper panel shows the DIC image of the human colonic crypt, and the pseudocolour Fura-2 ratio images with respective time (T) of Cch administration (blue pseudocolour = low Fura-2 ratio, red pseudocolour = high Fura-2 ratio) . The Ca^{2+} signal initiates at the apical pole of the 'initiator' cells at the base of the crypt (0.5s) and then spreads to the basal pole of the 'initiator' cells (6s) before further propagation along the entire crypt-axis in a unidirectional manner (10-30s). Bottom panels are traces of the Ca^{2+} signals that represent the change in Fura-2 ratio along the crypt-axis. Region of interests (ROIs, colour dots) were placed along the crypt-axis to detect the Fura-2 ratio changes with respect to time (Bottom left panel). The Ca^{2+} signal is progressively registered along the crypt-axis as demonstrated by the red ROI at the crypt base, first in the trace, which then spreads to pink, yellow and blue ROIs, with the green ROI at the mid region being last in the trace. ROIs were also placed at the basal and apical poles at the base and mid region of the crypt (bottom right panel). Ca^{2+} signal at the apical pole (red) at the base of crypt came first in the trace then spread to the basal pole (blue); similarly, the Ca^{2+} signal at the apical pole of mid region of crypt (purple) came first in the trace then spread to the basal pole (yellow). Images were taken with a x40 objective. This figure was provided courtesy of Mark Williams.

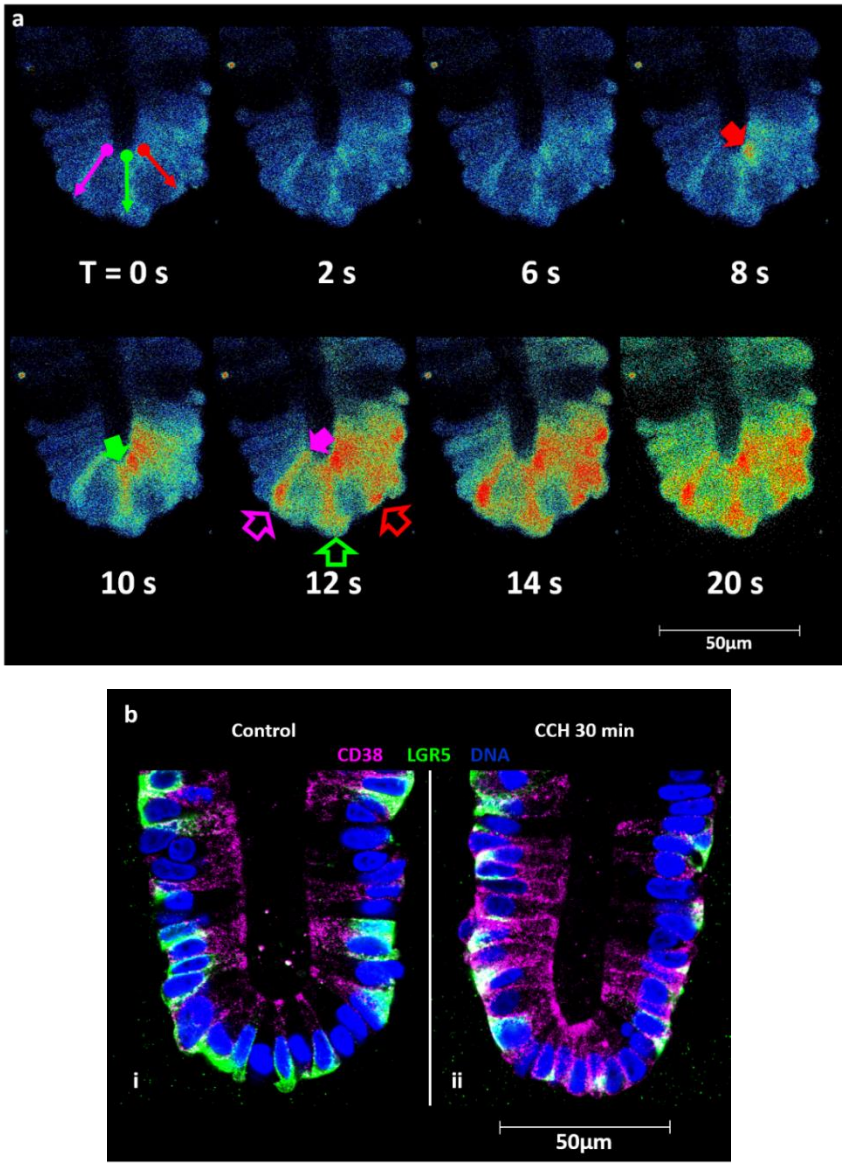

Figure 4.2B Potential Ca^{2+} initiator cells

Application of Cch (10µM) to a day-1 cultured human colonic crypt loaded with Fluo-4/AM (5µM). (a) Ca^{2+} signal initiates at the apical pole of the 'initiator' cells at the base of the crypt (8s) and then spreads to the basal pole of the 'initiator' cells (10-12s) before further propagation along the entire crypt-axis (20s). Filled colour arrows show the point of initiation in the initiator cells, while the open arrows show the propagation of the signals to the basal pole of initiator cells. Each of the red, pink and green arrows pointed to individual initiator cells at the base of the crypt. (b) Human colonic crypts were either unstimulated or stimulated with Cch (10µM) for 30 min. The samples were then fixed and stained with anti-CD38 (pink) and anti-LGR5 (green) antibodies, cell nuclei were stained with Hoechst (blue). Images were taken with a Zeiss confocal microscope with a x63 objective. (i) control, (ii) Cch stimulated for 30 min. Images are representative of N=2 subjects, n=6 crypts.

4.1.2 Characteristics of the Cch-induced calcium signals

The Ca^{2+} response evoked by repetitive stimulation (duration of 1-2 minutes; interval greater than 10 minutes) with Cch (10µM) at the base of the crypts were both reversible and reproducible (consistent peak, 0.99 ± 0.03, N= 6 subjects, n= 8 crypts, paired t-test p= 0.85, Figure 4.3A), making it possible to investigate the effects of Ca^{2+} channel blockers using a paired experimental design. The crypt to crypt peak amplitude of the response (from baseline to peak) ranged from approximately 0.3-1.5 between different crypts and individuals, with an average amplitude of approximately 0.5 Fura-2 ratio units observed in most crypts (e.g. Figure 4.3A). The variability in amplitude of the response could be a result of the different expression levels of the MAchR between individuals and the regions of the colon; this was not investigated in the current study. Moreover, a number of features associated with the Cch-induced Ca^{2+} transients were concentration-dependent (Figure 4.3B): these included the latency of the response (from point of stimulation to peak), the initial rate of increase and the peak amplitude, the persistence of the plateau phase, and the length of resolving phase (back to baseline level) of the response. The dose-dependent response of Cch has been described previously in our lab (Lindqvist, et al., 2002; Reynolds, et al., 2007). In this study, the concentration dependent effect of Cch was briefly investigated. Cch (1µM) was insufficient to evoke a regenerative Ca^{2+} wave (mean amplitude 0.026 ± 0.008, normalised to 1 ± 0, N= 2 subjects, n= 3 crypts), while Cch (10µM) is adequate to generate the Ca^{2+} waves along the entire crypt-axis (normalised mean amplitude 6.7 ± 0.86, N= 2 subjects, n= 3 crypts). In addition, a maximal amplitude of Ca^{2+} response was observed when the crypts were treated with 50µM Cch (normalised mean amplitude 22.6 ± 7.8) and 100µM Cch (normalised mean amplitude 15.9 ± 4.4, N= 2 subjects, n= 3 crypts), confirming that the Ca^{2+} response to Cch is concentration-dependent (Figure 4.3Bii). Furthermore, the mean amplitude of Ca^{2+} response to 100µM Cch was lower than that of 50µM Cch, this could possibly either be due to the short resting interval (about 10 min) between Cch (50µM) and Cch (100µM) treatment to allow refilling the ER store, or M3AchRs becoming desensitised after Cch (50µM) treatment.

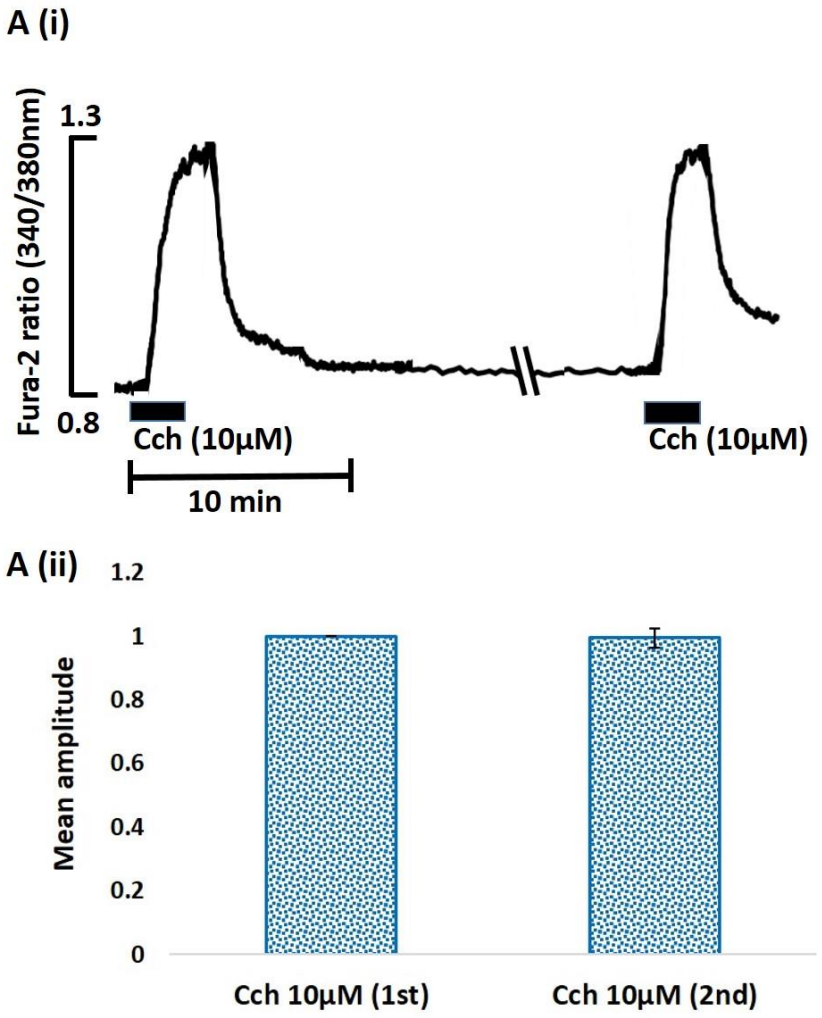

Figure 4.3A Reproducible Ca^{2+} response to successive pulse of Cch

(Ai) Representative Ca^{2+} trace showing response to successive Cch (10µM) treatment (duration=black bar). Fura-2 ratio changes along human colonic crypts pulsed with successive Cch (10µM), with a greater than 10 min resting interval after the first Cch administration. (Aii) The mean amplitude of the first and second Cch responses were calculated, before the mean amplitude of the 2nd response was then normalised to the 1st response and displayed as mean ± SE. Results were representative of N= 6 subjects, n= 8 crypts, paired t-test p= 0.85.

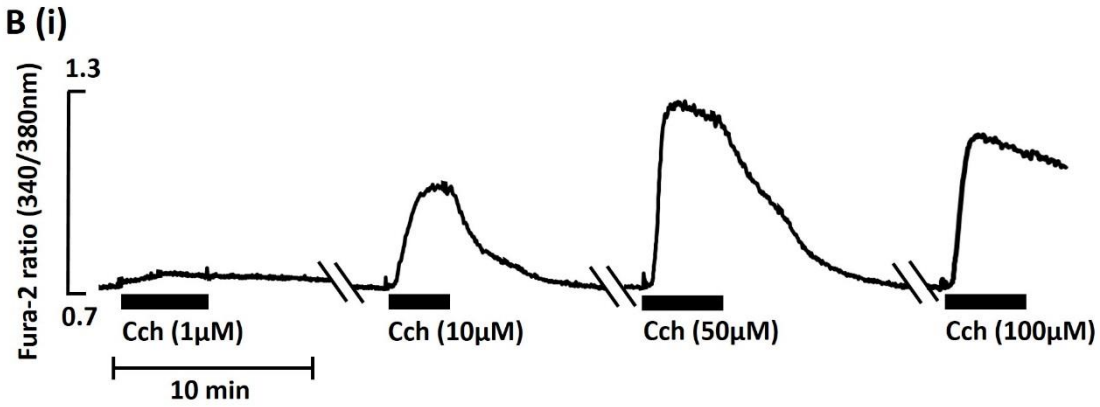

B (ii)

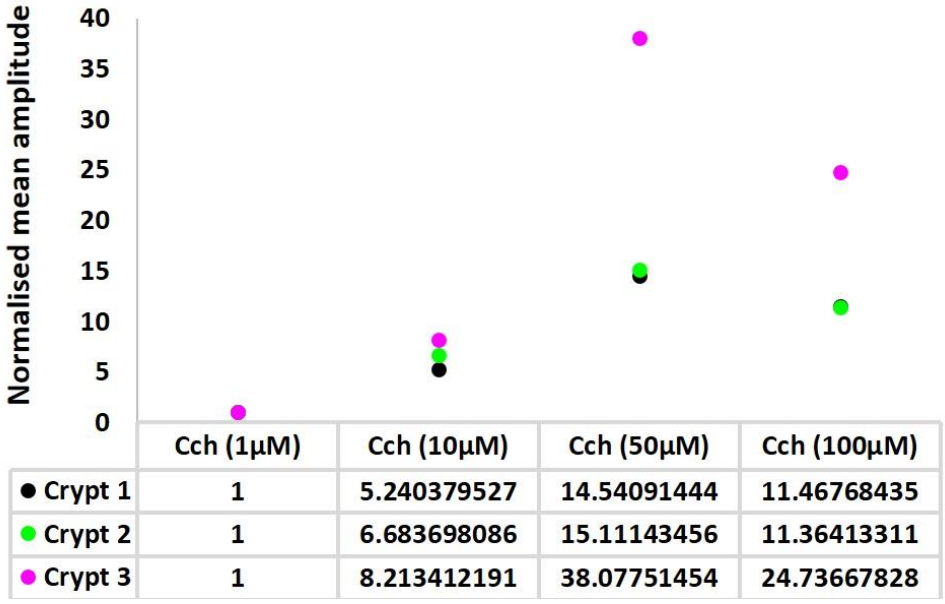

	Cch (1µM)	Cch (10µM)	Cch (50µM)	Cch (100µM)
● Crypt 1	1	5.240379527	14.54091444	11.46768435
● Crypt 2	1	6.683698086	15.11143456	11.36413311
● Crypt 3	1	8.213412191	38.07751454	24.73667828

Figure 4.3B Cch dosage response in human colonic crypts

(Bi) Traces are Fura-2 ratio changes in response to increasing concentrations of Cch (1µM, 10µM, 50µM and 100µM) (duration=black bar) along human colonic crypts loaded with Fura-2/AM (5µM). The crypt exhibited the same resting baseline ratio throughout the experiment. Intervals between each Cch administration were ≥ 10 min. (Bii) Concentration dependent features of the Cch-induced Ca^{2+} responses. Mean amplitudes of Ca^{2+} responses (from 4-5 ROIs) to each Cch dosage were calculated, then normalised to the lowest Cch (1µM) Ca^{2+} response and displayed as normalised mean values from N=2 subjects, n=3 crypts. Significance was assessed using a One-way ANOVA test, $F(3, 8) = 8.3$, $p = 0.008$; followed by Tukey's post hoc analysis. Significant difference ($p < 0.05$) was observed between pairs of mean values including (i) Cch (1µM) vs. Cch (50µM), (ii) Cch (1µM) vs. Cch (100µM), (iii) Cch (10µM) vs. Cch (50µM).

4.1.3 Cch-induced calcium release from intracellular calcium stores

In order to confirm whether the increase of intracellular [Ca^{2+}] is a result of Ca^{2+} release from intracellular stores (i.e. not from extracellular influx of Ca^{2+}), human colonic crypts were pre-incubated with Ca^{2+}-free HBS (supplemented with 1mM EGTA to chelate endogenous Ca^{2+}). Similar level Ca^{2+} transients in response to Cch were observed in the presence and absence of extracellular Ca^{2+} (Figure 4.4). The initial phase of the Ca^{2+} response (from initiation to peak) conducted with Ca^{2+}-free HBS was similar to the control. This phenomenon was observed in both the crypts stimulated with either Cch (10µM) or Cch (50µM, not shown). Thus, these results further confirmed the mobilisation of Ca^{2+} from intracellular stores into the cytosol upon Cch stimulation.

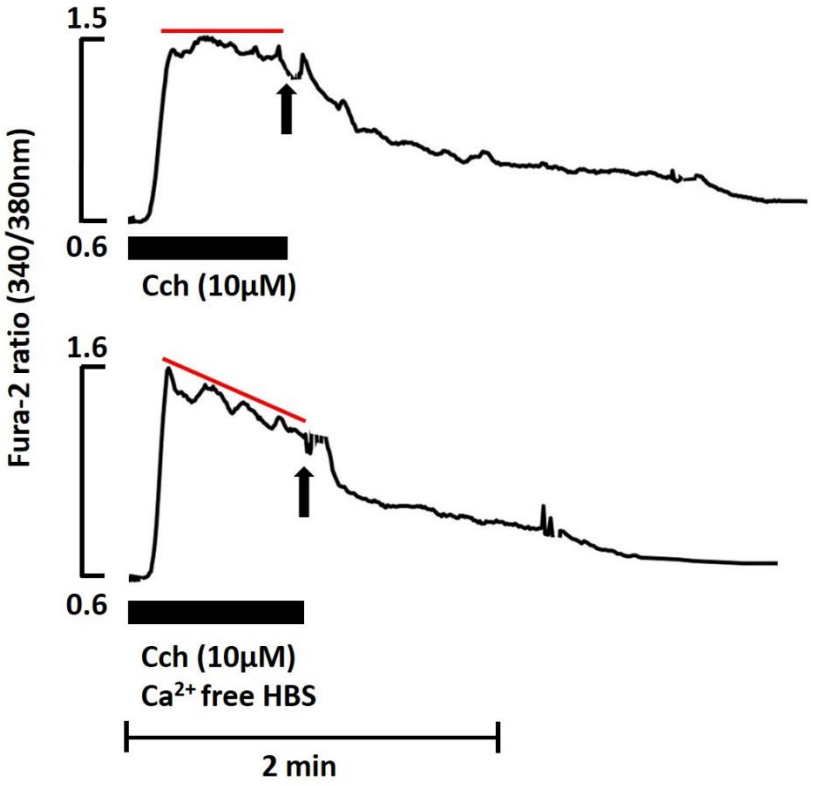

Figure 4.4 Effects of extracellular Ca^{2+} on Cch-induced Ca^{2+} responses

Traces represent Ca^{2+} signals in response to Cch (10µM) stimulation (black bar) in the presence (top) or absence (bottom) of Ca^{2+} in the bathing medium. Bottom trace shows cultured human colonic crypts pre-incubated with Ca^{2+}-free HBS for at least 5 min before the addition of Cch (10µM) prepared with Ca^{2+}-free HBS. The initial phase of the Ca^{2+} response was shown to be independent of extracellular Ca^{2+} (top and bottom traces). With extracellular Ca^{2+} (top), the Ca^{2+} response to Cch plateaued (flat red line) and remained high while SOCE is activate and continuously refilling the ER store. Upon removal of Cch (black arrow), the cytosolic Ca^{2+} levels gradually returned to baseline. In the absence of extracellular Ca^{2+} (bottom), the initial phase of Ca^{2+} response gradually decreased (slope red line). Upon

removal of Cch (black arrow), the rate at which cytosolic [Ca^{2+}] returned to baseline was increased compared to the control.

The relative contribution of different intracellular Ca^{2+} organelles such as the ER and lysosomes to generate the Cch-specific Ca^{2+} response in the human colonic epithelium is unclear. Thapsigargin (Tg) is a non-competitive inhibitor of the SERCA pump that is commonly used to deplete the ER Ca^{2+} store. In order to investigate the importance of the ER Ca^{2+} store in response to Cch induced Ca^{2+} signal generation, colonic crypts were pre-treated with thapsigargin (1µM) for 40 mins to deplete the ER store. In the presence of extracellular Ca^{2+}, a gradual increase of intracellular [Ca^{2+}] (high amplitude, 1.44 ± 0.12, N= 4 subjects, n= 4 crypts) was observed, which is consistent with ER store depletion followed by an activated influx of extracellular Ca^{2+} into the cytosol due to the inability of the SERCA pump to refill the depleted ER store (Figure 4.5A). The intracellular [Ca^{2+}] remained elevated and then slowly diminished. In the absence of extracellular Ca^{2+}, treatment with thapsigargin caused an increase of intracellular [Ca^{2+}], but the intracellular Ca^{2+} level quickly returned to the baseline level (0.2 ± 0.04, N= 2 subjects, n= 4 crypts, Figure 4.5B). Interestingly, the subsequent application of Cch (10µM) in the presence of Tg induced a small increase of intracellular [Ca^{2+}] in the human colonic crypt in both the presence of extracellular Ca^{2+} (0.14 ± 0.03, N= 4 subjects, n= 4 crypts, paired t-test p= 0.017, Figure 4.5A (ii)) and absence of extracellular Ca^{2+} (0.1 ± 0.03, N= 2 subjects, n= 4 crypts, paired t-test p=0.012, Figure 4.5B (ii)) as compared to Cch alone, suggesting that cholinergic stimulation was able to mobilise Ca^{2+} from organelles other than the ER.

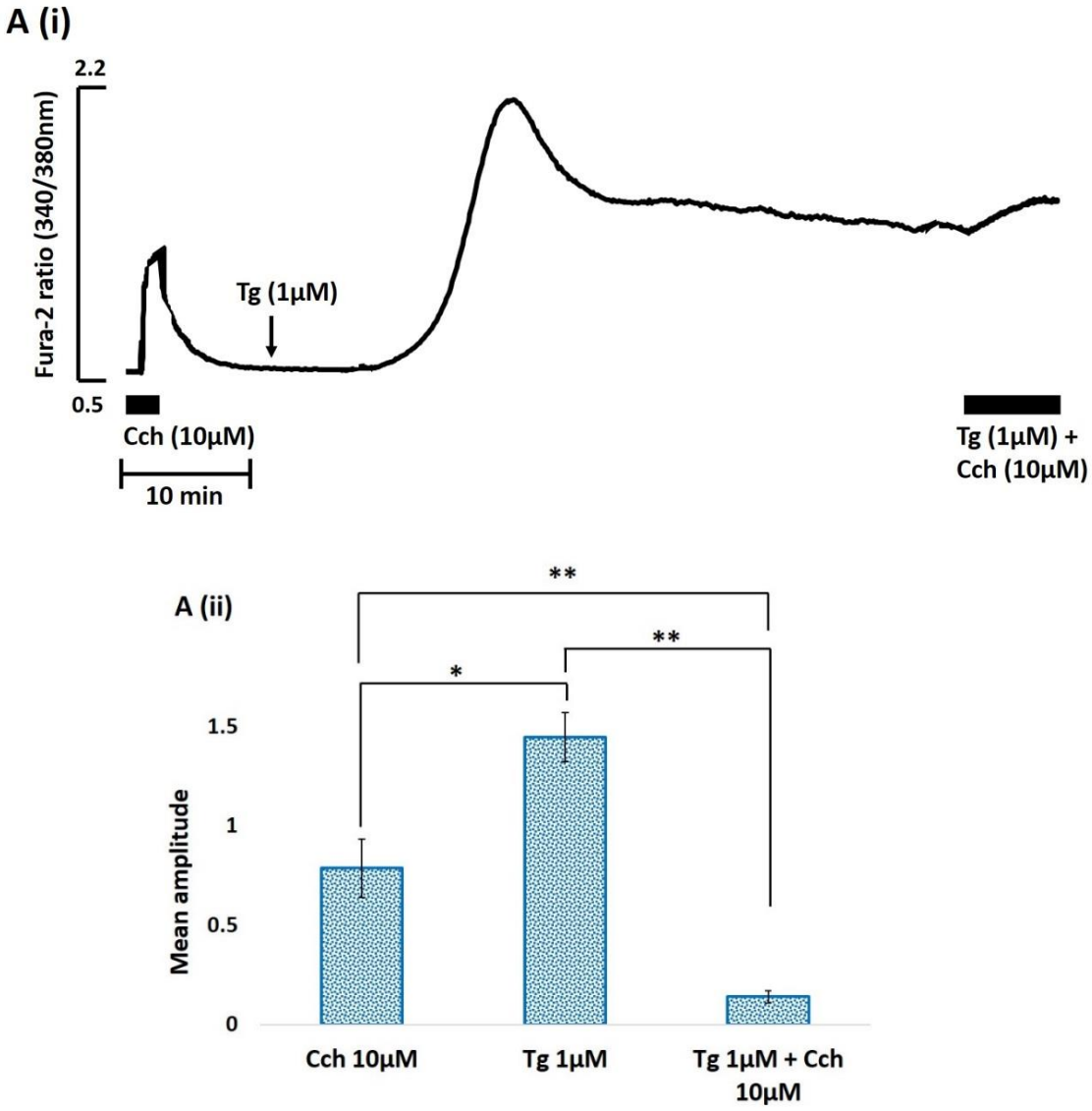

Figure 4.5A Effects of SERCA pump inhibition on the Ca^{2+} responses to Cch

(Ai) Control Ca^{2+} waves in response to Cch (10µM) (1st black bar) followed by thapsigargin (1µM) treatment to trigger depletion of the ER Ca^{2+} stores (arrows). In the presence of Ca^{2+} in the bathing medium, the Ca^{2+} peak contributed by the depletion of ER Ca^{2+} store is maintained by the influx of extracellular Ca^{2+} into the cytosol. A small Ca^{2+} response was observed when crypts were re-stimulated with Cch (10µM) (2nd black bar). (Aii) Mean amplitude of Ca^{2+} responses to all three treatments were calculated and displayed as mean ± SE. Representative data of N= 4 subjects and n= 4 crypts. Significant difference of the effect of thapsigargin (role of ER Ca^{2+} store) on Cch-induced Ca^{2+} response was assessed using One-way ANOVA test, $F(2,9)= 33.53$, $p= 0.00007$, followed by Bonferroni procedure and Tukey's post hoc analysis. Significant difference as indicated by asterisks (**) for $p< 0.01$ was observed between pairs of mean values including (i) Cch vs. Tg + Cch, (ii) Tg vs. Tg + Cch. Significant difference as indicated by asterisks (*) for $p< 0.05$ was observed between Cch vs. Tg.

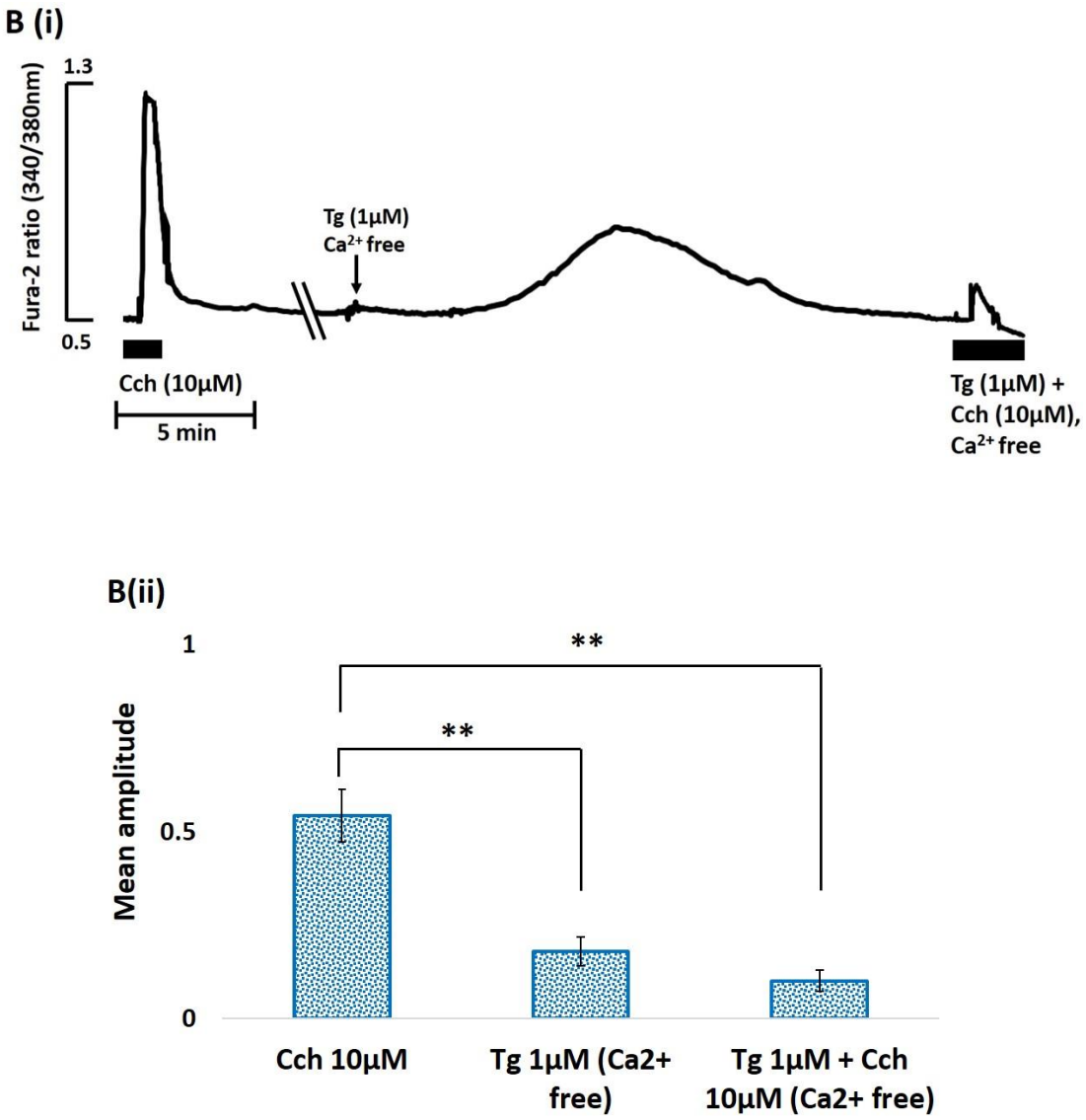

Figure 4.5B Role of SOCE to Cch-induced Ca^{2+} responses

(Bi) Control Ca^{2+} waves in response to Cch (10µM) (1st black bar) followed by thapsigargin (1µM) treatment to trigger depletion of the ER Ca^{2+} stores (arrows). In the absence of Ca^{2+} in the bathing medium, the latency of the Ca^{2+} signals in response to thapsigargin increased, and the Ca^{2+} peak quickly returned to baseline level. A small Ca^{2+} response was also observed when crypts were re-stimulated with Cch (10µM) (2nd black bar). (Bii) Mean amplitude of Ca^{2+} responses to all three treatments were calculated and displayed as mean ± SE. Data are representative of N= 2 subjects and n= 4 crypts. Statistical significant of the effect of thapsigargin (role of SOCE) on Cch-induced Ca^{2+} response was assessed using One-way ANOVA test, $F(2, 9)= 22.85$, $p= 0.0003$, followed by Bonferroni procedure and Tukey's post hoc analysis. Significant difference as indicated by asterisks (**) for $p< 0.01$ was observed between pairs of mean values including (i) Cch vs. Tg (Ca^{2+} free), (ii) Cch vs. Tg + Cch (Ca^{2+} free). No significant difference was observed between Tg (Ca^{2+} free) vs. Tg + Cch (Ca^{2+} free).

4.1.4 BAPTA abolished the Cch-induced calcium signals

In order to investigate whether chelation of intracellular Ca^{2+} blocks Cch-induced Ca^{2+} signals, cultured human colonic crypts were treated with the intracellular Ca^{2+} chelator BAPTA-AM (66µM) for 1 hour prior to the re-administration of Cch (10µM) (Figure 4.6 top panel). BAPTA-AM is taken up into cells like Fura-2/AM and de-esterified in the cytosol where it acts as a Ca^{2+} chelator which is highly selective for Ca^{2+} like EGTA. Chelation of intracellular Ca^{2+} decreased Cch-induced Ca^{2+} signals by greater than 85% (0.153 ± 0.03, N= 3 subjects, n= 10 crypts, paired t-test p< 0.01, Figure 4.6 bottom panel), and a similar level of inhibition was observed in experiments conducted with Ca^{2+}-free HBS (data not shown). These results suggested that 66µM of BAPTA-AM is an appropriate dosage for suppressing Cch-induced Ca^{2+} signals in the human colonic crypt.

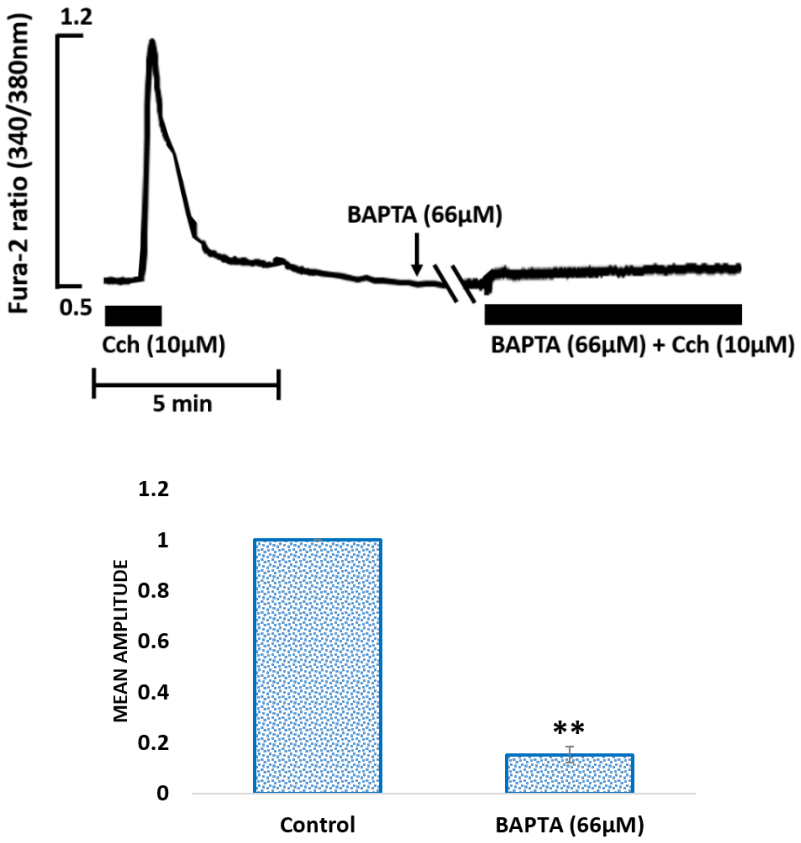

Figure 4.6 Role of BAPTA-AM on cholinergic mediated intracellular Ca^{2+} signals

Representative trace of Ca^{2+} responses (top). A control response to 10µM of Cch (amplitude 0.7) followed by pre-incubation with BAPTA-AM (66µM) for 1 hr. Crypts were then re-stimulated with Cch (10µM) with the presence of BAPTA-AM (black bar). The amplitude of the control and BAPTA treated Ca^{2+} responses were calculated and the mean values were plotted (bottom). Ca^{2+} responses were displayed as mean ± SE from N=3 subjects, n=10 crypts. Asterisks (**) denote a significant difference compared to the control (paired t-test, p< 0.01).

4.2 Characterisation of the calcium signal generation downstream of MAchR activation

A previous study from our laboratory used a range of MAchR antagonists to demonstrate that the Ca^{2+} signal is MAchR dependent, e.g. pre-incubation with atropine completely abolished colonic crypt Ca^{2+} signals stimulated with 10µM Cch (Lindqvist, et al., 2002). In keeping with the site of muscarinergic Ca^{2+} signal initiation at the crypt base, colonocytes at the base of the crypt have additionally been shown to be more sensitive to cholinergic stimulation and exhibited a higher expression level of M3AchRs (Lindqvist, et al., 2002). However, the intracellular molecular mechanism of Ca^{2+} signal generation at the base of the crypt is less well understood.

The MAchR signalling pathways involved in mobilising ER Ca^{2+} stores has been well described in numerous tissues. Activation of M3AchR by binding Ach (or Cch) promotes its association with the heterotrimeric G protein ($G\alpha_q\beta\gamma$). Dissociation of βγ subunits from the α-subunit frees the α-subunit to travel along the inner leaflet of the cell membrane and activate PLC molecules. PLC in turn catalyses PIP2 hydrolysis to generate DAG and IP3 (Felder, 1995; Budd, et al., 1999). IP3 then translocates to the ER where it binds to the IP3R and promotes Ca^{2+} release from the ER Ca^{2+} store into the cytosol (Felder, 1995; Nahorski, et al., 1997). Increase in cytosolic [Ca^{2+}] in turn activates the IP3R and RYR and induce the CICR response (Ca^{2+} waves) in the entire cell (Taylor and Dale, 2012). Meanwhile, DAG binds to and activates PKC (Felder, 1995). DAG can also be converted to PA by DAG kinase (Kanoh, et al., 2002). The most common MAchR signal transduction pathway is via the activation of PLC (Budd, et al., 1999), however, PLC and PLD have also been shown to be stimulated simultaneously after agonist induced receptor activation, but through independent processes (Liscovitch, 1991). In order to determine whether the Ca^{2+} signals generated upon Cch stimulation are PLC dependent, human colonic crypts were pre-treated with the PLC inhibitor U73122 (10µM) for 1 hour, prior to re-stimulation with Cch (10µM) (Figure 4.8A). U73122 significantly blocked the peak amplitude of the Ca^{2+} signals by 87% with respect to control (0.13 ± 0.026, N= 5 subjects, n= 19 crypts, paired t-test $p< 0.01$, Figures 4.8A and 4.9 bottom panel). This result suggests that the majority of the Ca^{2+} signals are downstream of the PLC pathway. Activation of PLC initiates the hydrolysis of PIP2 into IP3 and DAG. From this point onwards, the signals feed into two paths (Figure 4.7); while the IP3 pathway to Ca^{2+} mobilisation has been relatively well studied, signal transduction downstream of DAG and PKC is not yet clearly understood (Figure 4.7).

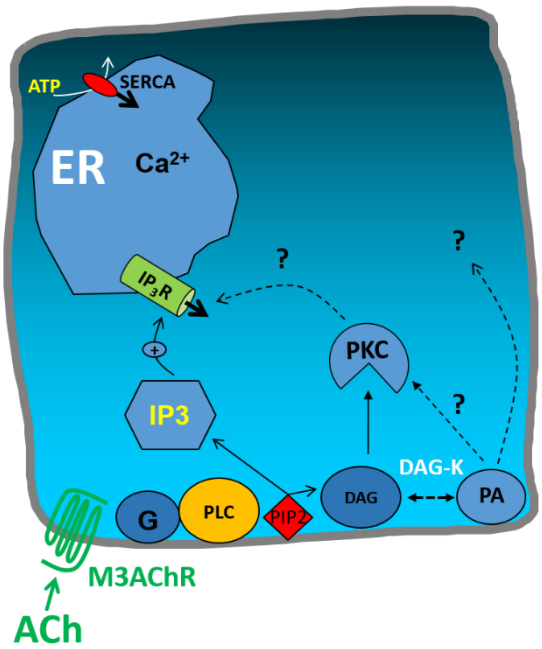

Figure 4.7 Schematic of the MAchR signalling pathways.

Binding of Ach (or Cch) to M3AchR promotes its association with the heterotrimeric G protein on the plasma membrane that further activates PLC molecules. PLC in turn catalyses PIP2 hydrolysis to generate DAG and IP3. IP3 then translocates to the ER where it binds to the IP3R and promotes Ca^{2+} release from the ER Ca^{2+} store into the cytosol. Meanwhile, DAG binds to and activates PKC. The 2nd messenger IP3 is the hallmark ER Ca^{2+} mobilising agent upon M3AchR activation that has been relatively well studied, while signal transduction downstream of DAG and PKC is not yet clearly understood as the downstream effector(s) of PKC is currently unknown. DAG can also converted to PA by DAG-kinase. It is currently unclear which PKC isoforms are activated by DAG or PA or both upon M3AchR activation in the human colonic epithelium, and the signalling pathway downstream of PA is also not known.

Under resting conditions, the activity of DAG kinase is low, which leaves DAG free to fulfill its various signalling roles, including activation of PKC (Mérida, et al., 2008). In order to gain an insight into the contribution of DAG kinase to cholinergic stimulated Ca^{2+} signal generation, human colonic crypts were treated with the DAG kinase inhibitor R59-022 (10µM) (Figure 4.8B). DAG kinase inhibition reduced the peak amplitude of the Ca^{2+} response to Cch by approx. 64% of control (0.36 ± 0.045, N= 2 subjects, n= 7 crypts, paired t-test $p< 0.01$, Figures 4.8B and 4.9 bottom panel). DAG kinase inhibition would be expected to increase levels of DAG by blocking the conversion to PA. The activation of PKC upon binding to DAG has been shown to activate downstream effectors involved in regulating proliferation, differentiation and secretion (Shearman, et al., 1989; Kikkawa, et al., 1989). Since Cch stimulation might activate more than one PKC isoform (and not all PKC isoforms are activated by DAG), the role of PKCs in the human colonic crypt Ca^{2+} signal generation were determined by using the pan-PKC-specific inhibitor sotrastaurin (20µM) (Figure 4.8C). Ca^{2+} signals were blocked by 45% in the presence of sotrastaurin (0.55 ± 0.06, N= 6 subjects, n= 14 crypts, paired t-test $p< 0.01$) compared to the control Ca^{2+} response (Figures 4.8C and 4.9 bottom panel), suggesting that the PKC pathway contributed to approximately half of the Ca^{2+} signals generated upon Cch stimulation. These observations suggest that PLC-mediated DAG formation can contribute to Ca^{2+} signal generation by activation of PKC and formation of PA. However, the relative contribution of PKC and PA, and their interdependency, to Ca^{2+} signal generation was not investigated.

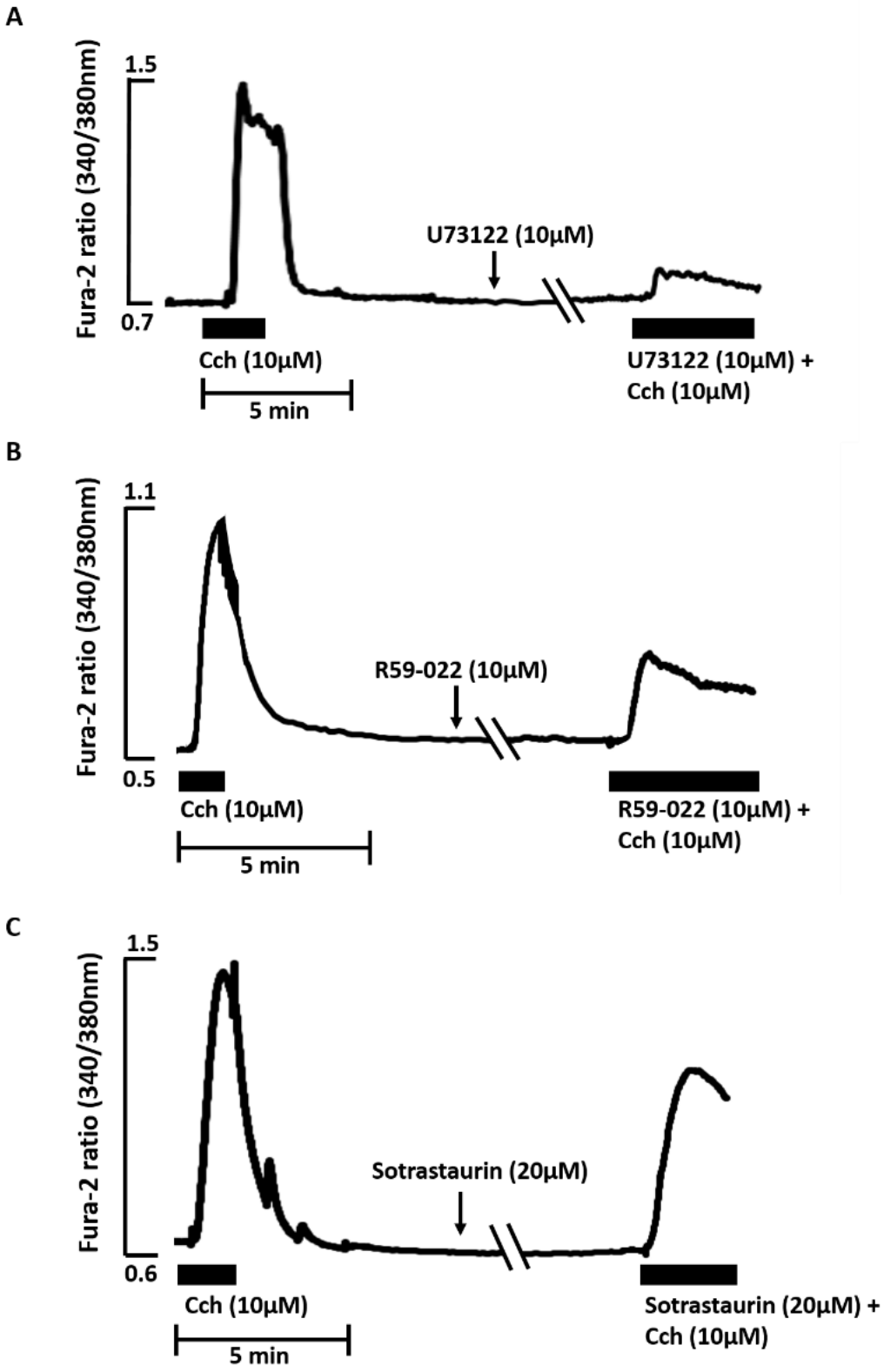
A
Fura-2 ratio (340/380nm)
1.5
0.7
U73122 (10μM)
Cch (10μM)
5 min
U73122 (10μM) +
Cch (10μM)
B
Fura-2 ratio (340/380nm)
1.1
0.5
R59-022 (10μM)
Cch (10μM)
5 min
R59-022 (10μM) +
Cch (10μM)
C
Fura-2 ratio (340/380nm)
1.5
0.6
Sotrastaurin (20μM)
Cch (10μM)
5 min
Sotrastaurin (20μM) +
Cch (10μM)

Figure 4.8 The roles of PLC, DAG kinase and PKC in Cch-mediated Ca^{2+} waves in the human colonic crypts (previous page)

Representative traces of the Ca^{2+} responses upon Cch stimulation of Fura-2 loaded human colonic crypts. A control response to 10µM of Cch was conducted in all experiments (first Ca^{2+} peak). Cch administration (duration) was indicated by the black bar. The amplitude of the control Cch-mediated Ca^{2+} responses ranged from 0.6- 1.2, measured from the peak to the baseline. After removal of the agonist and [Ca^{2+}] back to resting level, crypts were then treated with different inhibitors for 1 hour prior to subsequent re-administration of Cch (10µM) in the presence of the respective inhibitors (2nd black bar). (A) U73122 (PLC inhibitor, 10µM), representative result of N= 5 subjects, n= 19 crypts; (B) R59-022 (DAG kinase inhibitor, 10µM), representative result of N= 2 subjects, n= 7 crypts; (C) Sotrastaurin (PKC inhibitor, 20µM), representative result of N= 6 subjects, n= 14 crypts.

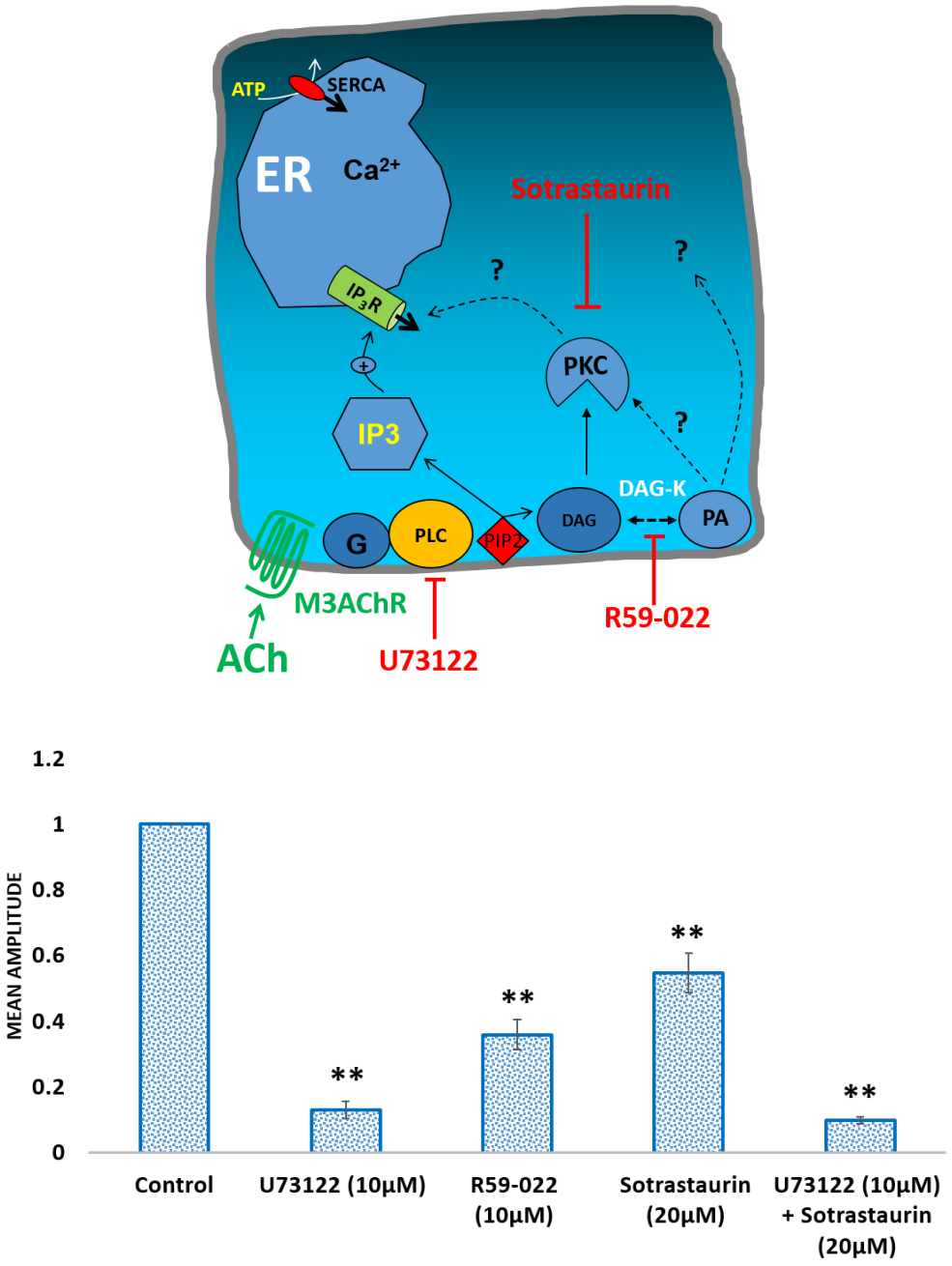

Figure 4.9 Probing downstream mediators of MAchR-coupled Ca^{2+} signalling pharmacological inhibitors.

Schematic representation of the MAchR signalling pathways (Top panel). The amplitude of the Ca^{2+} responses in the control group and the inhibitor treated groups as displayed in the previous figure (Figure 4.8) were calculated. The mean amplitude of each experimental groups were normalised to the control group, and displayed as mean ± SE (bottom panel). Significant difference was assessed by One-way ANOVA, $F(4, 73) = 209.3$, $p < 0.00001$; followed by Bonferroni procedures and Tukey's post hoc analysis. Significant difference between pairs of mean values (i.e control vs. each treatment group) were indicated by asterisks (**), $p < 0.01$. Significant differences ($p < 0.01$) were also observed between other pairs, but no significant difference was observed between U73122 and U73122 + Sotrastaurin ($p = 0.32$). Schematic diagram is courtesy of Mark Williams.

4.2.1 Involvement of IP3R-gated calcium release in Cch-induced calcium signals

IP3R is one of the major Ca^{2+} release channels expressed on the ER membranes of most cell types. Three IP3R isoforms (IP3R1, 2 and 3) have been identified in mammals, and all are regulated by both IP3 and Ca^{2+} (Finch, et al., 1991; Marchant and Taylor, 1997; Foskett, et al., 2007). In our human colonic crypt culture model, IP3Rs were found to be expressed in the ER area and also in the region where the acidic lysosomes reside (Chapter 3, Figure 3.17). However, whether they play any role in releasing Ca^{2+} from other intracellular organelles or not is unclear. Given that inhibition of PLC inhibits the Ca^{2+} response by 90%, while inhibition of DAG kinase or PKC inhibits by no more than 60%, it is conceivable IP3 mediated Ca^{2+} release via the IP3R upon Cch stimulation. In order to verify whether IP3 and IP3R are the major contributors to the Ca^{2+} signals in our model, human colonic crypts were pre-treated with either a non-specific IP3R inhibitor (2-APB, 50µM) or a specific IP3R inhibitor (Xes C, 2µM) for 1 hour prior to the re-application of the Cch (10µM) (Figure 4.10A and 4.10B). 2-APB is a non-specific IP3R antagonist because it can also block the TRP channels on the cell membrane. It acts to mobilise store-operated Ca^{2+} at low concentrations (<10µM), but also inhibits it at high concentrations (up to 50µM). At 50µM 2-APB, only 27% of inhibition (0.722 ± 0.085, N= 5 subjects, n= 16 crypts, paired t-test $p< 0.01$) of the Ca^{2+} signals was observed in comparison to the control (Figures 4.10A and 4.11 bottom panel). The role of IP3R was further confirmed by the specific inhibitor Xes C (2µM), however, similar levels of inhibition (31% reduction, 0.69 ± 0.036, N= 3 subjects, n= 6 crypts, paired t-test $p< 0.01$) compared to 2-APB were observed (Figures 4.10B and 4.11 bottom panel). Surprisingly, these findings suggest that the IP3R is not the major intracellular Ca^{2+} channel contributing to the Ca^{2+} signals upon Cch stimulation in the human colonic epithelium. This leaves the PKC and the PA pathways as the two other main possibilities. In order to eliminate one of the possibilities, crypts were treated simultaneously with the PKC inhibitor sotrastaurin (20µM) and 2-APB (50µM) (Figure 4.10C and Figure 4.11 top panel). The Ca^{2+} signal was blocked by 45% (0.55 ± 0.07, N=1 subject, n= 4 crypts, paired t-test $p< 0.01$) in the presence of these two inhibitors (Figure 4.11 bottom panel), but the percentage of inhibition was similar to the sotrastaurin-only treated groups (0.55 ± 0.06, N= 6 subjects, n= 14 crypts, paired t-test $p< 0.01$, Figure 4.9 bottom panel). Since there was no additive effect in the presence of 2-APB, it seems that the role of IP3R is dependent on some effectors or 2^{nd} messengers downstream of the PKC or PA pathways. Thus, these results suggest that the PA and PKC pathways – as well as potentially some other unknown pathways – are the major contributors to Cch-induced Ca^{2+} signals.

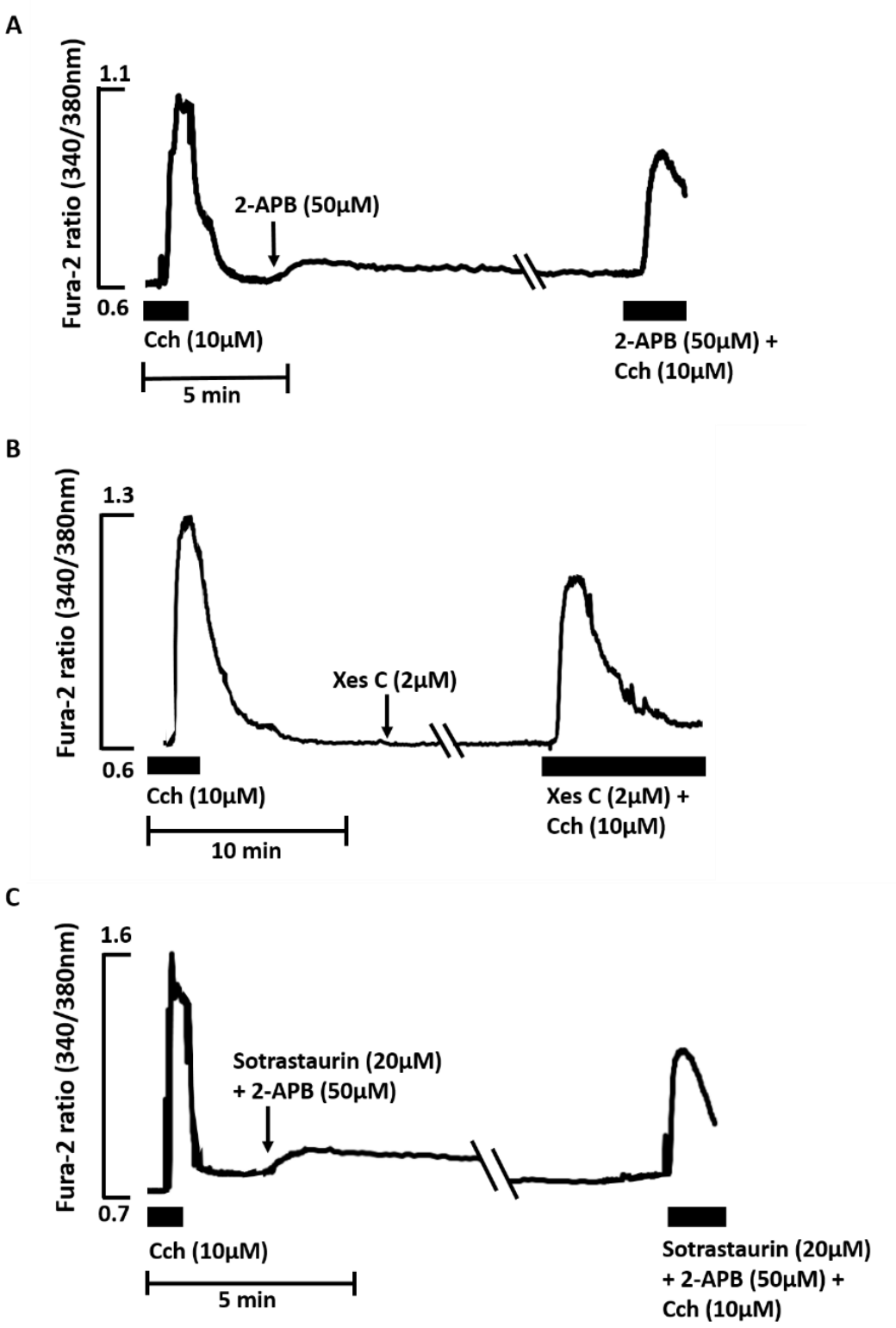
A
Fura-2 ratio (340/380nm)
1.1
0.6
2-APB (50μM)
Cch (10μM)
5 min
2-APB (50μM) +
Cch (10μM)
B
Fura-2 ratio (340/380nm)
1.3
0.6
Xes C (2μM)
Cch (10μM)
10 min
Xes C (2μM) +
Cch (10μM)
C
Fura-2 ratio (340/380nm)
1.6
0.7
Sotrastaurin (20μM)
+ 2-APB (50μM)
Cch (10μM)
5 min
Sotrastaurin (20μM)
+ 2-APB (50μM) +
Cch (10μM)

Figure 4.10 The role of IP3R in the Cch-induced Ca^{2+} waves in human colonic crypts (Previous page)

Representative traces of the Ca^{2+} responses upon Cch stimulation in the Fura-2 loaded human colonic crypts. A control response to 10μM of Cch was conducted in all experiments (first Ca^{2+} peak). Cch administration was indicated by the black bar. The amplitude of the control Ca^{2+} responses were ranging from 0.5-0.9. Upon removal of the agonist and the intracellular [Ca^{2+}] back to baseline, the crypts were then treated with different inhibitors for 1hr prior to subsequent re-administration of Cch (10μM) in the presence of the respective inhibitors (2nd black bar). (A) 2-APB (non-specific IP3R inhibitor, 50μM), representative result of N= 5 subjects, n= 16 crypts; (B) Xes C (specific IP3R inhibitor, 2μM), representative result of N= 3 subjects, n= 6 crypts; (C) Sotrastaurin (PKC inhibitor, 20μM) + 2-APB (50μM), representative result of N= 1 subject, n= 4 crypts.

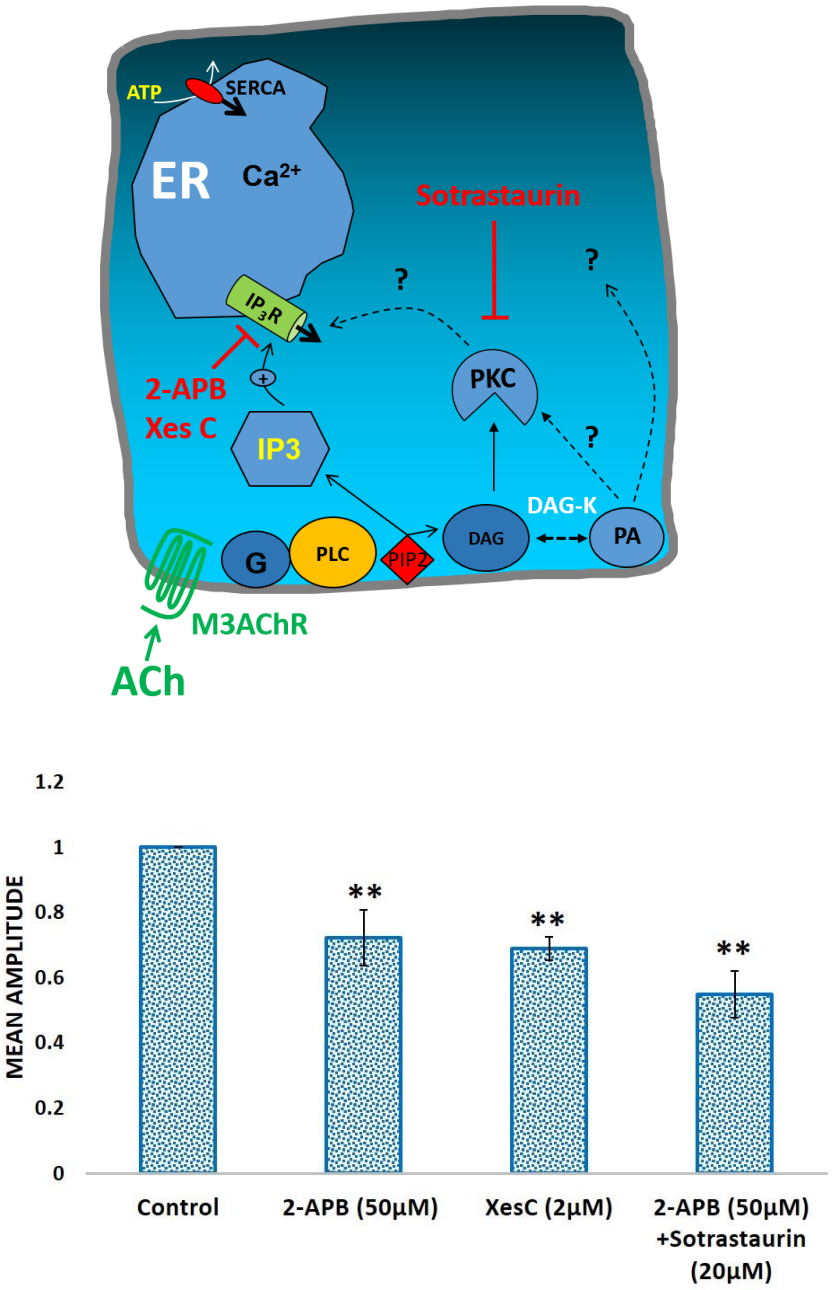

Figure 4.11 Pharmacological inhibition of the IP3Rs

Schematic representation of the MAchR signalling pathways (Top panel). The amplitude of the Ca^{2+} responses in the control group and the inhibitor treated groups as displayed in the previous figure (Figure 4.10) were calculated. The mean amplitude of each experimental groups were normalised to the control group, and displayed as mean ± SE (bottom panel). Significant difference was assessed by One-way ANOVA, $F(3, 38) = 7.27$, $p = 0.0006$; followed by Bonferroni procedures and Tukey's post hoc analysis. Significant difference between pairs of mean values (i.e control vs. each treatment group) were indicated by asterisks (**), $p < 0.01$. No significant difference were observed between 2-APB (0.722 ± 0.085) and XesC (0.69 ± 0.036), $p = 0.82$; and between 2-APB (0.722 ± 0.085) and 2-APB + Sotrastaurin (0.55 ± 0.073), $p = 0.34$. Schematic diagram is courtesy of Mark Williams.

4.2.2 Role of RYR-gated calcium release in generating Cch-induced calcium waves

Expressed primarily on the ER of non-muscle cell types, RYRs are other key regulators of intracellular Ca^{2+} release. In our human colonic crypt culture model, RYR1 is expressed on the ER near the basal membrane of the crypt (Chapter 3, Figure 3.17d). Although the activation mechanism of RYR has not been clearly elucidated, it has been previously demonstrated that RYR activation can be regulated by cADPR (Takasawa, et al., 1993; Ozawa, et al., 1999), Ca^{2+} (Lanner, et al., 2010), and pharmacologically by ryanodine. Low concentrations of ryanodine allow Ca^{2+} release from RYR, whereas high concentrations inhibit receptor opening (Meissner, et al., 1986; Lai, et al., 1989; McGrew, et al., 1989). In order to investigate the role of RYR in Cch-induced Ca^{2+} signals, crypts were treated with either low (10µM) or high (50µM) concentrations of ryanodine for 1 hour prior to re-stimulation with Cch (10µM), along with the respective concentration of ryanodine (Figure 4.12A). Low concentration ryanodine (10µM) slightly enhanced Ca^{2+} release in the presence of Cch (10µM), with approximately 12% increase in the Ca^{2+} signal amplitude observed (not significant, 1.125 ± 0.08, N= 5 subjects, n= 16 crypts, paired t-test $p> 0.05$, Figure 4.13 bottom panel). Conversely, high concentration ryanodine (50µM) blocked the Ca^{2+} signals by 36% (0.635 ± 0.04, N= 5 subjects, n= 12 crypts, paired t-test $p< 0.01$) upon Cch-stimulation in comparison to the control (Figures 4.12A and 4.13 bottom panel). To confirm the role of RYRs, crypts were treated with 8-Bromo-cADPR (30µM) for 1 hour prior to re-administration of Cch (10µM) in the presence of the inhibitor (Figure 4.12B). 8-Bromo-cADPR is an antagonist of cADPR, which is synthesised by ADP-ribosyl cyclase (CD38) in the cell. This dosage of 8-Bromo-cADPR only blocked the Ca^{2+} signals by approximately 9% (not significant, 0.91 ± 0.036, N= 4 subjects, n= 13 crypts, paired t-test $p> 0.05$, Figures 4.12B and 4.13 bottom panel). These results suggest two possibilities: (1) the dosage of 8-Bromo-cADPR was insufficient to suppress cADPR activity, or (2) cADPR did not play a role in the M3AchR mediated Ca^{2+} signals via the RYRs. Similar to IP3Rs, RYRs were also involved in the Cch-induced Ca^{2+} signal generation.

Both RYRs and IP3Rs are the major intracellular Ca^{2+} channels on the ER membrane. To determine the concomitant role of both channels on ER Ca^{2+} release, human colonic crypts were treated simultaneously with IP3R and RYR inhibitors (50µM 2-APB and ryanodine) for 1 hour, prior to re-stimulation with Cch (10µM) in the presence of both inhibitors (Figure 4.12C and Figure 4.13 top panel) and a 40% reduction (0.59 ± 0.055, N= 3 subjects, n= 11 crypts, paired t-test $p< 0.01$) of the Ca^{2+} signals was observed (Figure 4.13 bottom panel). The ER Ca^{2+} store was one of the major contributor to the Cch-induced Ca^{2+} signals, neither RYRs nor IP3Rs were the key trigger for the M3AchR signalling mediated Ca^{2+} signal

generation. Previous data from thapsigargin implicated other intracellular organelles might provide the activation signals to induce CICR response from the ER via RYRs and IP3Rs.

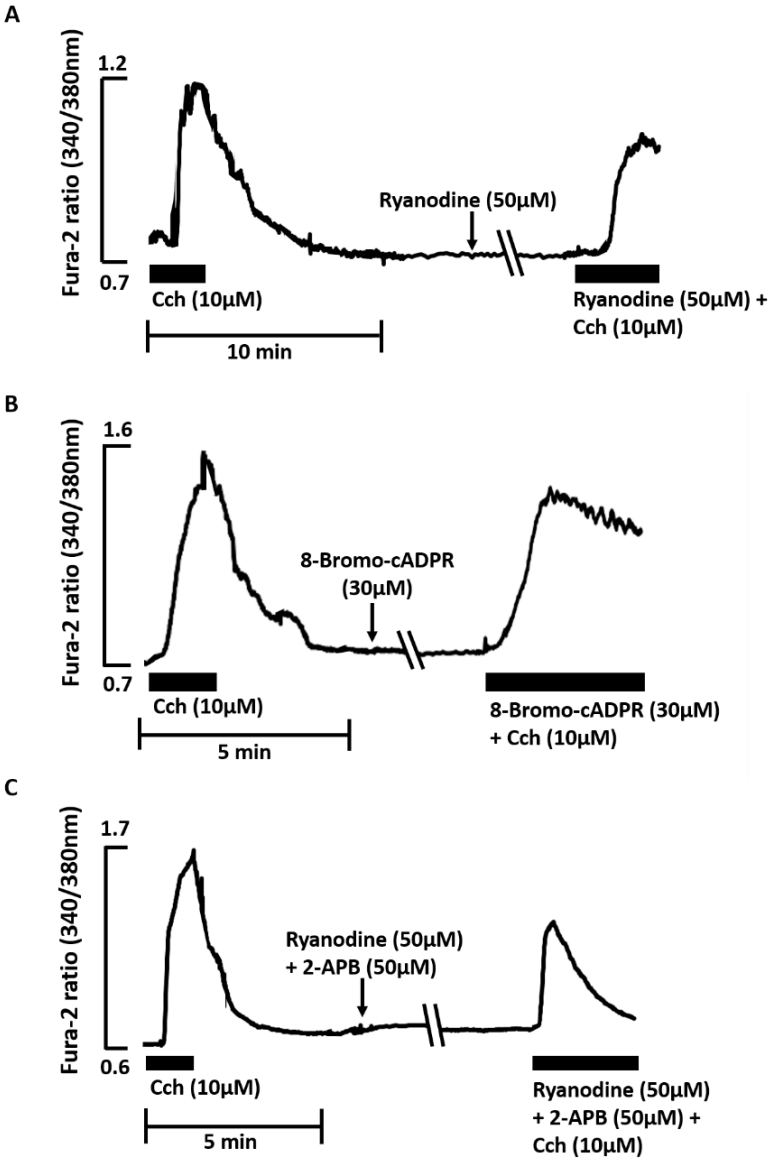

Figure 4.12 The role of RYRs on Cch-induced Ca^{2+} waves

Representative traces of the Ca^{2+} responses upon Cch stimulation in Fura-2 loaded human colonic crypts. A control response to 10µM of Cch was conducted in all experiments (first Ca^{2+} peak). Cch administration was indicated by the black bar. The amplitude of the control Ca^{2+} responses ranged from 0.5-1.2. After removal of the agonist and the intracellular [Ca^{2+}] returning to baseline, crypts were then treated with different inhibitors for 1 hour prior to subsequent re-administration of Cch (10µM) in the presence of the respective inhibitors (2^{nd} black bar). (A) Ryanodine (RYR inhibitor, 50µM), representative result of N= 5 subjects, n= 12 crypts; (B) 8-Bromo-cADPR (cADPR antagonist, 30µM), representative result of N= 4 subjects, n= 13 crypts; (C) Ryanodine (50µM) + 2-APB (IP3R inhibitor, 50µM), representative result of N= 3 subjects, n= 11 crypts.

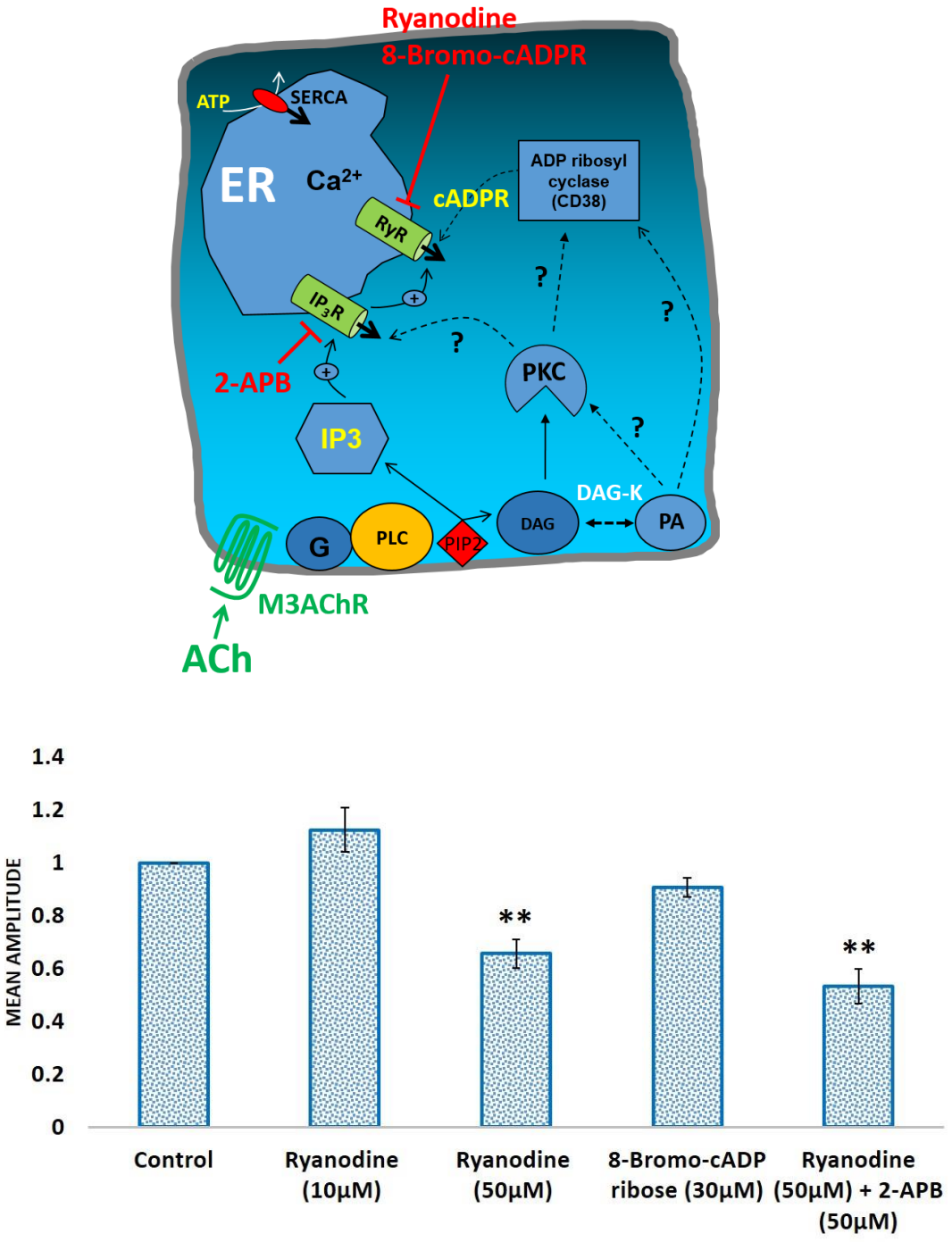

Figure 4.13 Pharmacological inhibition of the RYRs.

Schematic representation of the MAchR signalling pathways (Top panel). The amplitude of the Ca^{2+} responses in the control group and the inhibitor treated groups as displayed in the previous figure (Figure 4.12) were calculated, along with the results for low concentration (10µM) ryanodine, traces of which were not shown (N= 5 subjects, n= 16 crypts). The mean amplitude of each experimental groups were normalised to the control group, and displayed as mean ± SE (bottom panel). Statistical significance was assessed by One-way ANOVA, F (4, 63) = 18.12, p< 0.00001; followed by Bonferroni procedures and Tukey's post hoc analysis. Significant difference between pairs of mean values (i.e control vs. each treatment group) were indicated by asterisks (**), p< 0.01. Significant difference (p< 0.01) were also observed

between Ryanodine (10µM) vs. Ryanodine (50µM), and between Ryanodine (50µM) vs. 8-Bromo-cADPR. No significant difference were observed between (i) control vs. Ryanodine (10µM), p= 0.15, (ii) Ryanodine (50µM) vs. Ryanodine (50µM) + 2-APB, p= 0.53. Schematic diagram is courtesy of Mark Williams.

4.2.3 CD38 regulates intracellular calcium release upon Cch stimulation

CD38 was identified as the enzyme responsible for synthesising both cADPR (agonist of RYRs) and NAADP (agonist of TPCs) (Lee, 1997), as well as mediating the hydrolysis of cADPR to ADPR (Tohgo, et al., 1997). Both the cyclase and hydrolase activities of CD38 have been demonstrated in the mouse and human. CD38 expression is not restricted to the plasma membrane; in many cell types a soluble form of CD38 also exists which might be the product of enzymatic cleavage of the cell surface protein (Mehta, et al., 1996). In the rat brain, CD38 expression has been found in association with the ER, ribosomes, small vesicles and the mitochondria, thus it is spread in such a way that it could participate in many cellular events (Yamada, et al., 1997). Accumulating evidence suggests that the up-regulation of CD38 activity at the cell membrane is activated by GPCRs including MAchR (Higashida, et al., 1997a and b; Higashida, et al., 2001a and b). In mouse pancreatic acinar cells, activation of MAchR has been shown to cause an increase in the cellular content of cADPR that was not observed in CD38 knockout mice (Fukushi, et al., 2001). Activation of CD38 in B cells and human Namalwa cells (Burkitt's lymphoma cell line) has been demonstrated to result in vesicle-mediated internalisation of the enzyme (Xu, et al., 2013). As the catalytic domain of CD38 is localised at the extracellular side of the cell membrane (Tohgo, et al., 1994; Higashida, et al., 2001a and b), internalisation allows the active site access to the cytosolic substrates (NAD^+ or $NADP^+$) and hence exert its function intracellularly (Xu, et al., 2013). However, the mechanism of CD38 activation upon MAchR activation remains unclear.

A previous study has demonstrated the expression of CD38 on endosomes in pancreatic acinar cells, which appeared to be proximal to – but not co-localised with – the lysosomes (Cosker, et al., 2010). In the current study, the expression and localisation of CD38 was compared between the control and Cch treated group. Under resting (unstimulated) conditions, CD38 expression was detected in the cytoplasmic space of human colonic crypt epithelial cells where the acidic lysosomes reside. LAMP1 and CD38 were expressed in close proximity to each other, and some level of co-localisation was also observed (Chapter 3, Figure 3.18 and Figure 3.22A). CD38 was also in close association with the ER at the mid-cell region (Figure 4.14, control). It is still unclear which signals contribute to this CD38 (of a presumably endosomal origin) being continually internalised. Upon Cch (10µM) stimulation for 30 min, increased intensity of CD38 expression in the apical region of cells was observed (Figure 4.2B (b) and Figure 4.14, Cch). In addition, CD38 expression on the basal membrane was also increased. Thus, CD38 expression in human colonic epithelial cells is not restricted to the plasma membrane; instead, it is localised to the area where the acidic lysosomes and

mucus granules reside, indicating a possible role in synthesising 2nd messengers in response to signals.

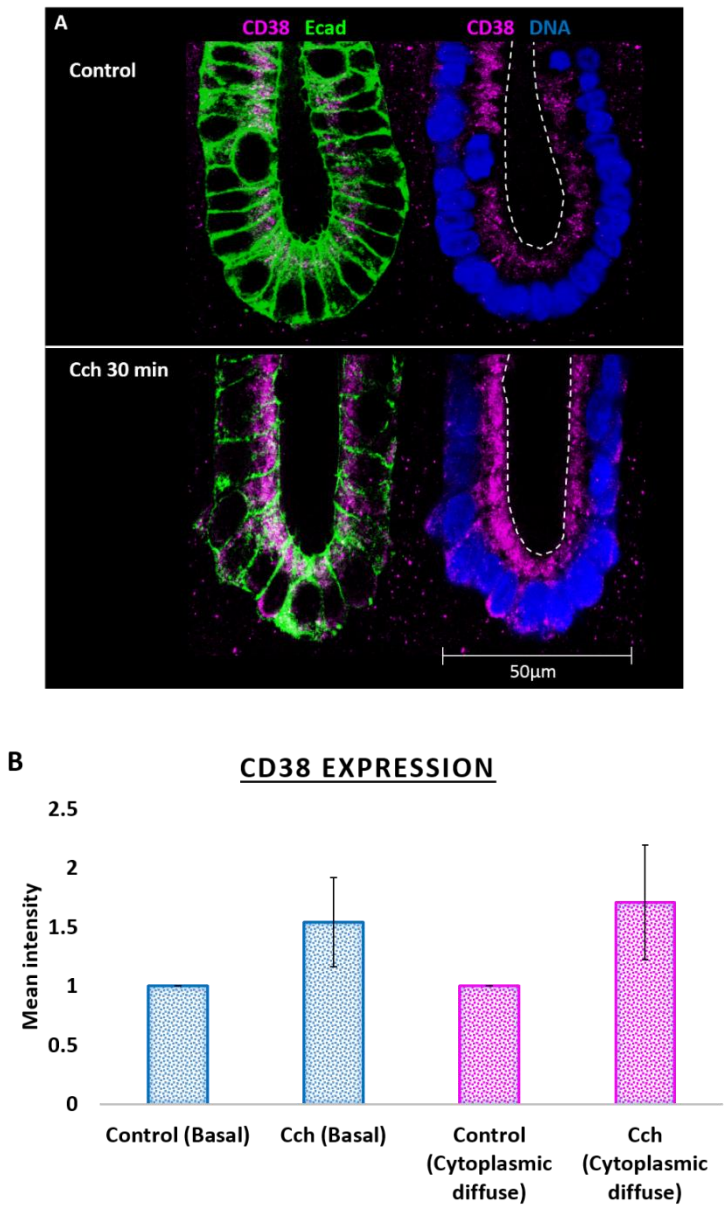

Figure 4.14 Expression of CD38 in the human colonic crypt in resting and stimulated state

Cultured human colonic crypts were either untreated or treated with Cch (10µM) for 30 min. Samples were fixed, labelled with anti-CD38 (pink) and anti-Ecad (green) antibodies, and visualised with Alexa-conjugated secondary antibodies; cell nuclei were stained with Hoechst (blue) (A). Representative images were taken with a Zeiss Meta 510 confocal microscope using a x63 objective. Left hand column show the overlay images of CD38 (pink) and Ecad (green); right hand column show the merged images of CD38 (pink) and cell nuclei (blue). White dotted lines show the boundary of the crypt lumen. The intensities of CD38 at the basal pole and cytoplasmic space of the crypt were measured by ImageJ software. Mean intensities of both regions were calculated and normalised to the control group, and

displayed as mean ± SE (B). Results were representative of N= 3 subjects, n= 12 crypts in each treatment group.

As mentioned previously, CD38 has been proposed to exert its function when it is internalised. Figure 4.14 suggests that there is an association between CD38 internalisation and the endocytic pathway in mediating Cch-induced Ca^{2+} signal generation in the human colonic crypt. The role of endocytosis in Cch evoked Ca^{2+} signal generation was briefly investigated. Dynasore, an inhibitor of clathrin mediated endocytosis did not inhibit the amplitude of the Cch-induced Ca^{2+} signal (1.16 ± 0.2, N= 2 subjects, n= 6 crypts, data not shown) as compared to the control (1 ± 0). Methyl-beta-cyclodextrin (MbetaC) is a commonly used inhibitor of endocytosis via lipid rafts by selectively extracts cholesterol from plasma membranes. Human colonic crypts were treated with MbetaC (10mM) for 1 hour prior to re-stimulation with Cch (10µM) in the presence of the inhibitor. MbetaC (10mM) reduced the Cch-induced Ca^{2+} signals by 56% (0.44 ± 0.09, N= 1 subject, n= 3 crypts, paired t-test p= 0.024, data not shown). This result supports the notion that CD38 internalisation upon Cch-stimulation is important for the downstream signalling cascade.

Nicotinamide is a compound that blocks CD38 activity. In order to investigate the cyclase activities of CD38 and its role in Ca^{2+} signal generation upon Cch-stimulation, human colonic crypts were treated with 20 or 50mM nicotinamide for 1 hour prior to re-stimulation with Cch (10µM), in the presence of the respective dose of nicotinamide (Figure 4.15 and Figure 4.16 top panel). The lower concentration of nicotinamide (20mM) significantly reduced the Ca^{2+} signal by 63% (0.36 ± 0.08, N= 2 subjects, n= 3 crypts, paired t-test $p< 0.01$), while the higher concentration (50mM) reduced the Ca^{2+} signal by 84% in comparison to the control (0.16 ± 0.03, N= 2 subjects, n= 5 crypts, paired t-test $p< 0.01$, Figures 4.15 and 4.16 bottom panel). Further statistical analysis shows no significant difference between Nicotinamide (20mM) and (50mM). These results suggest that CD38 plays a major role in the Cch-mediated Ca^{2+} signal generation.

However, as discussed previously, 8-Bromo-cADPR (a cADPR antagonist) failed to inhibit the Ca^{2+} signal in response to Cch-stimulation (Figure 4.12B), suggesting either that cADPR (one of the 2nd messengers synthesised by CD38) might not play any role in the Cch-induced Ca^{2+} response, suggesting that NAADP, also catalysed by CD38 activity, could be a key 2nd messenger. NAADP is renowned for mobilising Ca^{2+} from non-ER Ca^{2+} stores such as acidic endo-lysosomal organelle.

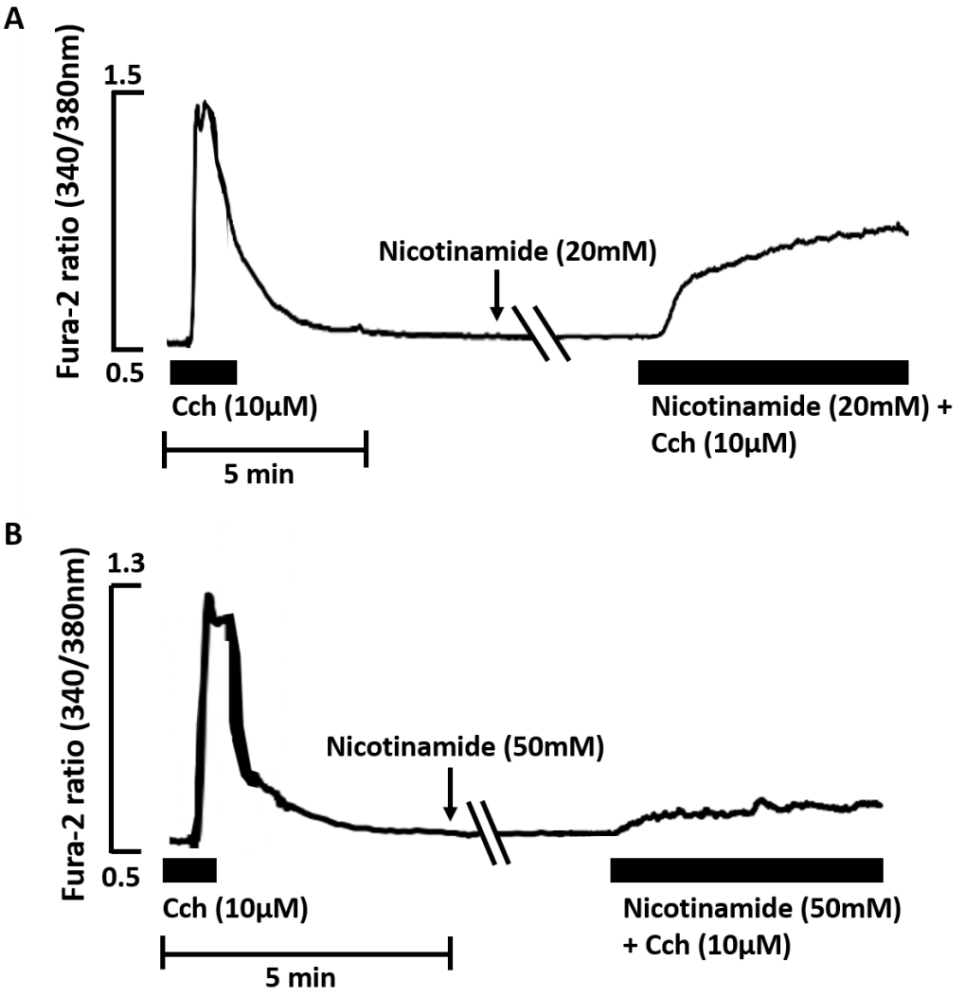

Figure 4.15 Effect of nicotinamide on Cch-stimulated Ca^{2+} waves

Representative traces of the Ca^{2+} responses upon Cch stimulation in Fura-2 loaded human colonic crypts. A control response to 10µM of Cch was conducted in all experiments (first Ca^{2+} peak). Cch administration was indicated by the black bar. The amplitude of the control Ca^{2+} responses ranged from 0.8-1. After removal of the agonist and return of the intracellular [Ca^{2+}] back to baseline, the crypts were then treated with different doses of nicotinamide for 1 hour prior to subsequent re-administration of Cch (10µM) while maintaining the same nicotinamide dose (2nd black bar). (A) Nicotinamide (CD38 inhibitor, 20mM), representative result of N= 2 subjects, n= 3 crypts; (B) Nicotinamide (50mM), representative result of N= 2 subjects, n= 5 crypts.

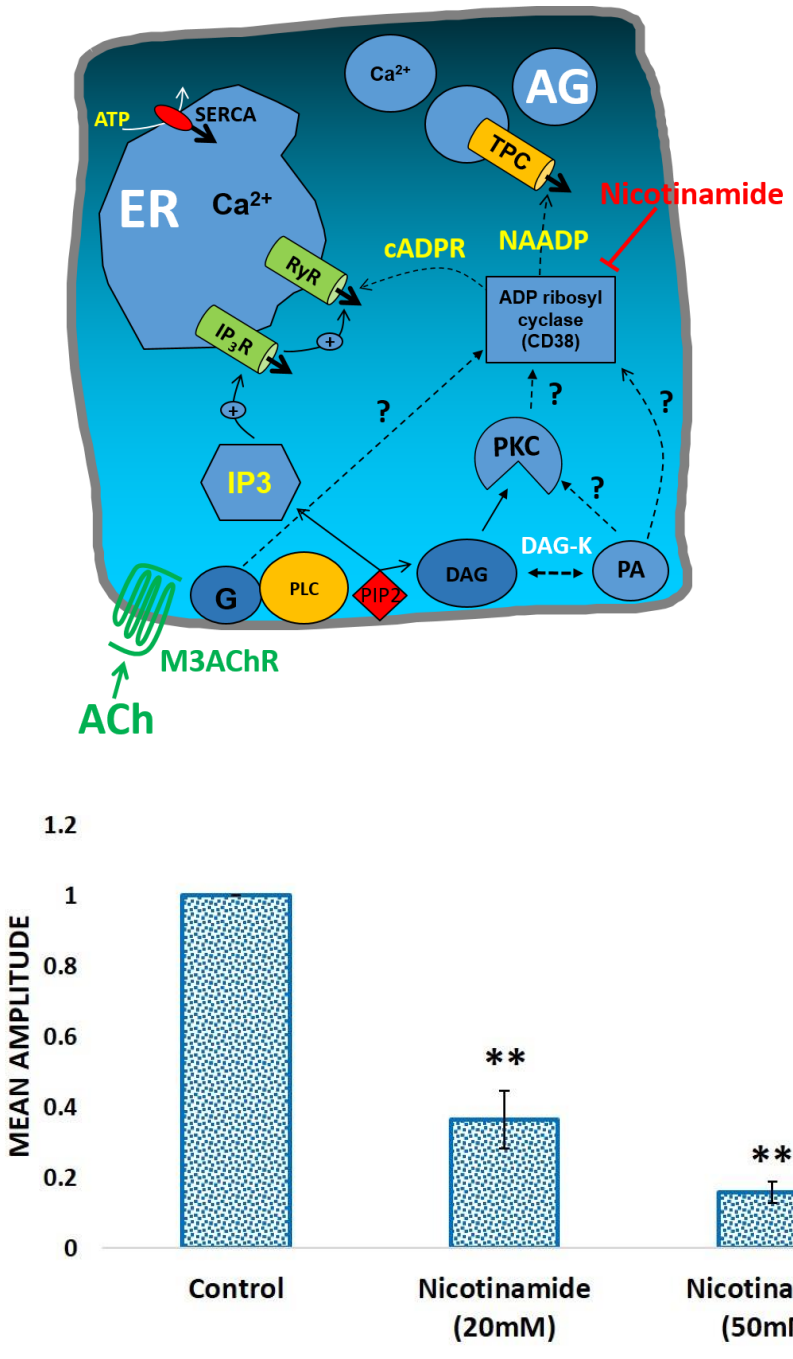

Figure 4.16 Pharmacological inhibition of CD38 and its role in Cch-mediated Ca^{2+} signals

Schematic representation of the MAchR signalling pathways (Top panel). The amplitude of the Ca^{2+} responses in the control group and the inhibitor treated groups as displayed in the previous figure (Figure 4.15) were calculated. The mean amplitude of each experimental groups were normalised to the control group and displayed as mean ± SE (bottom panel). Statistical significance was assessed by One-way ANOVA, $F(2, 10) = 162.3$, $p < 0.00001$; followed by Bonferroni procedures and Tukey's post hoc analysis. Significant difference between pairs of mean values (i.e control vs. each treatment group) were indicated by asterisks (**), $p < 0.01$. No significant difference was observed between Nicotinamide (20mM) and Nicotinamide (50mM). Schematic diagram is courtesy of Mark Williams.

4.2.4 Pharmacological disruption of lysosomal calcium stores inhibits Cch-induced calcium signals

The acidic lysosomes have recently emerged as important Ca^{2+} stores for regulating cellular and physiological functions (Morgan, et al., 2011). Ca^{2+} mobilisation from these stores have been shown to mediate vesicle trafficking (Ruas, et al., 2010; Ruas, et al., 2014) and exocytosis (Davis, et al., 2012). The thapsigargin data presented above implies that M3AchR activation mobilises Ca^{2+} from other intracellular Ca^{2+} stores (Figures 4.5A and B). In order to confirm whether MAchR activation mobilises Ca^{2+} from the acidic organelles, human colonic crypts were treated with different inhibitors targeting the acidic lysosomes in different ways (Figure 4.20 top panel). The continuous refilling with Ca^{2+} mediated by the V-type H^+ ATPase and a Ca^{2+}/H^+ exchanger on the lysosomal membrane is a basic requirement for a functional lysosomal store (Lemons and Thoene, 1991). This H^+ ATPase also promotes the acidification of lysosomal lumens (Beyenbach, et al., 2006). Bafilomycin acts to inhibit the V-type H^+ ATPase, and blocks Ca^{2+} refilling of the lysosomal stores (Galione, 2006).

Human colonic crypts were treated with bafilomycin (2.5µM) for at least 1 hour prior to re-stimulation with Cch (10µM, plus additional 2.5µM bafilomycin, Figure 4.17A). A significant reduction of Cch-induced Ca^{2+} signals by 65% (0.35 ± 0.1, N= 3 subjects, paired t-test $p< 0.01$) was observed (Figure 4.20 bottom panel). Chloroquine is a lysosomotropic agent that inhibits the acidification of the lysosomes by accumulating within the lysosomes and inhibiting the enzymes within, rendering the store inactive. Human colonic crypts were treated with chloroquine (100µM) for 1 hour prior to re-application of Cch (10µM) plus chloroquine (Figure 4.17B). Here Cch-induced Ca^{2+} signals were reduced even more dramatically than seen during bafilomycin treatment, by 94% (0.06 ± 0.03, N= 3 subjects, paired t-test $p< 0.01$, Figure 4.20 bottom panel). These data strongly suggest that the lysosomal Ca^{2+} stores are the key intracellular organelles responsible for the MAchR signal transduction.

In order to further confirm the role of acidic lysosomal Ca^{2+} stores, colon crypts were treated with glycyl-L-phenylalanine 2-naphthylamide (GPN). GPN is a substrate that is specifically hydrolysed by lysosomal cathepsin C; intralysosomal accumulation of its hydrolysis products cause 90% of the lysosomes in treated cells to burst under osmotic pressure (Berg, et al., 1994). Colonic crypts treated with GPN showed an irregular pattern of intracellular Ca^{2+} waves for 20-30 mins (Figure 4.18A), and the subsequent Cch-induced Ca^{2+} response was significantly reduced by an average of 87% (0.13 ± 0.03, N= 4 subjects, n= 8 crypts, paired t-test $p< 0.01$, Figure 4.20 bottom panel). Thus, these results further support the model that cholinergic activation of the M3AchR signalling pathway mobilises Ca^{2+} from acidic lysosomal

stores. As the acidic lysosomes are localised at the apical pole of the crypt, these findings are also in agreement with the observation that colonic crypt Ca^{2+} signals initiate at the apical pole of the initiator cells at the base of the crypt.

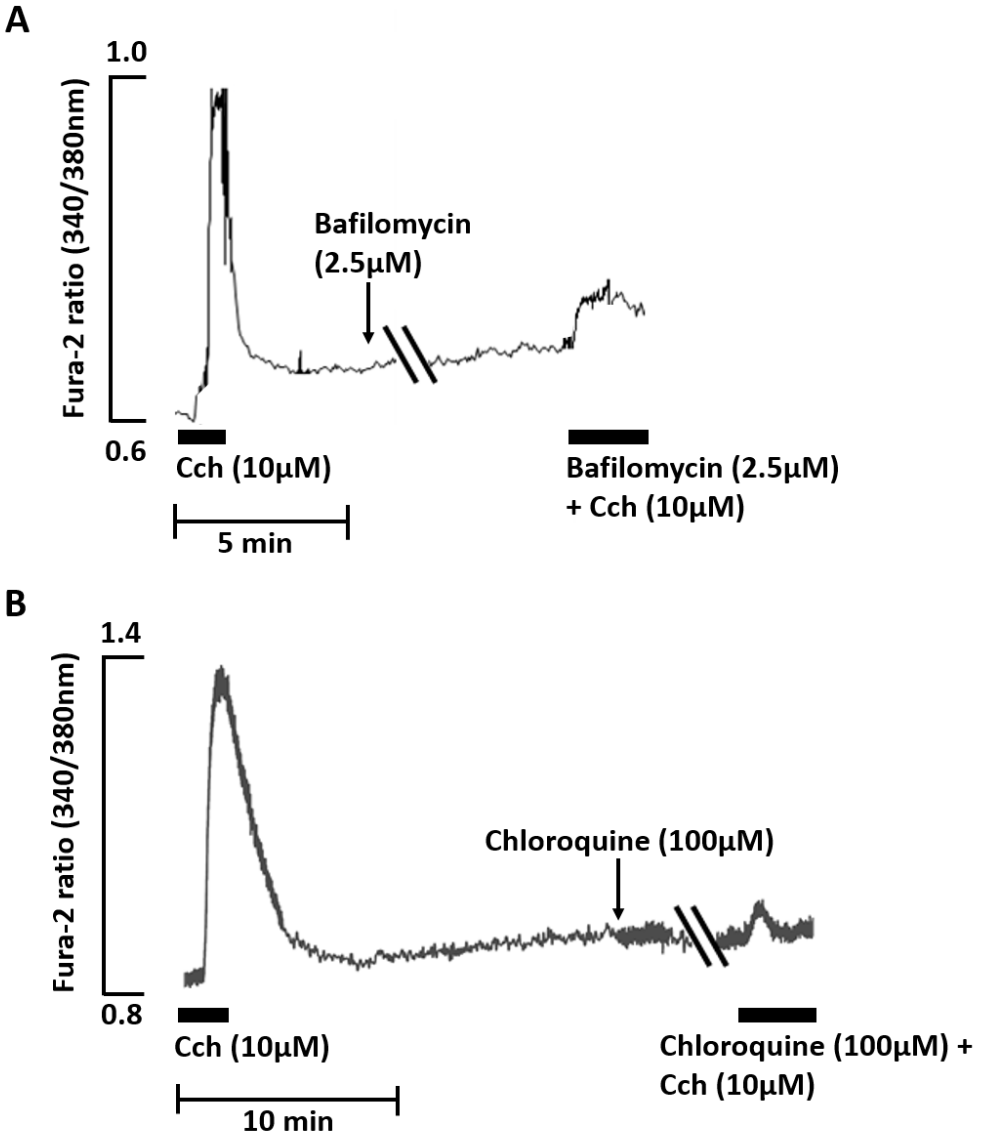

Figure 4.17 The role of acidic lysosomes on Cch-mediated Ca^{2+} mobilisation

Representative traces of Ca^{2+} responses upon Cch stimulation in Fura-2 loaded human colonic crypts. A control response to 10µM of Cch was conducted in all experiments (first Ca^{2+} peak). Cch administration was indicated by the black bar. The amplitude of the control Ca^{2+} responses ranged from 0.4-0.6. After removal of the agonist and return of the intracellular [Ca^{2+}] back to baseline, crypts were then treated with different inhibitors for 1 hour prior to subsequent re-administration of Cch (10µM) in the presence of the respective inhibitors (2nd black bar). (A) Bafilomycin (2.5µM); (B) Chloroquine (100µM). Both Ca^{2+} traces are courtesy of Martin loader, a student in the lab who collaborated on this section.

As discussed previously, CD38 immuno-localisation at the apical pole and the effects of the CD38 inhibitor nicotinamide on Ca^{2+} signal amplitude suggest that CD38 mediated generation of Ca^{2+} mobilising messengers plays a major role in Cch-mediated Ca^{2+} signal generation. Given that 8-Bromo-cADPR (a cADPR antagonist) failed to inhibit the Ca^{2+} signal in response to Cch-stimulation (Figure 4.12B), cADPR might not play any role in the Cch-induced Ca^{2+} response; however, NAADP could be the key 2^{nd} messenger downstream of the CD38 pathway upon M3AchR activation.

It is known that lysosomal Ca^{2+} release is mediated by TPCs, a family of proteins that have gained recognition in recent years as the major regulator/channel of Ca^{2+} release from acidic stores via the 2^{nd} messenger NAADP (Calcraft, et al., 2009; Brailoiu, et al., 2009). To further delineate the role of NAADP in mediating Ca^{2+} release from the acidic stores upon Cch stimulation, human colonic crypts were treated with Ned-19 (200µM), an NAADP antagonist, for 1 hour prior to re-stimulation with Cch (10µM) in the presence of Ned-19 (Figure 4.18B). The Cch-induced Ca^{2+} signals were drastically reduced by 94% in comparison to the control (0.057 ± 0.009, N= 4 subjects, n= 15 crypts, paired t-test $p< 0.01$, Figure 4.20 bottom panel). In addition, experiments conducted in Ca^{2+} free HBS gave the same results (Figure 4.19), suggesting that cholinergic signals mediated Ca^{2+} mobilisation from intracellular acidic stores, without the requirement for extracellular Ca^{2+}. The release of Ca^{2+} from acidic lysosomes seem to be the key trigger for the subsequent CICR response amplified by the ER store. Hence, NAADP is the key 2^{nd} messenger in mobilising lysosomal Ca^{2+} stores upon M3AchR activation.

Diltiazem (DZM), an L-type Ca^{2+} channel blocker that has been shown previously to also block NAADP receptors/TPCs (Zhang, et al., 2007). Human colonic crypts were treated with DZM (100µM) for 1 hour prior to re-administration of Cch (10µM) in the presence of the inhibitor (Figure 4.18C). The Cch-induced Ca^{2+} response was reduced by 79% (0.209 ± 0.028, N=4 subjects, n= 13 crypts, paired t-test $p< 0.01$, Figure 4.20 bottom panel). Thus, Cch stimulated Ca^{2+} release from lysosomal stores by NAADP via the TPCs. Since NAADP is synthesised by CD38, these results further suggest that CD38 is a requirement for the coupling of MAchR activation to NAADP-mediated Ca^{2+} mobilisation from lysosomal stores in the human colonic crypt.

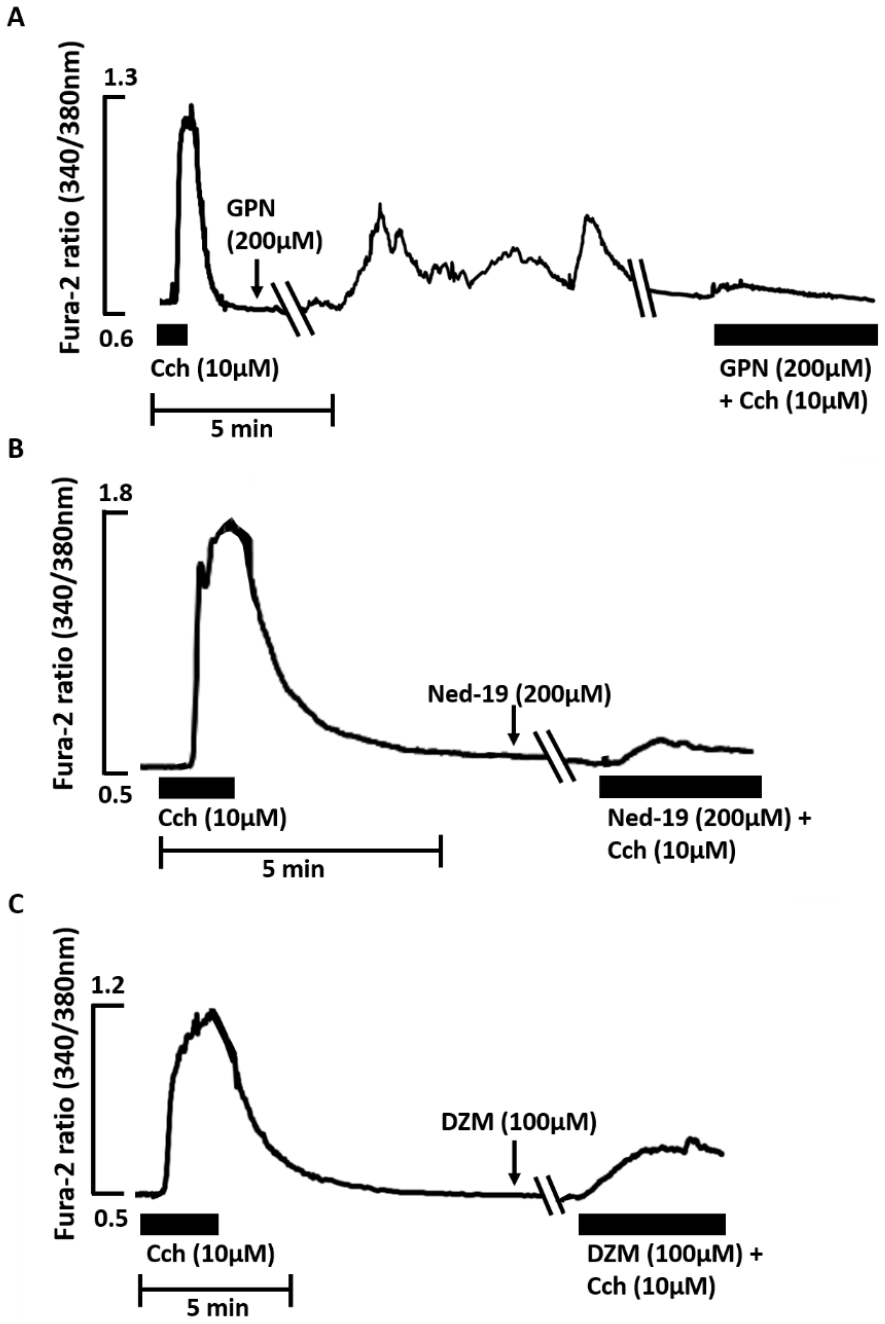

Figure 4.18 Role of NAADP and TPCs on Cch-stimulated Ca^{2+} mobilisation

Representative traces of the Ca^{2+} responses observed upon Cch stimulation in Fura-2 loaded human colonic crypts. A control response to 10µM of Cch was conducted in all experiments (first Ca^{2+} peak). Cch administration is indicated by the black bar. The amplitude of the control Ca^{2+} responses ranged from 0.6-1.3. After removal of the agonist and return of the intracellular [Ca^{2+}] back to baseline, crypts were treated with different inhibitors for 1hr prior to subsequent re-administration of Cch (10µM) in the presence of the respective inhibitors (2nd black bar). (A) GPN (200µM), representative result of N= 4 subjects, n= 8 crypts; (B) Ned-19 (200µM), representative result of N= 4 subjects, n= 15 crypts; (C) DZM (100µM), representative result of N= 4 subjects, n= 13 crypts.

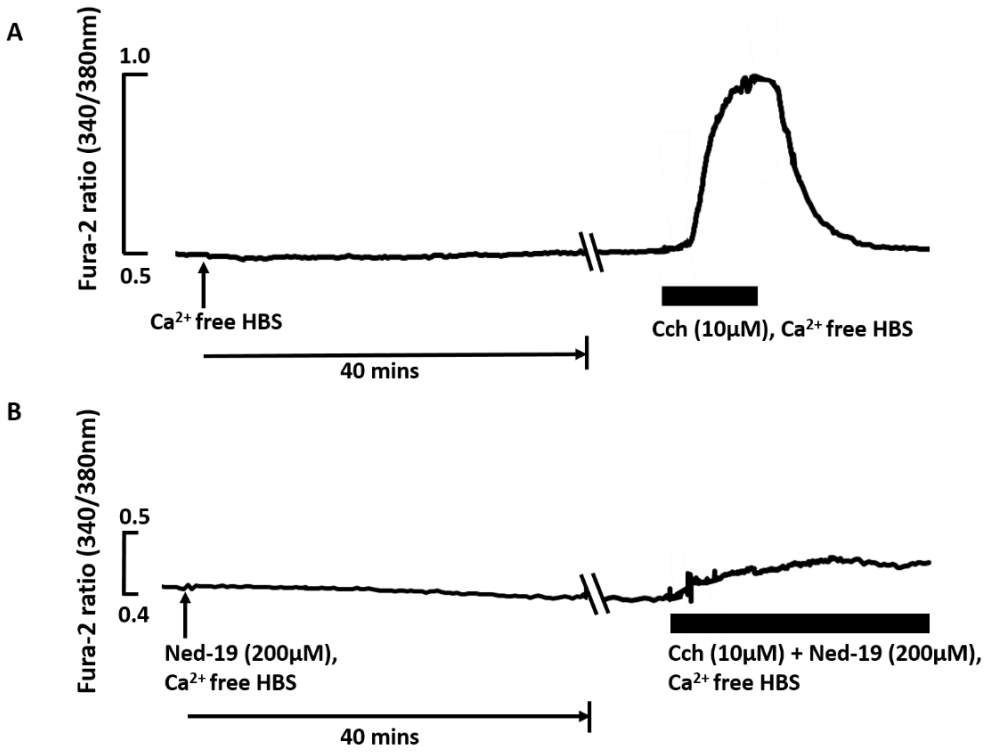

Figure 4.19 Cholinergic stimulation of Ca^{2+} mobilisation from intracellular acidic organelles

Cultured human colonic crypts were loaded with Fura-2/AM for 2 hours and then washed with Ca^{2+} free HBS. (A) The crypt was incubated with Ca^{2+} free HBS for 40 mins prior to stimulation with Cch (10µM) in Ca^{2+} free HBS (black bar). (B) The crypt was incubated with Ned-19 (200µM) in Ca^{2+} free HBS for 40 mins prior to Cch (10µM) challenge with the presence of Ned-19 (200µM) in Ca^{2+} free HBS (black bar). Intracellular Ca^{2+} changes were imaged at ROIs placed along the crypt-axis (not shown). Ca^{2+} trace is a representative of 5 ROIs. The Ca^{2+} responses and the level of inhibition were similar to the experiments conducted with normal HBS (Figure 4.18B). Data are derived from N= 1 subject, n= 2 crypts.

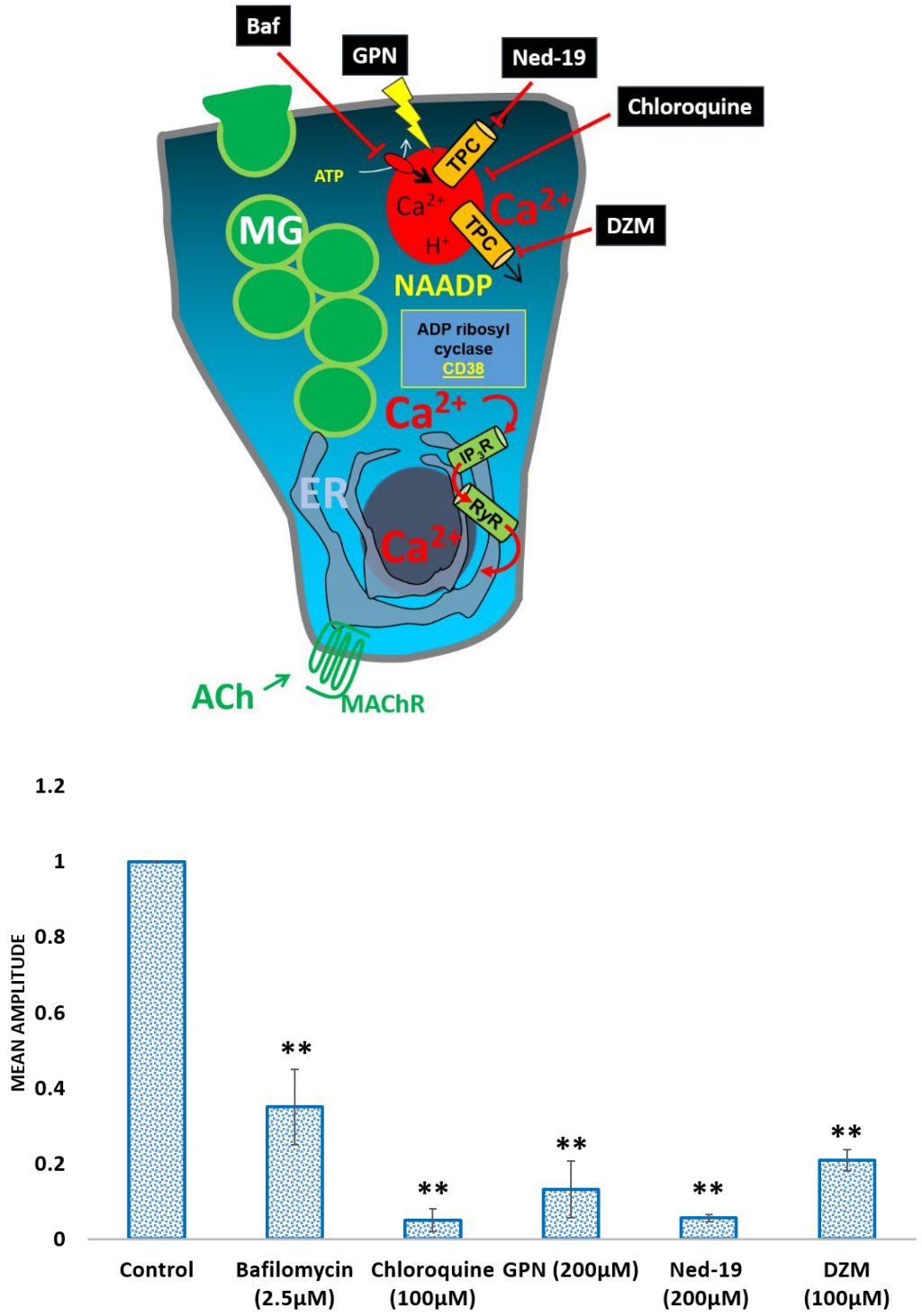

Figure 4.20 Pharmacological inhibition of the lysosomal Ca^{2+} stores

Schematic representation of the association between the acidic lysosomes and the mucus granules (Top panel). The amplitude of the Ca^{2+} responses in the control group and the inhibitor treated groups as displayed in the previous figures (Figure 4.17 and 4.18) were calculated. The mean amplitude of each experimental group was normalised to the control groups and displayed as mean ± SE (bottom panel). Significant differences were assessed using One-way ANOVA test, $F(5, 53) = 495$, $p < 0.00001$; followed by Bonferroni procedures and Tukey's post hoc analysis. Significant difference between pairs of mean values (i.e

control vs. each treatment group) were indicated by asterisks (**) for $p < 0.01$. Significant differences ($p < 0.01$) were also observed in the following pairs: (i) Bafilomycin vs. Chloroquine, (ii) Bafilomycin vs. GPN, (iii) Bafilomycin vs. Ned-19, (iv) GPN vs. Ned-19, (v) Ned-19 vs. DZM. No significant difference was observed in the following pairs: (i) Chloroquine vs. GPN, (ii) Chloroquine vs. Ned-19, (iii) Chloroquine vs. DZM, (iv) Bafilomycin vs. DZM, (v) GPN vs. DZM. Schematic diagram is courtesy of Mark Williams.

4.3 The interplay of calcium and ROS signalling pathways

Ca^{2+} and ROS are two important 2nd messengers that regulate a diverse range of cellular functions. Both Ca^{2+} and ROS signalling are intimately related, such that Ca^{2+} signals can be ROS dependent and vice versa (Yan, et al., 2006). In higher plants, systemic propagation of Ca^{2+} and ROS waves have been suggested to transmit long distance signals via cell-to-cell communication mechanisms (Gilroy, et al., 2014). ROS are generated by electron transfer reactions from molecular oxygen resulting in the formation of superoxide anion (O_2^-) and the subsequent conversion into hydrogen peroxide (H_2O_2) by superoxide dismutase (Yan, et al., 2006; Görlach, et al., 2015). There are various cellular sources of ROS such as the mitochondria, receptor activated enzyme NADPH oxidases (nicotinamide adenine dinucleotide phosphate-oxidase, NOX), xanthine oxidases and cytochrome P450 (Yan, et al., 2006). Our current understanding of the ROS and Ca^{2+} signalling cross talk has primarily been produced from studies focusing on mitochondrial derived ROS; the role of NOX-derived ROS in mediating intracellular Ca^{2+} signals remains poorly understood. It has been shown that NOX-derived ROS regulates Ca^{2+} mobilisation in smooth muscle cells in response to thrombin (Zimmerman, et al., 2011; Görlach, et al., 2015). In addition, increase in intracellular Ca^{2+} and NADPH oxidase activity has been suggested to be an upstream event of the apoptotic gene expression in pancreatic acinar cells in response to cerulein (Ji, H.Y. et al., 2006). Thus further support NOX-derived ROS and Ca^{2+} signalling cross talk mechanism. ROS can readily diffuse across the cell but they are relatively short-lived molecules, hence the subcellular localisation of NOX has been suggested to determine the downstream signalling cascade (Brown, et al., 2009). The idea of targeting specific ROS signals to a precise subcellular compartment upon receptor activation has been suggested to be mediated via the association of NOX with lipid rafts, caveolae and endosomes (reviewed by Ushio-Fukai, 2006a and b).

4.3.1 NADPH oxidase derived ROS

The NOX family of enzymes are one of the major sources of ROS generation upon receptor mediated signal transduction in mammals. These enzymes have gained considerable interest in recent years as NOX-derived ROS has been shown to contribute to a variety of cellular functions as well as pathophysiological conditions; in particular it plays an essential role in modulating inflammation, cell proliferation and migration (Fu, et al., 2014). In mammals, NOX can be divided into three subfamilies: (1) NOX1-NOX4, (2) NOX5 and (3) Duox (Fu, et al., 2014). Transmembrane NOX1-NOX4 isoforms form heterodimers with the p22phox subunit of NOX. The NOX1 isoform is highly expressed in the colon (Brown, et al., 2009) and the

assembly of the heterodimer (NOX1/p22phox) with the three cytosolic regulatory subunits (NOXO1, NOXA1 and a Rho GTPase RAC1) is necessary for its activation (Figure 4.21) (Yu, et al., 2006; Fu, et al., 2014; Görlach, et al., 2015). In particular, RAC1 activation has been shown to be the key trigger for NOX-dependent ROS generation (Cheng, et al., 2006). These transmembrane NOX enzymes have rapid kinetics of activation and inactivation in response to receptor activation for the generation of ROS (Yan, et al., 2006).

Both PA and DAG have previously been shown to be required for optimal activation of NOX in a cell free system (Palicz, et al., 2001). Other studies have also suggested the phosphorylation of cytosolic subunits of NOX2 by PKC before they translocate to the plasma membrane and form a complex with NOX2/p22phox (Görlach, et al., 2015), hence suggesting a role of PKC in NOX activation. Moreover, by using confocal microscopy, flow cytometry and membrane protein biotinylation assays, Xu and colleagues demonstrated that RAC1-dependent NOX-derived ROS mediates CD38 internalisation in coronary arterial myocytes (Xu, et al., 2013). All these findings suggest that NOX signalling pathway maybe downstream of M3AchR activation in human colonic crypts.

Signalling molecules including GPCR, PKC and NOX have been identified in caveolae and lipid rafts (plasma membrane micro-domains). By using immunofluorescence microscopy and biochemical fractionation, a previous study demonstrated the recruitment of NOX2 and the cytosolic subunits p47phox and RAC1 of NOX into lipid rafts upon Fas ligand stimulation of endothelial cells (Ushio-Fukai, 2006a and b). This recruitment facilitates the formation of the NOX complex and the subsequent increase of ROS production in endothelial cells. In addition, NOX has also been identified in endosomes: previous work by Li and colleagues demonstrated endocytosis of the IL1R complex upon activation which subsequently recruits RAC1 and NOX2 into the endosomal compartment (Li, et al., 2006). The recruitment of RAC1 into the endosomes is required for NOX2 translocation from the plasma membrane to the endosomal compartment. These endosomes then become the platform or source of NOX-mediated ROS (Li, et al., 2006; Ushio-Fukai, 2006a and b). Thus, it is feasible that M3AchR activation promotes localised ROS production at a specific subcellular compartment within a cell that is achieved by the recruitment and translocation of the NOX and RAC subunits to the endosomes

Currently, peptidic inhibitors specifically targeting NOX1 have not yet been developed. Due to this limitation, small molecule inhibitors such as Diphenyleneiodonium (DPI) and apocynin have been used historically as NOX inhibitors, yet they lack specificity (Cifuentes-Pagano, et

al., 2012). The difficulty in developing isoform-specific NOX inhibitors is that the different NOX isoforms are highly homologous. Despite these limitations, the currently available NOX inhibitors hold potential as pharmacological tools to dissect the role of NOX enzymes but their clinical potential is yet to be identified.

Information regarding the subcellular localisation of NOX1 is limited. However, a weak cytosolic and a strong nuclear immuno-labelling of NOX1 has been reported in keratinocytes; ER-proximal localisation has also been reported in vascular smooth muscle cells (Bedard, et al., 2007). In this study, the expression and localisation of the NOX signalling subunits NOX1 and RAC1 were investigated in the human colonic crypt model. Attempts have also been made to dissect the role of NOX-derived ROS in mobilising intracellular Ca^{2+} upon M3AchR activation.

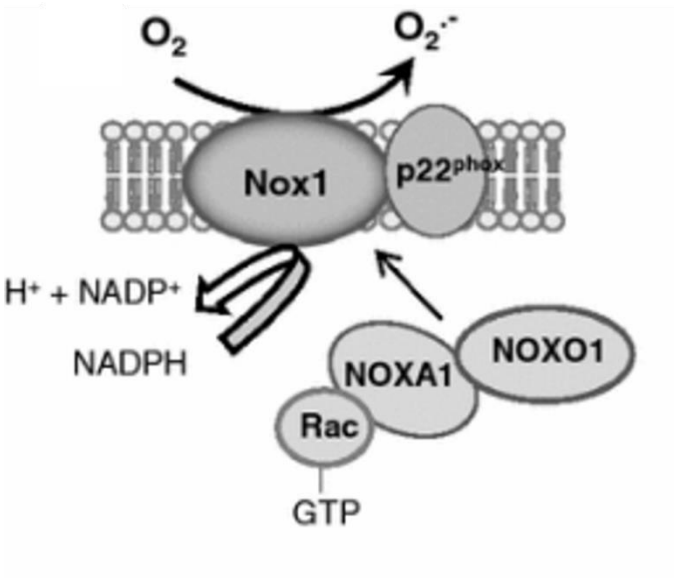

Figure 4.21 NOX1 and its regulatory subunits

NOX family enzymes generate ROS in response to a wide range of stimuli. NOX1 is the major isoform expressed in the colon. NOX1 uses NADPH as an electron donor to generate superoxide (O_2^-) from molecular oxygen. The NOX1 complex consists of the catalytic subunit NOX1 and the regulatory subunit p22phox, both are located in the membrane. The other regulatory subunits NOXO1, NOXA1 and the small GTPase Rac are normally located in the cytoplasm. Upon stimulation with agonists, the cytosolic subunits translocate to the membrane-bound complex leading to enzymatic activity. NOXO1 subunit of NOX is used to organize the enzyme assembly, while NOXA1 function to activate enzymatic activity.

(Figure from Sirker, et al., 2011)

4.3.2 Characterisation of NOX1 and RAC1 protein expression in the human colonic crypt

The activation of NOX1 for the generation of ROS is a RAC1 dependent process (Cheng, et al., 2006; Brandes, et al., 2014). The expression pattern of RAC1 proteins – both inactive and active forms – in human colonic crypts is unclear. In this current study, the protein expression of total RAC1, NOX1 and active RAC1-GTP were identified and confirmed in human colonic crypts. In order to investigate the effect of Cch on total RAC1 and NOX1 recruitment and translocation in colonic crypt epithelial cells, crypts were either stimulated with Cch (10µM) for 1 min or not (Figure 4.22). Under resting (unstimulated) conditions, total RAC1 was detected at the basal pole of the crypt, and in the cytoplasm of non-goblet cells. In goblet cells, total RAC1 was mainly detected at the basal pole of cells. After 1 min of Cch stimulation, the immune localisation of total RAC1 was increased both at the basal pole and in the cytoplasm of colonocytes, while in goblet cells the expression of total RAC1 seems to appear near the nuclei and at the lateral membrane towards the apical pole of cell in 2D view (Figure 4.22A). Compared to total RAC1, NOX1 expression is relatively greater under resting conditions. NOX1 is expressed at the basal pole of the crypt and also in the cytoplasm of non-goblet cells. In goblet cells, NOX1 was mainly detected near the ER area under the nuclei in the 2D view. After 1 min of Cch stimulation, the expression of NOX1 decreased at both the basal pole and in the cytoplasm of the crypt (Figure 4.22B). These results demonstrate the expression of both total RAC1 and NOX1 proteins in human colonic crypts.

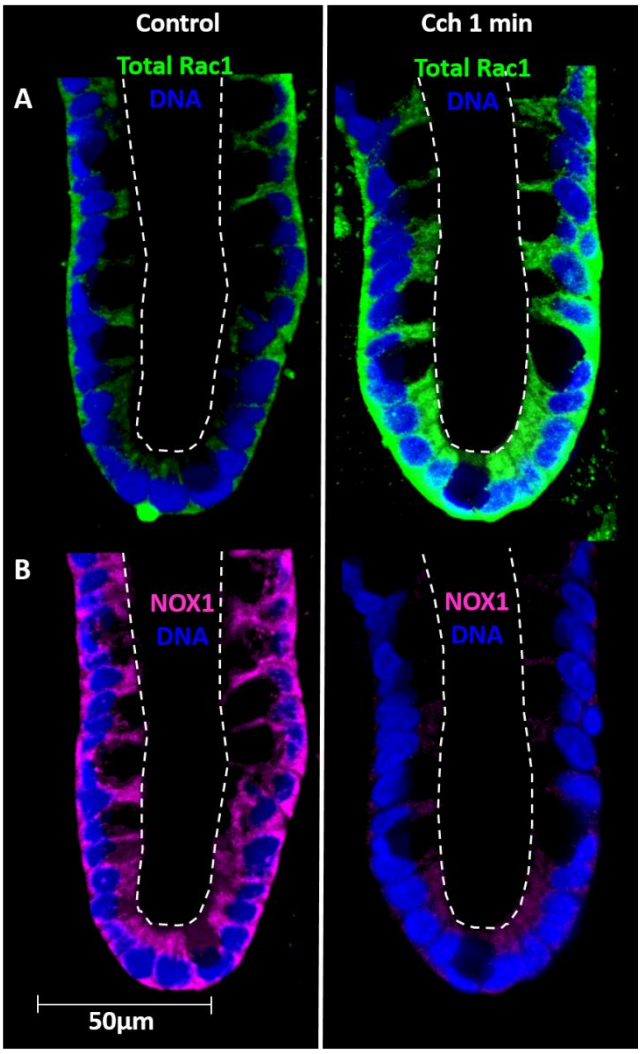

Figure 4.22 Expression patterns of total RAC1 and NOX1 proteins in human colonic crypts

Cultured human colonic crypts were separated into control and Cch treatment groups. Crypts were stimulated with Cch (10 µM) for 1 min. Both groups were fixed and stained with anti-total RAC1 (green) and anti-NOX1 (pink) antibodies; cell nuclei were stained with Hoechst (blue). White dotted lines show the boundary of the crypt lumen. Representative images were taken with a Zeiss Meta 510 confocal microscope using a x63 objective. (A) Composite image of total RAC1 (green) and DNA (blue). (B) Composite image of NOX1 (pink) and DNA (blue).

As discussed in previous sections 4.2.3 and 4.2.4, Cch-stimulated Ca^{2+} mobilisation from acidic organelles is mediated by the activation of CD38 and possibly the RAC1-dependent NOX signalling pathways. In order to demonstrate the correlation between the two pathways, the expression of both CD38 and total RAC1 proteins was investigated. Both CD38 and total RAC1 expression was detected at the basal pole of crypt cells and in the cytoplasm of non-goblet cells (Figure 4.23 A and B). In goblet cells, both CD38 and total RAC1 were expressed near the ER area below the nucleus and also below the lateral membrane towards the apical pole of the cell in 2D view. Some level of colocalisation of CD38 and total RAC1 was also observed at the basal pole and in the cytoplasm of crypt epithelial cells (Figure 4.23C). These results demonstrate the association between total RAC1 and CD38 proteins in human colonic crypts.

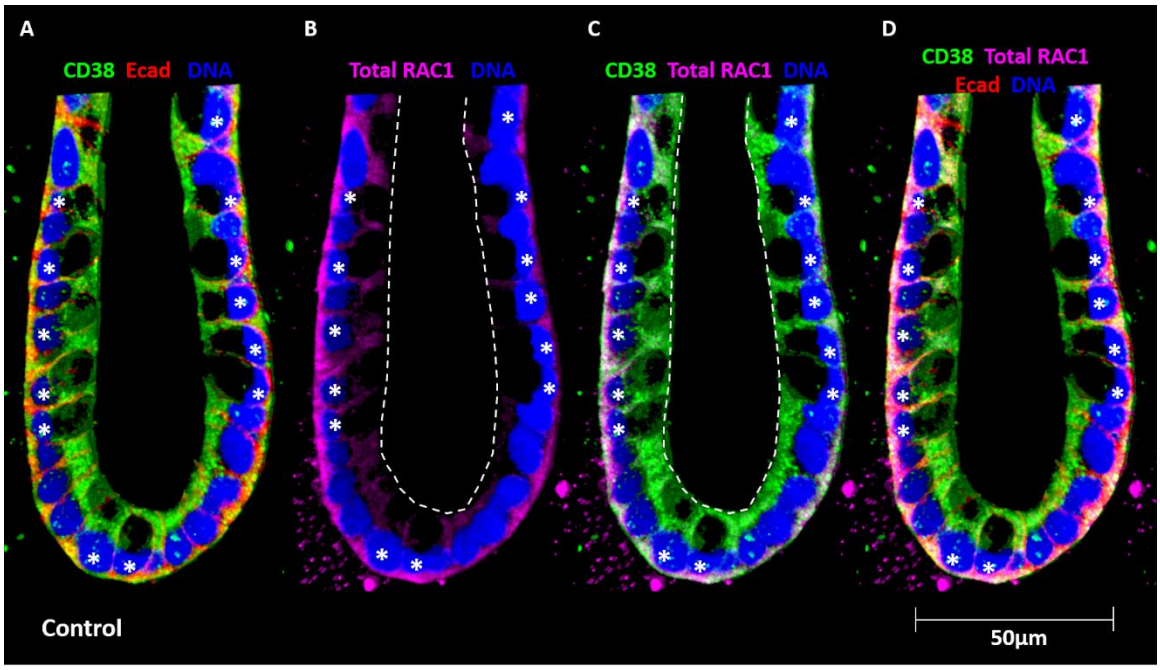

Figure 4.23 Localisation of CD38 and total RAC1 in human colonic crypts.

Cultured human colonic crypts were fixed and stained with anti-CD38 (green), anti-total RAC1 (pink) and anti-Ecad (red) antibodies; cell nuclei were stained with Hoechst (blue). Images were taken with a Zeiss Meta 510 confocal microscope using a x63 objective. Z stack confocal images were then reconstructed into 3D images using the Volocity software. White dotted lines show the boundary of the crypt lumen. (A) Composite image of CD38 (green), Ecad (red) and DNA (blue); (B) Composite image of Total RAC1 (pink) and DNA (blue); (C) Composite image of CD38 (green), Total RAC1 (pink) and DNA (blue); (D) Composite image of all four channels : CD38 (green); Total RAC1 (pink); Ecad (red) and DNA (blue). Goblet cells are highlighted with white asterisk.

4.3.3 Role of Cch in active RAC1-GTP and NOX1 recruitment and trafficking in human colonic crypts

RAC1 belongs to the Rho family of GTPases, and its downstream signalling is involved in a wide array of cellular responses including transcriptional dynamics, cell polarity and vesicular trafficking (Busetlo, et al., 2007). The conversion of inactive RAC1 to its active state is mediated by the guanine nucleotide exchange factors (GEFs) that catalyse the exchange of GDP with GTP. M3AchR activation has been shown previously to regulate RAC1 activation and translocation to cell junctions in Chinese Hamster Ovary (CHO) cells that were stably transfected with M3AchR (Ruiz-Velasco, et al., 2002). In this study, the role of Cch in the conversion and recruitment of active RAC1-GTP, and the trafficking of NOX1 in human colonic crypts were investigated. Cultured crypts were either unstimulated or stimulated with Cch (10μM) at different time points (30 sec, 1 min and 5 min). During resting (unstimulated) conditions, active RAC1-GTP was detected at the basal pole of the crypt, and also in the cytoplasm at the mid-cell region near the ER area of crypt epithelial cells; nuclear localisation was also observed in some colonocytes at the base of the crypt (Figure 4.24A i and ii). After Cch stimulation for 30 sec, the detection of active RAC1-GTP increased in the nuclei of some colonocytes, particularly at the crypt base (Figure 4.24A iii and iv), recruitment of active RAC1-GTP to the basal pole increased (by 94%, 1.94 ± 0.105, N= 4 subjects, n= 15 crypts, paired t-test $p< 0.01$) and possibly translocation of active RAC1-GTP from the basal pole to the apical pole of cells were also observed (intensity at apical pole/ cytoplasmic space increased by 82%, 1.82 ± 0.06, N= 4 subjects, n= 15 crypts, paired t-test $p< 0.01$, Figure 4.25A). After 1 min of Cch stimulation, the presence of active RAC1-GTP remained high at the basal pole, in particular in the nuclei of most colonocytes at the crypt base, while the amount in the cytoplasm was reduced in comparison to Cch 30 sec (0.98 ± 0.03, N= 3 subjects, n= 12 crypts, paired t-test $p< 0.01$, Figures 4.24A v and vi and 4.25A). With 5 min of Cch stimulation, the amount of active RAC1-GTP at the basal pole and nuclei returned to resting levels (1.005 ± 0.17, N= 4 subjects, n= 18 crypts) as compared to the unstimulated control, while the intensity in the cytoplasm slightly increased as compared to Cch 1 min (not significant, 1.19 ± 0.15, N= 4 subjects, n= 18 crypts, $p= 0.28$, Figures 4.24A vii and viii and 4.25A). Thus these results demonstrate the expression and localisation of active RAC1-GTP in human colonic crypts upon Cch stimulation; Cch not only increased the conversion of RAC1 to its active form, but it also seems to mediate the trafficking of active RAC1 in the cytosol of crypt epithelial cells.

Similar to active RAC1, the recruitment of NOX1 in colonic crypt epithelial cells was also observed upon Cch stimulation. Under resting (unstimulated) conditions, NOX1 protein was detected at the basal pole and in the cytosol of the crypt epithelial cells (Figure 4.24B, i and ii). Upon Cch stimulation for 30 sec, the intensity of NOX1 staining at the basal pole of crypt (1.8 ± 0.5) and in the cytosol of colonocytes (1.45 ± 0.23) slightly increased in comparison to the control group (not significant, p= 0.22, Figure 4.24B iii and iv and Figure 4.25B). After 1 min of Cch stimulation, both basal pole (1.3 ± 0.3) and cytoplasmic (0.98 ± 0.1) detection of NOX1 were similar to unstimulated condition (Figures 4.24B v and vi and 4.25B). With 5 min of Cch stimulation, NOX1 staining at both basal pole (0.9 ± 0.1) and cytoplasm (1.1 ± 0.2) remained similar to unstimulated condition and Cch 1 min treatment (Figure 4.24B vii and viii and 4.25B). These results suggest that there are some levels of co-regulation between active RAC1-GTP and NOX1 recruitment in the human colonic epithelium, in particular active RAC1-GTP trafficking to NOX complex upon Cch stimulation. Further experiments are required to confirm these findings and the mechanism of action.

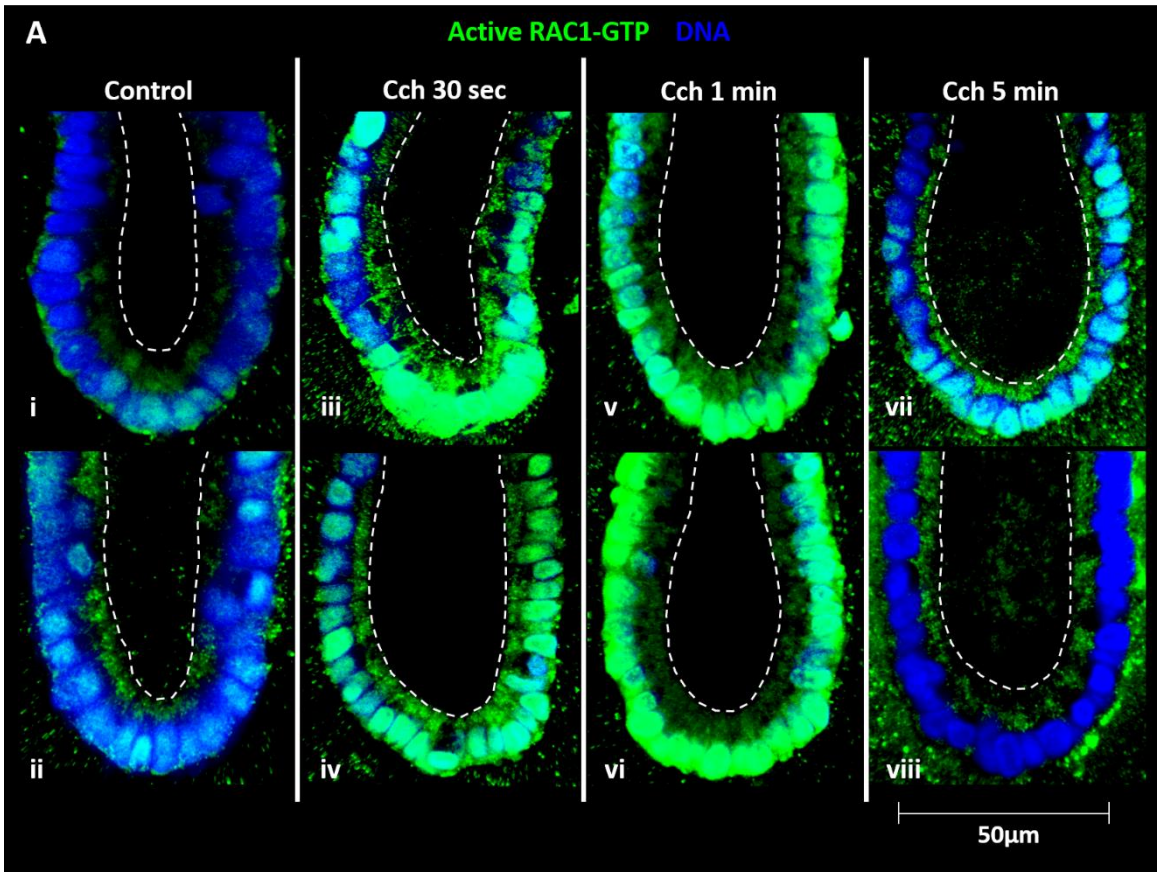

Figure 4.24A Expression patterns of active RAC1-GTP upon Cch stimulation in human colonic crypts

Cultured human colonic crypts were separated into control and Cch treatment groups. Crypts were stimulated with Cch (10 µM) for 30 sec, 1 min or 5 min. (A) Both treatment groups were fixed and stained with anti-active RAC1-GTP (green) antibody, cell nuclei were stained with Hoechst (blue). Dotted lines show the boundary of the crypt lumen. Representative images were taken with a Zeiss Meta 510 confocal microscope using a x63 objective. Composite images of active RAC1-GTP (green) and DNA (blue) (i-viii). Control group (i and ii); Cch 30 sec (iii and iv); Cch 1 min (v and vi); Cch 5 min (vii and viii).

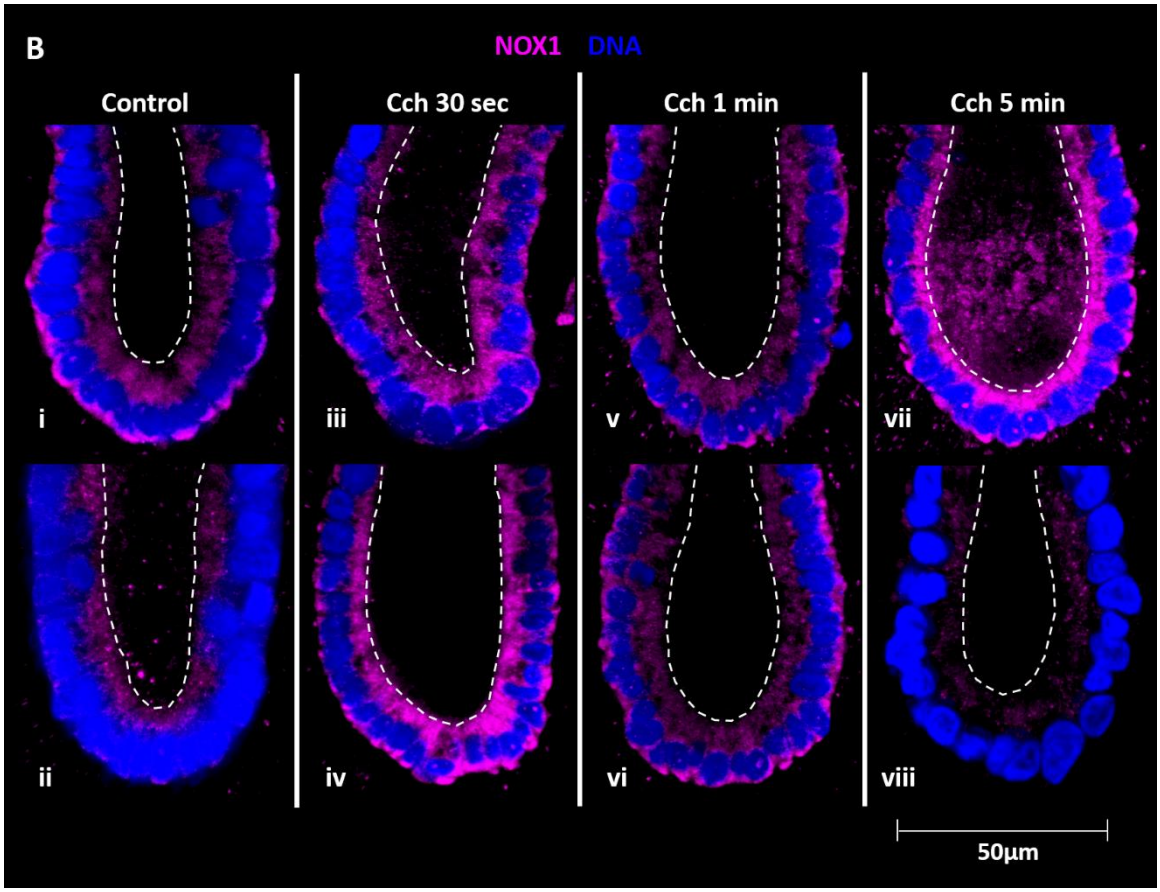

Figure 4.24B Expression patterns of NOX1 upon Cch stimulation in human colonic crypts

Cultured human colonic crypts were separated into control and Cch treatment groups. Crypts were stimulated with Cch (10 µM) for 30 sec, 1 min or 5 min. (B) Both groups were fixed and stained with anti-NOX1 (pink) antibody, cell nuclei were stained with Hoechst (blue). Dotted lines show the boundary of the crypt lumen. Representative images were taken with a Zeiss Meta 510 confocal microscope using a x63 objective. Composite images of NOX1 (pink) and DNA (blue) (i-viii). Control group (i and ii); Cch 30 sec (iii and iv); Cch 1 min (v and vi); Cch 5 min (vii and viii).

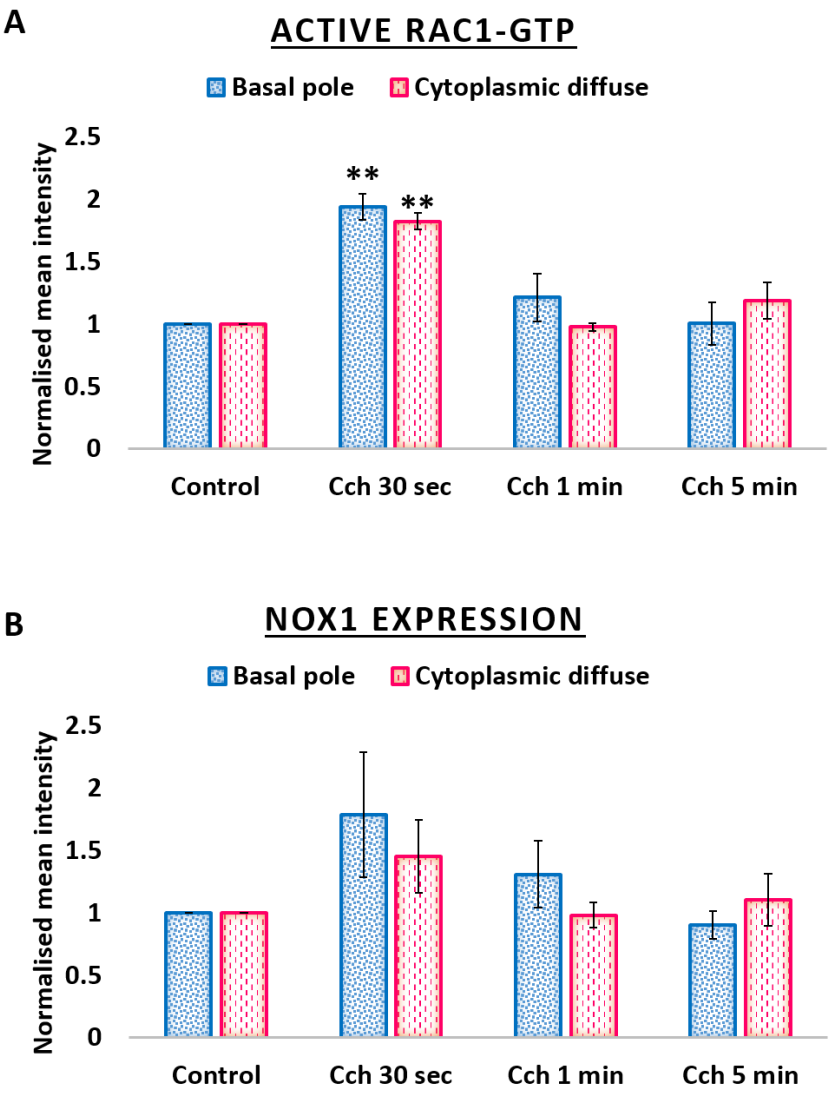

Figure 4.25 Intracellular trafficking of active RAC1-GTP and NOX1 upon Cch stimulation in human colonic crypts

Cultured human colonic crypts were separated into control and Cch treatment groups. Crypts were stimulated with Cch (10 µM) for 30 sec, 1 min or 5 min; both groups were then fixed and stained with anti-active RAC1-GTP (green) and anti-NOX1 (pink) antibodies, cell nuclei were stained with Hoechst (blue) (Figures 4.24A and B). The active RAC1-GTP (A) and NOX1 (B) intensities at the basal pole and cytoplasmic space of the crypt were quantified by ImageJ software. Mean intensities of both regions were calculated and normalised to the control group, and displayed as mean ± SE. Significant differences were assessed using One-way ANOVA test, [F (3, 11) = 11.1, p= 0.001] for basal active RAC1-GTP and [F (3, 11)= 21.1, p= 0.00007] for cytoplasmic active RAC1-GTP; followed by Bonferroni procedures and Tukey's post hoc analysis. Significant difference between pairs of mean values (ie. Cch 30 sec vs. each of the other group) were indicated by asterisks (**) for p< 0.01. No significant difference were observed between other pairs including (i) control vs. Cch 1 min, (ii) control vs. Cch 5 min, and (iii) Cch 1 min vs. Cch 5 min for both basal and cytoplasmic active RAC1-GTP. No significant difference were observed for both basal and cytoplasmic NOX1 upon Cch stimulation. Results were representative of N= 4 subjects, n≥ 11 crypts in each group.

4.3.4 Correlation of RAC1/NOX1 dependent ROS production and calcium signal generation at apical pole of crypt epithelial cells

Cross talk between ROS and Ca^{2+} signalling pathways has been shown to occur both in the plasma membrane and the cytosol (Yan, et al., 2006). In the human colonic epithelium, the role of RAC1/NOX1 dependent ROS production in mediating intracellular Ca^{2+} mobilisation or vice versa is unclear. In order to establish a correlation between ROS and Ca^{2+} signalling, the time course of RAC1/NOX1 recruitment or translocation to the apical pole of cells was compared to the latency (from the point of stimulation to the peak of response) of the Cch-induced Ca^{2+} signals. About 30 sec after Cch administration, there was an increase in active RAC1-GTP and NOX1 proteins at the basal pole of the crypt, and also in the cytoplasm towards the apical pole of the crypt (Figure 4.26A). The formation of RAC1/NOX1 complexes presumably generates ROS in the cytosol in close proximity to the acidic lysosomal Ca^{2+} stores. Coincidentally, the average latency of Cch-induced Ca^{2+} signals calculated from 15 human subjects is about 46 sec (Figure 4.26B). Hence, it is feasible that ROS acts as the second messenger that transfers the activation signals from the basal pole to the Ca^{2+} response at the apical pole of crypt cells. Due to the technical difficulties, it was unable to show the interactions/ events for less than 30 sec. The role of ROS/ Ca^{2+} signalling cross talk in the human colonic epithelium was then confirmed by pharmacological inhibitors (see section 4.3.5). As mentioned in section 4.2, M3AchR activation promotes the conversion of DAG into PA, while PA has been shown to stimulate NADPH oxidase activity (McPhail, et al., 1995; Zhang, Y. et al., 2009). The role of the PA pathway in NOX1 activation (subunit translocation) in human colonic crypts was briefly investigated. Crypt samples were treated with R59-022 (10μM) for 1 hour in order to block the conversion of DAG into PA. Inhibition of PA formation reduced the recruitment of active RAC1-GTP to the basal pole of the crypt as compared to the control, suggesting a role of the PA pathway in stimulating NOX1 activity in the human colonic epithelium upon Cch stimulation (data not shown). No obvious differences were observed in cytosolic RAC1-GTP. The initial recruitment of active RAC1-GTP to the basal membrane/pole of the crypt might be an important step for the subsequent recruitment or translocation of the active RAC1-GTP to the apical pole of crypt cells. In addition, no obvious difference were observed in NOX1 expression after treatment with R59-022 (data not shown).

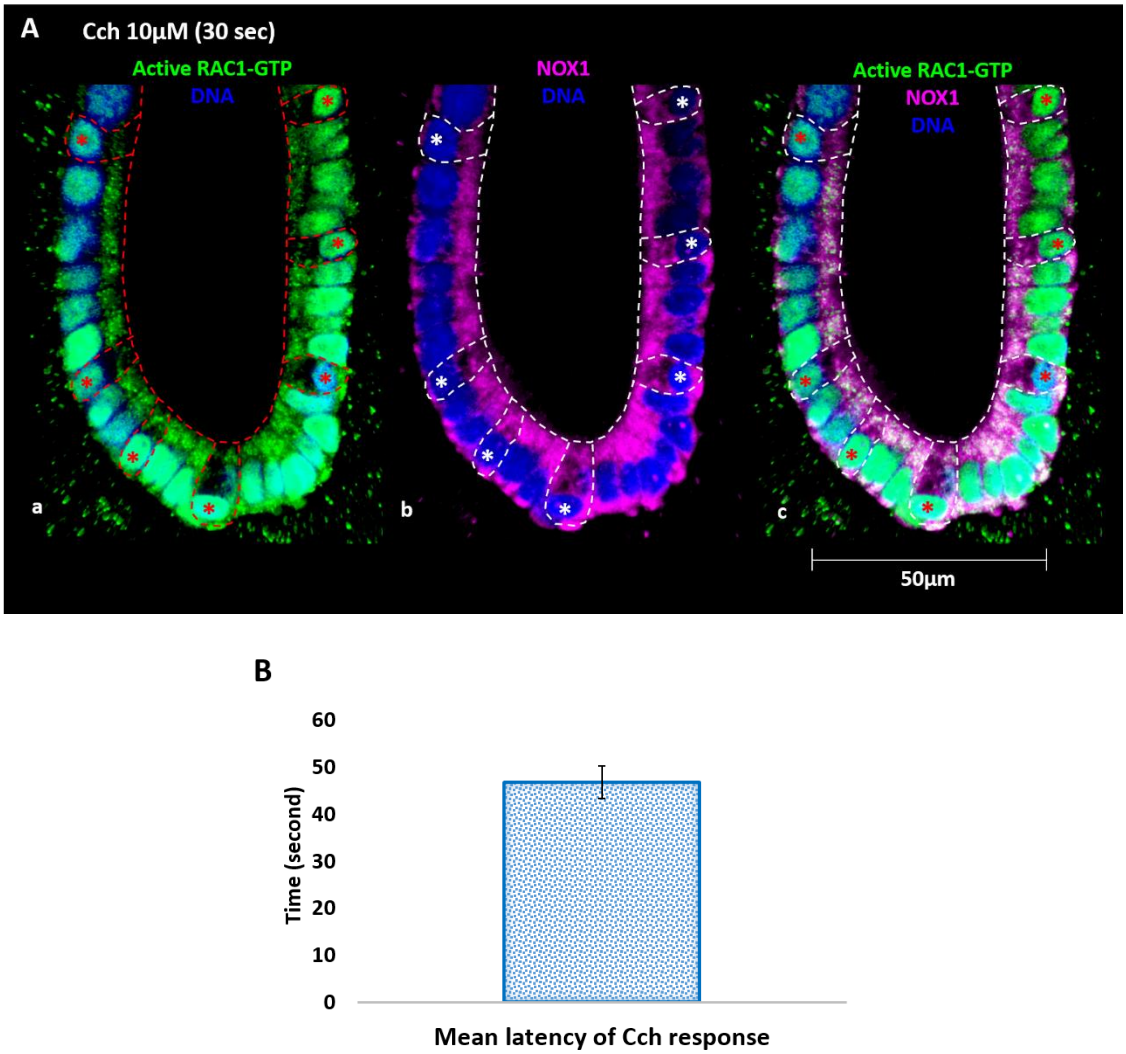

Figure 4.26 Correlation between active RAC1-GTP & NOX1 recruitment and Ca^{2+} signal generation upon Cch stimulation

Crypts were stimulated with Cch (10 µM) for 30 sec. (A) Crypts were then fixed and stained with anti-active RAC1-GTP (green) and anti-NOX1 (pink) antibodies, cell nuclei were stained with Hoechst (blue). Representative images were taken with a Zeiss Meta 510 confocal microscope using a x63 objective (Figures 4.24A (iv) & 4.24B (iv)).(a) Composite image of active RAC1-GTP (green) and DNA (blue); red dotted lines show the boundary of the crypt lumen and also the boundaries of each goblet cell. Goblet cells are highlighted with red asterisks. (b) Composite image of NOX1 (pink) and DNA (blue); white dotted lines show the boundary of the crypt lumen and also the boundaries of each goblet cell. Goblet cells are highlighted with white asterisks. (c) Composite image of all three channels: active RAC1-GTP (green), NOX1 (pink) and DNA (blue); white dotted lines show the boundary of the crypt lumen and also the boundaries of each goblet cell. Goblet cells are highlighted with red asterisks. (B) Mean latency of Cch stimulated Ca^{2+} responses in human colonic crypts (5-7 crypts per set of experiment) from 15 subjects. Mean response time is 46 sec.

4.3.5 Role of NOX1/RAC1 in Cch-induced calcium signal generation

NOX family enzymes are one of the major sources of ROS generation in mammals (Brandes, et al., 2014). The NOX1 isoform is dominantly expressed in the colon (Szanto, et al., 2005), however, the impact of NOX1-derived ROS on colonic physiology and M3AchR activation mediated Ca^{2+} mobilisation remains poorly understood. Due to the limitation and unavailability of peptide-based or other specific NOX1 inhibitors, small molecule inhibitors that lack specificity were used to investigate the role of NOX1-derived ROS in Cch-induced Ca^{2+} signal generation (Figure 4.28 top panel). Human colonic crypts were treated with a potent NOX inhibitor DPI (1µM) for 1 hr prior to re-stimulation with Cch (10µM) in the presence of the inhibitor (Figure 4.27A). DPI (1µM) significantly reduced the Cch-induced Ca^{2+} signals by 66% as compared to the control (0.34 ± 0.06, N= 2 subjects, n=6 crypts, paired t-test p= 0.0005, Figure 4.28 bottom panel). To test whether there is a dose dependent inhibition, human colonic crypts were treated in the same fashion with DPI (5µM) (Figure 4.27B). 5µM of DPI significantly blocked the Cch-induced Ca^{2+} signals by 94% (0.059 ± 0.02, N= 1 subject, n=2 crypts, paired t-test p= 0.016, Figure 4.28 bottom panel). However, further statistical analysis shows no significant difference between DPI (1µM) and DPI (5µM) (Figure 4.28 bottom panel). These data suggest NOX1-derived ROS contributes to the Cch-induced Ca^{2+} response. However, DPI has also been shown to block mitochondrial and other sources of ROS (Li, et al., 1998; Brandes, et al., 2014), therefore the role of NOX1-derived ROS was further verified by other inhibitors. Apocynin is a widely used NOX inhibitor; previous work in the vascular system has suggested this compound acts as an antioxidant that interferes with peroxides, but not superoxide (Heumüller, et al., 2008). To test the effect of this compound in our model system, human colonic crypts were treated with apocynin (100µM) for 1 hr prior to re-stimulation with Cch (10µM) + apocynin (Figure 4.27C). The Cch-induced Ca^{2+} signal was blocked by 49% (0.506 ± 0.05, N= 4 subjects, n= 12 crypts, paired t-test p< 0.00001, Figure 4.28 bottom panel). These results suggest that ROS is involved in generating the Cch-induced Ca^{2+} waves, yet it is still unclear whether these ROS were derived from NOX1 or other cellular sources.

The role of NOX1-derived ROS was further investigated with a specific pan-NOX inhibitor VAS2870. Human colonic crypts were treated with VAS2870 (56µM) for 1 hr prior to re-administration of Cch (10µM) in the presence of the inhibitor. The Cch-induced Ca^{2+} signal was blocked by 76% (0.24 ± 0.12, N= 3 subjects, n= 3 crypts, paired t-test p< 0.05, Figure 4.28 bottom panel). The level of inhibition is comparable to the effect of DPI (1µM), consistent with the hypothesis that NOX1-derived ROS is involved in the Ca^{2+} signal generation upon

Cch stimulation. In addition, the role of RAC1 in NOX-dependent ROS generation was further explored using the RAC1 activation inhibitor NSC23766. Cultured human colonic crypts were treated with NSC23766 (250µM) for 1 hr prior to re-administration of Cch (10µM) with the presence of the inhibitor (Figure 4.27D). The RAC1 inhibitor significantly blocked the Cch-induced Ca^{2+} signals by 95% (0.05 ± 0.02, N= 4 subjects, n= 10 crypts, paired t-test p< 0.00001) as compared to the control Ca^{2+} waves (Figure 4.28 bottom panel). This level of inhibition is comparable to the effect of DPI (5µM). Further statistical analysis shows no significant difference among treatments with NADPH oxidase inhibitors including DPI (5µM), VAS2870 and NSC23766 (Figure 4.28 bottom panel). Thus, these combined results suggest the involvement of NOX1-dependent ROS in Cch-mediated Ca^{2+} signal generation. Having established this involvement, the next step was to look into the effects of these inhibitors on mucus secretion in the human colonic epithelium.

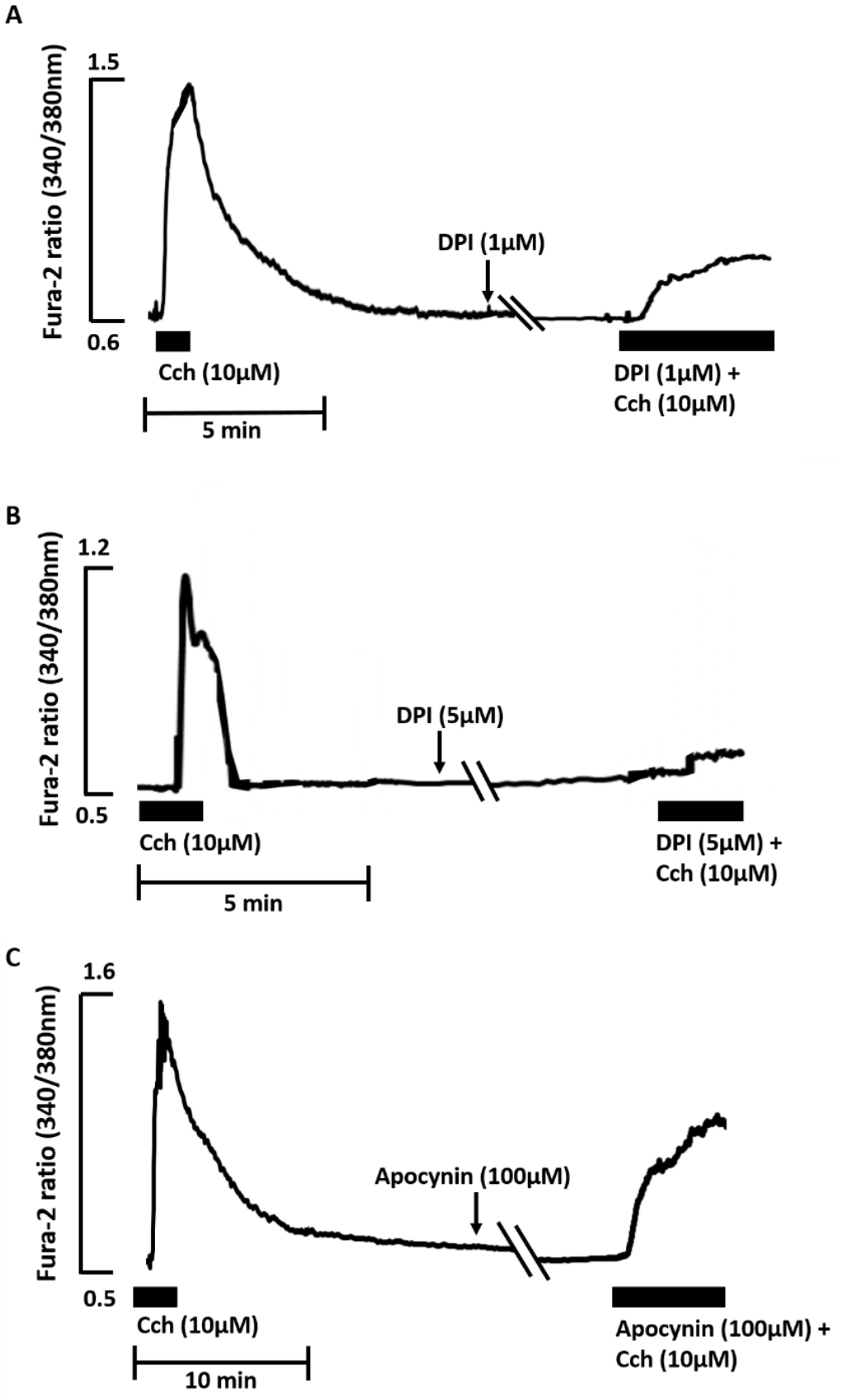
A
1.5
Fura-2 ratio (340/380nm)
0.6
DPI (1μM)
Cch (10μM)
5 min
DPI (1μM) +
Cch (10μM)
B
1.2
Fura-2 ratio (340/380nm)
0.5
DPI (5μM)
Cch (10μM)
5 min
DPI (5μM) +
Cch (10μM)
C
1.6
Fura-2 ratio (340/380nm)
0.5
Apocynin (100μM)
Cch (10μM)
10 min
Apocynin (100μM) +
Cch (10μM)

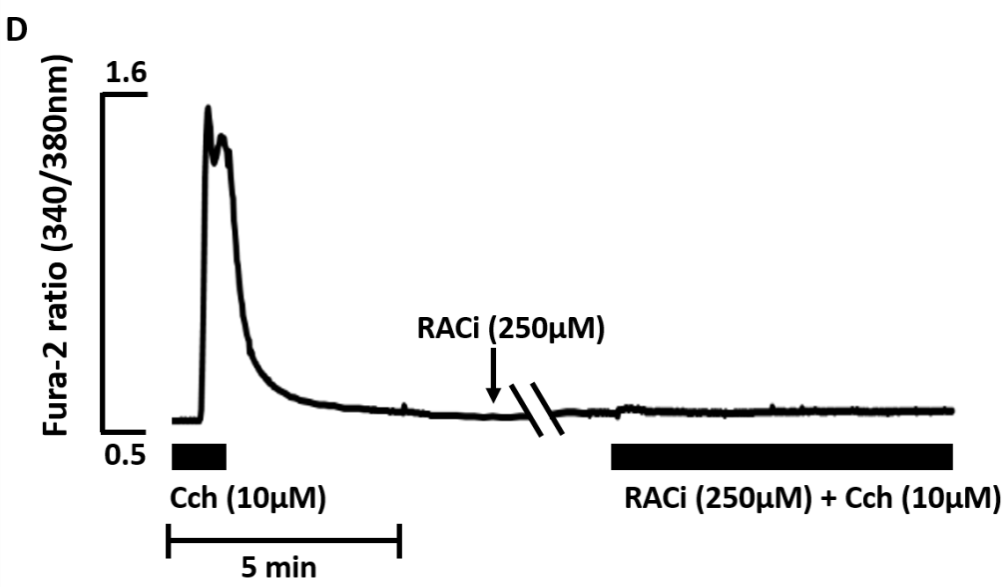

Figure 4.27 The role of NADPH oxidase inhibitors in Cch-induced Ca^{2+} signals in human colonic crypts

Representative traces of the Ca^{2+} response upon Cch stimulation in Fura-2 loaded human colonic crypts. A control response to 10µM of Cch was conducted in all experiments (first Ca^{2+} peak). Cch administration is indicated by the black bar (duration). The amplitude of the control Ca^{2+} responses ranged from 0.7-1.1. After removal of the agonist and return of the intracellular [Ca^{2+}] back to baseline, crypts were then treated with different inhibitors for 1 hour prior to subsequent re-administration of Cch (10µM) in the presence of the respective inhibitors (2^{nd} black bar). (A) DPI (1µM), representative result of N= 2 subjects, n= 6 crypts; (B) DPI (5µM), result derived from N= 1 subjects, n= 2 crypts; (C) Apocynin (100µM), representative result of N= 4 subject, n= 12 crypts; (D) RAC1 inhibitor (NSC23766, 250µM), representative result of N= 4 subjects, n= 10 crypts.

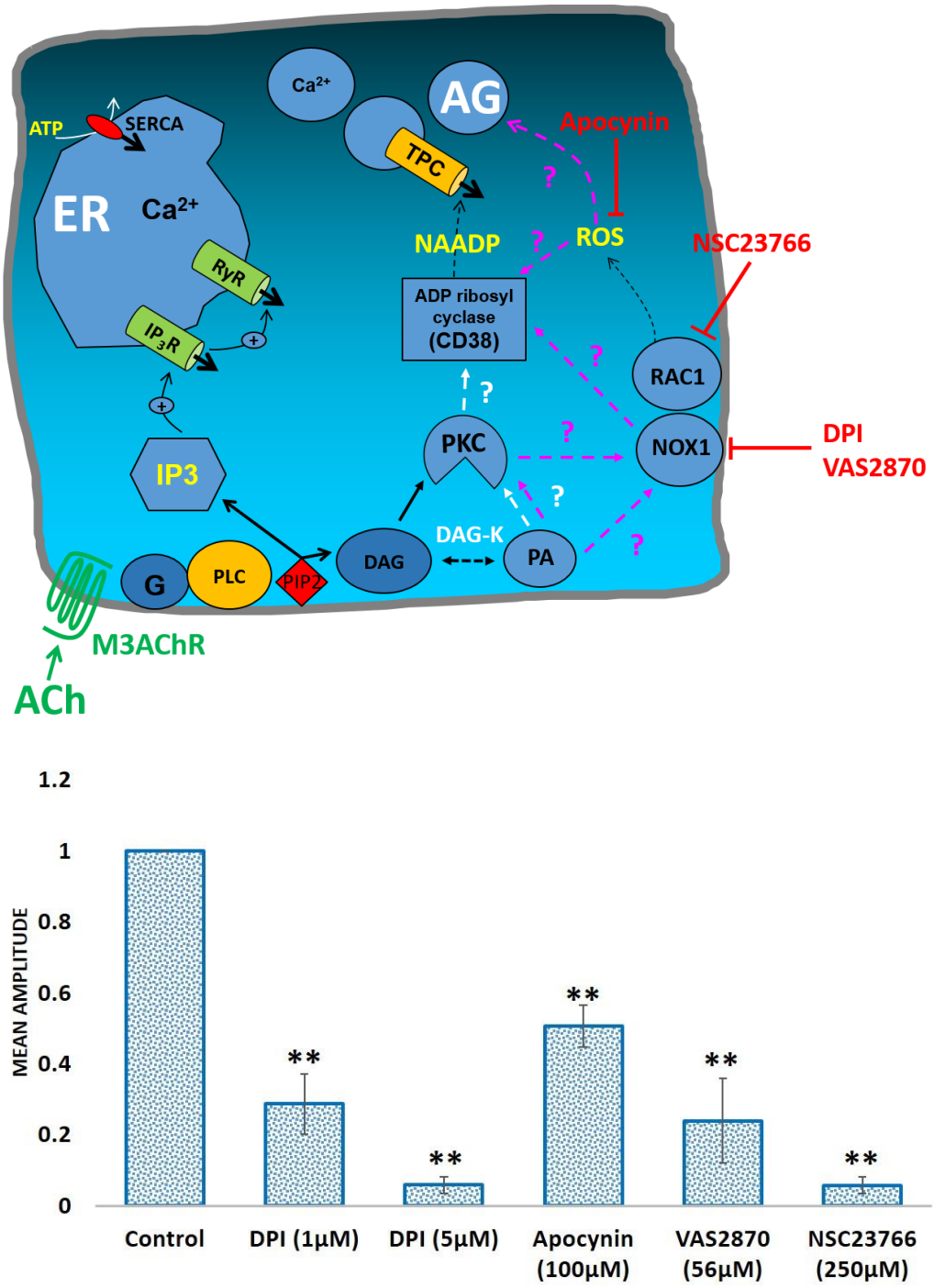

Figure 4.28 Pharmacological inhibition of NADPH oxidase 1 and RAC1

Schematic representation of the MAchR signalling pathways (top panel). The amplitude of the Ca^{2+} responses in the control group and the inhibitor treated groups as displayed in the previous figure (Figure 4.27) were calculated. The mean amplitude of each experimental group was normalised to the control group, and displayed as mean ± SE (bottom panel). Significant differences were assessed by One-way ANOVA test, $F(5, 38) = 91.3$, $p < 0.00001$; followed by Bonferroni procedures and Tukey's post hoc analysis. Significant difference between pairs of mean values (i.e control vs. each treatment group) were indicated by asterisks (**) for $p < 0.01$. Significant difference ($p < 0.01$) was also observed in the following pairs: (i) DPI (1µM) vs. NSC23766, (ii) DPI (5µM) vs. Apocynin, (iii) Apocynin vs. NSC23766.

No significant difference was observed in the following pairs: (i) DPI (1µM) vs. DPI (5µM), (ii) VAS2870 vs. NSC23766, (iii) Apocynin vs. VAS2870. (iv) DPI (1µM) vs. Apocynin, (v) DPI (1µM) vs. VAS2870, (vi) DPI (5µM) vs. VAS2870, (vii) DPI (5µM) vs. NSC23766. Schematic diagram is courtesy of Mark Williams. Ca^{2+} data for VAS2870 is courtesy of George Russam, a student in the lab who collaborated on this section.

4.4 Discussion

Ach is one of the many neurotransmitters that is synthesised and released by cholinergic neurons. In general, activation of MAchRs by Ach or Cch has been shown to trigger downstream signalling pathways. Generation of the 2nd messenger IP3 downstream of this signalling has been well established, which then causes release of Ca^{2+} from the ER store via the IP3R. The initial increase in intracellular [Ca^{2+}] can trigger the CICR response within the cell (Felder, 1995; Budd, et al., 1999). A link between MAchR activation and Ca^{2+} signal generation has been demonstrated previously in rat and human colonic crypts (Lindqvist, et al., 1998; Lindqvist, et al., 2002; Reynolds, et al., 2007). However, the underlying mechanism of the cholinergic mediated Ca^{2+} signal generation in the human colonic epithelium has never been demonstrated. In this part of the study, inhibitors of the MAchR signalling components and intracellular Ca^{2+} channels were used to delineate the key intracellular Ca^{2+} release channel and the Ca^{2+} store responsible for the generation of the Ca^{2+} signals upon Cch stimulation. In keeping with the topology and polarity of colonic crypt Ca^{2+} waves, and the expression characteristics of the colonic crypt Ca^{2+} signalling toolkit, the current data set indicate that mobilisation of acidic endolysosomal Ca^{2+} stores via a RAC1/NOX/CD38/NAADP/TPC pathway is instrumental in orchestrating human colonic crypt Ca^{2+} signals.

4.4.1 Cholinergic mediated calcium signalling in the human colonic crypt

Application of Ach to the human colonic crypt has repeatedly been shown extensively in our lab to mobilise Ca^{2+} in a wave-like manner via the activation of M3AchR. In order to avoid the hydrolysis of Ach by endogenous cholinesterases, Cch (a chemical analogue of Ach) was used for all of the experiments in this current study. Administration of 10µM Cch stimulates a Ca^{2+} response that is comparable to the Ach stimulated Ca^{2+} waves and dynamics as demonstrated from previous studies in our lab (Lindqvist, et al., 1998; Lindqvist, et al., 2002; Reynolds, et al., 2007). Specifically, these Ca^{2+} waves initiate at the apical pole of initiator cells located at the crypt base (Figure 4.2B (a)). It is currently unclear exactly which cell type (or types) make up the initiator cell population, however preliminary data from immunohistochemical labelling and Fluo-4 Ca^{2+} imaging suggests that the $LGR5^{+}$ stem cells at the base of crypt might be Ca^{2+} initiator cells (Figure 4.2B (b)). As the Ca^{2+} signals were initiated at the apical pole of crypt cells, this observation also suggests that some source of Ca^{2+} localised at the apical pole provides the initiation signal, and these Ca^{2+} signals then spread to neighbouring cells along the crypt-axis via gap junctional proteins or via a paracrine

route. In this current study, immunohistochemical labelling demonstrated the presence of the ER at the basal pole, whereas the acidic lysosomes are localised at the apical pole of the polarised colonic epithelial cells (Chapter 3, Figure 3.15). Hence, these findings strongly implicate the acidic lysosomes as having a pivotal role in Cch-induced Ca^{2+} signal generation. However, it is still unclear how the signals transfer to the apical pole when the M3AchRs are expressed on the basal membrane of the crypt (Chapter 3, Figures 3.10 and 3.15). One of the possibilities is the generation of another 2nd messenger upon M3AchR activation that spreads the signals to the other side of the cell. As the Ca^{2+} signals peaked between 30-100 seconds after Cch administration, this 2nd messenger must form very quickly and should be strongly associated with the Ca^{2+} signalling (see below section 4.4.6).

In this study, Cch-induced Ca^{2+} mobilisation from intracellular Ca^{2+} stores was also confirmed by conducting experiments in Ca^{2+}-free HBS buffer (Figure 4.4). The initial phase of the Ca^{2+} response (from initiation to peak) was similar to the control in both concentration of Cch (10µM and 50µM) tested. When the ER store was depleted with thapsigargin (Tg, 1µM), the SERCA pump is no longer capable to refill the depleted ER store. The differences in the Ca^{2+} response observed in the presence or absence of extracellular Ca^{2+} suggests that the SOCE (including the CRAC channels, ORAI1 and STIM1 proteins) are functional and operational in human colonic epithelial cells (Figures 4.5A and 4.5B). In addition, a small Ca^{2+} response observed after ER store depletion in both the control and Ca^{2+}-free conditions further suggests the M3AchR signalling might potentially induce Ca^{2+} release from additional intracellular Ca^{2+} stores (Figures 4.5A and 4.5B). Moreover, it also implies that global CICR Ca^{2+} signals are dependent on the ER store, as only minimal Ca^{2+} signals were observed when the ER store is depleted. These observations in human colonic epithelial cells are very similar to those in pancreatic acinar cells in a previous study which examined the requirement of acidic stores for the generation of local Ca^{2+} spikes upon IP3, cADPR or NAADP stimulation. Menteyne and colleagues demonstrated that both IP3- and NAADP-induced Ca^{2+} spikes were inhibited by bafilomycin A1 (150nM); while cADPR evoked Ca^{2+} spikes that were not inhibited by bafilomycin A1, which instead transformed hugely amplified the Ca^{2+} spike into a large response (Menteyne, et al., 2006). These results suggest that acidic stores are required for IP3- and NAADP-induced Ca^{2+} response in addition to the ER store in pancreatic acinar cells. Although acidic stores seem to play a role in cADPR-induced Ca^{2+} response but the level of regulation was unclear. Thus, Menteyne et al suggested Ca^{2+} spikes evoked by different agonists all require a different proportion of interactions between acidic lysosomal Ca^{2+} stores and the ER store (Menteyne, et al., 2006). In this thesis, based on the subcellular

localisation of the lysosomes, the initiation signals at the apical pole of the crypt, and the minimal Ca^{2+} signals evoked by Cch after ER store depletion, we can infer a strong link between the acidic lysosomal Ca^{2+} stores and the ER store during the M3AchR signal transduction pathways. However, the exact mechanisms of these interactions are as yet unclear.

4.4.2 Characterisation of the calcium signal generation downstream of M3AchR activation

The M3AchR signalling pathways which mobilise the ER Ca^{2+} stores via IP3R have been well established for decades (Felder, 1995; Nahorski, et al., 1997). However, the role of M3AchR signals in mobilising Ca^{2+} from other intracellular organelles is less clear. A study by Aley and colleagues have previously demonstrated a transient increase in NAADP levels upon Cch stimulation, and these NAADP were shown to increase intracellular [Ca^{2+}]. Inhibition of NAADP by Ned-19 suppressed intracellular Ca^{2+} mobilisation and blocked tracheal smooth muscle contraction (Aley, et al., 2013). These findings further support a role of MAchR activation in mobilising acidic lysosomal Ca^{2+} stores, however, the mechanism of regulation remains unclear. The most common MAchR signal transduction pathway operates via the activation of PLC (Budd, et al., 1999), however, simultaneous activation of PLC and PLD pathways have also been shown in most cells studied after receptor activation (Liscovitch, 1991). In this thesis, PLC was the dominant pathway upon M3AchR activation in human colonic crypts as demonstrated by the effect of the PLC inhibitor U73122 that blocked the Cch-induced Ca^{2+} signals (by 87%, Figure 4.8A). Activation of PLC initiates the hydrolysis of PIP2 into IP3 and DAG (Felder, 1995; Budd, et al., 1999), at which the signals diverge. DAG can be converted to PA by DAG kinase (Kanoh, et al., 2002). Under resting (unstimulated) conditions, the activity of DAG kinase is low, allowing DAG to exert its functions (e.g. PKC activation). Upon receptor activation of the PIP2 pathway, the increased activity of DAG kinase drives the conversion of DAG to PA, terminating signalling downstream of DAG (Mérida, et al., 2008). Given these findings, we would expect the effectors downstream of M3AchR activation should be IP3 and PA. In order to investigate the contribution of DAG, human colonic crypts were treated with the DAG kinase inhibitor R59-022, which blocks the conversion of DAG into PA. However, the DAG/PKC pathway only contributed to 36% of the Ca^{2+} signals as compared to the control (Figure 4.8B), suggesting some DAG dependent PKC isoforms are involved in the Cch-induced Ca^{2+} signal generation. Expressed in other terms, this means that blockade of the PA pathway reduced Cch-induced Ca^{2+} signals by 64%. PA

has also been shown to activate some isoforms of PKC including -zeta (DAG independent) and PKC-alpha (DAG dependent) in the absence and presence of Ca^{2+} respectively (Limatola, et al., 1994). Thus, it suggests that some effectors (including PKC) or 2nd messengers downstream of the PA pathway might play an important role in the generation of Cch-induced Ca^{2+} signals in the human colonic epithelium.

The PKC family of proteins consists of 15 isoforms in humans (Mellor, et al., 1998). They are divided into three subfamilies: conventional, novel, and atypical, based on their requirement for DAG and Ca^{2+} for activation (Shearman, et al., 1989; Kikkawa, et al., 1989). PKC isoforms including PKC-alpha (α), -beta (β), -delta (δ), -epsilon (ε), -zeta (ζ) and –eta (η) have previously been reported to be expressed in the human colonic mucosa (Davidson, et al., 1994). PKC-α, -β, and –ζ were found to be expressed predominantly in the cytosolic fraction, while PKC-δ, -ε and –η were detected in the membrane-associated fraction. It is speculated that more than one PKC isoform might be activated by Cch stimulation, and not all PKC isoforms are activated by DAG. In this study, the role of PKCs in Ca^{2+} signal generation was determined by the selective PKC inhibitor sotrastaurin, that blocked the Cch-induced Ca^{2+} signals (by 45%) relative to control Ca^{2+} waves (Figure 4.8C), suggesting that both DAG-dependent and -independent PKC isoforms are downstream of the M3AchR signal transduction which contribute to the Ca^{2+} signal generated upon Cch stimulation. As the expression of the different PKC isoforms was not measured in the current study, we are unable to determine which isoforms are involved in the signal transduction. Moreover, a previous study in the kidneys of diabetic rats demonstrated that some DAG-dependent PKC isoforms such as PKC-δ and PKC-ε can be sensitively regulated by oxidative stress (Ha, et al., 2001), suggesting another level of PKC regulation by ROS in the absence of DAG activation.

As discussed previously, blockade of the conversion of DAG into PA reduced Cch-induced Ca^{2+} signals by 64% (Figure 4.8B). In addition to activation of some PKC isoforms, PA has also been shown to regulate the activity of NADPH oxidases (NOXs) in plant cells (Zhang, Y. et al., 2009), and also mediate the phosphorylation of the neutrophil NOX component p47-phox in a cell free system (cytosolic and membrane fractions from neutrophils) (Waite, et al., 1997). This suggests that M3AchR activation may lead to activation of the NOX pathway via PA. NOX1 is the predominant NOX isoform expressed in the colon (Szanto, et al., 2005), and is involved in the generation of superoxide anion (O_2^-). The superoxide is then converted to hydrogen peroxide (H_2O_2) by superoxide dismutase (Yan, et al., 2006; Bedard, et al., 2007; Görlach, et al., 2015). Logically, if NOX is indeed activated upon cholinergic stimulation, it follows that ROS production might as well, necessitating an investigation of the role of ROS

in the Ca^{2+} signal generation upon Cch stimulation (See later section 4.4.6). PA can also be generated by the activation of PLD. PLD catalyses the hydrolysis of phosphatidylcholine producing PA and choline (Felder, 1995; Liscovitch, et al., 2000). Choline is the precursor of Ach, hence M3AchR-linked PLD activation might be important for the generation of endogenous (non-neuronal) Ach in the colonic epithelium.

4.4.3 Involvement of IP3R-gated and RYR-gated calcium release in generating Cch-induced calcium signals

IP3Rs are one of the types of Ca^{2+} release channel expressed on the ER membrane. They were also found to be expressed on the Golgi apparatus and secretory vesicles (Taylor, et al., 2009). In this current study, IP3Rs were indeed found in the ER area as well as in the area where the acidic lysosomes reside (Chapter 3, Figures 3.17A and B). However, it is still unclear whether IP3Rs play any role in releasing Ca^{2+} from other intracellular organelles. As discussed previously, if M3AchR activation of PIP2 promotes the conversion of DAG into PA by DAG kinase, the effectors downstream of this pathway should be IP3 and PA. The role of IP3/IP3R in Cch-induced Ca^{2+} signals in human colonic crypts was then investigated with a non-specific IP3R inhibitor (2-APB) and a specific IP3R inhibitor (Xes C). Surprisingly, both compounds were only observed to inhibit approximately 30% of the Ca^{2+} signals, in comparison to untreated controls (Figures 4.10A and B), suggesting that IP3/IP3R is not the key 2^{nd} messenger/Ca^{2+} release channel. This observation is quite unusual as it has been well established that M3AchR activation generates IP3, then IP3 mobilises Ca^{2+} from the ER store and subsequently induces CICR responses. These findings prompted our speculation that the PA pathway or some other pathways upstream of IP3 might be the key trigger for Cch-induced Ca^{2+} signals. As discussed previously, PA has been shown to activate the NOX pathway, and inhibition of PKC blocked the Cch-induced Ca^{2+} signals by 45%. The role of PA and the unknown (presumably NOX) pathways were further investigated with the application of both sotrastaurin (20μM) and 2-APB (50μM), the combination of which blocked the Ca^{2+} signal by 45% (Figure 4.10C). The lack of an additive effect of 2-APB suggests the role of IP3R in mediating Ca^{2+} release from the ER is probably downstream of PKC, and as R59-022 inhibited the Cch-induced Ca^{2+} signals by 64% (Figure 4.8B), the implication is that that PKC is activated by PA and/or NOX pathways that are downstream of M3AchR signal transduction upon Cch stimulation.

RYRs are other key players involved in regulating ER Ca^{2+} release. In this current study, the role of RYRs in Cch-induced Ca^{2+} signals were investigated by the application of ryanodine (50μM), which blocked the Cch evoked Ca^{2+} signal by 36% (Figure 4.12A). This level of inhibition was very similar that seen during IP3R blockade (27% reduction) (Figure 4.10A), suggesting that neither IP3Rs nor RYRs are the key intracellular Ca^{2+} channels mediating the Cch-stimulated Ca^{2+} signals. The role of RYR was further confirmed with the application of 8-Bromo-cADPR, which inhibits cADPR. 8-Bromo-cADPR only blocked the Ca^{2+} signals by approximately 9% (Figure 4.12B), these results suggest that M3AchR activation might not influence or regulate cADPR synthesis by CD38 in the human colonic epithelium; although coupling of MAchR to CD38 has been shown to regulate cADPR formation in neuronal cells (Higashida, et al., 1997b). An alternative explanation would be that cADPR did not get internalised and thus could not exert its function intracellularly via the RYR. As a previous study by Menteyne and colleagues demonstrated the lack of effect of bafilomycin on cADPR induced Ca^{2+} spikes (Menteyne, et al., 2006), it also implies that cADPR is not a part of the same pathway as NAADP.

In this current study, the role of the ER during Cch stimulation and the concomitant role of IP3Rs and RYRs in mediating ER Ca^{2+} release were further confirmed with the simultaneous application of 2-APB and ryanodine. However, the level of inhibition with the presence of two inhibitors was only 40% compared to 36% with the presence of RYR inhibitors alone (Figure 4.12C). This observation implies that the RYRs are probably more sensitive in triggering the Ca^{2+} signal from the ER upon Cch stimulation than IP3Rs, although both RYRs and IP3Rs are involved in ER Ca^{2+} release to generate the CICR response upon M3AchR activation.

4.4.4 CD38 regulation of Cch-induced calcium signals

CD38 is an enzyme that is responsible for the synthesis of two Ca^{2+} mobilising agents: cADPR (agonist of RYRs) and NAADP (agonist of TPCs) (Lee, 1997). In pancreatic acinar cells, a previous study demonstrated the expression of CD38 on endosomes, which appeared to be in close proximity to the lysosomes (Cosker, et al., 2010). In this thesis, CD38 expression was also detected in the cytoplasmic space where the acidic lysosomes and mucus granules reside (Chapter 3, Figures 3.18 and 3.22). In addition, CD38 was occasionally detected in the nuclei of colonic epithelial cells in 2D view (Chapter 3, Figure 3.22A). These expression patterns of CD38 are in line with those observed in rat brains that they are in primer positions

to theoretically participate in many cellular events (Yamada, et al., 1997). However, it is still unclear which signals contribute to endosomal CD38 constantly being internalised into the cytosol in the absence of external stimulation. MAchR activation has been suggested to up-regulate CD38 activity at the cell membrane (Higashida, et al., 1997b; Higashida, et al., 2001a and b). In this thesis, CD38 expression at the apical region and basal pole of the crypt was increased upon Cch (10µM) stimulation (Figure 4.2B (bii) and Figure 4.14 Cch), suggesting that M3AchR activation might enhance CD38 endocytosis and recycling.

Both exocytosis and endocytosis are Ca^{2+} dependent events. CD38 internalisation upon agonist-receptor activation has been suggested to be critical for its activity (Zocchi, et al., 1999). In this current study, MbetaC (10mM) significantly reduced the Cch-induced Ca^{2+} signals by approximately half (data not shown), and this level of inhibition is comparable to the inhibition of CD38 by nicotinamide (discussed below). Hence, there is a strong correlation between CD38 internalisation and the endocytic pathway in regulating Cch-induced Ca^{2+} signals. A previous study in platelets suggests that CD38 internalisation is mediated by PKC (Mushtaq, et al., 2011), while another study in diabetic kidney cells implicates NOX1 in the activation of PKC (Zhu, K. et al., 2015). Thus, it is feasible that RAC1/NOX1 activation in turn activates PKC, which could then mediate CD38 internalisation upon Cch stimulation. Coincidentally, a recent study has also suggested a role for NOX-derived ROS in the mediation of CD38 internalisation in coronary arterial myocytes (Xu, et al., 2013); all these findings suggest that the NOX signalling pathway is possibly downstream of the M3AchR activation and might possibly be involved in Cch-induced Ca^{2+} signal generation (see section 4.4.6).

Current knowledge regarding CD38 is mainly focused on the role of cADPR, yet CD38 is also responsible for the synthesis of NAADP in the acidic environment; information is still lacking about its pathways and significance in vivo. As the catalytic domain of membranous CD38 is located on the extracellular side of the cell membrane (Tohgo, et al., 1994; Higashida, et al., 2001a and b), two hypotheses have been proposed: the expression of membrane transporters (channels) or agonist mediated endocytosis that explain how the active site is rendered accessible to the intracellular substrate for the subsequent conversion into cADPR or NAADP. The first proposal is that the transporter connexin 43 hemichannel, which transfers intracellular NAD^+ to extracellular spaces in a Ca^{2+} dependent manner, pumps the substrate from the cell making it accessible to the CD38 active site (Bruzzone, et al., 2001). The cADPR would then need to transfer back into the cell via CD38 or some nucleoside transporters to be able to elevate intracellular [Ca^{2+}] (Guida, et al., 2002; Wei, et al., 2014). The increase in cytosolic [Ca^{2+}] induces a negative feedback mechanism that was shown to

be regulated by PKC, which limits NAD^+ transport out of the cell (Bruzzone, et al., 2001). Hence, it seems there are some intracellular regulatory mechanisms between CD38 and PKC pathways, both of which are activated upon MAchR activation. The second hypothesis, proposed by Zocchi and colleagues, is that CD38 undergoes vesicle-mediated internalisation upon activation (Zocchi, et al., 1999), for which supporting evidence has been demonstrated in B cells and human Namalwa cells (Burkitt's lymphoma cell line) (Xu, et al., 2013). Internalisation of CD38 provides the active site exposure to the intracellular substrates (NAD^+ and $NADP^+$), which could be shuttled into the endocytic vesicles by transmembrane transporters for the subsequent conversion into cADPR (Zocchi, et al., 1999); CD38 can then mediate the efflux of cADPR from the endosomal vesicles to the cytoplasm (Bruzzone, et al., 2001). Alternatively the conversion of $NADP^+$ into NAADP by CD38 could potentially occur when endosomes fused with lysosomes. However, many questions still remain regarding the CD38/NAADP pathway in vivo. For instance, a previous study has suggested that CD38 is not required for NAADP production in the myometrial cells (Soares, et al., 2007). In addition, the mechanism of CD38 activation upon MAchR activation still remains unclear.

In this current study, the cyclase activity of CD38 and its role in the Ca^{2+} signal generation upon Cch-stimulation in human colonic crypts was investigated with nicotinamide. Although no statistical significance were observed between the effects of 20mM and 50mM nicotinamide, significant level of inhibition of CD38 activity was observed suggests that CD38 plays a major role in Cch-mediated Ca^{2+} signal generation (average inhibition is 74%, Figure 4.15). However, based on this data, it is unclear whether the Ca^{2+} signals are mediated by cADPR or NAADP. Based on the current available knowledge, nicotinamide acts to reverse the cyclase activity of CD38 by forcing the conversion of cADPR back to NAD^+ (Aarhus, et al., 1995; Graeff, et al., 2002). One logical explanation for the above findings would be that cADPR is the key 2^{nd} messenger for the Cch-induced Ca^{2+} signals. However 8-Bromo-cADPR failed to suppress the Cch-induced Ca^{2+} signals, suggesting that cholinergic stimulation preferentially promotes the synthesis of NAADP as opposed to cADPR via CD38 internalisation in the human colonic epithelium; while NAADP is well-known in mobilising acidic lysosomal Ca^{2+} stores.

4.4.5 Cch-induced calcium signals are highly dependent on lysosomal calcium stores

As discussed in previous sections, M3AchR activation seems to mobilise Ca^{2+} from other intracellular Ca^{2+} stores that was observed after the depletion of the ER store. The acidic lysosomes have recently emerged as important Ca^{2+} stores involved in regulating various cellular and physiological functions (Morgan, et al., 2011). Ca^{2+} release from these endo-lysosomes has been shown to be regulated by the 2nd messenger NAADP (Churchill, et al., 2002). NAADP is synthesised by the ectoenzyme CD38, and inhibition of CD38 pathways also block the Cch-induced Ca^{2+} signals in human colonic crypts, thus prompting our investigations into the role of CD38/NAADP in Cch-induced Ca^{2+} signal generation.

In this current study, the role of the acidic organelles in the Cch-induced Ca^{2+} mobilisation upon M3AchR activation were investigated in human colonic crypts with different inhibitors which target the acidic lysosomes in different ways (Figure 4.20 top panel). Pharmacological agents such as bafilomycin that block the refilling of the stores or chloroquine that disrupt the lysosomal pH, both of which significantly reduced the Cch-induced Ca^{2+} signal generation (Figure 4.17). In addition, induction of lysosomal osmotic burst by GPN also suppressed the Cch-induced Ca^{2+} signals by nearly 90% (Figure 4.20 bottom panel). Thus, these results further support the model wherein cholinergic activation of the M3AchR signalling pathway mobilises Ca^{2+} from the acidic lysosomal stores; this initial Ca^{2+} signal (trigger) from the acidic lysosomes further activates the RYRs and IP3Rs on the ER store to trigger the CICR response. Furthermore, these findings are also consistent with the initial observation that the Ca^{2+} signals initiate at the apical pole of the initiator cells where the acidic lysosomes reside (Figure 4.2A top panel and Figure 4.2B (a)).

The role of NAADP in the generation of Cch-induced Ca^{2+} signal was further delineated in human colonic crypts through the application of the NAADP antagonist Ned-19. Ned-19 drastically reduced the Cch-induced Ca^{2+} signals by 94% (Figure 4.18B and Figure 4.20 bottom panel). To further support these findings, DZM was employed to test the role of the NAADP receptors (TPCs). DZM (100µM) significantly reduced the Cch-induced Ca^{2+} signal by 79% (Figure 4.18C and Figure 4.20 bottom panel). Hence, from these data we can infer that NAADP is the key 2nd messenger responsible for mobilising lysosomal Ca^{2+} stores via TPC upon M3AchR activation. These findings are very similar to those observed in the sea urchin egg homogenate model (Churchill, et al., 2002), in HEK293 cells overexpressing TPC2 (Calcraft, et al., 2009); and in pancreatic acinar cells (Gerasimenko, J.V. et al., 2015). As NAADP is synthesised by CD38, these results suggest that CD38 is a requirement for the

coupling of M3AchR activation to NAADP-mediated Ca^{2+} mobilisation from lysosomal stores in human colonic crypts. The current findings in the human colonic epithelium is in contrast to the findings in pancreatic acinar cells, as Menteyne and colleagues suggested that inhibition of the acidic stores failed to suppress the cADPR induced Ca^{2+} waves (Menteyne, et al., 2006). Data presented in the current study suggests cADPR might not play any role in the Cch-induced Ca^{2+} signal generation, while inhibition of the acidic stores almost completely suppressed the Cch-induced Ca^{2+} signals. In addition, Menteyne, et al also suggested the acidic stores are required for the IP3-induced Ca^{2+} waves, while inhibition of IP3R in the current study only showed about 30% of inhibition, suggests IP3 mediated Ca^{2+} release is downstream of the Ca^{2+} release from acidic stores.

4.4.6 The role of RAC1/NOX1/ROS in Cch-induced calcium signal generation

The expression of NOX1 has been shown previously in human colonic epithelial cells: in particular, high levels of NOX1 mRNA were detected within the crypts and on the luminal surface (Szanto, et al., 2005). Another study also noted the NOX1 protein expression towards the apical pole of crypt colonocytes (Laurent, et al., 2008); while the expression of RAC1 in the human colonic epithelium is currently unclear. In this current study, both total RAC1 (regulatory subunit) and NOX1 (catalytic subunit) of NOX were detected at the basal pole and in the cytoplasm towards the apical pole of crypt epithelial cells (Figures 4.22A and 4.22B control). This cytosolic expression pattern of NOX1 is in support from previous findings (Laurent, et al., 2008), and it seems there is a strong association between NOX1 and RAC1 localisation within the colonic epithelium. In human pancreatic islet cells, NOX2 protein was found to be localised to the membranes of the insulin granules and endo-lysosomes (Li, N. et al., 2012). These expression patterns are very similar to the expression of NOX1 in our human colonic crypt culture model, in that NOX1 was localised in the area where the acidic lysosomes and mucus granules reside (Figure 4.22B control and Figure 4.24B, i and ii), hence, suggesting their role in ROS production between mid-cell region to apical pole of crypt cells. In addition, a study by Patel and colleagues have demonstrated the localisation of p22phox subunit of NOX in $LC3^{+}$ autophagosomes. By using p22phox mutant mouse model, they demonstrated a greater level of mucin granules retention in mutant goblet cells as compared to the control, and they concluded that the LC3-associated NOX-derived ROS is critical for the regulation of mucus granule exocytosis (Patel, K.K. et al., 2013). Hence, these findings further support a role of NOX-derived ROS in mucus secretion; and the role of ROS in colonic goblet cell mucus secretion will be discussed in the next chapter.

The production of ROS is dependent on the assembly of the regulatory subunits in the cytosol with the catalytic subunit on the membrane. Upon agonist stimulation, the regulatory subunits (NOXO1, NOXA1 and RAC1) in the cytosol translocate to the membrane-bound complex (NOX1/p22phox) leading to the formation of ROS (Yu, et al., 2006; Fu, et al., 2014; Görlach, et al., 2015). In this current study, increased detection of total RAC1 protein was observed upon 1 min of Cch stimulation, both at the basal pole and in the cytoplasm towards the apical pole of crypt colonocytes (Figure 4.22A Cch). These results suggest that more total RAC1 proteins (in both inactive and active forms) were recruited to the basal pole of the crypt, and possibly translocate to other target sites in the cytosol upon M3AchR activation. In order to activate NOX1, inactive form of RAC1 is required to convert to its active state "RAC1-GTP". In this current study, the active RAC1-GTP immune-labelling was detected in the human colonic epithelium during unstimulated condition, and the expression of active RAC1 matched with the total RAC1 patterns except for the nuclear localisation of active RAC1-GTP in some colonocytes at the crypt base (Figure 4.24A i and ii). GTPases such as RAC1 contain a c-terminal polybasic region that resemble a nuclear localisation signal sequence; and the accumulation of RAC1 in the nucleus has been suggested to be enhanced by RAC1 activation (Lanning, et al., 2003). Data presented in the current study suggests there are some regulatory signals that target active RAC1-GTP to the nucleus in the absence of exogenous stimulation. However, it is currently unclear which signals mediate active RAC1 translocation to the nucleus in the human colonic epithelium in resting condition. To further dissect the role of cholinergic signals in NOX-derived ROS generation, the kinetics of active RAC1-GTP and NOX1 trafficking upon Cch stimulation was investigated in the current study. With 30 seconds of Cch stimulation, intensive labelling of active RAC1-GTP was observed at the basal pole and the apical pole of crypt colonocytes (Figure 4.24A iii and iv and Figure 4.25A). The expression of NOX1 at the basal pole of the crypt and in the cytosol of colonocytes was also slightly increased, but no significant difference were observed as compared to the control group (Figure 4.24B iii and iv and Figure 4.25B). This could possibly be due to the incapability of the antibody to detect NOX1 protein conformational change upon the formation of a complex with RAC1-GTP after 30s of Cch stimulation. In support of a previous study in CHO cells, activation of the MAchR has been shown to regulate RAC1 activation and translocation to cell junctions (Ruiz-Velasco, et al., 2002). Data presented in this study suggests the activation, recruitment and possibly translocation of active RAC1-GTP to the basal pole and also target sites (NOX1 expression sites) in the cytosol of the crypt upon M3AchR activation. It is currently unclear why the intensities of both active RAC1-GTP and

NOX1 proteins increased shortly after M3AchR activation. Gene expression analyses and time-lapse experiments are required to confirm these findings. RAC1 dependent ROS has also been shown to increase cyclin D1 expression, which drives hyper-proliferation and induces DNA damage in human tumours and cell lines (Daugaard, et al., 2013). In this current study, elevation of active RAC1-GTP levels was detected in the nucleus of some colonocytes at the crypt base upon Cch stimulation (Figure 4.24A iii and iv). These results suggest activation of M3AchR seems to increase the expression or translocation of active RAC1-GTP into the nuclei of proliferative colonocytes at the base of the crypt; further suggest the role of cholinergic signalling in proliferation by mediating the transcription of certain genes (possibly cyclin D1) in the human colonic epithelium.

Moreover, after 1 min of Cch stimulation, active RAC1-GTP levels remained high at the basal pole and in the nuclei of most colonocytes at the crypt base, and the expression in the cytoplasm was much reduced (Figure 4.24A v and vi); while NOX1 expression at both the basal pole and cytoplasm was also decreased that the level was similar to unstimulated condition (Figure 4.24B v and vi). These results suggest that both active RAC1-GTP and NOX1 were utilised for the generation of ROS in the cytosol, however, the mechanism of regulation in the human colonic epithelium is unclear. Previous studies have suggested that the deactivation of RAC1 protein by ubiquitylation and turn over by proteolytic degradation is necessary upon RAC1-induced ROS formation (Kovacic, et al., 2001). In addition, deactivation of RAC1 has been suggested to be the disassembly signal for the NOX complex, before the NOX complex then undergoes dissociation or degradation via proteolysis when it is no longer required (Yin, et al., 2013). This feedback mechanism presumably controls ROS production in cells, preventing aberrant oxidation. In human aortic endothelial cells, DPI (a potent NOX inhibitor) has been shown to decrease proteolytic degradation of RAC1, hence, suggesting the role of DPI in blocking the interactions between RAC1-GTP and NOX1 (Kovacic, et al., 2001). Furthermore, after 5 min of Cch stimulation, the intensities of active RAC1-GTP and NOX1 proteins returned to resting levels as compared to the control (Figure 4.24A vii and viii and Figure 4.24B vii and viii). These observations suggest a strong association between the catalytic (NOX1) and regulatory (RAC1) subunits of NOX in the cytosol following Cch stimulation. Thus, Cch seems to mediate the conversion of RAC1 to its active form, and the recruitment and translocation of active RAC1-GTP and NOX1 in the colonic crypt epithelial cells. It seems the recruitment patterns of active RAC1-GTP are dependent on the expression of NOX1 in the human colonic epithelium upon Cch stimulation.

In vascular endothelium, the increase in ROS production by NOX has been shown to regulate intracellular [Ca^{2+}] in the vasculature via the activation of IP3R, blockade of SERCA pumps, and stimulation of extracellular Ca^{2+} influx (Touyz, 2005). The functional role of NOX1-derived ROS in intracellular Ca^{2+} mobilisation or vice versa in the human colonic epithelium is unclear. Data presented in this study suggests: (1) both active RAC1-GTP and NOX1 were recruited to the apical pole of crypt cells upon 30 sec of Cch stimulation, (2) active RAC1-GTP was recruited to the NOX1 expression sites in the cytosol upon 30 sec of Cch stimulation, while the average latency of Cch-induced Ca^{2+} signals was about 46 sec (Figure 4.26); implicating a role of NOX-derived ROS in mediating Ca^{2+} mobilisation in the human colonic epithelium upon Cch stimulation. This is in compliment to the cytosolic CD38 and RAC1 expression in colonic crypt epithelial cells (Figure 4.23 A and B). However, the current study was unable to demonstrate the early event (less than 30 sec) for NOX1/ RAC1-GTP recruitment upon Cch stimulation due to technical difficulties. The role of NOX1-derived ROS in Ca^{2+} signal generation were further investigated by a range of NOX and RAC1 inhibitors. Both DPI (non-specific NOX inhibitor) and VAS2870 (pan-specific NOX inhibitor) significantly reduced the Cch-induced Ca^{2+} signals (Figure 4.28 bottom panel), and the level of inhibition were comparable to the inhibition of NAADP by Ned-19 (Figure 4.18B), suggesting NOX might be upstream of NAADP in the mediation of Ca^{2+} signal generation upon M3AchR activation. The role of NOX-derived ROS was further confirmed by the RAC1 activation inhibitor (NSC23766), and the level of inhibition was comparable to DPI treatment that further suggest the role of RAC1-dependent NOX1-derived ROS in Cch mediated Ca^{2+} mobilisation in the human colonic epithelium (Figure 4.28 bottom panel). However, due to the lack of specificity of both NOX1 inhibitors, further experiments including the use of siRNA silencing of NOX1 is required to confirm the current findings. In addition, NSC23766 has recently reported to be a competitive antagonist of MAchRs (Levay, et al., 2013), hence, the use of another RAC1 inhibitor such as W56 or siRNA silencing of RAC1 are required to confirm the role of RAC1 upon M3AchR activation. Other experiments including the measurement of ROS levels before and after Cch stimulation; the use of co-immunoprecipitation and western blotting to identify the physical interactions of NOX1 and active RAC1-GTP before and after Cch stimulation; and the quantification of NOX1 and RAC1 mRNA expression by quantitative real time PCR before and after Cch stimulation, etc. can be done to further confirm the role of cholinergic signals in the regulation of NOX-derived ROS generation in the human colonic epithelium.

In summary, the initial kinetic observations of the Cch-induced Ca^{2+} signals imply a strong link between the acidic lysosomal Ca^{2+} stores and the ER Ca^{2+} store. This is supported by the Ca^{2+} initiation signals beginning at the apical pole of initiator cells, the apical localisation of the lysosomes, and the effects of thapsigargin that revealed the interactions of the two intracellular organelles upon M3AchR activation. Inhibition of PLC downstream of M3AchR abolished the Cch-induced Ca^{2+} signals, which suggests that the signal transduction occurs predominantly via the PLC pathway. Surprisingly, the second messenger IP3 generated upon PLC activation in the conventional pathway did not show any dominant role in the generation of the Ca^{2+} signals via the IP3R. Intriguingly, signalling downstream of PA and the CD38 signalling pathways seem to play a major role in the Cch-induced Ca^{2+} signal generation. The PA pathway could possibly activate some PKC isoforms directly or via NOX1 and bypass the role of DAG. Inhibition of both IP3Rs and RYRs revealed that the role of the ER store is secondary to the initial signals but remained the major source of Ca^{2+} in response to Cch stimulation as demonstrated by using thapsigargin to deplete the ER store. In addition, RYRs might be more sensitive to the initiation Ca^{2+} signal than IP3R for the generation of CICR response upon Cch stimulation. Inhibition of the CD38 pathway by nicotinamide and blockade of endocytosis by MbetaC revealed the important role of CD38 in the Ca^{2+} signal generation upon Cch stimulation; and that CD38 could possibly be activated by PKC or the NOX signalling pathways. Pharmacological disruption of acidic lysosomal Ca^{2+} stores and inhibition of NAADP and TPCs blocked the Cch-induced Ca^{2+} signal generation, indicating lysosomal Ca^{2+} release mediated by NAADP is the key trigger for the subsequent CICR response generated by the ER Ca^{2+} release. Thus, CD38 is a requirement for the coupling of M3AchR activation to NAADP-mediated Ca^{2+} mobilisation from lysosomal stores via TPCs. NOX1-derived ROS has been suggested previously to mediate CD38 internalisation, while PA has been shown to activate NOX activity. Inhibition of the PA pathway seems to reduce the recruitment of active RAC1 to the basal pole of crypt that further suggests the NOX signalling pathway is downstream of M3AchR and PA. In addition, similar levels of inhibition of the Cch-induced Ca^{2+} signals were observed between inhibition of ROS by apocynin and inhibition of PKC by sotrastaurin, suggesting that PKC might be downstream of PA/NOX1 signalling. Furthermore, inhibition of NOX1 and RAC1 significantly reduced the Cch-evoked Ca^{2+} signals, suggesting that RAC1, NOX1 and O_2^- play an important role in Cch-induced Ca^{2+} signal generation, possibly by direct activation of CD38 or indirectly via PKC.

This results chapter details the experiments which were used to construct the proposed model for the mechanisms underlying Ca^{2+} signal generation in response to M3AchR

activation (Figure 4.29). The next step would be looking at how these intracellular Ca^{2+} signals couple mucus granule exocytosis in human colonic crypt goblet cells.

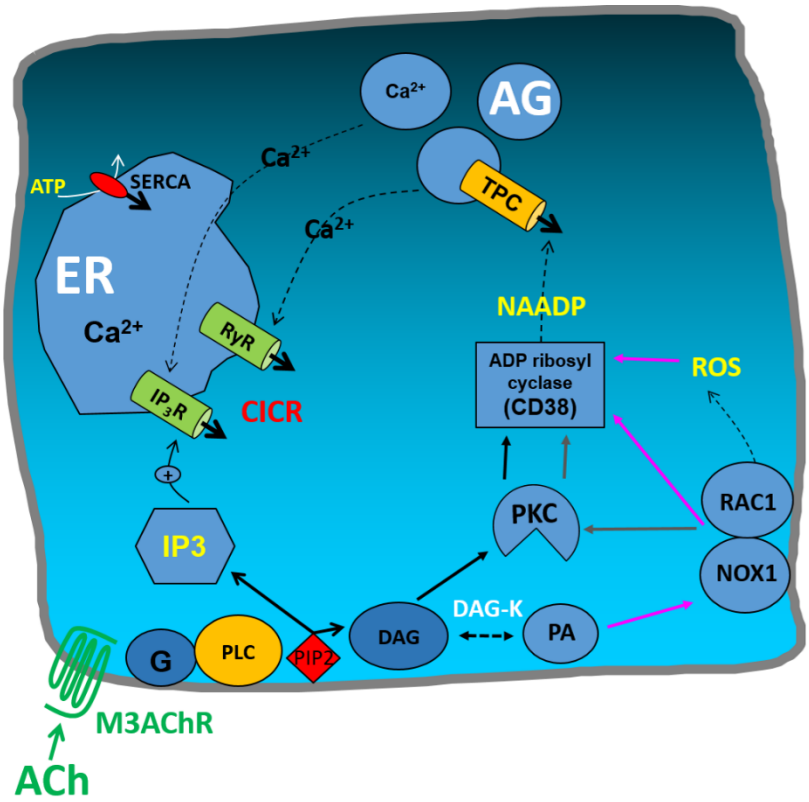

Figure 4.29 Proposed mechanisms of intracellular Ca^{2+} mobilisation upon M3AchR activation

M3AchR activation transduces its signal via the PLC pathway; activation of PLC in turn initiates PIP2 hydrolysis to generate DAG and IP3. Activation of PIP2 enhances DAG kinase activity that promotes the conversion of DAG into PA. PA then activates NOX1 by recruiting RAC1 to the plasma membrane or to vesicular membranes in the cytosol expressing NOX1. The RAC1/NOX1/ROS system possibly mediates CD38 internalisation or directly activates the CD38 on endosomes; alternatively RAC1/NOX1/ROS might mediate CD38 activity indirectly via PKC activation. CD38 then generates NAADP that mediates Ca^{2+} mobilisation from acidic lysosomes via the TPCs. This initial Ca^{2+} release triggers the IP3Rs and RYRs on the ER membrane and induces the CICR response within the cell.

Chapter 5 Results: Cholinergic regulation of calcium excitation-mucus secretion coupling in human colonic crypts

5.1 Introduction

The mucus barrier plays an important role in GI defence. The colon is normally protected by two layers of mucus that prevent the bacteria which inhabit the lumen, as well any host-derived digestive enzymes, from making contact with the epithelium (Johansson, et al., 2013). This mucus layer is continually being worn away by mechanical forces as the stool passes through. Thus, there is a requirement for the continuous replenishment of the mucus layers by goblet cells. Increased intestinal permeability due to a defective mucus barrier has been suggested as one of the contributing factors for IBD pathogenesis (Antoni, et al., 2014). The vast majority of current research into the pathophysiology of UC has mainly concentrated on the immunological aspects (Cader, et al., 2013; Geremia, et al., 2014). However, the role of defects in the production and maintenance of the mucus layer have not been extensively addressed. Anti-inflammatory therapy is currently the gold standard for treating IBD patients. Cholinergic signalling has been recently shown to mediate gut immune responses (Dhawan, et al., 2012), meaning that alternative therapies targeting cholinergic signalling pathways might feasibly be used to suppress abnormal inflammation in the GI tract (Pavlov, et al., 2008).

The link between cholinergic mediated MAchR activation and Ca^{2+} signal generation has been previously demonstrated in rat and human colonic crypts (Lindqvist, et al., 1998; Lindqvist, et al., 2002). These cholinergic stimulated Ca^{2+} signals have also been shown to regulate fluid secretion in the model of native human colonic epithelium (Reynolds, 2007). In addition, a close correlation between Ca^{2+} signalling and mucus secretion has been established in several model systems including animal GI tracts (Neutra, et al., 1982; Seidler, et al., 1989; Hamada, et al., 1997) and human colon cancer cell lines (Mitrovic, et al., 2013). Cholinergic stimulated mucus secretion was first demonstrated by Halm and Halm in isolated human colonic crypts (Halm and Halm, 2000). However, there are no specific reports targeting the underlying mechanism of cholinergic signal-mediated Ca^{2+} mobilisation in regulating mucus barrier function in the human colon published thus far.

In the previous chapter, a proposed mechanism of intracellular Ca^{2+} mobilisation upon M3AchR activation was established. M3AchR activation was shown to transduce its signal via the PLC pathway; activation of PLC in turn initiates PIP2 hydrolysis to generate DAG and IP3.

Activation of PIP2 enhances DAG kinase activity which promotes the conversion of DAG into PA. PA probably activates NOX1 by recruiting RAC1 to the plasma membrane or to NOX1-expressing vesicular membranes in the cytosol. The RAC1/NOX1/ROS system possibly mediates CD38 internalisation or directly activates CD38 on endosomes; alternatively RAC1/NOX1/ROS might mediate CD38 activity indirectly via PKC activation. CD38 then generates NAADP that mediates Ca^{2+} mobilisation from acidic lysosomes via the TPCs. This initial Ca^{2+} release from acidic lysosomes triggers the IP3Rs and RYRs on the ER membrane and induces the CICR response within the cell (Figure 4.29). In this chapter, the focus is to explore the coupling of the Ca^{2+} excitation to mucus secretion in the human colonic epithelium. In particular, the correlation between lysosomal Ca^{2+} release and mucus granule exocytosis will be established (Figure 5.1). Immunofluorescence labelling and confocal microscopy will be used to explore the specific role of the CD38/NAADP pathway and the potential upstream RAC1/ NOX1/ ROS pathway in the regulation of mucus granule exocytosis in human colonic crypt goblet cells.

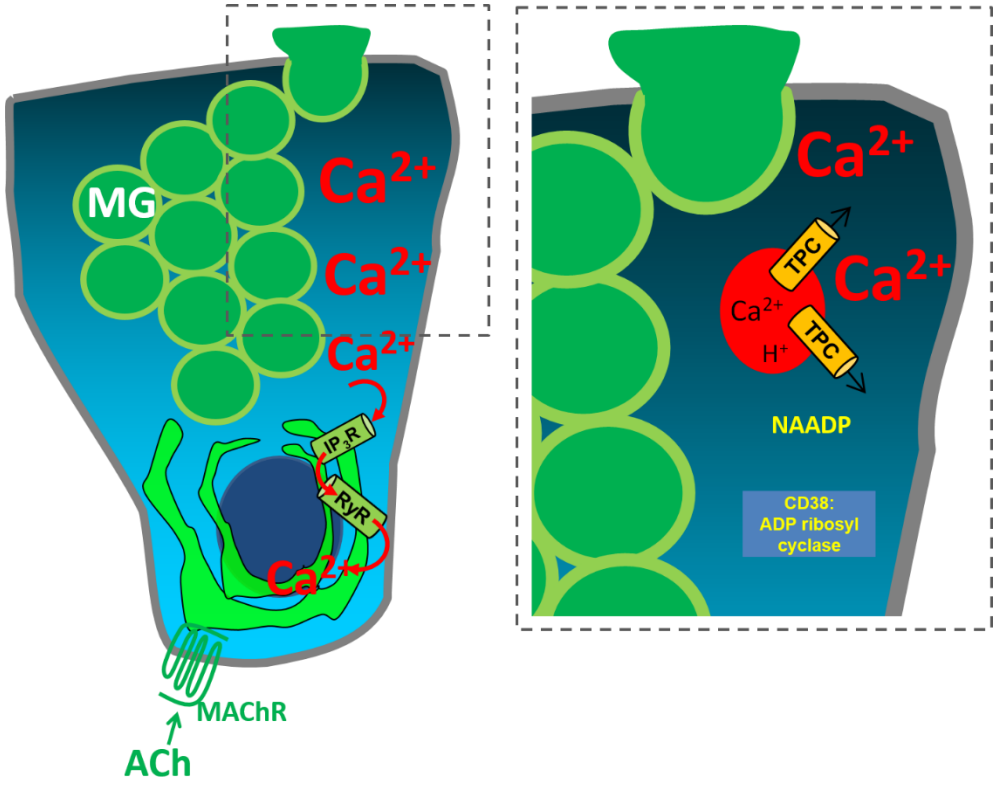

Figure 5.1 Proposed role for CD38/NAADP mediated lysosomal Ca^{2+} release in coupling mucus granule exocytosis in human colonic crypt goblet cells

Cch-stimulated lysosomal Ca^{2+} release has been shown to be regulated by the CD38/NAADP/TPC pathway. This initial Ca^{2+} spike further triggers the IP3R and RYR on the ER membrane and induces the CICR response. The increase in intracellular [Ca^{2+}] is proposed to couple exocytosis of mucus granules (MG) in goblet cells. Schematic diagram is courtesy of Mark Williams.

5.2 Cch-stimulated mucus secretion is dependent on intracellular calcium mobilisation

As discussed in the previous chapter, BAPTA-AM significantly reduced Cch-stimulated Ca^{2+} signals. The hypothesis that BAPTA-AM will decrease mucus secretion was then tested in human colonic crypts. Samples were separated into four groups: (1) untreated (control), (2) Cch treated, (3) BAPTA treated, and (4) treated with BAPTA and Cch. For Cch treated groups, colonic crypts were treated with Cch (10µM) for 30 min. For BAPTA treated groups, cultured crypts were pre-incubated with BAPTA-AM (66µM) for 1.5 hours or with BAPTA-AM (66µM) for 1 hour, subsequently treated with Cch (10µM) in the presence of BAPTA (66µM) for another 30 min. A significant depletion of intracellular MUC2 immuno-labelling, indicative of granule secretion, was observed in human colonic crypt goblet cells treated with 10µM Cch (0.49 ± 0.03), relative to untreated controls (1 ± 0, N= 4 subjects, ng≥ 181 goblet cells per group, paired t-test $p< 0.01$, Figures 5.2A and B). Pre-incubation with BAPTA-AM prevented Cch-stimulated mucus granule secretion, as evidenced by MUC2 retention in goblet cells at the crypt base, which displayed an approximate 106% increase (1.55 ± 0.19) compared to Cch alone (0.49 ± 0.03, N= 4 subjects, ng≥ 181 goblet cells per group, paired t-test $p= 0.012$, Figures 5.2A and B). Interestingly, there was a concomitant accumulation of immature MUC2 proteins (as detected by a mouse monoclonal antibody) detected in the perinuclear ER region of goblet cells when pre-treated with BAPTA-AM (66µM) (data not shown). Thus, these results further confirmed that cholinergic mediated intracellular Ca^{2+} signals play an important role in mucus secretion in human colonic crypt goblet cells.

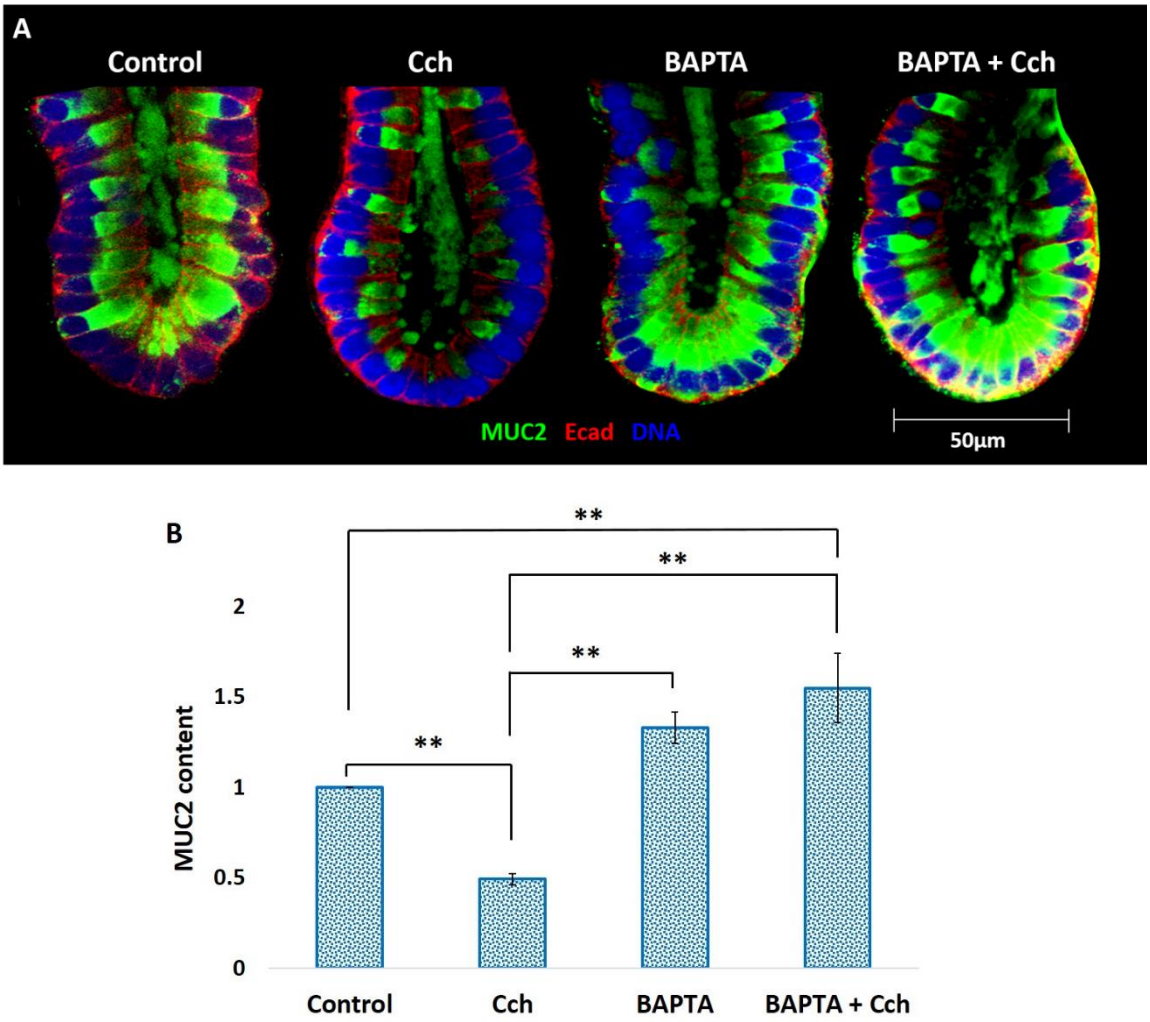

Figure 5.2 Effects of BAPTA-AM on colonic goblet cell mucus granules depletion

Cultured human colonic crypts were separated into four treatment groups, control untreated, Cch or BAPTA single-treated, and dual-treated. Crypts in the Cch group were stimulated with Cch (10µM) for 30 min. For BAPTA-AM treated groups, crypts were either pre-incubated with BAPTA (66µM) alone for 1.5 hr, or with BAPTA (66µM) for 1 hr, then with BAPTA (66µM) + Cch (10µM) for another 30 min. Samples were fixed and labelled with anti-MUC2 (green) and anti-Ecad (red) antibodies, and visualised with Alexa-conjugated secondary antibodies; cell nuclei were stained with Hoechst (blue) (A). Representative images taken with a Zeiss Meta 510 confocal microscope using a x63 objective. The amount of MUC2 mucin granule (i.e. immunofluorescence intensities) in goblet cells were measured from 3-5 slices of z-stack images using ImageJ software. Mean MUC2 intensities in goblet cells were calculated and normalised to the control group, and displayed as mean ± SE (B). Results were representative of N= 4 subjects, n≥ 13 crypts and ng≥ 181 goblet cells in each treatment group. Significance was assessed using a One-way ANOVA test, $F(3, 54) = 12.8$, $p < 0.0001$; followed by Bonferroni procedures and Tukey's post hoc analysis. Significant difference as indicated by asterisks (**) for $p < 0.01$ was observed between pairs of mean values including (i) control vs. Cch, (ii) Cch vs. BAPTA, (iii) Cch vs. BAPTA + Cch, (iv) control vs. BAPTA + Cch. No significant difference was observed between the following pairs: (i) Control vs. BAPTA, (ii) BAPTA vs. BAPTA + Cch.

5.3 CD38 has an essential role in Cch-mediated calcium coupling mucus secretion in human colonic crypts

As discussed in the previous chapter, nicotinamide (20mM) inhibits Cch-induced Ca^{2+} signal generation, suggesting an important role for CD38 upon M3AchR activation. The hypothesis that CD38 plays a role in Cch-mediated Ca^{2+} coupling mucus secretion was then tested; crypts were separated into four groups: (1) untreated (control), (2) Cch treated, (3) nicotinamide treated, and (4) treated with both nicotinamide and Cch. For the Cch treated group, colon crypts were stimulated with Cch (10µM) for 30 min. For nicotinamide treated groups, cultured crypts were pre-incubated with nicotinamide (20mM) for 2.5 hours or with nicotinamide (20mM) for 2 hours, then subsequently with Cch (10µM) in the presence of nicotinamide (20mM) for 30 min. Cch (10µM) induced significant levels of mucus depletion from colonic crypt goblet cells, an approximate 49% reduction (0.49 ± 0.03) of MUC2 immunofluorescence intensity in goblet cells as compared to the control (1 ± 0, N= 4 subjects, ng≥ 95 goblet cells per group, paired t-test $p< 0.01$, Figures 5.3A and B). During constitutive basal secretion, nicotinamide (20mM) showed no obvious effect on the retention of mucus granules (1.02 ± 0.07, N= 4 subjects, ng≥ 95 goblet cells per group) as the average mucus content in goblet cells was similar to those in the control (Figure 5.3B). In the presence of Cch (10µM), nicotinamide (20mM) counteracted the effect of Cch-stimulated (accelerated) mucus secretion (1.16 ± 0.09, N= 4 subjects, ng≥ 95 goblet cells per group, paired t-test $p< 0.01$) as compared to crypts treated only with 10µM Cch. Although mucus retention was more obvious in goblet cells at the base of the crypt (Figure 5.3A), the average mucus content (intensity) was similar to the control group (Figure 5.3B). These results confirm that Cch (10µM) induces or accelerates mucus granule exocytosis in human colonic crypt goblet cells, and this was counteracted by nicotinamide, an inhibitor of CD38 mediated Ca^{2+} mobilisation. This suggests mucus secretion in crypt goblet cells might be dependent on the CD38 pathway.

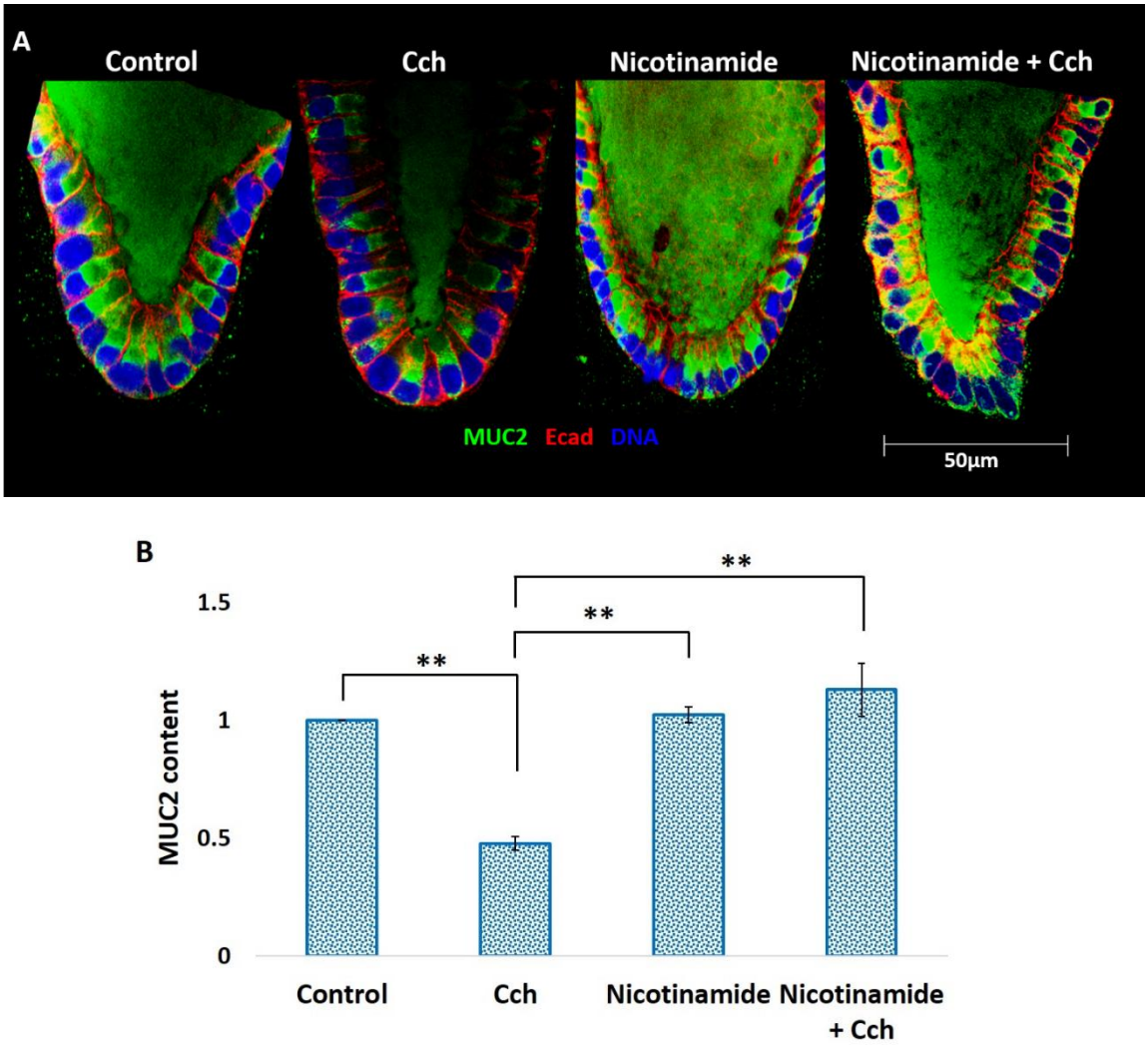

Figure 5.3 Effect of nicotinamide in Cch-mediated mucus secretion

Cultured human colonic crypts were separated into four treatment groups, control untreated, Cch treated, nicotinamide treated, and nicotinamide plus Cch treated. Colonic crypts in the Cch group were stimulated with Cch (10µM) for 30 min. For the nicotinamide treated group, crypts were either pre-incubated with nicotinamide (20mM) alone for 2.5 hours, or with nicotinamide (20mM) for 2 hours, then with nicotinamide (20mM) + Cch (10µM) for another 30 min. Samples were fixed and labelled with anti-MUC2 (green) and anti-Ecad (red) antibodies, and visualised with Alexa-conjugated secondary antibodies; cell nuclei were stained with Hoechst (blue) (A). Representative images were taken with a Zeiss Meta 510 confocal microscope using a x63 objective. The MUC2 mucin content (intensities) in goblet cells was measured from 3-5 slices of z-stack images using ImageJ. Mean MUC2 intensities in goblet cells were calculated and normalised to the control group, and displayed as mean ± SE (B). Results were representative of N= 4 subjects, n≥ 9 crypts and ng≥ 95 goblet cells in each group. Significant differences were assessed using One-way ANOVA tests, $F(3, 12) = 23.31$, $p < 0.0001$; followed by Bonferroni procedures and Tukey's post hoc analysis. Significant difference as indicated by asterisks (**) for $p < 0.01$ was observed between pairs of mean values including (i) control vs. Cch, (ii) Cch vs. Nic, (iii) Cch vs. Nic + Cch. No significant difference was observed in the following pairs: (i) control vs. Nic, (ii) control vs. Nic + Cch, (iii) Nic vs. Nic + Cch.

5.4 Cholinergic stimulated calcium mobilisation from acidic lysosomal stores couple mucus granule exocytosis in human colonic crypt goblet cells

Lysosomes are acidic organelles within a cell that are primarily expressed at the apical pole of the human colonic crypt (Chapter 3, Figures 3.15E and F). Use of the live tissue LysoTracker and fixed tissue LAMP1 antibody labelling reveals abundant expression of lysosomes in the mucus-granule storing region of goblet cells (Chapter 3, Figure 3.19A and Figure 5.4), which implies a potential role for these lysosomal Ca^{2+} stores in mucus granule exocytosis. Co-localisation of mucus granules and acidic lysosomes were also observed at the apical/ cytosolic region of goblet cells (Figure 5.4D iii and iv). As discussed in the previous chapter, Ned-19 not only inhibits Ca^{2+} mobilisation from lysosomes upon Cch stimulation, it also fluorescently labels the NAADP receptors on lysosomal membranes (Figure 5.5). This is consistent with the fixed tissue labelling with TPCs antibodies (Chapter 3, Figure 3.18).

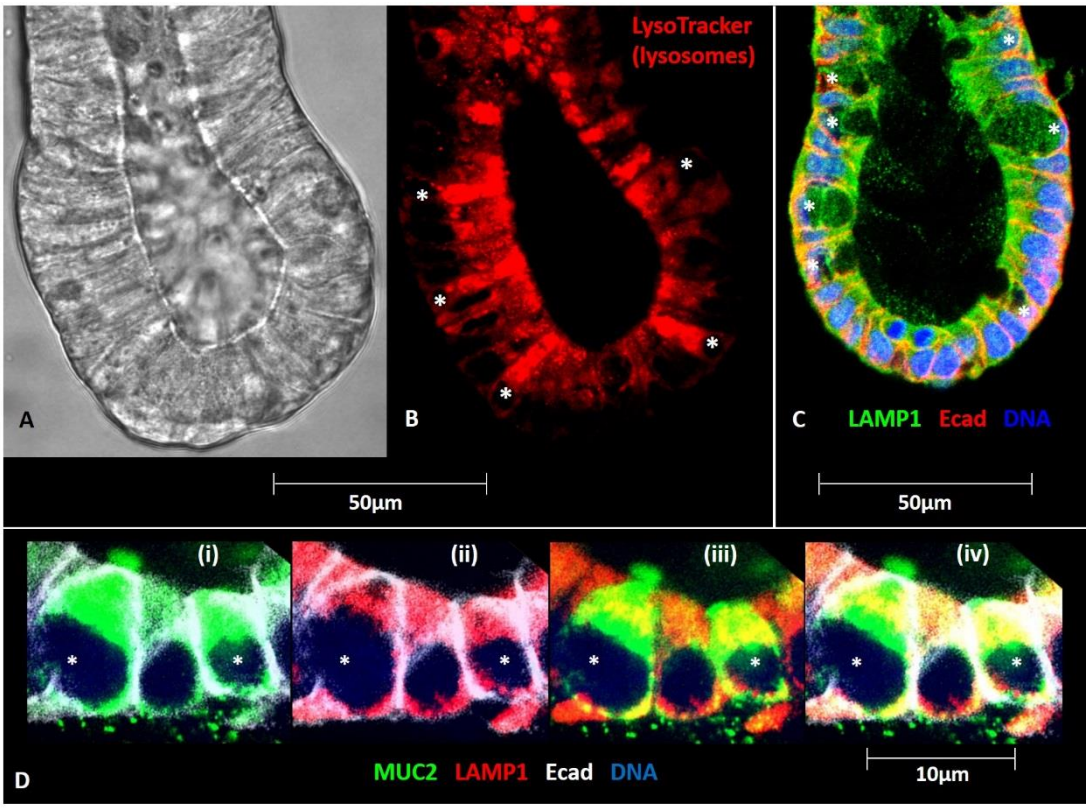

Figure 5.4 Correlation of acidic lysosomes and mucus granules in colonic crypt goblet cells

Human colonic crypts were labelled with LysoTracker (1µM), allowing the use of live cell imaging to reveal the expression and localisation of acidic lysosomes at the apical pole of crypt. Images were taken with a Zeiss Meta 510 confocal microscope using a x63 objective. (A) DIC image of a human colonic crypt; (B) LysoTracker labelling of the same crypt in (A). Images are representative of N= 3 subjects, n≥ 6 crypts. The expression of the lysosomes

were also detected by antibody labelling in fixed tissues. (C) Human colonic crypts were fixed and labelled with anti-LAMP1 (green), anti-Ecad (red) antibodies, cell nuclei were stained with Hoechst (blue). Image was taken with a Zeiss confocal microscope with a x63 objective. Representative image of N≥ 3 subjects, n≥ 10 crypts. (D) Enlarged images of human colonic epithelial cell layer stained with anti-MUC2 (green), anti-LAMP1 (red) and anti-Ecad (white) antibodies, cell nuclei were stained with Hoechst (blue). D(i) composite image of MUC2 (green), Ecad (white) and cell nuclei (blue), D (ii) merged image of LAMP1 (red), Ecad (white) and cell nuclei (blue), D (iii) overlay image of MUC2 (green), LAMP1 (red) and cell nuclei (blue), D (iv) composite image of all 4 channels. Asterisks (*) indicate goblet cells in situ. D (iii) shows co-localisation of mucus granules and lysosomes in yellow. Images are representative of N≥ 2 subjects, n≥ 6 crypts.

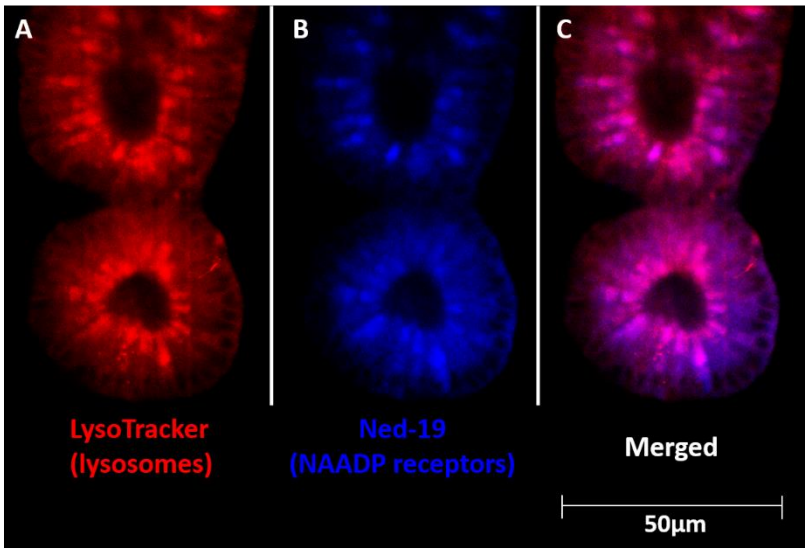

Figure 5.5 Colocalisation of NAADP receptors with lysosomes in the human colonic crypt

Human colonic crypts were loaded with LysoTracker (1µM) and Ned-19 (0.5mM) for 2 hours, live cell imaging revealed the colocalisation of NAADP receptor with lysosomes. Images were taken with the confocal microscope with a x63 objective. (A) Lysosomes labelled with LysoTracker (red); (B) NAADP receptors labelled with Ned-19 (blue); (C) merged image of LysoTracker (lysosomes, red) and Ned-19 (NAADP receptor, blue). Images are derived from N=1 subject, n=5 crypts.

M3AchR activation mobilising Ca^{2+} from acidic lysosomes was discussed extensively in the previous chapter. This effect can be significantly blocked by the NAADP antagonist Ned-19 or by pharmacological disruption of the lysosomal Ca^{2+} stores. Mucus granule exocytosis has been shown to be stimulated by Ach (Specian and Neutra, 1980). I then tested the hypothesis that Ned-19 blocks Cch-induced MUC2 mucin secretion in goblet cells; human colonic crypts were treated with Ned-19 (200µM) for 1.5 hours, or with Ned-19 (200µM) for 1 hour, then

with Cch (10μM) in the presence of the inhibitor for 30 min. Mucus secretion as demonstrated by reduced intensity of mucus staining relative to untreated control was observed in goblet cells upon Cch (10μM) stimulation (reduced by 48%, 0.52 ± 0.07, N= 4 subjects, ng≥ 228 goblet cells, paired t-test p< 0.01, Figures 5.6A and B). The level of mucus retained in goblet cells increased when crypts were pretreated with Ned-19 (200μM) as compared to the control group (an approximate 41% increase, 1.41 ± 0.14, N= 4 subjects, ng≥ 228 goblet cells, paired t-test p= 0.059). Ned-19 also inhibited the Cch-stimulated mucus depletion in goblet cells relative to the control group (an approximate 74% increase, 1.74 ± 0.09, N= 4 subjects, ng≥ 228 goblet cells, paired t-test p< 0.01) or the Cch only treated group (an approximate 123% increase, 1.74 ± 0.09, N= 4 subjects, ng≥ 228 goblet cells, paired t-test p< 0.01, Figures 5.6A and B). As antagonising CD38 and NAADP binding to its receptor block the majority of the phenotype, we can infer that NAADP is the key 2nd messenger in mediating Ca^{2+} coupling mucus secretion in human colonic crypt goblet cells.

In order to determine whether individual goblet cells can respond to the stimulus without a requirement for neighbouring signals, our lab is developing a single cell culture model, in which epithelial cells are isolated from human colonic crypts. Single epithelial cells were stimulated with Cch (10μM) for 30 min. The MUC2 content of goblet cells was then determined by antibody labelling (Figure 5.7A). Cch (10μM) significantly reduced the MUC2 intensity in single goblet cells by 50% (0.48 ± 0.06, N= 3 subjects, ng= 11 goblet cells, paired t-test p< 0.05, Figure 5.7B), suggesting that goblet cells were capable of responding to cholinergic signals in coupling mucus secretion in the absence of Ca^{2+} signals generated from neighbouring cells. The effect of Ned-19 on single goblet cells was briefly investigated. Preliminary data show the retention of mucus in single goblet cells that were pre-treated with Ned-19 (200μM) in both constitutive basal and Cch-stimulated conditions as compared to the control (data not shown), suggesting single goblet cells are responsive to Ned-19 treatment. Further experiments are required to confirm this finding.

With the addition of these mucus data, the proposed model can be expanded. First, MAchR activation from cholinergic stimulation mediates Ca^{2+} mobilisation from the lysosomal Ca^{2+} stores at the apical pole of the initiator cells; this initial increase in Ca^{2+} waves will then spread towards the basal pole and further activate the RYR and IP3R on the ER membrane and induce the CICR response in starting cells, before further spreading to the neighbouring cells via gap junctions. The induction of global Ca^{2+} waves along the crypt-axis will subsequently couple mucus granule exocytosis in goblet cells.

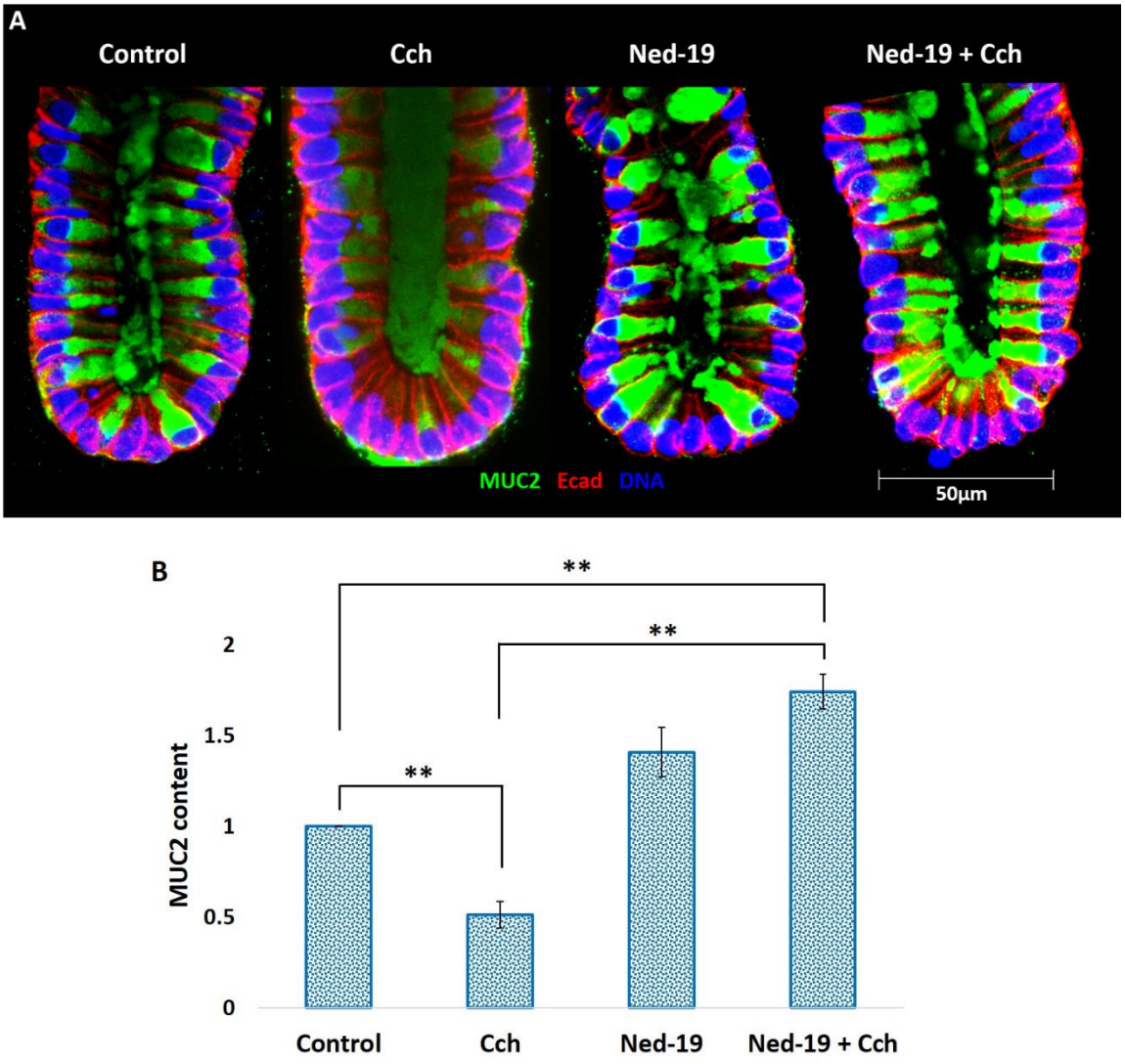

Figure 5.6 Role of lysosomal Ca^{2+} stores on MUC2 mucin secretion in human colonic crypt

Cultured human colonic crypts were separated into four treatment groups: control untreated crypts, singly treated with either Cch or Ned-19, or simultaneously treated with both. Colonic crypts in the Cch group were stimulated with Cch (10µM) for 30 min. For Ned-19 treated groups, crypts were either pre-incubated with Ned-19 (200µM) alone for 1.5 hour, or with Ned-19 (200µM) for 1 hour, then with Ned-19 (200µM) + Cch (10µM) for another 30 min. Samples were fixed and labelled with anti-MUC2 (green) and anti-Ecad (red) antibodies, cell nuclei were stained with Hoechst (blue) (A). Representative images taken with a confocal microscope using a x63 objective. The MUC2 intensities in goblet cells were measured from 3-5 slices of z-stack images using ImageJ. Mean MUC2 intensities in goblet cells were calculated and normalised to the control group, and displayed as mean ± SE (B). Results were representative of N= 4 subjects, n≥ 13 crypts and ng≥ 228 goblet cells in each treatment group. Significance differences were assessed using One-way ANOVA tests, $F(3, 49) = 18$, $p< 0.0001$; followed by Bonferroni procedures and Tukey's post hoc analysis. Significant difference as indicated by asterisks (**) for $p< 0.01$ was observed between pairs of mean values including (i) control vs. Cch, (ii) Cch vs. Ned-19, (iii) Cch vs. Ned-19 + Cch, (iv) control vs. Ned-19 + Cch. No significant difference was observed between (i) control vs. Ned-19, (ii) Ned-19 vs. Ned-19 + Cch.

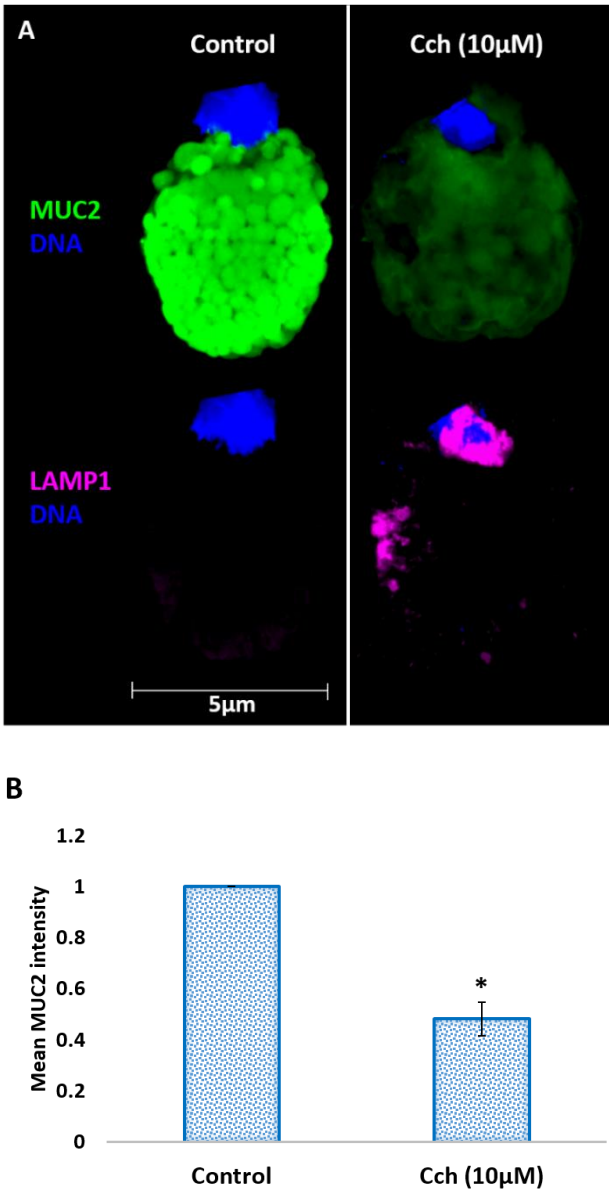

Figure 5.7 Goblet cell responsiveness to Cch stimulation in the absence of neighbouring signals

Single human colonic crypt epithelial cells (including goblet cells) were stimulated with Cch (10µM) for 30 min. The cells were then fixed and labelled with anti-MUC2 (green) and anti-LAMP1 (pink) antibodies, and cell nuclei were stained with Hoechst (blue). Enlarged images were taken with Zeiss LSM 510 Meta confocal microscope with a x63 objective. (A) Images are 3D reconstructed z-stack confocal images of single goblet cells, different channels were displayed separately with the respective treatment group. (B) MUC2 content (intensities) in single goblet cells were measured by Volocity 3D image analysis software. Mean MUC2 intensities in goblet cells were calculated and normalised to the control group, and displayed as mean ± SE. Results were representative of N= 3 subjects, ng=11 goblet cells derived from 3 subjects in each treatment group. Asterisks (*) denotes a significant difference compared to the control (paired t-test, $p < 0.05$).

5.5 Role of NOX1/RAC1/ROS in mucus granule exocytosis in human colonic crypts

As CD38 is the enzyme responsible for the synthesis of NAADP, it serves an important intermediate role in the signal transduction pathway downstream of M3AchR activation and upstream of NAADP. The synthesis of the two 2nd messengers cADPR and NAADP requires the availability of the substrates NAD^+ and $NADP^+$ respectively in the cytosol for the enzymatic reaction to occur. Intriguingly, both substrates of CD38 are side products of NADPH oxidase (NOX) (Xu, et al., 2013), hence establishing a link between CD38 and NOX signalling pathways.

Previous findings by Zocchi et al and Xu et al further support a role of NOX in regulating CD38 activity, which therefore merits investigation of the effect of CD38 modulation on mucus secretion in goblet cells (Zocchi, et al., 1999; Xu, et al., 2013). In addition, ROS derived from NOX enzymes on $LC3^+$ vacuoles has been suggested to regulate mucus granule accumulation in mouse colonic goblet cells; 60% of these $LC3^+$ vacuoles were shown to be co-localised with the NOX subunit p22phox (Patel, et al., 2013). In this thesis, the expression and localisation of $LC3^+$ autophagosomes in human colonic crypts were briefly investigated. $LC3^+$ autophagosomes were primarily detected at the basal pole of the crypt, at mid cell region near the ER, and also in the cytosol towards the apical pole of crypt epithelial cells (Figure 5.8A ii), while $LAMP1^+$ lysosomes were primarily localised at the basal and apical poles. Both LC3 and LAMP1 are in close proximity with each other at the mid-cell region but no co-localisation was observed (Figure 5.8A iii). In addition, NOX1 was detected in the cytosol at the apical pole of the crypt (Figure 5.8B i). Both NOX1 and LC3 are in close proximity with each other but no co-localisation was observed (Figure 5.8B iii). These results suggest the source of ROS is in close proximity to endosomal CD38 (Chapter 3, Figure 3.22) and the lysosomal Ca^{2+} stores at the apical pole of crypt cells.

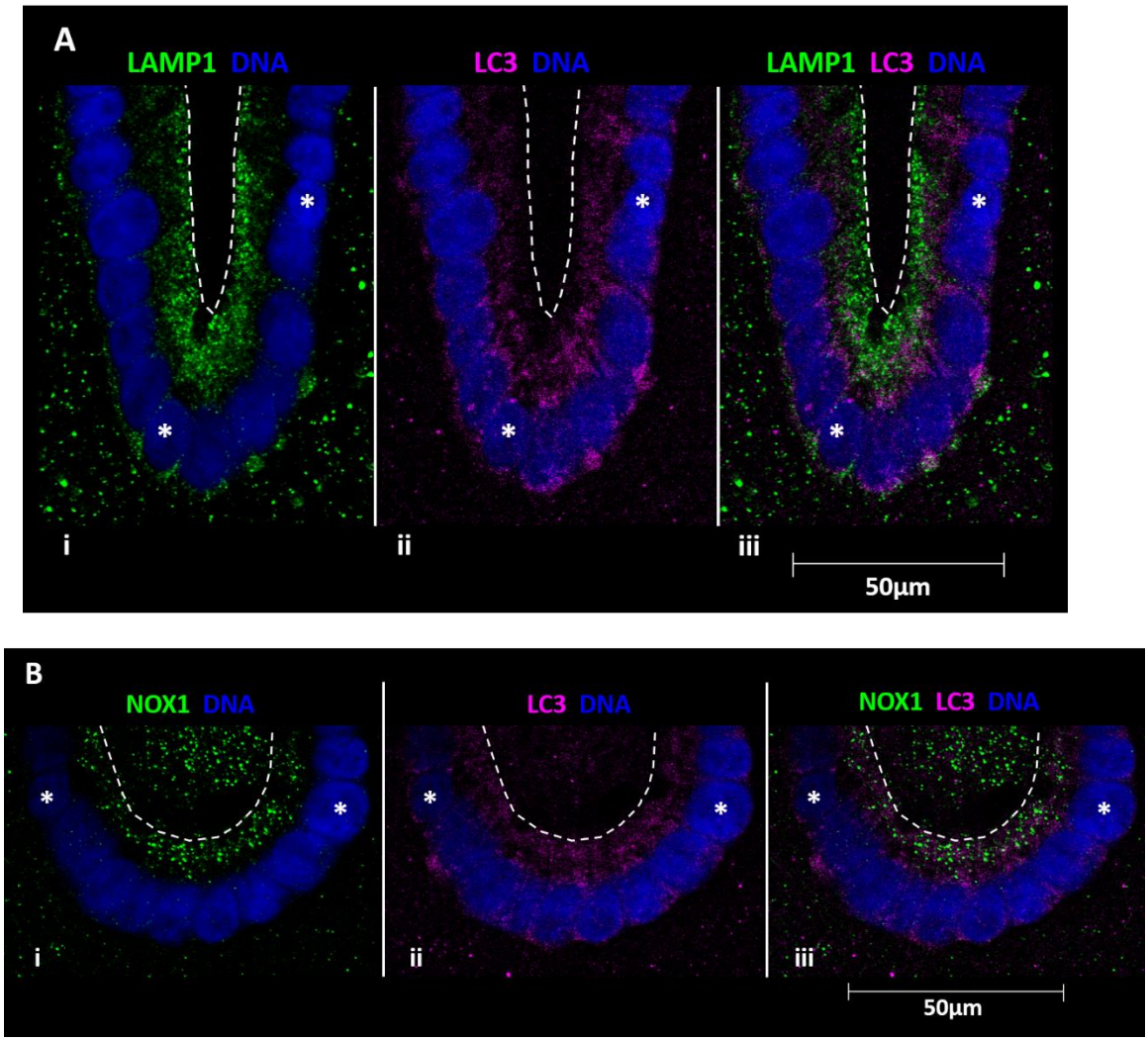

Figure 5.8 The expression and localisation of LC3^{+} autophagosomes and NOX1 in human colonic crypt

Human colonic crypts were fixed and stained with anti-LAMP1 (lysosomes, green) and anti-LC3 (autophagosomes, pink) antibodies, cell nuclei were stained with Hoechst (blue) (A). (i) Overlay image of LAMP1 (green) and DNA (blue); (ii) overlay image of LC3 (pink) and DNA (blue); (iii) merged image of all three channels: LAMP1 (green); LC3 (pink) and DNA (blue). To identify the association of NOX1 with LC3^{+} vacuoles, colon crypts were fixed and labelled with anti-NOX1 (green) and anti-LC3 (pink) antibodies, cell nuclei were stained with Hoechst (blue) (B). (i) Overlay image of NOX1 (green) and DNA (blue); (ii) overlay image of LC3 (pink) and DNA (blue); (iii) merged image of all three channels: NOX1 (green), LC3 (pink) and DNA (blue). Images were taken with a Zeiss confocal microscope with a x63 objective. White dotted lines show the boundary of the crypt lumen. Asterisks (*) denote goblet cells in situ. Images were derived from N=1 subject, n=3 crypts.

The role of NOX1-derived ROS in mucus granule exocytosis or retention in goblet cells was further investigated through the application of NOX inhibitors. Cultured human colonic crypts were treated with DPI (2.5µM) for 2.5 hours, or with DPI (2.5µM) for 2 hour then with DPI (2.5µM) + Cch (10µM) for another 30 min (Figure 5.9). During constitutive basal secretion, DPI (2.5µM) caused goblet cells to retain significantly more mucus (an approximate 100% increase, 2.07 ± 0.35, N= 4 subjects, ng≥ 187 goblet cells, paired t-test p= 0.05) when compared to the control group (1 ± 0, Figure 5.9B). In the presence of Cch (10µM), significant levels of mucus retention in goblet cells were still observed when crypts were pretreated with 2.5µM DPI (an approximate 115% increase, 2.15 ± 0.31, N= 4 subjects, ng≥ 187 goblet cells, paired t-test p= 0.034), in comparison to the control group and to the Cch only (0.53 ± 0.04) treated group (an approximate 162% increase, 2.15 ± 0.31, N= 4 subjects, ng≥ 187 goblet cells, paired t-test p= 0.01, Figure 5.9B). Hence, these results suggest that the availability of ROS can have profound quantitative effects on mucus granule exocytosis and accumulation under both resting (unstimulated) and Cch-stimulated conditions. As DPI has been shown to block mitochondrial and other sources of ROS (Wind, et al., 2010), the current data is unable to determine the specific source of ROS that was playing a role in mucus granule release.

The role of NOX-derived ROS in mucus secretion was further investigated using VAS2870, a specific pan-NOX inhibitor (Wingler, et al., 2012). Human colonic crypts were treated with VAS2870 (56µM) for 2.5 hours, or with VAS2870 (56µM) for 2 hours and then with VAS2870 (56µM) + Cch (10µM) for another 30 min (Figure 5.10A). During constitutive basal secretion, very little difference was observed in the amount of mucus retained in goblet cells of crypts pretreated with 56µM VAS2870 (1.3 ± 0.09, N= 2 subjects, ng≥ 85 goblet cells, paired t-test p= 0.19) or not (control, 1 ± 0, Figure 5.10B). In the presence of Cch (10µM), VAS2870 (56µM) failed to cause mucus granule retention in goblet cells as compared to the control group (0.712 ± 0.14, N= 2 subjects, ng≥ 85 goblet cells, paired t-test p= 0.29) or the Cch only (0.72 ± 0.13) treated group (0.712 ± 0.14, N= 2 subjects, ng≥ 85 goblet cells, paired t-test p= 0.98, Figure 5.10B). The current result of VAS2870 in human colonic crypts remained inconclusive as this dosage was sufficient to block Cch-induced Ca^{2+} signal generation. Hence, these findings seem to suggest that NOX1-derived ROS does not play a role in mucus granules retention in goblet cells. Further experiments including the use of ROSstar and MitoSOX are required to confirm the sources of ROS generated in response to Cch stimulation.

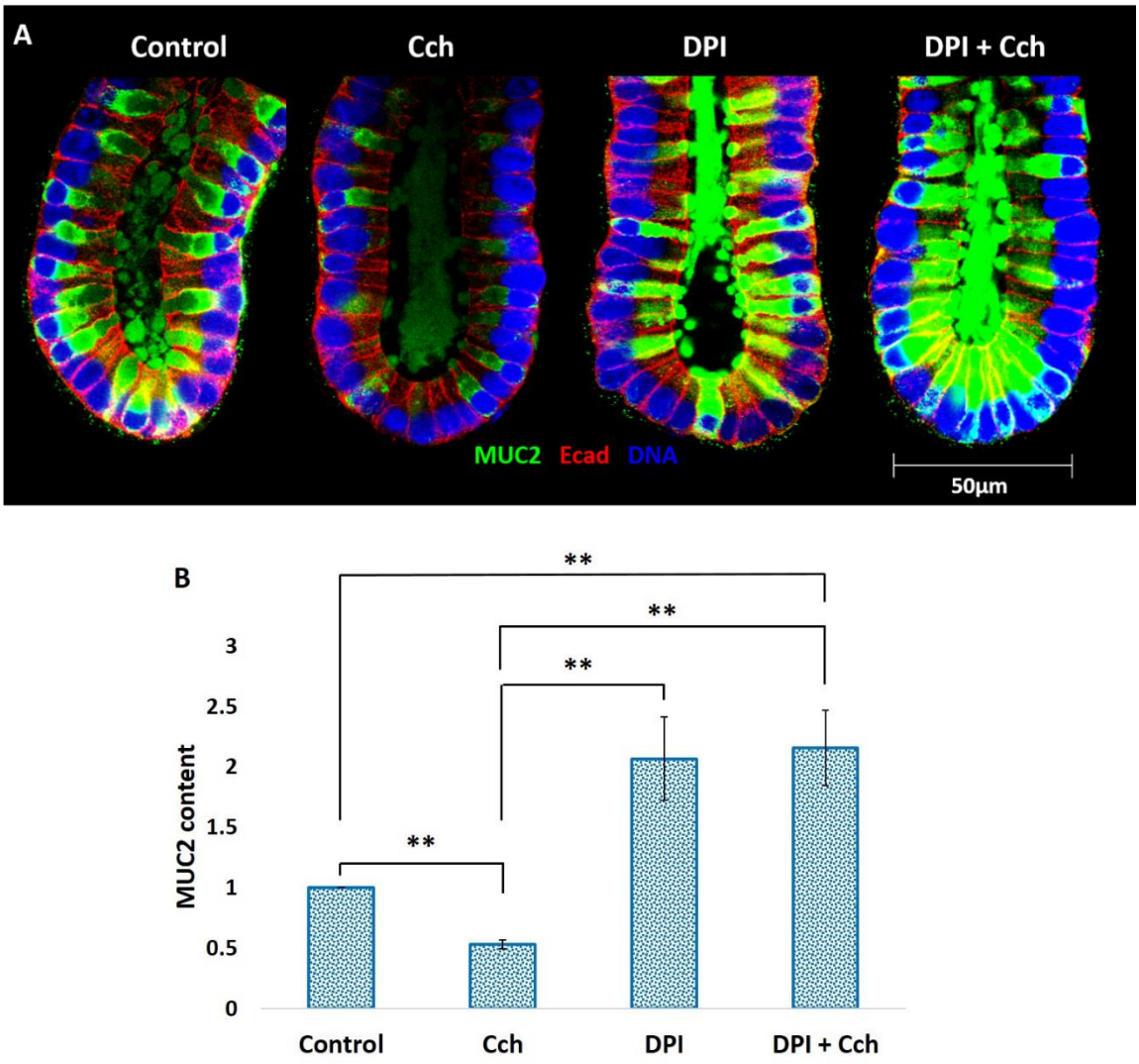

Figure 5.9 The role of NADPH oxidase in MUC2 mucin secretion in human colonic crypts

Cultured human colonic crypts were separated into four treatment groups as labelled above. Colonic crypts in the Cch group were stimulated with Cch (10µM) for 30 min. For DPI treated groups, crypts were either pre-incubated with DPI (2.5µM) alone for 2.5 hours, or with DPI (2.5µM) for 2 hours followed with DPI (2.5µM) + Cch (10µM) for another 30 min. (A) Samples were fixed and labelled with anti-MUC2 (green) and anti-Ecad (red) antibodies, and visualised with Alexa-conjugated secondary antibodies; cell nuclei were stained with Hoechst (blue). Representative images were taken with a Zeiss Meta 510 confocal microscope using a x63 objective. (B) The MUC2 mucin content (intensities) in goblet cells was measured from 3-5 slices of z-stack images using ImageJ. Mean MUC2 intensities in goblet cells were calculated and normalised to the control group, and displayed as mean ± SE. Results were representative of N= 4 subjects, n≥ 12 crypts and ng≥ 187 goblet cells in each treatment group. Significant difference was assessed by One-way ANOVA, $F(3, 49) = 74.3$, $p< 0.0001$; followed by Bonferroni procedures and Tukey's post hoc analysis. Significant difference as indicated by asterisks (**) for $p< 0.01$ was observed between pairs of mean values including (i) control vs. Cch, (ii) control vs. DPI, (iii) control vs. DPI + Cch, (iv) Cch vs. DPI, (v) Cch vs. DPI + Cch. No significant difference was observed between DPI vs. DPI + Cch.

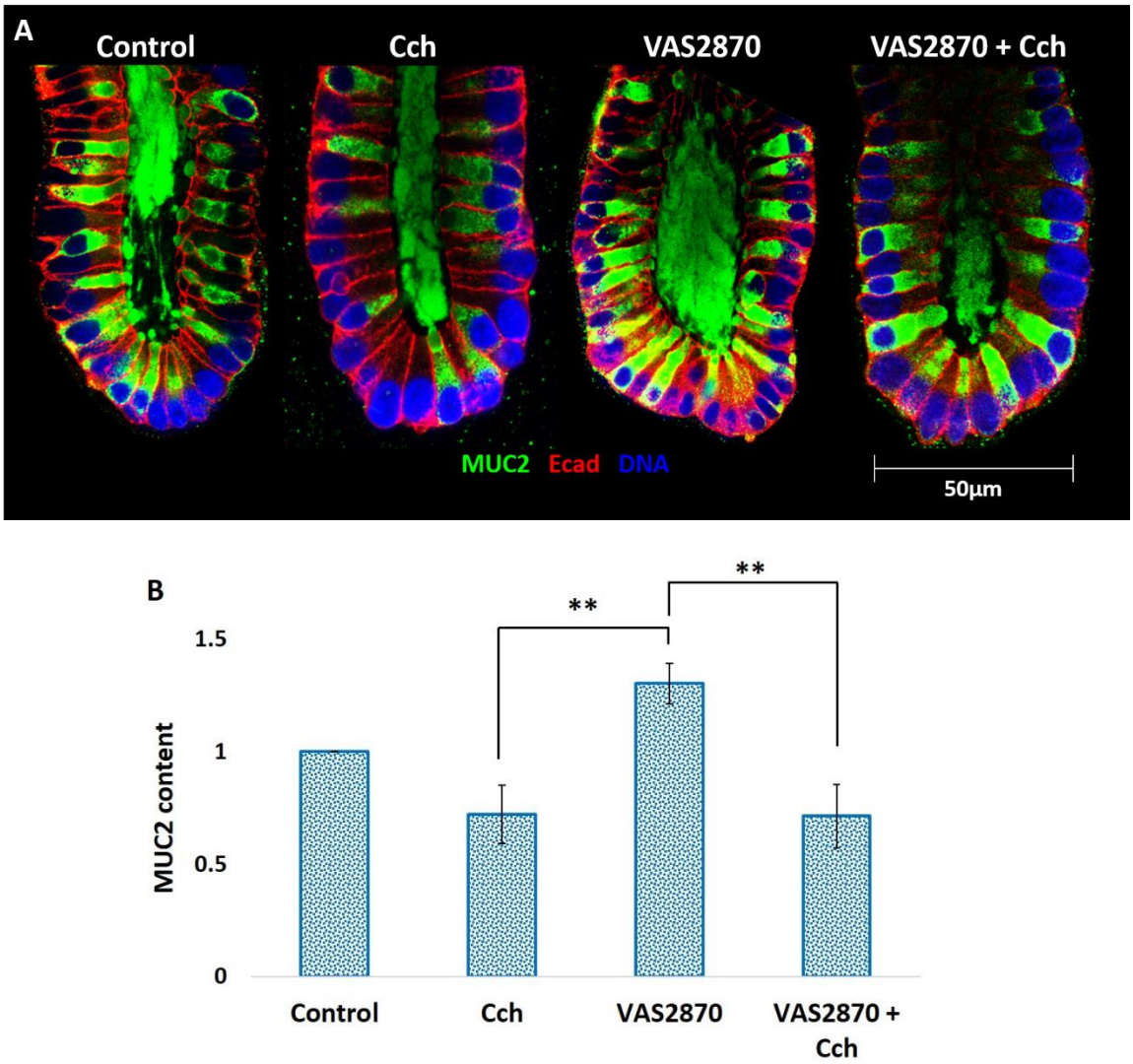

Figure 5.10 Effects of VAS2870 in MUC2 mucin secretion in human colonic crypts

Cultured human colonic crypts were separated into four treatment groups as labelled above. Colonic crypts in the Cch group were stimulated with Cch (10µM) for 30 min. For VAS2870 treated groups, crypts were either pre-incubated with VAS2870 (56µM) alone for 2.5 hours, or with VAS2870 (56µM) for 2 hours, then with VAS2870 (56µM) + Cch (10µM) for another 30 min. (A) Samples were fixed and labelled with anti-MUC2 (green) and anti-Ecad (red) antibodies, and visualised with Alexa-conjugated secondary antibodies; cell nuclei were stained with Hoechst (blue). Representative images were taken with a Zeiss Meta 510 confocal microscope using a x63 objective. (B) The MUC2 mucin content (intensities) in goblet cells was measured from 3-5 slices of z-stack images using ImageJ. Mean MUC2 intensities in goblet cells were calculated and normalised to the control group, and displayed as mean ± SE. Results were representative of N= 2 subjects, n≥ 6 crypts and ng≥ 85 goblet cells in each treatment group. Significant differences were assessed using One-way ANOVA tests, $F(3, 25) = 5.2$, $p= 0.0063$; followed by Bonferroni procedures and Tukey's post hoc analysis. Significant difference as indicated by asterisks (**) for $p< 0.01$ was observed between pairs of mean values including (i) Cch vs.VAS2870, (ii) VAS2870 vs. VAS2870 + Cch. No significant difference was observed between other pairs.

As is the case with NOX2, RAC1 is required for NOX1 activation (Ueyama, et al., 2006) and NOX1 dependent ROS formation (Cheng, et al., 2006). The role of RAC1-dependent NOX1-derived ROS in mucus secretion was further investigated using the RAC1 activation inhibitor NSC23766. Human colonic crypts were treated with NSC23766 (250µM) for 1.5 hour, or with NSC23766 (250µM) for 1 hour then with NSC23766 (250µM) + Cch (10µM) for another 30 min (Figure 5.11). During constitutive basal secretion, the level of mucus granules retained in goblet cells in NSC23766 treated crypts (1.08 ± 0.22) was similar to the control group (1 ± 0, N= 4 subjects, ng≥ 211 goblet cells, Figure 5.11B). In the presence of Cch (10µM), a significant level of mucus retention in goblet cells was observed when crypts were pre-incubated with NSC23766 (250µM) as compared to the control group (an approximate 100% increase, 1.99 ± 0.28, N= 4 subjects, ng≥ 211 goblet cells, paired t-test p= 0.038) and to the Cch only (0.54 ± 0.09) treated group (an approximate 146 % increase, 1.99 ± 0.28, N= 4 subjects, ng≥ 211 goblet cells, paired t-test p= 0.013, Figure 5.11B). These results imply that RAC1 is activated only upon Cch stimulation, as no obvious effect was seen in NSC23766-only treated group compared to the control group. Hence, the possible role of NOX1-derived ROS in mediating mucus granules exocytosis/retention seems likely, given the effects of DPI (NOX inhibitor) and NSC23766 (RAC1 inhibitor).

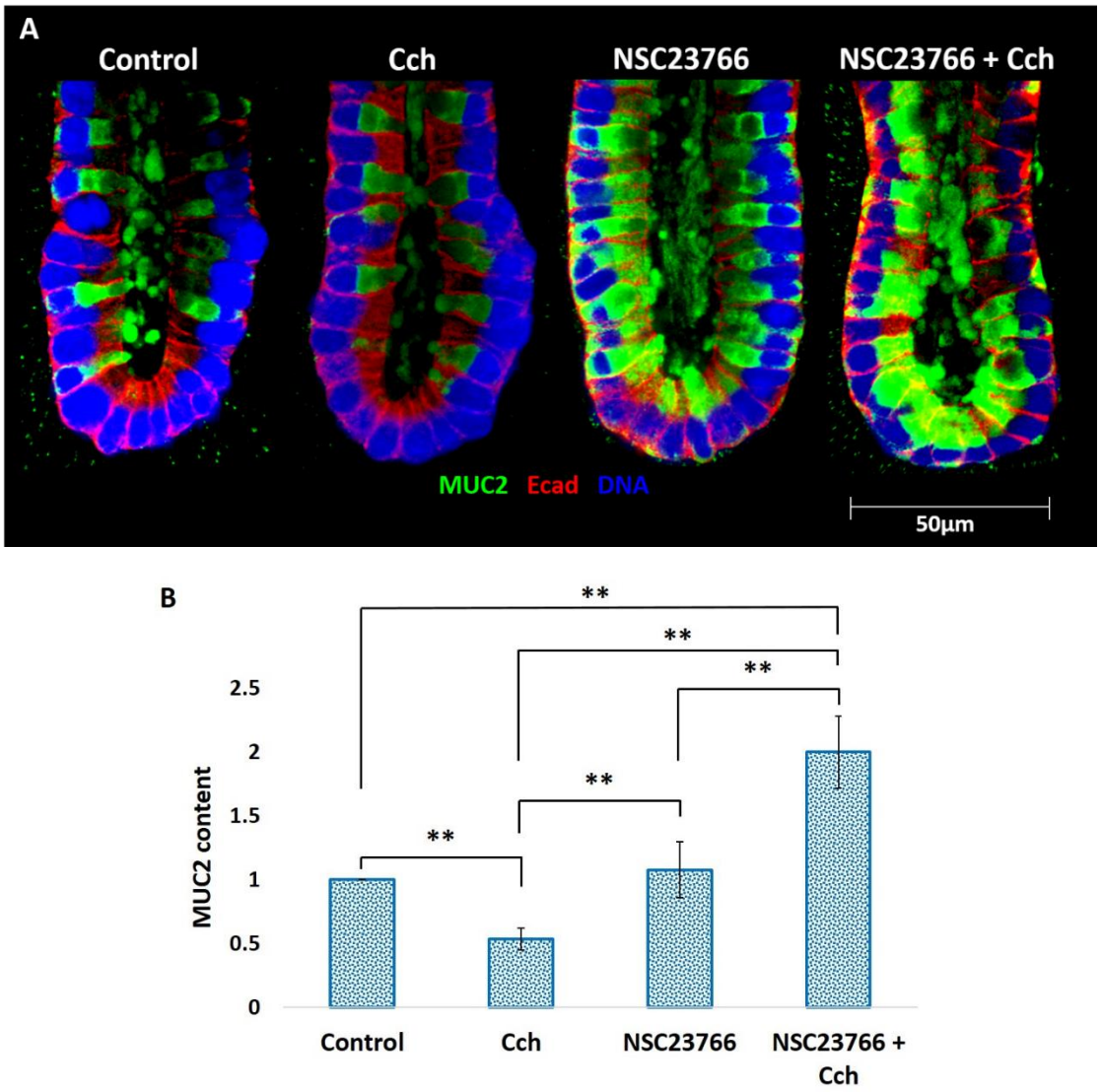

Figure 5.11 Role of RAC1 in MUC2 mucin secretion in human colonic crypts

Cultured human colonic crypts were separated into four treatment groups as labelled above. Colonic crypts in the Cch group were stimulated with Cch (10µM) for 30 min. For NSC23766 (RAC1 inhibitor) treated groups, crypts were either pre-incubated with NSC23766 (250µM) alone for 1.5 hours, or with NSC23766 (250µM) for 1 hour, then with NSC23766 (250µM) + Cch (10µM) for another 30 min. (A) Samples were fixed and labelled with anti-MUC2 (green) and anti-Ecad (red) antibodies, cell nuclei were stained with Hoechst (blue). Representative images were taken with a confocal microscope using a x63 objective. (B) The MUC2 mucin content (intensities) in goblet cells was measured from 3-5 slices of z-stack images using ImageJ. Mean MUC2 intensities in goblet cells were calculated and normalised to the control group and displayed as mean ± SE. Results were representative of N= 4 subjects, n≥ 12 crypts and ng≥ 211 goblet cells in each treatment group. Significance was assessed using One-way ANOVAs, $F(3, 51) = 12.7$, $p < 0.0001$; followed by Bonferroni procedures and Tukey's post hoc analysis. Significant difference as indicated by asterisks (**) for $p < 0.01$ was observed between pairs of mean values including (i) control vs. Cch, (ii) Cch vs. NSC23766, (iii) Cch vs. NSC23766 + Cch, (iv) control vs. NSC23766 + Cch, (v) NSC23766 vs. NSC23766 + Cch. No significant difference was observed between control vs. NSC23766.

5.6 Discussion

In the human GI tract, cholinergic signals have been shown to regulate intestinal ion transport (Kuwahara, et al., 1989; Mall, et al., 1998; Reynolds, et al., 2007) and gastric motility (Parkman, et al., 1999). In addition, Ach (or its analogue Cch) has been shown to regulate mucus secretion in rabbit colonic crypt goblet cells (Specian and Neutra, 1980), in the rat GI tract (Rubinstein, et al., 1994), and in the human colonic crypt goblet cells (Halm & Halm, 2000). All of these studies have demonstrated the effects of Ach in the acceleration of mucus granule exocytosis, reduction of goblet cell content, elevation of mucus thickness, and enhancement of mucus secretion rate. However, the mechanism of how Ach exerts its function is unclear.

MAchR is one of the Ach receptors that is expressed in the human colonic epithelium, of which M3AchR was found to be the predominant subtype expressed in human colonic crypts (Figure 3.10). Activation of M3AchR by Ach or Cch has been shown to trigger downstream signalling pathways, in particular the generation of the 2nd messenger IP3. IP3 releases Ca^{2+} from the ER store via the IP3R. The initial increase in intracellular [Ca^{2+}] triggers the CICR response within the cell (Felder, 1995; Budd, et al., 1999). Elevation of intracellular [Ca^{2+}] by cholinergic stimulation has been shown previously in coupling mucus secretion in rabbit gastric mucous cells, and the secretory response was blocked by the application of the intracellular Ca^{2+} chelator BAPTA (Seidler, et al., 1991), suggesting mucus secretion is a Ca^{2+} dependent process. In addition, the link between MAchR activation and Ca^{2+} signal generation was also demonstrated previously in the rat and human colonic crypts (Lindqvist, et al., 1998; Lindqvist, et al., 2002; Reynolds, et al., 2007). However, the underlying mechanism of cholinergic-mediated Ca^{2+} signal generation in coupling mucus secretion in the human colonic epithelium has never been shown.

In the previous chapter, BAPTA was shown to block Cch-induced Ca^{2+} signal generation (Figure 4.6). The hypothesis that mucus secretion is dependent on intracellular Ca^{2+} mobilisation was then tested by the application of the intracellular Ca^{2+} chelator BAPTA. BAPTA (66µM) significantly attenuated mucus secretion in human colonic crypt goblet cells at the base of the crypt upon Cch stimulation (approximately 100% increase of MUC2 content in goblet cells, Figure 5.2), suggests that mucus granule exocytosis in colonic crypt goblet cells are dependent on intracellular Ca^{2+} signal transduction. Intense labelling of immature MUC2 proteins was also detected in the ER/Golgi area in goblet cells when treated with BAPTA-AM (data not shown). These results suggest that newly synthesised MUC2 mucin protein, after all the glycosylation (maturation) processes in the ER and Golgi, was unable to

package into secretory vesicles due to the lack of Ca^{2+} ion in the environment. In support from previous findings in rabbit gastric mucous cells (Seidler, et al., 1991) and rat gastric epithelial cells (Tani, et al., 2002), the effect of BAPTA here confirmed that cholinergic mediated mucus secretion in human colonic crypts is dependent on intracellular Ca^{2+} mobilisation.

5.6.1 The essential role of CD38 in calcium coupling mucus secretion in human colonic crypts

In the previous chapter, CD38 is identified as one of the key players in Cch-evoked Ca^{2+} signal generation. In this chapter, the role of CD38 in regulating mucus secretion in human colonic crypt goblet cells was further investigated with the application of nicotinamide. Nicotinamide acts to reverse the cyclase activity of CD38 by forcing the conversion of cADPR back to NAD^+ (Aarhus, et al., 1995; Graeff, et al., 2002). Nicotinamide (20mM) has no obvious effect on mucus granule retention under constitutive basal condition but significantly retained mucus granules in Cch stimulated condition. The average mucus content in goblet cells in both nicotinamide only and nicotinamide + Cch treated groups were similar to the control group (Figure 5.3B). These results suggest that inhibition of cADPR has no obvious effect on either Cch-induced Ca^{2+} signal generation (Figure 4.12B) or mucus granule retention (Figure 5.3) in human colonic crypt goblet cells. However nicotinamide counteracts the Cch induced acceleration of mucus secretion as compared to the Cch only treated group (Figure 5.3B), these results further implicate the CD38/NAADP axis in mediating Ca^{2+} coupling mucus secretion in the human colonic epithelium.

CD38 has been shown to play a role in glucose-induced insulin secretion in pancreatic islet cells (Mehta, et al., 1996). One previous study reported that nicotinamide had no effect on insulin secretion and glucose kinetics in healthy human subjects, whereas nicotinic acid, a structurally similar compound, increased insulin secretion (Bingley, et al., 1993). Nicotinic acid is a substrate for CD38 for the generation of NAADP. The current model for the (acidic pH favoured) base-exchange reaction is: nicotinic acid + NADP → NAADP + nicotinamide (Cosker, et al., 2010; Lee, et al., 2012), suggests the acidic organelles might be a site of NAADP synthesis in vivo. Thus, these findings are consistent with our model system that further imply a role for NAADP as the key 2^{nd} messenger in Ca^{2+} coupling mucus secretion. However the mechanism of non-base-exchange NAADP synthesis is currently sparse; and whether CD38 is required for in vivo NAADP synthesis is unclear. A previous report has suggested that

both CD38 and base-exchange reaction are not required for in vivo NAADP synthesis in myometrial cells (Soares, et al., 2007). Hence, many questions still remain regarding the role of CD38/NAADP pathway in vivo.

Endocytosis has been suggested to modulate mucin granule accumulation and secretion. In differentiated mouse intestinal cells, a study by Patel and colleagues demonstrated the inhibition of clathrin-mediated endocytosis causes mucin granule accumulation in goblet cells (Patel, et al., 2013). Additionally CD38 activity has been suggested to be regulated by its internalisation (Zocchi, et al., 1999), which raises the possibility of a link between CD38 activation and endocytosis. As was briefly mentioned in the previous chapter, inhibition of endocytosis by MbetaC (10mM) reduced Cch evoked Ca^{2+} signals. Attempts have also been made to determine the role of endocytosis on mucus secretion in colonic crypt goblet cells, however, the viability of crypt cells decreased after a short period of incubation (30 min or 2 hours) with MbetaC (10mM). This finding is consistent with a previous study which reported that MbetaC significantly decreased the viability of some cell lines including Vero and HuH-7 cells, even after a short period of incubation with a dosage that is routinely used to inhibit endocytosis (Vercauteren, et al., 2010). Thus, the reduction of Cch evoked Ca^{2+} signals by MbetaC could be a false positive result due to decreased viability of the colonic epithelial cells. This technical barrier means that it is currently infeasible to show the specificity of this agent in inhibiting the endocytosis pathway and whether it causes the accumulation of mucus granules in human colonic crypt goblet cells. Further experiments using other endocytosis inhibitors such as chloroquine and pitstop 2 would be required to confirm these findings.

5.6.2 NAADP is the key 2nd messenger in mediating calcium coupling mucus secretion upon M3AchR activation

The results of this thesis demonstrate that in this model nicotinamide counteracts the effect of accelerated mucus secretion observed during Cch stimulation (Figure 5.3B), suggesting that the CD38/NAADP pathway plays a role in mediating mucus secretion in human colonic crypts. Similarly, the NAADP antagonist Ned-19 was able to inhibit Cch-induced Ca^{2+} signal generation and increase mucus retention inside goblet cells during both basal and stimulated conditions, blocking the majority of the phenotype when treated with Cch (Figures 4.18B and 5.6). Moreover, fluorescent staining of NAADP receptors reveals them to be localised to acidic lysosomes (Figure 5.5). These data thus suggest a model in which NAADP is the key 2nd

messenger responsible for mediating lysosomal Ca^{2+} coupling mucus secretion in human colonic crypt goblet cells.

Goblet cells are of course not alone in the crypt, and neighbouring colonic epithelial cells are interlinked via junctional proteins which provide a means of direct cellular communication. In a tissue explant model such as has been deployed here, it is therefore difficult to tell whether goblet cells (in particular those at the base of crypt) on their own are responsible for the response to cholinergic stimulation. In order to address this problem, our group is developing a colonic crypt derived single cell epithelial culture model, the preliminary data of which suggests that single goblet cells are indeed capable of responding to cholinergic stimulation even in the absence of signals from neighbouring cells (Figure 5.7), in a Ned-19 blockable manner (data not shown). This is consistent with the observation from chapter 3 that goblet cells are equipped with all of the necessary components required for Ca^{2+} signalling. The pitfall of this single cell model is that it cannot currently distinguish goblet cells derived from the crypt base from the mature goblet cells at the surface epithelium in a mixed population of epithelial cells. This presents a confounder, as previous studies have suggested that the colonic surface goblet cells are non-responsive to cholinergic stimulation (Gustafsson, et al., 2012a; Ermund, et al., 2013b), potentially as a result of the described decreasing MAchR expression along the crypt axis (Lindqvist, et al., 2002). Bereft of their ordered tissue structure it becomes difficult to identify goblet cells based on their morphology; MUC2 labelling is strictly required to distinguish them from other epithelial cell types. Hence, those goblet cells that were responsive to Cch stimulation in these experiments are likely to be from the base to mid region of the crypt. In future experiments it might be advantageous to use a concentrated pool of phenotyped goblet cells by using cell sorting, although this will require the identification of markers for immature and mature goblet cells. In addition, laser microdissection would possibly be another way to pick individual goblet cells from specific regions of crypts.

5.6.3 The potential role of NOX1, RAC1 and ROS in mucus secretion upon M3AchR activation

CD38 is the ectoenzyme responsible for the synthesis of the 2^{nd} messengers cADPR and NAADP (Lee, et al., 1997). Synthesis of both compounds requires the availability of the substrates NAD^+ and $NADP^+$ (for the production of cADPR and NAADP respectively) in the cytosol for the enzymatic reaction to occur. Interestingly, both substrates are produced by

NADPH oxidase (NOX) (Xu, et al., 2013), which raises the possibility of NOX (and therefore CD38) signalling lying downstream of MAchR activation. Previous studies have demonstrated the role of NAD^+ (Zocchi, et al., 1996) and NOX (Xu, et al., 2013) in mediating membrane CD38 activation via its internalisation. These findings further support a role of NOX in regulating CD38 activity and mucus secretion in goblet cells.

ROS derived from $LC3^+$ vacuole-associated NOX has been suggested to regulate mucus granule accumulation in mouse colonic goblet cells (Patel, et al., 2013). In this thesis, $LC3^+$ autophagosomes were detected at the apical pole of crypt epithelial cells (among other places), in close proximity to – but not precisely co-localised with – NOX1 (Figure 5.8B iii). NOX1 is known to form a heterodimer with the p22phox NOX complex subunit (Bedard, et al., 2007), which has been demonstrated previously to co-localise with $LC3^+$ vacuoles in mouse intestinal epithelial cells in a manner that was suggested to enhance the formation of these $LC3^+$ vacuoles (Patel, et al., 2013). There are several scenarios which might explain this discrepancy between our data and theirs. One is that the images analysed in Figure 5.8 were acquired at a greater resolution than in the Patel et al. data, allowing us to resolve separate LC3 and NOX1-p22phox proteins. However this scenario seems unlikely given they have used similar and greater resolution technologies in their image acquisition. The second possibility is that there is a difference in the underlying biology between the two models. The most likely scenarios in that case would likely be either that NOX1 and p22phox do not form stable heterodimers in human crypts, or NOX1-p22phox heterodimers do not associate with $LC3^+$ vacuoles in human cells. Given that the association between NOX1 and p22phox is reasonably well established (Sirker, et al., 2011) it seems unlikely that the first of these options is true: were the second option to be the case it might be possible that the NOX complex might be associating with LC3-negative organelles instead.

The role of NOX1-derived ROS in mucus granule exocytosis in goblet cells was further investigated through the application of different NOX-targeting small-molecule inhibitors. Pre-incubation with DPI – one of the small-molecule inhibitors often used to inhibit NOX-derived ROS production (Li, et al., 1998) –caused significant levels of mucus retention in goblet cells in both constitutive basal and Cch-stimulated conditions (Figure 5.9B). These results suggest that ROS is required for typical mucus secretion from both unstimulated or agonist stimulated colonic crypts. However a number of reports contest the specificity of DPI, with some suggestion that it can also block mitochondrial and other sources of ROS (Wind, et al., 2010). However, there appears to be a dose-dependent effect, with DPI preferentially blocking NOX enzymes over mitochondrial oxidative phosphorylation, even at high doses:

the effects of DPI are commonly attributed to NOX inhibition up to and above 10µM (Hancock and Jones, 1987; Bulua, et al., 2011). One study in HT-29 human colon cancer cell lines found that 10µM DPI blocked NOX-dependent ROS production and cell migration to a similar degree as NOX1 siRNA (Sadok, et al., 2008), suggesting DPI at these concentrations is specific in its NOX1-derived ROS blockade. Below this concentration, DPI as low as 0.5µM and 5µM has been shown to block mitochondrial ROS in monocytes/macrophages and in rat skeletal muscle respectively (Li, et al., 1998; Lambert, et al., 2008). Thus it appears that for certain concentrations of DPI, we can expect there to be reasonable NOX-specificity. In this current study, 2.5µM DPI caused significant mucus granule retention in human colonic crypt goblet cells during unstimulated and Cch-stimulated conditions. Therefore, it is still reasonable to interpret these data as suggesting that NOX-derived ROS plays a role in mucus secretion in human colonic crypt goblet cells. Future experiments including exogenous application of ROS and siRNA silencing of NOX1 gene are required to test the role or NOX1-derived ROS on mucus secretion in colonic goblet cells.

The role of NOX-derived ROS in mucus secretion was further investigated using the purportedly specific pan-NOX inhibitor VAS2870 (Wingler, et al., 2012). However, there was no significant difference in the level of mucus retention observed in goblet cells pretreated with VAS2870, during either constitutive basal or Cch stimulated secretion (Figure 5.10B). Contrary to the DPI and other data, these findings seem to suggest that NOX1-derived ROS does not play a role in mucus granules retention in goblet cells. Although the effectiveness of VAS2870 has been reported in multiple cell models, including neutrophils, smooth muscle and endothelial cells (Wingler, et al., 2012; Cifuentes-Pagano, et al., 2012), its mechanism of action and specificity towards NOX1 (among the various NOX isoforms) is unclear. It is possible that the effect of VAS2870 might be cell type or tissues specific, or below some dosage or other threshold for activity in this model. To illustrate this principle, we can consider a previous study which postulated that NOX is involved in influenza virus-induced ROS production and virus replication (Amatore, et al., 2015). In this study, while incubation with either DPI or VAS2870 significantly reduced viral load in infected cells, the effect of DPI was far more potent than VAS2870. The VAS2870 results shown in Figure 5.10B in human colonic crypts therefore remain inconclusive. Thus, further experiments including the use of MitoSOX and ROSstar in conjunction with time lapse imaging to identify and map the sources of ROS generation before and after Cch stimulation and/or NOX1 inhibition are required to confirm the effect of VAS2870 in NOX-derived ROS generation and mucus secretion.

RAC1 has been shown to be required for NOX1 activation (Ueyama, et al., 2006) and NOX1-dependent ROS formation (Cheng, et al., 2006). The small-molecule RAC1 activation inhibitor NSC23766 therefore provides another means of investigating the role of NOX1-derived ROS formation in mucus secretion. NSC23766 selectively inhibits the RAC1-GEF interaction, blocking the conversion of RAC1 to its active form RAC1-GTP, preventing the subsequent activation of the NOX1 complex. Incubation with NSC23766 had no obvious effect on mucus retention when observing constitutive basal secretion; however, it lead to a significantly greater amount of MUC2 being retained in goblet cells that were then stimulated with Cch (Figure 5.11B). This suggests that the effect of RAC1 might possibly lie downstream of M3AchR activation, and further supports the notion that NOX-derived ROS production is an important factor involved in MUC2 secretion. NSC23766 has been used for a decade as an antagonist of RAC1 activation since it was first reported by Gao et al in 2004 (Gao, et al., 2004). However, a recent report by Levay and colleagues suggested this compound also acts as a competitive MAchR antagonist (Levay, et al., 2013). NSC23766 was shown to bind to both M2AchR and M3AchR, and that the concentration ranges commonly used to block RAC1 activation also blocked MAchR activation. These findings were discovered after having done the above experiments. However, in the absence of ligand binding data in the Levay study, an alternative, and attractive, interpretation of their findings is that (i) NSC23766 is a specific inhibitor of RAC, (ii) NSC23766 blocks MAChR activated pathways by blocking downstream RAC1, and that (iii) some other GPCR functions are not blocked by NSC23766 because they are not coupled to RAC1. Further experiments using alternative RAC1 inhibitors such as W56 or siRNA silencing of RAC1 expression are required to confirm the coupling of MAChR to RAC1 and its role in Ca^{2+}-mediated mucus secretion.

To the best of our knowledge, there is no NOX1-specific inhibitor which could be used to support the current findings. Due to the lack of specificity of the small-molecule inhibitors, future work would benefit from the use of MitoSOX that targets mitochondrial superoxide in live cells, and also NOX1-specific siRNA to confirm the source of ROS in mediating mucus secretion. In addition, exogenous application of ROS and overexpression of NOX1 gene in laser microdissected goblet cells from crypt base provide another way to investigate the role of ROS/ NOX1-derived ROS in mucus secretion.

Chapter 6: General Discussion and future work

Ach is one of the many neurotransmitters that is synthesised by cholinergic neurons in the enteric nervous system (Furness, 2000). Activation of MAchRs by Ach or Cch has been shown to trigger various downstream signalling pathways. The generation of the 2nd messenger IP3 and the release of Ca^{2+} from the ER store via IP3R is a well-established example of such a pathway. The initial increase in intracellular [Ca^{2+}] further triggers the CICR response within the cell (Felder, 1995; Nahorski, et al., 1997; Budd, et al., 1999). The link between cholinergic mediated MAchR activation and Ca^{2+} signal generation has been demonstrated previously by our lab in both rat and human colonic crypts (Lindqvist, et al., 1998; Lindqvist, et al., 2002), while cholinergic stimulated mucus secretion has been demonstrated by others in isolated human colonic crypts (Halm and Halm, 2000), yet the underlying mechanism of cholinergic signal-mediated Ca^{2+} mobilisation and the expression of the Ca^{2+} signalling toolkit in regulating mucus barrier function in the human colon has not been published thus far. This thesis investigated the molecular and cellular basis of excitation-mucus secretion coupling in human colonic crypts – the intact unitary tissue structure of the polarised human colonic epithelium. This study has produced a number of findings, including descriptions of the arrangement of neuronal-epithelial cells, cholinergic receptors and polarised distribution of acidic Ca^{2+} storage organelles, and the discovery that their associated two pore Ca^{2+} channels trigger intracellular and intercellular colonic crypt Ca^{2+} waves throughout the intestinal stem cell niche. In goblet cells, these elevated Ca^{2+} levels stimulate mucus granule secretion into the colonic crypt lumen. This study identifies a novel neuronal-epithelial signal transduction pathway that orchestrates the highly complex release of mucus granules that is required to keep the luminal microflora at bay and maintain the barrier function of the intestinal epithelium. This study paves the way to investigate the status of this pathway in inflammatory bowel disease and cancer, which may lead to novel strategies for prevention and treatment.

6.1 Neuronal-epithelial cell interactions in the human colon

Both cholinergic and non-cholinergic neurons extend from the submucosal plexus into the mucosa (Furness, 2000). In this study, enteric neurons were found to be present at the sub-epithelial layers and also in the lamina propria surrounding the crypts. This observation is consistent with published findings regarding the location of enteric neurons in mouse

intestinal crypts (Bjerknes & Cheng, 2001) as well as in the human colonic epithelium (Reynolds, et al., 2007). These axonal projections are in close proximity with colonic crypts: 3D reconstructed images of colonic mucosal sections revealed that some axonal projections actually touch and clasp the surface of crypt cells. Given that there are gastric endocrine cells secreting gastrin under the control of vagal motor neurons (Furness, 2000), one might expect that these colonic axons represent motor neurons responsible for innervation of comparable enteroendocrine cell hormone secretion. In addition, some of these axon terminals were found to penetrate through the single epithelial cell layer towards the crypt lumen. This observation is in sharp contrast to the currently accepted view of enteric neurons, in which they are thought to lie in close proximity to – but do not penetrate – the colonic epithelium (Furness, 2006). Some nerve fibers, believed to be sensory, have been shown to penetrate the inner layers of stratified epithelium which line the oesophagus (Furness, 2006), thus these trans-epithelial colonic nerve fibers could potentially be sensory neurons responsible for sensing the luminal contents. Colon sensory neurons have been reported to detect extracellular acidosis via the transient receptor potential vanilloid receptor 1 in mice (Sugiura, et al., 2007). However, the actual function of these penetrating nerve fibers in the human colonic epithelium is as yet unknown, which presents an opportunity for the generation and testing of novel hypotheses regarding their functional roles. For instance, investigation into a similar neuronal-epithelial interaction revealed that neurons can play a role in the proliferation of epithelial cells and angiogenesis in the sub-epithelial layer – to the extent that these interactions were proposed to enhance cancer cell proliferation and neurogenesis in tumors (Garcia, et al., 2014). Viewed together with the findings of this thesis and similar studies, one might expect that a wide breadth of possible biological functions might fall under the control of such neuronal-epithelial cell communications.

The mechanisms underlying the production of these neuronal-epithelial interactions are also currently largely unknown. The field of neurology has identified a number of systems that govern the growth and orientation of developing axons, describing the interaction of axonal 'growth cones' which alter growth paths in response to a variety of guidance cues including physical interactions and chemical attractants, such as BMP, Wnt, neurotransmitters (Bovolenta, 2005; Tamariz, et al., 2015) and RAC1-dependent ROS (Zhang, et al., 2009). Future experiments co-culturing neurons and colonic crypts whilst modulating these neuron-targeting pathways might serve to investigate how neurons interact with the colonic epithelium and confirm whether the axon terminals extend and penetrate into the epithelial layer.

6.1.1 Neuronal and non-neuronal Ach system in the human colonic epithelium

Ach is primarily secreted by the cholinergic neurons of the enteric nervous system (Wessler, et al., 2008). In this thesis, cholinergic innervation was primarily found at the base of the crypt, as well as in the muscularis mucosae and submucosa. This observation further confirms the neuronal-epithelial interactions in the human colonic epithelium. The close proximity of cholinergic neurons to the colonic epithelium presumably provides the shortest distance for Ach diffusion. Epithelial cells from the skin and airways have been shown previously to express components of cholinergic systems that lack neuronal innervation. In the human placenta, CHAT was detected in multiple subcellular compartments such as the cell membrane, endosomes, cytoskeleton, mitochondria and the nucleus (Wessler, et al., 2003). This non-neuronally produced Ach is proposed to act as a local cellular signalling molecule due to its involvement in various nerve-independent cell functions such as proliferation, differentiation, cell trafficking and secretion, which are different from Ach functioning as a neurotransmitter (Wessler, et al., 2003). While data regarding the cellular localisation of non-neuronal Ach is increasing, knowledge of the biological significance of the system remains limited. Jönsson and colleagues were the first group to demonstrate the possible existence of a non-neuronal Ach system in the human colon (Jönsson, et al., 2007). In this thesis, the expression of CHAT-positive cells, the basal expression of M3AchR and CHAT proteins, and the cytoplasmic expression of VAChT further confirmed the existence of colonic epithelial self-regulation in the absence of neuronal innervation. In agreement with the findings of Jönsson, et al, CHAT-positive signals were detected in enteroendocrine cells in this study. Because MAchR subtypes 1, 3 and 5 were found to be expressed on the basal membrane of the crypt, it is a reasonable supposition that these CHAT-positive enteroendocrine cells synthesise and secrete Ach into the basolateral compartment where it can bind to MAchR in an autocrine or paracrine manner. In mouse models, CHAT positive cells which were identified in the intestinal epithelium have been proposed to have chemosensory traits, through which they might participate in protective reflexes by paracrine Ach signalling (Schutz, et al., 2015); it is therefore possible that the CHAT-positive cells identified in this thesis might have comparable functions.

In neurons, Ach is stored in vesicles in the nerve terminals and released when required for effective neurotransmission. Non-neuronal cells described so far do not appear to be endowed with storage organelles, and the mechanism of non-neuronal Ach release is currently unknown (Wessler, et al., 2003). Recent studies on rat colonic epithelium have suggested the involvement of organic cation transporters (OCT) in regulating non-neuronal

Ach release in the rat colon (Yajima, et al., 2011; Bader, et al., 2014). This hypothesis is further supported by observations from human placenta that non-neuronal Ach is released via OCT (subtypes 1 and 3) (Wessler, et al., 2003), and from human skin, in which OCTs have been shown to contribute to non-neuronal Ach release (albeit in a non-dominant role) (Schlereth, et al., 2006). During the work of this thesis, detection of VAChT expression was used to identify colonic crypt-associated neurons; staining for this protein however also revealed the presence of non-neuronal VAChT expression in epithelial crypt cells. Given the literature cited above, it is currently unclear whether this VAChT has any functional role in non-neuronal Ach release in the human colon, which makes this observation difficult to interpret. As non-neuronal Ach release was not the focus of this project, OCT gene expression was not assessed, although we might expect this family to be responsible for mediating such release. OCTN2 (a recently described member of the OCT family) has been found to be highly expressed in human intestines, from the jejunum to the colon (Terada, et al., 2005; Liu, et al., 2013), making the hypothesis that it could be mediating non-neuronal Ach release feasible. Two functional variants of the OCTN genes have also been identified to be associated with Crohn's diseases (Peltekova, et al., 2004), suggesting an important role for OCTNs in colon physiology. Further research is required to identify the mechanism of non-neuronal Ach release and the functional role of VAChT and OCTN in the human colonic epithelium. Experiments that could be conducted include (1) measurement of crypt Ach content before and after inhibition of VAChT and OCTN2 expression by siRNA; (2) measurement of Ach content in the presence or absence of pharmacological inhibitors, such as quinine or omeprazole for OCTN2 inhibition and inhibition of VAChT by vesamicol, or (3) study the effect of these inhibitors on Ca^{2+} signal generation and their functional role in mucus secretion in the absence of exogenous stimulation (such as Ach or other MAchR agonists).

6.2 Cch-induced colonic crypt calcium signals upon MAchR activation

In this study, immunohistochemical analysis demonstrated the protein expression of MAchR subtypes 1, 3 and 5 at the basal pole of human colonic crypts, with M3AchR being the predominant subtype. Exogenous application of Cch induced coordinated Ca^{2+} signals in the 3D human colonic crypt culture model, the pattern of which being consistent with the application of Ach in previous studies in the same model (Lindqvist, et al., 2002; Reynolds, et al., 2007). Specifically, Ca^{2+} signals initiate at the apical pole of initiator cells at the base of the crypt, before spreading to the basal pole of those cell and then further propagating along

the crypt axis by intercellular communication via the gap junctional proteins. Preliminary data in this study suggests that the Ca^{2+} initiator cells at the base of the crypt are $LGR5^{+}$ stem cells, whose increased Ca^{2+} signal sensitivity could be due to the higher intensity of MAchR expression in this region (Lindqvist, et al., 2002). These unidirectional Ca^{2+} waves along the crypt axis have previously been shown in our lab to impact both short term and long term physiological consequences in the colonic epithelium, such as fluid secretion and epithelial homeostasis respectively (Lindqvist, et al., 2002; Reynolds, et al., 2007). This current study focusses on the short term process of mucus secretion following Cch stimulation, and aimed to delineate the molecular mechanism of the Ca^{2+} signal generation.

Immunohistochemical data presented here demonstrate the polarised location of the intracellular Ca^{2+} stores, with ER at the basal pole of crypt cells, while the acidic lysosomes at the apical poles. The subcellular localisation of these acidic lysosomes coincide with the initiation site of the Cch-induced Ca^{2+} signals, which led to the speculation that these acidic Ca^{2+} stores might play an important role in Ca^{2+} signal generation. The typically accepted major role of these lysosomes is to degrade and recycle macromolecules (Appelqvist, et al., 2013), however recent studies have increasingly shown the importance of the Ca^{2+} signals released from these acidic organelles. NAADP has been shown to be the key 2^{nd} messenger responsible for mobilising acidic Ca^{2+} stores via TPCs (Galione, 2010); these lysosomal Ca^{2+} signals have been shown to regulate diverse cellular functions such as cell differentiation (Brailoiu, et al., 2006; Aley, et al., 2010; Zhang, et al., 2013), vesicle trafficking (Ruas, et al., 2010; Ruas, et al., 2014), exocytosis (Davis, et al., 2012) and autophagy (Medina, et al., 2015). The role of NAADP in recruiting Ca^{2+} from different sources has been studied previously in various models, including arterial smooth muscle cells (Boittin, et al., 2002), pancreatic acinar cells (Cancela, et al., 1999; Menteyne, et al., 2006) and Jurkat T cells (Steen, et al., 2007). In smooth muscle cells, depletion of sarcoplasmic reticulum (SR) Ca^{2+} stores with thapsigargin or inhibition of RYR with ryanodine selectively blocked NAADP mediated global Ca^{2+} waves (Boittin, et al., 2002), suggesting that the NAADP mediated initial phase of Ca^{2+} release from other intracellular organelles triggers global Ca^{2+} release from the ER, while in pancreatic acinar cells or T cells, thapsigargin-depletion of the ER store abolished NAADP evoked Ca^{2+} signals (Menteyne, et al., 2006; Steen, et al., 2007). Thus the role of NAADP in recruiting intracellular Ca^{2+} seems to be cell type specific. In this study, depletion of ER Ca^{2+} stores with thapsigargin did not abolish Cch-induced Ca^{2+} signals in human colonic crypts: instead a small Ca^{2+} wave was observed, suggesting that M3AchR activation mobilises Ca^{2+} from other

intracellular organelles (in line with the findings in smooth muscle cells but in contrast to pancreatic acinar cell and T cell data). In tracheal smooth muscle cells, Cch has been shown to induce a rapid and transient elevation of NAADP levels (Aley, et al., 2013), which provides a line of reasoning to question whether MAchR activation by Cch induces NAADP-mediated Ca^{2+} mobilisation from acidic stores in human colonic crypts, which has never been reported previously. In addition to the activation of PLC and the subsequent generation of the 2nd messenger IP3 in mediating ER store Ca^{2+} release via the IP3R, MAchR activation has been shown to regulate CD38 activity by an unknown mechanism in airway smooth muscle cells (Gosens, et al., 2006). Activation of M3AchR has also been shown to lead to cADPR generation by CD38 (Higashida, et al., 1997a and b). These findings suggest a potential involvement of CD38 pathways in the regulation of Ca^{2+} signal generation upon MAchR activation in the human colonic epithelium, and generate a level of complexity regarding how intracellular Ca^{2+} stores interact in the presence of multiple Ca^{2+} releasing messengers to generate the cholinergic-specific Ca^{2+} signature in the human colonic epithelium.

6.2.1 Molecular mechanism of calcium signal generation upon M3AchR activation

Activation of each of the three MAchR subtypes detected here in the human colonic epithelium could be expected to simultaneously activate both PLC and PLD pathways (Liscovitch, 1991). The subsequent PLC pathway is then well described: activated PLC initiates the hydrolysis of PIP2 into IP3 and DAG; IP3 then mediates ER Ca^{2+} release via the IP3R, while DAG binds to and activates PKC (Felder, 1995; Budd, et al., 1999). Inhibition experiments in this thesis demonstrated that PLC is the major signal transduction pathway responsible for generating Ca^{2+} signals upon M3AchR activation in the human colonic epithelium, thus we expected these signals to be transduced via the subsequent generation of IP3 and DAG. Surprisingly, inhibition of IP3R did not have any significant effect on Cch-induced Ca^{2+} waves, suggesting that IP3 was not the key 2nd messenger for the Ca^{2+} signal generation.

In addition to activating PKC, DAG can be converted to PA by DAG kinase (Kanoh, et al., 2002). The activity of DAG kinase remains low during unstimulated condition, allowing DAG to exert its function (i.e. contribute to the activation of PKC). Elevation of DAG kinase activity upon receptor activation of the PIP2 pathway drives the conversion of DAG to PA, which terminates signalling downstream of DAG (Mérida, et al., 2008). In rabbit neutrophils, inhibition of DAG kinase activity using the compound R59-022 has been shown to potentiate superoxide production, a phenotype which can be blocked by PKC inhibitors, suggesting a

role for PKC in ROS generation (Gomez-Cambronero, et al., 1987). In this thesis, inhibition of PA formation using R59-022 significantly reduced Cch-induced Ca^{2+} signal generation by more than 60%, suggesting a dominant role for PA (or some member of its downstream signalling pathways) in Ca^{2+} signal generation upon M3AchR activation in human colonic epithelium. PA has also been shown to activate some isoforms of PKC in COS cells including PKC-zeta (which is DAG-insensitive) and PKC-alpha in the absence and presence of Ca^{2+} respectively (Limatola, et al., 1994). These findings collectively suggest that PKC isoforms can be activated either by DAG or PA or both. As the expression of PKC isoforms was not addressed in the current study, we are unable to determine which isoforms were activated in response to M3AchR activation; inhibition of PKC suppressed approximately half of the Cch-induced Ca^{2+} signals; considered with the observation that R59-022 did not completely abolish Cch-induced Ca^{2+} signals, we can infer that both DAG-sensitive and -insensitive PKC isoforms were involved in the Ca^{2+} signal generation in the human colonic epithelium.

Having established the importance of PA in signal transduction between cholinergic stimulation and production of Ca^{2+} waves, the target molecules mediating further signalling needed to be established. As discussed in Section 6.2, CD38 is responsible for the production of two 2nd messengers which are known to mediate Ca^{2+} secretion, which makes it an attractive potential target. In this study, inhibition of CD38 activity by nicotinamide significantly reduced Cch-induced Ca^{2+} signals in human colonic crypts, to a similar degree as observed during R59-022 treatment, demonstrating that CD38 does indeed play a role, in a manner which is consistent with a model in which CD38 activity lies downstream of PA. However the mechanism of CD38 activation upon M3AchR activation remains unclear.

Identification of the steps in the pathway of M3AchR activation between PA generation and CD38 activation requires some speculation. The major possibility considered here involves the NADPH oxidase (NOX) family of enzymes, which are responsible for the generation of superoxide and the subsequent conversion into ROS. The activity of NOX enzymes has been shown to be stimulated by PA in various models; in terms of mammalian NOX such studies are largely confined to the study of neutrophils, in which NOX-produced reactive oxygen compounds serves a microbicidal role (McPhail, et al., 1995; Erickson, et al., 1999; Zhang, Y. et al., 2009). As mentioned previously, inhibition of PA formation in rabbit neutrophils potentiates superoxide production, an effect which could be blocked by PKC inhibitors, suggesting a role for DAG or PKC in ROS generation (Gomez-Cambronero, et al., 1987), a

finding which might be argued to run counter to the role that PA plays in stimulating NOX. Another report has suggested a synergistic role for PA and DAG in the activation of NOX in human neutrophils (Qualliotine-Mann, et al., 1993), while Erickson et al suggested that the activity of DAG in the activation of NOX is dependent on its conversion into PA but not via PKC (Erickson, et al., 1999). However, a study by Fontayne and colleagues demonstrated the phosphorylation of p47phox subunit of NOX by PKC isoforms including α, βII, δ and ζ in human neutrophils (Fontayne, et al., 2002). Therefore while some details require clarification, PA seems to be the key regulator of neutrophil NOX activation. However it is currently unclear (1) whether PA activates NOX in other cell systems, such as the human colonic epithelium upon Cch stimulation, (2) whether NOX activation is dependent or independent of PKC activation, and (3) whether DAG and Ca^{2+} dependent or independent PKC isoforms are involved in the process. It has been previously reported that high levels of glucose-induced ROS production occur via PKC-dependent NOX activation in vascular smooth muscle and endothelial cells, and that the increase in ROS production can be blocked by both PKC and NOX inhibitors, however the specific PKC isoforms involved in the process were not identified (Inoguchi, et al., 2000). In this thesis, inhibition of ROS with apocynin significantly reduced the Cch-induced Ca^{2+} signals in human colonic crypts, to a level of inhibition similar to that observed during blockade of PKC. These findings not only demonstrate a role for ROS in the Ca^{2+} signal generation downstream of M3AchR activation, but also suggest a link between NOX activity and PKC. The NOX1 isoform is highly expressed in the colon (Brown, et al., 2009), and the assembly of the transmembrane heterodimer (NOX1/p22phox) with three cytosolic regulatory subunits (NOXO1, NOXA1 and a Rho GTPase RAC1) is necessary for NOX activation (Yu, et al., 2006; Fu, et al., 2014; Görlach, et al., 2015), with activation of the cytosolic RAC1 subunit being the key trigger for NOX-dependent ROS generation (Cheng, et al., 2006). Preliminary data in this thesis demonstrated that the DAG kinase inhibiting chemical R59-022 blocked the recruitment of active RAC1-GTP to the basal pole of crypts (where NOX1 is expressed), suggesting a role for PA in mediating NOX assembly and activation. This supports previous findings that DAG kinase alpha mediates RAC activation by recruiting PKC zeta (which is DAG and Ca^{2+} independent), that dissociate RAC from the inhibitory complex with RhoGDI (Chianale, et al., 2010). Another study also suggested that inhibition of PKC zeta blocks NOX-derived ROS production in cultured neurons (Brennan, et al., 2009). However, the role of different PKC isoforms in NOX activation in the human colonic epithelium remains unclear. Because data presented in this study suggest a dominant role for the PA pathway in Ca^{2+} signal generation, NOX is most likely to be activated by the DAG-

insensitive PKC isoforms. There is currently no direct evidence to suggest the activation of NOX in plant and animal cells is mediated by the PKC-RAC pathway in a Ca^{2+} manner (Jiang, et al., 2011). As PA has been shown to activate PKC-zeta (Limatola, et al., 1994), one possible configuration of the signalling pathway for ROS production in the human colonic epithelium would be M3AchR→ PA → PKC (DAG and Ca^{2+} independent)→ NOX → ROS. Further experiments are required to compare the level of ROS production before and after the application of DAG kinase inhibitor. PKC and NOX inhibitors could also be employed following M3AchR activation in the human colonic epithelium to confirm the role of PKC and the upstream pathway for ROS generation.

The role of NOX-derived ROS in mediating intracellular Ca^{2+} signals remains poorly understood, although one study has previously demonstrated that NOX1-derived ROS regulates Ca^{2+} mobilisation in smooth muscle cells in response to thrombin (Zimmerman, et al., 2011). In this thesis, inhibition of NOX1 by two commonly used NOX inhibitors (DPI and VAS2870), and inhibition of RAC1 activation (by NSC23766) potently blocked the Cch-induced Ca^{2+} signals in the human colonic epithelium by more than 70%. These results further support a potential role of NOX-derived ROS in mediating intracellular Ca^{2+} mobilisation in the human colonic epithelium upon M3AchR activation. However, due to the lack of specificity of these small molecule inhibitors, further research using more specific techniques, such as siRNAs directed against NOX1 and RAC1, is required to confirm these findings. A recent study by Xu and colleagues suggested that NOX-derived ROS mediates CD38 internalisation and activation in coronary arterial myocytes upon MAchR agonist stimulation (Xu, et al., 2013). This is consistent with the data discussed earlier in this section that CD38 activation possibly exists downstream of PA upon M3AchR activation in the human colonic epithelium, as demonstrated by the similar level of Ca^{2+} signal inhibition seen during either DAG kinase or CD38 inhibition. CD38 function has been suggested to be regulated by its internalisation, and ligand-induced CD38 internalisation (endocytosis) has been shown to mediate intracellular Ca^{2+} mobilisation (Zocchi, et al., 1999). Preliminary data in this thesis demonstrated that the inhibition of endocytosis reduced the Cch-induced Ca^{2+} signal by half, suggesting endocytosis is important for Ca^{2+} signal generation in the human colonic epithelium. The level of Ca^{2+} signal inhibition observed during endocytosis blockade is comparable to the inhibition of PKC and ROS, which again provide suggests that a link between NOX-derived ROS and CD38 endocytosis is plausible. Combined, these data can be summarised in the following proposed signalling pathway: M3AchR → PA → RAC1 → NOX → ROS → CD38.

ROS are relatively short-lived molecules but they are readily diffusible through the cytoplasm, hence the subcellular localisation of NOX has been suggested to determine the downstream signalling cascade (Brown, et al., 2009). The idea of targeting specific ROS signals to a precise subcellular compartment upon receptor activation has been suggested to occur via the association of NOX with lipid rafts, caveolae and endosomes (reviewed by Ushio-Fukai, 2006a and b). In this thesis, expression of both NOX1 and active RAC1-GTP protein was detected in the cytoplasm of human colonic crypt epithelial cells. After 30 sec of Cch stimulation, there was an increase in both staining intensity and translocation towards the apical pole of cells where the acidic lysosomes reside (also the Ca^{2+} initiation sites) observed for both proteins. As there was translocation of NOX occurs within the first 30 seconds of a Cch response and the average latency of the induced Ca^{2+} signal was about 46 sec, it is feasible that NOX-derived ROS acts as the second messenger that transfers the M3AchR-mediated activation signals from the basal pole to the response at the apical pole of crypt cells, and that CD38 should be the key regulator of the Ca^{2+} signal generation at the apical pole of cells. As with NOX1, CD38 expression was detected in the cytoplasmic space of human colonic crypt epithelial cells, where the acidic lysosomes reside. This finding is in line with the previous report in pancreatic acinar cells that CD38 expression was detected on endosomes which are in close proximity with the lysosomes (Cosker, et al., 2010). Data presented in this thesis also showed an increase in CD38 expression in the apical region of cells after a prolonged Cch incubation (30 min) in human colonic crypts, possibly representing Cch-mediated CD38 internalisation over a period of time. However, the early events of NOX-dependent CD38 internalisation in the human colonic crypt remain unclear. In the absence of neuronal innervation and the lack of exogenous stimulation with Cch, one possible explanation for the continued endosomal CD38 expression in the cytoplasm of crypt epithelial cells might be that the non-neuronal Ach system is mediating CD38 internalisation via NOX, although such a form of regulation is currently not known. Non-neuronal Ach can be negatively regulated by endogenous cholinesterase, which we would expect to present in these epithelial cells (Montenegro, et al., 2005), which could possibly explain why there wasn't excessive accumulation of endosomal CD38 in the cytoplasm of crypt epithelial cells as compared to the effect of prolonged Cch incubation.

CD38 is responsible for the synthesis of both cADPR and NAADP (Lee, 1997). Data presented in chapter 4 showed that Cch-induced Ca^{2+} signals were reduced when CD38 activity is blocked by nicotinamide, however this finding cannot differentiate between whether the effect was mediated by cADPR or NAADP. The cADPR antagonist 8-bromo-cADPR had no

obvious effect on blocking Cch-induced Ca^{2+} signals, suggesting that cADPR might not play any role in Cch mediated Ca^{2+} signal generation: it is possible that cADPR in these cells does not get transported into the cytoplasm and hence cannot exert its function via the RYR on the ER. Thus our inference that NAADP is likely the CD38-produced messenger responsible for Ca^{2+} signal generation (although it is also possible that the 8-bromo-cADPR inhibitor treatment suffered from some technical flaw such as an incorrect dosage, and that cADPR might play some role). In guinea pig tracheal smooth muscle cells, Cch has been shown to induce a transient increase in NAADP levels, and NAADP was also shown to elevate cytosolic [Ca^{2+}] following microinjection into cells (Aley, et al., 2013), findings which further support the role of CD38/NAADP pathway in mediating Ca^{2+} mobilisation upon M3AchR activation in the human colonic epithelium. In this thesis, some level of co-localisation between LAMP1 lysosomes and CD38 was observed, suggesting that these could be feasible sites of NAADP production. This is in support of previous findings that NAADP synthesis is favoured at an acidic pH (Lee, 1999). However, information is still lacking about how NAADP is generated in vivo. A previous report has suggested that CD38 is not a requirement for NAADP production in myometrial cells (Soares, et al., 2007), while another showed that pancreatic acinar cells derived from CD38 knockout mice produced no NAADP in response to CCK stimulation, in contrast to wild type mice, demonstrating that it was required (Cosker, et al., 2010). Development of protocols for the measurement of intracellular NAADP levels is underway in our lab to allow direct investigation of the effect of Cch in NAADP synthesis in the human colonic crypt.

Since NAADP was first discovered in sea urchin egg homogenates it has been shown to potently mobilise Ca^{2+} from acidic stores in a wide range of cell types (Galione, 2006). Functional coupling between different Ca^{2+} releasing 2nd messengers such as IP3, cADPR and NAADP has also been reported previously (Patel, S. et al., 2001; Menteyne, et al., 2006). Notably, one previous study suggested that NAADP mediated Ca^{2+} released from acidic stores may further trigger Ca^{2+} release from the ER store via IP3Rs and RYRs (Patel, S. et al., 2001). In this thesis, inhibition of both IP3R and RYR revealed that the ER Ca^{2+} store was indeed involved in Cch-induced Ca^{2+} signal generation in the human colonic epithelium, but was not the key trigger for the process. This finding is entirely complementary with the thapsigargin data, in which depletion of the ER store did not abolish the Cch-induced Ca^{2+} signals, but reduce it to a small Ca^{2+} wave, suggesting that the initial M3AchR signal mobilises Ca^{2+} from other intracellular organelles (see section 6.2). The role of acidic lysosomes was investigated

with the NAADP antagonist Ned-19, which potently suppressed Cch-induced Ca^{2+} signals. The importance of NAADP was further confirmed by targeting the NAADP receptor (TPC) with diltiazem (DZM), which caused strong inhibition of the Ca^{2+} signals. These results further support the role of NAADP as the key 2nd messenger responsible for mobilising acidic lysosomal Ca^{2+} stores upon M3AchR activation. Several other drugs such as bafilomycin, chloroquine and GPN were also employed to confirm the importance of the acidic lysosomes. Because the level of inhibition by these inhibitors were more profound than the inhibition of IP3R and RYR on the ER, these observation further suggests the initial increase in local [Ca^{2+}] from acidic stores is the key trigger that further activates RYRs and IP3Rs on the ER membrane to initiate the CICR response in human colonic crypt epithelial cells. These findings are very similar to those experiments in the sea urchin egg homogenate model (Churchill, et al., 2002), in HEK293 cells overexpressing TPC2 (Calcraft, et al., 2009), and in pancreatic acinar cells (Gerasimenko, et al., 2015). All of these findings further confirm the important role of acidic lysosomes in M3AchR signal transduction via a CD38-NAADP-TPC pathway in the human colonic epithelium, although further experiments such as siRNA knockdown of CD38 and TPC genes would be useful in confirming these findings. Incorporating the information from this section, the updated proposed pathway is: M3AchR→ PA→ RAC1→NOX→ CD38→ NAADP→TPC→ Ca^{2+}.

6.3 Cholinergic regulation of mucus secretion in human colonic crypt goblet cells

The role of Ca^{2+} signalling in the regulation of GI tract mucus secretion has been reported from as early as in the 1980s in several animal models (Neutra, et al., 1982; Seidler, et al., 1989; Hamada, et al., 1997; Yang, et al., 2013). The link between cholinergic signalling and intracellular Ca^{2+} mobilisation has been demonstrated previously in our lab (Lindqvist, et al., 2002; Reynolds, et al., 2007). Cholinergic regulation of mucus secretion was first reported in the airway epithelium in 1990 (Rogers, et al., 1990; Widdicombe, et al., 1991), and then in isolated human colonic crypt in 2000 (Halm and Halm, 2000). In this thesis, the role of cholinergic-mediated Ca^{2+} coupling mucus secretion was demonstrated in human colonic crypts. Due to the higher intensity of M3AchR expression at the crypt base, this region of the crypt has been suggested to be more sensitive to cholinergic signals (Lindqvist, et al., 2002). Data presented in chapter 5 confirmed that intracellular Ca^{2+} mobilisation upon M3AchR activation is a requirement for mucus granule exocytosis in human colonic crypt goblet cells,

as the application of the intracellular Ca^{2+} chelator BAPTA caused significant retention of mucus granules in goblet cells at the base of the crypt. The effect of BAPTA in blocking Cch-induced mucus secretion supports previous findings in rabbit gastric mucous cells (Seidler, et al., 1989) and in rat gastric epithelial cells (Tani, et al., 2002).

As discussed previously in section 6.2.1, the lysosomal Ca^{2+} stores play an important role in the generation of Cch-induced Ca^{2+} signals, leading to the proposal that Ca^{2+} mobilisation from these acidic stores couple mucus granule exocytosis in human colonic crypt goblet cells. To confirm this hypothesis, inhibitors targeting NOX, CD38 and NAADP were employed to investigate how these transitional mediators regulate mucus granule secretion in goblet cells. Both DPI (NOX1 inhibitor) and NSC23766 (RAC1 activation inhibitor) caused significant upregulation of mucus granule retention in goblet cells upon Cch stimulation, which suggests a potential role for NOX-derived ROS in the upstream pathway controlling Ca^{2+} signal generation and thus mucus secretion. This is consistent with previous studies which suggested NOX1 and DUOX2 are the predominant sources of ROS in the GI tract which play important roles in limiting bacterial pathogenicity and enforcing barrier integrity (Patel, et al., 2013; Hayes, et al., 2015). In addition, Hayes et al has also identified novel missense variants in the NOX1 and DUOX2 genes that are associated with very early onset IBD (VEOIBD). Patients possessing certain variants of both genes showed abnormal Paneth cell metaplasia, reduced ROS production, and impaired resistance to *Campylobacter jejuni* infection (Hayes, et al., 2015). However, DPI has been shown to block other sources of ROS (Wind, et al., 2010), while NSC23766 was shown to act as a competitive MAchR antagonist (Levay, et al., 2013), hence the data presented here remain inconclusive due to the lack of specificity of these agents. Yet, other reports have suggested that DPI is less potent in blocking mitochondrial oxidative phosphorylation than NOX enzymes (Hancock and Jones, 1987; Bulua, et al., 2011). Due to this complexity, NOX-derived ROS was further investigated by a pan-NOX inhibitor called VAS2870, (Wingler, et al., 2012). In this thesis, both DPI and VAS2870 showed similar levels of inhibition of the Cch-induced Ca^{2+} signals, but VAS2870 failed to retain mucus granules in goblet cells upon Cch stimulation. It is currently unclear about its mechanism of action and its specificity towards NOX1 in the human colonic epithelium. However, in a study of MDCK cells infected with H3N2 viruses, the effect of DPI is far more effective in reducing viral load than VAS2870 (Amatore, et al., 2015), which suggests DPI might be a more potent NOX inhibitor. There is currently no NOX1-specific inhibitor which could be used to confirm the current findings, hence future work including

the use of MitoSOX (which specifically targets mitochondrial superoxide in live cells) as well as NOX1 and RAC1 specific siRNAs are required to confirm the source of ROS in mediating mucus secretion in human colonic crypt goblet cells upon M3AchR activation.

In this study, inhibition of CD38 by nicotinamide has no obvious effect on mucus granule retention under constitutive basal condition but significantly retained mucus granules in Cch stimulated condition. As nicotinamide acts to block cADPR generation, one logical explanation is that inhibition of cADPR has no effect on mucus granules retention. However nicotinamide does prevent the observed acceleration in mucus secretion which occurs following Cch stimulation. These results further implicate the CD38-NAADP axis in mediating Ca^{2+} coupling mucus secretion in the human colonic epithelium. These observations are consistent with the findings in a clinical trial on healthy human subjects, in which nicotinamide was shown to have no effect on insulin secretion rates and glucose kinetics, whereas nicotinic acid – a structurally similar compound to nicotinamide that is the substrate for NAADP (Cosker, et al., 2010; Lee, et al., 2012) – increased insulin secretion (Bingley, et al., 1993). The role of NAADP in mucus secretion was further confirmed using Ned-19, which behaved as predicted and lead to significantly more mucus granules being retained in goblet cells upon Cch stimulation. Thus, NAADP is the key 2nd messenger in mediating Ca^{2+} coupling mucus secretion in human colonic crypt goblet cells (Figure 6.1). Further experiments such as siRNA silencing of CD38 and TPC would help to confirm these findings.

6.4 IBD treatment and therapy

The colon is normally protected by two layers of mucus which play an important role in GI defence (Johansson, et al., 2013). The mucus layer is continually being worn away as the stool passes through. Thus, there is strong need for the continuous replenishment of the mucus layers by goblet cells. One of the major contributing factors for IBD pathogenesis is a defective mucus barrier (Antoni, et al., 2014). The vast majority of current research into the pathophysiology of UC has mainly concentrated on immunological aspects (Cader, et al., 2013; Geremia, et al., 2014), and anti-inflammatory therapy is currently the gold standard for treating IBD patients. However, the role of defects in the production and maintenance of the mucus layer have not been extensively addressed, and there is no specific report thus far targeting the underlying mechanism of cholinergic signal mediated Ca^{2+} mobilisation in regulating mucus barrier function in the human colon. This thesis offers a novel therapeutic target for treating IBD. Both cADPR and NAADP have been shown to regulate Ca^{2+} mediated secretion coupling in pancreatic β cells (Takasawa, et al., 1993b; Takasawa, et al., 1998; Johnson, et al., 2002; Arredouani, et al., 2015), while both diltiazem (Fehmann, et al., 1988) and Ned-19 (Arredouani, et al., 2015) have been shown to inhibit glucose induced insulin secretion in the pancreas. In this thesis, inhibition of NAADP significantly blocked Cch induced Ca^{2+} coupling mucus secretion. Thus, NAADP not only acts as a 2^{nd} messenger for mobilising lysosomal Ca^{2+} that couples mucus secretion, its pathway could also be a potential target for treating IBD.

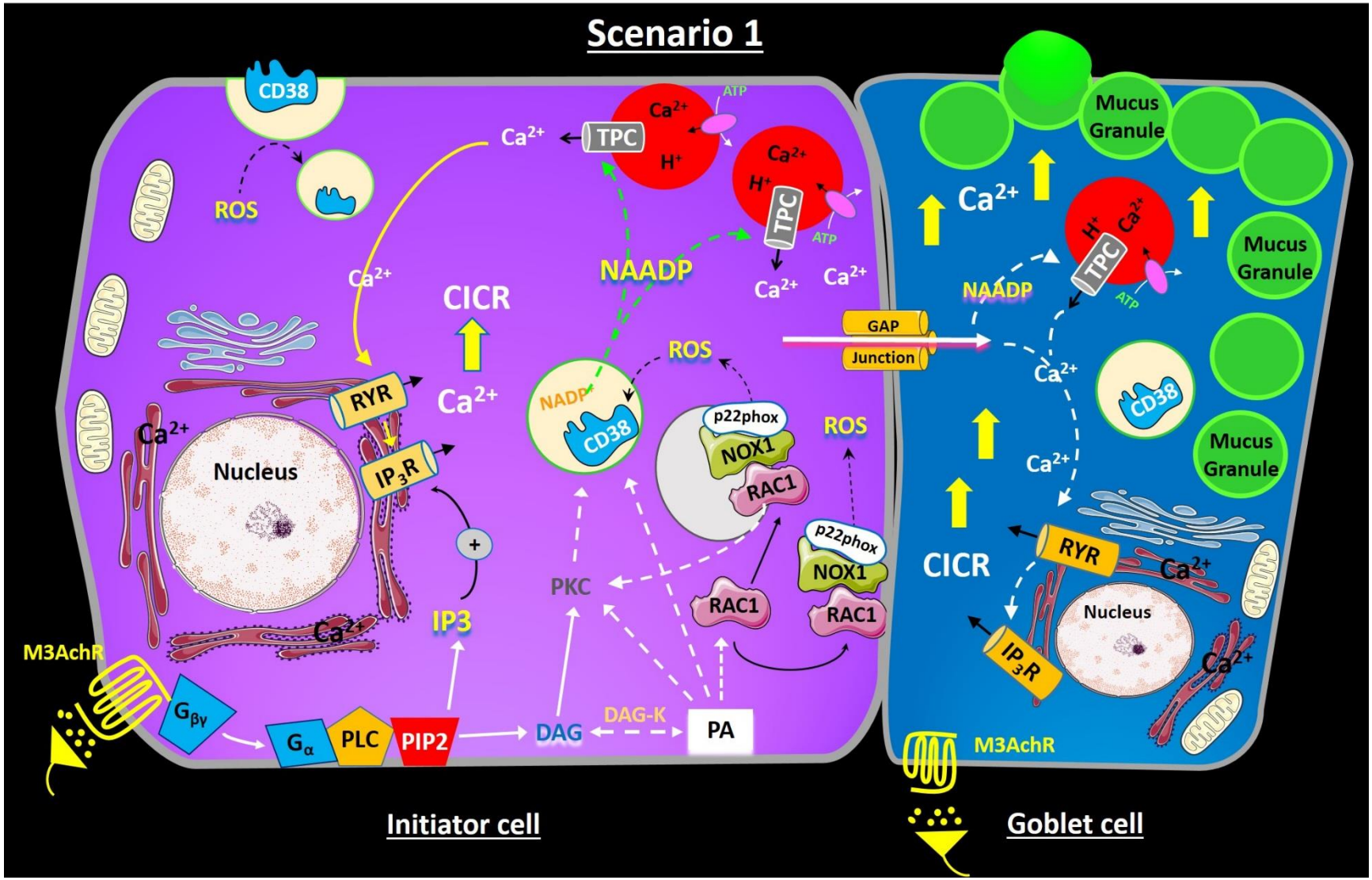
Scenario 1
CD38
ROS
Ca2+
TPC
H+
ATP
NAADP
CICR
RYR
IP3R
Nucleus
IP3
PKC
DAG
DAG-K
PA
PIP2
PLC
Gα
Gβγ
M3AchR
p22phox
NOX1
RAC1
NADP+
GAP
Junction
Mucus Granule
Initiator cell
Goblet cell

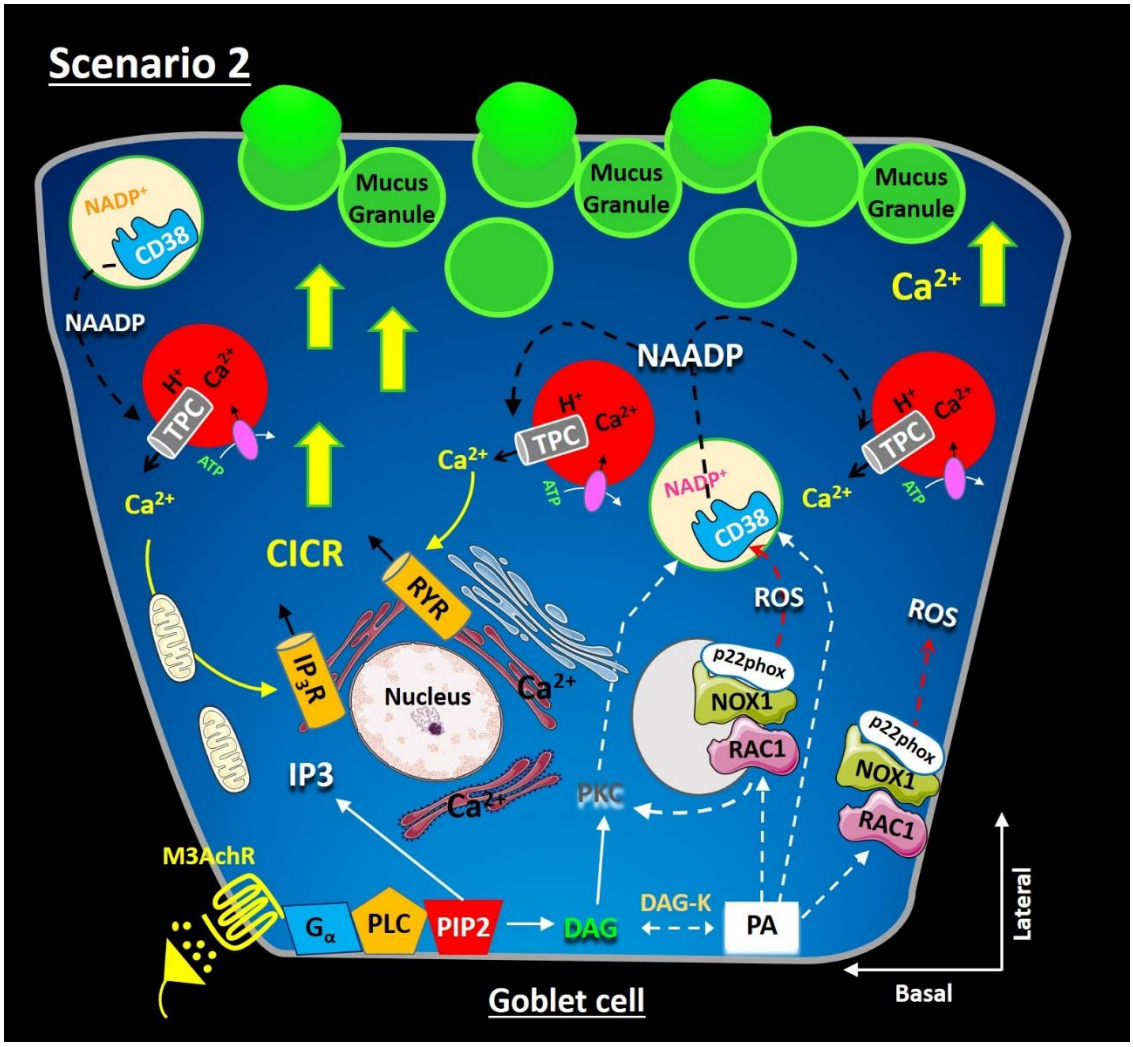
Scenario 2
Mucus Granule
Mucus Granule
Mucus Granule
NADP+
CD38
NAADP
Ca2+
H+
Ca2+
TPC
ATP
Ca2+
CICR
RYR
IP3R
IP3
Nucleus
Ca2+
Ca2+
NADP+
CD38
ROS
ROS
p22phox
NOX1
RAC1
PKC
M3AchR
Gα
PLC
PIP2
DAG
DAG-K
PA
Lateral
Basal
Goblet cell

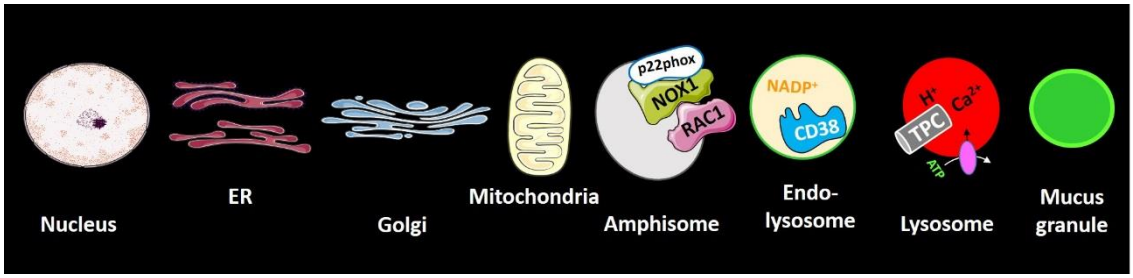
Nucleus
ER
Golgi
Mitochondria
p22phox
NOX1
RAC1
Amphisome
NADP+
CD38
Endo-lysosome
H+
Ca2+
TPC
ATP
Lysosome
Mucus granule

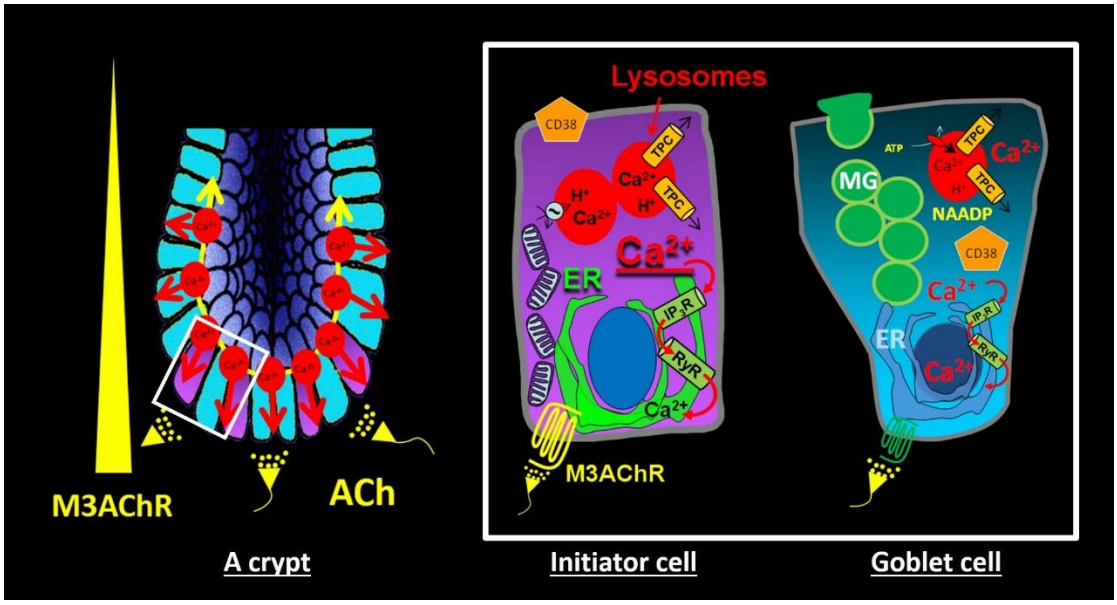

Figure 6.1 Summary diagram of the consequences of cholinergic stimulation

(Scenario 1, pg 236) Binding of Ach (or Cch) to M3AchR at the basal pole of crypt/ initiator cell promotes its association with the heterotrimeric G protein on the plasma membrane that further activates PLC molecules. PLC in turn initiates PIP2 hydrolysis to generate DAG and IP3. Activation of PIP2 enhances DAG kinase activity that promotes the conversion of DAG into PA. PA then activates NOX1 by recruiting RAC1 to the plasma membrane or to vesicular membranes in the cytosol (amphisome) expressing NOX1/p22phox complex. The RAC1/NOX1/ROS system possibly mediates CD38 internalisation or directly activates the CD38 on endosomes; alternatively RAC1/NOX1/ROS might mediate CD38 activity indirectly via PKC activation. CD38 then generates NAADP (presumably in acidic endo-lysosome) that mediates Ca^{2+} mobilisation from acidic lysosomes via the TPCs. These initial Ca^{2+} release from lysosome triggers the IP3Rs and RYRs on the ER membrane and induces the CICR response within the cell. Both Ca^{2+} and NAADP could potentially translocate to the neighbouring goblet cell via Gap junctional protein and subsequently activate the IP3Rs and RYRs on the ER membrane and TPCs on lysosomes respectively. The induction of CICR response in goblet cell mediates the exocytosis of mucus granules. These regenerative Ca^{2+} waves from the Ca^{2+} initiator cells at the base of crypt then propagate to all cell types along the crypt axis, and further mediates mucus granule exocytosis in goblet cells.

(Scenario 2, pg 237) Binding of Ach (or Cch) to M3AchR at the basal pole of goblet cell promotes its association with the heterotrimeric G protein on the plasma membrane that further activates PLC molecules. PLC in turn initiates PIP2 hydrolysis to generate DAG and IP3. Activation of PIP2 enhances DAG kinase activity that promotes the conversion of DAG into PA. PA then activates NOX1 by recruiting RAC1 to the plasma membrane or to vesicular membranes in the cytosol (amphisome) expressing NOX1/p22phox complex. The RAC1/NOX1/ROS system possibly mediates CD38 internalisation or directly activates the CD38 on endosomes; alternatively RAC1/NOX1/ROS might mediate CD38 activity indirectly via PKC activation. CD38 then generates NAADP (presumably in acidic endo-lysosome) that mediates Ca^{2+} mobilisation from acidic lysosomes via the TPCs. These initial Ca^{2+} release from lysosome triggers the IP3Rs and RYRs on the ER membrane and induces the CICR response within the cell, followed by mucus granule exocytosis.

6.5 Limitations of the current study

The mucosal samples used in the current study were derived from histologically healthy tissues, and the spatial characteristics of the Cch induced Ca^{2+} signals were similar regardless of the age and sex of the donor patient. However there might still be some patient bias could theoretically impact on the general applicability of the current findings: clinical history and demographic data such as medication and family history, sex, ethnicity, age, social status and life style (which might include various disease risk-factors, e.g. diet or smoking) were not collected or considered in the current study. The fact that these colonic mucosal samples were obtained from patients for whom there was a suspected need to undergo a surgical resection or colonoscopy could be used to argue that they may be derived from a pool enriched for certain demographics that do not represent the majority and thus could bias the current results.

There is also of course the possibility that explanted colon tissue might not behave the same way as native, in situ colonic crypts. Surgical removal of colon tissue causes ischemia and basal inflammation in the mucosa, which is known to alter gene expression and cause tissue damage (Huang, et al., 2001; Santos, et al., 2015). Although explants were immediately kept on ice, both for rapid transit to the lab and throughout the isolation process, it is entirely feasible that the extraction and culture conditions (which uses various supplements and growth factors) might alter the transcriptional profile of certain genes and affect physiological responses. Whether or not the extraction process itself unduly affects crypts must remain a philosophical question, as we are unable to assay human crypts in vivo. The expression profiles of the genes of interest were not compared before and after crypt culture in this thesis due to the technical difficulties involved in collecting sufficient crypts from Matrigel for further RNA isolation.

Another consideration is that native colonic crypts are constantly under physical and mechanical forces and strains, including compression, shear stress and pressure resulting from peristalsis and passing stool, which is not currently replicated or simulated in our culture model. As the intestinal mucosal cells respond differently to the type of forces that might influence proliferation, differentiation and motility, the lack of such mechanical forces may affect the biology of these cells (Gayer, et al., 2009). It is possible that a flow based culture system could be used to address whether this is an important consideration.

A major technical limitation was the inability to directly measure NAADP or ROS, which means that many effects need to be measured indirectly. Protocols for the measurement of

the intracellular levels of these chemicals before and after Cch treatment are currently being developed in our laboratory, which should provide means to more directly investigate the findings of this thesis.

6.6 Future work

The data described in this thesis details how cholinergic signals in human colonic crypts can translate into mucus secretion via Ca^{2+} signalling. While these results are of interest in untangling molecular pathways and providing insights into the basic biology and physiology of this system, as yet they do not provide much in the way of clinical or translational insight. Therefore the next steps in this body of work would be geared towards using the methodologies and discoveries of this thesis to explore how the systems described here are perturbed in human pathologies. This would best be achieved by conducting a comparative study of mucus excitation secretion coupling in the colonic crypts of healthy and IBD subjects. Such a study would necessarily involve characterisation of the intracellular Ca^{2+} signalling machinery in crypts from IBD patients, and response to cholinergic stimulation. Similarly calcium-mediated excitation-mucus secretion coupling would need to be investigated in IBD crypts. Crucially, pharmacological or genetic modulation of components of the signalling pathway identified here would allow determination of the functional role of Ca^{2+} signalling in rescuing mucus secretion in IBD crypts.

There are a number of techniques that could be employed to further investigate and expand upon the current findings. Techniques such as proteomics and other molecule sensing technologies could be used to identify other molecular changes upon cholinergic stimulation. This might identify the currently unknown intermediate signalling molecules downstream of MAchR activation. Metabolomics may be used to measure the generation of NAD and NADP (substrate of CD38) by NOX upon cholinergic stimulation, and similarly the generation of cADPR and NAADP by CD38, which may provide more accurate quantification of signalling responses. Phosphoproteomics and glycoproteomics could be used to try to identify the effect of Ach on RAC1 activation and MUC2 maturation respectively. Mass spectrometry can be used to measure non-neuronal Ach release before and after the application of the OCT or VAChT inhibitors. Genome-wide transcriptomics may identify larger or unanticipated transcriptional changes before and after cholinergic stimulation in the human colonic epithelium. It might also be instructive to develop or adopt an assay to measure the mucus content of stool, which should be easily extractable using standard centrifugation and

filtration equipment (White, et al., 2009). Rectal mucus discharge is one of the most common symptoms of patients suffering from irritable bowel syndrome (IBS). Similarly, patients with IBD have defective mucus barriers, hence sufferers might be expected to have less mucus in their stool. Such an assay might have use as a prognostic tool to identify candidates who have these or similar gut pathologies. The crypt culture model can also be employed to investigate other gut phenotypes and pathologies such as IBS, coeliac disease, diverticulitis and colon cancer.

Acetylcholine has been shown to play a variety of physiological and cellular functions such as colonic epithelial cell proliferation (Takahashi, et al., 2014), axon guidance (Xu, et al., 2011), muscle contraction (intestinal motility) (Furness, 2000), fluid secretion (Reynolds, et al., 2007) and mucus granule exocytosis (Halm and Halm, 2000); suggesting an important role for this neurotransmitter in gut health. The binding of Ach to the MAchR causes intracellular Ca^{2+} mobilisation, and interfering with the generation of these Ca^{2+} signals also has an impact on cellular events, which suggests an inter-relationship between cholinergic and Ca^{2+} signalling systems. Cholinergic-mediated mucus secretion has been shown previously in the human colonic epithelium (Halm and Halm, 2000), and understanding of the molecular mechanism of both the cholinergic and Ca^{2+} signalling system could enhance our knowledge on how mucus secretion is regulated. This thesis identifies a novel cholinergic-mediated Ca^{2+} signal transduction pathway that orchestrates the highly complex release of mucus granules. Perturbation of these pathways is therefore likely to lead to either gut inefficiencies or even pathologies, making their constituents potential therapeutic targets. Perturbation of mucus production may influence the microbiota compositions, which is increasingly reported to have wide impacts on gut health (Manichanh, et al., 2012; Guinane, et al., 2013; Ohkusa, et al., 2015; Li, H. et al., 2015), and hence it might be instructive to assess gut microbial contents in people who have variation in their cholinergic-epithelial secretion systems. The possibility of therapeutically targeting perturbed neuronal-epithelial secretion systems which are causing gut pathologies may also even be relevant to the treatment of other diseases which involve a similar interface, such as chronic obstructive pulmonary disease (COPD). As in human bronchial epithelial cells, exposure to titanium dioxide (TiO_2) nanoparticles have been shown to evoke Ca^{2+} coupling mucus secretion and led to mucus hypersecretion (Chen, E.Y.T. et al., 2011). Finally, I believe that this thesis demonstrates the need for interdisciplinary investigations, as they might yield results of translational significance that are less likely to be produced from fields which focus on one biological system alone.

Bibliography

Aarhus, R., Graeff, R. M., Dickey, D. M., Walseth, T. F., & Lee, H. C. (1995). ADP-ribosyl cyclase and CD38 catalyze the synthesis of a calcium-mobilizing metabolite from NADP. *Journal of Biological Chemistry*, *270*(51), 30327–30333. DOI:10.1074/jbc.270.51.30327

Abdel-Latif, A. A. (1986). Calcium-mobilizing receptors, polyphosphoinositides, and the generation of second messengers. *Pharmacological Reviews*, *38*(3), 227–272.

Abdul Khalek, F. J., Gallicano, G. I., & Mishra, L. (2010). Colon cancer stem cells. *Gastrointestinal Cancer Research : GCR*, (Suppl 1), S16–S23. DOI:10.1002/9780470151808.sc0301s7

Adkins, C., & Taylor, C. (1999). Lateral inhibition of inositol 1, 4, 5-trisphosphate receptors by cytosolic Ca^{2+}. *Current Biology*, 1115–1118.

Adler, K. B., Tuvim, M. J., & Dickey, B. F. (2013). Regulated mucin secretion from airway epithelial cells. *Frontiers in Endocrinology*, *4*(SEP), 1–9. DOI:10.3389/fendo.2013.00129

Aley, P. K., Mikolajczyk, A. M., Churchill, G. C., Galione, A., Berger, F., Aley, P. K., Galione, A. (2010). Nicotinic acid adenine dinucleotide phosphate regulates skeletal muscle differentiation via action at two-pore channels. *Proceedings of the National Academy of Sciences of the United States of America*, *107*(46), 19927–19932. DOI:10.1073/pnas.1102690108

Aley, P. K., Singh, N., Brailoiu, G. C., Brailoiu, E., & Churchill, G. C. (2013). Nicotinic acid adenine dinucleotide phosphate (NAADP) is a second messenger in muscarinic receptor-induced contraction of guinea pig trachea. *The Journal of Biological Chemistry*, *288*(16), 10986–93. DOI:10.1074/jbc.M113.458620

Allen, A., & Flemström, G. (2005). Gastroduodenal mucus bicarbonate barrier: protection against acid and pepsin. *American Journal of Physiology. Cell Physiology*, *288*(1), C1–C19. DOI:10.1152/ajpcell.00102.2004

Alvarez, J., & Montero, M. (2002). Measuring $[Ca^{2+}]$ in the endoplasmic rerticulum with aequorin. *Cell Calcium*, *32*(5-6), 251–260. DOI: 10.1016/S0143416002001860

Amatore, D., Sgarbanti, R., Aquilano, K., Baldelli, S., Limongi, D., Civitelli, L., Palamara, A. T. (2015). Influenza virus replication in lung epithelial cells depends on redox-sensitive pathways activated by NOX4-derived ROS. *Cellular Microbiology*, *17*(1), 131–145. DOI:10.1111/cmi.12343

Anatomy of the human colon. Colorectal Cancer Association of Canada. Retrieved from http://www.colorectal-cancer.ca/en/

Antoni, L., Nuding, S., Wehkamp, J., & Stange, E. F. (2014). Intestinal barrier in inflammatory bowel disease. *World Journal of Gastroenterology : WJG*, *20*(5), 1165–79. DOI:10.3748/wjg.v20.i5.1165

Appelqvist, H., Wäster, P., Kågedal, K., & Öllinger, K. (2013). The lysosome: From waste bag to potential therapeutic target. *Journal of Molecular Cell Biology*, *5*(4), 214–226. DOI:10.1093/jmcb/mjt022

Arai, M., Matsui, H., & Periasamy, M. (1994). Sarcoplasmic reticulum gene expression in cardiac hypertrophy and heart failure. *Circulation Research*, *74*(4), 555–564. DOI:10.1161/01.RES.74.4.555

Arndt, L., Castonguay, J., Arlt, E., Meyer, D., Hassan, S., Borth, H., Boekhoff, I. (2014). NAADP and the two-pore channel protein 1 participate in the acrosome reaction in mammalian spermatozoa. *Molecular Biology of the Cell*, *25*(6), 948–64. DOI:10.1091/mbc.E13-09-0523

Arredouani, A., Ruas, M., Collins, S. C., Parkesh, R., Clough, F., Pillinger, T., Galione, A. (2015). NAADP and endolysosomal two-pore channels modulate membrane excitability and stimulus-secretion coupling in mouse pancreatic β cells. *Journal of Biological Chemistry*, jbc.M115.671248. DOI:10.1074/jbc.M115.671248

Arslan, G., Atasever, T., Cindoruk, M., & Yildirim, I. S. (2001). (51)CrEDTA colonic permeability and therapy response in patients with ulcerative colitis. *Nuclear Medicine Communications*, *22*(9), 997–1001.

Asada, R., Saito, A., Kawasaki, N., Kanemoto, S., Iwamoto, H., Oki, M., Imaizumi, K. (2012). The endoplasmic reticulum stress transducer OASIS is involved in the terminal differentiation of goblet cells in the large intestine. *The Journal of Biological Chemistry*, *287*(11), 8144–53. DOI:10.1074/jbc.M111.332593

Ashkenazi, A., Peralta, E. G., Winslow, J. W., Ramachandran, J., & Capon, D. J. (1989). Functionally distinct G proteins selectively couple different receptors to PI hydrolysis in the same cell. *Cell*, *56*(3), 487–493. DOI: 10.1016/0092-8674(89)90251-1

Atuma, C., Strugala, V., Allen, a, & Holm, L. (2001). The adherent gastrointestinal mucus gel layer: thickness and physical state in vivo. *American Journal of Physiology. Gastrointestinal and Liver Physiology*, *280*(5), G922–G929.

Bader, S., Klein, J., & Diener, M. (2014). Choline acetyltransferase and organic cation transporters are responsible for synthesis and propionate-induced release of acetylcholine in colon epithelium. *European Journal of Pharmacology*, *733*(1), 23–33. DOI:10.1016/j.ejphar.2014.03.036

Balzola, F., Cullen, G., Hoentjen, F., Ho, G. T., & Russell, R. (2013). Bacteria penetrate the normally impenetrable inner colon mucus layer in both murine colitis models and patients with ulcerative colitis. *Inflammatory Bowel Disease Monitor*, *13*(4), 156–157. DOI: 10.1136/gutjnl-2012-303207

Banks, M. R., Golder, M., Farthing, M. J. G., & Burleigh, D. E. (2004). Intracellular potentiation between two second messenger systems may contribute to cholera toxin induced intestinal secretion in humans. *Gut*, *53*, 50–57.

Bargal, R., Avidan, N., Ben-Asher, E., Olender, Z., Zeigler, M., Frumkin, a, Bach, G. (2000). Identification of the gene causing mucolipidosis type IV. *Nature Genetics*, *26*(1), 118–123. DOI: 10.1038/79095

Barker, N., van Es, J. H., Kuipers, J., Kujala, P., van den Born, M., Cozijnsen, M., Clevers, H. (2007). Identification of stem cells in small intestine and colon by marker gene Lgr5. *Nature*, *449*(7165), 1003–7. DOI: 10.1038/nature06196

Barsukova, A., Komarov, A., Hajnoczky, G., Bernardi, P., Bourdette, D., & Forte, M. (2011). Activation of the mitochondrial permeability transition pore modulates Ca^{2+} responses to physiological stimuli in adult neurons. *European Journal of Neuroscience*, *33*(5), 831–842. DOI:10.1111/j.1460-9568.2010.07576.x

Basseri, R. J., Basseri, B., & Papadakis, K. A. (2011). Dysplasia and cancer in inflammatory bowel disease. *Expert Review of Gastroenterology & Hepatology*, *5*(1), 59–66. DOI:10.1586/egh.10.77

Bedard, K., & Krause, K.-H. (2007). The NOX family of ROS-generating NADPH oxidases: physiology and pathophysiology. *Physiological Reviews*, *87*(1), 245–313. DOI:10.1152/physrev.00044.2005

Begue, B., Verdier, J., Rieux-Laucat, F., Goulet, O., Morali, A., Canioni, D., Ruemmele, F. M. (2011). Defective IL10 signaling defining a subgroup of patients with inflammatory bowel disease. *The American Journal of Gastroenterology*, *106*(8), 1544–1555. DOI:10.1038/ajg.2011.112

Belmonte, S. L., & Blaxall, B. C. (2011). G Protein Coupled Receptor Kinases as Therapeutic Targets in Cardiovascular Disease. *Circulation Research*, *109*(3), 309–319. Doi:10.1161/CIRCRESAHA.110.231233

Berg, T. O., Strømhaug, E., Løvdal, T., Seglen, O., & Berg, T. (1994). Use of glycyl-L-phenylalanine 2-naphthylamide, a lysosome-disrupting cathepsin C substrate, to distinguish between lysosomes and prelysosomal endocytic vacuoles. *The Biochemical Journal*, *300*, 229–236.

Berger, E., & Haller, D. (2011). Structure-function analysis of the tertiary bile acid TUDCA for the resolution of endoplasmic reticulum stress in intestinal epithelial cells. *Biochemical and Biophysical Research Communications*, *409*(4), 610–5. DOI:10.1016/j.bbrc.2011.05.043

Bergström, J. H., Berg, K. A., Rodríguez-Piñeiro, A. M., Stecher, B., Johansson, M. E. V, & Hansson, G. C. (2014). AGR2, an Endoplasmic Reticulum Protein, Is Secreted into the Gastrointestinal Mucus. *PLoS ONE*, *9*(8), e104186. DOI:10.1371/journal.pone.0104186

Berridge, M., & Irvine, R. (1984). Inositol trisphosphate, a novel second messenger in cellular signal transduction. *Nature*, *312*, 315–320.

Berridge, M., Lipp, P., & Bootman, M. (1999). Calcium signalling. *Current Biology : CB*, *9*(5), R157–R159.

Berridge, M. J. (1990a). Calcium Oscillations. *The Journal of Biological Chemistry*, *265*(17), 9583–9586.

Berridge, M. J. (2002). The endoplasmic reticulum: A multifunctional signaling organelle. *Cell Calcium*, *32*(5-6), 235–249. DOI: 10.1016/S0143416002001823

Berridge, M. J., Bootman, M. D., & Roderick, H. L. (2003). Calcium signalling: dynamics, homeostasis and remodelling. *Nature Reviews. Molecular Cell Biology*, *4*(7), 517–29. DOI: 10.1038/nrm1155

Berridge, M. J., & Irvine, R. F. (1989). Inositol phosphates and cell signalling. *Nature*, *341*, 197–205.

Berridge, M. (1993). Inositol trisphosphate and calcium signaling. *Nature*, *361*, 315–325.

Berridge, M. (1990b). Temporal aspects of calcium signalling. *Advances in Second Messenger and Phosphoprotein Research*, *24*, 108–114.

Bers, D. M. (2002). Cardiac excitation-contraction coupling. *Nature*, *415*, 198–205.

Bertrand, C. A., Laboisse, C. L., & Hopfer, U. (1999). Purinergic and cholinergic agonists induce exocytosis from the same granule pool in HT29-Cl.16E monolayers. *The American Journal of Physiology*, *276*, C907–C914.

Bevans, C. G., Kordel, M., Rhee, S. K., & Harris, A. L. (1998). Isoform composition of connexin channels determines selectivity among second messengers and uncharged molecules. *Journal of Biological Chemistry*, *273*(5), 2808–2816. DOI:10.1074/jbc.273.5.2808

Beyenbach, K. W., & Wieczorek, H. (2006). The V-type H^+ ATPase: molecular structure and function, physiological roles and regulation. *The Journal of Experimental Biology*, *209*, 577–589. DOI:10.1242/jeb.02014

Billington, C. K., & Penn, R. B. (2002). M3 Muscarinic Acetylcholine Receptor Regulation in the Airway. *American Journal of Respiratory Cell and Molecular Biology*, *26*(25), 27–29.

Bingley, P., Caldas, G., Bonfanti, R., & Gale, E. (1993). Nicotinamide and insulin secretion in normal subjects. *Diabetologia*, *36*(7), 675–677.

Biosynthesis of ACh and release of ACh in cholinergic synapse. Quizlet.com. Retrieved from https://quizlet.com/76473836/nerve-histology-nervous-system-ch12-flash-cards/

Birchenough, G. M. H., Johansson, M. E., Gustafsson, J. K., Bergström, J. H., & Hansson, G. C. (2015). New developments in goblet cell mucus secretion and function. *Mucosal Immunology*, *8*(4). DOI:10.1038/mi.2015.32

Bird, G. S. J., & Putney, J. W. (2005). Capacitative calcium entry supports calcium oscillations in human embryonic kidney cells. *The Journal of Physiology*, *562*, 697–706. DOI:10.1113/jphysiol.2004.077289

Bjerknes, M., & Cheng, H. (2001). Modulation of specific intestinal epithelial progenitors by enteric neurons. *Proceedings of the National Academy of Sciences of the United States of America*, *98*(22), 12497–12502. DOI:10.1073/pnas.211278098

Bjerknes, M., & Cheng, H. (1981a). The stem-cell zone of the small intestinal epithelium.V. Evidence for controls over orientation of boundaries between the stem-cell zone, proliferative zone, and the maturation zone. *American Journal of Anatomy*, *160*(1), 105–112.

Bjerknes, M., & Cheng, H. (1981b). The stem-cell zone of the small intestinal epithelium. III. Evidence from columnar, enteroendocrine, and mucous cells in the adult mouse. *The American Journal of Anatomy*, *160*(1), 77–91. DOI:10.1002/aja.1001600107

Bjerknes, M., Khandanpour, C., Möröy, T., Fujiyama, T., Hoshino, M., Klisch, T. J., Cheng, H. (2012). Origin of the brush cell lineage in the mouse intestinal epithelium. *Developmental Biology*, *362*(2), 194–218. DOI:10.1016/j.ydbio.2011.12.009

Boittin, F. X., Galione, A., & Evans, A. M. (2002). Nicotinic acid adenine dinucleotide phosphate mediates Ca^{2+} signals and contraction in arterial smooth muscle via a two-pool mechanism. *Circulation Research*, *91*(12), 1168–1175. DOI:10.1161/01.RES.0000047507.22487.85

Bonner, T. I., Buckley, N. J., Young, A. C., & Brann, M. R. (1987). Identification of a family of muscarinic acetylcholine receptor genes. *Science*, *237*(4814), 527–532.

Bootman, M., Niggli, E., Berridge, M., & Lipp, P. (1997). Imaging the Hierarchical Ca^{2+} signalling system in HeLa cells. *Journal of Physiology*, *499*(2), 307–314.

Bootman, M. D., Collins, T. J., Mackenzie, L., Roderick, H. L., Berridge, M. J., & Peppiatt, C. M. (2002). 2-aminoethoxydiphenyl borate (2-APB) is a reliable blocker of store-operated Ca^{2+} entry but an inconsistent inhibitor of InsP3-induced Ca^{2+} release. *The FASEB Journal : Official Publication of the Federation of American Societies for Experimental Biology*, *16*(10), 1145–1150. DOI:10.1096/fj.02-0037rev

Bou-Hanna, C., Berthon, B., Combettes, L., Claret, M., & Laboisse, C. L. (1994). Role of calcium in carbachol- and neurotensin-induced mucin exocytosis in a human colonic goblet cell line and cross-talk with the cyclic AMP pathway. *The Biochemical Journal*, *299*, 579–585.

Bovolenta, P. (2005). Morphogen signaling at the vertebrate growth cone: a few cases or a general strategy? *Journal of Neurobiology*, *64*(4), 405–416.

Bowen, R. (2006). The Enteric Nervous System. Retrieved from http://www.vivo.colostate.edu/hbooks/pathphys/digestion/basics/gi_nervous.html

Bradbury, J., Black, J., & Wyllie, J. (1980). Stimulation of mucus output from rat colon in vivo. *European Journal of Pharmacology*, *68*(4), 417–425.

Brailoiu, E., Churamani, D., Cai, X., Schrlau, M. G., Brailoiu, G. C., Gao, X., Patel, S. (2009). Essential requirement for two-pore channel 1 in NAADP-mediated calcium signaling. *Journal of Cell Biology*, *186*(2), 201–209. DOI:10.1083/jcb.200904073

Brailoiu, E., Churamani, D., Pandey, V., Brailoiu, G. C., Tuluc, F., Patel, S., & Dun, N. J. (2006). Messenger-specific role for nicotinic acid adenine dinucleotide phosphate in neuronal differentiation. *Journal of Biological Chemistry*, *281*(23), 15923–15928. DOI:10.1074/jbc.M602249200

Brailoiu, E., Hoard, J. L., Filipeanu, C. M., Brailoiu, G. C., Dun, S. L., Patel, S., & Dun, N. J. (2005). Nicotinic acid adenine dinucleotide phosphate potentiates neurite outgrowth. *The Journal of Biological Chemistry*, *280*(7), 5646–5650. DOI:10.1074/jbc.M408746200

Brailoiu, E., Rahman, T., Churamani, D., Prole, D. L., Brailoiu, G. C., Hooper, R., Patel, S. (2010a). An NAADP-gated two-pore channel targeted to the plasma membrane uncouples triggering from amplifying Ca^{2+} signals. *Journal of Biological Chemistry*, *285*(49), 38511–38516. DOI:10.1074/jbc.M110.162073

Brailoiu, G. C., Gurzu, B., Gao, X., Parkesh, R., Aley, P. K., Trifa, D. I., Brailoiu, E. (2010b). Acidic NAADP-sensitive calcium stores in the endothelium: agonist-specific recruitment and role in regulating blood pressure. *The Journal of Biological Chemistry*, *285*(48), 37133–7. DOI:10.1074/jbc.C110.169763

Brandes, R. P., Weissmann, N., & Schröder, K. (2014). Nox family NADPH oxidases: Molecular mechanisms of activation. *Free Radical Biology & Medicine*, *76C*, 208–226. DOI:10.1016/j.freeradbiomed.2014.07.046

Brennan, A. M., Won Suh, S., Joon Won, S., Narasimhan, P., Kauppinen, T. M., Lee, H., Swanson, R. A. (2009). NADPH oxidase is the primary source of superoxide induced by NMDA receptor activation. *Nature Neuroscience*, *12*(7), 857–863. DOI:10.1038/nn.2334

Brini, M., & Carafoli, E. (2009). Calcium pumps in health and disease. *Physiological Reviews*, *89*(4), 1341–1378. DOI:10.1152/physrev.00032.2008

Brough, D., Schell, M. J., & Irvine, R. F. (2005). Agonist-induced regulation of mitochondrial and endoplasmic reticulum motility. *The Biochemical Journal*, *392*, 291–297. DOI: 10.1042/BJ20050738

Brouland, J.-P., Gélébart, P., Kovàcs, T., Enouf, J., Grossmann, J., & Papp, B. (2005). The loss of sarco/endoplasmic reticulum calcium transport ATPase 3 expression is an early event during the multistep process of colon carcinogenesis. *The American Journal of Pathology*, *167*(1), 233–42. DOI: 10.1016/S0002-9440(10)62968-9

Brown, D., & Griendling, K. (2009). Nox proteins in signal transduction. *Free Radical Biology and Medicine*, *47*(9), 1239–1253. DOI:10.1016/j.freeradbiomed.2009.07.023.Nox

Brown, D., & O'Grady, S. (1997). Regulation of ion transport in the porcine intestinal tract by enteric neurotransmitters and hormones. *Comparative Biochemistry and Physiology*, *118*(2), 309–317.

Brownlee, I., Havler, M., Dettmar, P., Allen, A., & Pearson, J. (2003). Colonic mucus: secretion and turnover in relation to dietary fibre intake. *Proceedings of the Nutrition Society*, *62*, 245–249.

Brownlee, I. A., Knight, J., Dettmar, P. W., & Pearson, J. P. (2007). Action of reactive oxygen species on colonic mucus secretions. *Free Radical Biology and Medicine*, *43*(5), 800–808. DOI:10.1016/j.freeradbiomed.2007.05.023

Bruzzone, S., Franco, L., Guida, L., Zocchi, E., Contini, P., Bisso, A., De Flora, A. (2001). A Self-restricted CD38-connexin 43 Cross-talk Affects NAD^+ and Cyclic ADP-ribose Metabolism and Regulates Intracellular Calcium in 3T3 Fibroblasts. *Journal of Biological Chemistry*, *276*(51), 48300–48308. DOI:10.1074/jbc.M107308200\rM107308200 [pii]

Budarf, M. L., Labbé, C., David, G., & Rioux, J. D. (2009). GWA studies: rewriting the story of IBD. *Trends in Genetics*, *25*(3), 137–146. DOI:10.1016/j.tig.2009.01.001

Budd, D. C., Challiss, R. A., Young, K. W., & Tobin, A. B. (1999). Cross talk between m3-muscarinic and beta (2)-adrenergic receptors at the level of receptor phosphorylation and desensitization. *Molecular Pharmacology*, *56*(4), 813–823.

Bulua, A. C., Simon, A., Maddipati, R., Pelletier, M., Park, H., Kim, K.-Y., Siegel, R. M. (2011). Mitochondrial reactive oxygen species promote production of proinflammatory cytokines and are elevated in TNFR1-associated periodic syndrome (TRAPS). *Journal of Experimental Medicine*, *208*(3), 519–533. DOI:10.1084/jem.20102049

Busetlo, X. R., Sauzeau, V., & Berenjeno, I. M. (2007). GTP-binding proteins of the Rho/Rac family: regulation, effectors and functions in vivo. *Bioessays*, *29*(4), 356–370. DOI:10.1016/j.biotechadv.2011.08.021.Secreted

Cader, M. Z., & Kaser, A. (2013). Recent advances in inflammatory bowel disease: mucosal immune cells in intestinal inflammation. *Gut*, *62*(11), 1653–64. DOI: 10.1136/gutjnl-2012-303955

Cahalan, M. D. (2009). STIMulating store-operated Ca^{2+} entry. *Cell Regulation*, *11*(6), 669–677. DOI:10.1038/ncb0609-669.STIMulating

Calcraft, P. J., Ruas, M., Pan, Z., Cheng, X., Arredouani, A., Hao, X., Zhu, M. X. (2009). NAADP mobilizes calcium from acidic organelles through two-pore channels. *Nature*, *459*(7246), 596–600. DOI: 10.1038/nature08030

Caldara, M., Friedlander, R. S., Kavanaugh, N. L., Aizenberg, J., Foster, K. R., & Ribbeck, K. (2012). Mucin biopolymers prevent bacterial aggregation by retaining cells in the free-swimming state. *Current Biology*, *22*(24), 2325–2330. DOI:10.1016/j.cub.2012.10.028

Camilleri, M., Murphy, R., & Chadwick, V. (1982). Pharmacological inhibition of chenodeoxycholate-induced fluid and mucus secretion and mucosal injury in the rabbit colon. *Digestive Diseases and Sciences*, *27*(10), 865–869.

Cancela, J. M., Churchill, G. C., & Galione, A. (1999). Coordination of agonist-induced Ca^{2+}-signalling patterns by NAADP in pancreatic acinar cells. *Nature*, *398*(6722), 74–76. DOI: 10.1038/18032

Cang, C., Zhou, Y., Navarro, B., Seo, Y. J., Aranda, K., Shi, L., Ren, D. (2013). MTOR regulates lysosomal ATP-sensitive two-pore Na^+ channels to adapt to metabolic state. *Cell*, *152*(4), 778–790. DOI:10.1016/j.cell.2013.01.023

Carafoli, E. (2012). The interplay of mitochondria with calcium: an historical appraisal. *Cell Calcium*, *52*(1), 1–8.

Carulli, A. J., Samuelson, L. C., & Schnell, S. (2014). Unraveling intestinal stem cell behavior with models of crypt dynamics. *Integrative Biology*, *6*(3), 243–57. DOI: 10.1039/c3ib40163d

Caulfield, M. P. (1993). Muscarinic receptors--characterization, coupling and function. *Pharmacology & Therapeutics*, *58*(3), 319–379. DOI: 10.1016/0163-7258(93)90027-B

Caulfield, M. P., & Birdsall, N. J. (1998). International Union of Pharmacology. XVII. Classification of muscarinic acetylcholine receptors. *Pharmacological Reviews*, *50*(2), 279–290.

CDC. (2015). Inflammatory Bowel Disease. Retrieved September 1, 2015, from http://www.cdc.gov/ibd/

CDC. (2014). Ulcerative colitis World-wide incidence rate. Retrieved from http://www.cdc.gov/ibd/

Cereijido, M., González-Mariscal, L., Contreras, R., Gallardo, J., García-Villegas, R., & Valdés, J. (1993). The making of a tight junction. *Journal of Cell Science*, *17 suppl*, 127–132.

Chen, E. Y. T., Garnica, M., Wang, Y.-C., Chen, C.-S., & Chin, W.-C. (2011). Mucin secretion induced by titanium dioxide nanoparticles. *PLoS One*, *6*(1), e16198. DOI:10.1371/journal.pone.0016198

Chen, E. Y. T., Yang, N., Quinton, P. M., & Chin, W.-C. (2010). A new role for bicarbonate in mucus formation. *American Journal of Physiology. Lung Cellular and Molecular Physiology*, *299*(4), L542–L549. DOI:10.1152/ajplung.00180.2010

Chen, G., & Nunez, G. (2011). Inflammasomes in Intestinal Inflammation and Cancer. *Gastroenterology*, *141*(6), 1986–1999. DOI:10.1016/j.biotechadv.2011.08.021.Secreted

Chen, G. Y., & Stappenbeck, T. S. (2014). Mucus, it is not just a static barrier. *Science Signaling*, *7*(323), pe11. DOI:10.1126/scisignal.2005357

Cheng, G., Diebold, B. a, Hughes, Y., & Lambeth, J. D. (2006). Nox1-dependent reactive oxygen generation is regulated by Rac1. *The Journal of Biological Chemistry*, *281*(26), 17718–26. DOI:10.1074/jbc.M512751200

Cheng, H. (1974a). Origin, differentiation and renewal of the four main epithelial cell types in the mouse small intestine. II. Mucous cells. *The American Journal of Anatomy*, *141*(4), 481–501.

Cheng, H., & Leblond, C. P. (1974b). Origin, differentiation and renewal of the four main epithelial cell types in the mouse small intestine. V. Unitarian Theory of the origin of the four epithelial cell types. *The American Journal of Anatomy*, *141*(4), 537–561. DOI:10.1002/aja.1001410407

Chianale, F., Rainero, E., Cianflone, C., Bettio, V., Pighini, A., Porporato, P. E., Graziani, A. (2010). Diacylglycerol kinase alpha mediates HGF-induced Rac activation and membrane ruffling by regulating atypical PKC and RhoGDI. *Proceedings of the National Academy of Sciences of the United States of America*, *107*(9), 4182–4187. DOI:10.1073/pnas.0908326107

Choi, W.-G., Toyota, M., Kim, S.-H., Hilleary, R., & Gilroy, S. (2014). Salt stress-induced Ca^{2+} waves are associated with rapid, long-distance root-to-shoot signaling in plants. *Proceedings of the National Academy of Sciences of the United States of America*, *111*(17), 6497–502. DOI:10.1073/pnas.1319955111

Churamani, D., Hooper, R., Rahman, T., Brailoiu, E., & Patel, S. (2013). The N-terminal region of two-pore channel 1 regulates trafficking and activation by NAADP. *The Biochemical Journal*, *453*(1), 147–51. DOI: 10.1042/BJ20130474

Churchill, G., Okada, Y., Thomas, J., Genazzani, A., Patel, S., & Galione, A. (2002). NAADP mobilizes Ca^{2+} from reserve granules, lysosome-related organelles, in sea urchin eggs. *Cell*, *111*, 703–708.

Cifuentes-Pagano, E., Csanyi, G., & Pagano, P. J. (2012). NADPH oxidase inhibitors: a decade of discovery from Nox2ds to HTS. *Cellular and Molecular Life Sciences*, *69*(14), 2315–25. DOI: 10.1007/s00018-012-1009-2

Clapham, D. E. (2007). Calcium signaling. *Cell*, *131*(6), 1047–58. DOI:10.1016/j.cell.2007.11.028

Clapper, D., Walseth, T., Dargie, P., & Lee, H. C. (1987). Pyridine nucleotide metabolites stimulate calcium release from sea urchin eggs desensitized to IP3. *Journal of Biological Chemistry*, *264*, 1608–1612.

Clevers, H. (2013a). The intestinal crypt, a prototype stem cell compartment. *Cell*, *154*(2), 274–284. DOI:10.1016/j.cell.2013.07.004

Clevers, H., & Batlle, E. (2013b). SnapShot: the intestinal crypt. *Cell*, *152*(5), 1198–1198.e2. DOI:10.1016/j.cell.2013.02.030

Cliff, W. H., Duffey, M. E., & Packianathan, N. (1998). Acetylcholine-activated chloride current in the T-84 colonic cell line. *Pflugers Archiv European Journal of Physiology*, *436*(1), 90–94. DOI: 10.1007/s004240050608

Colorectal Cancer Association of Canada. Anatomy of the human colon. Retrieved September 1, 2015, from http://www.colorectal-cancer.ca/en/

Cooke, H. J. (2000). Neurotransmitters in neuronal reflexes regulating intestinal secretion. *Annals of the New York Academy of Sciences*, *915*, 77–80.

Cosker, F., Cheviron, N., Yamasaki, M., Menteyne, A., Lund, F. E., Moutin, M. J., Cancela, J. M. (2010). The ecto-enzyme CD38 is a Nicotinic Acid Adenine Dinucleotide Phosphate (NAADP) synthase that couples receptor activation to Ca^{2+} mobilization from lysosomes in pancreatic acinar cells. *Journal of Biological Chemistry*, *285*(49), 38251–38259. DOI:10.1074/jbc.M110.125864

Costa, M., Brookes, S. J., & Hennig, G. W. (2000). Anatomy and physiology of the enteric nervous system. *Gut*, *47* (Suppl 4), iv15–v19; discussion iv26. DOI:10.1136/gut.47.suppl_4.iv15

Coussens, L. M., & Werb, Z. (2002). Inflammation and cancer. *Nature*, *420*(6917), 860–867. DOI:10.1038/nature01322.Inflammation

Crompton, M., & Heid, I. (1978). The cycling of calcium, Sodium, and Protons across the inner mitochondrial membrane of cardiac mitochondria. *European Journal of Biochemistry*, *91*, 599–608.

Crosnier, C., Stamataki, D., & Lewis, J. (2006). Organizing cell renewal in the intestine: stem cells, signals and combinatorial control. *Nature Reviews. Genetics*, *7*(5), 349–359. DOI: 10.1038/nrg1840

Crosnier, C., Vargesson, N., Gschmeissner, S., Ariza-McNaughton, L., Morrison, A., & Lewis, J. (2005). Delta-Notch signalling controls commitment to a secretory fate in the zebrafish intestine. *Development (Cambridge, England)*, *132*(5), 1093–1104. DOI:10.1242/dev.01644

Dartt, D. A., Rios, J. D., Kanno, H., Rawe, I. M., Zieske, J. D., Ralda, N., Rios, J. R. (2000). Regulation of conjunctival goblet cell secretion by Ca^{2+} and protein kinase C. *Experimental Eye Research*, *71*(6), 619–28. DOI:10.1006/exer.2000.0915

Date, S., & Sato, T. (2015). Mini-Gut Organoids: Reconstitution of the Stem Cell Niche. *Annual Review of Cell and Developmental Biology*, *31*(1), 269–89. DOI: 10.1146/annurev-cellbio-100814-125218

Daugaard, M., Nitsch, R., Razaghi, B., McDonald, L., Jarrar, A., Torrino, S., Sorensen, P. H. (2013). Hace1 controls ROS generation of vertebrate Rac1-dependent NADPH oxidase complexes. *Nature Communications*, *4*, 2180. DOI: 10.1038/ncomms3180

Davidson, L. A., Jiang, Y.-H., Derr, J. N., Aukema, H. M., Lupton, J. R., & Chapkin, R. S. (1994). Protein Kinase C Isoforms in Human and Rat Colonic Mucosa. *Archives of Biochemistry and Biophysics*, *312*(2), 547–553.

Davis, C. W., & Dickey, B. F. (2008). Regulated airway goblet cell mucin secretion. *Annual Review of Physiology*, *70*, 487–512. DOI:10.1146/annurev.physiol.70.113006.100638

Davis, L. C., Morgan, A. J., Chen, J.-L., Snead, C. M., Bloor-Young, D., Shenderov, E., Galione, A. (2012). NAADP activates two-pore channels on T cell cytolytic granules to stimulate exocytosis and killing. *Current Biology*, *22*(24), 2331–7. DOI:10.1016/j.cub.2012.10.035

Dellis, O., Dedos, S., Tovey, S., Taufig, U., Dubel, S., & Taylor, C. (2006). Ca^{2+} entry through plasma membrane IP3 receptors. *Science*, *313*(5784), 229–233.

Deluca, H. F., & Engstrom, G. W. (1961). Calcium Uptake by Rat Kidney Mitochondria. *Biochemistry*, *47*, 1744–1750.

Demuro, A., & Parker, I. (2008). Multi-dimensional resolution of elementary Ca^{2+} signals by simultaneous multi-focal imaging. *Cell Calcium*, *43*(4), 367–74. DOI:10.1016/j.ceca.2007.07.002

Denning, G. M., Railsback, M. A., Rasmussen, G. T., Cox, C. D., & Britigan, B. E. (1998). Pseudomonas pyocyanine alters calcium signaling in human airway epithelial cells. *The American Journal of Physiology*, *274*(6), L893–L900.

Devi, L. A. (2001). Heterodimerization of G-protein coupled receptors: pharmacology, signalling and trafficking. *Trends in Pharmacological Sciences*, *22*(10), 532.

Dhawan, S., Cailotto, C., Harthoorn, L. F., & De Jonge, W. J. (2012). Cholinergic signalling in gut immunity. *Life Sciences*, *91*(21-22), 1038–1042. DOI:10.1016/j.lfs.2012.04.042

Diener, M., Knobloch, S. F., Bridges, R. J., Keilmann, T., & Rummel, W. (1989). Cholinergic-mediated secretion in the rat colon: neuronal and epithelial muscarinic responses. *European Journal of Pharmacology*, *168*(2), 219–229. DOI: 10.1016/0014-2999(89)90568-2

Dolman, N. J., Gerasimenko, J. V., Gerasimenko, O. V., Voronina, S. G., Petersen, O. H., & Tepikin, A. V. (2005). Stable Golgi-mitochondria complexes and formation of Golgi Ca^{2+} gradients in pancreatic acinar cells. *Journal of Biological Chemistry*, *280*(16), 15794–15799. DOI:10.1074/jbc.M412694200

Dupont, G., Combettes, L., Bird, G. S., & Putney, J. W. (2011). Calcium oscillations. *Cold Spring Harbor Perspectives in Biology*, *3*(3), 1–18. DOI:10.1101/cshperspect.a004226

Dziadek, M. a., & Johnstone, L. S. (2007). Biochemical properties and cellular localisation of STIM proteins. *Cell Calcium*, *42*(2), 123–132. DOI:10.1016/j.ceca.2007.02.006

Eaden, J., Abrams, K., McKay, H., Denley, H., & Mayberry, J. (2001). Inter-observer variation between general and specialist gastrointestinal pathologists when grading dysplasia in ulcerative colitis. *Journal of Pathology*, *194*(2), 152–157. DOI:10.1002/path.876

Ebashi, S., & Lipmann, F. (1962). Adenosine triphosphate-linked concentration of calcium ions in a particulate fraction of rabbit muscle. *The Journal of Cell Biology*, *14*(30), 389–400.

Ehlert, F., Pak, K., & Griffin, M. (2011). Muscarinic Agonists and Antagonists: Effects on Gastrointestinal Function. *Muscarinic Receptors*, *208*, 343–374.

Eisenhoffer, G. T., Loftus, P. D., Yoshigi, M., Otsuna, H., Chien, C.-B., Morcos, P. A, & Rosenblatt, J. (2012). Crowding induces live cell extrusion to maintain homeostatic cell numbers in epithelia. *Nature*, *484*(7395), 546–9. DOI: 10.1038/nature10999

Elinav, E., Strowig, T., Kau, A. L., Henao-Mejia, J., Thaiss, C. A., Booth, C. J., Flavell, R. A. (2011). NLRP6 inflammasome regulates colonic microbial ecology and risk for colitis. *Cell*, *145*(5), 745–57. DOI:10.1016/j.cell.2011.04.022

Elrod, J. W., Wong, R., Mishra, S., Vagnozzi, R. J., Sakthievel, B., Goonasekera, S. A., Molkentin, J. D. (2010). Cyclophilin D controls mitochondrial pore - Dependent Ca^{2+} exchange, metabolic flexibility, and propensity for heart failure in mice. *Journal of Clinical Investigation*, *120*(10), 3680–3687. DOI: 10.1172/JCI43171

Endo, M. (1977). Calcium Release from the Sarcoplasmic Reticulum. *Physiological Reviews*, *57*(1), 71–108.

Enteric nervous system. *Human Physiology (2000, 12th edition).* McGraw-Hill Education.

Erickson, J., Weihe, E., Schäfer, M., Neale, E., Williamson, L., Bonner, T., Eiden, L. (1996). The VAChT/ChAT "cholinergic gene locus": new aspects of genetic and vesicular regulation of cholinergic function. *Progress in Brain Research*, *109*, 69–82.

Erickson, R., Langel-Peveri, P., & Traynor-, A. (1999). Activation of human neutrophil NADPH oxidase by phosphatidic acid or diacylglycerol in a cell-free system. *Journal of Biological Chemistry*, *274*(32), 22243–22250.

Ermund, A., Gustafsson, J. K., Hansson, G. C., & Keita, Å. V. (2013a). Mucus properties and goblet cell quantification in mouse, rat and human ileal Peyer's patches. *PLoS ONE*, *8*(12), 1–7. DOI:10.1371/journal.pone.0083688

Ermund, A., Schütte, A., Johansson, M. E. V, Gustafsson, J. K., & Hansson, G. C. (2013b). Studies of mucus in mouse stomach, small intestine, and colon. I. Gastrointestinal mucus layers have different properties depending on location as well as over the Peyer's patches. *American Journal of Physiology. Gastrointestinal and Liver Physiology*, *305*(5), G341–7. DOI:10.1152/ajpgi.00046.2013

Fabiato, A. (1983). Calcium-induced release of calcium from the cardiac sarcoplasmic reticulum. *The American Journal of Physiology*, *245*(1), C1–C14. DOI: 10.1016/0022-2828(92)90114-F

Falk, M. M., Buehler, L. K., Kumar, N. M., & Gilula, N. B. (1997). Cell-free synthesis and assembly of connexins into functional gap junction membrane channels. *EMBO Journal*, *16*(10), 2703–2716. DOI:10.1093/emboj/16.10.2703

Fehmann, H., Stöckmann, F., Haverich, R., & Creutzfeldt, W. (1988). Diltiazem inhibition of glucose-induced insulin secretion from the isolated perfused rat pancreas. *European Journal of Pharmacology*, *156*(3), 415–417.

Felder, C. (1995). Muscarinic acetylcholine receptors: signal transduction through multiple effectors. *The FASEB Journal*, *9*(8), 619–625.

Ferré, S., Casadó, V., Devi, L. a, Filizola, M., Jockers, R., Lohse, M. J., Guitart, X. (2014). G protein-coupled receptor oligomerization revisited: functional and pharmacological perspectives. *Pharmacological Reviews*, *66*(2), 413–34. DOI:10.1124/pr.113.008052

Finch, E. A., Turner, T. J., & Goldin, S. M. (1991). Calcium as a co-agonist of inositol 1,4,5-trisphosphate-induced calcium release. *Science*, *252*(5004), 443–446. DOI:10.1126/science.2017683

Florio, V. A., & Sternweis, P. C. (1989). Mechanisms of muscarinic receptor action on G (o) in reconstituted phospholipid vesicles. *Journal of Biological Chemistry*, *264*(7), 3909–3915.

Fontayne, A., Dang, P., Gougerot-Pocidalo, M., & Benna, J. El. (2002). Phosphorylation of p47 phox sites by PKC alpha, beta II, delta, and zeta: Effect on Binding to p22phox and on NADPH Oxidase Activation. *Biochemistry*, *41 (24)*, 7743–7750.

Foskett, J. K., White, C., Cheung, K., & Mak, D. D. (2007). Inositol Trisphosphate Receptor Ca^{2+} Release Channels. *Physiological Reviews*, *87*(2), 593–658. DOI:10.1152/physrev.00035.2006

Franke, A., Balschun, T., Karlsen, T. H., Sventoraityte, J., Nikolaus, S., Mayr, G., Schreiber, S. (2008). Sequence variants in IL10, ARPC2 and multiple other loci contribute to ulcerative colitis susceptibility. *Nature Genetics*, *40*(11), 1319–1323. DOI:10.1038/ng.221

Fre, S., Huyghe, M., Mourikis, P., Robine, S., Louvard, D., & Artavanis-Tsakonas, S. (2005). Notch signals control the fate of immature progenitor cells in the intestine. *Nature*, *435*(7044), 964–968. DOI: 10.1038/nature03589

Frieden, M., Arnaudeau, S., Castelbou, C., & Demaurex, N. (2005). Subplasmalemmal mitochondria modulate the activity of plasma membrane Ca^{2+}-ATPases. *Journal of Biological Chemistry*, *280*(52), 43198–43208. DOI:10.1074/jbc.M510279200

Fristrom, D. (1988). The cellular basis of epithelial morphogenesis. *Tissue and Celle*, *20*(5), 645–690. DOI: 10.1016/0040-8166(88)90015-8

Fritz, T., Niederreiter, L., Adolph, T., Blumberg, R. S., & Kaser, A. (2011). Crohn's disease: NOD2, autophagy and ER stress converge. *Gut*, *60*(11), 1580–8. DOI: 10.1136/gut.2009.206466

Fu, X. J., Peng, Y. B., Hu, Y. P., Shi, Y. Z., Yao, M., & Zhang, X. (2014). NADPH oxidase 1 and its derived reactive oxygen species mediated tissue injury and repair. *Oxidative Medicine and Cellular Longevity*, *2014*. DOI:10.1155/2014/282854

Fukada, K., Kubo, T., Akiba, I., Maeda, A., Mishina, M., & Numa, S. (1987). Molecular distinction between muscarinic acetylcholine receptor subtypes. *Nature*, *327*, 623–625.

Fukushi, Y., Kato, I., Takasawa, S., Sasaki, T., Ong, B. H., Sato, M., Maruyama, Y. (2001). Identification of cyclic ADP-ribose-dependent mechanisms in pancreatic muscarinic Ca^{2+} signaling using CD38 knockout mice. *Journal of Biological Chemistry*, *276*(1), 649–655. DOI:10.1074/jbc.M004469200

Function of Large Intestine. National Cancer Institute. Retrieved September 1, 2015, from http://www.cancer.gov/publications/dictionaries/cancer-terms?cdrid=45097

Furness, J. B. (2000). Types of neurons in the enteric nervous system. *Journal of the Autonomic Nervous System*, *81*, 87–96.

Furness, J. B. (2008). The enteric nervous system: Normal functions and enteric neuropathies. *Neurogastroenterology and Motility*, *20*(SUPPL. 1), 32–38. DOI: 10.1111/j.1365-2982.2008.01094.x

Furness, J., Callaghan, B., Rivera, L., & Cho, H. (2014). The enteric nervous system and gastrointestinal innervation: integrated local and central control. *Microbial Endocrinology*, *817*, 39–71.

Furness, J. B. (2006). The Enteric Nervous System. In *Blackwell Publishing*. DOI:10.1038/sj.jcbfm.9600419.Transport

Gafni, J., Munsch, J. A., Lam, T. H., Catlin, M. C., Costa, L. G., Molinski, T. F., & Pessah, I. N. (1997). Xestospongins: Potent membrane permeable blockers of the inositol 1,4,5-trisphosphate receptor. *Neuron*, *19*(3), 723–733. DOI:10.1016/S0896-6273(00)80384-0

Galione, A. (2006). NAADP, a new intracellular messenger that mobilizes Ca^{2+} from acidic stores. *Biochemical Society Transactions*, *34*(5), 922–926. DOI: 10.1042/BST0340922

Galione, A., & Petersen, O. (2005). The NAADP receptor: new receptors or new regulation. *Molecular Interventions*, *5*(2), 73–79.

Galione, A. (2015). A primer of NAADP-mediated Ca^{2+} signalling: From sea urchin eggs to mammalian cells. *Cell Calcium*, *58*(1), 27–47. DOI: 10.1016/j.ceca.2014.09.010

Galione, A., & Churchill, G. C. (2002). Interactions between calcium release pathways: Multiple messengers and multiple stores. *Cell Calcium*, *32*(5-6), 343–354. DOI: 10.1016/S0143416002001902

Galione, A., Morgan, A. J., Arredouani, A., Davis, L. C., Rietdorf, K., Ruas, M., & Parrington, J. (2010). NAADP as an intracellular messenger regulating lysosomal calcium-release channels. *Biochemical Society Transactions*, *38*(6), 1424–1431. DOI: 10.1042/BST0381424

Gamberucci, A., Innocenti, B., Fulceri, R., Bànhegyi, G., Giunti, R., Pozzan, T., & Benedetti, A. (1994). Modulation of Ca^{2+} Influx Dependent on Store Depletion by Intracellular Adenine-Guanine Nucleotide Levels. *Journal of Biological Chemistry*, *269*(38), 23597–23602.

Gao, Y., Dickerson, J. B., Guo, F., Zheng, J., & Zheng, Y. (2004). Rational design and characterization of a Rac GTPase-specific small molecule inhibitor. *Proceedings of the National Academy of Sciences of the United States of America*, *101*(20), 7618–7623. DOI: 10.1073/pnas.0307512101

Garcia SB, Stopper H, K. V. (2014). The contribution of neuronal-glial-endothelial-epithelial interactions to colon carcinogenesis. *Cell and Molecular Life Sciences*, *71*(17), 3191–3197.

Garcia, M. A. S., Yang, N., & Quinton, P. M. (2009). Normal mouse intestinal mucus release requires cystic fibrosis transmembrane regulator – dependent bicarbonate secretion. *The Journal of Clinical Investigation*, *119*(9), 2613–2622. DOI: 10.1172/JCI38662

Gayer, C. P., & Basson, M. D. (2009). The effects of mechanical forces on intestinal physiology and pathology. *Cellular Signalling*, *21*(8), 1237–44. DOI: 10.1016/j.cellsig.2009.02.011

Gees, M., Colsoul, B., & Nilius, B. (2010). The Role of Transient Receptor Potential Cation Channels in Ca^{2+} Signaling. *Cold Spring Harbor Perspectives in Biology*, *2*(10), a003962–a003962. DOI: 10.1101/cshperspect.a003962

Genazzani, A. A., & Galione, A. (1996). Nicotinic acid-adenine dinucleotide phosphate mobilizes Ca^{2+} from a thapsigargin-insensitive pool. *The Biochemical Journal*, *315 (3)*, 721–725.

Gerasimenko, J. V., Charlesworth, R. M., Sherwood, M. W., Ferdek, P. E., Mikoshiba, K., Parrington, J., Gerasimenko, O. V. (2015). Both RyRs and TPCs are required for NAADP-induced intracellular Ca^{2+} release. *Cell Calcium*, *58*(3), 237–245. DOI:10.1016/j.ceca.2015.05.005

Gerasimenko, O. V., Gerasimenko, J. V., Belan, P. V., & Petersen, O. H. (1996). Inositol trisphosphate and cyclic ADP-ribose-mediated release of Ca^{2+} from single isolated pancreatic zymogen granules. *Cell*, *84*(3), 473–480.

Gerasimenko, O. V, Gerasimenko, J. V, Tepikin, A. V, & Petersen, O. H. (1995). ATP-Dependent Accumulation and Inositol Trisphosphate or Cyclic ADP-Ribose-Mediated Release of Calcium from the Nuclear Envelope. *Cell*, *80*(3), 439–444.

Gerbe, F., Legraverend, C., & Jay, P. (2012). The intestinal epithelium tuft cells: Specification and function. *Cellular and Molecular Life Sciences*, *69*(17), 2907–2917. DOI: 10.1007/s00018-012-0984-7

Gerbe, F., van Es, J. H., Makrini, L., Brulin, B., Mellitzer, G., Robine, S., Jay, P. (2011). Distinct ATOH1 and Neurog3 requirements define tuft cells as a new secretory cell type in the intestinal epithelium. *The Journal of Cell Biology*, *192*(5), 767–80. DOI:10.1083/jcb.201010127

Geremia, A., Biancheri, P., Allan, P., Corazza, G. R., & Di Sabatino, A. (2014). Innate and adaptive immunity in inflammatory bowel disease. *Autoimmunity Reviews*, *13*(1), 3–10. DOI:10.1016/j.autrev.2013.06.004

Gersemann, M., Stange, E. F., & Wehkamp, J. (2011). From intestinal stem cells to inflammatory bowel diseases. *World Journal of Gastroenterology : WJG*, *17*(27), 3198–203. DOI: 10.3748/wjg.v17.i27.3198

Gerthoffer, W. T. (2005). Signal-transduction pathways that regulate visceral smooth muscle function. III. Coupling of muscarinic receptors to signaling kinases and effector proteins in gastrointestinal smooth muscles. *American Journal of Physiology. Gastrointestinal and Liver Physiology*, *288*(5), G849–G853. DOI:10.1152/ajpgi.00530.2004

Ghaleb, A. M., Aggarwal, G., Bialkowska, A. B., Nandan, M. O., & Yang, V. W. (2008). Notch inhibits expression of the Krüppel-like factor 4 tumor suppressor in the intestinal epithelium. *Molecular Cancer Research*, *6*(12), 1920–1927. DOI:10.1158/1541-7786.MCR-08-0224

Ghaleb, A. M., McConnell, B. B., Kaestner, K. H., & Yang, V. W. (2011). Altered intestinal epithelial homeostasis in mice with intestine-specific deletion of the Kruppel-like factor 4 gene. *Developmental Biology*, *349*(2), 310–320. DOI:10.1016/j.ydbio.2010.11.001

Giepmans, B. N. G., & van IJzendoorn, S. C. D. (2009). Epithelial cell-cell junctions and plasma membrane domains. *Biochimica et Biophysica Acta - Biomembranes*, *1788*(4), 820–831. DOI:10.1016/j.bbamem.2008.07.015

Gilmor, M. L., Nash, N. R., Roghani, A., Edwards, R. H., Yi, H., Hersch, S. M., & Levey, a I. (1996). Expression of the putative vesicular acetylcholine transporter in rat brain and localization in cholinergic synaptic vesicles. *The Journal of Neuroscience*, *16*(7), 2179–2190.

Gilroy, S., Suzuki, N., Miller, G., Choi, W.-G., Toyota, M., Devireddy, A. R., & Mittler, R. (2014). A tidal wave of signals: calcium and ROS at the forefront of rapid systemic signaling. *Trends in Plant Science*, 1–8. DOI:10.1016/j.tplants.2014.06.013

Giorgi, C., Romagnoli, A., Pinton, P., & Rizzuto, R. (2008). Ca^{2+} signaling, mitochondria and cell death. *Current Molecular Medicine*, *8*(2), 119–30.

Giorgi, C., Agnoletto, C., Bononi, A., Bonora, M., de Marchi, E., Marchi, S., Pinton, P. (2012). Mitochondrial calcium homeostasis as potential target for mitochondrial medicine. *Mitochondrion*, *12*(1), 77–85. DOI:10.1016/j.mito.2011.07.004

Goldhaber, J., & Qayyum, M. (2000). Oxygen free radicals and excitation-contraction coupling. *Antioxidants & Redox Signaling*, *2*(1), 55–64.

Gomez-Cambronero, J., Molski, T. F. P., Becker, E. L., & Sha'afi, R. I. (1987). The diacylglycerol kinase inhibitor R59022 potentiates superoxide production but not secretion induced by fMET-LEU-PHE: effects of leupeptin and the protein kinase C inhibitor H-7. *Biochemical and Biophysical Research Communications*, *148*(1), 38–46.

Goodenough, D. A., Goliger, J. A., & Paul, D. L. (1996). Connexins, Connexons, and Intercellular Communication. *Annual Review of Biochemistry*, *65*, 475–502.

Gordon, J., Schmidt, G., & Roth, K. (1992). Studies of intestinal stem cells using normal, chimeric, and transgenic mice. *The FASEB Journal*, *6*, 3039–3050.

Görlach, A., Bertram, K., Hudecova, S., & Krizanova, O. (2015). Calcium and ROS: A mutual interplay. *Redox Biology*, REDOXD1500102. DOI:10.1016/j.redox.2015.08.010

Gosens, R., Zaagsma, J., Meurs, H., & Halayko, A. J. (2006). Muscarinic receptor signaling in the pathophysiology of asthma and COPD. *Respiratory Research*, *7*, 73. DOI: 10.1186/1465-9921-7-73

Graeff, R., & Lee, H. C. (2002). A novel cycling assay for nicotinic acid-adenine dinucleotide phosphate with nanomolar sensitivity. *The Biochemical Journal*, *367*(Pt 1), 163–168. DOI: 10.1042/BJ20020644

Grando, S. A., Kawashima, K., Kirkpatrick, C. J., Meurs, H., & Wessler, I. (2012). The non-neuronal cholinergic system: Basic science, therapeutic implications and new perspectives. *Life Sciences*, *91*(21-22), 969–972. DOI:10.1016/j.lfs.2012.10.004

Grando, S., Kist, D., Qi, M., & Dahl, M. (1993). Human keratinocytes synthesize, secrete, and degrade acetylcholine. *Journal of Investigative Dermatology*, *101*(1), 32–36.

Grays, H. (1918). Structure of human colon. *Gray's Anatomy*.

Gregorieff, A., & Clevers, H. (2005). Wnt signaling in the intestinal epithelium: from endoderm to cancer. *Genes & Development*, *19*(8), 877–90. DOI:10.1101/gad.1295405

Gregorieff, A., Stange, D. E., Kujala, P., Begthel, H., van den Born, M., Korving, J., Clevers, H. (2009). The ets-domain transcription factor Spdef promotes maturation of goblet and paneth cells in the intestinal epithelium. *Gastroenterology*, *137*(4), 1333–45.e1–3. DOI:10.1053/j.gastro.2009.06.044

Grootjans, J., Hundscheid, I. H., & Buurman, W. A. (2013). Goblet cell compound exocytosis in the defense against bacterial invasion in the colon exposed to ischemia-reperfusion. *Gut Microbes*, *4*(3), 232–235. DOI:10.4161/gmic.23866

Groschwitz, K., & Hogan, S. (2009). Intestinal Barrier Function: Molecular Regulation and Disease Pathogenesis. *Journal of Allergy and Clinical Immunology*, *124*(1), 3–22. DOI:10.1016/j.jaci.2009.05.038

Guagnozzi, D. (2012). Colorectal cancer surveillance in patients with inflammatory bowel disease: What ¡s new? *World Journal of Gastrointestinal Endoscopy*, *4*(4), 108. DOI:10.4253/wjge.v4.i4.108

Guida, L., Bruzzone, S., Sturla, L., Franco, L., Zocchi, E., & De Flora, A. (2002). Equilibrative and concentrative nucleoside transporters mediate influx of extracellular cyclic ADP-ribose into 3T3 murine fibroblasts. *Journal of Biological Chemistry*, *277*(49), 47097–47105. DOI:10.1074/jbc.M207793200

Guinane, C. M., & Cotter, P. D. (2013). Role of the gut microbiota in health and chronic gastrointestinal disease: understanding a hidden metabolic organ. *Therapeutic Advances in Gastroenterology*, *6*(4), 295–308. DOI: 10.1177/1756283X13482996

Gustafsson, J. K., Hansson, G. C., & Sjövall, H. (2012a). Ulcerative colitis patients in remission have an altered secretory capacity in the proximal colon despite macroscopically normal mucosa. *Neurogastroenterology and Motility*, *24*(8), e381–91. DOI:10.1111/j.1365-2982.2012.01958.x

Gustafsson, J. K., Ermund, a., Ambort, D., Johansson, M. E. V., Nilsson, H. E., Thorell, K., Hansson, G. C. (2012b). Bicarbonate and functional CFTR channel are required for proper mucin secretion and link cystic fibrosis with its mucus phenotype. *Journal of Experimental Medicine*, *209*(7), 1263–1272. DOI:10.1084/jem.20120562

Gustafsson, J. K., Ermund, A., Johansson, M. E. V., Schutte, A., Hansson, G. C., & Sjovall, H. (2012c). An ex vivo method for studying mucus formation, properties, and thickness in human colonic biopsies and mouse small and large intestinal explants. American Journal of Physiology. *AJP: Gastrointestinal and Liver Physiology*, *302*(4), G430–G438. DOI:10.1152/ajpgi.00405.2011

Ha, H., Yu, M., Choi, Y., & Lee, H. (2001). Activation of protein kinase c-delta and c-epsilon by oxidative stress in early diabetic rat kidney. *American Journal of Kidney Diseases*, *38*(4 suppl1), S204–207.

Haberberger, R., Schultheiss, G., & Diener, M. (2006). Epithelial muscarinic M1 receptors contribute to carbachol-induced ion secretion in mouse colon. *European Journal of Pharmacology*, *530*(3), 229–233.

Halestrap, A. P., & Pasdois, P. (2009). The role of the mitochondrial permeability transition pore in heart disease. *Biochimica et Biophysica Acta*, *1787*(11), 1402–1415. DOI:10.1016/j.bbabio.2008.12.017

Halm, D. R., & Halm, S. T. (2000). Secretagogue response of goblet cells and columnar cells in human colonic crypts. *American Journal of Physiology. Cell Physiology*, *278*(1), C212–C233.

Hamada, E., Nakajima, T., Hata, Y., Hazama, H., Iwasawa, K., Takahashi, M., Omata, M. (1997). Effect of caffeine on mucus secretion and agonist-dependent Ca^{2+} mobilization in human gastric mucus secreting cells. *Biochimica et Biophysica Acta*, *1356*(2), 198–206.

Hancock, J. T., & Jones, O. T. (1987). The inhibition by diphenyleneiodonium and its analogues of superoxide generation by macrophages. *The Biochemical Journal*, *242*(1), 103–107.

Hansson, G. C., & Johansson, M. E. V. (2010). The inner of the two Muc2 mucin-dependent mucus layers in colon is devoid of bacteria. *Gut Microbes*, *1*(1), 51–54. DOI:10.1073/pnas.0803124105

Hardie, R. C., & Minke, B. (1992). The trp gene is essential for a light-activated Ca^{2+} channel in Drosophila photoreceptors. *Neuron*, *8*(4), 643–651. DOI: 10.1016/0896-6273(92)90086-S

Hardie, R.C., & Minke, B. (1993). Novel Ca^{2+} channels underlying transduction in Drosophila photoreceptors: implications for phosphoinositide-mediated Ca^{2+} mobilization. *Trends in Neurosciences*, *16*(9), 371–376

Harr, M. W., & Distelhorst, C. W. (2010). Apoptosis and autophagy: decoding calcium signals that mediate life or death. *Cold Spring Harbor Perspectives in Biology*, *2*(10). DOI:10.1101/cshperspect.a005579

Harrington, A. M., Peck, C. J., Liu, L., Burcher, E., Hutson, J. M., & Southwell, B. R. (2010). Localization of muscarinic receptors M1R, M2R and M3R in the human colon. *Neurogastroenterology and Motility : The Official Journal of the European Gastrointestinal Motility Society*, *22*(9), 999–1008, e262–3. DOI:10.1111/j.1365-2982.2009.01456.x

Harris, A. (2007). Connexin Channel Permeability to Cytoplasmic Molecules. *Progress in Biophysics and Molecular Biology*, *94*(1-2), 120–143.

Harrop, C. A., Thornton, D. J., & McGuckin, M. A. (2012). Detecting, Visualising, and Quantifying Mucins. In *Methods in molecular biology 842 Mucins Methods and Protocols* (Vol. 842, pp. 49–66). DOI: 10.1007/978-1-61779-513-8_1

Hasnain, S. Z., Tauro, S., Das, I., Tong, H., Chen, A. H., Jeffery, P. L., McGuckin, M. A. (2013). IL-10 promotes production of intestinal mucus by suppressing protein misfolding and endoplasmic reticulum stress in goblet cells. *Gastroenterology*, *144*(2), 357–368.e9. DOI:10.1053/j.gastro.2012.10.043

Hassan, H. A., Cheng, M., & Aronson, P. S. (2012). Cholinergic signaling inhibits oxalate transport by human intestinal T84 cells. *American Journal of Physiology. Cell Physiology*, *302*(1), C46–58. DOI:10.1152/ajpcell.00075.2011

Hattrup, C. L., & Gendler, S. J. (2008). Structure and function of the cell surface (tethered) mucins. *Annual Review of Physiology*, *70*, 431–457. DOI:10.1146/annurev.physiol.70.113006.100659

Hayes, P., Dhillon, S., O'Neill, K., Thoeni, C., Hui, K. Y., Elkadri, A., Knaus, U. G. (2015). Defects in Nicotinamide-adenine Dinucleotide Phosphate Oxidase Genes NOX1 and DUOX2 in Very Early Onset Inflammatory Bowel Disease. *CMGH Cellular and Molecular Gastroenterology and Hepatology*, *1*(5), 489–502. DOI:10.1016/j.jcmgh.2015.06.005

Heazlewood, C. K., Cook, M. C., Eri, R., Price, G. R., Tauro, S. B., Taupin, D., McGuckin, M. A. (2008). Aberrant mucin assembly in mice causes endoplasmic reticulum stress and spontaneous inflammation resembling ulcerative colitis. *PLoS Medicine*, *5*(3), e54. DOI:10.1371/journal.pmed.0050054

Hering, N. A., Fromm, M., & Schulzke, J.-D. (2012). Determinants of colonic barrier function in inflammatory bowel disease and potential therapeutics. *The Journal of Physiology*, *590*(5), 1035–1044. DOI:10.1113/jphysiol.2011.224568

Hess, P., Lansman, J., Nilius, B., & Tsien, R. (1986). Calcium channel types in cardiac myocytes: modulation by dihydropyridines and beta-adrenergic stimulation. *Journal of Cardiovascular Pharmacology*, *8*(Suppl 9), S11–S21.

Heumüller, S., Wind, S., Barbosa-Sicard, E., Schmidt, H. H. H. W., Busse, R., Schröder, K., & Brandes, R. P. (2008). Apocynin is not an inhibitor of vascular NADPH oxidases but an antioxidant. *Hypertension*, *51*(2), 211–217. DOI:10.1161/HYPERTENSIONAHA.107.100214

Hidalgo, C., & Donoso, P. (2008). Crosstalk between calcium and redox signaling: from molecular mechanisms to health implications. *Antioxidants & Redox Signaling*, *10*(7), 1275–1312. DOI:10.1089/ars.2007.1886

Higashida, H. (1997a). ADP-ribosyl cyclase coupled with receptors via G protiens. *FEBS Letters*, *418*(3), 355–356. DOI: 10.1016/S0014-5793(97)01410-5

Higashida, H., Hashii, M., Yokoyama, S., Hoshi, N., Asai, K., & Kato, T. (2001a). Cyclic ADP-ribose as a potential second messenger for neuronal Ca^{2+} signaling. *Journal of Neurochemistry*, *76*(2), 321–331. DOI:10.1046/j.1471-4159.2001.00082.x

Higashida, H., Hashii, M., Yokoyama, S., Hoshi, N., Chen, X. L., Egorova, A., Zhang, J. S. (2001b). Cyclic ADP-ribose as a second messenger revisited from a new aspect of signal transduction from receptors to ADP-ribosyl cyclase. *Pharmacology and Therapeutics*, *90*(2-3), 283–296. DOI: 10.1016/S0163-7258(01)00142-5

Higashida, H., Yokoyama, S., Hashii, M., Taketo, M., Higashida, M., Takayasu, T., Noda, M. (1997b). Muscarinic receptor-mediated dual regulation of ADP-ribosyl cyclase in NG108-15 neuronal cell membranes. *Journal of Biological Chemistry*, *272*(50), 31272–31277. DOI:10.1074/jbc.272.50.31272

Himmerkus, N., Vassen, V., Sievers, B., Goerke, B., Shan, Q., Harder, J., Bleich, M. (2010). Human β-defensin-2 increases cholinergic response in colon epithelium. *Pflugers Archiv European Journal of Physiology*, *460*(1), 177–186. DOI: 10.1007/s00424-009-0780-x

Hirota, C. L., & McKay, D. M. (2006). Cholinergic regulation of epithelial ion transport in the mammalian intestine. *British Journal of Pharmacology*, *149*(5), 463–479. DOI:10.1038/sj.bjp.0706889

Hirota, J., Michikawa, T., Natsume, T., & Furuichi, T. (1999). Calmodulin inhibits inositol 1,4,5-trisphosphate-induced calcium release through the purified and reconstituted inositol 1,4,5-trisphosphate receptor type 1. *FEBS Letters*, *456*, 322–326.

Höfer, D., & Drenckhahn, D. (1996). Cytoskeletal markers allowing discrimination between brush cells and other epithelial cells of the gut including enteroendocrine cells. *Histochemistry and Cell Biology*, *105*(5), 405–412. DOI: 10.1007/BF01463662

Hollander, D. (1988). Leading article Crohn's disease - a permeability disorder of the tight junction? *Gut*, *29*, 1621–1624.

Holm, L., & Phillipson, M. (2012). Assessment of mucus thickness and production in situ. *Methods Molecular Biology*, *842*, 217–227.

Hoth, M., & Penner, R. (1992). Depletion of intracellular calcium stores activates a calcium current in mast cells. *Nature*, *355*, 353–356.

Howe, S. E., Lickteig, D. J., Plunkett, K. N., Ryerse, J. S., & Konjufca, V. (2014). The uptake of soluble and particulate antigens by epithelial cells in the mouse small intestine. *PLoS ONE*, *9*(1), 1–11. DOI:10.1371/journal.pone.0086656

Huang J, Qi R, Quackenbush J, Dauway E, Lazaridis E, Y. T. (2001). Effects of ischemia on gene expression. *The Journal of Surgical Research*, *99*(2), 222–227.

Hugot, J. P., Chamaillard, M., Zouali, H., Lesage, S., Cézard, J. P., Belaiche, J., Thomas, G. (2001). Association of NOD2 leucine-rich repeat variants with susceptibility to Crohn's disease. *Nature*, *411*(6837), 599–603. DOI: 10.1038/35079107

Hulme, E. C., Spalding, T. A., Curtis, C. A., Birdsall, N. J., & Corrie, J. E. (1990). Blockade of muscarinic receptors by alkylating agonist analogues. *Biochemical Society Transactions*, *18*(3), 440–441.

Hurst, R. S., Zhu, X., Boulay, G., Birnbaumer, L., & Stefani, E. (1998). Ionic currents underlying HTRP3 mediated agonist-dependent Ca^{2+} influx in stably transfected HEK293 cells. *FEBS Letters*, *422*, 333–338.

Ichikawa, T., Ajiki, K., Matsuura, J., & Misawa, H. (1997). Localization of two cholinergic markers, choline acetyltransferase and vesicular acetylcholine transporter in the central nervous system of the rat: In situ hybridization histochemistry and immunohistochemistry. *Journal of Chemical Neuroanatomy*, *13*(1), 23–39. DOI: 10.1016/S0891-0618(97)00021-5

Iino, M. (1987). Calcium dependent inositol triphosphate-induced calcium release in the guinea-pig taenia caeci. *Biochemical and Biophysical Research Communications*, *142*(1), 47–52.

Imai, Y., Yamagishi, H., Fukuda, K., Ono, Y., Inoue, T., & Ueda, Y. (2013). Differential mucin phenotypes and their significance in a variation of colorectal carcinoma. *World Journal of Gastroenterology : WJG*, *19*(25), 3957–68. DOI:10.3748/wjg.v19.i25.3957

Inoguchi, T., Li, P., Umeda, F., Yu, H. Y., Kakimoto, M., Imamura, M., Nawata, H. (2000). High Glucose Level and Free Fatty Acid Stimulate Protein Kinase C – Dependent Activation of NAD(P)H Oxidase in Cultured Vascular Cells. *Diabetes*, *49*, 1939–1945. DOI:10.2337/diabetes.49.11.1939

Ishibashi, K., Suzuki, M., & Imai, M. (2000). Molecular cloning of a novel form (two-repeat) protein related to voltage-gated sodium and calcium channels. *Biochemical and Biophysical Research Communications*, *270*(2), 370–376. DOI:10.1006/bbrc.2000.2435

Itzkovitz, S., Blat, I. C., Jacks, T., Clevers, H., & Van Oudenaarden, A. (2012). Optimality in the development of intestinal crypts. *Cell*, *148*(3), 608–619. DOI:10.1016/j.cell.2011.12.025

Iwai, M., Michikawa, T., Bosanac, I., Ikura, M., & Mikoshiba, K. (2007). Molecular basis of the isoform-specific ligand-binding affinity of inositol 1,4,5-trisphosphate receptors. *Journal of Biological Chemistry*, *282*(17), 12755–12764. DOI:10.1074/jbc.M609833200

Jackson, T. R., Patterson, S. I., Thastrup, O., & Hanley, M. R. (1988). A novel tumour promoter, thapsigargin, transiently increases cytoplasmic free Ca^{2+} without generation of inositol phosphates in NG115-401L neuronal cells. *The Biochemical Journal*, *253*(1), 81–86.

Jaladanki, R. N., & Wang, J.-Y. (2011). Regulation of Gastrointestinal Mucosal Growth. *Colloquium Series on Integrated Systems Physiology: From Molecule to Function*, *3*(2), 1–114. DOI: 10.4199/C00028ED1V01Y201103ISP015

Javed, N. H., & Cooke, H. J. (1992). Acetylcholine release from colonic submucous neurons associated with chloride secretion in the guinea pig. *The American Journal of Physiology*, *262*(1), G131–G136.

Jawad, N., Direkze, N., & Leedham, S. (2011). Inflammatory bowel disease and colon cancer. *Recent Results in Cancer Research*, *185*, 99–115.

Jha, A., Ahuja, M., Patel, S., Brailoiu, E., & Muallem, S. (2014). Convergent regulation of the lysosomal two-pore channel-2 by Mg^{2+}, NAADP, PI(3,5) P2 and multiple protein kinases. *EMBO Journal*, *33*, 501–511.

Ji, H. Y., Kyung, H. K., & Kim, H. (2006). Role of NADPH oxidase and calcium in cerulein-induced apoptosis: Involvement of apoptosis-inducing factor. *Annals of the New York Academy of Sciences*, *1090*, 292–297. DOI:10.1196/annals.1378.031

Jiang, F., Zhang, Y., & Dusting, G. J. (2011). NADPH Oxidase-Mediated Redox Signaling: Roles in Cellular Stress Response, Stress Tolerance, and Tissue Repair. *Pharmacological Reviews*, *63*(1), 218–242. DOI:10.1124/pr.110.002980.218

Johansson, M. E. V, Phillipson, M., Petersson, J., Velcich, A., Holm, L., & Hansson, G. C. (2008). The inner of the two Muc2 mucin-dependent mucus layers in colon is devoid of bacteria. *Proceedings of the National Academy of Sciences*, *105*(39), 15064–15069. DOI:10.1073/pnas.0803124105

Johansson, M., & Hansson, G. (2013a). Mucus and the Goblet Cell. *Digestive Diseases*, *31*(0), 305–309. DOI:10.1016/j.biotechadv.2011.08.021.Secreted

Johansson, M. E. V. (2012). Fast renewal of the distal colonic mucus layers by the surface goblet cells as measured by in vivo labeling of mucin glycoproteins. *PLoS One*, *7*(7), e41009. DOI:10.1371/journal.pone.0041009

Johansson, M. E. V, Larsson, J. M. H., & Hansson, G. C. (2011). The two mucus layers of colon are organized by the MUC2 mucin, whereas the outer layer is a legislator of host-microbial interactions. *Proceedings of the National Academy of Sciences of the United States of America*, *108 (Suppl 1)*, 4659–4665. DOI:10.1073/pnas.1006451107

Johansson, M. E. V, Sjövall, H., & Hansson, G. C. (2013). The gastrointestinal mucus system in health and disease. *Nature Reviews. Gastroenterology & Hepatology*, *10*(6), 352–61. DOI:10.1038/nrgastro.2013.35

Johnson, J. D., & Misler, S. (2002). Nicotinic acid-adenine dinucleotide phosphate-sensitive calcium stores initiate insulin signaling in human beta cells. *Proceedings of the National Academy of Sciences of the United States of America*, *99*(22), 14566–71. DOI:10.1073/pnas.222099799

Jönsson, M., Norrgård, Ö., & Forsgren, S. (2007). Presence of a marked non-neuronal cholinergic system in human colon: Study of normal colon and colon in ulcerative colitis. *Inflammatory Bowel Diseases*, *13*(11), 1347–1356. DOI:10.1002/ibd.20224

Kai, H., & Yoshitake, K. (1994). Involvement of protein kinase C in mucus secretion by hamster tracheal epithelial cells in culture. *American Journal of Physiology. Lung Cellular and Molecular Physiology*, *267*, L526–L530.

Kanoh, H., Yamada, K., & Sakane, F. (2002). Diacylglycerol kinases: emerging downstream regulators in cell signaling systems. *Journal of Biochemistry*, *131*(5), 629–633.

Karam, S. (1999). Lineage commitment and maturation of epithelial cells in the gut. *Frontiers in Bioscience*, *4*, 286–298.

Kaser, A., Lee, A., Franke, A., & Glickman, J. (2008). XBP1 links ER stress to intestinal inflammation and confers genetic risk for human inflammatory bowel disease. *Cell*, *134*(5), 743–756. DOI:10.1016/j.cell.2008.07.021.XBP1

Katz, A., Wu, D., & Simon, M. I. (1992). Subunits βγ of heterotrimeric G protein activate β2 isoform of phospholipase C. *Nature*, *360*, 686–689.

Katz, J. P., Perreault, N., Goldstein, B. G., Lee, C. S., Labosky, P. A., Yang, V. W., & Kaestner, K. H. (2002). The zinc-finger transcription factor Klf4 is required for terminal differentiation of goblet cells in the colon. *Development*, *129*(11), 2619–28

Kawashima, K., & Fujii, T. (2000). Extraneuronal cholinergic system in lymphocytes. *Pharmacology and Therapeutics*, *86*(1), 29–48. DOI: 10.1016/S0163-7258(99)00071-6

Keely, S. J. (2011). Epithelial acetylcholine--a new paradigm for cholinergic regulation of intestinal fluid and electrolyte transport. *The Journal of Physiology*, *589*, 771–2. DOI:10.1113/jphysiol.2010.204263

Kikkawa, U., Kishimoto, a, & Nishizuka, Y. (1989). The protein kinase C family: heterogeneity and its implications. *Annual Review of Biochemistry*, *58*, 31–44. DOI:10.1146/annurev.biochem.58.1.31

Kim, Y. S., & Ho, S. B. (2010). Intestinal goblet cells and mucins in health and disease: recent insights and progress. *Current Gastroenterology Reports*, *12*(5), 319–30. DOI: 10.1007/s11894-010-0131-2

Kinnear, N. P., Boittin, F. X., Thomas, J. M., Galione, A., & Evans, a. M. (2004). Lysosome-sarcoplasmic reticulum junctions: A trigger zone for calcium signaling by nicotinic acid adenine dinucleotide phosphate and endothelin-1. *Journal of Biological Chemistry*, *279*(52), 54319–54326. DOI:10.1074/jbc.M406132200

Kinnear, N. P., Wyatt, C. N., Clark, J. H., Calcraft, P. J., Fleischer, S., Jeyakumar, L. H., Evans, A. M. (2008). Lysosomes co-localize with ryanodine receptor subtype 3 to form a trigger zone for calcium signalling by NAADP in rat pulmonary arterial smooth muscle. *Cell Calcium*, *44*(2), 190–201. DOI:10.1016/j.ceca.2007.11.003

Kirkpatrick, C. J., Bittinger, F., Unger, R. E., Kriegsmann, J., Kilbinger, H., & Wessler, I. (2001). The non-neuronal cholinergic system in the endothelium: evidence and possible pathobiological significance. *Japanese Journal of Pharmacology*, *85*(1), 24–28. DOI:10.1254/jjp.85.24

Klapproth, H., Reinheimer, T., Metzen, J., Münch, M., Bittinger, F., Kirkpatrick, C., Wessler, I. (1997). Non-neuronal acetylcholine, a signalling molecule synthesized by surface cells of rat and man. *Naunyn Schmiedebergs Archieves of Pharmacology*, *355*(4), 515–523.

Klaren, P., Hardcastle, J., Evans, S., Colledge, W., Evans, M., Taylor, C., White, S. (2001). Acetylcholine induces cytosolic Ca^{2+} mobilization in isolated distal colonic crypts from normal and cystic fibrosis mice. *Journal of Pharmacy and Pharmacology*, *53*(3), 371–377.

Knoop, K. A., McDonald, K. G., McCrate, S., McDole, J. R., & Newberry, R. D. (2015). Microbial sensing by goblet cells controls immune surveillance of luminal antigens in the colon. *Mucosal Immunology*, *8*(1), 198–210. DOI:10.1038/mi.2014.58

Kocks, S., Schultheiss, G., & Diener, M. (2002). Ryanodine receptors and the mediation of Ca^{2+}-dependent anion secretion across rat colon. *Pflugers Archiv European Journal of Physiology*, *445*(3), 390–397. DOI: 10.1007/s00424-002-0947-1

Kong, K. C., & Tobin, A. B. (2011). The role of M3-muscarinic receptor signaling in insulin secretion. *Communicative and Integrative Biology*, *4*(4), 489–491. DOI:10.4161/cib.4.4.15716

Kovacic, H. N., Irani, K., & Goldschmidt-Clermont, P. J. (2001). Redox regulation of human Rac1 stability by the proteasome in human aortic endothelial cells. *The Journal of Biological Chemistry*, *276*(49), 45856–45861. DOI:10.1074/jbc.M107925200

Kühn, R., Löhler, J., Rennick, D., Rajewsky, K., & Müller, W. (1993). Interleukin-10-deficient mice develop chronic enterocolitis. *Cell*, *75*(2), 263–274.

Kummer, W., Wiegand, S., Akinci, S., Schinkel, A. H., Wess, J., Koepsell, H., Lips, K. S. (2006). Role of acetylcholine and muscarinic receptors in serotonin-induced bronchoconstriction in the mouse. *Journal of Molecular Neuroscience*, *30*(1-2), 67–68. DOI: 10.1186/1465-9921-7-65

Kuwahara, A, Bowen, S., Wang, J., Condon, C., & Cooke, H. J. (1987). Epithelial responses evoked by stimulation of submucosal neurons in guinea pig distal colon. *The American Journal of Physiology*, *252*(5), G667–G674.

Kuwahara, A., Cooke, H. J., Carey, H. V, Mekhjian, H., Ellison, E. C., & McGregor, B. (1989). Effects of enteric neural stimulation on chloride transport in human left colon in vitro. *Digestive Diseases and Sciences*, *34*(2), 206–213. DOI: 10.1007/BF01536052

Kwon, M.-C., Koo, B.-K., Kim, Y.-Y., Lee, S.-H., Kim, N.-S., Kim, J.-H., & Kong, Y.-Y. (2009). Essential role of CR6-interacting factor 1 (Crif1) in E74-like factor 3 (ELF3)-mediated intestinal development. *The Journal of Biological Chemistry*, *284*(48), 33634–41. DOI:10.1074/jbc.M109.059840

Kwong, T. C., Liu, X., Hwei, L. O., & Ambudkar, I. S. (2008). Functional requirement for Orai1 in store-operated TRPC1-STIM1 channels. *Journal of Biological Chemistry*, *283*(19), 12935–12940. DOI:10.1074/jbc.C800008200

Lai, F. A., Misra, M., Xu, L., Smith, H. A., & Meissner, G. (1989a). The ryanodine receptor-Ca^{2+} release channel complex of skeletal muscle sarcoplasmic reticulum. *Journal of Biological Chemistry*, *264*(28), 16776–16785.

Lai, F., & Meissner, G. (1989b). The muscle ryanodine receptor and its intrinsic Ca^{2+} channel activity. *Journal of Bioenergetics and Biomembranes*, *21*(2), 227–246.

Lamb, G. D. (2000). Excitation-contraction coupling in skeletal muscle: comparisons with cardiac muscle. *Clinical and Experimental Pharmacology and Physiology*, *27*, 216–224.

Lambert, A. J., Buckingham, J. A., Boysen, H. M., & Brand, M. D. (2008). Diphenyleneiodonium acutely inhibits reactive oxygen species production by mitochondrial complex I during reverse, but not forward electron transport. *Biochimica et Biophysica Acta - Bioenergetics*, *1777*(5), 397–403. DOI:10.1016/j.bbabio.2008.03.005

Lamkanfi, M., & Dixit, V. M. (2014). Mechanisms and functions of inflammasomes. *Cell*, *157*(5), 1013–1022. DOI:10.1016/j.cell.2014.04.007

Lanner, J. T., Georgiou, D. K., Joshi, A. D., & Hamilton, S. L. (2010). Ryanodine receptors: structure, expression, molecular details, and function in calcium release. *Cold Spring Harbor Perspectives in Biology*, *2*(11), a003996. DOI:10.1101/cshperspect.a003996

Lanning, C. C., Ruiz-Velasco, R., & Williams, C. L. (2003). Novel mechanism of the co-regulation of nuclear transport of SmgGDS and Rac1. *Journal of Biological Chemistry*, *278*(14), 12495–12506. DOI:10.1074/jbc.M211286200

Laurent, E., McCoy, J. W., Macina, R. A., Liu, W., Cheng, G., Robine, S., Lambeth, J. D. (2008). Nox1 is over-expressed in human colon cancers and correlates with activating mutations in K-Ras. *International Journal of Cancer*, *123*(1), 100–7. DOI:10.1002/ijc.23423

Laver, D. R., Owen, V. J., Junankar, P. R., Taske, N. L., Dulhunty, A. F., & Lamb, G. D. (1997). Reduced inhibitory effect of Mg^{2+} on ryanodine receptor-Ca^{2+} release channels in malignant hyperthermia. *Biophysical Journal*, *73*(4), 1913–1924. DOI: 10.1016/S0006-3495(97)78222-5

Leblond, C., & Stevens, C. (1947). Rate of renewal of the cells of the intestinal epithelium in the rat. *The Anatomical Record*, *97*(3), 373.

Lechleiter, J., Girard, S., Peralta, E., & Clapham, D. (1991a). Spiral calcium wave propagation and annihilation in Xenopus laevis oocytes. *Science*, *252*, 123–126. DOI:10.1126/science.2011747

Lechleiter, J., Girard, S., Clapham, D., & Peralta, E. (1991b). Subcellular patterns of calcium release determined by G protein-specific residues of muscarinic receptors. *Nature*, *350*, 505–508.

Lee, H. C. (1997). Mechanisms of calcium signaling by cyclic ADP-ribose and NAADP. *Physiological Reviews*, *77*(4), 1133–1164.

Lee, H. (1999). A unified mechanism of enzymatic synthesis of two calcium messengers: cyclic ADP-ribose and NAADP. *Biological Chemistry*, *380*(7-8), 785–793.

Lee, H., & Aarhus, R. (1995). A Derivative of NADP Mobilizes Calcium Stores Insensitive to Inositol Trisphosphate and Cyclic ADP-ribose. *The Journal of Biological Chemistry*, *270*(5), 2152–2157.

Lee, H. C. (2012). Cyclic ADP-ribose and nicotinic acid adenine dinucleotide phosphate (NAADP) as messengers for calcium mobilization. *The Journal of Biological Chemistry*, *287*(38), 31633–40. DOI:10.1074/jbc.R112.349464

Lemons, R. M., & Thoene, J. G. (1991). Mediated calcium transport by isolated human fibroblast lysosomes. *The Journal of Biological Chemistry*, *266*(22), 14378–14382.

Levay, M., Krobert, K. A., Wittig, K., Voigt, N., Bermudez, M., Wolber, G., Wieland, T. (2013). NSC23766, a widely used inhibitor of Rac1 activation, additionally acts as a competitive antagonist at muscarinic acetylcholine receptors. *The Journal of Pharmacology and Experimental Therapeutics*, *347*(1), 69–79. DOI:10.1124/jpet.113.207266

Levine, B., Mizushima, N., & Virgin, H. W. (2011). Autophagy in immunity and inflammation. *Nature*, *469*(7330), 323–335. DOI: 10.1038/nature09782

Lewartowksi, B. (2000). Excitation-Contraction Coupling In Cardiac Muscle Revisited. *Journal of Physiology and Pharmacology*, *51*(3), 371–386.

Li, H., Limenitakis, J. P., Fuhrer, T., Geuking, M. B., Lawson, M. A., Wyss, M., Macpherson, A. J. (2015). The outer mucus layer hosts a distinct intestinal microbial niche. *Nature Communications*, *6*, 8292. DOI: 10.1038/ncomms9292

Li, N., Li, B., Brun, T., Deffert-Delbouille, C., Mahiout, Z., Daali, Y., Maechler, P. (2012). NADPH oxidase NOX2 defines a new antagonistic role for reactive oxygen species and cAMP/PKA in the regulation of insulin secretion. *Diabetes*, *61*(11), 2842–2850. DOI: 10.2337/db12-0009

Li, Q., Harraz, M. M., Zhou, W., Zhang, L. N., Ding, W., Zhang, Y., Engelhardt, J. F. (2006). Nox2 and Rac1 Regulate H 2 O 2 -Dependent Recruitment of TRAF6 to Endosomal Interleukin-1 Receptor Complexes. *Molecular and Cellular Biology*, *26*(1), 140–154. DOI:10.1128/MCB.26.1.140

Li, Y., & Trush, M. A. (1998). Diphenyleneiodonium, an NAD(P)H oxidase inhibitor, also potently inhibits mitochondrial reactive oxygen species production. *Biochemical and Biophysical Research Communications*, *253*(2), 295–299. DOI:10.1006/bbrc.1998.9729

Limatola, C., Schaap, D., Moolenaar, W. H., & van Blitterswijk, W. J. (1994). Phosphatidic acid activation of protein kinase C-zeta overexpressed in COS cells: comparison with other protein kinase C isotypes and other acidic lipids. *The Biochemical Journal*, *304*, 1001–1008.

Lindqvist, S. M., Sharp, P., Johnson, I. T., Satoh, Y., & Williams, M. R. (1998). Acetylcholine-induced calcium signaling along the rat colonic crypt axis. *Gastroenterology*, *115*(5), 1131–43.

Lindqvist, S. (2000). *Colonic Crypt Calcium Signalling*. Thesis, University of East Anglia.

Lindqvist, S., Hernon, J., Sharp, P., Johns, N., Addison, S., Watson, M., Williams, M. (2002). The colon-selective spasmolytic otilonium bromide inhibits muscarinic M(3) receptor-coupled calcium signals in isolated human colonic crypts. *British Journal of Pharmacology*, *137*(7), 1134–1142. DOI:10.1038/sj.bjp.0704942

Lin-Moshier, Y., Keebler, M. V., Hooper, R., Boulware, M. J., Liu, X., Churamani, D., Marchant, J. S. (2014). The Two-pore channel (TPC) interactome unmasks isoform-specific roles for TPCs in endolysosomal morphology and cell pigmentation. *Proceedings of the National Academy of Sciences*, *111*(36), 13087–13092. DOI:10.1073/pnas.1407004111

Lin-Moshier, Y., Walseth, T. F., Churamani, D., Davidson, S. M., Slama, J. T., Hooper, R., Marchant, J. S. (2012). Photo-affinity labeling of nicotinic acid adenine dinucleotide phosphate (NAADP) targets in mammalian cells. *The Journal of Biological Chemistry*, *287*(4), 2296–307. DOI:10.1074/jbc.M111.305813

Liou, J., Kim, M. L., Won, D. H., Jones, J. T., Myers, J. W., Ferrell, J. E., & Meyer, T. (2005). STIM is a Ca^{2+} sensor essential for Ca^{2+}-store- depletion-triggered Ca^{2+} influx. *Current Biology*, *15*(13), 1235–1241. DOI:10.1016/j.cub.2005.05.055

Lips, K. S., Volk, C., Schmitt, B. M., Pfeil, U., Arndt, P., Miska, D., Koepsell, H. (2005). Polyspecific cation transporters mediate luminal release of acetylcholine from bronchial epithelium. *American Journal of Respiratory Cell and Molecular Biology*, *33*(1), 79–88. DOI:10.1165/rcmb.2004-0363OC

Liscovitch, M. (1991). Signal-dependent activation of phosphatidylcholine hydrolysis: role of phospholipase D. *Biochemical Society Transactions*, *19*(2), 402–407.

Liscovitch, M., Czarny, M., Fiucci, G., & Tang, X. (2000). Phospholipase D: molecular and cell biology of a novel gene family. *The Biochemical Journal*, *345*, 401–415.

Liu, Z., & Liu, K. (2013). The transporters of intestinal tract and techniques applied to evaluate interactions between drugs and transporters. *Asian Journal of Pharmaceutical Sciences*, *8*(3), 151–158. DOI:10.1016/j.ajps.2013.07.020

López, J. J., Dionisio, N., Berna-Erro, A., Galán, C., Salido, G. M., & Rosado, J. A. (2012). Two-pore channel 2 (TPC2) modulates store-operated Ca2+ entry. *Biochimica et Biophysica Acta (BBA) - Molecular Cell Research*, *1823*(10), 1976–1983. DOI:10.1016/j.bbamcr.2012.08.002

Luik, R., Wang, B., Prakriya, M., Wu, M., & Lewis, R. (2008). Oligomerization of STIM1 couples ER calcium depletion to CRAC channel activation. *Nature*, *454*(7203), 538–542. DOI: 10.1038/nature07065

Luzio, J. P., Gray, S. R., & Bright, N. A. (2010). Endosome-lysosome fusion. *Biochemical Society Transactions*, *38*(6), 1413–1416. DOI: 10.1042/BST0381413

Luzio, J. P., Pryor, P. R., & Bright, N. A. (2007). Lysosomes: fusion and function. *Nature Reviews. Molecular Cell Biology*, *8*(8), 622–632. DOI: 10.1038/nrm2217

Mak, D.-O. D., McBride, S. M. J., & Foskett, J. K. (2003). Spontaneous channel activity of the inositol 1,4,5-trisphosphate (InsP3) receptor (InsP3R). Application of allosteric modeling to calcium and InsP3 regulation of InsP3R single-channel gating. *The Journal of General Physiology*, *122*(5), 583–603. DOI:10.1085/jgp.200308809

Mall, M., Bleich, M., Schürlein, M., Kühr, J., Seydewitz, H. H., Brandis, M., Kunzelmann, K. (1998). Cholinergic ion secretion in human colon requires coactivation by cAMP. *The American Journal of Physiology*, *275*(6), G1274–G1281.

Manichanh, C., Borruel, N., Casellas, F., & Guarner, F. (2012). The gut microbiota in IBD. *Nature Reviews. Gastroenterology & Hepatology*, *9*(10), 599–608. DOI:10.1038/nrgastro.2012.152

Marchant, J. S., & Taylor, C. W. (1997). Cooperative activation of IP3 receptors by sequential binding of IP3 and Ca^{2+} safeguards against spontaneous activity. *Current Biology*, *7*(7), 510–518. DOI: 10.1016/S0960-9822(06)00222-3

Marchenko, S. M., Yarotskyy, V. V, Kovalenko, T. N., Kostyuk, P. G., & Thomas, R. C. (2005). Spontaneously active and InsP3-activated ion channels in cell nuclei from rat cerebellar Purkinje and granule neurones. *The Journal of Physiology*, *565*, 897–910. DOI:10.1113/jphysiol.2004.081299

Marshall, I. C. B., & Taylor, W. (1993). Biphasic Effects of Cytosolic Ca^{2+} of Ins (1,4,5)P3-stimulated Ca^{2+} Mobilization in Hepatocytes. *The Journal of Biological Chemistry*, *268*(18), 13214–13220.

Marshall, I. C., & Taylor, C. W. (1994). Two calcium-binding sites mediate the interconversion of liver inositol 1,4,5-trisphosphate receptors between three conformational states. *The Biochemical Journal*, *301*, 591–598.

Maruyama, T., Kanaji, T., Nakade, S., Kanno, T., & Mikoshiba, K. (1997). 2APB, 2-Aminoethoxydiphenyl Borate, a Membrane-Penetrable Modulator of Ins (1,4,5)P3-Induced Ca^{2+} Release. *Journal of Biochemistry*, *122*, 498–505.

Matsuo, K., Akamatsu, T., & Katsuyama, T. (1997). Histochemistry of the surface. *Gut*, *40*, 782–789.

Mattson, M. P., & Chan, S. L. (2003). Neuronal and glial calcium signaling in Alzheimer's disease. *Cell Calcium*, *34*(4-5), 385–397. DOI: 10.1016/S0143-4160(03)00128-3

McCulloch, C., Kuwahara, A., Condon, C., & Cooke, H. (1987). Neuropeptide modification of chloride secretion in guinea pig distal colon. *Regulatory Peptides*, *19*(1-2), 35–43.

McDole, J. R., Wheeler, L. W., McDonald, K. G., Wang, B., Konjufca, V., Knoop, K. A. , Miller, M. J. (2012). Goblet cells deliver luminal antigen to $CD103^{+}$ dendritic cells in the small intestine. *Nature*, *483*(7389), 345–9. DOI: 10.1038/nature10863

McGrew, S., Wolleben, C., Siegl, P., Inui, M., & Fleischer, S. (1989). Positive cooperativity of ryanodine binding to the calcium release channel of sarcoplasmic reticulum from heart and skeletal muscle. *Biochemistry*, *28*(4), 1686–1691.

McGuckin, M. A., Eri, R. D., Das, I., Lourie, R., & Florin, T. H. (2010). ER stress and the unfolded protein response in intestinal inflammation. *American Journal of Physiology. Gastrointestinal and Liver Physiology*, *298*(6), G820–32. DOI:10.1152/ajpgi.00063.2010

McGuckin, M. A., Eri, R. D., Das, I., Lourie, R., & Florin, T. H. (2011a). Intestinal secretory cell ER stress and inflammation. *Biochemical Society Transactions*, *39*(4), 1081–1085. DOI: 10.1042/BST0391081

McGuckin, M. A., Lindén, S. K., Sutton, P., & Florin, T. H. (2011b). Mucin dynamics and enteric pathogens. *Nature Reviews. Microbiology*, *9*(4), 265–78. DOI: 10.1038/nrmicro2538

McPhail, L. C., Qualliotine-Mann, D., & Waite, K. A. (1995). Cell-free activation of neutrophil NADPH oxidase by a phosphatidic acid-regulated protein kinase. *Proceedings of the National Academy of Sciences of the United States of America*, *92*(17), 7931–7935. DOI:10.1073/pnas.92.17.7931

Medema, J. P., & Vermeulen, L. (2011). Microenvironmental regulation of stem cells in intestinal homeostasis and cancer. *Nature*, *474*(7351), 318–26. DOI: 10.1038/nature10212

Medina, D. L., Di Paola, S., Peluso, I., Armani, A., De Stefani, D., Venditti, R., Ballabio, A. (2015). Lysosomal calcium signalling regulates autophagy through calcineurin and TFEB. *Nature Cell Biology*, *17*(3), 288–299. DOI: 10.1038/ncb3114

Mehta, K., & Shahid, U. (1996). Human CD38, a cell-surface protein with multiple functions. *The FASEB Journal*, *10*, 1408–1417.

Meissner, G. (1986). Ryanodine activation and inhibition of the Ca^{2+} release channel of sarcoplasmic reticulum. *The Journal of Biological Chemistry*, *261*(14), 6300–6306.

Meissner, G., Rios, E., Tripathy, A., & Pasek, D. A. (1997). Regulation of skeletal muscle Ca^{2+} release channel (ryanodine receptor) by Ca^{2+} and monovalent cations and anions. *The Journal of Biological Chemistry*, *272*(3), 1628–1638.

Mellor, H., & Parker, P. J. (1998). The extended protein kinase C superfamily. *The Biochemical Journal*, *332*, 281–292.

Menteyne, A., Burdakov, A., Charpentier, G., Petersen, O. H., & Cancela, J. M. (2006). Generation of Specific Ca^{2+} Signals from Ca^{2+} Stores and Endocytosis by Differential Coupling to Messengers. *Current Biology*, *16*(19), 1931–1937. DOI:10.1016/j.cub.2006.07.070

Mérida, I., Avila-Flores, A., & Merino, E. (2008). Diacylglycerol kinases: at the hub of cell signalling. *The Biochemical Journal*, *409*(1), 1–18. DOI: 10.1042/BJ20071040

Merzel, J., & Leblond, C. (1969). Origin and renewal of goblet cells in the epithelium of the mouse small intestine. *The American Journal of Anatomy*, *124*(3), 281–305.

Mignery, G. A., Sudhof, T. C., Takei, K., & Camilli, P. De. (1989). Putative receptor for inositol 1,4,5-trisphosphate similar to ryanodine receptor. *Nature*, *342*, 192–195.

Miller, D. J. (2004). Sydney Ringer; physiological saline, calcium and the contraction of the heart. *The Journal of Physiology*, *555*, 585–587. DOI:10.1113/jphysiol.2004.060731

Milligan, G. (2009). G protein-coupled receptor hetero-dimerization: Contribution to pharmacology and function. *British Journal of Pharmacology*, *158*(1), 5–14. DOI:10.1111/j.1476-5381.2009.00169.x

Mitrovic, S., Nogueira, C., Cantero-Recasens, G., Kiefer, K., Fernández-Fernández, J. M., Popoff, J.-F., Malhotra, V. (2013). TRPM5-mediated calcium uptake regulates mucin secretion from human colon goblet cells. *eLife*, *2*, e00658. DOI:10.7554/eLife.00658

Miyamoto, H., & Racker, E. (1982). Mechanism of calcium release from skeletal sarcoplasmic reticulum. *The Journal of Membrane Biology*, *66*(3), 193–201.

Montell, C., & Rubin, G. M. (1989). Molecular characterization of the Drosophila trp locus: a putative integral membrane protein required for photo-transduction. *Neuron*, *2*(4), 1313–1323. DOI: 10.1016/0896-6273(89)90069-X

Montell, C., Birnbaumer, L., & Flockerzi, V. (2002). The TRP channels, a remarkably functional family. *Cell*, *108*(5), 595–598. DOI: 10.1016/S0092-8674(02)00670-0

Montenegro, M. F., Nieto-Cerón, S., Ruiz-Espejo, F., Cadena, M. P. de la, Rodríguez-Berrocal, F. J., & Vidal, C. J. (2005). Cholinesterase activity and enzyme components in healthy and cancerous human colorectal sections. *Chemico-Biological Interactions*, *157-158*, 429–430. DOI:10.1016/j.cbi.2005.10.091

Morgan, A. J., Platt, F. M., Lloyd-Evans, E., & Galione, A. (2011). Molecular mechanisms of endolysosomal Ca^{2+} signalling in health and disease. *The Biochemical Journal*, *439*(3), 349–74. DOI: 10.1042/BJ20110949

Morgan, A. J., Davis, L. C., Ruas, M., & Galione, A. (2015). TPC: the NAADP discovery channel? *Biochemical Society Transactions*, *43*(3), 384–389. DOI: 10.1042/BST20140300

Muñoz, J., Stange, D. E., Schepers, A. G., van de Wetering, M., Koo, B.-K., Itzkovitz, S., Clevers, H. (2012). The Lgr5 intestinal stem cell signature: robust expression of proposed quiescent "+4" cell markers. *The EMBO Journal*, *31*(14), 3079–3091. DOI:10.1038/emboj.2012.166

Mushtaq, M., Nam, T.-S., & Kim, U.-H. (2011). Critical role for CD38-mediated Ca^{2+} signaling in thrombin-induced procoagulant activity of mouse platelets and hemostasis. *The Journal of Biological Chemistry*, *286*(15), 12952–8. DOI:10.1074/jbc.M110.207100

Myant, K. B., Scopelliti, A., Haque, S., Vidal, M., Sansom, O. J., & Cordero, J. B. (2013). Rac1 drives intestinal stem cell proliferation and regeneration. *Cell Cycle*, *12*(18), 2973–2977. doi:10.4161/cc.26031

Nadif Kasri, N., Bultynck, G., Sienaert, I., Callewaert, G., Erneux, C., Missiaen, L., De Smedt, H. (2002). The role of calmodulin for inositol 1,4,5-trisphosphate receptor function. *Biochimica et Biophysica Acta*, *1600*(1-2), 19–31. DOI:10.1016/S1570-9639(02)00440-5

Nahorski, S. R., Tobin, A. B., & Willars, G. G. (1997). Muscarinic M3 Receptor Coupling and Regulation. *Life Sciences*, *60*(13-14), 1039–1045.

Nakai, J., Sekiguchi, N., Rando, T. a, Allen, P. D., & Beam, K. G. (1998). Two regions of the ryanodine receptor involved in coupling with L-type Ca^{2+} channels. *The Journal of Biological Chemistry*, *273*(22), 13403–13406. DOI:10.1074/jbc.273.22.13403

Nathanson, N. M. (2000). A multiplicity of muscarinic mechanisms: enough signaling pathways to take your breath away. *Proceedings of the National Academy of Sciences of the United States of America*, *97*(12), 6245–6247. DOI:10.1073/pnas.97.12.6245

Navarro-Borelly, L., Somasundaram, A., Yamashita, M., Ren, D., Miller, R. J., & Prakriya, M. (2008). STIM1-Orai1 interactions and Orai1 conformational changes revealed by live-cell FRET microscopy. *The Journal of Physiology*, *586*(22), 5383–5401. DOI:10.1113/jphysiol.2008.162503

Naylor, E., & Arredouani, A. (2009). Identification of a chemical probe for NAADP by virtual screening. *Nature Chemical Biology*, *5*(4), 220–226. DOI:10.1038/nchembio.150

Nervous system- neurons. New World Encyclopedia. Retrieved September 1, 2015, from http://www.newworldencyclopedia.org/entry/Nervous_system

Neutra, M. R., O'Malley, L. J., & Specian, R. D. (1982). Regulation of intestinal goblet cell secretion. II. A survey of potential secretagogues. *The American Journal of Physiology*, *242*(4), G380–G387.

Neutra, M. R. (1998). Role of M cells in transepithelial transport of antigens and pathogens to the mucosal immune system. *Current Concepts in Mucosal Immunity*, 455–458.

Ng, A. Y.-N., Waring, P., Ristevski, S., Wang, C., Wilson, T., Pritchard, M., Kola, I. (2002). Inactivation of the transcription factor Elf3 in mice results in dysmorphogenesis and altered differentiation of intestinal epithelium. *Gastroenterology*, *122*(5), 1455–1466. DOI:10.1053/gast.2002.32990

Noah, T. K., Kazanjian, A., Whitsett, J., & Shroyer, N. F. (2010). SAM pointed domain ETS factor (SPDEF) regulates terminal differentiation and maturation of intestinal goblet cells. *Experimental Cell Research*, *316*(3), 452–65. DOI:10.1016/j.yexcr.2009.09.020

Ogaki, S., Shiraki, N., Kume, K., & Kume, S. (2013). Wnt and Notch signals guide embryonic stem cell differentiation into the intestinal lineages. *Stem Cells*, *31*(6), 1086–1096. DOI:10.1002/stem.1344

Ogunbayo, O. A., Zhu, Y., Rossi, D., Sorrentino, V., Ma, J., Zhu, M. X., & Evans, A. M. (2011). Cyclic adenosine diphosphate ribose activates ryanodine receptors, whereas NAADP activates two-pore domain channels. *Journal of Biological Chemistry*, *286*(11), 9136–9140. DOI:10.1074/jbc.M110.202002

Ogura, Y., Bonen, D. K., Inohara, N., Nicolae, D. L., Chen, F. F., Ramos, R., Cho, J. H. (2001). A frameshift mutation in NOD2 associated with susceptibility to Crohn's disease. *Nature*, *411*(6837), 603–606. DOI: 10.1038/35079114

Ohkusa, T., & Koido, S. (2015). Intestinal microbiota and ulcerative colitis. *Journal of Infection and Chemotherapy : Official Journal of the Japan Society of Chemotherapy*, *21*(11), 761–768. DOI:10.1016/j.jiac.2015.07.010

O'Malley, K. E., Farrell, C. B., O'Boyle, K. M., & Baird, A. W. (1995). Cholinergic activation of Cl^- secretion in rat colonic epithelia. *European Journal of Pharmacology*, *275*(1), 83–89. DOI: 10.1016/0014-2999(94)00758-Y

Ong, H. L., de Souza, L. B., Zheng, C., Cheng, K. T., Liu, X., Goldsmith, C. M., Ambudkar, I. S. (2015). STIM2 enhances receptor-stimulated Ca^{2+} signaling by promoting recruitment of STIM1 to the endoplasmic reticulum-plasma membrane junctions. *Science Signaling*, *8*(359), ra3. DOI:10.1126/scisignal.2005748

Oprins, J. C., Meijer, H. P., & Groot, J. A. (2000). Tumor necrosis factor-alpha potentiates ion secretion induced by muscarinic receptor activation in the human intestinal epithelial cell line HT29cl.19A. *Annals of the New York Academy of Sciences*, *915*, 102–106.

Otsu, K., Willard, H. F., Khanna, V. K., Zorzato, F., Green, N. M., & MacLennan, D. H. (1990). Molecular cloning of cDNA encoding the Ca^{2+} release channel (ryanodine receptor) of rabbit cardiac muscle sarcoplasmic reticulum. *The Journal of Biological Chemistry*, *265*(23), 13472–13483.

Ozawa, T. (1999). Ryanodine-sensitive Ca ($^{2+}$) release mechanism of rat pancreatic acinar cells is modulated by calmodulin. *Biochimica et Biophysica Acta*, *1452*(3), 254–262.

Palicz, A., Foubert, T. R., Jesaitis, A. J., Marodi, L., & McPhail, L. C. (2001). Phosphatidic Acid and Diacylglycerol Directly Activate NADPH Oxidase by Interacting with Enzyme Components. *Journal of Biological Chemistry*, *276*(5), 3090–3097. DOI:10.1074/jbc.M007759200

Parker, B. Y. I., & Ivorra, I. (1991). Caffeine inhibits inositol trisphosphate-mediated liberation of intracellular calcium in Xenopus oocytes. *Journal of Physiology*, *433*, 229–240.

Parkman, H. P., Trate, D. M., Knight, L. C., Brown, K. L., Maurer, A. H., & Fisher, R. S. (1999). Cholinergic effects on human gastric motility. *Gut*, *45*(3), 346–354. DOI:10.1136/gut.45.3.346

Parris, A., & Williams, M. R. (2015). A Human Colonic Crypt Culture System to Study Regulation of Stem Cell-Driven Tissue Renewal and Physiological Function. *Methods in Molecular Biology 1212* (pp. 141–161). Humana Press. DOI: 10.1007/7651_2015_197

Parsons, S. M. (2000). Transport mechanisms in acetylcholine and monoamine storage. *The FASEB Journal*, *14*(15), 2423–2434. DOI:10.1096/fj.00-0203rev

Parsons, S. M., Bahr, B. A., Gracz, L. M., Kaufman, R., Kornreich, W. D., Nilsson, L., & Rogers, G. A. (1987). Acetylcholine transport: fundamental properties and effects of pharmacologic agents. *Annals of the New York Academy of Sciences*, *493*, 220–233.

Patel, K. K., Miyoshi, H., Beatty, W. L., Head, R. D., Malvin, N. P., Cadwell, K., Stappenbeck, T. S. (2013). Autophagy proteins control goblet cell function by potentiating reactive oxygen species production. *The EMBO Journal*, *32*(24), 3130–44. DOI:10.1038/emboj.2013.233

Patel, S., Churchill, G. C., & Galione, A. (2001). Coordination of Ca^{2+} signalling by NAADP. *Trends in Biochemical Sciences*, *26*(8), 482–9.

Patel, S., Ramakrishman, L., Rahman, T., Hamdoun, A., Marchant, J., Taylor, C., & Brailoiu, E. (2011). The endo-lysosomal system as an NAADP-sensitive acidic calcium store: Role for the two-pore channels. *Cell Calcium*, *50*(2), 157–167. DOI:10.1016/j.biotechadv.2011.08.021.Secreted

Patel, S., Marchant, J. S., & Brailoiu, E. (2010). Two-pore channels: Regulation by NAADP and customized roles in triggering calcium signals. *Cell Calcium*, *47*(6), 480–490. DOI:10.1016/j.ceca.2010.05.001

Patterson, R. L., Boehning, D., & Snyder, S. H. (2004). Inositol 1,4,5-trisphosphate receptors as signal integrators. *Annual Review of Biochemistry*, *73*, 437–65. DOI:10.1146/annurev.biochem.73.071403.161303

Pavlov, V. A. (2008). Cholinergic modulation of inflammation. *International Journal of Clinical and Experimental Medicine*, *1*(3), 203–212.

Pavlov, V. A., Wang, H., Czura, C. J., Friedman, S. G., & Tracey, K. J. (2003). The Cholinergic Anti-inflammatory Pathway: A Missing Link in Neuroimmunomodulation. *Molecular Medicine*, *9*(5-8), 125–134.

Pearson, A. D., Eastham, E. J., Laker, M. F., Craft, A. W., & Nelson, R. (1982). Intestinal permeability in children with Crohn's disease and coeliac disease. *British Medical Journal*, *285*(6334), 20–21. DOI:10.1136/bmj.285.6334.20

Peinelt, C., Vig, M., Koomoa, D. L., Beck, A., Nadler, M. J. S., Koblan-Huberson, M., Kinet, J.-P. (2006). Amplification of CRAC current by STIM1 and CRACM1 (Orai1). *Nature Cell Biology*, *8*(7), 771–773. DOI: 10.1038/ncb1435

Peiter, E., Maathuis, F. J. M., Mills, L. N., Knight, H., Pelloux, J., Hetherington, A. M., & Sanders, D. (2005). The vacuolar Ca^{2+}-activated channel TPC1 regulates germination and stomatal movement. *Nature*, *434*(7031), 404–408. DOI: 10.1038/nature03381

Peltekova, V. D., Wintle, R. F., Rubin, L. A., Amos, C. I., Huang, Q., Gu, X., Siminovitch, K. A. (2004). Functional variants of OCTN cation transporter genes are associated with Crohn disease. *Nature Genetics*, *36*(5), 471–475. DOI: 10.1038/ng1339

Peralta, E. G., Ashkenazi, A., Winslow, J. W., Ramachandran, J., & Capon, D. J. (1988). Differential regulation of PI hydrolysis and adenylyl cyclase by muscarinic receptor subtypes. *Nature*, *334*, 434–437. DOI: 10.1038/334242a0

Perez-Moreno, M., Jamora, C., & Fuchs, E. (2003). Sticky Business: Orchestrating Cellular Signals at Adherens Junctions. *Cell*, *112*(4), 535–548. DOI: 10.1016/S0092-8674(03)00108-9

Periasamy, M., & Kalyanasundaram, A. (2007). SERCA pump isoforms: Their role in calcium transport and disease. *Muscle and Nerve*, *35*(4), 430–442. DOI:10.1002/mus.20745

Petersen, O. H., Burdakov, D., & Tepikin, A. V. (1999). Polarity in intracellular calcium signaling. *BioEssays*, *21*(10), 851–860.

Phillips, T. E., Phillips, T. H., & Neutra, M. R. (1984). Regulation of intestinal goblet cell secretion. III. Isolated intestinal epithelium. *The American Journal of Physiology*, *247*(6), G674–81.

Phillips, T., & Wilson, J. (1993). Signal transduction pathways mediating mucin secretion from intestinal goblet cells. *Digestive Diseases and Sciences*, *38*(6), 1046–1054.

Pinto, D., Gregorieff, A., Begthel, H., & Clevers, H. (2003). Canonical Wnt signals are essential for homeostasis of the intestinal epithelium. *Genes & Development*, *17*, 1709–1713. DOI: 10.1101/ gad.267103

Pinton, P., Pozzan, T., & Rizzuto, R. (1998). The Golgi apparatus is an inositol 1,4,5-trisphosphate-sensitive Ca^{2+} store, with functional properties distinct from those of the endoplasmic reticulum. *The EMBO Journal*, *17*(18), 5298–5308.

Pitt, S. J., Funnell, T. M., Sitsapesan, M., Venturi, E., Rietdorf, K., Ruas, M., Sitsapesan, R. (2010). TPC2 is a novel NAADP-sensitive Ca^{2+} release channel, operating as a dual sensor of luminal pH and Ca^{2+}. *The Journal of Biological Chemistry*, *285*(45), 35039–46. DOI:10.1074/jbc.M110.156927

Pitt, S. J., Lam, A. K. M., Rietdorf, K., Galione, A., & Sitsapesan, R. (2014). Reconstituted Human TPC1 Is a Proton-Permeable Ion Channel and Is Activated by NAADP or Ca^{2+}. *Science Signaling*, *7*(326), ra46. DOI:10.1126/scisignal.2004854

Plaisancié, P., Barcelo, A., Moro, F., Claustre, J., Chayvialle, J. A., & Cuber, J. C. (1998). Effects of neurotransmitters, gut hormones, and inflammatory mediators on mucus discharge in rat colon. *The American Journal of Physiology*, *275*(5), G1073–G1084.

Potten, C. S., Gandara, R., Mahida, Y. R., Loeffler, M., & Wright, N. A. (2009). The stem cells of small intestinal crypts: Where are they? *Cell Proliferation*, *42*(6), 731–750. DOI:10.1111/j.1365-2184.2009.00642.x

Potten, C. S., Booth, C., Tudor, G. L., Booth, D., Brady, G., Hurley, P., Okano, H. (2003). Identification of a putative intestinal stem cell and early lineage marker; musashi-1. *Differentiation*, *71*(1), 28–41. DOI:10.1046/j.1432-0436.2003.700603.x

Pozzan, T., Rizzuto, R., Volpe, P., & Meldolesi, J. (1994). Molecular and cellular physiology of intracellular calcium stores. *Physiological Reviews*, *74*(3), 595–636.

Prakriya, M., Feske, S., Gwack, Y., Srikanth, S., Rao, A., & Hogan, P. G. (2006). Orai1 is an essential pore subunit of the CRAC channel. *Nature*, *443*(7108), 230–233. DOI: 10.1038/nature05122

Prakriya, M., & Lewis, R. S. (2001). Potentiation and inhibition of Ca^{2+} release-activated Ca^{2+} channels by 2-aminoethyldiphenyl borate (2-APB) occurs independently of IP3 receptors. *The Journal of Physiology*, *536*(1), 3–19. DOI:10.1111/j.1469-7793.2001.t01-1-00003.x

Prince, W. T., & Berridge, M. J. (1973). The Role of Calcium in the Action of 5-Hydroxytryptamine and Cyclic Amp on Salivary Glands. *The Journal of Experimental Biology*, *58*(2), 367–384.

Prinz, G., & Diener, M. (2008). Characterization of ryanodine receptors in rat colonic epithelium. *Acta Physiologica*, *193*(2), 151–62. DOI:10.1111/j.1748-1716.2007.01802.x

Puertollano, R., & Kiselyov, K. (2009). TRPMLs: in sickness and in health. American Journal of Physiology. *AJP: Renal Physiology*, *296*(6), F1245–F1254. DOI:10.1152/ajprenal.90522.2008

Putney Jr, J. (1986). A model for receptor-regulated calcium entry. *Cell Calcium*, *7*(1), 1–12.

Putney, J. W. (2011). The Physiological Function of Store-operated Calcium Entry. *Neurochemical Research*, *36*(7), 1157–1165. DOI: 10.1007/s11064-010-0383-0

Putney, J. (2014). Origins of the concept of store-operated calcium entry. *Frontiers in Bioscience*, *3*, 980–984.

Putney, J. W., Broad, L. M., Braun, F. J., Lievremont, J. P., & Bird, G. S. (2001). Mechanisms of capacitative calcium entry. *Journal of Cell Science*, *114* (12), 2223–2229.

Putney, J. W., & Bird, G. S. (2008). Cytoplasmic calcium oscillations and store-operated calcium influx. *The Journal of Physiology*, *586*(13), 3055–3059. DOI:10.1113/jphysiol.2008.153221

Qualliotine-Mann, D., Agwu, D. E., Ellenburg, M. D., McCall, C. E., & McPhail, L. C. (1993). Phosphatidic acid and diacylglycerol synergize in a cell-free system for activation of NADPH oxidase from human neutrophils. *Journal of Biological Chemistry*, *268*(32), 23843–23849.

Radwan, K., Oliver, M., & Specian, R. (1990). Cytoarchitectural reorganization of rabbit colonic goblet cells during baseline secretion. *The American Journal of Anatomy*, *189*(4), 365–376.

Rao, J. N. (2006). TRPC1 functions as a store-operated Ca^{2+} channel in intestinal epithelial cells and regulates early mucosal restitution after wounding. American Journal of Physiology. *AJP: Gastrointestinal and Liver Physiology*, *290*, G782–G792. DOI:10.1152/ajpgi.00441.2005

Reynolds, A., Parris, A., Evans, L. A., Lindqvist, S., Sharp, P., Lewis, M., Williams, M. R. (2007). Dynamic and differential regulation of NKCC1 by calcium and cAMP in the native human colonic epithelium. *The Journal of Physiology*, *582*(2), 507–24. DOI:10.1113/jphysiol.2007.129718

Reynolds, A., Wharton, N., Parris, A., Mitchell, E., Sobolewski, A., Kam, C., Williams, M. R. (2014). Canonical Wnt signals combined with suppressed TGFβ/BMP pathways promote renewal of the native human colonic epithelium. *Gut*, *63*(4), 610–21. DOI: 10.1136/gutjnl-2012-304067

Ribeiro, F. M., Black, S. A. G., Prado, V. F., Rylett, R. J., Ferguson, S. S. G., & Prado, M. A. M. (2006). The "ins" and "outs" of the high-affinity choline transporter CHT1. *Journal of Neurochemistry*, *97*(1), 1–12. DOI:10.1111/j.1471-4159.2006.03695.x

Ridley, C., Kouvatsos, N., Raynal, B. D., Howard, M., Collins, R. F., Desseyn, J. L., Thornton, D. J. (2014). Assembly of the respiratory Mucin MUC5B a new model for a gel-forming Mucin. *Journal of Biological Chemistry*, *289*(23), 16409–16420. DOI:10.1074/jbc.M114.566679

Rizzuto, R., Pinton, P., Carrington, W., Fay, F. S., Fogarty, K. E., Lifshitz, L. M., Pozzan, T. (1998). Close contacts with the endoplasmic reticulum as determinants of mitochondrial Ca^{2+} responses. *Science*, *280*(5370), 1763–1766. DOI:10.1126/science.280.5370.1763

Rizzuto, R., De Stefani, D., Raffaello, A., & Mammucari, C. (2012). Mitochondria as sensors and regulators of calcium signalling. *Nature Reviews Molecular Cell Biology*, *13*(9), 566–578. DOI: 10.1038/nrm3412

Rogers, D., & Dewar, A. (1990). Neural control of airway mucus secretion. *Biomedicine and Pharmacotherapy*, *44*(9), 447–453.

Rooney, T. A., & Thomas, A. P. (1993). Intracellular calcium waves generated by Ins (1,4,5)P3-dependent mechanisms. *Cell Calcium*, *14*(10), 674–690.

Rose, B. (1971). Intercellular communication and some structural aspects of membrane junctions in a simple cell system. *Journal of Membrane Biology*, *5*(1), 1–19.

Rothenberg, M. E., Nusse, Y., Kalisky, T., Lee, J. J., Dalerba, P., Scheeren, F., Clarke, M. F. (2012). Identification of a $cKit^{+}$ Colonic Crypt Base Secretory Cell That Supports $Lgr5^{+}$ Stem Cells in Mice. *Gastroenterology*, *142*(5), 1195–1205.e6. DOI:10.1053/j.gastro.2012.02.006

Rottenberg, H., & Scarpa, A. (1974). Calcium uptake and membrane potential in mitochondria. *Biochemistry*, *13*(23), 4811–4817.

Ruas, M., Chuang, K.-T., Davis, L. C., Al-Douri, a., Tynan, P. W., Tunn, R., Parrington, J. (2014). TPC1 Has Two Variant Isoforms, and Their Removal Has Different Effects on Endo-Lysosomal Functions Compared to Loss of TPC2. *Molecular and Cellular Biology*, *34*(21), 3981–3992. DOI:10.1128/MCB.00113-14

Ruas, M., Davis, L. C., Chen, C., Morgan, A. J., Chuang, K., Walseth, T. F., Galione, A. (2015). Expression of Ca^{2+}-permeable two-pore channels rescues NAADP signalling in TPC-deficient cells. *The EMBO Journal*, *34*(13), 1743–1758. DOI:10.15252/embj.201490009

Ruas, M., Rietdorf, K., Arredouani, A., Davis, L. C., Lloyd-Evans, E., Koegel, H., Galione, A. (2010). Purified TPC Isoforms Form NAADP Receptors with Distinct Roles for Ca^{2+} Signaling and Endolysosomal Trafficking. *Current Biology*, *20*(8), 703–709. DOI:10.1016/j.cub.2010.02.049

Rubinstein, A., & Tirosh, B. (1994). Mucus gel thickness and turnover in the gastrointestinal tract of the rat: response to cholinergic stimulus and implication for mucoadhesion. *Pharmacology Research*, *11*(6), 794–799.

Ruiz-Velasco, R., Lanning, C. C., & Williams, C. L. (2002). The activation of Rac1 by M3 muscarinic acetylcholine receptors involves the translocation of Rac1 and IQGAP1 to cell junctions and changes in the composition of protein complexes containing Rac1, IQGAP1, and actin. *Journal of Biological Chemistry*, *277*(36), 33081–33091. DOI:10.1074/jbc.M202664200

Rümenapp, U., Asmus, M., Schablowski, H., Woznicki, M., Han, L., Jakobs, K. H., Schmidt, M. (2001). The M3 muscarinic acetylcholine receptor expressed in HEK-293 cells signals to phospholipase D via G12 but not Gq-type G proteins. Regulators of G proteins as tools to dissect pertussis toxin-resistant G proteins in receptor-effector coupling. *Journal of Biological Chemistry*, *276*(4), 2474–2479. DOI:10.1074/jbc.M004957200

Rybalchenko, V., Ahuja, M., Coblentz, J., Churamani, D., Patel, S., Kiselyov, K., & Muallem, S. (2012). Membrane potential regulates Nicotinic Acid Adenine Dinucleotide Phosphate (NAADP) dependence of the pH- and Ca^{2+}-sensitive organellar two-pore channel TPC1. *Journal of Biological Chemistry*, *287*(24), 20407–20416. DOI:10.1074/jbc.M112.359612

Sadok, A., Bourgarel-Rey, V., Gattacceca, F., Penel, C., Lehmann, M., & Kovacic, H. (2008). Nox1-dependent superoxide production controls colon adenocarcinoma cell migration. *Biochimica et Biophysica Acta*, *1783*(1), 23–33. DOI:10.1016/j.bbamcr.2007.10.010

Salim, S. Y., & Söderholm, J. D. (2011). Importance of disrupted intestinal barrier in inflammatory bowel diseases. *Inflammatory Bowel Diseases*, *17*(1), 362–381. DOI:10.1002/ibd.21403

Sanchez-Wandelmer, J., & Reggiori, F. (2013). Amphisomes: out of the autophagosome shadow? *The EMBO Journal*, *32*(24), 3116–8. DOI:10.1038/emboj.2013.246

Sanders, K. M. (1998). G Protein-Coupled Receptors in Gastrointestinal Physiology IV. Neural regulation of gastrointestinal smooth muscle. *American Journal of Physiology. Gastrointestinal and Liver Physiology*, *275*(38), G1–G7.

Sanderson, M. J., Charles, A. C., Boitano, S., & Dirksen, E. R. (1994). Mechanisms and function of intercellular calcium signaling. *Molecular and Cellular Endocrinology*, *98*(2), 173–187. DOI: 10.1016/0303-7207(94)90136-8

Sanderson, M. J., Charles, A. C., & Dirksen, E. R. (1990). Mechanical stimulation and intercellular communication increases intracellular Ca^{2+} in epithelial cells. *Cell Regulation*, *1*(8), 585–596.

Sandow, A., Taylor, S., & Preiser, H. (1965). Role of the action potential in excitation-contraction coupling. *Federation Proceedings*, *24*(5), 1116–1123.

Santos, M., Tannuri, A., Coelho, M., Gonçalves, J., Serafini, S., Silva, L., & Tannuri, U. (2015). Immediate expression of c-fos and c-jun mRNA in a model of intestinal autotransplantation and ischemia-reperfusion in situ. *Clinics*, *70*(5), 373–379. DOI:10.6061/clinics/2015(05)12

Sastry, R., & Sadavongvivad, C. (1979). Cholinergic Systems in Non-nervous Tissues. *Pharmacological Reviews*, *30*(1), 66–132.

Sato, T., Stange, D. E., Ferrante, M., Vries, R. G. J., Van Es, J. H., Van den Brink, S., Clevers, H. (2011). Long-term expansion of epithelial organoids from human colon, adenoma, adenocarcinoma, and Barrett's epithelium. *Gastroenterology*, *141*(5), 1762–72. DOI:10.1053/j.gastro.2011.07.050

Satoh, Y., Habara, Y., Ono, K., & Kanno, T. (1995). Carbamylcholine- and catecholamine-induced intracellular calcium dynamics of epithelial cells in mouse ileal crypts. *Gastroenterology*, *108*(5), 1345–1356. DOI: 10.1016/0016-5085(95)90681-9

Scarpa, A., & Azzone, G. F. (1970). The mechanism of ion translocation in mitochondria. 4. Coupling of K^+ efflux with Ca^{2+} uptake. *European Journal of Biochemistry*, *12*(2), 328–335.

Schafer, M., Eiden, L., & Weihe, E. (1998). Cholinergic neurons and terminal fields revealed by immunohistochemistry for the vesicular ACh transporter II. *Neuroscience*, *84*(2), 361–376.

Schieder, M., Rötzer, K., Brüggemann, A., Biel, M., & Wahl-Schott, C. A. (2010). Characterization of two-pore channel 2 (TPCN2)-mediated Ca^{2+} currents in isolated lysosomes. *The Journal of Biological Chemistry*, *285*(28), 21219–22. DOI:10.1074/jbc.C110.143123

Schlereth, T., Birklein, F., Haack, K. an., Schiffmann, S., Kilbinger, H., Kirkpatrick, C. J., & Wessler, I. (2006). In vivo release of non-neuronal acetylcholine from the human skin as measured by dermal microdialysis: effect of botulinum toxin. *British Journal of Pharmacology*, *147*(2), 183–187. DOI:10.1038/sj.bjp.0706451

Schonhoff, S. E., Giel-Moloney, M., & Leiter, A. B. (2004). Minireview: Development and differentiation of gut endocrine cells. *Endocrinology*, *145*(6), 2639–2644. DOI:10.1210/en.2004-0051

Schrlau, M.G., Brailoiu, E., Patel, S., Gogotsi, Y., Dun, N.J. (2008). Carbon nanopipettes characterize calcium release pathways in breast cancer cells. *Nanotechnology*, *19*(32), 325102.

Schutz, B., Jurastow, I., Bader, S., Ringer, C., Engelhardt, von. J., Chubanov, V., Weihe, E. (2015). Chemical coding and chemosensory properties of cholinergic brush cells in the mouse gastrointestinal and biliary tract. *Frontiers in Physiology*, *6*, 1–14. DOI:10.3389/fphys.2015.00087

Scoote, M., & Williams, A. J. (2004). Myocardial calcium signalling and arrhythmia pathogenesis. *Biochemical and Biophysical Research Communications*, *322*(4), 1286–1309. DOI:10.1016/j.bbrc.2004.08.034

Sebille, S., Pereira, M., Millot, J. M., Jacquot, J., Delabroise, A.M., Arnaud, M., & Manfait, M. (1998). Extracellular Mg^{2+} inhibits both histamine-stimulated Ca ($^{2+}$)-signaling and exocytosis in human tracheal secretory gland cells. *Biochemical and Biophysical Research Communications*, *246*(1), 111–116. DOI:10.1006/bbrc.1998.8494

Seidler, U., & Pfeiffer, A. (1991). Inositol phosphate formation and [Ca^{2+}] i in secretagogue-stimulated rabbit gastric mucous cells. *The American Journal of Physiology*, *260*(1), G133–G141.

Seidler, U., & Sewing, K. (1989). Ca^{2+}-dependent and-independent secretagogue action on gastric mucus secretion in rabbit mucosal explants. *American Journal of Physiology. Gastrointestinal and Liver Physiology*, *19* (G739-G746).

Sellon, R. K., Tonkonogy, S., Schultz, M., Dieleman, L. A., Grenther, W., Balish, E., Sartor, R. B. (1998). Resident enteric bacteria are necessary for development of spontaneous colitis and immune system activation in interleukin-10-deficient mice. *Infection and Immunity*, *66*(11), 5224–5231.

Selwyn, M. J., Dawson, A. P., & Dunnett, S. J. (1970). Calcium Transport in Mitochondria. *FEBS Letters*, *10*(1), 1–5.

Sham, J. S., Cleemann, L., & Morad, M. (1995). Functional coupling of Ca^{2+} channels and ryanodine receptors in cardiac myocytes. *Proceedings of the National Academy of Sciences of the United States of America*, *92*(1), 121–125.

Shearman, M. S., Sekiguchi, K., & Nishizuka, Y. (1989). Modulation of ion channel activity: a key function of the protein kinase C enzyme family. *Pharmacological Reviews*, *41*(2), 211–237.

Sheng, Y. H., Lourie, R., Lindén, S. K., Jeffery, P. L., Roche, D., Tran, T. V, McGuckin, M. A. (2011). The MUC13 cell-surface mucin protects against intestinal inflammation by inhibiting epithelial cell apoptosis. *Gut*, *60*(12), 1661–70. DOI:10.1136/gut.2011.239194

Shibao, K., Fiedler, M. J., Nagata, J., Minagawa, N., Hirata, K., Nakayama, Y., Yamaguchi, K. (2010). The type III inositol 1,4,5-trisphosphate receptor is associated with aggressiveness of colorectal carcinoma. *Cell Calcium*, *48*(6), 315–23. DOI:10.1016/j.ceca.2010.09.005

Shim, A., Tirado-Lee, L., & Prakriya, M. (2015). Structure and functional mechanisms of CRAC channel regulation. *Journal of Molecular Biology*, *427*(1), 77–93. DOI:10.1016/j.jmb.2014.09.021.Structural

Shkoda, A., Ruiz, P. A., Daniel, H., Kim, S. C., Rogler, G., Sartor, R. B., & Haller, D. (2007). Interleukin-10 Blocked Endoplasmic Reticulum Stress in Intestinal Epithelial Cells: Impact on Chronic Inflammation. *Gastroenterology*, *132*(1), 190–207. DOI:10.1053/j.gastro.2006.10.030

Siefjediers, A., Hardt, M., Prinz, G., & Diener, M. (2007). Characterization of inositol 1,4,5-trisphosphate (IP3) receptor subtypes at rat colonic epithelium. *Cell Calcium*, *41*(4),303–15. DOI:10.1016/j.ceca.2006.07.009

Simons, B. D., & Clevers, H. (2011a). Stem cell self-renewal in intestinal crypt. *Experimental Cell Research*, *317*(19), 2719–2724. DOI:10.1016/j.yexcr.2011.07.010

Simons, B. D., & Clevers, H. (2011b). Strategies for homeostatic stem cell self-renewal in adult tissues. *Cell*, *145*(6), 851–62. DOI:10.1016/j.cell.2011.05.033

Singh, P. K., & Hollingsworth, M. A. (2006). Cell surface-associated mucins in signal transduction. *Trends in Cell Biology*, *16*(9), 467–476. DOI:10.1016/j.tcb.2006.07.006

Sirker, A., Zhang, M., & Shah, A. M. (2011). NADPH oxidases in cardiovascular disease: Insights from in vivo models and clinical studies. *Basic Research in Cardiology*, *106*(5), 735–747. DOI: 10.1007/s00395-011-0190-z

Slater, E. C., & Cleland, K. W. (1953). The effect of calcium on the respiratory and phosphorylative activities of heart-muscle sarcosomes. *The Biochemical Journal*, *55*(4), 566–590.

Sneyd, J., Keizer, J., & Sanderson, M. J. (1995). Mechanisms of calcium oscillations and waves: a quantitative analysis. *The FASEB Journal*, *9*, 1463–1472.

Soares, S., Thompson, M., White, T., Isbell, A., Yamasaki, M., Prakash, Y., Chini, E. N. (2007). NAADP as a second messenger: neither CD38 nor base-exchange reaction are necessary for in vivo generation of NAADP in myometrial cells. *American Journal of Physiology. Cell Physiology*, *292*(1), C227–C239. DOI:10.1152/ajpcell.00638.2005

Soboloff, J., Spassova, M. A., Tang, X. D., Hewavitharana, T., Xu, W., & Gill, D. L. (2006). Orai1 and STIM reconstitute store-operated calcium channel function. *Journal of Biological Chemistry*, *281*(30), 20661–20665. DOI:10.1074/jbc.C600126200

Specian, R. D., & Neutra, M. R. (1980). Mechanism of rapid mucus secretion in goblet cells stimulated by acetylcholine. *The Journal of Cell Biology*, *85*(3), 626–40.

Stanger, B. Z., Datar, R., Murtaugh, L. C., & Melton, D. A. (2005). Direct regulation of intestinal fate by Notch. *Proceedings of the National Academy of Sciences of the United States of America*, *102*(35), 12443–12448. DOI:10.1073/pnas.0505690102

Stanley, C., & Phillips, T. (1999). Selective secretion and replenishment of discrete mucin glycoforms from intestinal goblet cells. *American Journal of Physiology. Gastrointestinal and Liver Physiology*, *277*, 191–200.

Stappenbeck, T. S. (2009). Paneth Cell Development, Differentiation, and Function: New Molecular Cues. *Gastroenterology*, *137*(1), 30–33. DOI:10.1053/j.gastro.2009.05.013

Steen, M., Kirchberger, T., & Guse, A. H. (2007). NAADP mobilizes calcium from the endoplasmic reticular Ca^{2+} store in T-lymphocytes. *Journal of Biological Chemistry*, *282*(26), 18864–18871. DOI:10.1074/jbc.M610925200

Streb, H., Bayerdörffer, E., Haase, W., Irvine, R., & Schulz, I. (1984). Effect of inositol-1,4,5-trisphosphate on isolated subcellular fractions of rat pancreas. *The Journal of Membrane Biology*, *81*(3), 241–253.

Structure of the colonic mucosa. Encyclopaedia Britannica. Retrieved September 1, 2015, from http://www.britannica.com/science/human-digestive-system

Sugiura, T., Bielefeldt, K., & Gebhart, G. F. (2007). Mouse colon sensory neurons detect extracellular acidosis via TRPV1. *American Journal of Physiology. Cell Physiology*, *292*(5), C1768–C1774. DOI:10.1152/ajpcell.00440.2006

Szanto, I., Rubbia-Brandt, L., Kiss, P., Steger, K., Banfi, B., Kovari, E., Krause, K. H. (2005). Expression of NOXI, a superoxide-generating NADPH oxidase, in colon cancer and inflammatory bowel disease. *Journal of Pathology*, *207*(2), 164–176. DOI:10.1002/path.1824

Szasz, I., Sarkadi, B., Schubert, A., Gardos, G. (1978). Effects of Lanthanum on Calcium-dependent phenomena in human red cells. *Biochemica et Biophysica Acta*, *512*(2), 331–340. DOI:10.1085/jgp.71.6.721

Tabcharani, J., Harris, R., Boucher, A., Eng, J., & Hanrahan, J. (1994). Basolateral K channel activated by carbachol in the epithelial cell line T84. *The Journal of Membrane Biology*, *142*(2), 241–254.

Takahashi, T., Ohnishi, H., Sugiura, Y., Honda, K., Suematsu, M., Kawasaki, T., Yuba, S. (2014). Non-neuronal acetylcholine as an endogenous regulator of proliferation and differentiation of Lgr5-positive stem cells in mice. *The FEBS Journal*, *281*, 4672–4690. DOI:10.1111/febs.12974

Takasawa, S., Akiyama, T., Nata, K., Kuroki, M., Tohgo, A., Noguchi, N., Okamoto, H. (1998). Cyclic ADP-ribose and Inositol 1,4,5-Trisphosphate as Alternate Second Messengers for Intracellular Ca^{2+} Mobilization in Normal and Diabetic beta-Cells. *Journal of Biological Chemistry*, *273*(5), 2497–2500. DOI:10.1074/jbc.273.5.2497

Takasawa, S., Nata, K., Yonekura, H., & Okamoto, H. (1993b). Cyclic ADP-Ribose in Insulin Secretion from Pancreatic beta cells. *Science*, *259*, 370–372.

Takasawa, S., Tohgo, A., Noguchi, N., Koguma, T., Nata, K., Sugimoto, T., Okamoto, H. (1993). Synthesis and Hydrolysis of Cyclic ADP-Ribose by Human Leukocyte Antigen CD38 and Inhibition of the Hydrolysis by ATP. *The Journal of Biological Chemistry*, *268*(35), 26052–26054.

Takemura, H., & Putney, J. W. (1989). Capacitative calcium entry in parotid acinar cells. *The Biochemical Journal*, *258*(2), 409–412.

Takens-Kwak, B., & Jongsma, H. (1992). Cardiac gap junctions: three distinct single channel conductances and their modulation by phosphorylating treatments. *Pflugers Archiv-European Journal of Physiology*, *422*(2), 198–200.

Takeshima, H., Nishimura, S., Matsumoto, T., Ishida, H., Kangawa, K., Minamino, N., Numa, S. (1989). Primary structure and expression from complementary DNA of skeletal muscle ryanodine receptor. *Nature*, *339*, 439–445.

Tamaoki, J., Nakata, J., Takeyama, K., Chiyotani, A., & Konno, K. (1997). Histamine H2 receptor-mediated airway goblet cell secretion and its modulation by histamine-degrading enzymes. *Journal of Allergy and Clinical Immunology*, *99*(2), 233–238. DOI: 10.1016/S0091-6749(97)70102-7

Tamariz, E., & Varela-Echavarría, A. (2015). The discovery of the growth cone and its influence on the study of axon guidance. *Frontiers in Neuroanatomy*, *9*, 1–9. DOI:10.3389/fnana.2015.00051

Tanabe, T., Mikami, A., Numa, S., & Beam, K. G. (1990). Cardiac-type excitation-contraction coupling in dysgenic skeletal muscle injected with cardiac dihydropyridine receptor cDNA. *Nature*, *334*, 451–453.

Tani, S., Suzuki, T., Kano, S., Tanaka, T., Sunaga, K., Morishige, R., & Tsuda, T. (2002). Mechanisms of gastric mucus secretion from cultured rat gastric epithelial cells induced by carbachol, cholecystokinin octapeptide, secretin, and prostaglandin E2. *Biological & Pharmaceutical Bulletin*, *25*(1), 14–18. DOI:10.1248/bpb.25.14

Taylor, C. W., & Dale, P. (2012). Intracellular Ca^{2+} channels – A growing community. *Molecular and Cellular Endocrinology*, *353*(1-2), 21–28. DOI:10.1016/j.mce.2011.08.028

Taylor, C. W., & Laude, A. J. (2002). IP_3 receptors and their regulation by calmodulin and cytosolic Ca^{2+}. *Cell Calcium*, *32*(5-6), 321–334. DOI: 10.1016/S0143-4160(02)00185-9

Taylor, C. W., & Tovey, S. C. (2010). IP3 Receptors: Toward Understanding Their Activation. *Cold Spring Harbor Perspectives in Biology*, *2*(12), 1–22.

Taylor, G. (2009). Non-neuronal release of Ach plays a key role in secretory response to luminal proprionate in rat colon. *Journal of Physiology*, 252–256. DOI:10.1017/CBO9780511609749.016

Terada, T., Shimada, Y., Pan, X., Kishimoto, K., Sakurai, T., Doi, R., Inui, K. I. (2005). Expression profiles of various transporters for oligopeptides, amino acids and organic ions along the human digestive tract. *Biochemical Pharmacology*, *70*(12), 1756–1763. DOI:10.1016/j.bcp.2005.09.027

Thastrup, O., Cullen, P. J., Drøbak, B. K., Hanley, M. R., & Dawson, A. P. (1990). Thapsigargin, a tumor promoter, discharges intracellular Ca^{2+} stores by specific inhibition of the endoplasmic reticulum Ca^{2+}-ATPase. *Proceedings of the National Academy of Sciences of the United States of America*, *87*(7), 2466–2470.

Thomas, A. P., Bird, G. S., Hajnóczky, G., Robb-Gaspers, L. D., & Putney, J. W. (1996). Spatial and temporal aspects of cellular calcium signaling. *The FASEB Journal*, *10*(13), 1505–17.

Toescu, E. C., & Verkhratsky, A. (2004). Ca^{2+} and mitochondria as substrates for deficits in synaptic plasticity in normal brain ageing. *Journal of Cellular and Molecular Medicine*, *8*(2), 181–190. DOI:10.1016/j.ceca.2004.02.020

Tohgo, A., Munakata, H., Takasawa, S., Nata, K., Akiyama, T., Hayashi, N., & Okamoto, H. (1997). Lysine 129 of CD38 (ADP-ribosyl cyclase/cyclic ADP-ribose hydrolase) participates in the binding of ATP to inhibit the cyclic ADP-ribose hydrolase. *Journal of Biological Chemistry*, *272*(7), 3879–3882. DOI:10.1074/jbc.272.7.3879

Tohgo, A., Takasawa, S., Noguchi, N., Koguma, T., Nata, K., Sugimoto, T., Okamoto, H. (1994). Essential cysteine residues for cyclic ADP-ribose synthesis and hydrolysis by CD38. *Journal of Biological Chemistry*, *269*(46), 28555–28557.

Toumi, F., Frankson, M., Ward, J. B., Kelly, O. B., Mroz, M. S., Bertelsen, L. S., & Keely, S. J. (2011). Chronic regulation of colonic epithelial secretory function by activation of G protein-coupled receptors. *Neurogastroenterology and Motility*, *23*(2), 178-186. DOI:10.1111/j.1365-2982.2010.01610.x

Touyz, R. M. (2005). Reactive oxygen species as mediators of calcium signaling by angiotensin II: implications in vascular physiology and pathophysiology. *Antioxidants & Redox Signaling*, *7*(9-10), 1302–1314. DOI:10.1089/ars.2005.7.1302

Tsubouchi, S., & Leblond, C. P. (1979). Migration and turnover of entero-endocrine and caveolated cells in the epithelium of the descending colon, as shown by radioautography after continuous infusion of 3H-thymidine into mice. *The American Journal of Anatomy*, *156*(4), 431–451. DOI:10.1002/aja.1001560403

Tu, H., Wang, Z., & Bezprozvanny, I. (2005a). Modulation of mammalian inositol 1,4,5-trisphosphate receptor isoforms by calcium: a role of calcium sensor region. *Biophysical Journal*, *88*(2), 1056–1069. DOI:10.1529/biophysj.104.049601

Tu, H., Wang, Z., Nosyreva, E., De Smedt, H., & Bezprozvanny, I. (2005b). Functional characterization of mammalian inositol 1,4,5-trisphosphate receptor isoforms. *Biophysical Journal*, *88*(2), 1046–1055. DOI:10.1529/biophysj.104.049593

Tuček, S. (1983). Acetylcoenzyme A and the synthesis of acetylcholine in neurons: Review of recent progress. *General Physiology and Biophysics*, *2*, 313–324.

Turner, J. R. (2009). Intestinal mucosal barrier function in health and disease. *Nature Reviews. Immunology*, *9*(11), 799–809. DOI: 10.1038/nri2653

Ueyama, T., Geiszt, M., & Leto, T. L. (2006). Involvement of Rac1 in activation of multicomponent Nox1- and Nox3-based NADPH oxidases. *Molecular and Cellular Biology*, *26*(6), 2160–2174. DOI:10.1128/MCB.26.6.2160-2174.2006

University of Tokyo. Intercellular communications. *Life Science Web Textbook*. Retrieved from http://csls-text.c.u-tokyo.ac.jp/active/11_04.html

Ushio-Fukai, M. (2006a). Localizing NADPH oxidase-derived ROS. *Science Signalling*, *349*, re8. DOI:10.1126/stke.3492006re8

Ushio-Fukai, M. (2006b). Redox signaling in angiogenesis: Role of NADPH oxidase. *Cardiovascular Research*, *71*(2), 226–235. DOI:10.1016/j.cardiores.2006.04.015

Vais, H., Foskett, J. K., & Daniel Mak, D.-O. (2010). Unitary Ca^{2+} current through recombinant type 3 InsP (3) receptor channels under physiological ionic conditions. *The Journal of General Physiology*, *136*(6), 687–700. DOI:10.1085/jgp.201010513

van der Flier, L. G., & Clevers, H. (2009). Stem cells, self-renewal, and differentiation in the intestinal epithelium. *Annual Review of Physiology*, *71*, 241–60. DOI:10.1146/annurev.physiol.010908.163145

van der Sluis, M., Bouma, J., Vincent, A., Velcich, A., Carraway, K. L., Büller, H. A., Renes, I. B. (2008). Combined defects in epithelial and immunoregulatory factors exacerbate the pathogenesis of inflammation: mucin 2-interleukin 10-deficient mice. *Laboratory Investigation; a Journal of Technical Methods and Pathology*, *88*(6), 634–642. DOI:10.1038/labinvest.2008.28

Van der Sluis, M., De Koning, B. A. E., De Bruijn, A. C. J. M., Velcich, A., Meijerink, J. P. P., Van Goudoever, J. B., Einerhand, A. W. C. (2006). Muc2-deficient mice spontaneously develop colitis, indicating that MUC2 is critical for colonic protection. *Gastroenterology*, *131*(1), 117–29. DOI:10.1053/j.gastro.2006.04.020

VanDussen, K. L., Carulli, A. J., Keeley, T. M., Patel, S. R., Puthoff, B. J., Magness, S. T., Samuelson, L. C. (2012). Notch signaling modulates proliferation and differentiation of intestinal crypt base columnar stem cells. *Development*, *139*(3), 488–97. DOI:10.1242/dev.070763

van Es, J. H., de Geest, N., van de Born, M., Clevers, H., & Hassan, B. A. (2010). Intestinal stem cells lacking the Math1 tumour suppressor are refractory to Notch inhibitors. *Nature Communications*, *1*(2), 18. DOI: 10.1038/ncomms1017

van Es, J. H., Sato, T., van de Wetering, M., Lyubimova, A., Yee Nee, A. N., Gregorieff, A., Clevers, H. (2012). $Dll1^{+}$ secretory progenitor cells revert to stem cells upon crypt damage. *Nature Cell Biology*, *14*(10), 1099–1104. DOI: 10.1038/ncb2581

van Es, J. H., van Gijn, M. E., Riccio, O., van den Born, M., Vooijs, M., Begthel, H., Clevers, H. (2005). Notch/gamma-secretase inhibition turns proliferative cells in intestinal crypts and adenomas into goblet cells. *Nature*, *435*(7044), 959–963. DOI: 10.1038/nature03659

van Koppen, C. J., & Kaiser, B. (2003). Regulation of muscarinic acetylcholine receptor signaling. *Pharmacology & Therapeutics*, *98*(2), 197–220. DOI: 10.1016/S0163-7258(03)00032-9

Van Leeuwen, I. M. M., Mirams, G. R., Walter, a., Fletcher, a., Murray, P., Osborne, J., Byrne, H. M. (2009). An integrative computational model for intestinal tissue renewal. *Cell Proliferation*, *42*(5), 617–636. DOI:10.1111/j.1365-2184.2009.00627.x

Van Limbergen, J., Wilson, D. C., & Satsangi, J. (2009). The genetics of Crohn's disease. *Annual Review of Genomics and Human Genetics*, *10*, 89–116. DOI: 10.1146/annurev-genom-082908-150013

Vanuytsel, T., Senger, S., Fasano, A., & Shea-Donohue, T. (2013). Major Signaling Pathways in Intestinal Stem Cells. *Biochimica et Biophysica Acta*, *1830*(2), 2410–2426. DOI:10.1016/j.bbagen.2012.08.006.Major

Varoqui, H., & Erickson, J. D. (1996). Active Transport of Acetylcholine by the Human Transporter. *Journal of Biological Chemistry*, *271*(44), 27229–27232.

Vasington, F., & Murphy, J. (1962). Calcium Uptake by Rat Kidney Mitochondria and Its Dependence on Respiration and Phosphorylation. *The Journal of Biological Chemistry*, *237*(8), 2671–2677.

Veenstra, R., Wang, H., Beblo, D., Chilton, M., Harris, A., Beyer, E., & Brink, P. (1995). Selectivity of connexin-specific gap junctions does not correlate with channel conductance. *Circulation Research*, *77*(6), 1156–1165.

Velcich, A., Yang, W., Heyer, J., Fragale, A., Nicholas, C., Viani, S., Augenlicht, L. (2002). Colorectal cancer in mice genetically deficient in the mucin Muc2. *Science*, *295*(5560), 1726–1729. DOI:10.1126/science.1069094

Vembar, S., & Brodsky, J. (2008). One step at a time: endoplasmic reticulum-associated degradation. *Nature Reviews Molecular Cell Biology*, *9*(12), 944–957. DOI: 10.1038/nrm2546

Vercauteren, D., Vandenbroucke, R. E., Jones, A. T., Rejman, J., Demeester, J., De Smedt, S. C., Braeckmans, K. (2010). The use of inhibitors to study endocytic pathways of gene carriers: optimization and pitfalls. *Molecular Therapy*, *18*(3), 561–569. DOI:10.1038/mt.2009.281

Verma, V., Carter, C., Keable, S., Bennett, D., & Thorn, P. (1996). Identification and function of type-2 and type-3 ryanodine receptors in gut epithelial cells. *The Biochemical Journal*, *319 (2)*, 449–454.

Waite, K. a, Wallin, R., Qualliotine-Mann, D., & McPhail, L. C. (1997). Phosphatidic acid-mediated phosphorylation of the NADPH oxidase component p47-phox. *Journal of Biological Chemistry*, *272*(24), 15569–15578.

Walseth, T. F., Lin-Moshier, Y., Jain, P., Ruas, M., Parrington, J., Galione, A., Slama, J. T. (2012). Photoaffinity labeling of high affinity nicotinic acid adenine dinucleotide phosphate (NAADP)-binding proteins in sea urchin egg. *Journal of Biological Chemistry*, *287*(4), 2308–2315. DOI:10.1074/jbc.M111.306563

Walter, P., & Ron, D. (2011). The unfolded protein response: from stress pathway to homeostatic regulation. *Science*, *334*(6059), 1081–6. DOI:10.1126/science.1209038

Wang, X., Zhang, X., Dong, X., Samie, M., Li, X., Cheng, X., Xu, H. (2012). TPC Proteins Are Phosphoinositide-Activated Sodium-Selective Ion Channels in Endosomes and Lysosomes. *Cell*, *151*(2), 372–383. DOI:10.1016/j.cell.2012.08.036

Wei, W., Graeff, R., & Yue, J. (2014). Roles and mechanisms of the CD38/cyclic adenosine diphosphate ribose/Ca^{2+} signaling pathway. *World Journal of Biological Chemistry*, *5*(1), 58–67. DOI:10.4331/wjbc.v5.i1.58

Weiss, E. R., Kelleher, D. J., Woon, C. W., Soparkar, S., Osawa, S., Heasley, L. E., & Johnson, G. L. (1988). Receptor activation of G proteins. *FASEB Journal : Official Publication of the Federation of American Societies for Experimental Biology*, *2*, 2841–2848.

Welcker, K., Martin, A., Kölle, P., Siebeck, M., & Gross, M. (2004). Increased intestinal permeability in patients with inflammatory bowel disease. *European Journal of Medical Research*, *9*(10), 456–460.

Wess, J., Brann, M. R., & Bonner, T. I. (1989). Identification of a small intracellular region of the muscarinic m3 receptor as a determinant of selective coupling to PI turnover. *FEBS Letters*, *258*(1), 133–136. DOI: 10.1016/0014-5793(89)81633-3

Wess, J. (2003). Novel insights into muscarinic acetylcholine receptor function using gene targeting technology. *Trends in Pharmacological Sciences*, *24*(8), 414–420. DOI: 10.1016/S0165-6147(03)00195-0

Wessler, I., & Kirkpatrick, C. J. (2008). Acetylcholine beyond neurons: the non-neuronal cholinergic system in humans. *British Journal of Pharmacology*, *154*(8), 1558–1571. DOI:10.1038/bjp.2008.185

Wessler, I., Kilbinger, H., Bittinger, F., Unger, R., & Kirkpatrick, C. J. (2003). The non-neuronal cholinergic system in humans: Expression, function and pathophysiology. *Life Sciences*, *72*(18-19), 2055–2061. DOI: 10.1016/S0024-3205(03)00083-3

Westphalen, C. B., Asfaha, S., Hayakawa, Y., Takemoto, Y., Lukin, D. J., Nuber, A. H., Wang, T. C. (2014). Long-lived intestinal tuft cells serve as colon cancer-initiating cells. *Journal of Clinical Investigation*, *124*(3), 1283–1295. DOI: 10.1172/JCI73434

White, B. D., Chien, A. J., & Dawson, D. W. (2012). Desregulation of Wnt/beta-catenin Signaling in Gastrointestinal Cancer. *Gastroenterology*, *142*(2), 219–232. DOI:10.1053/j.gastro.2011.12.001.Dysregulation

White, V., Scarpini, C., Barbosa-Morais, N. L., Ikelle, E., Carter, S., Laskey, R. A., Coleman, N. (2009). Isolation of stool-derived mucus provides a high yield of colonocytes suitable for early detection of colorectal carcinoma. *Cancer Epidemiology, Biomarkers & Prevention*, *18*(7), 2006–13. DOI:10.1158/1055-9965.EPI-08-1145

Widdicombe, J. G. (1991). Neural Control of Airway Vasculature and Edema. *American Review of Respiratory Disease*, *143*, S18–S21.

Williams, A., Lüter, C., & Cusack, M. (2001). The nature of siliceous mosaics forming the first shell of the brachiopod Discinisca. *Journal of Structural Biology*, *134*(1), 25–34. DOI:10.1006/jsbi.2001.4366

Wind, S., Beuerlein, K., Eucker, T., Müller, H., Scheurer, P., Armitage, M. E., Wingler, K. (2010). Comparative pharmacology of chemically distinct NADPH oxidase inhibitors. *British Journal of Pharmacology*, *161*(4), 885–898. DOI:10.1111/j.1476-5381.2010.00920.x

Wingler, K., Altenhoefer, S. A., Kleikers, P. W. M., Radermacher, K. A., Kleinschnitz, C., & Schmidt, H. H. H. W. (2012). VAS2870 is a pan-NADPH oxidase inhibitor. *Cellular and Molecular Life Sciences*, *69*(18), 3159–3160. DOI: 10.1007/s00018-012-1107-1

Wlodarska, M., Thaiss, C. A., Nowarski, R., Henao-Mejia, J., Zhang, J.-P., Brown, E. M., Flavell, R. A. (2014). NLRP6 inflammasome orchestrates the colonic host-microbial interface by regulating goblet cell mucus secretion. *Cell*, *156*(5), 1045–59. DOI:10.1016/j.cell.2014.01.026

Woods, N. M., Cuthbertson, K. S., & Cobbold, P. H. (1987). Agonist-induced oscillations in cytoplasmic free calcium concentration in single rat hepatocytes. *Cell Calcium*, *8*(1), 79–100. DOI: 10.1016/0143-4160(87)90038-8

Worley, P. F., Baraban, J. M., Supattapone, S., Wilson, V., & Snyder, S. H. (1987). Characterization of inositol trisphosphate receptor binding in brain. *The Journal of Biological Chemistry*, *262*(25), 12132–12136.

Wurtman, R., Cansev, M., & Ulus, I. (2008). Choline and its products acetylcholine and phosphatidylcholine. In *Handbook of Neurochemistry*, Vol. 8, Chapter 3.2.

Wuytack, F., Raeymaekers, L., & Missiaen, L. (2002). Molecular physiology of the SERCA and SPCA pumps. *Cell Calcium*, *32*(5-6), 279–305. DOI: 10.1016/S0143416002001847

Wyatt, J., Vogelsang, H., Hübl, W., Waldhöer, T., & Lochs, H. (1993). Intestinal permeability and the prediction of relapse in Crohn's disease. *Lancet*, *341*(8858), 1437–1439.

Xu, M., Li, X.-X., Ritter, J. K., Abais, J. M., Zhang, Y., & Li, P.-L. (2013). Contribution of NADPH Oxidase to Membrane CD38 Internalization and Activation in Coronary Arterial Myocytes. *PLoS ONE*, *8*(8), e71212. DOI:10.1371/journal.pone.0071212

Xu, Y., Ren, X. C., Quinn, C. C., & Wadsworth, W. G. (2011). Axon response to guidance cues is stimulated by acetylcholine in Caenorhabditis elegans. *Genetics*, *189*(3), 899–906. DOI:10.1534/genetics.111.133546

Yajima, T., Inoue, R., Matsumoto, M., & Yajima, M. (2011). Non-neuronal release of ACh plays a key role in secretory response to luminal propionate in rat colon. *The Journal of Physiology*, *589*(4), 953–62. DOI:10.1113/jphysiol.2010.199976

Yamada, M., Mizuguchi, M., Otsuka, N., Ikeda, K., & Takahashi, H. (1997). Ultrastructural localization of CD38 immunoreactivity in rat brain. *Brain Research*, *756*(1-2), 52–60.

Yamasaki, M., Masgrau, R., Morgan, A. J., Churchill, G. C., Patel, S., Ashcroft, S. J. H., & Galione, A. (2004). Organelle Selection Determines Agonist-specific Ca^{2+} Signals in Pancreatic Acinar and β Cells. *Journal of Biological Chemistry*, *279*(8), 7234–7240. DOI:10.1074/jbc.M311088200

Yamasaki, M., Thomas, J. M., Churchill, G. C., Garnham, C., Lewis, A. M., Cancela, J.-M., Galione, A. (2005). Role of NAADP and cADPR in the induction and maintenance of agonist-evoked Ca^{2+} spiking in mouse pancreatic acinar cells. *Current Biology : CB*, *15*(9), 874–8. DOI:10.1016/j.cub.2005.04.033

Yan, K., Chia, L., & Li, X. (2012). The intestinal stem cell markers Bmi1 and Lgr5 identify two functionally distinct populations. *Proceedings of the National Academy of Sciences*, *109*(2), 466–471. DOI:10.1073/pnas.1118857109

Yan, Y., Wei, C. L., Zhang, W. R., Cheng, H. P., & Liu, J. (2006). Cross-talk between calcium and reactive oxygen species signaling. *Acta Pharmacologica Sinica*, *27*(7), 821–826. DOI:10.1111/j.1745-7254.2006.00390.x

Yang, N., Garcia, M. A. S., & Quinton, P. M. (2013). Normal mucus formation requires cAMP-dependent HCO_3^- secretion and Ca^{2+}-mediated mucin exocytosis. *The Journal of Physiology*, *591*(18), 4581–4593. DOI:10.1113/jphysiol.2013.257436

Yang, Q., Bermingham, N. A., Finegold, M. J., & Zoghbi, H. Y. (2001). Requirement of Math1 for secretory cell lineage commitment in the mouse intestine. *Science*, *294*(5549), 2155–2158. DOI:10.1126/science.1065718

Yi, M., Weaver, D., & Hajnóczky, G. (2004). Control of mitochondrial motility and distribution by the calcium signal: A homeostatic circuit. *Journal of Cell Biology*, *167*(4), 661–672. DOI:10.1083/jcb.200406038

Yin, W., & Voit, E. O. (2013). Function and design of the Nox1 system in vascular smooth muscle cells. *BMC Systems Biology*, *7*(1), 20. DOI: 10.1186/1752-0509-7-20

Yoo, S. H. (2010). Secretory granules in inositol 1,4,5-trisphosphate-dependent Ca^{2+} signaling in the cytoplasm of neuroendocrine cells. *The FASEB Journal : Official Publication of the Federation of American Societies for Experimental Biology*, *24*(3), 653–664. DOI:10.1096/fj.09-132456

Yu, J., Kim, K., & Kim, H. (2006). Role of NADPH Oxidase and Calcium in Cerulein-induced Apoptosis. *Annuals of The New York Academy Of Sciences*, *1090*, 292–297.

Yu, K., Lujan, R., Marmorstein, A., Gabriel, S., & Hartzell, H. C. (2010). Bestrophin-2 mediates bicarbonate transport by goblet cells in mouse colon. *Journal of Clinical Investigation*, *120*(5), 1722–1735. DOI: 10.1172/JCI41129

Yu, T., Chen, X., Zhang, W., Li, J., Xu, R., Wang, T. C., Liu, C. (2012). Krüppel-like factor 4 regulates intestinal epithelial cell morphology and polarity. *PLoS One*, *7*(2), e32492. DOI:10.1371/journal.pone.0032492

Yuan, J. P., Zeng, W., Dorwart, M. R., Choi, Y., Paul, F., & Muallem, S. (2009). SOAR and the polybasic STIM1 domains gate and regulate the Orai channels. *Nature Cell Biology*, *11*(3), 337–343. DOI:10.1038/ncb1842.SOAR

Zecchini, V., Domaschenz, R., Winton, D., & Jones, P. (2005). Notch signaling regulates the differentiation of post-mitotic intestinal epithelial cells. *Genes & Development*, 1686–1691. DOI:10.1101/gad.341705.1686

Zhang, F., Jin, S., Yi, F., & Li, P. L. (2009). TRP-ML1 functions as a lysosomal NAADP-sensitive Ca^{2+} release channel in coronary arterial myocytes. *Journal of Cellular and Molecular Medicine*, *13*(9B), 3174–3185. DOI:10.1111/j.1582-4934.2008.00486.x

Zhang, F., & Li, P. L. (2007). Reconstitution and characterization of a Nicotinic Acid Adenine Dinucleotide Phosphate (NAADP)-sensitive Ca^{2+} release channel from liver lysosomes of rats. *Journal of Biological Chemistry*, *282*(35), 25259–25269. DOI:10.1074/jbc.M701614200

Zhang, S., Yu, Y., Roos, J., Kozak, A., Deerinck, T., Ellisman, M., Cahalan, M. (2005). STIM1 is a Ca^{2+} sensor that activates CRAC channels and migrates from the Ca^{2+} store to the plasma membrane. *Nature*, *437*(7060), 902–905. DOI:10.2190/OM.58.2.b.Six-Year

Zhang, W., Chen, X., Kato, Y., Evans, P. M., Yang, J., Rychahou, P. G., Yuan, S. (2006). Novel Cross Talk of Krüppel-Like Factor 4 and β -Catenin Regulates Normal Intestinal Homeostasis and Tumor Repression. *Molecular and Cellular Biology*, *26*(6), 2055–2064. DOI:10.1128/MCB.26.6.2055

Zhang, X., & Forscher, P. (2009). Rac1 Modulates Stimulus-evoked Ca^{2+} Release in Neuronal Growth Cones via Parallel Effects on Microtubule/Endoplasmic Reticulum Dynamics and Reactive Oxygen Species Production. *Molecular Biology of the Cell*, *20*, 3700–3712. DOI:10.1091/mbc.E08-07-0730

Zhang, Y., Zhu, H., Zhang, Q., Li, M., Yan, M., Wang, R., Wang, X. (2009). Phospholipase D-alpha1 and phosphatidic acid regulate NADPH oxidase activity and production of reactive oxygen species in ABA-mediated stomatal closure in Arabidopsis. *The Plant Cell*, *21*(8), 2357–2377. DOI:10.1105/tpc.108.062992

Zhang, Z.-H., Lu, Y.-Y., & Yue, J. (2013). Two pore channel 2 differentially modulates neural differentiation of mouse embryonic stem cells. *PLoS One*, *8*(6), e66077. DOI:10.1371/journal.pone.0066077

Zhao, W., Hisamuddin, I. M., Nandan, M. O., Babbin, B. A., & Neil, E. (2004). Identification of Kruppel-like factor 4 as a potential tumor suppressor gene in colorectal cancer. *Oncogene*, *23*(2), 395–402.

Zheng, H., Pritchard, D. M., Yang, X., Bennett, E., Liu, G., Liu, C., & Ai, W. (2009). KLF4 gene expression is inhibited by the notch signaling pathway that controls goblet cell differentiation in mouse gastrointestinal tract. *American Journal of Physiology. Gastrointestinal and Liver Physiology*, *296*(3), G490–G498. DOI:10.1152/ajpgi.90393.2008

Zhernakova, A., van Diemen, C. C., Wijmenga, C., C, W., Zhernakova, A., van Diemen, C. C., & Wijmenga, C. (2009). Detecting shared pathogenesis from the shared genetics of immune-related diseases. *Nature Reviews Genetics*, *10*(1), 43–55. DOI: 10.1038/nrg2489

Zhu, K., Kakehi, T., Matsumoto, M., Iwata, K., Ibi, M., Ohshima, Y., Yabe-Nishimura, C. (2015). NADPH oxidase NOX1 is involved in activation of protein kinase C and premature senescence in early stage diabetic kidney. *Free Radical Biology and Medicine*, *83*, 21–30. DOI:10.1016/j.freeradbiomed.2015.02.009

Zhu, M. X., Ma, J., Parrington, J., Galione, A., & Evans, A. M. (2010). TPCs: Endolysosomal channels for Ca^{2+} mobilization from acidic organelles triggered by NAADP. *FEBS Letters*, *584*(10), 1966–74. DOI:10.1016/j.febslet.2010.02.028

Zimmerman, M. C., Takapoo, M., Jagadeesha, D. K., Stanic, B., Banfi, B., Bhalla, R. C., & Miller, F. J. (2011). Activation of NADPH Oxidase 1 Increases Intracellular Calcium and Migration of Smooth Muscle Cells. *Hypertension*, *58*(3), 446–453. DOI:10.1161/HYPERTENSIONAHA.111.177006

Zimmerman, T. W., Dobbins, J. W., & Binder, H. J. (1982). Mechanism of cholinergic regulation of electrolyte transport in rat colon in vitro. *The American Journal of Physiology*, *242*(2), G116–G123.

Zocchi, E., Franco, L., Guida, L., Piccini, D., Tacchetti, C., & De Flora, A. (1996). NAD^+-dependent internalization of the transmembrane glycoprotein CD38 in human namalwa B cells. *FEBS Letters*, *396*(2-3), 327–332. DOI:10.1016/0014-5793(96)01125-8

Zocchi, E., Usai, C., Guida, L., Franco, L., Bruzzone, S., Passalacqua, M., & De Flora, A. (1999). Ligand-induced internalization of CD38 results in intracellular Ca^{2+} mobilization: role of NAD^+ transport across cell membranes. *The FASEB Journal*, *13*(2), 273–283.

Zong, X., Schieder, M., Cuny, H., Fenske, S., Gruner, C., Rötzer, K., Wahl-Schott, C. (2009). The two-pore channel TPCN2 mediates NAADP-dependent Ca^{2+}-release from lysosomal stores. *Pflügers Archiv : European Journal of Physiology*, *458*(5), 891–9. DOI: 10.1007/s00424-009-0690-y

Appendix

Proceedings of the Physiological Society, Epithelia and Membrane Transport Abstract

Epithelia and Smooth Muscle Interactions in Health and Disease (Dublin) (2013) Proc Physiol Soc 30, PC18

Mobilisation from endo/lysosomal calcium stores is fundamental to the cellular polarity and tissue topology of human colonic crypt calcium signals

Christy Kam[1], Alyson Parris[1], Martin Loader[1], Nathalie Juge[2], Mike Lewis[3], Mark Williams[1]

1. Biological Sciences, University of East Anglia, Norwich, United Kingdom.
2. Gut Health and Food, Institute of Food Research, Norwich, United Kingdom.
3. General Surgery, Norfolk and Norwich University Hospital, Norwich, United Kingdom.

The human large intestinal epithelium comprises millions of invaginations called colonic crypts, which are highly innervated by cholinergic neurons. Spatiotemporal characteristics of cholinergic induced calcium waves along the human colonic crypt-axis suggest that calcium signals play a central role in co-ordinating the physiological function and perpetual renewal of the human colonic epithelium. However, the mechanism of colonic crypt calcium signalling is unknown. The aim of the current study was to characterise the cellular and molecular basis of human colonic crypt calcium signal generation. Methods: Human colonic crypts were isolated from colorectal biopsy samples (NRES approval) and placed in a 3D culture system. Intracellular calcium was monitored by Fura-2 ratio imaging. mRNA expression was assessed by real-time RT-PCR and protein localisation was visualised by fluorescence immunolabelling and confocal microscopy. Results: Application of carbachol (10µM) initiated calcium signals at the apical pole of M3AChR-positive cells located in the stem cell niche at the colonic crypt-base. Calcium signals spread from the apical to basal pole of initiator cells and from initiator cells to all neighbouring cell types (e.g. goblet cells) along the crypt-axis. The absence of extracellular calcium attenuated the duration of the biphasic calcium response at the crypt-base, but did not alter the initial peak amplitude (n=5). Thapsigargin pre-treatment did not abolish the carbachol-induced calcium signal at the apical pole of crypt cells (n=14). Immunolabelling revealed the presence of ER (anti-Kdel) at the basal pole and lysosomes (anti-LAMP1) at the apical pole of polarised crypt cells (n=16). Lysosomal lysis by GPN (200 µM) invoked a calcium increase at the apical pole and abolished subsequent responses to carbachol stimulation (n=5), as did pre-treatment with other lysosomotropic agents, chloroquine (100µM, n=4) and bafilomycin (5µM, n=4). Colonic crypts expressed mRNA for

InsP3R1-3, RyR1&2 and TPC1&2 intracellular calcium channels (N=5 subjects). Carbachol induced calcium signals were profoundly inhibited (peak amplitude inhibition >80%, P<0.05) by the PLC inhibitor U73122 (10μM, n=15) or the NAADP antagonist NED-19 (20-200μM, n=10) and partially inhibited (peak amplitude inhibition <40%, P<0.05) by InsP3R (Xestospongin C, n=5; 2-APB, n=10) or RyR (ryanodine, n=10; 8-bromo cADP ribose, n=10) antagonists. Conclusions: Cholinergic stimulation of M3AChR mobilises calcium from lysosomes located at the apical pole of cells within the colonic crypt stem cell niche. The effects of pharmacological agents suggest that dynamic interplay between NAADP-, InsP3- and cADP ribose-sensitive stores determines the spatiotemporal characteristics, and the physiological outcomes, of colonic crypt calcium signalling.

Proceedings of the Physiological Society, GI Tract Abstract

Physiology 2014 (London, UK) (2014) Proc Physiol Soc 31, C26

Inhibition of CD38-NAADP-TPC-induced calcium signalling blocks cholinergic excitation-mucus secretion coupling in native human colonic crypt goblet cells

Christy Kam[1], Alyson Parris[1], Martin Loader[1], Nathalie Juge[2], Mike Lewis[3], Mark Williams[1]

1. Biological Sciences, University of East Anglia, Norwich, United Kingdom.
2. Gut Health and Food, Institute of Food Research, Norwich, United Kingdom.
3. General Surgery, Norfolk and Norwich University Hospital, Norwich, United Kingdom.

The lumen of the large intestine houses approximately 10^{13} -10^{14} microorganisms. In order to defend itself, the intestinal epithelium secretes a protective coating of mucus, the major component of which is Muc2 mucin protein. There is much interest in the mechanism of excitation-mucus secretion coupling because compromised mucus layer formation in Muc2 knock-out mice and human disease is associated with direct contact of bacteria with the epithelium, inflammation, bloody diarrhoea and colon cancer. Previously, cholinergic stimulation has been shown to promote mucus secretion, but the mechanism for excitation-mucus secretion coupling is not fully understood. The aim of the current study was to elucidate the mechanism of calcium (Ca^{2+}) signal generation in native human colonic crypt goblet cells in situ and determine the role of Ca^{2+} signalling in Muc2 protein secretion. Methods: Human colonic crypts were isolated from colorectal tissue samples obtained at surgical resection (NRES approval) and placed in a 3D culture system. Intracellular Ca^{2+} was monitored by Fura-2/Fluo-4 imaging. To complement previous qRT-PCR mRNA expression analyses, localisation of M3AChR, CD38 (which catalyses NAADP synthesis), TPC1&2 (i.e. Ca^{2+} channels stimulated by NAADP) and endolysosomes (LAMP-1 positive puncta) within $Muc2^{+}$ goblet cells was visualised by fluorescence immunolabelling and confocal microscopy. Ca^{2+} signal generation and Muc2 depletion from goblet cells was assessed following stimulation with carbachol (Cch,10µM) in the presence and absence of nicotinamide (20mM, an inhibitor of CD38-mediated NAADP synthesis) or NED-19 (200µM, an NAADP receptor inhibitor). Results: Application of Cch evoked a Ca^{2+} signal at the human colonic crypt base which spread to all cell types located along the human colonic crypt-axis, including goblet cells. $Muc2^{+}$ goblet cells expressed: M3AChRs on the basal membrane; CD38 in the cytoplasm and nucleus; cytoplasmic TPC1&2 associated with apical LAMP-1 positive intracellular puncta. Cch-induced colonic crypt Ca^{2+} signals were suppressed by pre-treatment with nicotinamide (64.5±5% reduction, N=2 subjects, n=5 crypts) and were inhibited profoundly by pre-

incubation with NED-19 (85±5% reduction, N=5 subjects, n=15 crypts). Goblet cell Muc2 immunofluorescence was dramatically reduced following a 30 minute exposure to Cch (44±4.7 % reduction, N=4 subjects, n=4 crypts) and this was inhibited by NED-19 (150±45%, N=4 subjects, n=4 crypts). Conclusions: Goblets cells in the human large intestine express the molecular machinery to synthesise NAADP. Inhibition of the CD38-NAADP-TPC pathway suppressed Ca^{2+} signal generation and Muc2 depletion. The CD38-NAADP-TPC-calcium pathway plays a central role in cholinergic excitation-mucus secretion coupling in human colonic crypt goblet cells in situ.

Biochemical Society Focused Meeting, Calcium Signalling: The Next Generation (2014) Abstract P025

https://www.biochemistry.org/Events/tabid/379/View/Posters/Page/2/MeetingNo/SA166/Default.aspx

Cryptic calcium signals maintain the fitness of the human intestinal stem cell niche

Christy Kam[1], Alyson Parris[1], Martin Loader[1], Nathalie Juge[2], Mike Lewis[3] and Mark Williams[1]

1. Biological Sciences, University of East Anglia, Norwich, United Kingdom.
2. Gut Health and Food, Institute of Food Research, Norwich, United Kingdom.
3. General Surgery, Norfolk and Norwich University Hospital, Norwich, United Kingdom.

Spatiotemporal characteristics of cholinergic-induced calcium waves along the human colonic crypt-axis suggest that calcium signals play a central role in coordinating the physiological function and perpetual renewal of the human colonic epithelium. One aim of the work in our lab is to characterise the cellular and molecular basis of human colonic crypt calcium signal generation and ascertain their influence on the intestinal stem cell niche. Methods: Human colonic crypts were isolated from tissue biopsy samples obtained at sigmoidoscopy (NRES approval) and placed in a 3D culture system. Intracellular calcium was monitored by Fura-2/Fluo-4 fluorescence imaging. mRNA expression was assessed by RT-PCR and protein localisation was visualised by fluorescence immunolabelling and confocal microscopy. Results: Methacholine initiated calcium signals at the apical pole of M3AChR-positive, LGR5-positive, intestinal stem cells at the colonic crypt-base. Calcium signals spread from the apical to basal pole of initiator stem cells and from initiator cells to all neighbouring cell types (e.g. goblet cells) along the crypt-axis. RT-PCR and immunofluorescence analyses confirmed the expression of InsP3R, RyR and TPC subtypes. TPCs were expressed at the apical pole on endolysosomes. Accordingly, NED-19, a blocker of NAADP/TPC-mediated calcium release, inhibited the calcium signal amplitude by ~90%. NED-19 also inhibited cholinergic-induced mucus secretion from goblet cells and colonic crypt cell proliferation in the intestinal stem cell niche. Conclusions: Cholinergic-induced calcium signals maintain the fitness of the human intestinal stem cell niche.

Published article

Reynolds, A., Wharton, N., Parris, A., Mitchell, E., Sobolewski, A., **Kam, C**., Bigwood, L., El Hadi, A., Münsterberg, A., Lewis, M., Speakman, C., Stebbings, W., Wharton, R., Sargen, K., Tighe, R., Jamieson, C., Hernon, J., Kapur, S., Oue, N., Yasui, W., Williams, MR. (2014) Canonical Wnt signals combined with suppressed TGFβ/BMP pathways promote renewal of the native human colonic epithelium. *Gut 63(4):610-621*.